UNIVERSITY OF THE
WITWATERSRAND,
JOHANNESBURG

The development of new synthetic methods for the assembly of the angucycline skeleton and xanthones. A foray at utilizing a bio-renewable carbon resource and greener chemical reactions

Fatema Jagot

Supervised by C B de Koning and K J Ngwira

A thesis submitted to the Faculty of Science, University of the Witwatersrand, Johannesburg, in fulfilment of the requirements for the degree of Doctor of Philosophy

July 2022

Declaration

I declare that the work presented in this thesis is my own, unaided work carried out under the supervision of Prof. Charles B. de Koning and Dr Kennedy J. Ngwira. It is being submitted for the degree of Doctor of Philosophy at the University of the Witwatersrand, Johannesburg. It has not been submitted before for any degree or any examination in any other University.

Fatema Jagot

29 July 2022

Abstract

The work detailed in this PhD thesis can be broadly separated into two parts, both focusing on the use of certain principles of Green Chemistry in organic synthesis. The aim of the first part was to feature catalysis as our major application of Green Chemistry in the formal synthesis of the angucycline natural product 1,8-dihydroxy-3-methyltetraphene-7,12-dione, also known as tetrangulol. Other principles of Green Chemistry were also integrated as part of our design strategy, where possible.

Previously in our laboratory, a methodology was developed for the synthesis of tetrangulol, that involved a $PtCl_2$- and a $AuCl_3$- mediated cycloisomerization as the key step to construct the B ring of the angucycline. However, significant amounts of the side product 1,10,12-trimethoxy-8-methylchrysene were produced. We therefore set out to attempt to improve this synthesis of tetrangulol, and in so doing incorporate some principles of Green Chemistry. We anticipated using the recently developed carbonyl-olefin metathesis catalyzed by the earth abundant $FeCl_3$ as the key step to construct the B ring of tetrangulol. A palladium- catalyzed Suzuki-Miyaura coupling reaction was used to synthesize the highly congested, carbonyl-olefin containing biaryl intermediate 2-[1,4-dimethoxy-3-(2-methylprop-1-en-1-yl)naphthalen-2-yl]-3-methoxy-5-methylbenzaldehyde. This precursor was then subjected to carbonyl-olefin metathesis conditions, in the presence of 27 mol% of $FeCl_3$, to furnish the desired tetracyclic core, 1,7,12-trimethoxy-3-methyltetraphene. The unexpected formation of quinone 1-methoxy-3-methyltetraphene-7,12-dione was also observed as a side product of this reaction, albeit in poor yields. A late-stage C-H functionalization protocol was subsequently used to introduce a hydroxyl group, however; this led instead to the unforeseen formation of the two chlorocyclinones 2,4-dichloro-11-hydroxy-1-methoxy-3-methyltetraphene-7,12-dione and 2,4-dichloro-6-hydroxy-1-methoxy-3-methyltetraphene-7,12-dione, rather than tetrangulol.

The second part of this PhD thesis details the use of cashew nut shell liquid-derived cardanol as a bio-renewable feedstock to synthesize a small library of UV-absorbing hydroxy-xanthones. A ceric ammonium sulfate-mediated oxidation that was developed in our laboratory was used to efficiently construct the xanthones, for example 2-methoxy-6-pentadecyl-9*H*-xanthen-9-one, from benzophenone intermediates, such as (2,5-dimethoxyphenyl)(2-hydroxy-4-pentadecylphenyl)methanone. Late-stage oxidation procedures were subsequently used to introduce a hydroxyl functionality *ortho* to the carbonyl moiety of the xanthones, to deliver for

example 1-hydroxy-7-methoxy-3-pentadecyl-9*H*-xanthen-9-one. The hydroxy-containing xanthones, as well as benzophenone intermediates, were tested for their UV absorption capabilities. Although all compounds tested displayed good UV absorption profiles, the hydroxy-xanthone 1-hydroxy-6,7-dimethoxy-3-pentadecyl-9*H*-xanthen-9-one was found to show excellent UV absorption in both the UVA and UVB regions of the UV spectrum with molar extinction coefficients of 20320 L mol^{-1} cm^{-1} at 290 nm, and 13949 L mol^{-1} cm^{-1} at 368 nm, qualifying it for a broad-spectrum UV protectant.

List of abbreviations

Ac_2O	Acetic anhydride
AcOH	Acetic acid
B_2Pin_2	Bis(pinacolato)diboron
BPO	Benzoyl peroxide
LiO*t*Bu	Lithium *tert*-butoxide
CAN	Ammonium cerium(IV) nitrate
dba	Dibenzylideneacetone
DBU	1,8-Diazabicyclo[5.4.0]undec-7-ene
DCE	1,2-Dichloroethane
DDQ	2,3-Dichloro-5,6-dicyano-1,4-benzoquinone
DME	Dimethoxyethane
DMF	Dimethylformamide
DMPU	*N*,*N*′-Dimethylpropyleneurea
DMSO	Dimethyl sulfoxide
dppf	1,1′-Bis(diphenylphosphino)ferrocene
HBPin	Pinacolborane
hv	Photon of light
IBX	2-Iodoxybenzoic acid
KO*t*Bu	Potassium *tert*-butoxide
NBS	*N*-Bromosuccinimide
n-BuLi	*n*-Butyllithium
NHPI	*N*-hydroxyphthalimide

NIS	*N*-Iodosuccinimide
NMR	Nuclear magnetic resonance
PCC	Pyridinium chlorochromate
PDC	Pyridinium dichromate
PIDA	(Diacetoxyiodo)benzene
PIFA	(Bis(trifluoroacetoxy)iodo)benzene
PINO	Phthalimide-*N*-oxyl
PKS	Polyketide synthase
TBABr	Tetrabutyl ammonium bromide
TBAF	Tetrabutyl ammonium fluoride
TBAI	Tetrabutyl ammonium iodide
TFA	Trifluoroacetic acid
TFAA	Trifluoroacetic anhydride
TMEDA	Tetramethylethylenediamine
UV	Ultraviolet

Acknowledgements

Thank you to my supervisor Prof. Charles de Koning for his constant guidance, encouragement, patience, and humor. I have benefitted greatly from your wealth of knowledge and am truly honored to have been a part of your research group. Thank you also for all the laughs and jokes we shared in the lab when things got too serious! I am grateful for my co-supervisor Dr Kennedy Ngwira, who has been a part of my academic journey since my undergrad years. Thank you for all your support through the years, and for helping me to grow as a scientist.

I would like to acknowledge all my lab mates for the moments we shared, both high and low, and for ensuring that there never was a dull moment in the lab. Thank you especially to Bianca, Edward, and Nompumelelo for their assistance when I needed it. Thank you also to Prof. Manuel Fernandes for his generous assistance with resolving my crystal structures. Your help is much appreciated.

Many thanks to Prof Dr Till Opatz and his entire research group at the Johannes-Gutenberg-Universität Mainz, Germany, for a wonderful two-months experience in their laboratory.

I am truly grateful for my friends Samaneh, Pierre, Phumlile, and Rudo for constantly checking up on me and keeping me sane.

A very special thanks to Songz for all your valuable inputs and suggestions throughout the course of my project, and for taking the time to read my thesis and providing me with valuable feedback. Thank you also for the confidence you showed in me, for inspiring me, and always being there for me.

I also wish to express my deepest gratitude to my mum and dad for their constant support and unconditional love. Thank you to Umar for his unwavering belief in me, and to Hali for being with me every step of the way. Without you loved ones, I would not have made it this far. Thank you also to all other members of my wonderful family. I am truly blessed.

Finally, and yet in no small measure, I would like to send my heartfelt gratitude to all members of the Khatri Association of Malawi, for sponsoring the first three undergraduate years of my study. Thank you for giving me the opportunity to embark on this incredible journey. I am also very grateful for the National Research Foundation of South Africa for generously sponsoring my Masters through to this PhD degree, as well as the University of the Witwatersrand for awarding me with a Postgraduate Merit Award.

Dedication

This is for you ma and dad.

Table of Contents

CHAPTER 1

1.1 Green Chemistry

The first major chemical discovery made by mankind was the smelting of rocky ore to release copper metal.[1] Since then, chemistry has undoubtedly had an enormous impact on the course of history over the years. From the futile chasing of gold and immortality by the alchemists of more than a thousand years ago, to the eventual transition of alchemy to, and the rise of, modern chemistry, enormous strides have been made.

Following the 'accidental' synthesis of urea by Friedrich Wöhler in 1828,[2] the first planned total synthesis of an organic molecule, acetic acid, was accomplished in 1845 by the German chemist Hermann Kolbe.[3] Subsequently came the syntheses of a plethora of well-known organic molecules such as ethyl alcohol, methyl alcohol, and benzene, among others, by the French chemist Berthalot in the 1850s.[4] This set the stage for the beginning of organic synthesis which would eventually progress and flourish into a discipline with unparalleled respect from the other sciences.[5] From the manufacture of dyes that revolutionized the textile industry, to the synthesis of soaps that improved hygiene practices, organic and chemical synthesis has contributed significantly to the many improvements in our way of life.[5] Perhaps most important of all, is the manufacture of drugs of ever-increasing complexity that have helped tremendously in the fight against diseases.

The problem, however, is that many chemical processes have the potential to cause immediate or long term negative impacts on the environment.[6-7] A prime example was the surprising and yet disturbing discovery by American chemists of the British Antarctic Survey, that the springtime levels of ozone in the Antarctic had eroded by 40% between 1977 and 1984.[8] To put it simply, the ozone layer which is vital to living organisms,[9] was in danger of depletion. It was later identified that the primary cause of this depletion were chlorofluorocarbons (CFCs) generated by industry, and this then led to the establishment of the Montreal Protocol in 1989, calling for a reduction in the amounts of CFCs produced.[10] Another leading global scientific and environmental issue in recent times is that of the global warming effect.[11] There are rising concerns over the increasing levels of atmospheric greenhouse gases,[12] and the negative impact that this is having on climate change globally.

Chemical disasters differ in their nature of occurrence as well as in their mode of action. A prototype of a chemical disaster that had a major immediate impact on humans was the Bhopal disaster of 1984, when 30 metric tons of methyl isocyanate was accidentally released into the atmosphere. It is reported that 3800 people were killed immediately,[13] and the long term effects could be seen in the casualties that ran as high as 20,000 over a period of 2 decades.[14]

These types of disasters lead to increased pressure among synthetic organic chemists to try and minimize the risks to the environment, and yet achieve the desired synthetic products in a cost-effective manner. In its most simple form, risk can be expressed as: **Risk = Hazard × Exposure**.[6] The more traditional option to minimize risk is by minimizing exposure, through improved handling, treatment and disposal of chemicals.[6] This method however is costly as it requires that funds be directed away from research and development, and rather towards the proper handling and treatment of chemical waste.[15]

Another option is to minimize risk through the elimination of the use of chemicals that are likely to cause environmental damage or are known to be toxic to humans, i.e., reducing the hazard factor of the risk equation. Hence, new reaction pathways that reduce or eliminate substances that are hazardous to human health and the environment, are designed, developed, and thereafter, implemented.[6, 16] This approach towards organic synthesis is what is most commonly referred to as 'Green Chemistry'.

The term 'Green Chemistry' was first coined in the early 1990s by the US Environmental Protection Agency Office of Pollution prevention and Toxins, although it had been in practice long before that.[7] In 1998, a set of design principles were published by Anastas and Warner in their seminal book (**Figure 1**). These principles are a set of guidelines to help guide chemists in the design of more sustainable routes towards the synthesis of chemical compounds.[6-7, 16-17]

The focus of this PhD thesis will be mainly on two of the principles of Green Chemistry (refer to **Figure 1**), namely principle 7, *The Use of Renewable Feedstock* which details the use of chemicals which are made from bio-renewable sources, rather than other equivalent chemicals originating from finite sources. The second major focus of this PhD thesis is principle 9, *Catalysis*, which details the use of catalytic instead of stoichiometric reagents in reactions.

While particular emphasis is placed on these Green Chemistry principles in this thesis, other principles such as atom economy, reduced use of derivatives, i.e. protecting groups, and less hazardous chemical synthesis are aspects that were also considered.

The focus of Chapter 1 and Chapter 2 of this thesis will be on the use of catalysts as one of the major design principles of Green Chemistry. The use of bio renewable feedstock as another major design principle will be the focus of Chapter 3 and Chapter 4 of this thesis.

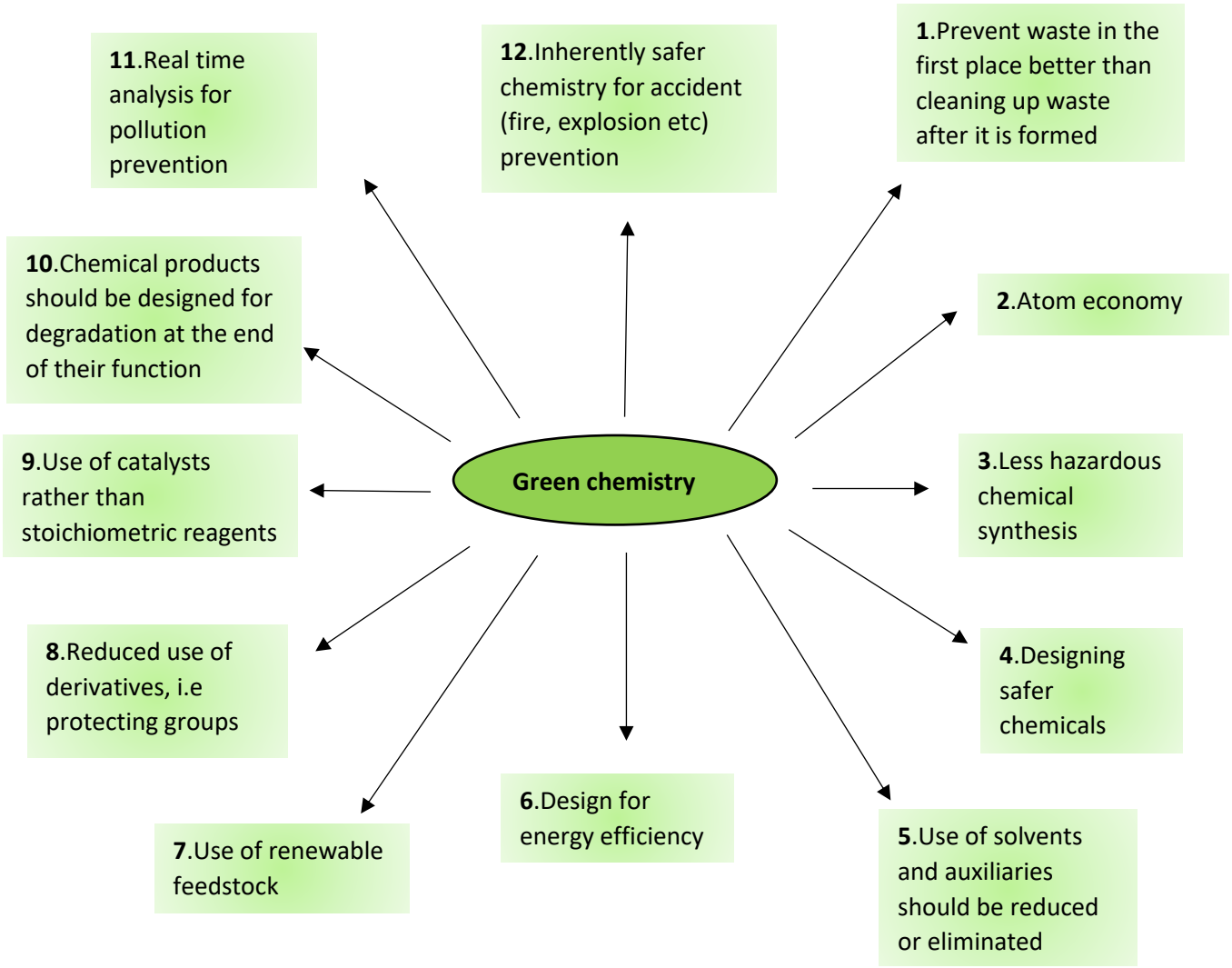

Figure 1: The twelve principles of Green Chemistry.[6-7, 16-17]

1.1.1 Catalysis

Of the twelve principles of Green Chemistry (see **Figure 1**), catalysis is often identified as one of the most important in the drive towards sustainability at the molecular level.[18-19] The use of catalysts is significant in achieving several Green Chemistry benefits, one example being improved selectivity. In fact, it was in 1968, long before the birth of Green Chemistry, that the first ever selective catalyst to promote asymmetric hydrogenation was developed by William. S. Knowles.[20] The catalyst, Rh-DiPAMP, was used in the first catalytic asymmetric industrial synthesis of L-DOPA **1**, an amino acid used in the treatment of Parkinson's disease (**Scheme**

1).[20-21] Asymmetric catalytic hydrogenation of acrylic acid **2**, followed by deacetylation of the amide **3**, yields L-DOPA exclusively. In addition to improved selectivity, this synthesis also demonstrates improved waste reduction due to the lesser number of steps required in the synthesis. This pioneering work was recognized by the Nobel Prize in chemistry that was awarded in part to Knowles in 2001.[20] He shared this award with Ryoji Noyori for his work on catalytic asymmetric hydrogenations,[22] and with Barry Sharpless for his work on catalytic asymmetric oxidations.[23]

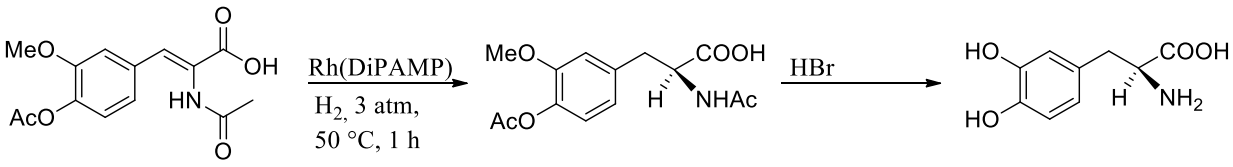

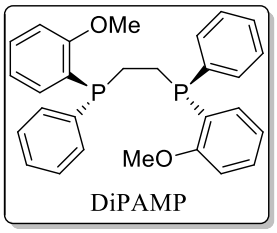

Scheme 1: Catalytic asymmetric synthesis of L-DOPA using Rh(DiPAMP).

The use of catalysts also helps in promoting waste reduction. The amount of waste generated in a chemical process per kilogram of product produced can be measured by the environmental (E) factor introduced by Roger Sheldon.[24] The E factor takes into account all the reagents as well as solvents that are used in the chemical process, and of which the atoms thereof are not incorporated into the final product. The more the number of steps in a chemical process, the more waste that is generated, and therefore, the higher will be the E Factor for that process. Ideally, a green reaction must have an E factor of zero.[24-25]

As an example, the traditional synthesis of the drug ibuprofen required six **stoichiometric** steps, with the first step utilizing the environmentally undesirable $AlCl_3$.[26] The amount of waste generated in this process was immense. An improvement in this synthesis was made by the Bausch Health Companies (BHC), in which liquid HF is used as both the catalyst as well as the solvent in the acetylation of **4**, and is recovered and recycled with a 99% efficiency.[27] Ibuprofen **5** is formed in two steps thereafter, which comprise of a catalytic hydrogenation, followed by a catalytic carbonylation. As no other solvent is required in the process, and, the number of synthetic steps is reduced to three (**Scheme 2**), with an overall calculated atom

economy of 77%,[19, 28] consequently the E factor is significantly less than that of the conventional process.

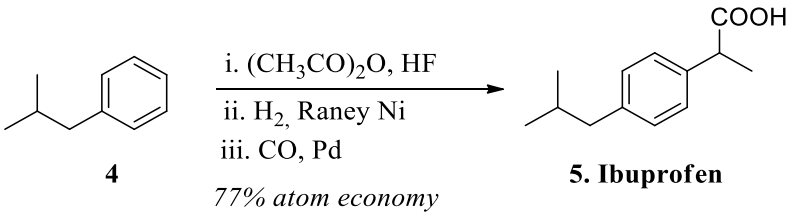

Scheme 2: Synthesis of ibuprofen using HF as the catalyst.

Additionally, catalysts often result in reduced energy consumption. An illustration of this would be in the synthesis of propylene glycol **6** from glycerol **7** (**Scheme 3**). The process mechanism involves the initial dehydration of glycerol **7**, followed by the hydrogenation of the resulting intermediate acetol **7a**. The conventional process involves hydrogen pressures of 10 MPa and a reaction temperature of 350 °C for the hydrogenation step.[15, 29] The use of a copper-chromite catalyst, which is recyclable, however, allows the reaction to be carried out under a significantly reduced hydrogen pressure of 1.4 MPa and a lower reaction temperature of 200 °C,[15, 29] resulting in substantially less overall energy consumption.

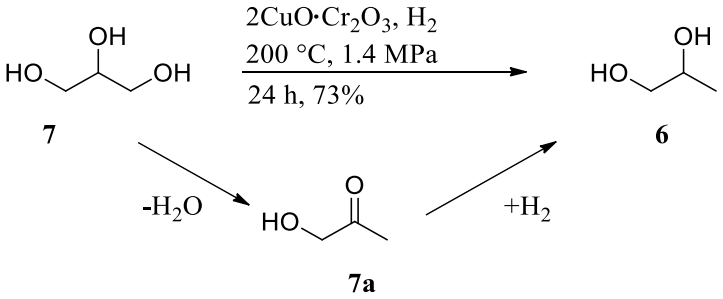

Scheme 3: Synthesis of propylene glycol from glycerol.

As a result of the advantages gained when using catalysts, they have now become an integral part of several important organic reactions, such as C-C bond forming reactions. One such example is the olefin metathesis reaction for which Chauvin, Grubbs and Schrock received the Nobel prize in 2005. The catalytic olefin metathesis reaction was recognized by the Royal Swedish Academy of Sciences as contributing to "greener" chemistry.[30]

1.2 General introduction to olefin metathesis

Olefin metathesis consists of the mutual exchange of alkylidene groups that takes place between substituted alkenes, in the presence of catalytic amounts of metal alkylidene

catalyst.[31-32] This reaction was initially discovered in 1964 by Natta *et al.*,[33-35] and later developed into the synthetically versatile method of forming C-C bonds that it is today. Depending on the substrates used, and on the reaction conditions, different types of olefin metathesis can be affected, as showcased in **Figure 2,** leading to its astonishingly wide range of applications. Ring-opening metathesis polymerization (ROMP) and acyclic diene metathesis polymerization (ADMET) are mostly used in industry for the synthesis of polymers.[36] Widely employed in organic synthesis, however, is the ring-closing metathesis (RCM), as well as cross metathesis (CM).[37]

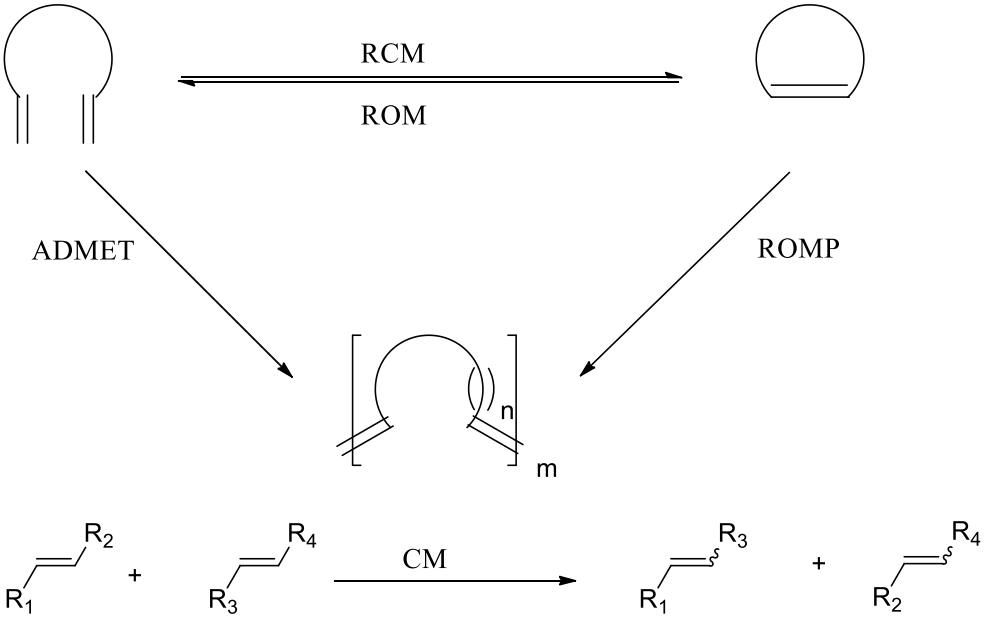

Figure 2: Types of metathesis reactions. RCM = Ring-closing metathesis, ROM = Ring-opening metathesis, ROMP = Ring-opening metathesis polymerization, ADMET = Ayclic diene metathesis polymerization, CM = Cross metathesis.

The success of olefin metathesis in industry and in organic synthesis is due partly to the availability of the highly active alkylidene catalyst systems. Initially, the first class of catalysts for metathesis, referred to as "Ziegler-Natta type" catalysts, included transition metal salts combined with main group organometallic compounds.[31-32] Although generally very active, these catalysts displayed poor functional group tolerance, which limited their application in organic synthesis.[31-32] Important advancements in catalyst development later led to the introduction of stable alkylidene-metal complexes as catalysts. Although quite a number of transition metal complexes have been investigated as potential catalysts for olefin metathesis,[38] the most popular of these include ruthenium-based Grubbs first and second generation catalysts, molybdenum-based Schrock catalyst, and the second generation Hoveyda-Grubbs

catalyst.[39] Of importance was that these catalysts were soluble in organic solvents and hence were characterizable homogenous catalysts. In particular, the ruthenium-based catalysts have received much attention as a result of their wide tolerance for a variety of functional groups.[38]

1.2.1 Mechanism of olefin metathesis

It is now generally accepted that olefin metathesis follows the "Chauvin mechanism", [32, 39] which was first proposed by Chauvin and Herisson in 1970.[40] The mechanism, which is shown in **Figure 3**, consists of a reversible formal [2+2] cycloaddition of an olefin, e.g. **8**, with a metal carbene catalyst, resulting in the formation of a metallacyclobutane intermediate **8a**. This is followed by a reversible formal [2+2] cycloreversion, generating the metal-alkylidene **8b**. A second reversible formal [2+2] cycloaddition ensues, this time intramolecular, followed by a subsequent formal [2+2] cycloreversion to deliver a new olefin **9**.

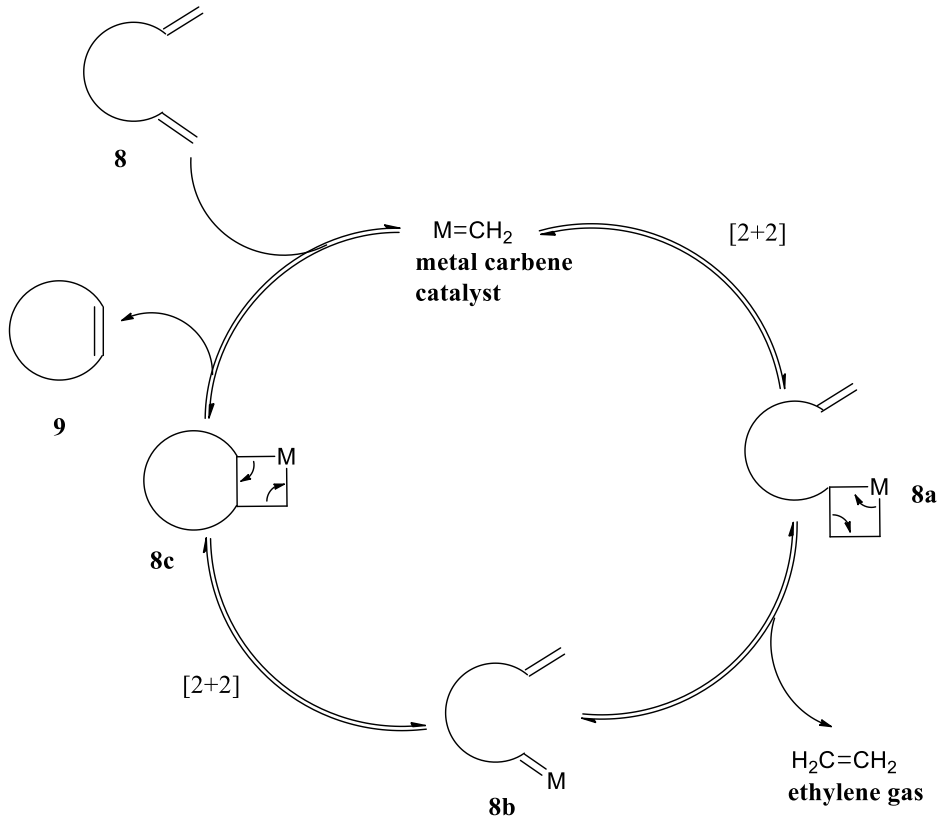

Figure 3: Ring-closing olefin metathesis catalytic cycle.

1.2.2 Ring-closing alkene metathesis

Due to its versatility, alkene ring-closing metathesis has been used widely in the synthesis of a wide array of ring systems, including aromatic and heterocyclic rings, and therefore features in

several natural product syntheses.[37, 39] As an example, de Koning and coworkers from our laboratories used a Grubbs-II catalyzed olefin ring-closing metathesis of **10** as the key step to form the central aromatic ring of the core **11a** of the natural product rebeccamycin **11** (**Scheme 4**).[41] This was one of the first examples of the use of metathesis in the construction of a polyaromatic system.[41]

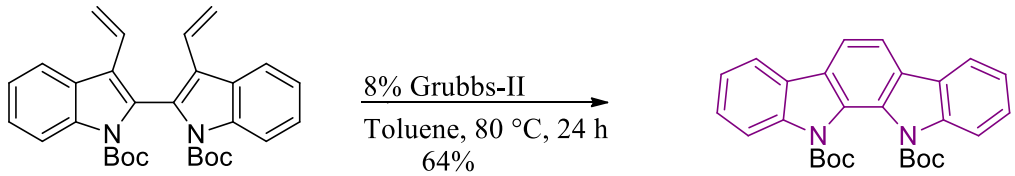

10 **11a**

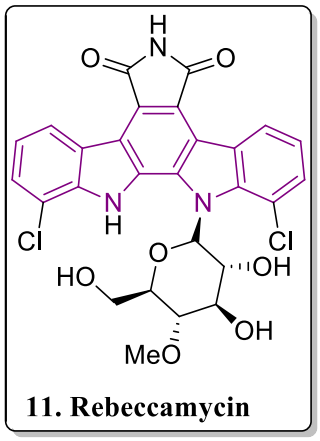

11. Rebeccamycin

Scheme 4: Synthesis of an aromatic ring using a ring-closing alkene metathesis.

Olefin metathesis has therefore found great use in the formation of C-C bonds in the petroleum, pharmaceutical, agricultural, and materials industry.[42] The related carbonyl-olefin metathesis reaction has been, however, considerably less developed, and hence not applied as widely in industry. It has nevertheless gained some interest towards its development in recent years due to its potentiality to have a similar impact on synthetic strategies as the olefin metathesis.[43]

1.3 Carbonyl-olefin metathesis

The exchange reaction between an alkene and a carbonyl compound, to yield a new olefin and a new carbonyl compound, is described as a carbonyl-olefin metathesis (**Scheme 5**).

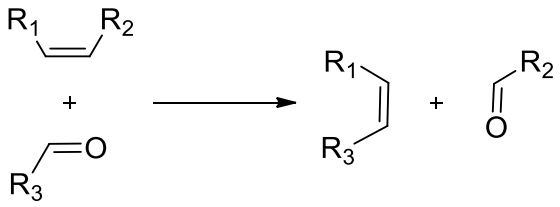

Scheme 5: General scheme for a carbonyl-olefin metathesis reaction.

The first example, albeit an accidental one, of carbonyl-olefin metathesis, was reported in 1963 by Scharf and Korte.[44] During their investigation of the photodimerization of norbornene **12**, small amounts of benzophenone were introduced to function as photosensitizers (**Scheme 6**). This led instead to the photoinduced formation of oxetane **12a** (a Paternò-Büchi reaction), the structure of which was confirmed by acid-induced cleavage, in the event generating the fragmented product **13**. This is representative of a ring-opening carbonyl-olefin metathesis.[45]

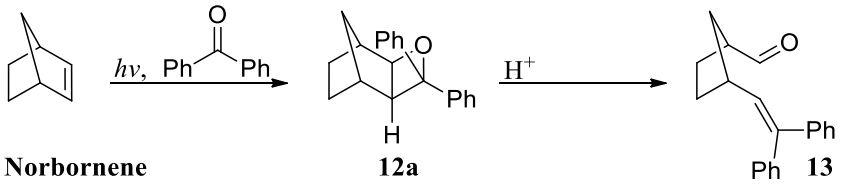

Scheme 6: Ring-opening carbonyl-olefin metathesis by Scharf and Korte.

Following this, in 1973, Jones and his team investigated the formation of carbonyl-olefin metathesis products *via* the thermal cleavage of oxetane photoadducts.[46] The oxetane intermediates were heated to temperatures of 280-300 °C (!), inducing pyrolysis and thus generating carbonyl-olefin metathesis products. In 1975, the same team employed the sequence of photolysis-pyrolysis for carbonyl-olefin metathesis in the synthesis of long chain enals.[45, 47] Over the years, a number of research groups have investigated and explored this methodology for carbonyl-olefin metathesis, however, its use in industry and organic synthesis has remained very limited.[45] The lack of functional group tolerance as a result of the very high temperatures required for pyrolysis of the oxetane intermediates limited its practicality in synthesis.

Subsequent developments led to the introduction of non-catalytic, metal-alkylidene-mediated carbonyl-olefin metathesis. This method consists of two different strategies (**Scheme 7**).[45] Strategy I involves the formal [2+2] cycloaddition between a metal alkylidene **14** and an olefin **15** to generate the metallacyclobutane intermediate **14a**. This then undergoes a formal [2+2] cycloreversion to generate the new metal alkylidene **14b**, which takes part in a carbonyl olefination with carbonyl **16** to generate olefin **17**, and metal-oxo byproduct **18** which prevents catalyst turnover. This strategy was utilized, for example, by Grubbs and Stille in the synthesis of the natural product (±)-Δ (9,12)-capnellane, using a titanium-based alkylidene reagent.[48]

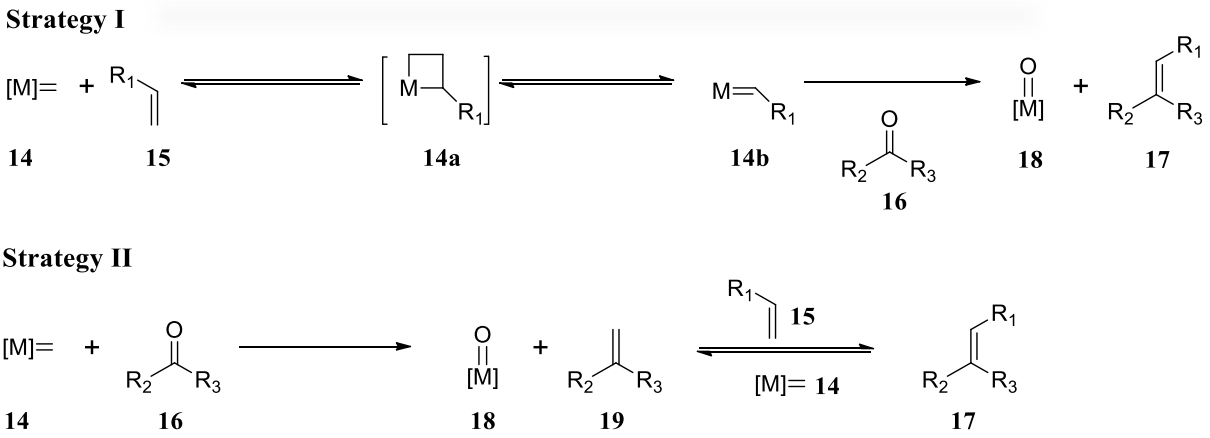

Scheme 7: Strategy I and II for metal alkylidene mediated carbonyl-olefin metathesis.

Strategy II, on the other hand, involves an initial carbonyl olefination between the metal alkylidene **14** and carbonyl **16** to generate metal-oxo byproduct **18** and alkene intermediate **19**. This is then followed by an olefin metathesis between alkene **15** and alkene intermediate **19** to generate olefin **17**. This strategy hence requires excess amounts of the metal alkylidene reagent, and was applied by Nicolaou *et al.* in the synthesis of cyclic enol ethers from olefins and esters.[49]

Despite featuring in some natural product syntheses, the use of stoichiometric and, in the case of strategy II, super-stoichiometric amounts of metal alkylidene reagents renders this approach highly atom uneconomical.

A significant breakthrough in the arena of carbonyl-olefin metathesis occurred in 2012 through the contributions made by Lambert and co-workers, in the form of a symmetric hydrazine organocatalyst.[50] This was the first ever effective carbonyl-olefin metathesis catalyst to be developed. Their strategy centres on the use of a thermally allowed [3+2] cycloaddition, rather than the symmetry forbidden [2+2] cycloaddition employed in normal metathesis reactions. As for the reaction scope, the team reported the successful ring-opening carbonyl-olefin metathesis between various cyclopropene derivatives **20** bearing *O*-linkages as well as thioethers, and aryl aldehydes **21** bearing alkyl substituents as well as electron-withdrawing substituents, in the presence of hydrazine organocatalyst **22** in its bis-hydrochloride form.[50]

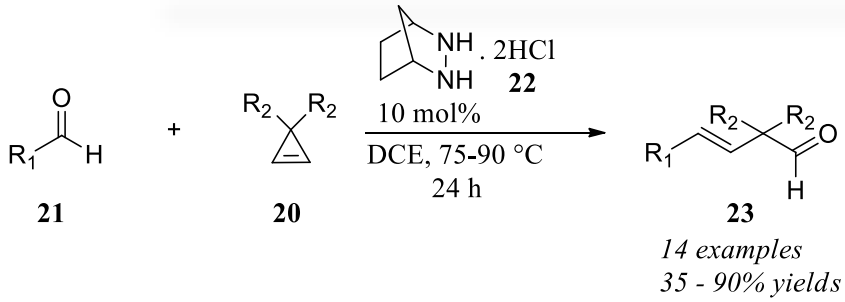

Scheme 8: Ring-opening carbonyl-olefin metathesis catalyzed by a hydrazine organocatalyst.

The mechanistic rationale, which was supported by computational and mechanistic studies, involves an initial condensation of the hydrazine catalyst **22** with the aldehyde **21** to generate an azomethine imine salt **24** (**Figure 4**).[50-51] A 1,3-dipolar cycloaddition of the azomethine imine derived from **24** with the alkene substrate **20** generates a pseudosymmetric pyrazolidine cycloadduct **25**, which undergoes a ring strain relieving [3+2] cycloreversion to generate the new azomethine imine salt **26**. Hydrolysis of **26** yields the aldehyde product **23** and regenerates the hydrazine catalyst **22**.

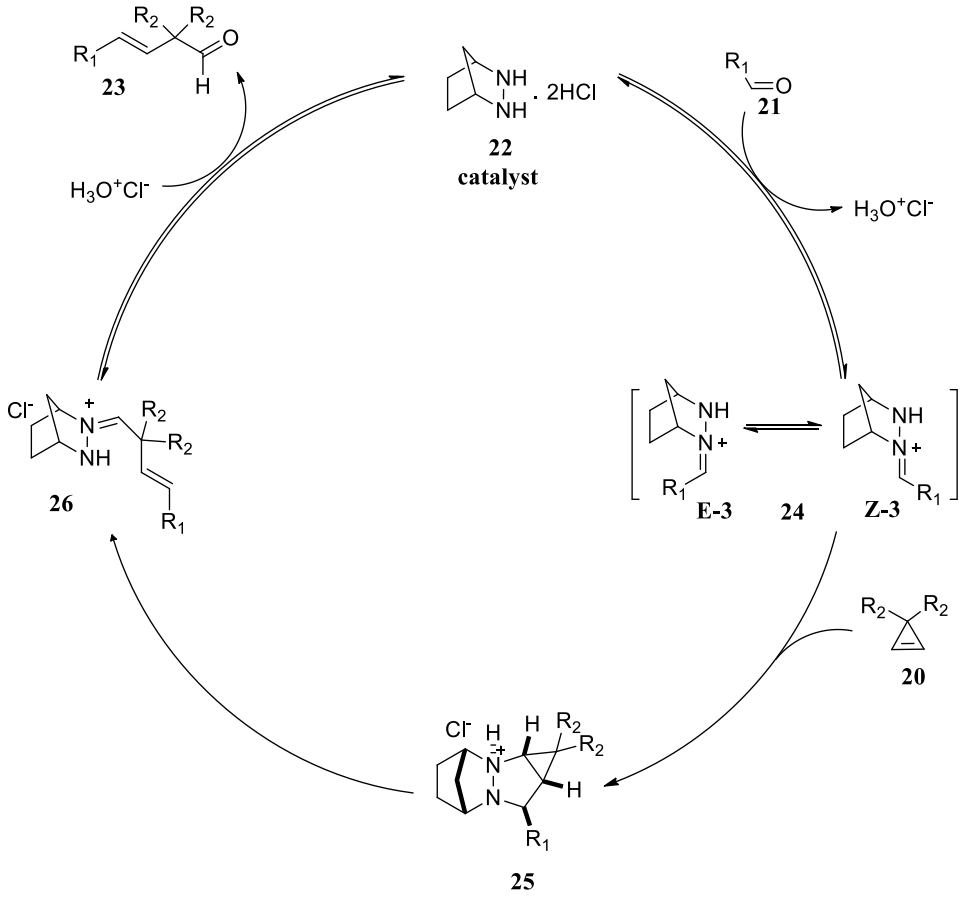

Figure 4: General catalytic cycle for an organocatalyzed carbonyl-olefin metathesis.[50]

However, the stability of the five membered cycloadduct **25** compared to the less stable, four membered ring intermediates **12a** and **14a**, renders this method applicable only for highly strained alkene substrates that can destabilize the cycloadduct intermediates.[45] Nevertheless, ongoing research by the Lambert group is being focused on the development of a hydrazine organocatalyst that would allow for the use of less strained substrates.[52] Lambert and co-workers have also reported the successful formation of *2H*-chromenes,[53] and 1,2-dihydroquinolines,[54] through organocatalyzed ring-closing carbonyl-olefin metathesis.

1.3.1 $FeCl_3$-catalyzed carbonyl-olefin metathesis

In their studies towards the synthesis of carotol sesquiterpenes in 1971, Demole *et al.* discovered the formation of an oxetane intermediate **27**, mediated by the reaction of ketone **28** with $SnCl_4$ (20 mol%, **Scheme 9i**).[55] A few years later, Snider and his team realized the potential of Lewis acids for mediating carbonyl-olefin metathesis, when they subjected the same ketone **28** to a stoichiometric mixture of $MeAlCl_2$/Me_2AlCl, and obtained the metathesis product **29**, *via* oxetane intermediate **27** (**Scheme 9ii**).[56] Although there have been several reports in this area since then, Lewis acid-*catalyzed* carbonyl olefin metathesis has only been actively pursued in recent years.

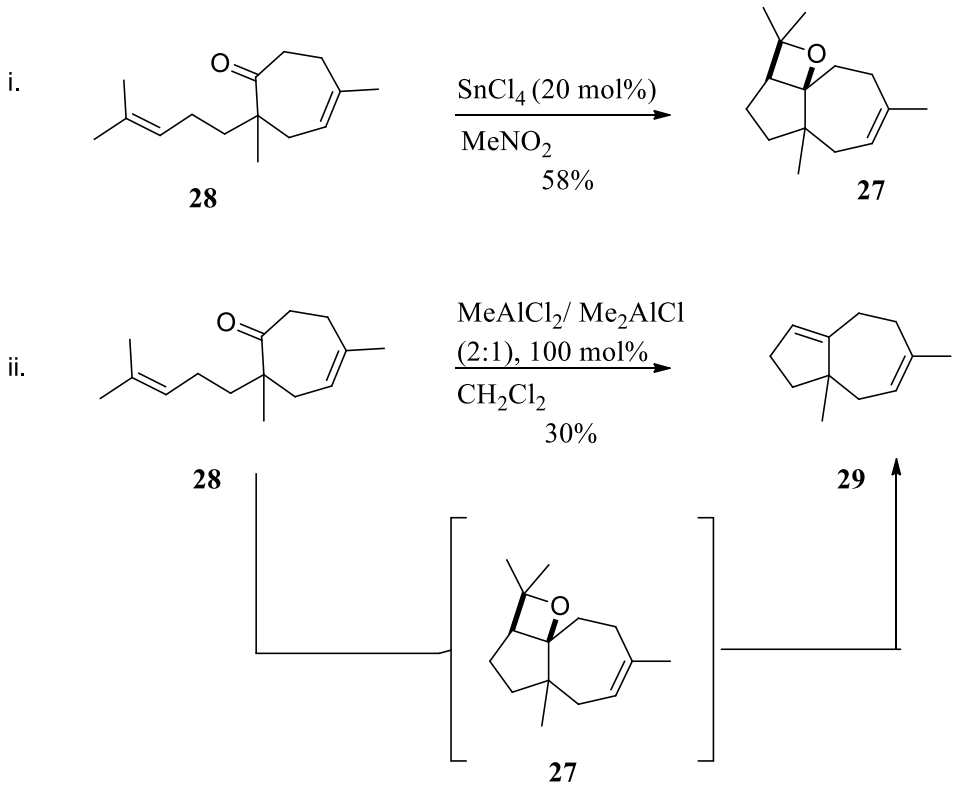

Scheme 9: Earliest examples of Lewis acid-mediated carbonyl-olefin metathesis.

Building on the work done earlier by Bickelhaupt,[57] Khripach,[58] and Schmalz,[59] Schindler and coworkers in 2016 described an $FeCl_3$-catalyzed carbonyl-olefin ring-closing metathesis protocol.[60] The use of iron, an environmentally benign and abundant metal, as a catalyst, represents a major advancement in carbonyl-olefin metathesis. This catalyzed reaction would prove to be more tolerant of a variety of functional groups, requires milder reaction conditions and is therefore operationally simple.[45, 61]

The design principle for such a Lewis acid catalyzed system was based on the *in situ* formation of an oxetane intermediate (**Scheme 10**).[60] This differs from the oxo-metallacyclobutane intermediate that is formed as part of the transition metal-mediated carbonyl-olefin metathesis, and which fragments to yield a very stable metal-oxo complex that prevents catalyst turnover. In contrast, the oxetane intermediate undergoes fragmentation directly to yield the new olefin and carbonyl compound, releasing the Lewis acid, thus allowing the reaction to proceed catalytically.

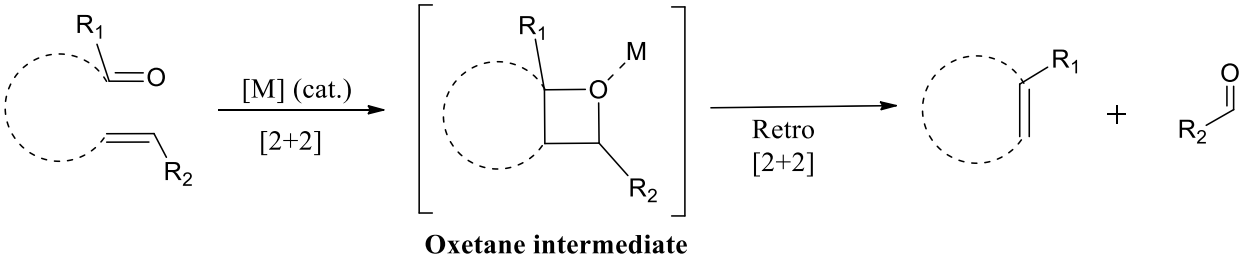

Scheme 10: Formation of oxetane intermediate using a Lewis acid as a catalyst for carbonyl-olefin metathesis.

This design principle requires a potent catalyst that would be able to promote both a formal [2+2] cycloaddition as well as a formal [2+2] cycloreversion, hence promoting both oxetane formation as well as fragmentation. It was hypothesized that metal-based Lewis acids could best achieve this essentially by activating the carbonyl component and yielding the desired oxetane intermediate.[60] After the screening of a variety of potential Lewis acid catalysts, it was found that $FeCl_3$ gave the desired metathesis products in excellent yield and with minimal side products.[60] Although initially, this was attributed to the high Lewis acidity and oxophilicity of $FeCl_3$, further investigations proved that there is something unique about the inherent reactivity of $FeCl_3$ towards carbonyl-olefin metathesis rather than competing side reactions.[62]

1.3.2 Mechanism of $FeCl_3$-catalyzed carbonyl-olefin metathesis

Based on computational, kinetic, and synthetic experiments, two possible mechanisms, concerted (**Figure 5**) or stepwise (**Figure 6**), have been proposed depending on the metathesis substrates.[60-61, 63-64] Prenylated substrates undergo the concerted mechanism, which involves initial coordination of a carbonyl- and olefin- containing substrate **30** to iron(III) to form an activated Lewis acid complex **31**. This complex undergoes a concerted asynchronous [2+2] cycloaddition to yield a reactive oxetane intermediate **32**, which then undergoes a concerted asynchronous [2+2] cycloreversion leading to a new olefin **33** and carbonyl product **34**, and ultimately regenerating the $FeCl_3$ catalyst.[60, 63]

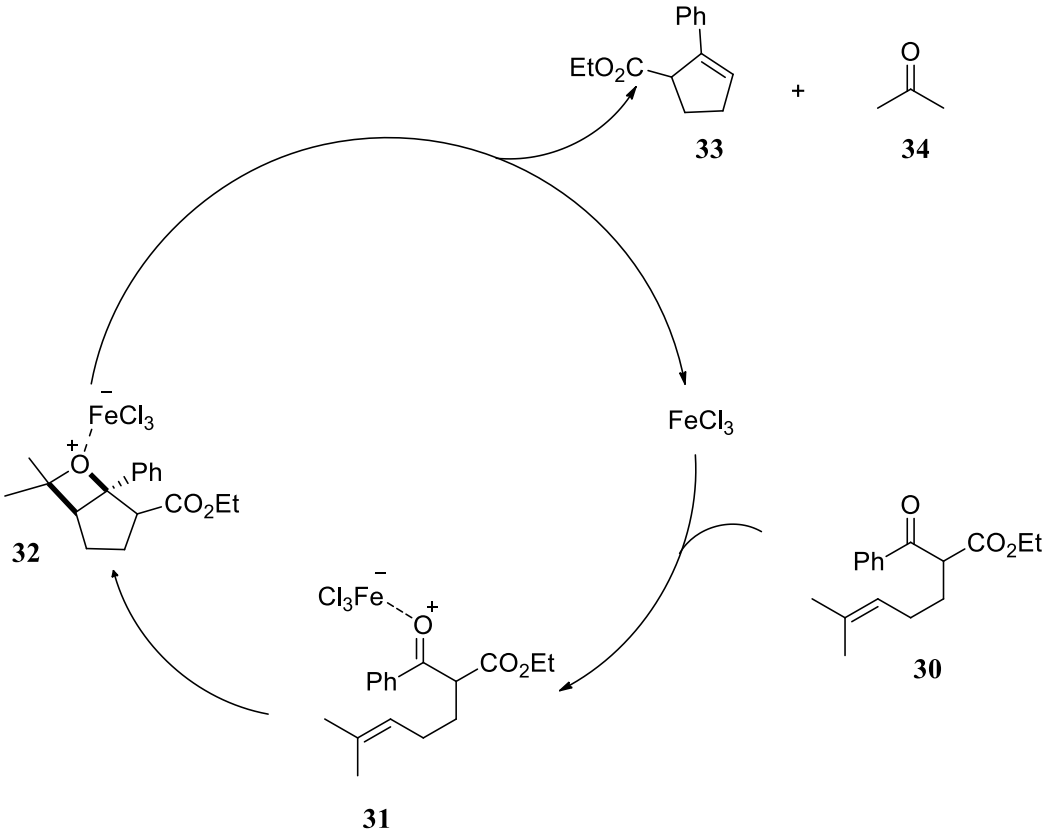

Figure 5: Proposed concerted mechanism for iron(III)-catalyzed carbonyl-olefin metathesis.[63]

The alternative, stepwise pathway, which is followed by styrenyl substrates, involves initial coordination of the substrate **35** to iron(III) to generate a Lewis acid adduct **36** (**Figure 6**). The olefin moiety of the substrate can then undergo an intramolecular nucleophilic attack on the activated carbonyl component on either face to generate *cis* **37a** and *trans* **37b** carbocycles.[60, 63] It is only the *cis* **37a** carbocycle that can proceed further to undergo an intramolecular

trapping of the carbocation to generate the reactive oxetane intermediate **38**.[60, 63] The *trans* **37b** carbocycle is non-reactive as intramolecular trapping of the carbocation would be geometrically improbable.[61] The oxetane intermediate **38** undergoes an iron(III)-mediated ring-opening to generate a carbocation intermediate **39** which, upon hydrolysis, yields the carbonyl-olefin metathesis products **40** and **41**.

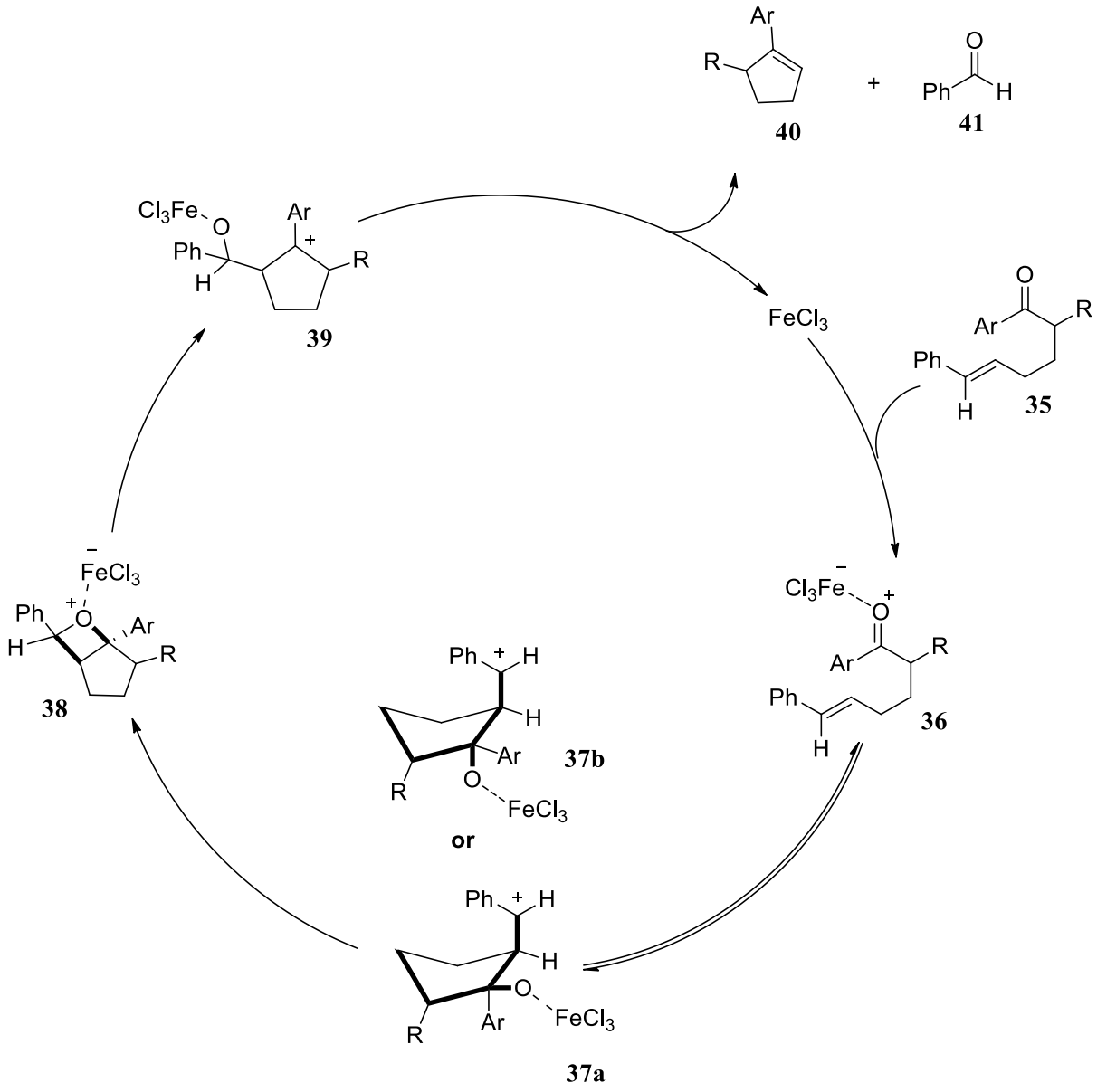

Figure 6: Proposed stepwise mechanism for iron(III)-catalyzed carbonyl-olefin metathesis.[63]

1.3.3 Scope of the $FeCl_3$-catalyzed carbonyl-olefin metathesis

To establish the scope of the $FeCl_3$-mediated metathesis, initial studies were conducted on β-keto esters **42**.[60] Under optimal reaction conditions, these substrates resulted in the successful

formation of five- and six-membered rings **43** (**Scheme 11**). The iron(III)-catalyzed metathesis reaction demonstrated an excellent tolerance to a variety of arene functional groups bearing both electron-withdrawing as well as electron-donating substituents. A wide tolerance of various olefinic substituents was also observed; however yields generally decreased with styrenyl olefin substrates.

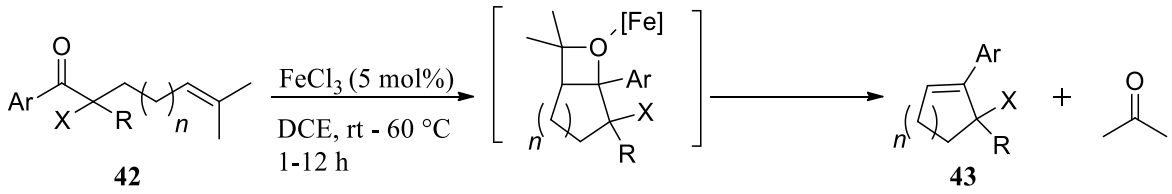

Variations of *n,* X, R, and Ar with *n* = 1,2
X = CO_2R, SO_2Ar, CONHAr, alkyl
R = H, alkyl, aryl, allyl

41 examples
52 - 99% yields

Scheme 11: Formation of 5 and 6 membered rings *via* iron(III)-catalyzed carbonyl-olefin metathesis.[60]

In 2016, Li and coworkers also reported the use of iron(III)-catalyzed carbonyl-olefin metathesis for the formation of five- and six-membered rings.[64] Five-membered rings were generally obtained in high yields of 71-84%. Six-membered rings however were formed with a lower efficiency compared to five-membered rings, with yields obtained averaging at about 50%. The construction of nitrogen-containing heterocycles was also investigated and it was found that 2,5-dihydropyrrole products **44a-d** were synthesized generally in good yields from carbonyl- and olefin- containing precursors **45**, provided that allyltrimethylsilane, the exact function of which was not clear, is used as an additive (**Scheme 12**).[64]

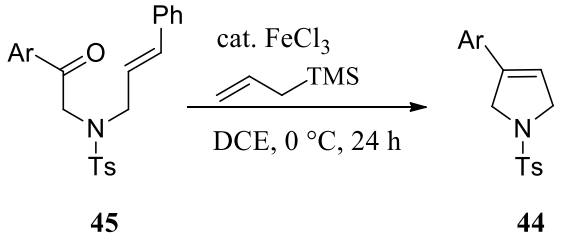

44a Ar = C_6H_5, 91%
44b Ar = *p*-BrC_6H_4, 80%
44c Ar = *p*-ClC_6H_4, 73%
44d Ar = *p*-Tol, 71%

Scheme 12: Formation of five-membered, nitrogen-containing heterocycles using iron(III)-catalyzed carbonyl-olefin metathesis.[64]

In 2017, the formation of polycyclic aromatic compounds **46** (PACs) using iron(III)-catalyzed carbonyl-olefin metathesis was investigated by McAtee *et al.* (**Scheme 13**).[65] Investigation of

the two reaction partners revealed that the olefin moiety of the substrate **47** readily reacts intramolecularly with a variety of substituted aryl-ketones, sterically and electronically differentiated, as well as aryl aldehydes to form the corresponding PACs in good yields.

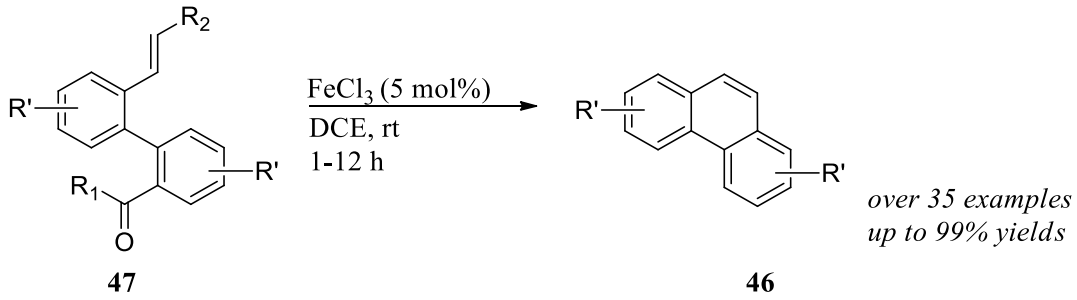

Scheme 13: Formation of PACs *via* $FeCl_3$-catalyzed carbonyl-olefin metathesis.[65]

In 2018, Schindler and coworkers demonstrated the successful formation of chiral 3-pyrrolines,[66] as well as tetrahydronaphthalenes,[67] using $FeCl_3$-catalyzed carbonyl-olefin metathesis. This catalyzed reaction has thus, in a short period of time, proved its versatility by being used in the synthesis of various scaffolds, some of them important structural motifs that are used in the synthesis of biologically active natural products.[66-68]

Most importantly, this strategy has been used to replace the previously harsh conditions that have been used to synthesize these motifs, with the much milder reaction conditions that $FeCl_3$-catalyzed carbonyl-olefin metathesis employs. Furthermore, the use of iron, an earth abundant and benign metal, as a catalyst, is in definite conjunction with Green Chemistry principles.

Iron(III)-catalyzed carbonyl-olefin metathesis reaction therefore displays promising utility particularly in the synthesis of complex biologically active molecules. For the purposes of this PhD thesis the well-known polyaromatic class of compounds that were targeted for synthesis using the iron(III)-catalyzed carbonyl-olefin metathesis reaction were the angucyclines. An introduction to this class of compounds is given below, followed by our strategy for the synthesis of the angucyclines utilizing the carbonyl-olefin metathesis reaction as a key step.

1.4 Introduction to angucyclines

In the year 1966, a new type of natural product bearing interesting biological properties derived from microorganisms of the genus *Streptomyces* was defined, and much later given the names ‘angucycline’ and ‘angucyclinone’.[69-70] The angucycline/angucyclinone class of natural products all share the common structural feature of an unsymmetrical tetracyclic benz[α]anthracene moiety **48** (**Figure 7**), which is derived biosynthetically from a decaketide

chain.[69] The first of these natural products to be discovered was tetrangomycin **49** in 1965,[71] which was isolated from cultures of a variant strain of *Streptomyces rimosus*, and tetrangulol **50**, which is coproduced with tetrangomycin by the same organism, in 1966.[72] Subsequently, the structure of ochromycinone **51** was published in 1967,[73] followed by rabelomycin **52** in 1970.[74] These early published structures are all examples of 'angucyclinones' as they do not possess hydrolysable sugar moieties as part of their structure.

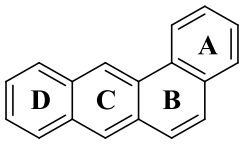

48 Benz[***a***]anthracene framework

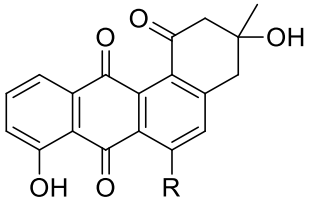

49. Tetrangomycin R = H
52. Rabelomycin R = OH

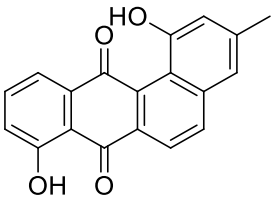

50. Tetrangulol

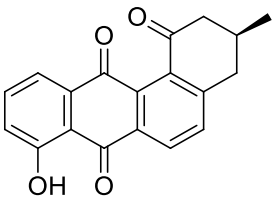

51. Ochromycinone

Figure 7: Benz[α]anthracene backbone and the structures of tetrangomycin, tetrangulol, ochromycinone, and rabelomycin.

Also in 1970 came the publication of the structure of aquayamycin **53** (**Figure 8**), the first angucyclinone containing a non-hydrolysable sugar moiety.[75] Although an angucyclinone, aquayamycin serves as the parent compound for a large group of glycosidic angucyclines. Angucyclines, in contrast to angucyclinones, possess a hydrolysable sugar moiety. A well-known set of examples being the landomycins, discovered in 1990, which comprise of compounds containing a hydrolysable saccharide component chemically attached to the benz[α]anthracene skeleton by means of a C-glycosidic linkage.[76] The structure of landomycin A **54** is shown in **Figure 8**.

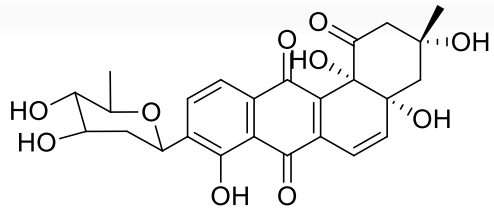

53. Aquayamycin

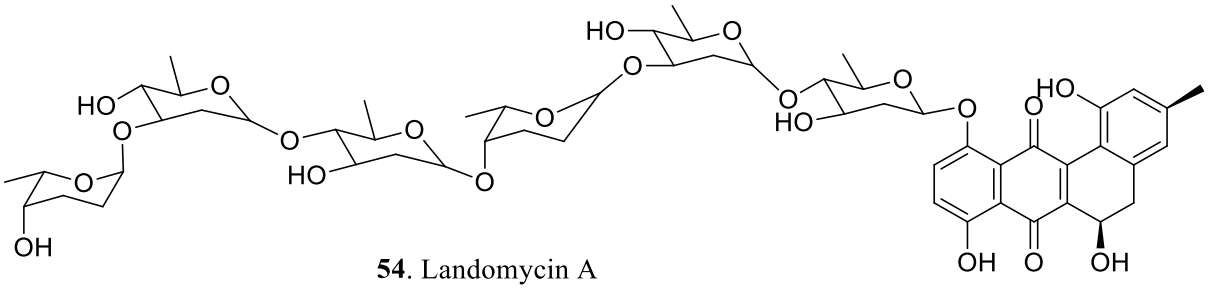

54. Landomycin A

Figure 8: Chemical structures of aquayamycin and the carbohydrate rich landomycin A.

1.4.1 Biological properties of angucyclines

The large number of publications related to the synthesis and biological properties of angucyclines highlights the interest of biologists as well as synthetic chemists in this group of natural products. This is because angucyclines are rich in biological activities.[69, 77] Not only have they been found to have antibacterial properties, some angucyclines also act as hydroxylase and mono oxygenase inhibitors, as well as inhibitors of platelet aggregation.[69] In addition, angucyclines exhibit very interesting cytotoxic properties.[77] The landomycins belong to the most active angucycline group of anti-cancer drugs.[77] Landomycin A **54** promotes disruption of the cell cycle, and has shown promising activity against prostate cancer cell lines.[78] Landomycin E exhibits potent anti-cancer properties against multiple drug resistant cell lines by acting as an inducer of apoptosis in these cells.[77, 79] Jadomycins, a group of glycosylated, polyketide-derived angucyclines, are known to be involved in DNA cleavage of cancerous cells and have been found to be active against breast cancer cell lines.[80-81] Kinamycins, originally isolated from *Streptomyces murayamaensis*, are a unique group of angucycline antibiotics that are endowed with a diazo group, and a five-membered ring (ring B).[77] The kinamycins have also received much attention as a result of their ability to disrupt the cell cycle and bring about anti-proliferation of affected, cancerous cells.[82]

1.4.2 Biosynthesis of the benz[α]anthracene framework

Angucyclines are biosynthesized by means of the polyketide-derived biosynthetic pathway.[77] The enzyme Type II polyketide synthase (PKS) plays a major role in this pathway as it is responsible for the synthesis of a decaketide intermediate (**Figure 9**) from which the benz[α]anthracene framework is generated. PKS utilizes acetyl CoA as the starter unit and 9-malonyl CoA as an extender unit to synthesize the decaketide backbone.[77] Depending on the nature of the angucycline, there are two different routes leading to the formation of benz[α]anthracenes. The first, most common, route (**Figure 9**, **route 1**) proceeds *via* the decaketide intermediate **55** which folds in an angular fashion, bringing about ring-closing reactions that lead to a benz[α]anthracene moiety.[83] The alternative route involves the formation of an anthracyclinone intermediate **56** from the decaketide backbone **57**. The anthracyclinone then undergoes an oxidative disconnection at the bond between C10a and C11, possibly through a pathway specific Baeyer-Villiger oxygenase, and eventually a rearrangement and recyclization to generate the benz[α]anthracene moiety.[84]

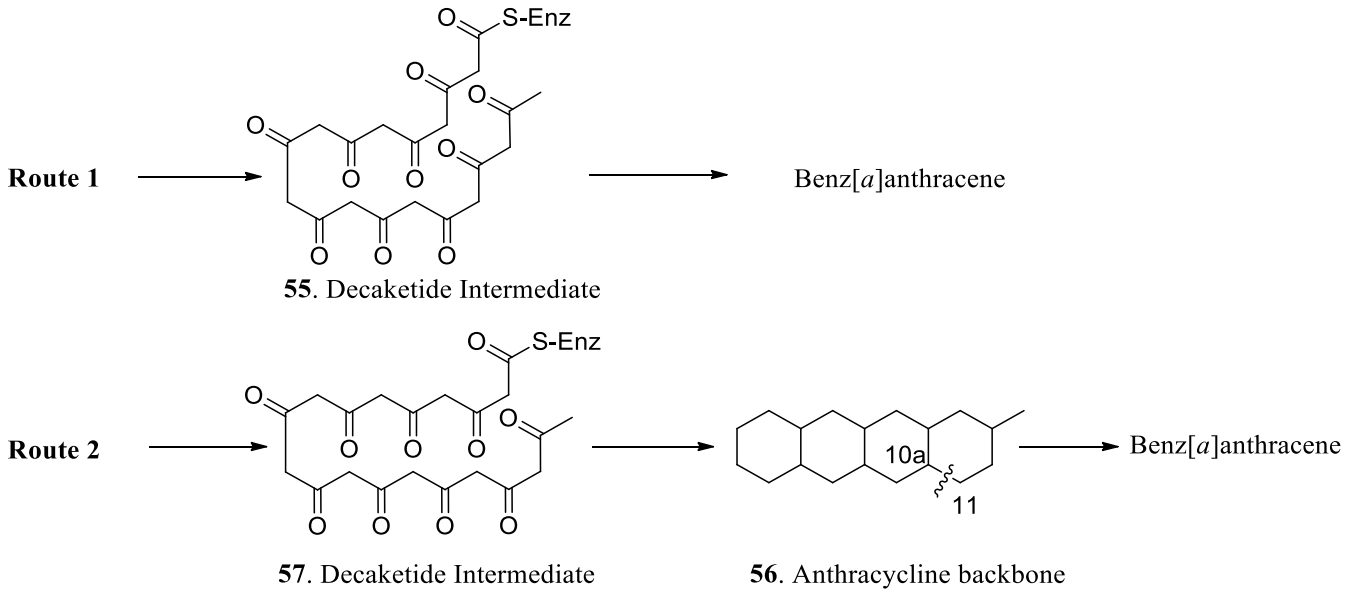

Figure 9: Benz[α]anthracene synthesis *via* route 1 or route 2 of the polyketide biosynthetic pathway.[77]

1.4.3 Chemical synthesis of angucyclines

The synthesis of tetrangulol **50**, ten years after it was first discovered, marked the first total synthesis of the angucyclinone natural product.[85] Since then, due to the wide range of biological activities exhibited by angucyclines, a lot of interest has been enthused in their total synthesis

by organic chemists. Numerous strategies have been developed for their synthesis, and these can be grouped into five categories as follows; i) Diels-Alder; ii) Nucleophilic addition; iii) Friedel-Crafts acylation; iv) Intramolecular cyclization; and v) Transition metal-catalyzed strategies.

1.4.3.1 Diels-Alder strategy

The Diels-Alder reaction, which was discovered in 1928 by Otto Diels and his then student Kurt Alder, has featured in many total syntheses of natural products.[86] Following the pioneering work in 1987 by Guingant and Barreto in the synthesis of ochromycinone **51**,[87] several of the earlier syntheses of angucycline natural products employed the Diels-Alder reaction as the key step in the synthesis of the tetracyclic ring skeleton.

As an example, Krohn *et al.* adopted the approach of Guingant and Barreto in the synthesis of 6-deoxybrasiliquinone **58**, the C-3 ethyl analogue of ochromycinone **51** (**Scheme 14**).[88] The synthesis of the diene **59** was accomplished in three steps from 5-ethyl-1,3-cyclohexanedione **60**. This was followed by a boron triacetate-mediated Diels-Alder cyclization reaction between the chiral racemic diene **59** and juglone **61**, to form the B ring of the tetracyclic framework **62** in a 71% yield as a single diastereomer. This was then followed by an epoxidation using dimethyldioxirane to yield the *cis* epoxide **63** stereoselectively. Aromatization of this epoxide was achieved in a modest yield of 26% using boron triacetate, which also caused the acetylation of the free hydroxyl group, producing hydroxy-quinone **64**. Subsequent hydrolysis, followed by photo-oxidation of the intermediate alcohol, generated the desired 6-deoxybrasiliquinone **58**.

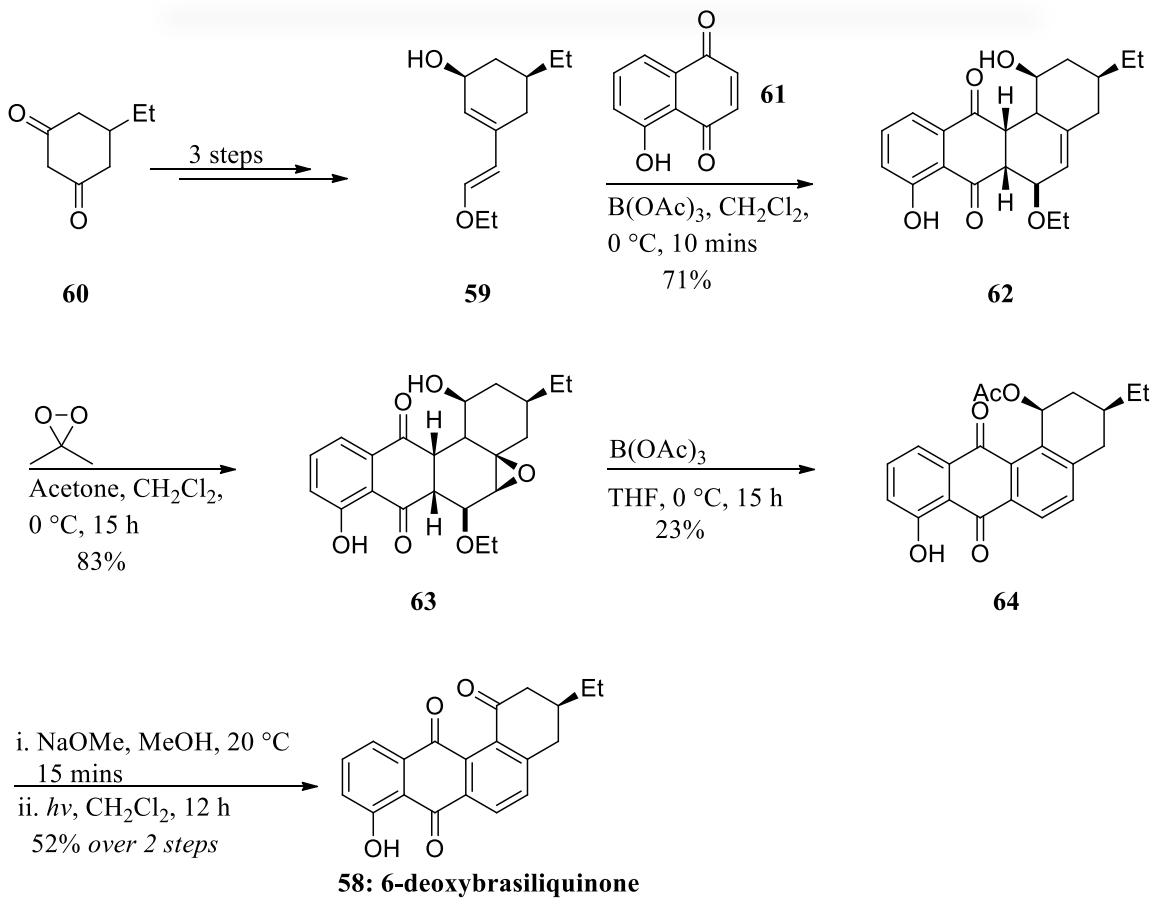

Scheme 14: Synthesis of 6-deoxybrasiloquinone by Krohn *et al*.[88]

More recently, as a second example, Kaliappan and Ravikumar used the Diels-Alder reaction as the key step to construct the B ring, in the synthesis of the angucycline natural product YM-181741 **65** (**Scheme 15**).[89] Ene-yne-containing compound **66** was synthesized in four steps from hexenoic acid, and subjected to ene-yne metathesis reaction conditions to construct the key diene **67**. Diene **67** was then exposed to bromojuglone acetate **68** in the presence of toluene at 80 °C to generate an intermediate cycloadduct, which upon treatment with K_2CO_3 in MeOH, underwent an aromatization, generating the angucyclinone skeleton **69**. Photo-oxidation to introduce the C-1 carbonyl group, followed by deprotection of the silyl group, yielded the desired natural product **65**.

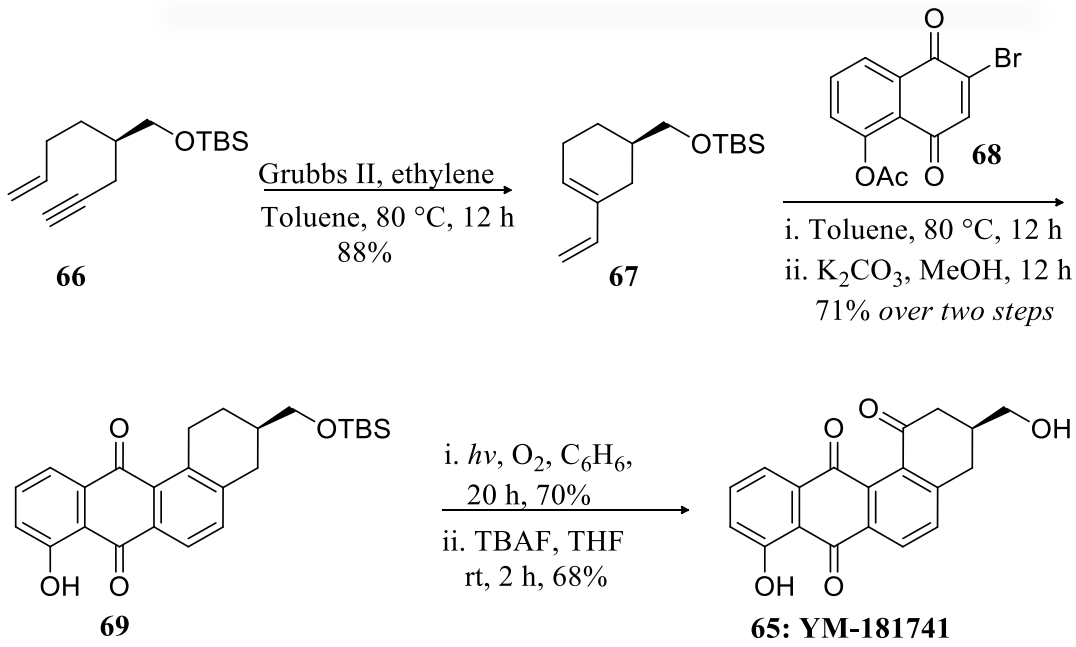

Scheme 15: Synthesis of YM-181741 by Kaliappan and Ravikumar using a Diels-Alder reaction as the key step.[89]

Although the construction of the B ring of the tetracyclic framework utilizing the Diels-Alder reaction is the most commonly applied strategy, there exist in the literature some examples of different modes of disconnections that have been effected. As an example, Suzuki and coworkers achieved the total synthesis of tetrangulol **50** using a benzyne-furan cycloaddition as the key step to form the C ring of the tetracyclic framework (**Scheme 16**).[90] This strategy makes use of benzyne **70** as the dienophile constituting the D ring, and siloxyfuran **71** as the diene constituting the AB rings of the tetracyclic framework. Beginning the synthetic sequence with tetralone **72**, intermediate siloxyfuran **71**, which was too moisture sensitive for isolation, was generated in five steps. Triflate **73** was added to the mixture containing intermediate **71**, and after careful addition of *n*-BuLi, generated benzyne species **70**, immediately underwent a Diels-Alder cycloaddition with siloxyfuran **71**. This produced a mixture of the regioisomeric tetracyclic structures **74** and **75** which were too unstable to isolate and purify. Upon oxidation with CAN in MeCN and H_2O, quinones **76** and **77** were produced in an overall yield of 76%, with quinone **76** being the major isomer. Quinone **76** was aromatized by refluxing in 1,4-dioxane in the presence of DBU, followed by exposure to air. This compound was then deprotected by treatment with BBr_3 to yield tetrangulol **50** in a moderate yield.[90]

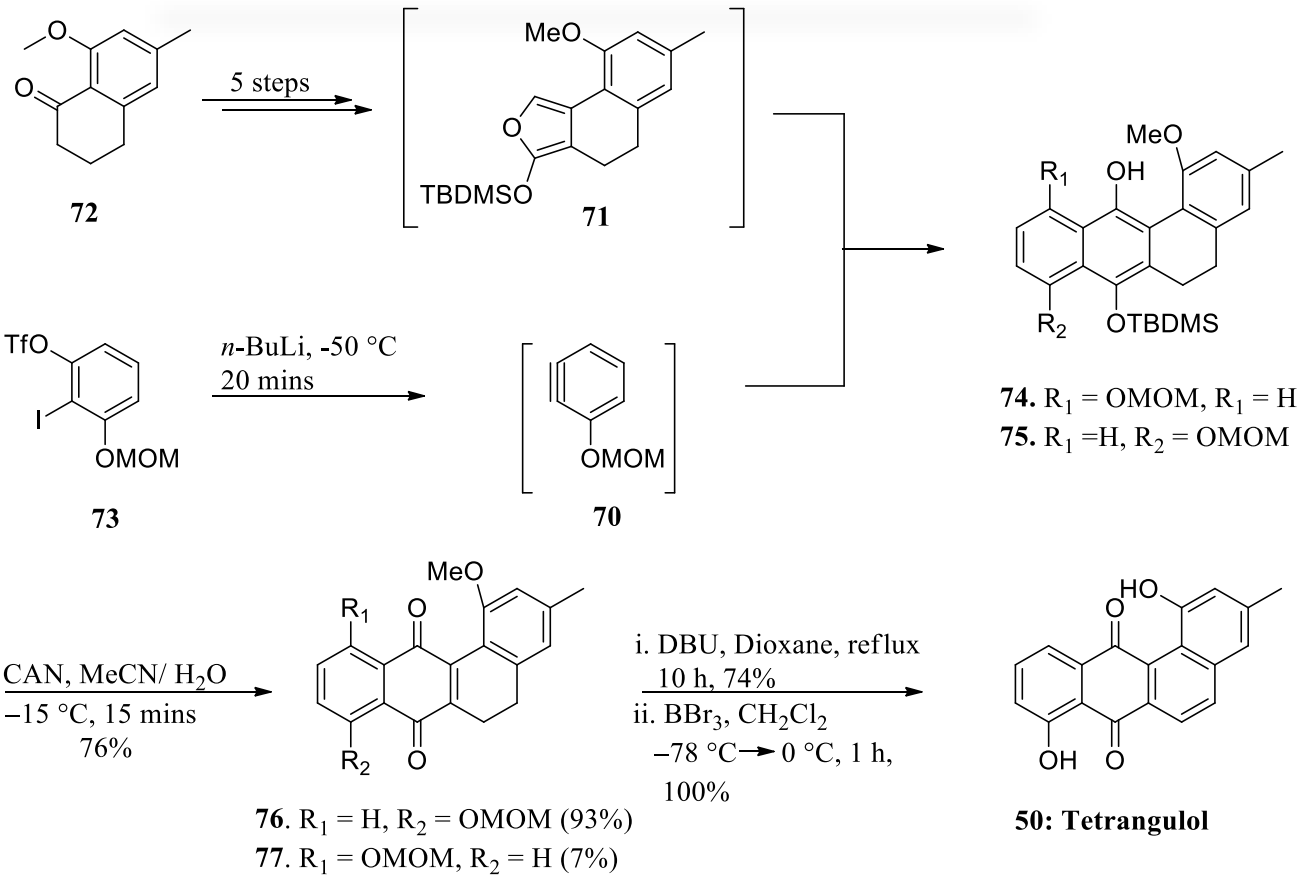

Scheme 16: Synthesis of tetrangulol by Suzuki and coworkers.[90]

Despite being widely employed in the synthesis of angucyclines, the Diels-Alder approach is not without its challenges. Foremost of these is the common issue of regioselectivity, as well as the need for an additional step to aromatize the B ring of the tetracyclic framework. Furthermore, often harsh reaction conditions are used in the synthesis of the diene and dienophile intermediates.

1.4.3.2 Nucleophilic addition-type strategies

Beginning with the first ever synthesis of tetrangulol by Brown and Thomson in 1976,[85] inter- and intra-molecular nucleophilic addition-cyclization type strategies have since been used in the formation of the benz[α]anthracene core. The synthesis of 3-deoxyrabelomycin **78** was realized by Kraus and Wu,[91] using an inter-molecular Michael addition reaction between acetylated naphthoquinone **79** and cyclohexanedione **80** (as the preferred enol tautomer) as the key step (**Scheme 17**). The addition reaction proceeded at room temperature, without a catalyst, most likely due to the superior Michael-acceptor properties of naphthoquinone **79**. Subsequent methylation afforded adduct **81**. This was then followed by an intra-molecular Michael addition and the subsequent elimination of methanol, in the presence of base and heat, resulting in the

formation of the B ring of tetracycle. Subsequent demethylation generated 3-deoxyrabelomycin **78** in a very modest yield of 17%.

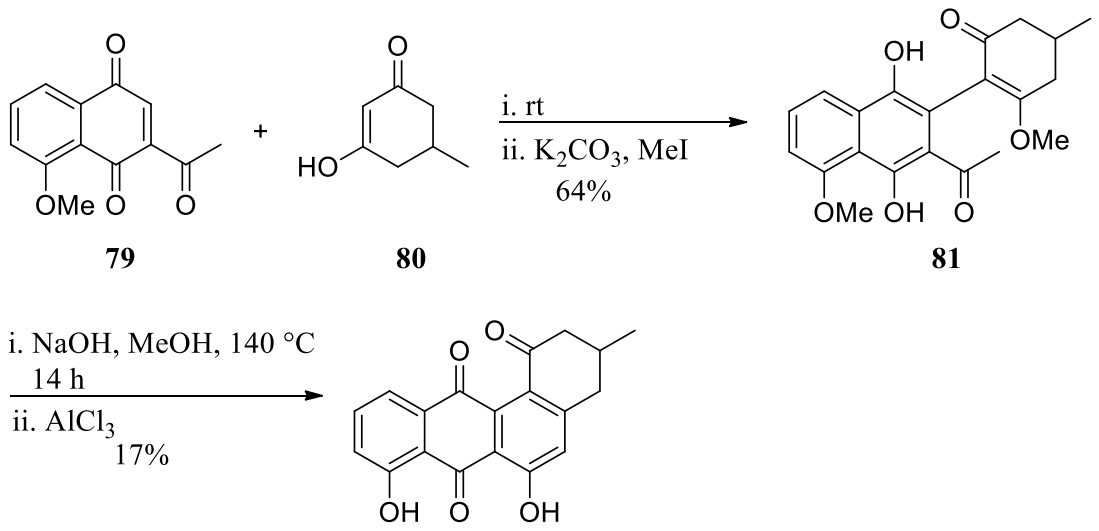

Scheme 17: Synthesis of 3-deoxyrabelomycin by Kraus and Wu.[91]

In recent years however, a specific type of Michael addition reaction, the Hauser-Kraus annulation, has gained a surge in its use for the formation of the tetracyclic framework of angucyclinones. Discovered in 1978,[92] the Hauser annulation is generally defined as the annulation reaction between a C-3 nucleofugal phthalide (also termed the Hauser donor) and a corresponding polarized Michael acceptor, resulting in a naphthalene-1,4-diol, or a 1,4-napthoquinone. Of the many Hauser donors that are available, the most commonly employed are the Hauser donors **82**, the Kraus donors **83**, and the Kraus-Mal donors **84** (**Figure 10**), although the Kraus donors have shown greater potential in their reactivity and applicability. In general, the reaction involves a Michael addition followed by a cyclization between a base generated stabilized anion, formed from the substituted phthalide, and the Michael acceptor.

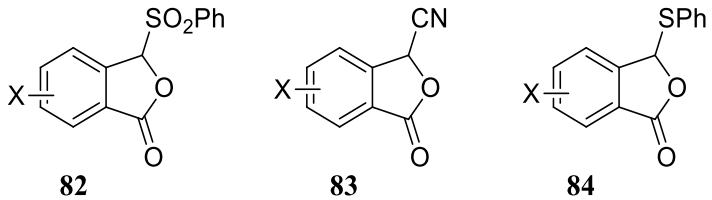

Figure 10: Hauser, Kraus and Mal donors.

Mal for example, demonstrated the versatility of this method in the synthesis of several benz[α]anthraquinones.[93] To effect the Hauser annulation, they utilized Hauser donors, and

naphthoquinone monoketals, furnishing benz[α]anthraquinones in good yields, demonstrating for the first time that phthalide annulation can effectively be used for the synthesis of benz[α]anthraquinones of angucyclinones.

This strategy was again adopted in 2006, due to its regiochemical integrity and convergence, as the key step in the synthesis by Mal and Dey, of BE-23254 **85**, a chlorinated angucyclinone natural product possessing antibiotic properties (**Scheme 18**).[94] The Kraus donor **86** was prepared in six steps from cyclohexenone **87**. Quinone monoketal **88**, the Michael acceptor, was prepared from 6-methoxytetralone in seven steps. The Hauser annulation between *t*-BuOLi generated stabilized phthalide anion and quinone monoketal **88** generated tetracyclic intermediate **89** in a moderate yield of 71%. This is an illustration of the formation of a C ring of the benz[α]anthracene framework from AB and D synthons. Aromatization of the A ring of tetracycle **89** was achieved using DDQ in refluxing benzene in a modest yield of 43%. Demethylation using $AlCl_3$, followed by base catalyzed hydrolysis furnished BE-23254 **85**.

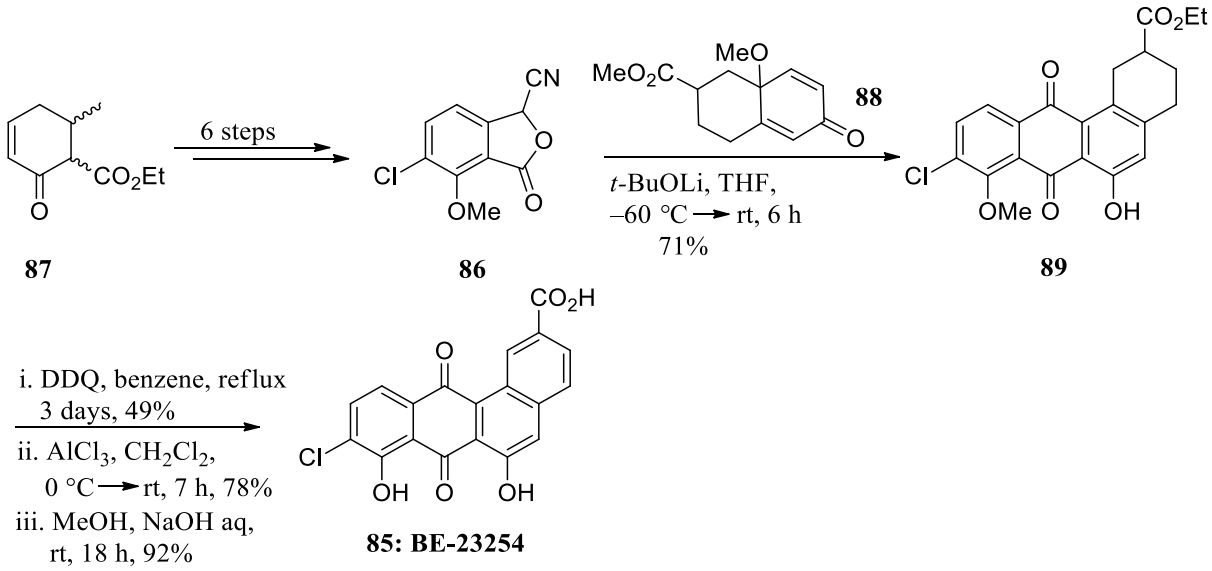

Scheme 18: Synthesis of BE-23254 by Mal and Dey.[94]

In addition to the Hauser annulation, other nucleophilic addition-type strategies have also been used in the formation of the benz[α]anthracene moiety. One such example is in the synthesis of landomycinone **90** by Roush and Neitz (**Scheme 19**).[95] Their reaction strategy involved the use of NaOEt to mediate an intramolecular nucleophilic addition and cyclization reaction of substituted naphthoquinone **91**, followed by oxidation in air of the resulting hydroquinone, to generate the tetracyclic quinone **92**. Substituted naphthoquinone **91** was prepared from chromium carbene **93** and alkyne **94** using a Dötz benzannulation reaction. Chromium carbene

93 was synthesized from a MOM-protected hydroquinone in three steps, whereas alkyne **94** was prepared from *m*-cresol in a thirteen-step reaction sequence. Deprotection of the MOM and TBS protecting groups of tetracycle **92** furnished landomycinone **90**.

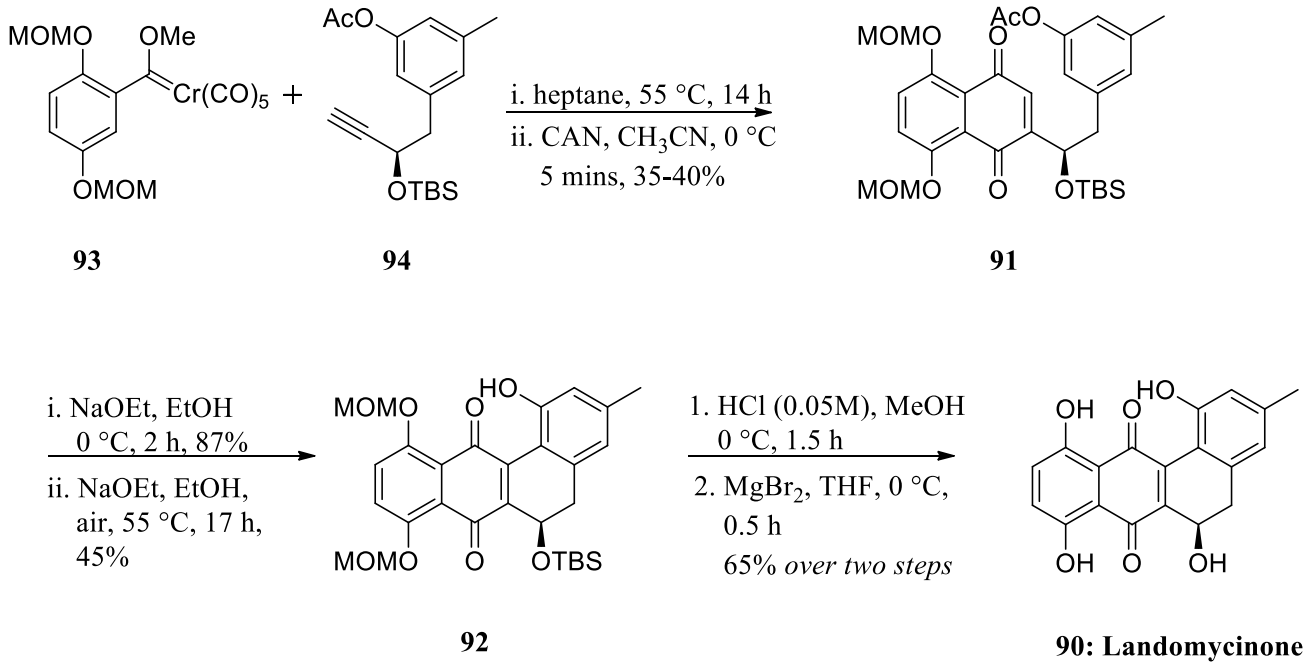

93 **94** **91**

92 **90: Landomycinone**

Scheme 19: Synthesis of landomycinone by Roush and Neitz.[95]

Despite the regiochemical integrity associated with the nucleophilic addition-type strategy, the key Michael acceptors, and donors, are often tedious to synthesize, often requiring long reaction times and sometimes harsh reaction conditions.

1.4.3.3 Friedel-Crafts reaction strategy

Although not as popular as the two methods already discussed, the use of the Friedel-Crafts reaction in the synthesis of angucyclinones has been demonstrated as early as 1985, for example in the synthesis of ochromycinone **51** by Katsuura and Snieckus (**Scheme 20**).[96] Their synthesis started with dithiane **95**, which in a total of eight steps, generated the substituted benzoic acid precursor **96**. Exposure of **96** to TFAA in CH_2Cl_2 mediated an intramolecular Friedel-Crafts acylation, resulting in the formation of ring C. This was followed by base catalyzed aerial oxidation in methanol, to yield benz[α]anthraquinone **97** in a good yield. To introduce the carbonyl group at the C-1 position, selenohydroxylation of **97** yielded an intermediate hydroxyselenide which was thereafter oxidized with chromate, and deselenated

in the presence of AIBN and Ph_3SnH to yield anthraquinone **98**. Demethylation using $AlCl_3$ afforded ochromycinone **51**.

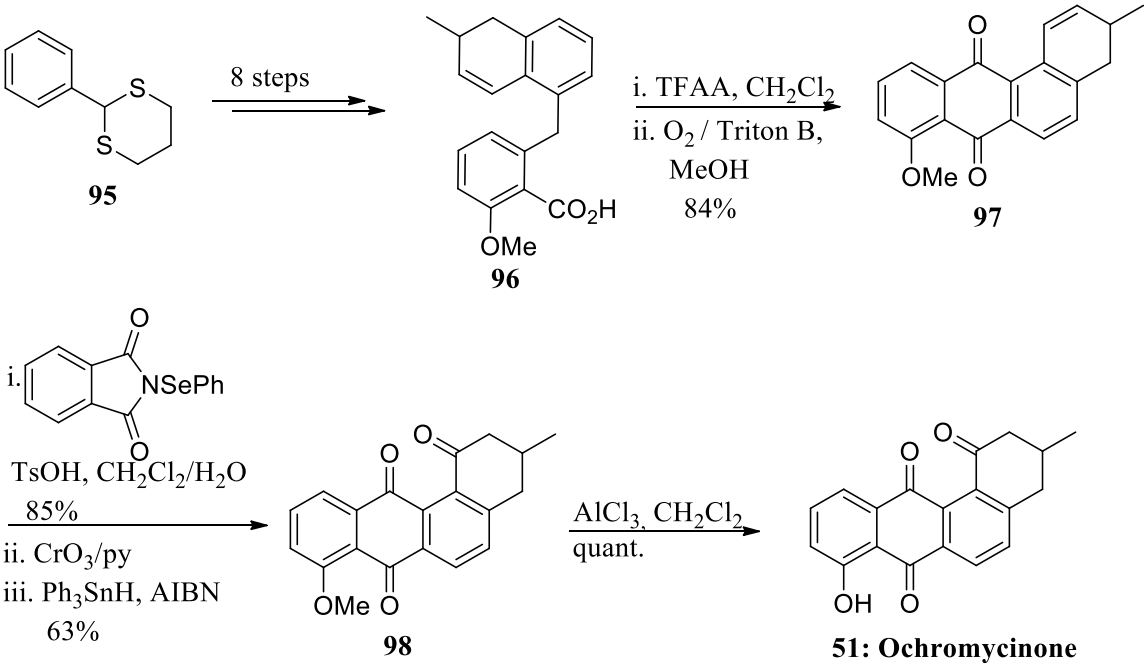

Scheme 20: Synthesis of ochromycinone by Katsuura and Snieckus.[96]

More recently, Kimura *et al.* used a Friedel-Crafts acylation reaction in their synthesis of prekinamycin **99** to construct the tetracyclic ring system **100** (**Scheme 21**).[97] Biaryl benzaldehyde **101** was synthesized using a Suzuki-Miyaura cross coupling reaction of the boronic acid **102** with bromo aldehyde **103**. Biaryl benzaldehyde **101** was then oxidized to the acid **104** in the presence of hydrogen peroxide**.** An ensuing intramolecular Friedel-Crafts reaction in the presence of $AlCl_3$ produced the tetracyclic skeleton **100**. Subsequent demethylation, followed by hydrazone formation and oxidation yielded the corresponding prekinamycin **99** in moderate yields.

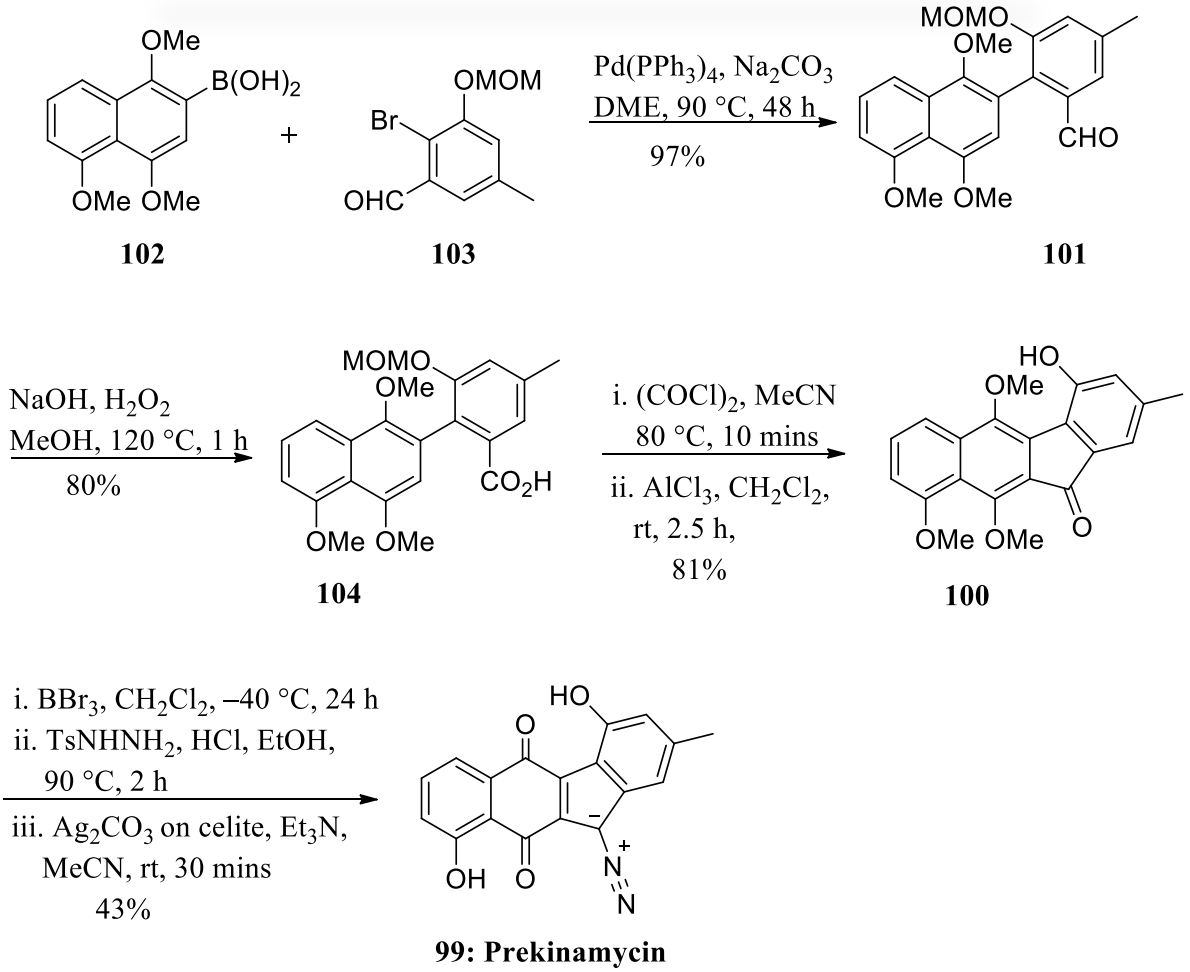

Scheme 21: Synthesis of prekinamycin by Kimura *et al.* [97]

1.4.3.4 Intramolecular cyclization strategy

Transition metals such as Co and Au have been used to effect intramolecular cycloaddition reactions in the formation of the tetracyclic framework of angucyclines and angucyclinones. An example is the synthesis of (-)-tetrangomycin **105** by Groth and coworkers (**Scheme 22**).[98] The primary step of their synthesis entailed an expedient intramolecular Co mediated [2+2+2] cycloaddition of a chiral triyne **106**, forming rings A,B, and C of tetracycle **107** in one step. The synthesis of the chiral triyne **106** was achieved in a total of eighteen steps. Oxidation of tetracycle **107** using $Ag(Py)_2MnO_4$ and silica gel, and subsequent deprotection of the MOM group generated benz[α]anthraquinone **108**. TBS deprotection, followed by a photooxidation to insert a C=O group at C-1 afforded (-)-tetrangomycin **105** regioselectively.

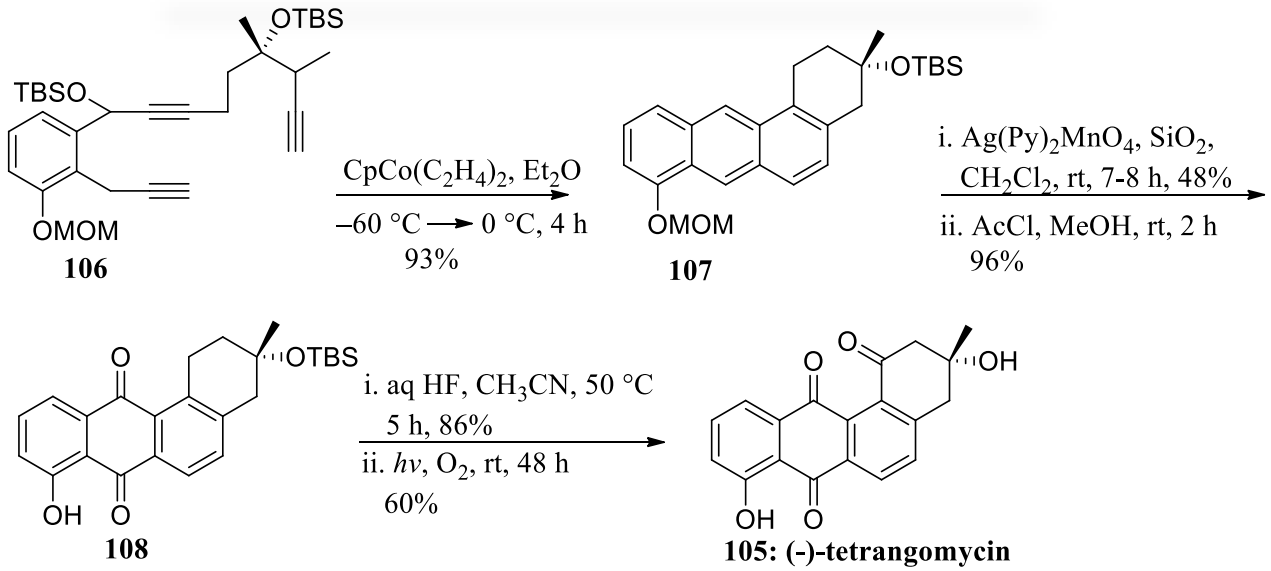

Scheme 22: Synthesis of (-)-tetrangomycin by Groth and coworkers.[98]

Another example is the Sato *et al.* synthesis of (+)-ochromycinone **51** and (+)-rubiginone B_2 **109** (**Scheme 23**).[99] An $AuCl_3$-mediated [4+2] intramolecular cycloaddition of alkynyl enynal **110** was used as the crucial step, forming rings A and B of tetracycle **111** in one step. Alkynyl enynal **110** was prepared in a total of eleven steps with an overall yield of 88%. Tetracyclic benz[α]anthracene **111** was oxidized using CAN to yield (+)-rubiginone B_2 **109**, which after deprotection with BCl_3 furnished (+)-ochromycinone.

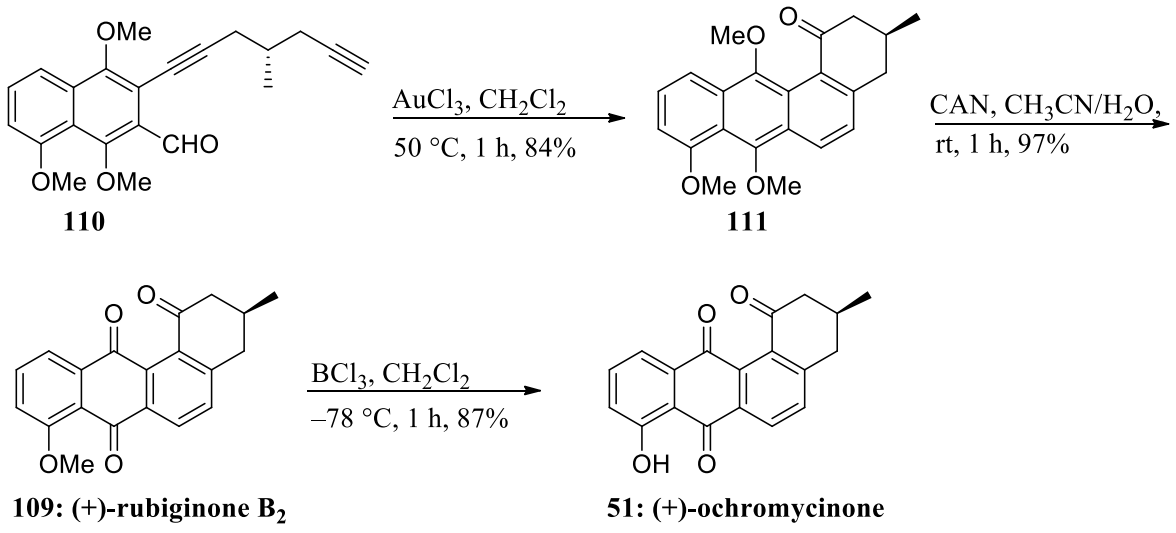

Scheme 23: Synthesis of (+)-ochromycinone and (+)-rubiginone B_2 by Sato *et al*.[99]

Although intramolecular cyclization strategies establish an impressive ability to form more than one ring in one step, the synthesis of the key precursors can be challenging, often requiring many synthetic steps to synthesize.

1.4.3.5 Transition metal catalyzed cross-coupling strategies

Of insurmountable significance, especially in the fields of organic synthesis, medicinal and process chemistry, as well as in chemical biology, are the transition metal-catalyzed coupling reactions that are used to forge new carbon-carbon bonds within and between functionalized substrates.[100] Of these coupling reactions, the palladium-catalyzed coupling reactions, which include the Heck, Suzuki-Miyaura, Sonogashira, Stille, Tsuji-Trost, and the Negishi reactions, have been demonstrated particularly to play a significant role in total synthesis, forging bonds that lead to complex natural products.

An example of the use of a palladium-catalyzed cross-coupling reaction as a key step in the formation of the tetracyclic framework of angucyclines is the synthesis of C-3' desmethyl analogues **112** and **113** of marmycin A by Ding *et al.* (**Scheme 24**).[101] Substituted bromo-naphthoquinone **114** was prepared in an overall six steps reaction sequence. The primary step of the synthesis involved an intramolecular Heck coupling reaction of the key intermediate **114**, catalyzed by $Pd(OAc)_2$ to effect the ring closure, forming ring B of tetracycle **115** as a single regioisomer. Quinone **115** was used in the following step without purification, where ring B was aromatized using DDQ in refluxing benzene generating benz[α]anthraquinone **116**. Following a series of modifications, involving transamination, and simultaneous C- and N-glycosidations, 3-desmethylmarmycin A **112** and its diastereomer **113** were generated in decent yields.

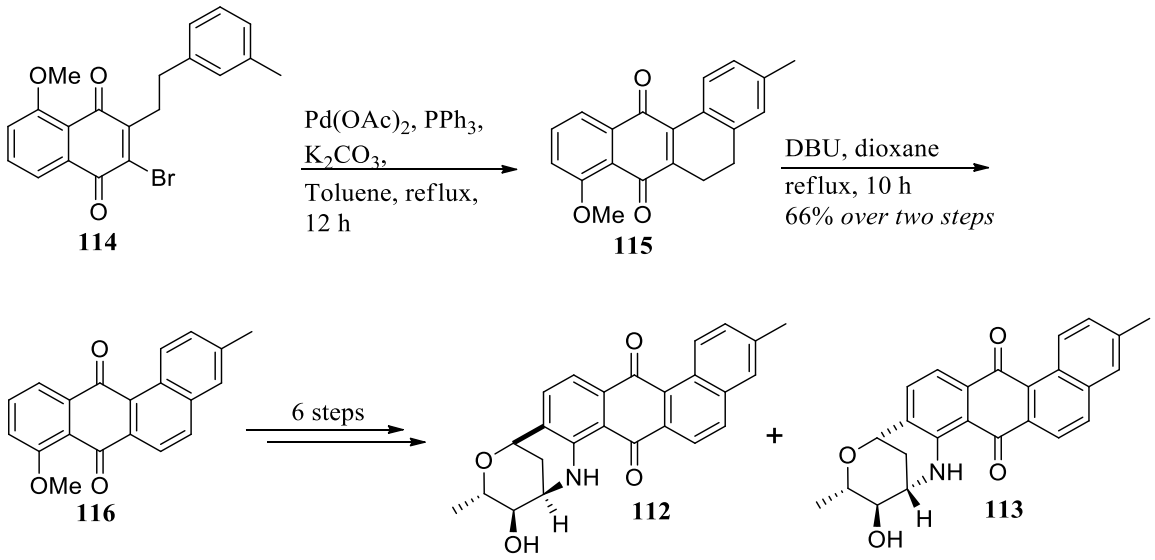

Scheme 24: Synthesis of C-3' desmethyl analogues of Marmycin A by Ding *et al.*[101]

There is therefore no doubt that palladium-catalyzed cross-coupling reactions have considerably advanced the ability of synthetic organic chemists to synthesize complex molecular frameworks. Recognizing this potential, the organic research group in our laboratory have been especially interested in the use of these coupling reactions as key steps in the synthesis of angucycline frameworks. The palladium-catalyzed cross-coupling reaction of primary interest in our group is the Suzuki-Miyaura coupling reaction, a brief overview of which is given in the next section.

1.5 Suzuki-Miyaura coupling reaction

The Suzuki-Miyaura coupling reaction has been developed into a robust and efficient method for forming new carbon-carbon bonds.[100, 102-103] It comprises of a reaction between organic electrophiles such as aryl or alkyl halides, triflates and other pseudohalides, with an organoboron compound, in the presence of a base, to yield stereospecific polyene compounds as well as biaryl systems.[104-105] The first example of a Suzuki-Miyaura coupling reaction between alkenylboranes and alkenyl or alkynyl halides was demonstrated by the Suzuki group in 1979,[104-105] and the first synthesis of unsymmetrical biaryls through the coupling of arylboronic acids with haloarenes was demonstrated in 1981.[106] In 1992, Suzuki and co-workers reported conditions for the Suzuki-Miyaura cross-coupling of sterically hindered substrates.[107] Since then, several developments have been made in terms of improved reaction conditions, increasing the range of applicability of this reaction, and rendering it a ubiquitous occurrence in the synthesis of pharmaceuticals and natural products.

The preference of this reaction over others is also as a result of the often mild conditions that are used, and the sole generation of non-toxic by-products. Furthermore, the organoboron compounds are relatively easy to prepare and handle, and are environmentally benign compared to other organometallic reagents.[102]

1.5.1 Mechanism of Suzuki-Miyaura coupling reaction

As with most other cross-coupling reactions, the catalytic cycle of the Suzuki-Miyaura coupling reaction is thought to follow the general sequence of oxidative addition, followed by a transmetallation, and ending with a reductive elimination **(Figure 11**). Oxidative addition of the aryl or alkenyl halide to the palladium(0) catalyst generates the palladium(II) complex R^1-Pd-X. This is then followed by a transmetallation with the organoborane to form the diarylpalladium intermediate R^1-Pd-R^2, which undergoes a reductive elimination generating a biaryl product and regenerating palladium(0) catalyst. Although the exact mechanism of the

transmetallation step is still unknown. It is however, generally accepted that to accelerate this step, a base is used, and this occurs by either of two pathways.[108-109] The base can interact with organoborane species, quaternizing the boron atom, and thus making the organic group more nucleophilic to exchange with the R^1-Pd-X complex, generating the diarylpalladium(II) complex R^1-Pd-R^2 (**Path A**).[108-109] Alternatively, a base-halogen exchange between R^1-Pd-X and the base takes place, forming an oxo-palladium(II) species which then facilitates an intramolecular transmetallation with the organoborane species, generating the diarylpalladium(II) complex R^1-Pd-R^2 (**Path B**).[108-109]

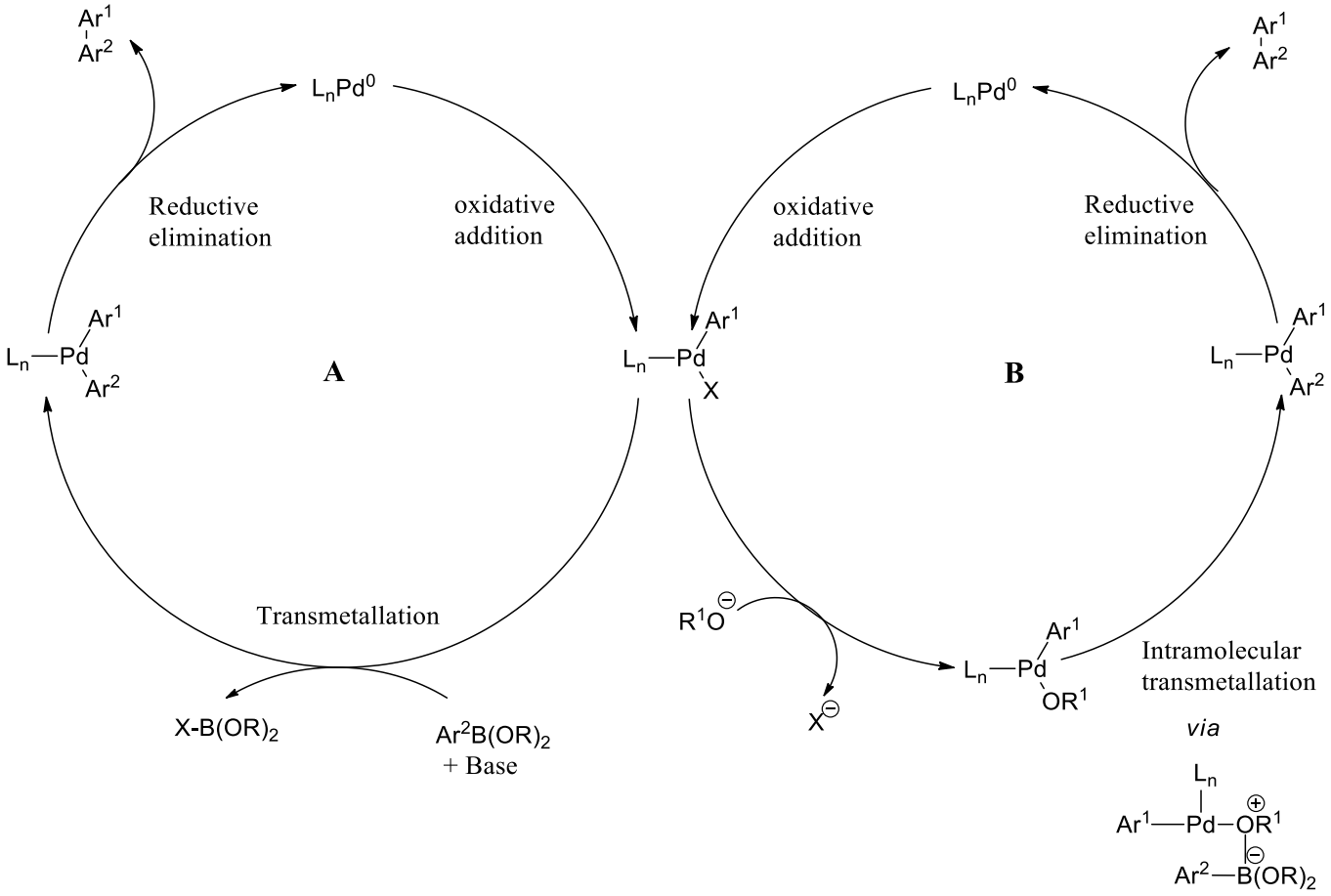

Figure 11: Mechanism of the Suzuki-Miyaura cross-coupling reaction.[109]

1.5.2 Use of the Suzuki-Miyaura coupling reaction in the synthesis of tetrangulol

The work involving the use of Suzuki cross-coupling reaction in the synthesis of angucycline backbone **117** was pioneered in our labs by Myron Johnson, under the supervision of Prof. Charles de Koning. The cross-coupling reaction between bromonaphthalene **118** and boronic acid **119** was utilized as the most crucial step in order to form a biaryl axis, resulting in the formation of biaryl intermediate **120** (**Scheme 25**).[110] The second key step of the synthesis

involved a Grubbs-II catalyzed olefin metathesis of intermediate **121** forming ring B of the tetracyclic framework **117**. However, the drawback with this methodology is that a Wittig reaction (highly atom uneconomical!) was used in order to form the alkene precursor **122**.

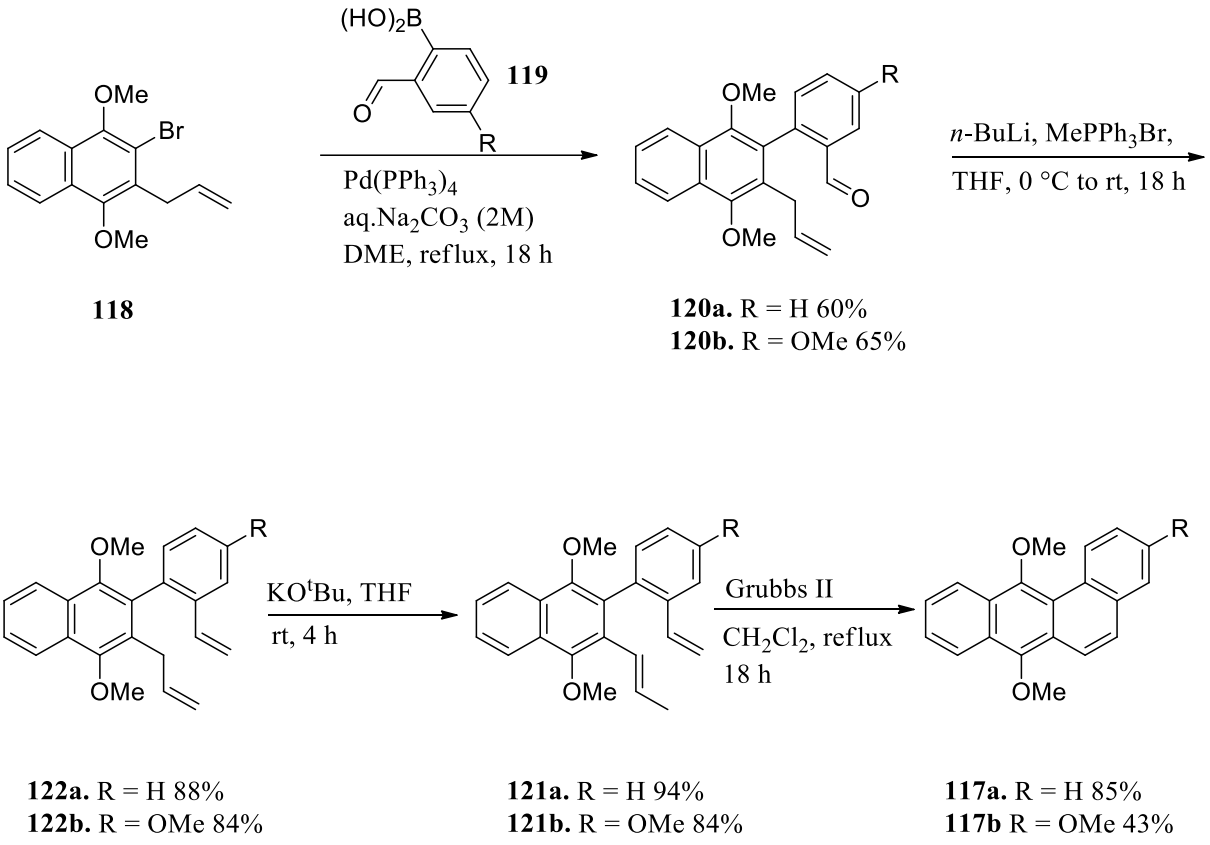

Scheme 25: Synthesis of benz[α]anthracene backbone by Johnson *et al.*[110]

This work was then continued by a former PhD student, Dr Kennedy Ngwira, and later developed into a methodology for the synthesis of the angucycline natural product tetrangulol **50**.[111] Ngwira *et al.* used a Suzuki-Miyaura coupling reaction between boronic acid **123** and iodo-compound **124** as the key step in forming biaryl compound **125** (**Scheme 26**).[111] Using Corey-Füchs methodology, **125** was converted to acetylene intermediate **126**, the precursor to the second key step of this synthesis. A $PtCl_2$- or a $AuCl_3$-catalyzed cycloisomerization was subsequently used to construct the B ring of tetracyclic framework **127**, the precursor to tetrangulol.

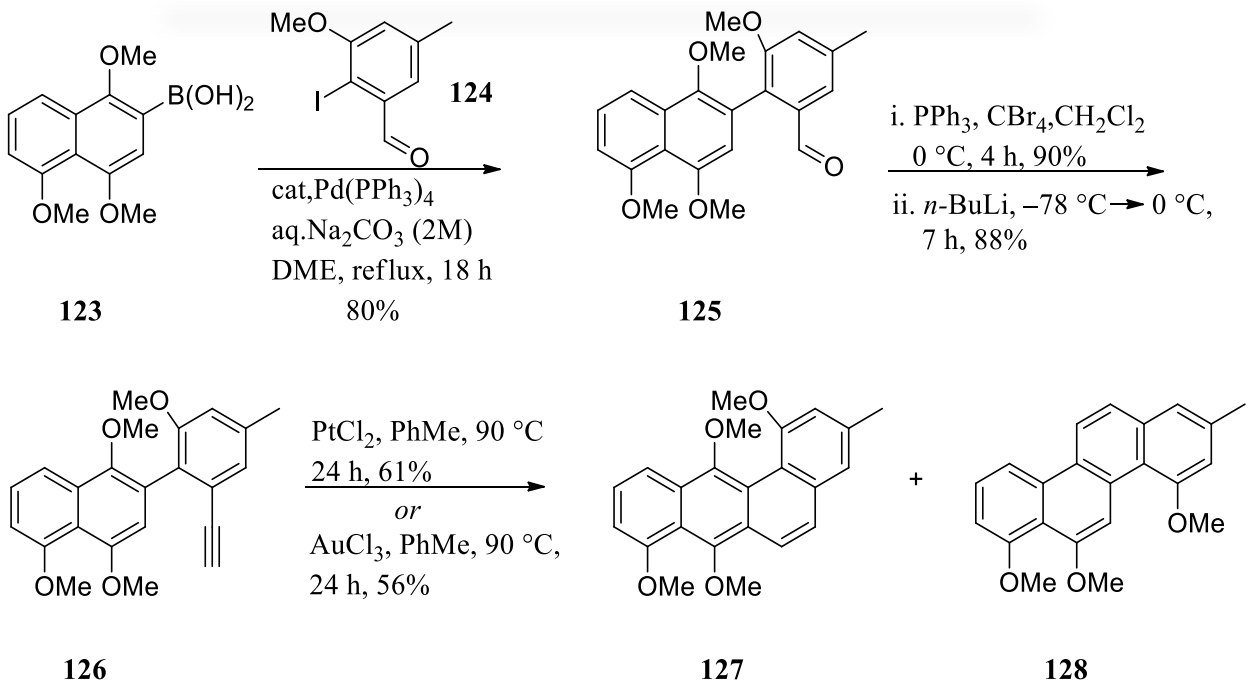

Scheme 26: Key steps in the synthesis of tetrangulol by Ngwira *et al.*[111]

However, the cost of $PtCl_2$ or $AuCl_3$ renders this method highly inefficient, especially for large scale synthesis. This inefficiency is further elaborated by the lack of selectivity of the key cycloisomerization step, as can be seen from the side product **128** which formed in a 1:0.5 ratio of **127:128**. An improved synthetic strategy was therefore necessitated.

1.6 Aim and objectives

Therefore the aim of the first part of this PhD was to attempt to improve the efficiency of the methodology developed in our laboratory (**Scheme 26**) to synthesize the angucycline tetrangulol, and apply principles of Green Chemistry in so doing, where possible. One crucial way that we anticipated to achieve this was to use the much milder, environmentally benign, $FeCl_3$-catalyzed carbonyl olefin metathesis described in section **1.3** to construct the B ring of the tetracyclic framework of tetrangulol. We also envisaged using the palladium-catalyzed Suzuki-Miyaura coupling reaction as a key reaction in bringing together the A and CD rings of the benz[α]anthracene scaffold. This would essentially enable us to incorporate Green Chemistry principle 9 i.e. *Catalysis* into our synthetic strategy. Additionally, we expected *to reduce the number of derivatives in terms of protecting groups* by starting the synthesis with naphthoquinone rather than the more commonly used juglone, thus integrating principle 8. It was envisaged that the oxygen at C-8 would be introduced at a later stage by C-H functionalization, a rather risky move, but nonetheless one that would promote step-wise

economy. Principles 1 and 12, i.e. *preventing waste in the first place which is better than cleaning up waste,* and, *the use of inherently safer chemicals for accident prevention* were also aspects that were considered in our synthetic strategy.

CHAPTER 2

2.1 Overview

Our initial foray into the construction of the angucycline natural product tetrangulol began with a simple model study, the primary aim of which was to investigate the use of carbonyl-olefin metathesis to construct the tetracyclic framework of angucyclines. This will be discussed in the first part of this section. Thereafter, our attempts towards the formal synthesis of tetrangulol are described.

2.2 Model study on the synthesis of a benz[α]anthracene skeleton

Initially, we selected biaryl compound **129** as our target molecule to be subjected to carbonyl-olefin metathesis conditions. In a forward sense, we anticipated that this would lead to the desired benz[α]anthracene skeleton **117b**. Biaryl compound **129** could in turn be prepared by means of an olefin isomerization of intermediate **120b**, which, adopting the same strategy as previously used in our laboratory, was to be furnished by means of a Suzuki-Miyaura coupling reaction between allyl-bromonaphthalene **118** and boronic acid **119b** (**Scheme 27**).

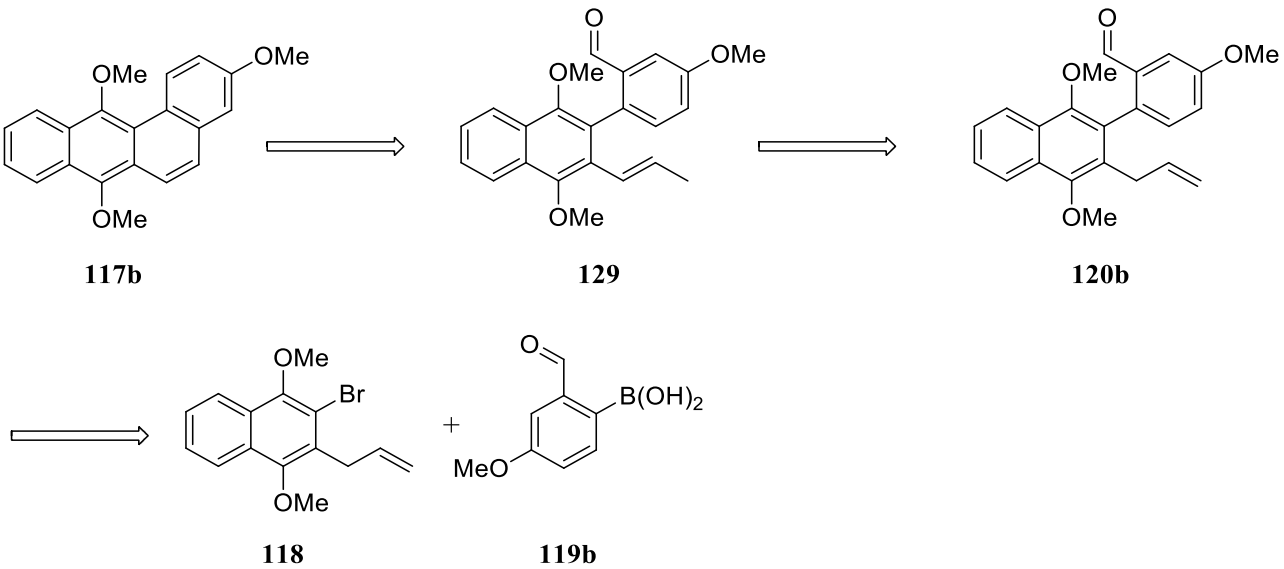

117b **129** **120b**

118 **119b**

Scheme 27: Retrosynthetic strategy for the formation of a benz[α]anthracene skeleton

2.2.1 Synthesis of allyl-bromo-dimethoxynaphthalene 118

Our model study began with the synthesis of the ally-bromonaphthalene **118** (**Scheme 28**). This was initiated by the oxidative bromination of naphthol **130** to 2-bromo-1,4-

naphthoquinone **131** in the presence of NBS and aqueous AcOH, following literature precedent.[112] This reaction proceeded smoothly to yield the desired quinone **131** as a yellow solid in a good yield. Care was taken not to expose the crude product to silica gel for a prolonged period of time as this resulted in significant discoloration of the quinone. The characteristic quinone carbons were observed in the ^{13}C NMR spectrum at δ 182.2 and 177.6 ppm, confirming the oxidation of naphthol **130**. The ^{1}H NMR spectrum was identical to that described in the literature for quinone **131**.[113]

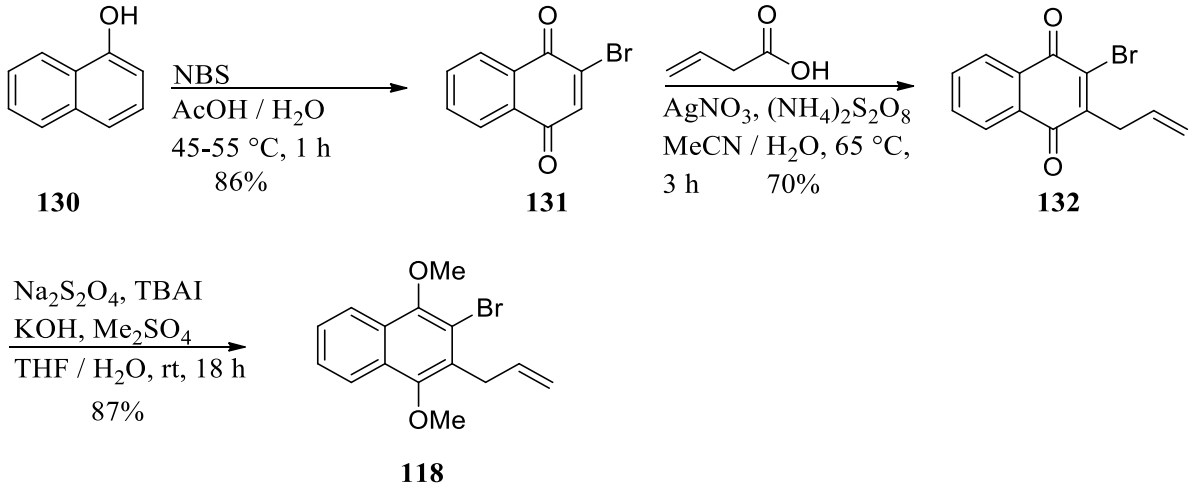

130 **131** **132** **118**

Scheme 28: Synthesis of allyl-bromonaphthalene intermediate 118

The next step involved the Kochi-Anderson[114] allylation of bromonaphthoquinone **131** (**Scheme 28**). This reaction proceeds by way of a two-step mechanism involving, initially, a persulfate/silver(I)-mediated decarboxylation of 3-butenoic acid, in aqueous MeCN, to generate an intermediate ally radical. The radical then reacts with 2-bromonaphthoquinone **131**, generating ally-naphthoquinone **132**[115] in a decent yield of 70%. ^{1}H NMR spectral analysis established the presence of an allyl group by the appearance of four new signals. The two protons at H-1′ were observed at δ 3.61 ppm, split into a doublet of triplet, whereas proton H-2′ appeared further downfield at δ 5.85 ppm as a peak split into a doublet of doublet of triplets. The two olefinic protons at H-3′ were observed as separate signals at δ 5.26 and 5.14 ppm. This was complemented by the ^{13}C NMR spectrum which showed the appearance of two new peaks in the aromatic region, and a peak at δ 35.4 ppm representing C-1′.

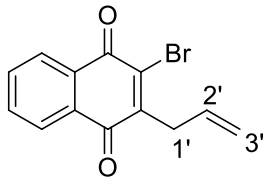

132

With the synthesis of allyl-bromonaphthalene **118** in mind, naphthoquinone **132** had to be reduced to a 1,4-dihydroxynaphthalene intermediate, followed by protection as the di-*O*-methyl ethers. This was accomplished using an aqueous solution of sodium dithionite to generate an unstable hydroxynaphthalene intermediate. The hydroquinone was immediately deprotonated with an aqueous solution of KOH, and then *O*-alkylated using Me_2SO_4. The reaction proceeded satisfactorily to furnish allylated-1,4-dimethoxynaphthalene **118**[116] in a good yield of 87%. In agreement with literature, the presence of methoxy groups was verified by ^{1}H NMR spectral analysis that showed the appearance of two singlet peaks, each integrating for 3 protons at δ 4.02 and 3.96 ppm. The disappearance of the highly deshielded quinone carbon peaks from the ^{13}C NMR spectrum, and the appearance, instead, of peaks at δ 150.9 and 150.1 ppm representing ArC-OMe carbons, further established the successful reduction and protection of the quinone carbons. In addition, peaks at δ 62.5 and 61.1 ppm were observed which are representative of methoxy group carbons.

2.2.2 Synthesis of biaryl compound 129

Having successfully synthesized intermediate **118**, the stage was now set for the union of commercially-available formyl-boronic acid **119b** and intermediate **118** to form biaryl naphthalene **120b** (**Scheme 29**). A 2-formylphenyl-boronic acid was chosen, as it would provide the requisite aldehyde appendage to perform a carbonyl-olefin metathesis. The union of the two fragments was undertaken by means of the highly versatile Suzuki-Miyaura coupling reaction utilizing conditions that have previously been successful in our group.[110] In the presence of $Pd(PPh_3)_4$ as a catalyst, and aqueous Na_2CO_3 as a base, the reaction was allowed to proceed. Purification by silica gel column chromatography generated biaryl compound **120b**[110] in an acceptable yield of 60%. The presence of a deshielded signal, in the ^{1}H NMR spectrum, at δ 9.58 ppm representing an aldehyde proton, as well as the appearance of three singlets at δ 3.89, 3.86, and 3.37 ppm representing the three methoxy group protons, proved the successful union of the two fragments. This was well corresponded to by the ^{13}C NMR spectrum which showed the appearance of a carbonyl peak at δ 192.1 ppm, and three signals at δ 62.4, 61.1, and 55.5 ppm corresponding to the three methoxy group carbons.

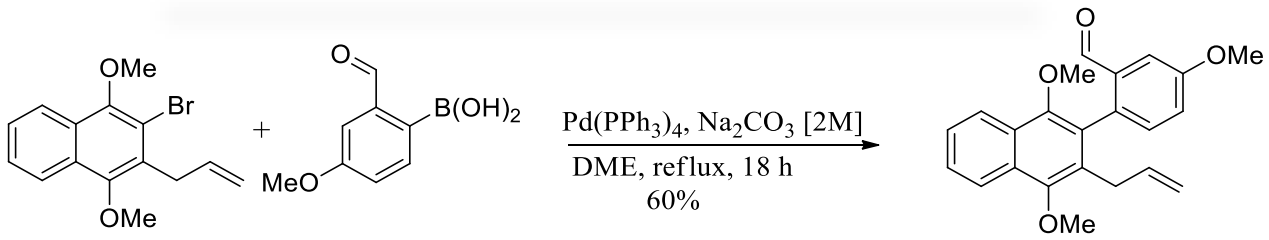

118 **119b** **120b**

Scheme 29: Synthesis of biaryl compound 120b *via* Suzuki-Miyaura coupling.

We then anticipated that exposing biaryl compound **120b** to KO*t*Bu would isomerize the double bond in order to deliver the desired carbonyl-olefin containing compound **129**, which would serve as the precursor to our key carbonyl-olefin metathesis. Our attempts at this reaction, however, were unsuccessful. Upon NMR spectral analysis of the sample obtained after the reaction, it was noted that the aldehyde peak was missing. We then concluded that the KO*t*Bu was acting as a nucleophile, attacking the carbonyl group rather than mediating an isomerization. The identity of the compound generated, however, was not confirmed.

2.2.3 An alternative approach

Overcoming this obstacle would prove to be facile, as we then decided to initially isomerize the allylated naphthalene **118** (**Scheme 30**), before carrying out the Suzuki-Miyaura coupling operation.

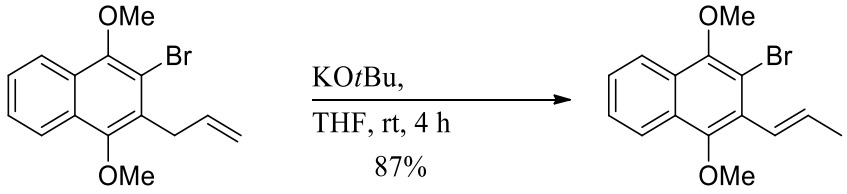

118 **133**

Scheme 30: Isomerization of allyl-bromo-naphthalene 118.

Exposing allyl-bromonaphthalene **118** to a solution of KO*t*Bu in dry THF, at room temperature, efficiently delivered the desired isomerized bromo-naphthalene **133** upon chromatographic purification, in a good yield of 87%. ^{1}H NMR spectral analysis proved without a doubt that the isomerization was successful. The appearance of a doublet signal integrating for 3 protons at δ 1.92 ppm established the presence of methyl protons H-3′. The

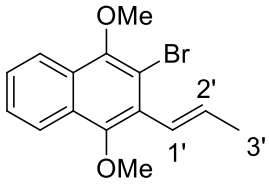

133

doublet at δ 6.50 ppm, with a *J*-coupling of 16.1 Hz pointing towards *trans* coupling, clearly indicated the presence of proton H-1′, whereas proton H-2′ was seen as a multiplet in the region of δ 6.44 – 6.30 ppm. A shift of the ^{13}C NMR spectral signal peak in the alkyl region from δ 34.3 to 19.5 ppm was observed which confirms the disappearance of methylene protons and the appearance of methyl protons as expected. It should be noted that trace amounts of the *E* isomer were observed in the ^{1}H NMR spectrum, however no attempt was made to isolate it.

At this point, the stage was set to construct the carbonyl-olefin precursor to our desired benz[α]anthracene skeleton, by means of the Suzuki-Miyaura coupling reaction. Due to the unavailability in our lab, at that time, of boronic acid **119b** we decided to perform the coupling operation with commercially available boronic acid **119a** instead, which bears the formyl group at the desired position (**Scheme 31**).

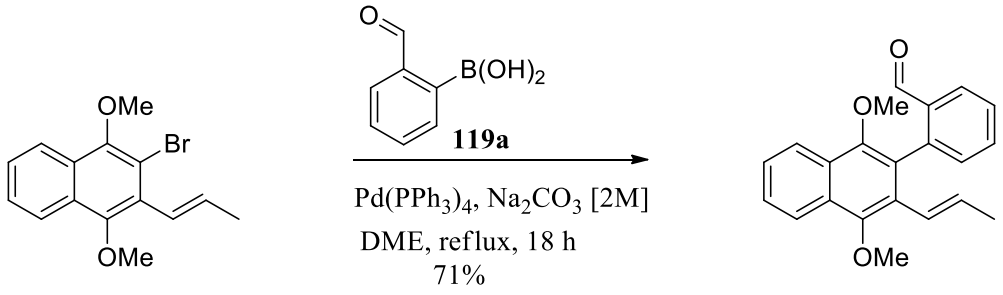

Scheme 31: Synthesis of biaryl compound 134 *via* Suzuki-Miyaura coupling.

The coupling was performed in the same manner as described for the synthesis of **120b**. DME was used as the solvent and was de-oxygenated before being added to the reaction flask, by bubbling nitrogen gas through the solvent for a minimum of 10 minutes. Following the completion of the reaction, column chromatography was performed; resulting in the isolation of the desired tetra-substituted-naphthalene biaryl compound **134** as a yellow solid in a yield of 71%. The success of the reaction was pronounced by the distinct presence of the deshielded signal for an aldehyde proton at δ 9.80 ppm, the presence of which was also confirmed by the highly deshielded peak at δ 192.2 ppm in the ^{13}C NMR spectrum. A total of eight aromatic protons were seen in the ^{1}H NMR spectrum as expected. The presence of the vinyl substituent of the naphthalene fragment of the molecule was ascertained by the downfield doublet peak at δ 6.13 ppm indicating the presence of proton H-1″, and the doublet of quartet peak at δ 5.90 ppm, indicating the presence of proton H-2″. The methyl group protons H-3″ appeared upfield at δ 1.68 ppm as a doublet as expected. These results were also

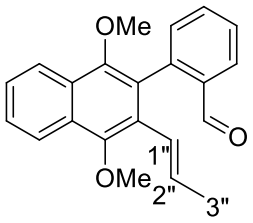

134

complemented by the presence of methoxy group protons at δ 3.86 and 3.41 ppm, and methoxy carbons at δ 60.9 and 60.8 ppm. Trace amounts of the possible *cis* isomer were visible in the ^{1}H NMR spectrum of the isolated *trans* product; however, due to the extremely minute amounts present, we were unable to isolate it. The mass of the compound was determined using HRMS, and was found to be 333.1458 corresponding to $[M + H]^+$, which correlates well with the calculated mass of 333.1491.

Pleased that rings A, C, and D were now in place with the required aldehyde and alkene functional groups, we proceeded to the most crucial step of our model study, i.e., the construction of ring B of the benz[α]anthracene skeleton *via* carbonyl-olefin metathesis. This reaction would proceed by means of a formal [2+2] cycloaddition between the $FeCl_3$-coordinated aldehyde moiety, and the olefin moiety, followed by a formal cycloreversion of the resulting oxetane intermediate **134a**, generating ring B of the tetracycle **135** (**Scheme 32**).

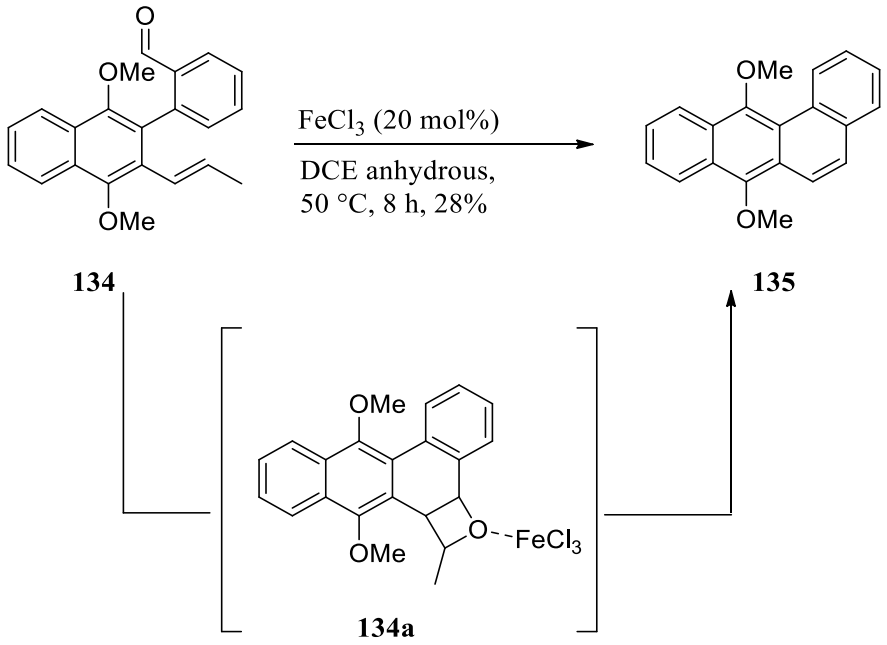

Scheme 32: $FeCl_3$-catalyzed carbonyl-olefin metathesis of biaryl compound 134.

Initially, at the outset of our investigation, the metathesis was attempted using a catalyst loading of 10 mol% of $FeCl_3$. Due to the highly hygroscopic nature of $FeCl_3$, it was weighed directly into the round bottom flask and placed under an inert atmosphere. Anhydrous DCE was then added, and the resulting solution was stirred for 5 minutes before a separate solution of biaryl compound **134** in anhydrous DCE was added. Upon complete consumption of starting material, the solution was passed through a short silica plug, and then purified *via* silica gel column chromatography. To our delight, tetracycle **135** was furnished as a yellow solid, albeit in a poor yield of 24%. NMR spectral analysis proved that the tetracycle had indeed formed successfully,

especially by the disappearance of the aldehyde signal, as well as the disappearance of the vinylic and methyl protons. The two singlet peaks at δ 4.11 and 3.97 ppm indicated the presence of two methoxy groups as expected. This was accompanied by the expected number of ten aromatic protons. The ^{13}C NMR spectrum also corresponded to this by the disappearance of the carbonyl peak, as well as the presence of eighteen aromatic carbon signals. The mass of the sample was confirmed by HRMS, and was found to be 289.1246 corresponding to $[M + H]^+$, which is in good agreement with the calculated mass of 289.1229, further establishing the success of the reaction.

Although pleased with the successful demonstration that a benz[α]anthracene skeleton can be formed using cheap, and environmentally abundant $FeCl_3$ as opposed to using expensive catalysts, the yield was poor and needed to be optimized. We hoped to improve the yield by trying several different conditions as described below (**Table 1**).

$FeCl_3$ (mol%)	**Solvent**	**Yield (%)**
10	DCE (anhydrous)	24
20	DCE (anhydrous)	28
20	Toluene	14
50	DCE (anhydrous)	28
100	DCE (anhydrous)	6 + 7% Quinone **136**

Table 1: Optimization of carbonyl olefin metathesis.

As is clear to see from Table 1, optimization was performed with limited success. In all cases, only uncharacterizable material was isolated in addition to the desired product. The best, so to speak, optimized yield of 28% was obtained using a catalyst loading of 20 mol% of $FeCl_3$ using anhydrous DCE as the solvent. Interestingly, when stoichiometric amounts of $FeCl_3$ were used, only 6% of the benz[α]anthracene was generated, but this was accompanied by small amounts (7%) of the corresponding benz[α]anthraquinone **136**. Although $FeCl_3$ is a mild oxidizing agent and has been used in the oxidation of benzimidazoles to benzimidazolequinones,[117-119] the use of $FeCl_3$ in establishing a metathesis reaction followed by the concomitant oxidation of the resulting methoxy-containing benz[α]anthracene was an exciting result. The NMR spectra of compound **136** matched those found in literature.[120] The diagnostic disappearance of methoxy protons in the ^1H NMR spectrum, as well as the distinct appearance

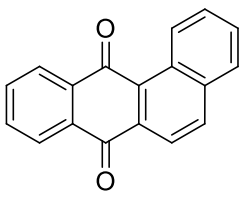

136

of deshielded quinone carbon peaks at δ 185.9 and 183.7 ppm in the ^{13}C NMR spectrum, conclusively proved that oxidation of the methoxy groups to a quinone had taken place. The observance of ten aromatic protons, as expected, further confirmed this result.
Inevitably, attempts were made to optimize the reaction further to see if we could improve the yield of the quinone **136**. This endeavor, unfortunately, was not met with success.

The poor yield obtained for the formation of tetracycle **135** however, is not surprising. Schindler and coworkers have reported the possibility of competing side reactions such as the Prins reaction and carbonyl-ene reactions when using olefin substrates with a crotyl moiety, as was the case with our substrate.[60, 65] Although the side products that we obtained were undiscernible, we eventually realized that the only possible way to optimize the yield was by attempting the reaction using a substrate bearing a tri-substituted alkene fragment. Even though Schindler and coworkers[65] report the best yields with styrenyl substrates, we chose rather to replace the 1-propenyl moiety of biaryl compound **134** with a 1-isobutenyl l moiety, as this would result in less waste after the ene-carbonyl metathesis reaction, in terms of atom economy as compared to using a styrenyl containing substrate. We therefore then focused our efforts towards the synthesis of biaryl compound **137**, as we envisioned that using this substrate would result in improved carbonyl-olefin metathesis yields, and therefore justifying its application in the formal synthesis of tetrangulol.

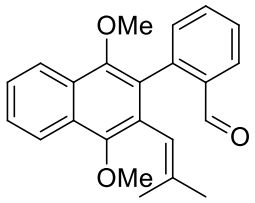

137

2.2.4 Towards improving carbonyl-olefin metathesis yields

In our initial foray into the construction of biaryl compound **137**, the Suzuki-Miyaura coupling reaction was to be used as the key step in forging the desired biaryl axis between 1-isobutenyl-substituted naphthalene **138** and boronic acid **119a** (**Scheme 33**). For the formation of 1-isobutenyl-substituted naphthalene **138**, we reasoned that because this was just a model study, the use of a Wittig reaction between aldehyde **139** and phosphonium salt **140**, could be permitted. We anticipated forming aldehyde **139** *via* ozonolysis of bromo-naphthalene **133**.

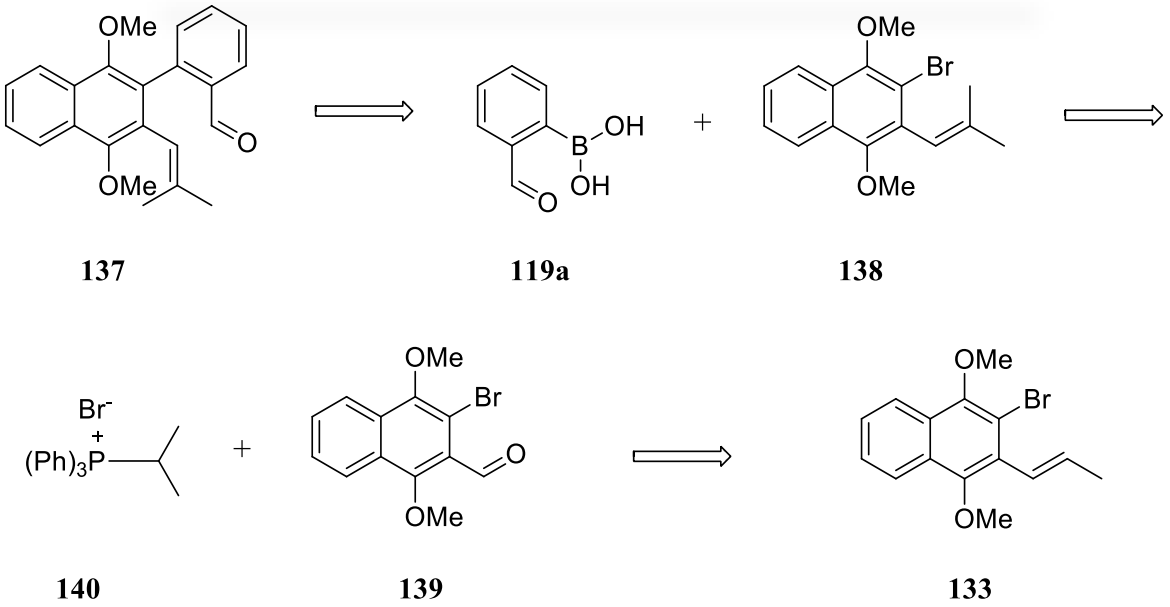

Scheme 33: Retrosynthetic strategy for the formation of carbonyl-olefin-bearing biaryl compound 137.

As an initial step in the synthesis of **137**, naphthalene **133** was subjected to ozonolysis conditions (**Scheme 34**). Ozone, from an ozone generator, was bubbled through a solution of naphthalene **133** in dichloromethane at –78 °C. Immediately after, the solution was purged with nitrogen gas to eliminate any residual ozone, and thereafter quenched with Me_2S to reduce the trioxolane intermediate formed through ozonolysis.

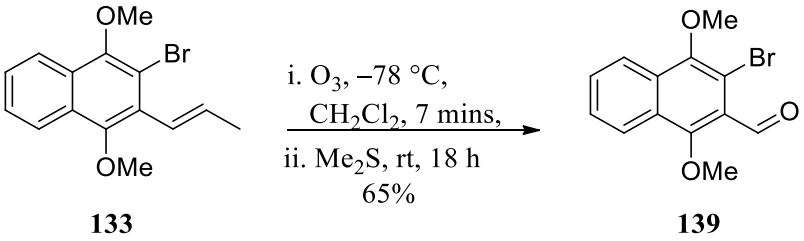

Scheme 34: Formation of aldehyde 139 *via* ozonolysis.

Purification using silica gel column chromatography afforded aldehyde **139** as a pale yellow solid in a decent yield of 65%. From NMR spectral analysis, it was plain to see that the desired aldehyde **139** was present. The distinct singlet at δ 10.52 ppm in the ^{1}H NMR spectrum clearly marked the presence of an aldehyde proton, which was additionally confirmed by the presence of a signal at δ 190.5 ppm in the ^{13}C NMR spectrum. In addition, the disappearance of methyl group protons and alkene protons further concluded that the ozonolysis was a success. The presence of methoxy group protons was confirmed by the two singlet peaks at δ 4.05 and 3.98 ppm, and this was accompanied by the expected number of four aromatic protons.

With naphthaldehyde **139** in hand, we next set out to perform the Wittig reaction in order to generate naphthalene **138** (**Scheme 35**), all the while being acutely conscious of the extremely low atom economy of this reaction.

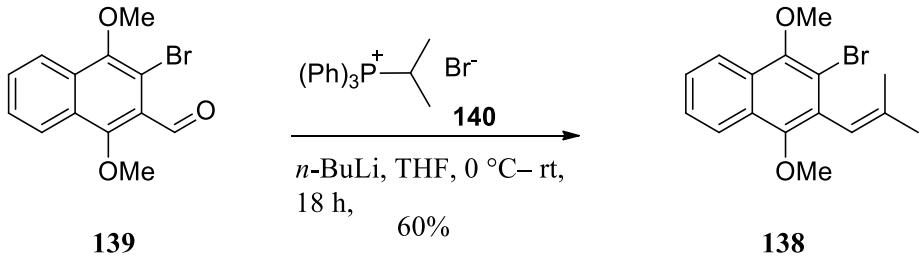

139 **138**

Scheme 35: Synthesis of naphthalene 138 *via* Wittig reaction.

The first step was to synthesize the phosphonium bromide salt **140**. Following literature precedent,[121] triphenylphosphine and 2-bromopropane were added to a sealed autoclave glass tube and placed in an autoclave high pressure reactor at 150 °C for 48 hours. After recrystallizing the residue from ethanol, the phosphonium salt was used in the next step without characterization.

To form the ylide, a solution of *n*-BuLi was added dropwise *via* syringe to a suspension of phosphonium salt **140** in dry THF at room temperature. The suspension rapidly turned orange and was allowed to stir for 30 minutes before being cooled to 0 °C. Thereafter, a solution of naphthaldehyde **139** in dry THF was added dropwise *via* syringe to the resulting ylide, and the reaction was allowed to warm to room temperature and stirred. Following purification by column chromatography, isobutenyl-substituted naphthalene **138** was isolated as a yellow oil in 60% yield. The disappearance of the aldehyde signal in the ^{1}H NMR spectrum confirmed nucleophilic attack of the ylide on the carbonyl carbon. The appearance of two doublet peaks in the alkyl region at δ 2.01 and 1.59 ppm, confirmed the presence of two methyl groups. An apparent septet peak at δ 6.18 ppm was also observed, which established the presence of vinylic proton H-1′. Analysis of the ^{13}C NMR spectrum showed, in addition to the disappearance of the carbonyl carbon, two signals in the alkyl region, at δ 25.4 and 20.1 ppm which were consistent with methyl group carbons. Based on 2D NMR analysis, the signal at δ 138.5 ppm was in accord with the vinylic carbon at C-2′, and the peak at δ 120.15 ppm was consistent with the vinylic carbon at C-1′. The mass of the compound was confirmed by HRMS, and was found to be 321.0465 which corresponds to $[M + H]^{+}$, and this is in good agreement with the expected mass of 321.0490.

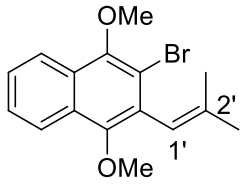

138

Pleased with the successful synthesis of naphthalene **138**, the subsequent step was to couple it with the commercially available boronic acid **119a**. Consequently, the stitching of the two fragments was performed *via* the amenable Suzuki-Miyaura coupling reaction. The same procedure was followed as described for the synthesis of biaryl compound **134**, and after purification by column chromatography, biaryl compound **137** was afforded in a yield of 47% as a yellow solid (**Scheme 36**). Presumably due to the increased steric bulk of substituted naphthalene **138**, the yield for this coupling is much lower than that attained for the synthesis of biaryl compound **134**.

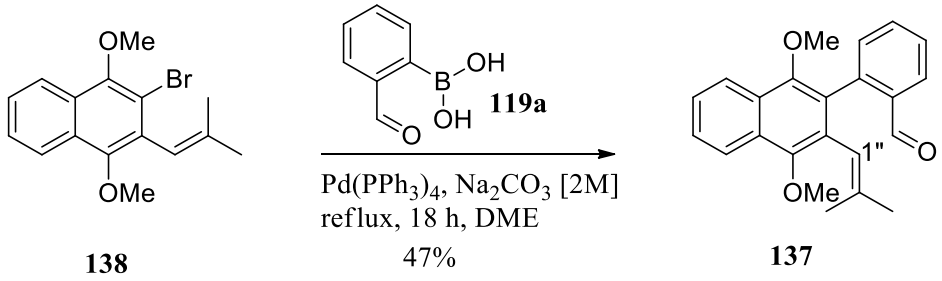

Scheme 36: Suzuki-Miyaura coupling to form biaryl compound 137.

Analysis of the ^{1}H NMR spectrum evidently showed the presence of an aldehydic proton by the distinct signal at δ 9.70 ppm. This was accompanied by an apparent septet peak at δ 5.75 ppm corresponding to vinylic proton H-1″, and two doublet peaks at δ 1.67 and 1.46 ppm corresponding to the methyl group protons. The methoxy group protons were seen at δ 3.79 and 3.43 ppm, as expected, confirming the successful coupling of the two fragments. This conclusion was further ascertained by analysis of the ^{13}C NMR spectrum which displayed the carbonyl peak at δ 192.1 ppm, as well as eighteen aromatic carbons as expected.

Bearing in mind that the objective of this endeavor was to investigate if the yield for the formation of tetracycle **135** could be improved using a tri-substituted olefin and carbonyl containing compound, the final step of our model study was ready to be executed (**Scheme 37**).

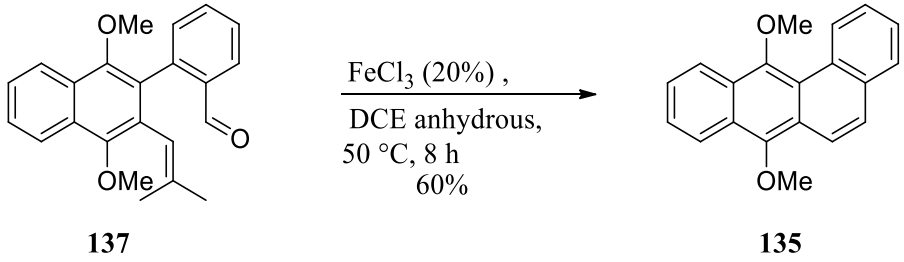

Scheme 37: $FeCl_3$-catalyzed carbonyl-olefin metathesis of biaryl compound 137.

A solution of biaryl compound **137** in anhydrous DCE was treated with $FeCl_3$ (20 mol%), following the same procedure as before. After complete consumption of starting material, and purification *via* silica gel column chromatography, tetracycle **135** was generated in a significantly improved yield of 60%! Corresponding with Schindler and coworkers' results,[65] it is evident that blocking the terminal alkene proton with a substituent consequently results in the elimination of competing side reactions, thus resulting in much improved yields.

Extremely pleased with this result, and based on the model study, we could safely come to the conclusion that $FeCl_3$-catalyzed carbonyl-olefin metathesis can successfully be applied in the formation of a benz[α]anthracene framework.

The stage was now set to begin the formal synthesis of the target natural product, tetrangulol **50**.

2.3 Formal synthesis of tetrangulol

We planned to commence our formal synthesis of tetrangulol **50** with naphthalene **138**, which would provide the C and D rings of the benz[α]anthracene, with the requisite 1-isobutenyl group in place (**Scheme 38**). This, rather than starting the synthesis with juglone, as has previously been done, would result in the use of fewer derivatives in terms of protecting groups. We anticipated that methoxy-protected tetrangulol **50a** could be formed *via* a late-stage, carbonyl-directed, oxidation of benz[α]anthraquinone **141**. We envisioned that the hydroxy group would append to the desired position for steric reasons.

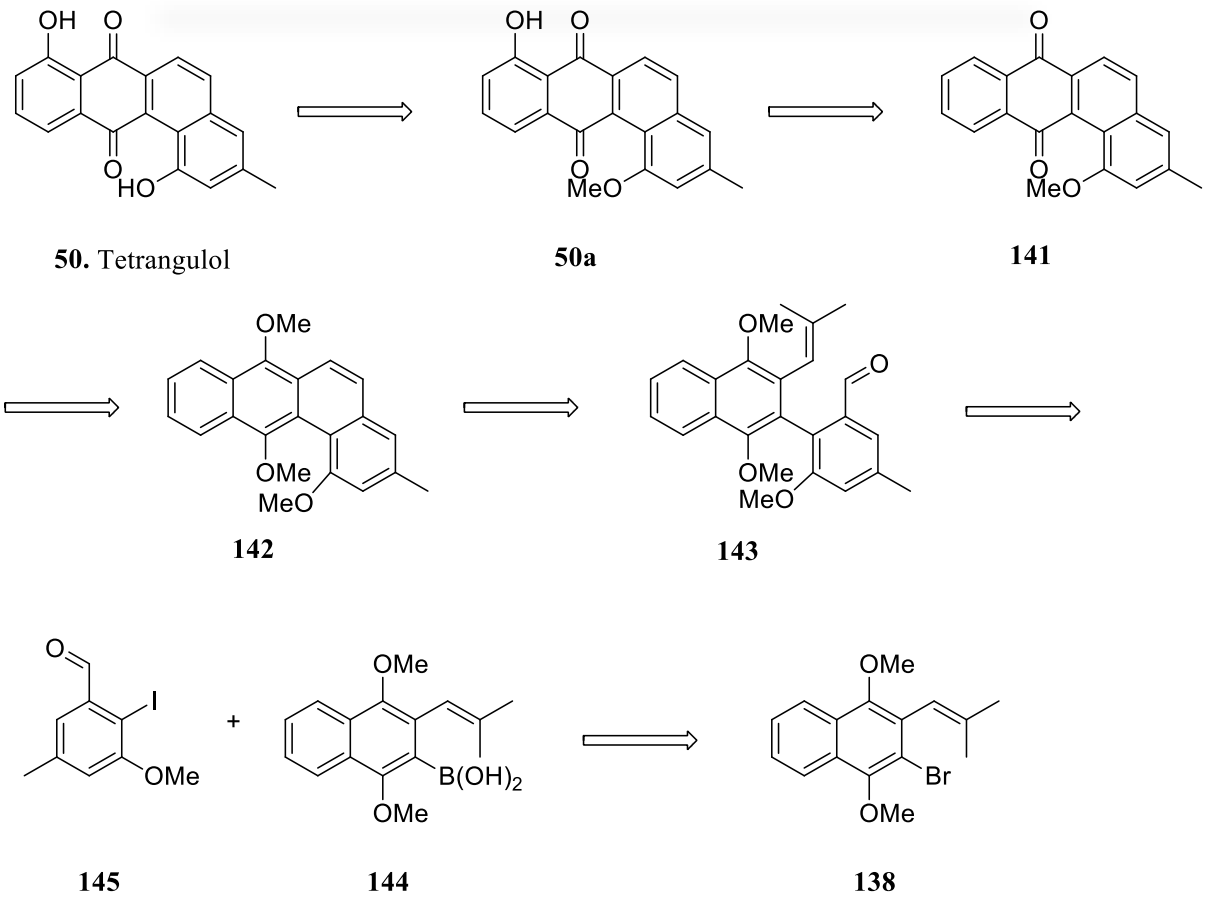

50. Tetrangulol **50a** **141**

142 **143**

145 **144** **138**

Scheme 38: Retrosynthetic plan for tetrangulol.

Benz[α]anthraquinone **141** was to be synthesized by means of a CAN-mediated oxidation of benz[α]anthracene **142**. The B ring of **142** could be constructed by $FeCl_3$-catalyzed carbonyl-olefin metathesis of carbonyl- and olefin-containing compound **143**. The classical Suzuki-Miyaura coupling between boronic acid **144**, which was to be synthesized *via* borylation of naphthalene **138**, and iodo-benzaldehyde **145** was anticipated to generate the desired biaryl compound **143**, the precursor to the key metathesis reaction.

Upon embarking on this formal synthesis, the first step was to improve the synthesis of naphthalene **138** in terms of atom economy. We had employed the Wittig reaction in our model study to synthesize naphthalene **138**; however, as mentioned earlier, this reaction is notoriously well-known for its poor atom economy.[17] An entirety of three aromatic rings and a phosphorous atom, not to mention a bromine atom, totaling a mass of 342 amu, are released as waste products. The requirement to synthesize naphthalene **138** in a more atom economical manner was therefore primary.

2.3.1 Attempts at improving the synthesis of naphthalene 138 in terms of atom economy

2.3.1.1 Use of the McMurry coupling

Initially, we planned to use the McMurry coupling reaction to couple naphthaldehyde **139** with acetone in order to generate naphthalene **138** (**Scheme 39**). The McMurry coupling reaction was reported simultaneously, and independently, by the groups of McMurry,[122] Mukaiyama,[123] and Tyrlik[124] in 1973. This coupling reaction has been used widely in the synthesis of highly strained olefins.[125] It involves the use of low-valent titanium reagents to mediate the reductive dimerization, or the cross coupling, of ketones and aldehydes. The systems used to generate the low-valent titanium species vary with the three different research groups. The Mukaiyama group utilized a $TiCl_4$/Zn system, and this is the system that we adopted for our synthesis due to easy availability of the reagents.

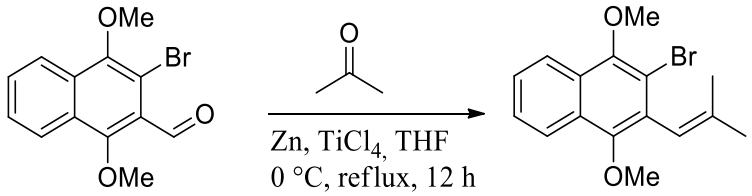

139 **138**

Scheme 39: McMurry coupling between naphthaldehyde 139 and acetone.

To perform the coupling, we first suspended zinc powder in dry THF under an inert atmosphere at 0 °C, and then $TiCl_4$ was carefully added dropwise *via* syringe. After complete addition, the solution was refluxed for 1.5 hours before a solution of naphthaldehyde **139** and acetone in dry THF was added dropwise (**Scheme 39**). The solution was then allowed to reflux for 12 hours. Disappointingly however, the reaction did not yield the desired product, even after several repeated attempts. From NMR spectral analysis, it seemed that the starting material was decomposing under the various conditions employed.

2.3.1.2 Use of Friedel-Crafts acylation: Route 1

Having frustratingly failed at the McMurry coupling of the two carbonyl moieties, we then set out to search for an alternative route, eventually calling upon the venerable Friedel-Crafts acylation. A direct acylation of 1,4-dimethoxynaphthalene would lead to an acylated naphthalene which could later be brominated, reduced and dehydrated to deliver the desired naphthalene **138**. We were however concerned that using the commonly employed, strong Lewis acids would easily allow for *O*-demethylation. Sure enough, using $AlCl_3$, $SnCl_4$ or $TiCl_4$

resulted in either demethylation, or decomposition, depending on the conditions used. It was then that our attention was drawn to a paper by Bensari and Zaveri,[126] describing a procedure for the *ortho*-acylation of phenols and naphthols, mediated by $TiCl_4$. We envisaged that, using this procedure, we could attempt to acylate 4-methoxynaphthalene-1-ol **146**, and the resulting compound could then be *O*-alkylated and, thereafter, brominated.

The first step was to synthesize 4-methoxynaphthalene-1-ol **146**, which we anticipated to achieve *via* a reduction of commercially available naphthoquinone **147** followed by mono-alkylation of the resulting hydroxynaphthalene intermediate (**Scheme 40**).

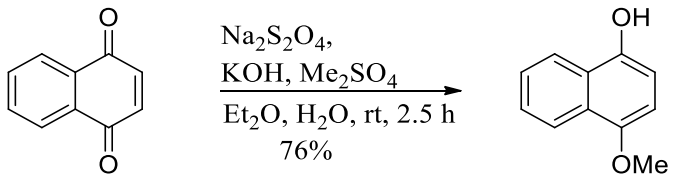

147 **146**

Scheme 40: Synthesis of naphthol 146

Sodium dithionite was used as the reducing agent, which was added to a deoxygenated solution of naphthoquinone **147** in Et_2O and water. The reaction was stirred under an inert atmosphere for an hour. The solution was then transferred to a separating funnel to run off the aqueous layer, as we found that adding the base KOH to the aqueous solution of the intermediate hydroxynaphthalene disappointingly resulted in the formation of significant amounts of the di-methoxylated naphthalene, in addition to mono-methoxylated naphthol **146**. The organic layer was then immediately transferred into the reaction flask, minimizing exposure to air, and only then, under an inert atmosphere, were KOH pellets added. The solution was stirred for 30 minutes, before the dropwise addition of dimethyl sulfate. It was also observed that using dilute conditions for this reaction eliminated the formation of di-methoxylated naphthalene.

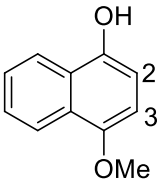

146

Purification *via* silica gel column chromatography yielded hydroxynaphthalene **146** as a white solid with a slight purple tinge in 76% yield. ^{1}H NMR spectral analysis proved unequivocally that the mono-methoxylated compound had been formed, especially by the presence of only one singlet peak at δ 4.00 ppm integrating for 3 protons, corresponding to the methoxy group protons. In addition, the presence of a broad singlet peak at δ 5.01 ppm integrating for 1 proton corresponded to the OH proton. Protons H-2 and H-3 were observed at δ 6.68 and 6.77 ppm respectively. This was complemented by the ^{13}C NMR spectrum which showed the appearance

of one methoxy carbon at δ 56.1 ppm and the corresponding aromatic carbon at δ 150.2 ppm. The peak at δ 145.4 ppm corresponded to the ArC-OH carbon, as expected. Both the ^{1}H NMR spectrum and the ^{13}C NMR spectrum compared well to that found in literature for compound **146**.[127]

With the naphthol precursor in hand, we were ready to explore the *ortho*-directed Friedel-Crafts acylation (**Scheme 41**). The acylation uses solvent free conditions, and $TiCl_4$ as a Lewis acid which simultaneously co-ordinates to the hydroxyl group and the carbonyl group of the acid chloride **148**, and this directs acylation *ortho* to the hydroxyl group.

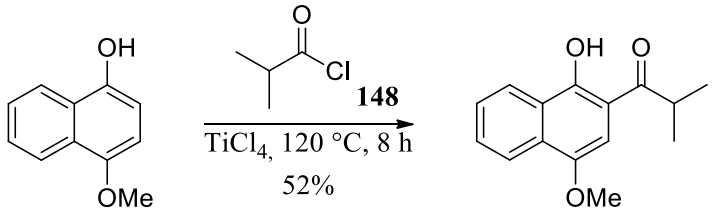

146 **149**

Scheme 41: Friedel-Crafts acylation of mono-hydroxylated naphthalene 146

The acid chloride **148** was synthesized from isobutyric acid and thionyl chloride, and was used immediately without purification. To carry out the acylation, naphthol **146** was added to a round bottom flask under inert gas. $TiCl_4$ was then carefully added dropwise. Once all the ensuing gas evolution had ceased, the acid chloride was injected into the flask at room temperature, and the resulting paste was left at 120 °C for 8 hours. Purification by silica gel column chromatography furnished acylated hydrogen-bonded naphthalene **149** as a yellow solid in an average yield of 52%. The presence of a hydrogen-bonded phenol group was established by ^{1}H NMR spectral analysis of the product which showed the presence of the deshielded signal at δ 14.09 ppm, confirming *ortho*-acylation to the phenol moiety. This was accompanied by the disappearance of an aromatic proton, and the presence of a singlet signal at δ 6.95 ppm representing proton H-3′, and proving unambiguously that mono substitution had taken place. The appearance of a septet peak at δ 3.65 ppm for proton H-2, coupling with the two methyl group protons which appear as a doublet peak at δ 1.35 ppm, ascertained the presence of the acyl group. In support of this, the ^{13}C NMR spectrum showed the appearance of a carbonyl peak at δ 210.2 ppm, as well as the occurrence of a peak at δ 35.6 ppm representing C-2, and δ 19.5 ppm representing the methyl carbons. The mass of

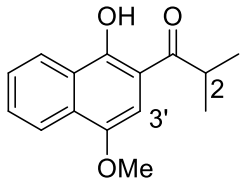

149

the compound was confirmed by HRMS, and was found to be 245.1171 corresponding to [M + H]$^+$, which agrees very well with the calculated mass of 245.1178.

Delighted that the acylation worked, and that no sign of demethylation had taken place, we then moved on to methylate the free naphthol group. This was achieved using KOH as the base and dimethyl sulfate as the alkylating agent (**Scheme 42**).

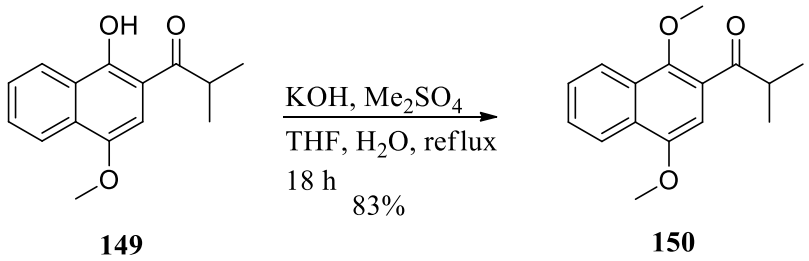

149 **150**

Scheme 42: *O*-alkylation of naphthol 149.

Purification *via* silica gel column chromatography generated **150** as a yellow oil in 83% yield. The identity of the product was clear to see from the ^{1}H NMR spectrum which now displayed two peaks at δ 3.99 and 3.90 ppm, corresponding to two methoxy group protons. This was also accompanied by the disappearance of the deshielded peak at δ 14.09 ppm as expected. This was complemented by the ^{13}C NMR spectrum which showed the appearance of two peaks in the alkoxy region at δ 64.1 and 55.7 ppm representing the two methoxy group carbons.

In the meantime, and alongside this synthesis, we were also investigating direct acylation. Intuitively, we felt that the direct Friedel-Crafts acylation of 1,4-dimethoxynaphthalene deserved a second chance. This seemingly easy task, however, proved not to be so trivial.

2.3.1.3 Friedel-Crafts acylation: Route 2

Initially, before attempting the Friedel-Crafts acylation of 1,4-dimethoxynaphthalene, we endeavored to perform the acylation of bromo-naphthalene **151**, as we anticipated that this would be much easier than having to brominate the acylated compound. To this end, bromo-naphthalene **151** was synthesized from 2-bromo-1,4-naphthoquinone **131** using sodium dithionite as reductant, KOH as the base, and dimethyl sulfate as the alkylating agent (**Scheme 43**).

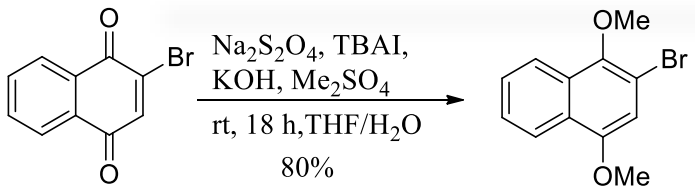

131 **151**

Scheme 43: Synthesis of 2-bromo-1,4-dimethoxynaphthalene 145

The characteristic methoxy group protons were easily observed in the ^{1}H NMR spectrum at δ 3.97 and 3.95 ppm. This also corresponded to the appearance of two peaks in the alkoxy region of the ^{13}C NMR spectrum at δ 61.4 and 55.9 ppm, which was accompanied by the disappearance of the quinone carbon peaks.

Unfortunately, however, we were unable to acylate bromo-naphthalene **151**, even after several attempts. Using conventional Lewis acids ($AlCl_3$, $TiCl_4$, $SnCl_4$) resulted in either decomposition or demethylation, whereas using milder conditions with trifluoroacetic anhydride led to the recovery of starting material.

In the meantime, a second foray into the direct acylation of 1,4-dimethoxynaphthalene **152** was being explored. 1,4-dimethoxynaphthalene **152** was synthesized from naphthoquinone **147** in quantitative yields following the same reduction and alkylation procedure as described for naphthoquinone **131** (**Scheme 44**). The presence of a singlet peak integrating for 6 protons at δ 3.90 ppm, as well as the appearance of a peak at δ 55.7 ppm established unequivocally that the formation of 1,4-dimethoxynaphthalene **152** was a success. Thereafter, using the milder reaction conditions described by de Koning,[128] commercially available acid **153** was treated with TFAA to form an anhydride which we envisioned would react with naphthalene **152** dissolved in CH_2Cl_2. This, unfortunately, only led to recovered starting material, even after leaving the reaction to stir for 5 days. Heating the reaction gave the same result.

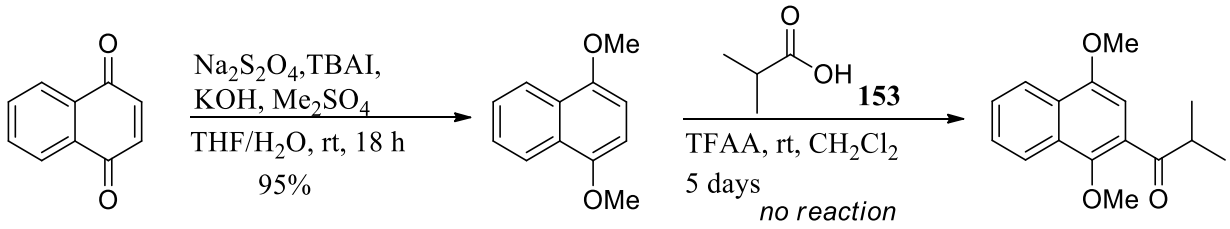

147 **152** **150**

Scheme 44: Friedel-Crafts acylation of 1,4-dimethoxynaphthalene 152.

Disappointed, yet not willing to give up, we decided to soldier on, eventually coming across a recently published paper by Liu and Xu[129] describing the use of TFAA and hydrogen-bonding TFA in the metal and halogen-free Friedel-Crafts acylation of aromatic compounds.

Following their procedure, isobutyric acid **153** was dissolved in TFAA to form the corresponding anhydride at room temperature for 15 minutes. Thereafter 1,4-dimethoxynaphthalene **152** was added, followed by TFA and the reaction was stirred at 70 °C for 24 hours (**Scheme 45**). To our delight the reaction resulted in the formation of acylated naphthalene **150**, albeit in a poor yield of 23% yield. Despite this being a very low yield, we were nevertheless excited. Analysis of the ^{1}H NMR spectrum proved undoubtedly that acylation had taken place by the presence of the septet peak at δ 3.71 ppm representing the α-proton H-2, as well as the doublet at δ 1.22 ppm integrating for 6 protons, corresponding to the two methyl group protons. Furthermore, the aromatic singlet peak at δ 6.85 ppm representing the aromatic proton H-3′ was indicative of mono-acylation. Complementing this, the presence of a carbonyl peak at δ 208.6 ppm was observed in the ^{13}C NMR spectrum. Also present were peaks at δ 39.9 and 18.8 ppm corresponding to the C-2 carbon and methyl group carbons respectively.

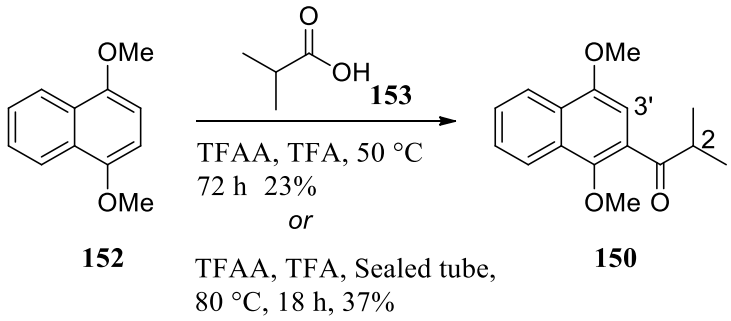

Scheme 45: Friedel-Crafts acylation using TFAA and TFA.

In an attempt to improve the yield, the decision was taken to carry out the reaction in a sealed pressure tube. The same procedure was followed as before, and the sealed tube was sealed with a Teflon lined cap and stirred at 80 °C for 18 hours. Purification by column chromatography furnished acylated naphthalene **150** in a slightly improved yield of 37% (**Scheme 45**).

Armed with a renewed enthusiasm, we reasoned that since the stronger Lewis acid, triflic acid is also a strong hydrogen-bond donor, replacing TFA with triflic acid might improve the acylation yields. Following the same procedure but replacing TFA with triflic acid, the reaction was stirred in a round bottom flask at room temperature until all starting material had been consumed (**Scheme 46**). Purification led to the isolation of acylated naphthalene **150** in a significantly improved yield of 66%.

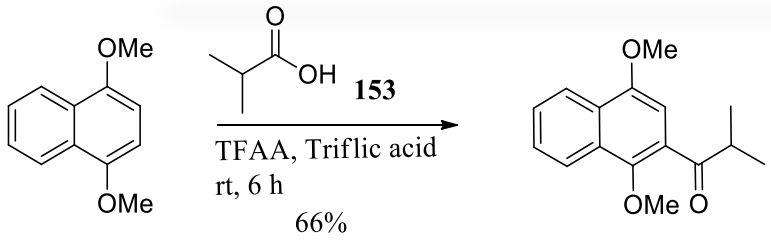

152 **150**

Scheme 46: Friedel-Crafts acylation using TFAA and Triflic acid.

Whilst very pleased with this result, we were not fully satisfied due to the high cost of triflic acid, as well as its highly fuming nature which makes it an unpleasant acid to work with. We therefore chose to see how the reaction would proceed if we replaced triflic acid with the much milder, cheaper, and environmentally friendly, methanesulfonic acid. Gratifyingly, purification of the reaction mixture led to the isolation of acylated naphthalene **150** in an even better yield of 84% (**Scheme 47**).

This Friedel-Crafts acylation condition can be termed 'green' as it is completely halogen and metal free, and uses the environmentally-acceptable methanesulfonic acid as solvent. It will of course be interesting, in the future, to investigate these reaction conditions on other aromatic scaffolds.

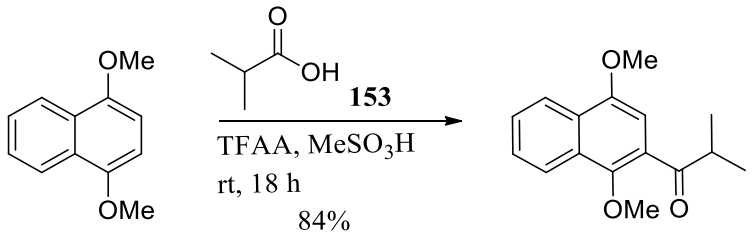

152 **150**

Scheme 47: Friedel-Crafts acylation using TFAA and methanesulfonic acid.

Route 2 therefore results in the formation of acylated compound **150** in 2 steps starting from naphthoquinone **147**, whereas *Route 1* requires three steps with a lower overall yield. Accordingly, we opted to use the sequence in *Route 2* for our formal synthesis.

2.3.1.4 Bromination

Having secured the acylated intermediate **150**, the subsequent step was to perform a nuclear bromination. For this we initially used NBS as the brominating agent in CH_2Cl_2. After heating at reflux for 2 hours, the reaction was pronounced complete (from TLC analysis), and purification by chromatography showed that instead of nuclear bromine insertion, bromination

had taken place at the α-position of the carbonyl group, forming brominated compound **154** in a yield of 79%. This was clearly seen in the ^{1}H NMR spectrum by the disappearance of the septet peak at δ 3.65 ppm, whereas the aromatic singlet peak at δ 6.96 ppm was still present. This was also complemented by the shift of the α-carbon from δ 39.9 to 55.8 ppm in the ^{13}C NMR spectrum. To further confirm that the bromine atom was present, the mass of the compound was determined by HRMS, and was found to be 337.0402 corresponding to $[M + H]^+$, which is in reasonable agreement with the expected mass of 337.0439. Looking back at this, it made sense that bromination was taking place at the α-carbon as the α-proton is acidic and therefore easily attacked by the bromine radical from NBS.

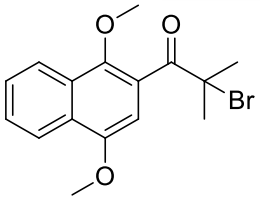

154

Deciding then to use molecular bromine instead of NBS, a solution of molecular bromine in CH_2Cl_2 was added dropwise to a solution of acylated naphthalene **150** in CH_2Cl_2 at room temperature, and then heated at reflux for 2 hours, after which another equivalent of bromine in acetic acid was added and further refluxed for 3 hours. Upon completion, the reaction was quenched and purified using silica gel column chromatography, this time yielding brominated compound **155** as a yellow solid in 70% yield (**Scheme 48**). It was observed that performing the reaction in the absence of acetic acid gave **154** as the major product, accompanied by small amounts of dibromonaphthalene **155**. It is therefore possible that the substrate is prone to enolization, especially under acidic conditions. Thus, in the presence of AcOH, α-bromination proceeds quicker, and thereafter the desired nuclear bromination takes place. In the absence of AcOH, α-bromination proceeds much slower, hindering nuclear bromination. NMR spectral analysis of the product confirmed that dibromination had taken place, by the disappearance of the septet peak at δ 3.65 ppm, as well as the absence of the aromatic singlet peak at δ 6.99 ppm. This was also corresponded to by the shift in the peak at δ 102.2 to 107.7 ppm representing the ArC-Br carbon, and the shift of the α-carbon peak from δ 39.9 to 63.6 ppm. To further confirm that dibromination had indeed taken place, an HRMS was run on the sample **155**, and a mass of 414.9514 was found corresponding to $[M + H]^+$ of the compound containing the ^{79}Br isotope, which agrees reasonably well with the calculated mass of 414.9544.

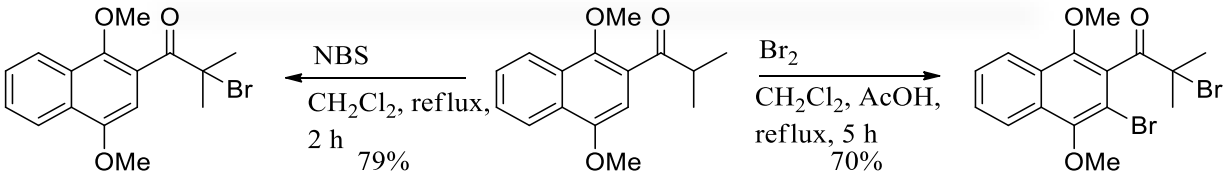

154 **150** **155**

Scheme 48: Bromination reactions of naphthalene 150.

Eventually coming to the unfortunate realization that it would not be possible to brominate the nuclear position without first brominating the α-carbon, it was inevitable that we would have to think of an alternative plan. Nevertheless, we did initially attempt to utilize 2 equivalents of $LiAlH_4$ to reduce the carbonyl group to an alcohol as well as lithiate the α-bromine, thus eliminating it. However, this resulted in a very messy reaction, with selectivity, in terms of lithiating the α-bromine *vs* nuclear bromine, being a major problem.

Alas, getting back to the drawing board, we revisited our retrosynthetic plan. To circumvent the inevitable α-bromination, it was decided to reduce the carbonyl group on **150**. This would lead to an alcohol, thus providing an opportunity to perform *ortho* directed lithium halogen exchange, ensuring nuclear halogenation at the desired position. The refined plan is detailed in **Scheme 49**. Thus we envisioned generating an iodinated-isobutenyl-substituted naphthalene **156** and this would serve instead as the perfect precursor to our desired boronic acid **144**. Naphthalene **156** could be formed *via* dehydration of iodo-alcohol **157**. It was anticipated that a simple reduction of the acylated compound **150** would generate alcohol **158**, which could be subjected to directed *ortho*-metalation conditions leading to iodo-alcohol **157**.

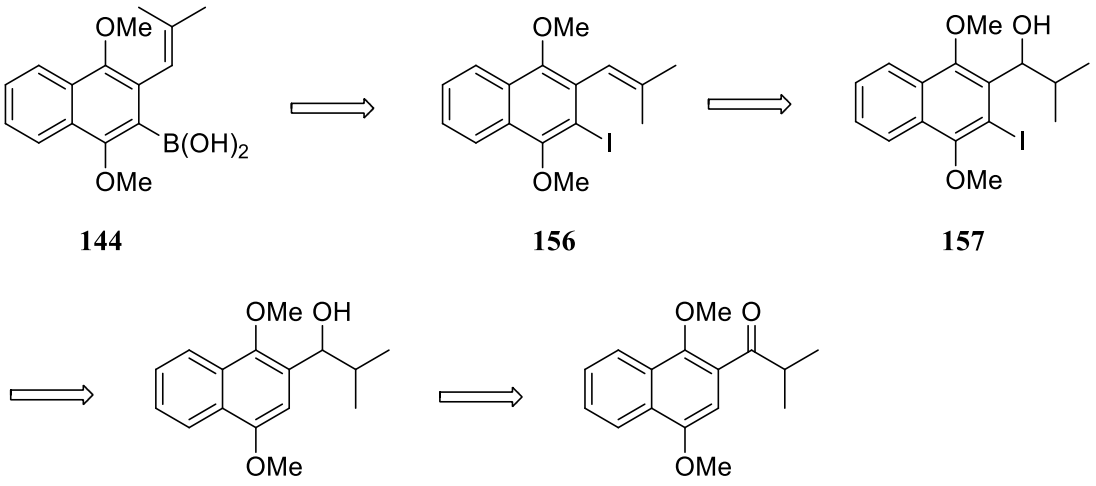

144 **156** **157**

158 **150**

Scheme 49: An alternative retrosynthetic plan for the synthesis of boronic acid 144.

2.3.2 Synthesis of iodinated-isobutenyl-substituted naphthalene 156

The reduction of acylated naphthalene **150** proceeded smoothly in the presence of $NaBH_4$ at 0 °C using a solvent system of THF and MeOH (**Scheme 50**). Purification by column chromatography furnished alcohol **158** in quantitative yields as a yellow low melting solid. NMR spectral analysis proved unequivocally that the reduction was successful by the presence, in the ^{1}H NMR spectrum, of a doublet peak at δ 4.83 ppm which integrated for one proton, corresponding to H-1 which couples to proton H-2. The OH signal appears as a broad singlet at δ 2.71 ppm, whereas proton H-2 appears as a multiplet in the region of δ 2.12 – 1.98 ppm. This was accompanied by the disappearance of the carbonyl peak at δ 208.6 ppm in the ^{13}C NMR spectrum as well as by the appearance of a peak at δ 74.1 ppm which corresponds to slightly deshielded carbon C-1.

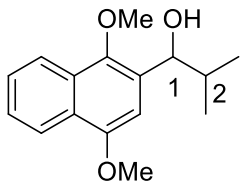

158

Thereafter, alcohol **158** was iodinated under directed *ortho*-metalation conditions (**Scheme 50**). This was achieved using *n*-BuLi, with the hydroxyl and methoxy functionalities as directing groups. Alcohol **158** was dissolved in dry Et_2O and at –78 °C *n*-BuLi was added to the solution *via* syringe. The reaction was allowed to warm to room temperature and stirred for four hours before being cooled to 0 °C and stirred further for an hour. Thereafter a solution of iodine in dry THF was added dropwise *via* dropping funnel at 0 °C. After complete addition, the solution was allowed to warm to room temperature, and stirred for 18 hours. Purification *via* silica gel column chromatography led to the isolation of iodinated alcohol **157** in a yield of 45%, and a calculated yield of 77% based on recovered starting material. The disappearance of the singlet peak at δ 6.85 ppm in the ^{1}H NMR spectrum indicated that iodination had taken place at the desired position. In support of this, the shift of a peak, in the ^{13}C NMR spectrum, to δ 93.7 ppm clearly indicated the presence of a C-I bond. Additionally, the peaks at δ 4.96 and 2.40 ppm confirmed that protons H-1 and H-2 (refer to **158**), respectively, were still intact, as was the OH signal at δ 3.49 ppm. An HRMS of the compound was run to confirm the mass, and a mass of 369.0330 was found corresponding to $[M - H_2O + H]^+$, being in accord with the expected mass of 369.0352 of the iodinated compound.

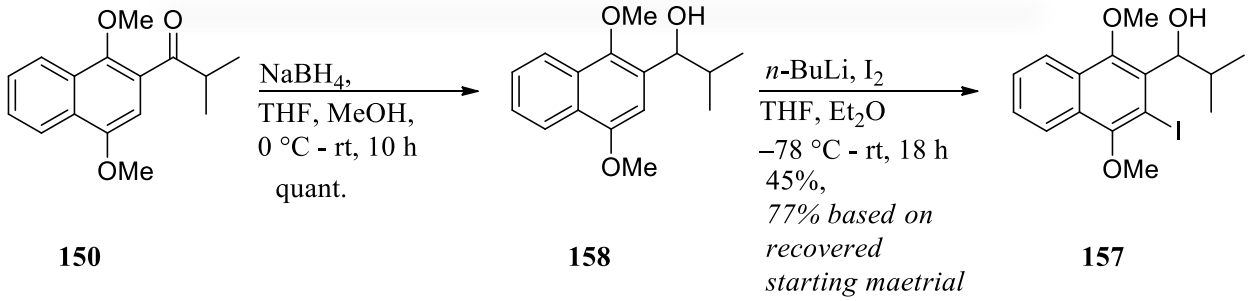

150 **158** **157**

Scheme 50: Synthesis of iodinated-alcohol 157.

Even though the reaction was clean, producing only iodinated-alcohol **157**, significant amounts of starting material were recovered. All our attempts at achieving complete conversion, however, were unsuccessful. Performing the reaction using only THF as the solvent led to the complete isolation of starting material, whereas using only Et_2O as the solvent gave the same yields as when using a mixture of Et_2O and THF. Since Et_2O is considered a highly hazardous solvent,[130-131] it was more practical to rather use a mixture of Et_2O and THF.

Furthermore, it was observed during one of our many efforts at attaining complete conversion, that adding TMEDA as an additive to the reaction led to the formation of an unknown side product that was formed in 36% yield, whereas iodinated-alcohol **157** was isolated in a yield of only 10%. ^{1}H NMR spectral analysis of the side-product showed the presence of two methoxy group protons at δ 3.91 and 3.78 ppm, as well as two methyl group protons at δ 1.23 and 0.83 ppm. Also present were the OH peak at δ 3.41 ppm, and the methine protons at δ 4.98 and 2.49-2.42 ppm, indicating that the alcohol substituent of the naphthalene was still intact. Upon examination of the aromatic region, it was observed that only three aromatic protons were present, which pointed towards a di-iodo-substituted compound **159**. It seemed that one iodine had substituted in the same position as with compound **157** whereas the position of the second iodine was confirmed by 2D NMR spectral analysis. The methoxy ArC-OMe carbon C-1′ was identified based on its correlation with methine proton at δ 4.98 ppm. Based on the HMBC, only one aromatic proton at δ 8.11 ppm was interacting with the second ArC-OMe carbon C-4′ at δ 152.9 ppm, whereas no aromatic proton was interacting with carbon C-1′, thus confirming that substitution had taken place at carbon C-8′. To ensure that di-iodination had indeed taken place, an HRMS of the sample was run, and a mass of 494.9390 was found, corresponding to $[M - H_2O + H]^+$, which was in concurrence with the calculated mass of 494.9318.

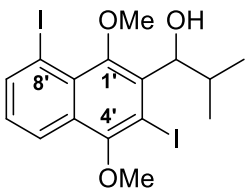

159

At this point, it had dawned on us that we would not be able to achieve complete conversion. One positive aspect, however, was the starting material that was recovered could be recycled, and in essence no starting material was wasted. The decision was undertaken, therefore, to continue with the synthesis. Consequently, a solution of iodinated-alcohol **157** in toluene was dehydrated in the presence of catalytic amounts of *p*-toluenesulfonic acid, under reflux using a Dean-Stark apparatus (**Scheme 51**).

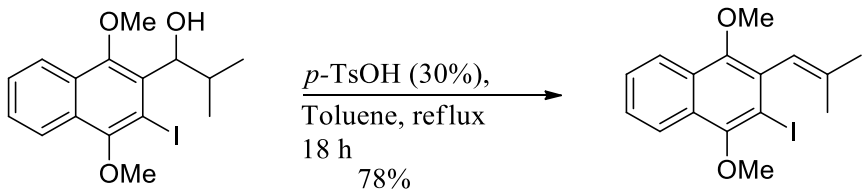

157 **156**

Scheme 51: Dehydration of iodinated-alcohol 157.

Purification by column chromatography led to the isolation of 1-isobutenyl-substituted naphthalene **156** as a yellow oil, in a decent yield of 78%. Analysis of the ^{1}H NMR spectrum proved undoubtedly that dehydration had taken place by the noticeable disappearance of the peaks for protons H-1 and H-2 (refer to **158**) at δ 4.96 ppm and δ 2.40 ppm. The signal for the OH proton had also disappeared, with the only peaks present in the alkyl region being for the two methyl group protons at δ 1.89 and 1.44 ppm, and the two peaks in the alkoxy region at δ 3.82 and 3.63 ppm being for the two methoxy protons. The appearance of a singlet peak at δ 6.03 ppm clearly represents the alkene proton, and this was accompanied by the expected number of four aromatic protons. Complementing this was the disappearance of the peaks at δ 83.3 and 34.9 ppm representing C-OH and C-2 (refer to **158**), as well as the appearance of two extra peaks in the aromatic region representing the alkene carbons.

2.3.3 Synthesis of iodo-benzaldehyde 145

In the meantime, iodo-benzaldehyde **145**, the requisite building block for biaryl intermediate **143**, had also to be constructed. Initially, to do this, we adopted the same strategy that Ngwira *et al.* implemented.[111] The synthesis began with 3,5-dimethylanisole **160** (**Scheme 52**) which was expediently converted into a dibrominated intermediate, in the presence of toxic CCl_4, with NBS as the brominating agent, and BPO as the radical initiator.

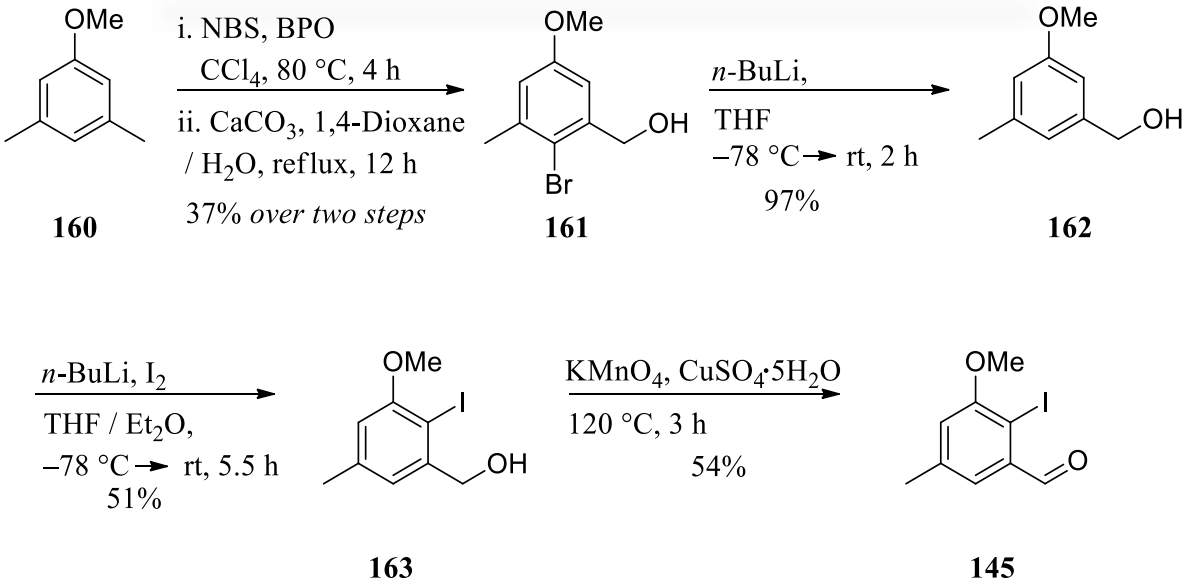

160 **161** **162** **163** **145**

Scheme 52: Synthesis of iodo-benzaldehyde 145.

As was reported by Ngwira *et al.* exclusive benzylic bromination of 3,5-dimethylanisole was not possible without first brominating the nuclear position.

The crude product was used in the next step without further purification, and was treated with $CaCO_3$ in aqueous 1,4-dioxane to generate alcohol **161** in an overall yield of 37% over two steps. ^{1}H NMR spectral analysis was used to confirm the structure of alcohol **161**, and particularly distinct was the peak at δ 4.71 ppm which was representative of benzylic proton H-1. The signal for methoxy protons appeared at δ 3.79 ppm, whereas the methyl protons appeared at δ 2.39 ppm. The presence of two aromatic protons at δ 6.90 and 6.74 ppm were observed, representing protons H-6′ and H-4′ respectively. The assignment of these protons were based on the HMBC correlation of C-4′ at δ 139.3 ppm with methyl protons and C-6′ at δ 140.9 ppm with benzylic proton H-1. The presence of the benzylic carbon C-1 was also established by the ^{13}C NMR spectrum which showed the appearance of a signal in the slightly deshielded region of δ 65.6 ppm.

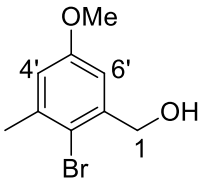

161

Having synthesized the alcohol, which would later be oxidized to an aldehyde, the subsequent step involved the elimination of bromine. To achieve this, brominated-alcohol **161** was treated with *n*-BuLi in dry THF. Purification led to the isolation of alcohol **162** in 97% yield. Thereafter, using the methoxy and alcohol functionalities as *ortho* directing groups, a solution of alcohol **162** in Et_2O was treated with *n*-BuLi, followed by a solution of iodine in THF. Purification by column chromatography led to the isolation of iodinated alcohol **163** in an average

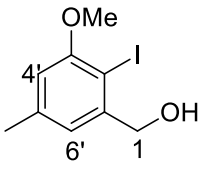

163

yield of 51%. The presence of iodine was confirmed by the appearance of a C-I peak in the ^{13}C NMR spectrum at δ 85.4 ppm. As expected, signals for two aromatic protons were observed at δ 6.92 and 6.59 ppm. Ensuring that the iodine had indeed gone *ortho* to the methoxy and alcohol groups, an analysis of the HMBC showed a correlation of the carbon at δ 121.9 ppm representing C-6′ with benzylic proton H-1 at δ 4.67 ppm as well as the methyl protons at δ 2.35 ppm; whereas the carbon at δ 111.2 ppm representing C-4′ only showed a correlation with methyl protons.

To access the desired benzaldehyde intermediate **145**, iodinated alcohol **163** was subjected to oxidizing conditions. We were able to improve on the previous oxidation of this molecule by making use of a solvent free method that uses $KMnO_4$ and $CuSO_4 \cdot 5H_2O$ as oxidants. The oxidants and alcohol **163** were ground together to a fine powder. The entire homogenous mixture was then heated to 120 °C for 3 hours, after which purification eventually led to the isolation of iodo-benzaldehyde **145** in an average yield of 54%**.** The diagnostic aldehyde peak at δ 10.14 ppm in the ^{1}H NMR spectrum confirmed that oxidation had taken place. This of course correlated well with the carbonyl peak at δ 196.4 ppm that was observed in the ^{13}C NMR spectrum. Both ^{1}H and ^{13}C NMR spectra compared well with that found in literature for compound **145**.[111]

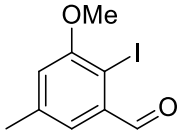

145

Although pleased with this slight improvement in the previous synthesis, the use of CCl_4 was still problematic. Furthermore, the formation a di-brominated compound was highly atom uneconomical, and that had to be remedied. To circumvent these problems, we rationalized that an alternative approach would be to selectively oxidize one of the methyl groups of 3,5-dimethylanisole **160** to an aldehyde, and thereafter attempt a direct iodination. The oxidation, however, occupied us for several months, as various conditions were tried (**Scheme 53**), each being met with failure, despite literature reports of success on simpler model systems.[132-135]

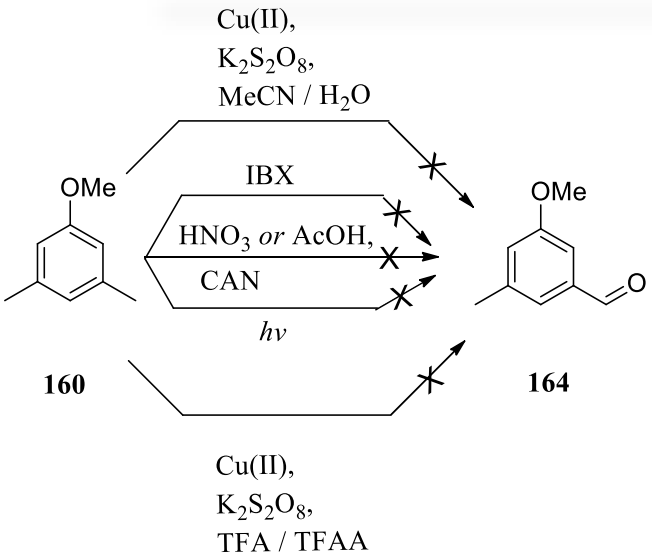

Scheme 53: Unsuccessful attempts at oxidizing 3,5-dimethylanisole.

It was only later during the year, that we were alerted to a paper by Ishii *et al.* reporting the use of NHPI (*N*-hydroxyphthalimide) and Co(II) catalysts in the radical-induced oxidation of benzylic side chains.[136-137] They reported the successful conversion of terminal methyl groups to carboxylic acids under ambient conditions, in the presence of dioxygen (air). The reaction proceeds principally by means of a PINO (phthalimide-*N*-oxyl) radical induced abstraction of a proton from the terminal side chain carbon to form a radical that is then trapped by dioxygen, eventually forming a carboxylic acid/ ketone or alcohol. The key PINO radical is generated from a Co(III)-oxygen complex under ambient conditions.[136-137] Excited about this, we anticipated that if we managed to oxidize the methyl group to a carboxylic acid, it could thereafter be reduced to an aldehyde. Following their reaction protocol however, led disappointingly only to recovery of starting material. Determined not to give up yet, the conditions were experimented with, until we were eventually successful. 3,5-Dimethylanisole **160**, NHPI, $Co(OAc)_2 \cdot 4H_2O$, $K_2S_2O_8$, and acetic acid were placed in a sealed pressure tube and the solution was bubbled with oxygen gas for 15 minutes before being sealed and heated to 105 °C. The reaction was left to stir for 3 days, and oxygen was bubbled through every 10 hours. Much to our delight, purification *via* column chromatography resulted in the isolation of aldehyde **164**. This came as a rather pleasant surprise, as we were expecting to isolate the corresponding carboxylic acid. Although the yield was poor (20%), a significant amount of starting material was recovered, which could then be recycled, rendering the overall yield 56% based on recovered starting material. The distinct aldehyde signal at δ 9.93 ppm in the ^{1}H NMR spectrum was clearly observed, that also corresponded to the carbonyl peak at δ 192.3 ppm in

the ^{13}C NMR spectrum. Signals for three aromatic protons were observed as expected, and these were accompanied by the peak at δ 3.85 ppm representing the methoxy protons, and a signal for one set of methyl protons at δ 2.40 ppm.

Although we were unsuccessful in our attempts at iodinating aldehyde **164**, the reduction of **164** to alcohol **162** proceeded smoothly in the presence of $NaBH_4$ using a solvent system of THF / MeOH (**Scheme 54**). Alcohol **162** was then iodinated to **163**, followed by oxidation to **145** using the same procedures as described before.

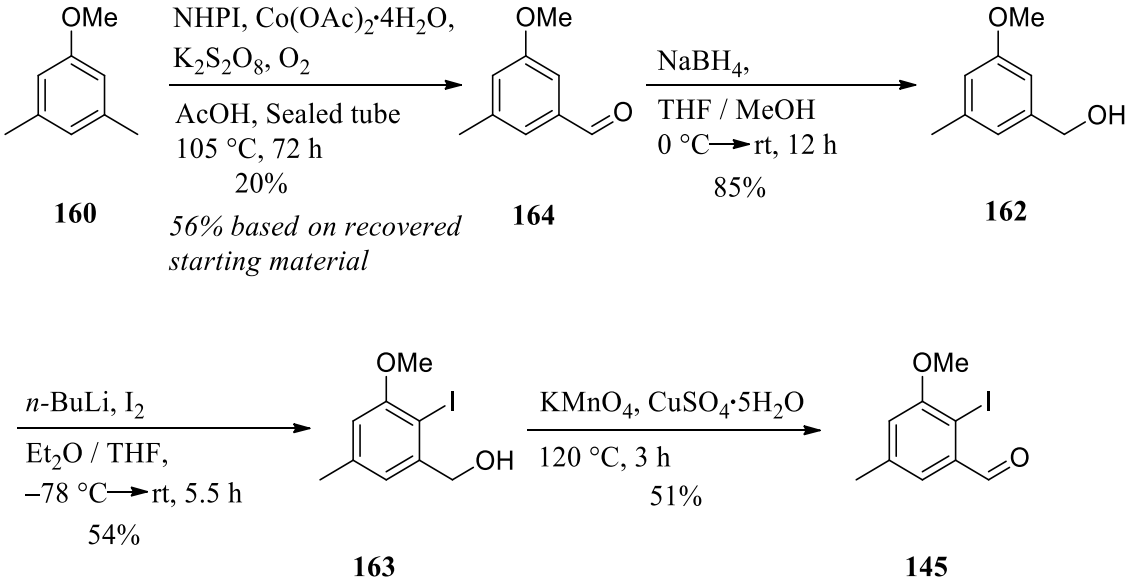

Scheme 54: Second approach to synthesis of benzaldehyde 145

2.3.4 Borylation

With the requisite iodinated building block in hand, we were now ready to construct the boronic acid **144** which would serve as the organoborane for the subsequent Suzuki-Miyaura coupling reaction. We rationalized choosing to convert iodinated naphthalene **156**, rather than iodinated benzaldehyde **145**, to the organoborane coupling partner, since the overall yield of **156** is much higher than the overall yield of **145**.

To perform the operation, naphthalene **156** was dissolved in dry THF. This was cooled to –78 °C, after which a solution of *n*-BuLi was added dropwise *via* syringe. The solution was maintained at –78 °C for 30 minutes before freshly distilled tri-isopropyl borate was added, maintaining an inert atmosphere. The solution was stirred for a further 30 minutes, at –78 °C, before being allowed to warm to room temperature. The reaction was thereafter

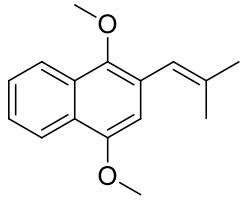

165

subjected to an acidic work-up. To our dismay, the reaction was unsuccessful, even after several attempts, and would lead instead to the sole formation of de-iodinated compound **165**. The same result was observed, even after employing freshly distilled tri-methyl borate as the borylating agent. It seemed from this result that lithiation by *n*-BuLi was taking place; however, borylation was failing to occur, conceivably due to steric hindrance.

Another approach to the organoborane-coupling partner was to synthesize a boronic ester instead of a boronic acid. Boronic esters are generally more stable than their boronic acid counterparts, and are therefore much easier to purify and characterize. We also came to the realization that we would have greater flexibility in terms of changing conditions (catalyst, temperature, solvent) to allow the formation of boronic ester to proceed with success, compared to the formation of a boronic acid. Eager to try the reaction, we initially resolved to follow the traditional Miyaura borylation conditions developed by Miyaura and co-workers in 1995,[138] to construct a pinacol boronic ester from substituted naphthalene **156**. Naphthalene **156** was added to a three-necked round bottom flask flushed with inert gas. To this flask was also added bis(pinacolato)diboron as the borylating agent, KOAc that was oven dried for 24 hours, and $PdCl_2$(dppf) as the catalyst. DMSO that was de-oxygenated by bubbling through with nitrogen gas, was then added to the flask and the reaction was stirred at 80 °C for 18 hours. Much to our pleasure, purification furnished boronic ester **166** as a yellow oil in an average yield of 50%. De-iodinated naphthalene **165** was also formed as a side product in 30% yield.

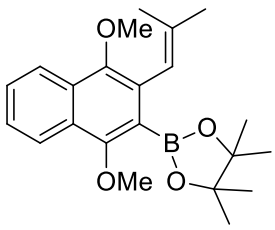

166

^{1}H NMR spectral analysis clearly established the presence of a pinacol ester by the presence of a singlet peak integrating for 12 protons at δ 1.38 ppm. A total of four aromatic protons were observed as expected, and the singlet peak at δ 6.39 ppm confirmed that the alkene moiety was still intact. The ^{13}C NMR spectrum also corresponded to this by the appearance of a signal at δ 20.0 ppm corresponding to the pinacol methyl group carbons, in addition to the two peaks at δ 25.5 and 24.8 ppm corresponding to the methyl carbons of the isoprenyl substituent. The mass of the compound was confirmed using HRMS. A mass of 369.2241 was observed corresponding to $[M + H]^+$, comparing agreeably to the expected mass of 369.2237.

We next set about trying to optimize the conditions to see if the yield of the pinacol ester could be improved. Some of the most notable of these conditions are tabulated below (**Table 2**).

Entry number	Borylating agent	Catalyst (mol%)	Base	Solvent	Temperature (° C)	Yield 166	Yield 165
1	B_2Pin_2	$PdCl_2(dppf)$ (3.0)	KOAc	DMSO	80	50	30
2	B_2Pin_2	$PdCl_2(dppf)$ (10.0)	KOAc	DMSO	80	41	45
3	B_2Pin_2	$PdCl_2(dppf)$ (5.0)	KOAc	DMSO	80	50	25
4	B_2Pin_2	$Pd(PPh_3)_4$ (10.0)	KOAc	DMF	80	30	_
5	B_2Pin_2	$Pd(PPh_3)_4$ (10.0)	KOAc	DMSO	90	65	22
6	HBPin	$PdCl_2(dppf)$ (3.0)	Et_3N	Dioxane	80	n.r	n.r
7	HBPin	$PdCl_2(dppf)$ (3.0)	Et_3N	Toluene	80	45	43

Table 2: Optimization of Miyaura borylation; n.r = no reaction, Yield **166 =** isolated yield of desired boronic ester; Yield **165** = isolated yield of de-iodinated naphthalene; B_2Pin_2 = Bis(pinacolato)diboron; HBPin = pinacolborane.

The best yield of 65% was attained when $Pd(PPh_3)_4$ was used as the catalyst, and DMSO as the solvent (**Table 2, entry 5**). These are the conditions that were employed henceforth for the synthesis of boronic ester **166** (**Scheme 55**).

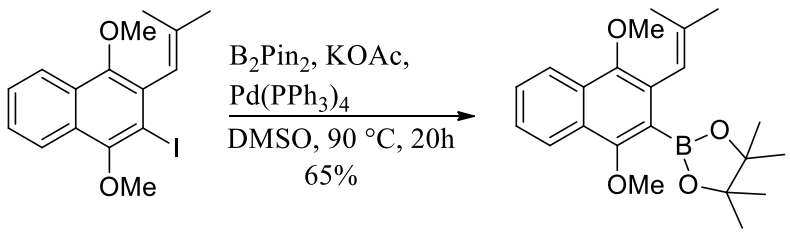

156 **166**

Scheme 55: Optimized conditions for the Miyaura borylation of naphthalene 156.

As can be noted from the last two entries in the table, our attempts at using HBPin as a more atom economical alternative borylating agent to B_2Pin_2, were not as fruitful as hoped. Nevertheless, pleased with our results so far, we moved on to the subsequent and perhaps most important step.

2.3.5 Suzuki-Miyaura coupling

With the two fragments of the molecule in place, it was now time to elaborate the boronic ester **166** into the complex biaryl-compound **143**, by means of a Suzuki-Miyaura coupling reaction with iodo-benzaldehyde **145**. Noting the extremely sterically hindered nature of the biaryl-compound, we knew from the onset that this would not be a trivial task to accomplish..

This phase of our formal synthesis could be considered one of the most crucial, as failure to couple the two fragments **166** and **145** was to result in an obstacle that would not be easily circumvented. We were certain that using the conventional Suzuki-Miyaura procedure normally followed in our laboratory (refer to **Scheme 36**), would result in very low yields, if at all, of biaryl-compound **143** due to competitive deboronation, as reported by Suzuki and coworkers for sterically hindered substrates.[107] Rather, we chose to follow Suzuki's protocol for sterically hindered, functionalized biaryl compounds.[107] Benzaldehyde **145** was added to a three necked round bottom flask flushed with inert gas. To this flask was also added K_3PO_4 as the base and $Pd(PPh_3)_4$ as the catalyst. Boronic ester **166** was dissolved in DMF and de-oxygenated using nitrogen gas for 10 minutes before being added to the flask. The reaction was heated to 100 °C and stirred for 18 hours. To our delight, purification *via* silica gel column chromatography delivered the desired biaryl compound **143** as a yellow, very sticky oil, in a yield of 32%. Although the yield was poor, we were relieved that some coupling had taken place.

Unfortunately, this feeling of relief was short-lived, as we were later unable to reproduce the reaction, even after several attempts. The only difference in the conditions between the first attempt and the following trials, was the batch of the catalyst, $Pd(PPh_3)_4$ that was being employed. A new, fresh batch was made after the first trial, and this is what was used for subsequent trials. It is therefore conceivable that an impurity in the old batch is what promoted the reaction to occur. After having failed at all subsequent attempts, we resolved to change the conditions. Experimenting with a number of catalysts, changing the solvents and bases, were all met with frustrating failure, until, eventually we resorted to using $Pd_2(dba)_3$ as catalyst in combination with tri-*o*-tolyl phosphine as ligand. Deciding to keep K_3PO_4 as the base and DMF

as the solvent, the reaction was performed in the same manner as before, at 100 °C for 18 hours. Gratifyingly, biaryl-compound **143** was isolated in a significantly improved, reproducible yield of between 61 and 64% (**Scheme 56**). The only downside of this reaction was the long and arduous purification required to separate dibenzylideneacetone which was released as a side product that eluted together with the desired product.

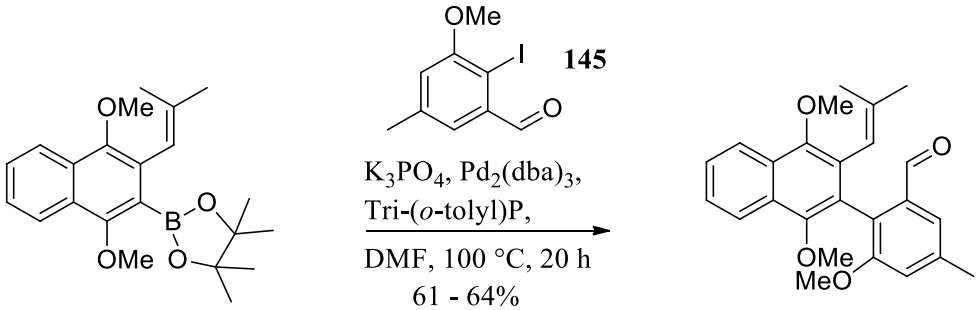

166 **143**

Scheme 56: Suzuki-Miyaura coupling of boronic ester 166 with iodo-anisole 145.

Confirmation of the successful union of the two fragments was provided by analysis of the NMR spectra. The diagnostic aldehyde signal in the ^{1}H NMR spectrum was observed at δ 9.64 ppm. Protons H-6 and H-4 were represented by the singlet peaks at δ 7.47 and 7.01 ppm respectively, based on 2D NMR analysis. They were accompanied by signals between δ 8.24 and 7.49 ppm integrating for four protons, representing the naphthalene aromatic protons, whereas proton H-1″ appeared at δ 5.74 ppm as a singlet peak. Also present were the signals for three methoxy group protons at δ 3.79, 3.73, and 3.47 ppm as expected, and methyl group protons at δ 2.48, 1.66, and 1.44 ppm. Complementing this was the ^{13}C NMR spectrum from which was observed a carbonyl peak at δ 192.8 ppm establishing the presence of the aldehyde, as well as three ArC-OMe peaks at δ 157.1, 149.9, 149.6 ppm, as expected. In support of this was the presence of the characteristic methoxy carbon peaks at δ 60.9, 60.8, and 55.7 ppm. Methyl carbons were observed at δ 25.3, 21.7, 19.9 ppm. Furthermore, the mass of the compound was established by HRMS, and a mass of 391.1914 was found, corresponding to $[M + H]^+$, concurring well with the calculated mass of 391.1909.

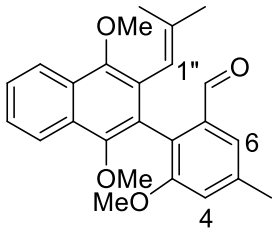

143

2.3.6 Carbonyl-olefin metathesis

With rings A, C, and D in place with the requisite carbonyl and alkene moieties, the stage was now set for the formation of ring B to construct tetracycle **142**. This was to be the next most

crucial step of our formal synthesis. Based on our findings from the model study, we were hopeful that the $FeCl_3$-catalyzed carbonyl-olefin metathesis of biaryl compound **143** would proceed smoothly.

To perform this key operation, into a round bottom flask, $FeCl_3$ was weighed out directly, minimizing exposure to air due to its highly hygroscopic nature. To this, under an inert atmosphere, was added anhydrous DCE and the solution stirred for 5 minutes. A solution of biaryl compound **143** in anhydrous DCE was then added dropwise *via* syringe to the $FeCl_3$ solution and the reaction was stirred at room temperature for 4.5 hours. After running the solution through a short silica plug, the crude product was purified using silica gel column chromatography to furnish, much to our delight, tetracycle **142** as a yellow solid in 67% yield (**Scheme 57**). We observed that using solution concentrations of higher than 0.01 M gave significantly lower yields, thus, it was essential to use dilute conditions. It was also observed during optimization that using a catalyst loading of 27 mol% gave the best results.

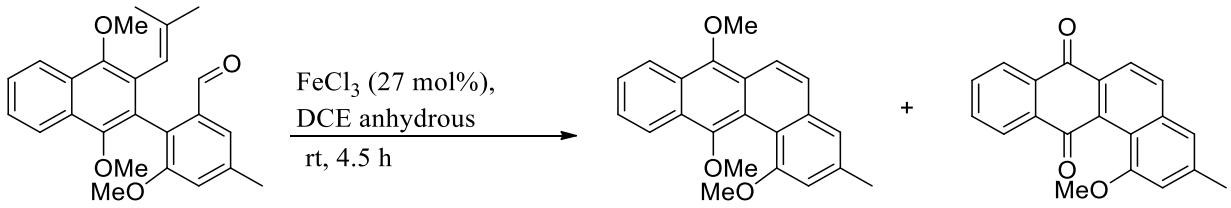

143 **142** 67% **141** 17%

Scheme 57: Carbonyl-olefin metathesis of biaryl compound 143

The disappearance of the aldehyde signal at δ 9.64 ppm in the ^{1}H NMR spectrum, which was also complemented by the disappearance of the carbonyl peak at δ 192.8 ppm in the ^{13}C NMR spectrum, were key in establishing the success of the metathesis reaction. The absence of two methyl group protons in the ^{1}H NMR spectrum, as well as the lack of the singlet peak at δ 5.74 ppm representing proton H-1″ of biaryl compound **143** (refer to **Section 2.3.5**) provided further confirmation that the metathesis had taken place. Accompanying this were the two doublet peaks at δ 7.99 and 7.41 ppm representing the two aromatic protons of the newly formed ring B. We were also successful in obtaining suitable crystals of **142** for single-crystal X-ray crystallography, which further verified the structure of tetracycle **142** (**Figure 12**).

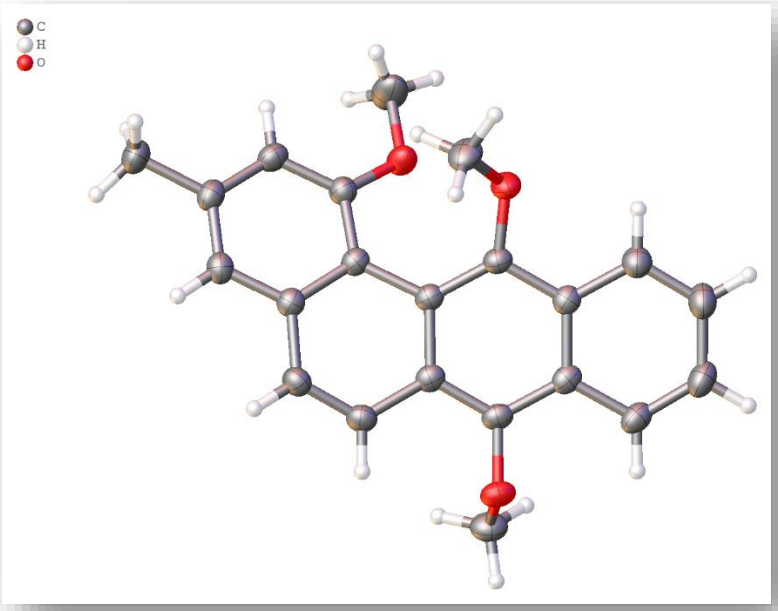

Figure 12: X-ray crystal structure of tetracycle 142; orthorhombic, space group Pccn (no. 56), *a* = 11.4925(6) Å, *b* = 36.9186(17) Å, *c* = 8.6409(4) Å.

Just as was observed with the model study, we suspected that the identity of the side product that was formed in a yield of 17% pointed towards quinone **141**. This was verified by the ^{1}H NMR spectrum, from which was noted that only one methoxy group protons signal was present at δ 3.99 ppm, confirming our suspicion that it had been oxidized to a quinone. Complimenting this was the ^{13}C NMR spectrum which showed the appearance of quinone carbons at δ 186.1 and 183.1 ppm. The ^{1}H NMR spectrum displayed peaks integrating for eight aromatic protons as expected, with two doublets at δ 8.23 and 7.94 ppm representing protons H-6 and H-5 respectively. These two doublets appear more deshielded than those for tetracycle **142** and this can be rationalized by the presence of quinone carbonyl groups. Two singlets at δ 7.28 and 6.91 ppm were also present, signifying protons H-4 and H-2 respectively. This conclusion was further ascertained by running an HRMS of the sample, which gave a mass of 303.1017 corresponding to $[M + H]^{+}$, and this agrees very well with the calculated mass of the quinone of 303.1021.

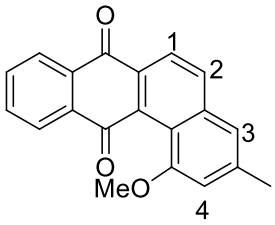

141

This is of course, an interesting result, and can possibly be further investigated and exploited to achieve the one step formation of a benz[α]anthraquinone from a carbonyl- and olefin-containing precursor.

As for the possible mechanistic pathway, it is likely that it proceeds in a similar way to the CAN-mediated oxidation of alkoxyarenes to quinones (**Scheme 58**).[139] An initial co-ordination of Fe(III) to one of the methoxy groups of tetracycle **142** is followed by a one-electron reduction generating intermediate **167**. Electron transfer, followed by attack of water and proton transfer eventually leads to the formation of mono-quinone **168**. The same process is repeated with the second methoxy group, leading to the formation of quinone **141**. Although great care was taken to perform the metathesis under anhydrous conditions, it is possible that traces of water were still present in the system due to the highly hygroscopic nature of $FeCl_3$.

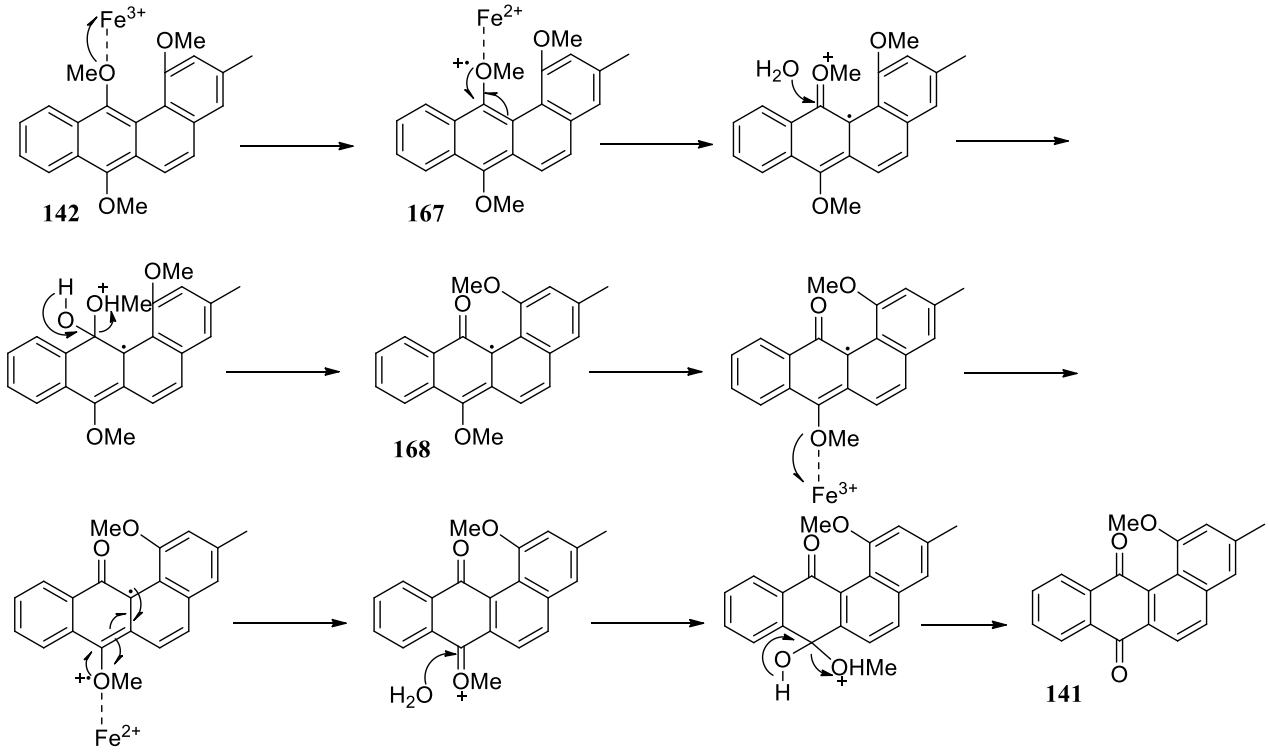

Scheme 58: Possible mechanism for the formation of quinone in the presence of $FeCl_3$.

2.3.7 Late-stage oxidation

Almost at the end of our journey, with the benz[α]anthracene scaffold in hand, and all requisite functional groups for tetrangulol present, the final step was to introduce a hydroxyl group at the C-8 position (**Scheme 59**). We envisaged to do this by exploiting the recently developed transition metal-catalyzed late-stage oxidation.[140-142] The last decade has witnessed a growing interest in the development of, and the use of, C-H activation, as a result of the increased stepwise economy and atom economy associated with this strategy.[140, 143] Although several protocols for C-H activation have been reported in literature, we anticipated to apply the OH-functionalization protocol by Ackermann and coworkers,[142] that makes use of inexpensive

ruthenium catalysts. The reaction proceeds by way of a carbonyl-directed C-H ruthenation, which activates the proton *ortho* to the carbonyl group. This is followed by an oxidation of the ruthenium(II) complex to a ruthenium(IV) complex, which thereafter undergoes a carbon-oxygen bond forming reductive elimination.[140, 142] Acidic aqueous work up then results in the formation of the hydroxylated carbonyl-containing product. We envisioned, perhaps naively, that the hydroxyl group would be directed to the desired C-8 position of the benz[α]anthraquinone scaffold **141** as that position is the least sterically encumbered.

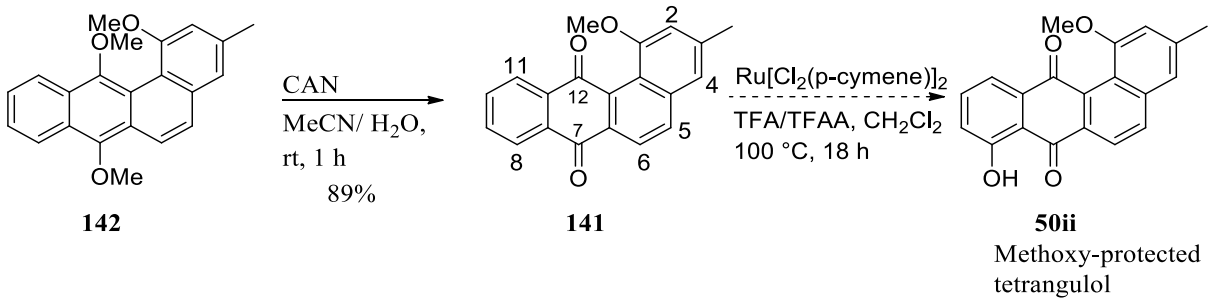

142 **141** **50ii** Methoxy-protected tetrangulol

Scheme 59: Proposed synthesis of methoxy-protected tetrangulol.

Inevitably, we first had to convert tetracycle **142** into quinone **141**. This was achieved following the standard oxidation procedure using CAN in aqueous MeCN (**Scheme 59**). The reaction proceeded uneventfully, generating quinone **141** in a decent yield of 89% as a bright orange solid. The NMR spectra of this compound matched the one obtained for the metathesis side product, with the diagnostic quinone carbonyl signals clearly observed in the ^{13}C NMR spectrum at δ 186.1 and 183.1 ppm.

We were now set to perform the final key step of our formal synthesis of tetrangulol. Following literature precedent,[142] quinone **141** was added to a sealed tube. To the same tube were added Ru[(p-cymene)Cl_2]$_2$ catalyst, PIFA as the oxidant, TFA and TFAA in a ratio of 0.02: 1, and CH_2Cl_2. The tube was sealed and stirred at 100 °C for 18 hours. Following purification by silica gel chromatography, to our fascination two unknown compounds **169** and **170** were isolated, albeit in 9% and 20% yields respectively, with similar NMR spectra except for the splitting patterns of the aromatic protons (**Figure 13** and **Figure 15**).

*2.3.7.1 Compound **169***

Analyzing the spectra of compound **169**, we were immediately pleased to observe, in the ^1H NMR spectrum, the presence of a hydroxyl proton that is *ortho* to a carbonyl group by a deshielded peak at δ 11.51 ppm signifying a hydrogen bonded hydroxyl proton. This was

indicative of a successful late-stage oxidation. The signal for methoxy group protons was clearly visible at δ 3.75 ppm, and so was that for the methyl protons at δ 2.76 ppm, establishing that these functional groups were still present. Since very small amounts of compounds were isolated, the NMR spectra are not the cleanest, with grease peaks from our hexane dominating. Looking at the aromatic protons, it was immediately obvious that the two singlet protons representing H-2 and H-4 (refer to quinone **141, Scheme 59**) were missing.

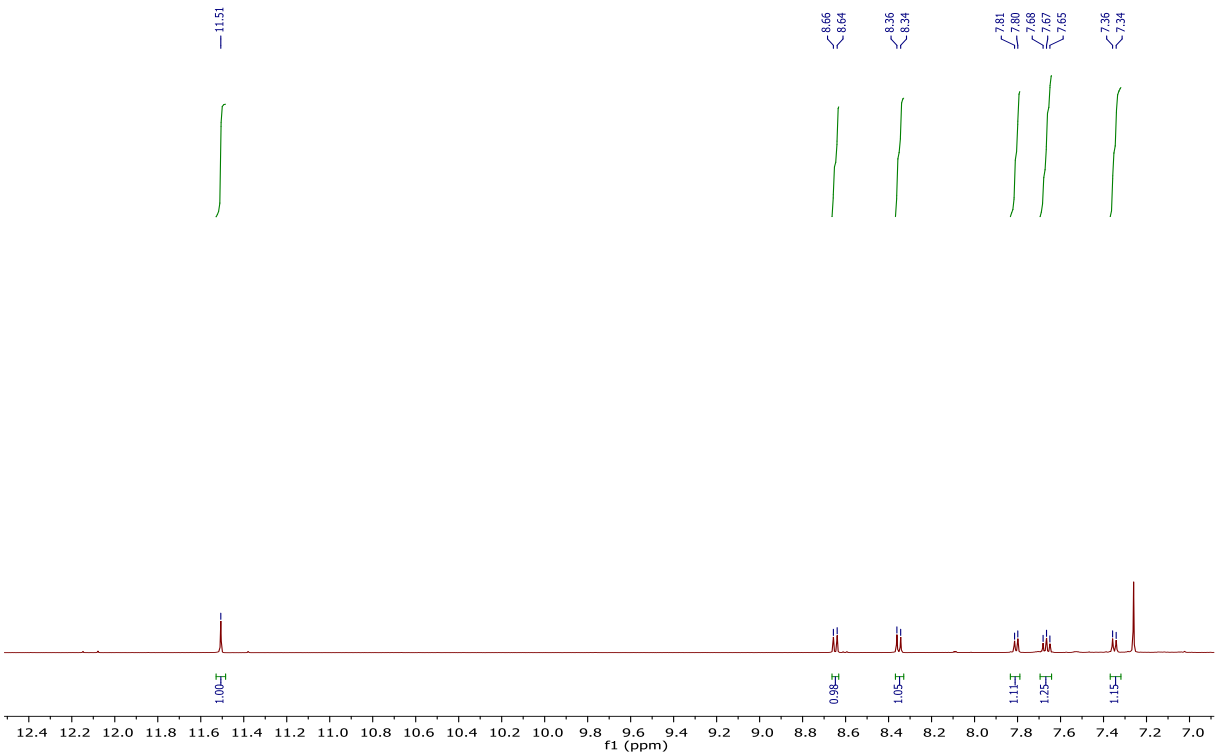

Figure 13: Aromatic region of the ^{1}H NMR spectrum of unknown compound 169

Signals for only five aromatic protons were present, whereas seven aromatic protons for the hydroxylated compound were expected. It was clear that substituents that were made up of neither protons nor carbons were attached to the H-2 and H-4 positions. The ^{13}C NMR spectrum showed 18 aromatic carbons as expected, with the quinone carbon peaks appearing at δ 187.4 and 182.3 ppm. The signals at δ 160.3 and 152.9 ppm were in concurrence with the expected shifts for ArC-OMe and ArC-OH carbons. In this case, NMR spectral analysis was not going to hint at the possible identity of the substituent/s. Notwithstanding this, we also had to determine if the hydroxyl group had been directed to the desired C-8 position of the three possible positions that it could have been directed to (C-6, 8 or 11). From the COSY spectrum (**Figure 14**), it was clear that protons H-5 and H-6 were still present, being the only two protons that couple with each other only, with a coupling constant of 8.8 Hz, and represented by the

doublet peaks at δ 8.65 and 8.35 ppm. This meant that the OH had gone to either C-8 or C-11, and we were unable to determine which of these positions, despite 2D NMR analysis.

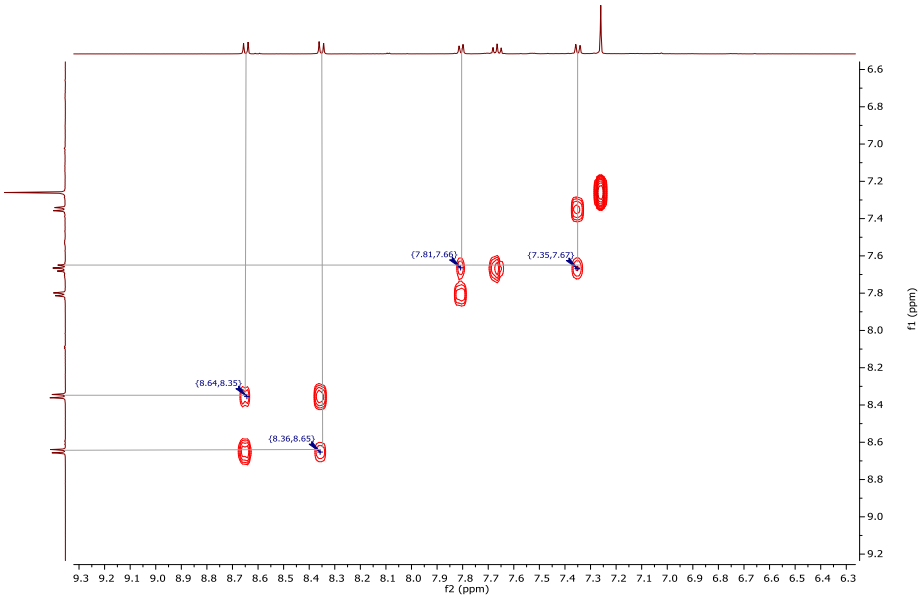

Figure 14: COSY spectrum in the aromatic region of unknown compound 169

*2.3.7.2 Compound **170***

Analyzing the ^{1}H NMR spectrum for compound **170**, similarly to compound **169**, a hydrogen bonded hydroxyl proton was present, represented by the peak at δ 12.07 ppm. This was accompanied by the signal for methoxy group protons at δ 3.81 ppm and methyl protons at δ 2.70 ppm. Just as with compound **169**, only five aromatic protons were observed, with the two singlet peaks representing protons H-2 and H-4 missing.

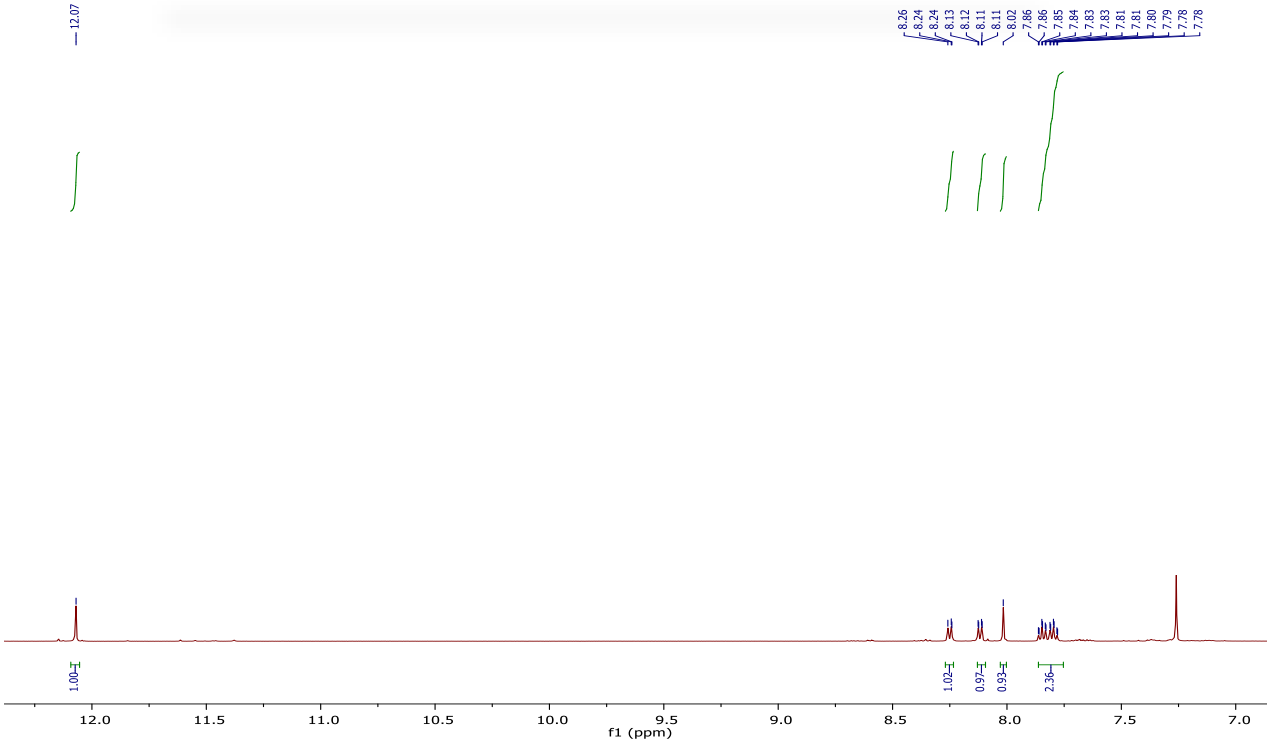

Figure 15: Aromatic region of the ^{1}H NMR spectrum of unknown compound 170

To establish the position of the OH group, it was clear from the COSY spectrum (**Figure 16**) that the naphthalene protons were all present based on their interactions with each other. A deshielded singlet peak at δ 8.02 ppm indicated to the OH position being directed to the C-6 position, with the singlet peak representing proton H-5.

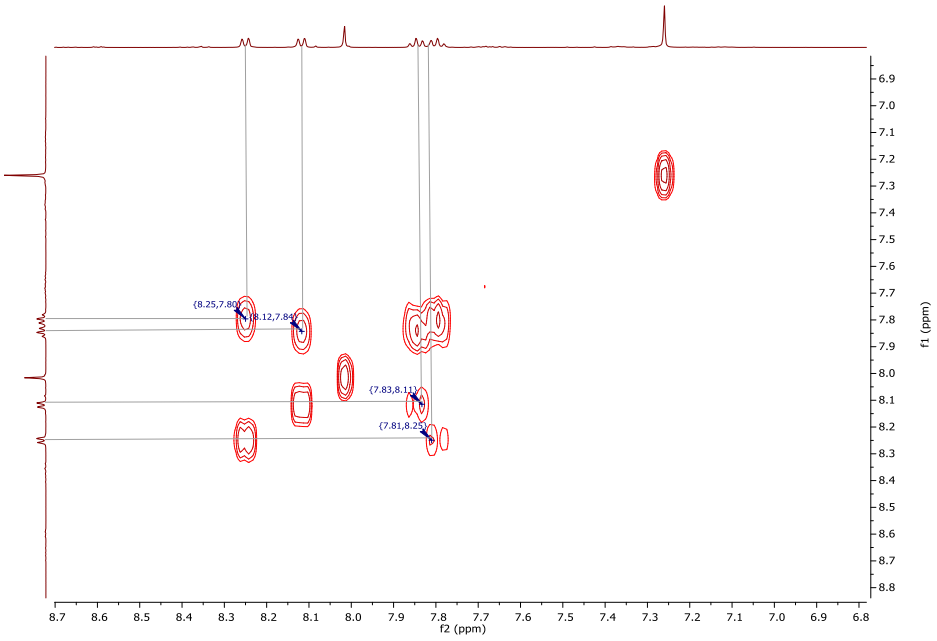

Figure 16: COSY spectrum in the aromatic region for unknown compound 170

Based on NMR spectroscopic analysis, the structures of compounds **169** and **170** that we had deduced so far are shown in **Figure 17**.

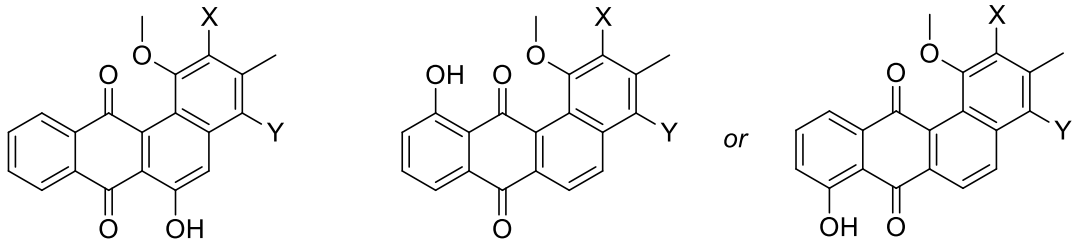

170 **169**

Figure 17: Possible structures of unknown compounds 169 and 170.
X and Y = unknown substituents

*2.3.7.3 Elucidation of the structures of compounds **169** and **170***

We were eventually able to grow suitable single crystals of the two compounds, despite having minute quantities of each. The crystals were grown from solvent mixtures of EtOAc and $CHCl_3$ and were used in single crystal X-ray structure elucidation experiments.

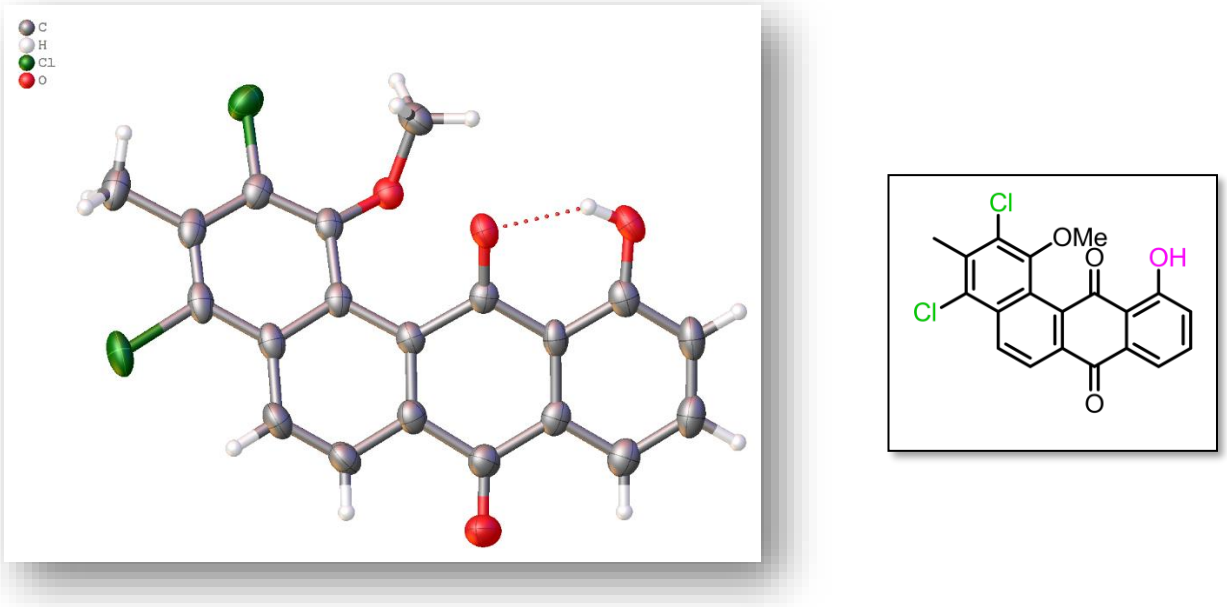

Figure 18: Crystal structure of compound 169; monoclinic, space group $P2_1/c$ (no. 14), *a* = 16.284(3) Å, *b* = 3.8310(7) Å, *c* = 26.131(4) Å.

X-ray crystallographic analysis beautifully revealed the structures of compounds **169** and **170** (**Figures 18** and **19**). We were astonished to find that the unknown substituents were actually chlorine! Although the yields were poor, we had successfully managed to add not only a

hydroxyl group, but also and unexpectedly two chlorine atoms, on our benz[α]anthracene scaffold, and this was an interesting result.

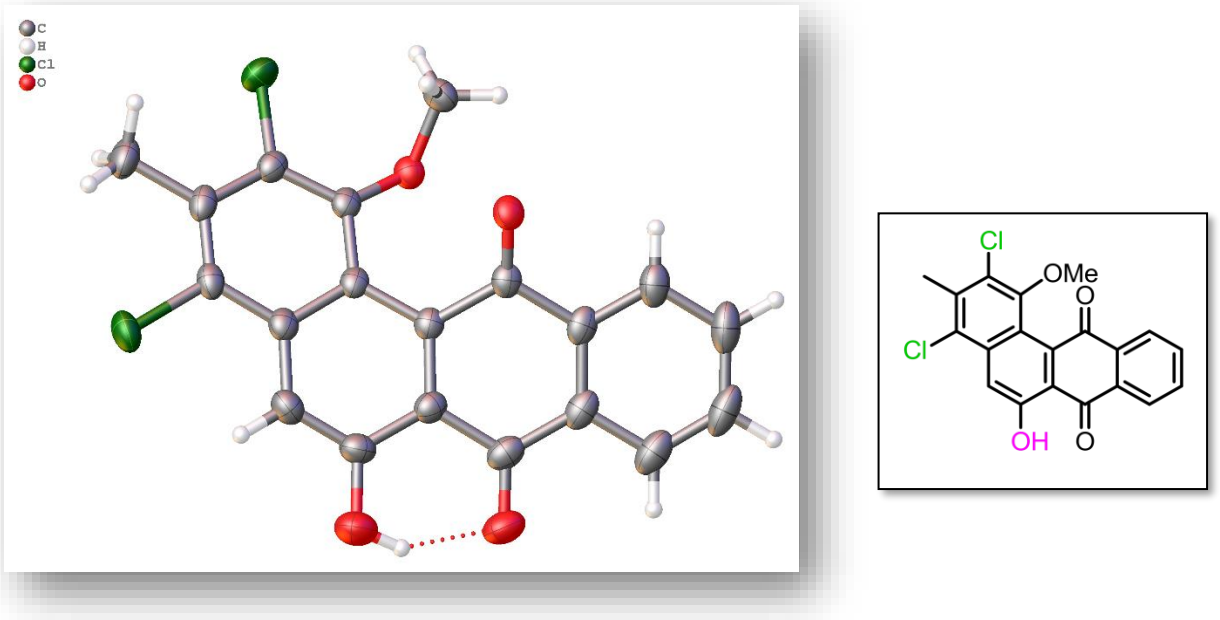

Figure 19: Crystal structure for compound 170; monoclinic, space group $P2_1/c$ (no. 14), a = 3.8487(2) Å, b = 25.7577(15) Å, c = 15.8388(10) Å.

The crystal structure for compound **169** revealed that the hydroxyl group was indeed directed to the naphthalene ring as we predicted, but to position C-11 instead of C-8 as we had hoped. Of course, it is possible that the methoxy group had some influence in directing the ruthenium catalyst to coordinate to the oxygen at C-12 (refer to quinone **141, Scheme 59**). The crystal structure for compound **170** confirmed our prediction that the hydroxyl functionality had been directed to C-6. From our results, it seems that, contrary to the report by Ackermann and coworkers,[144] electronic effects far outweighed steric effects. As position C-6 is more electron-rich than positions C-8 and C-11, it made sense that compound **170** was formed in a higher yield compared to **169**.

Although a detailed mechanistic study is not the scope of the present work, one possible mechanistic pathway to explain the substitution of chlorines could involve an initial ruthenium insertion of the catalyst into the C-H bond to form an intermediate **A** (**Scheme 60**). This most likely happens due to that position being the most electron-rich. This could then be followed by a reductive elimination, resulting in an Ar-Cl bond, forming intermediate **B**. This is then repeated for the second C-H bond by the second ruthenium component of the dimer, ultimately

resulting in the formation of a di-chloro substituted compound (**C**⟶**D**). The utilization of the catalyst in this way could also explain the very low yields obtained. However, it is also possible that the reaction proceeds *via* a different mechanism whereby the chlorine atoms are sourced from CH_2Cl_2 by a radical induced pathway. The dichloro-compound then undergoes a carbonyl directed C-H functionalization to introduce the hydroxyl group.

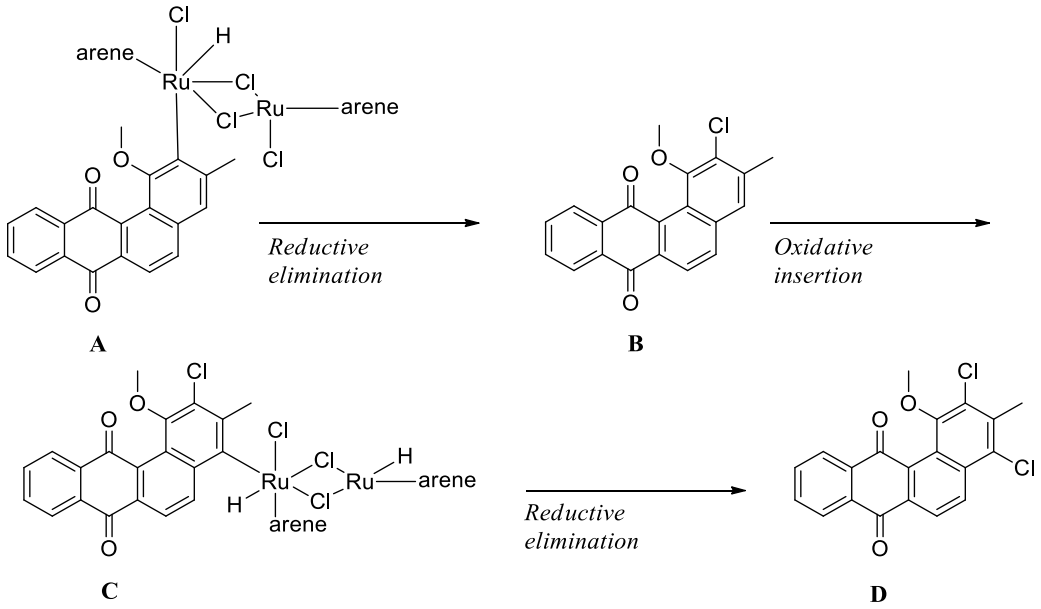

Scheme 60: Possible mechanistic pathway for the insertion of chlorine atoms by Ru[(p-cymene)Cl_2]$_2$

2.4 Conclusion and future work

We began this program with the aim of improving the synthesis of tetrangulol by the implementation of certain Green Chemistry principles in our design strategy. Although we were unsuccessful in the formation of tetrangulol, several interesting results and discoveries were made along the way. Among the most prominent of these was the development and use of a 'green' Friedel-Crafts acylation methodology that makes use of the environmentally acceptable methanesulfonic acid. We were also successful in developing a synthesis for iodo-benzaldehyde **145** that is more elegant than the previously employed synthetic strategy, as we were able to eliminate the use of toxic CCl_4, and avoid waste in terms of atom economy.

Particularly key to this project, was to demonstrate if an $FeCl_3$-catalyzed carbonyl-olefin metathesis could be used in the formation of a benz[α]anthracene scaffold. We were able to establish that this reaction can indeed be used, with ease, to construct the tetracyclic core of angucyclines, from carbonyl and olefin containing precursors. Moreover, it was found that, under the conditions used, the formation of a quinone was promoted, albeit in poor yield. This

could therefore be investigated as part of future work, to enable the one-step synthesis of a benz[α]anthraquinone from a biaryl carbonyl-olefin containing precursor. Also of significance to our synthesis was the use of a palladium-catalyzed Suzuki-Miyaura coupling reaction, which we were successful in utilizing to construct a sterically congested biaryl intermediate.

This work also revealed that a late-stage oxidation can be used to introduce a hydroxyl group on a benz[α]anthraquinone; however, regioselectivity proved to be problematic. Furthermore, rather than a single hydroxylated compound, we observed the formation of two unexpected isomeric hydroxy-dichloro-benzoquinones as our final products in 0.6% and 1.3% overall yields starting from 1,4-dimethoxynaphthalene, not taking into account recycled starting material.

Seeing that a group of chlorine-containing angucyclines have recently been isolated from the mycelium of *streptomyces* sp., and have been found to display interesting biological properties,[145] this synthetic strategy, and in particular the late-stage oxidation could therefore be useful in the formation of chlorocyclinones, as part of future work, that may possess attractive biological profiles. As a starting point, the novel chlorocyclinones **169** and **170** must be tested for their potential antimicrobial as well as potential anticancer properties. Thereafter, the late-stage oxidation procedure must be optimized, through the use of alternative ruthenium-based catalysts targeted specifically for CH activation reactions. This will allow for an efficient one-step addition of hydroxyl- and chloro-functionalities on quinone containing scaffolds.

CHAPTER 3

3.1 Bio-renewable feedstock

3.1.1 An introduction

Organic synthesis, which involves the construction of target molecules comprising of carbon and hydrogen atoms often in combination with other atoms, has revolutionized the world, as we know it. Only until recently, however, has the sustainability of the final product been a major concern. Amongst other factors, where the carbon atoms of the target molecule come from is an important aspect of the sustainability of the final product. Presently, chemical industries worldwide are largely dependent on petroleum based starting materials for chemical synthesis. It is said that, in estimate, more than 98% of all organic chemicals are derived from petroleum.[146] Being a fossil fuel, this resource is classified as being non-renewable, and its significant extent of use in the chemical industry is not only rendering it in danger of depletion but is also causing a carbon imbalance in our ecosystem.[147-149] In order to address these issues, a major goal of green chemistry is to make the switch from petroleum based resources to bio-renewable feedstock for chemical synthesis, and this constitutes one of the major design principles of Green Chemistry as defined by Anastas and Warner (refer to **Figure 1**, Chapter 1).[15-17, 146, 150] Bio-renewable feedstock comprises primarily of biomass, which can easily be replenished by Nature.[147] Biomass is the term that is used to describe all material that is derived from wood and plant based sources, that are in possession of stored energy from the sun through photosynthesis.[147]

The use of biomass as an alternative feedstock for chemicals affords several advantages over those derived from petroleum-based feedstock. Principally, starting material derived from biomass-based resources are most often endowed with a high degree of functionalization, for example in the form of possession of heteroatoms or stereogenic centers.[148, 151] This in turn has the potential to cut down the number of steps it takes to get to the final product as compared to using hydrocarbons derived from fossil fuels, which typically have no organic functional groups.[148, 151] Step-economy in synthesis is favored as the consequence is most often a reduction of overall waste generated, which is in accordance with the principles of Green Chemistry.

Additionally, it may be possible that bio-based products may have unique properties compared to products derived from non-renewable, petroleum-based hydrocarbons in that they may possess useful qualities such as biodegradability.[151] This would allow chemical products, at the end of their life cycle, to degrade into innocuous by-products rather than remaining in their original form in the environment.

Despite the recent emerging interest in the use of bio-renewable feedstock, chemical synthesis from biomass-derived starting materials is essentially not a recent development. In point of fact, before petrochemical sources were discovered as a more economical alternative, organic molecules such as methanol, ethanol, benzaldehyde, and benzoic acid were all biomass-derived.[148] This being the case, one remarkable example of a natural product synthesis in the 1800s was by Adolf von Baeyer in his second synthesis of indigo **171**, using cinnamic acid **172**, which was made from benzaldehyde **173** derived from bitter almond oil (**Scheme 61**).[148, 152-153]

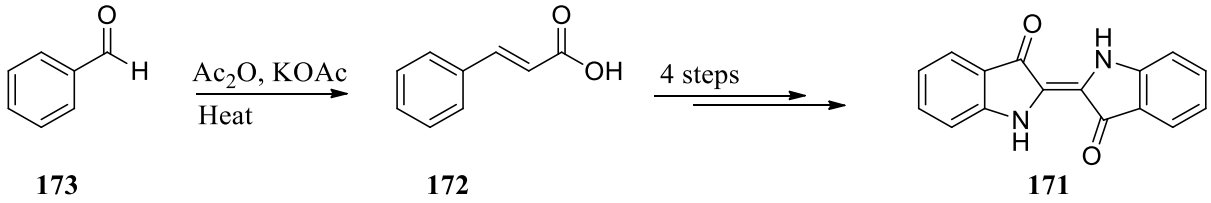

173 **172** **171**

Scheme 61: Synthesis of Indigo by Adolf von Baeyer from benzaldehyde.[148, 152]

Baeyer was later awarded the Nobel prize in chemistry in 1905 for 'his services in the advancement of organic chemistry and the chemical industry, through his work on organic dyes and hydroaromatic compounds'.[154]

3.1.2 Types of bio-renewable feedstock

Indeed Nature provides us with an armory of abundant biorenewable resources in the form of biomass that could potentially be used in the future to replace the petrochemical industry. Various classes of these naturally-occurring resources abound, which can then be converted into platform molecules, each possessing its own level and degree of functionalization that could contribute to a specific natural product synthesis. Fats and oils that are derived from either plant or animal sources for example, are principally used in the production of bio-fuels.[148, 155-156] However, they can also be used in natural product synthesis particularly to introduce alkyl chains, after the valorization of the free fatty acids and glycerol of which they are a source.[148, 155-156] An amenable example would be the synthesis of the alkaloid (+)-azimic

acid, by Naito and coworkers,[157] from **175** which is derived from eicos-5-enoic acid **176**, a constituent of meadowfoam seed oil (**Scheme 62**).[155]

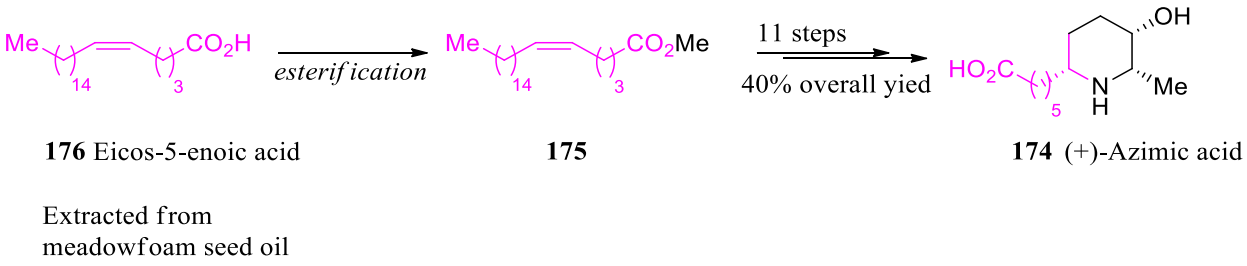

176 Eicos-5-enoic acid

Extracted from meadowfoam seed oil

175

174 (+)-Azimic acid

Scheme 62: Synthesis of (+)-azimic acid using a fatty acid as a biorenewable starting material.[148, 157]

The use of fats and oils in the chemical industry, however, is a debatable issue as it can bring about competition with the global population for food, which altogether leads to concern of increased food prices universally.[158]

A much nobler alternative would be to use inedible bio-renewable sources, which eliminates competition of these resources with food consumption. A plethora of examples exist, such as cellulose, chitin, and lignin. Lignin is a major waste product of the paper and pulp industry and hence comprises of a large portion of biomass not utilized by humans.[159] It is a biopolymer, which in addition to other functions, confers mechanical strength to plants, and is one of the largest sources of carbon on earth.[15] Through various valorization approaches, lignin can be used to deliver a plethora of platform molecules such as vanillin, resorcinol, syringaldehyde, veratrole and piperonal which can then be used as starting materials for natural product synthesis.[148, 160-161] The total synthesis of organic compounds, where all starting materials are wood-derived, is referred to as 'xylochemistry'; work that was pioneered by Arduengo and Opatz.[149] Although the valorization and transformation of wood into platform molecules still needs to be optimized, the xylochemical approach is a sizeable step forward in the synthesis of sustainable natural products.

To this end, another bio-renewable starting material that has gained prominence for synthesis in recent times is cashew nut shell liquid (CNSL), which is a major waste product of the cashew nut industry.

3.2 Cashew nut shell liquid

The cashew tree (*Anacardium occidentale* L), which is native to South America, was first introduced, early in the 1500s, to India, before spreading to other parts of the world.[162] It is

now a significant cash crop in several countries such as Vietnam, Tanzania, Mozambique, Brazil, and India.[163] From the cashew plant stems the comestible cashew apple, at the base of which grows the cashew nut, often eaten as a snack. The cashew nut is encompassed within a shell that comprises of an inner and an outer layer, in between which lies a honeycomb-like structure.

The global production of cashew nuts is estimated to be around 2.1 million tons annually.[164] Traditionally, the shells of these cashew nuts would be discarded as waste; however in recent times, these shells have proved to be immensely valuable due to the isolation of a red-brown oil acknowledged as the cashew nut shell liquid (CNSL), derived from the honeycomb-like structure. CNSL, in addition to its ubiquitous occurrence in Nature and inexpensiveness, further demonstrates an admirable potential as a bio-renewable feedstock for the synthesis of several value-added products, making this a classic example of a 'cradle-to-gate' approach for agricultural waste.[162, 164-167]

Remarkably, the chemical composition of CNSL was investigated as early as 1847 by Stadeler,[168] and thereafter in 1887 by Ruhemann and Skinner.[169] Several publications have followed since then,[170-172] and it is now widely accepted that CNSL comprises chiefly of a mixture of four phenolic compound scaffolds, namely anacardic acids **177a-d**, cardanols **178a-d**, cardols **179a-d**, and 2-methylcardols **180a-d** (**Figure 20**). Each of these sets of compounds possess a long hydrocarbon side chain with varying degrees of unsaturation **a-d** in the *meta* position to the phenol group, and this, in addition to the phenol functionality, render CNSL a valued resource for the synthesis of chemicals.[164] The percentages of the anacardic acids and cardanols differ depending on the extraction method used, where solvent extraction or cold-press methods result in 60-65% anacardic acids. The more commonly applied technical extraction methods involving heating result in a higher percentage of the cardanols (65%) due to the ensuing decarboxylation of the anacardic acids, making the cardanols the most widely employed constituent of CNSL, [162-164] hence our focus will be centered primarily on this versatile constituent.

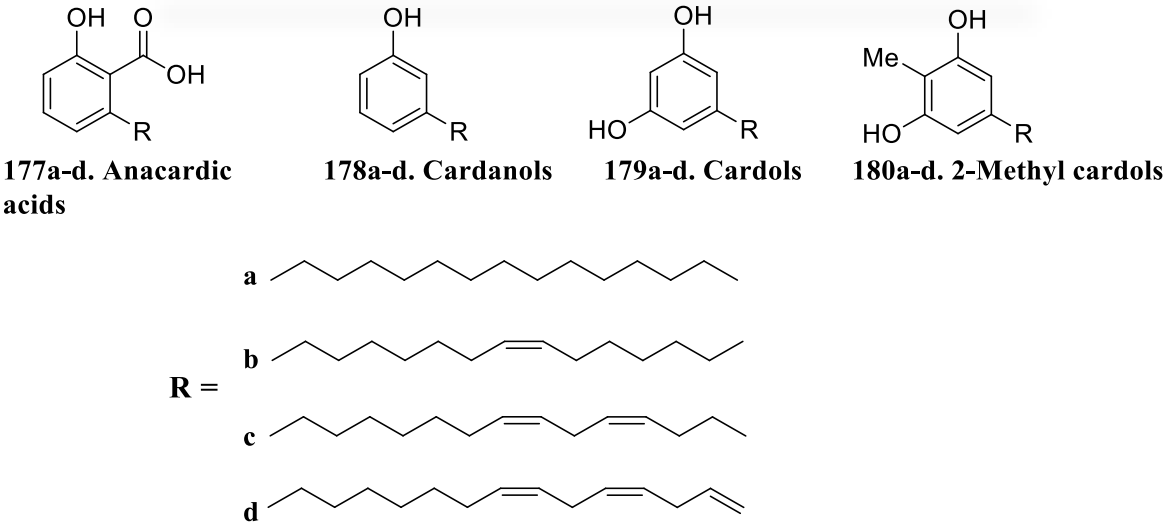

177a-d. Anacardic acids **178a-d. Cardanols** **179a-d. Cardols** **180a-d. 2-Methyl cardols**

Figure 20: Chemical composition of CNSL.

3.2.1 Cardanols as bio-renewable starting materials for synthesis

Owing to their inherent functionality, the cardanols **178a-d** boast a myriad of versatile applications such as in the synthesis of polymers,[163] phenolic resins,[164] nanomaterials,[173-174] stabilizers,[175] as well as a bio-renewable source of energy in the form of a biofuel.[176] Although the cardanols have been used for such applications as these since the early 1900s,[170] their conversion into value-added chemical products has only recently been described, and as such few examples have been reported in literature. A prominent case, seemingly simple yet representing a step forward in the replacement of petrochemically-derived resources with biochemically-derived sources, was the hydrogenation of the cardanols **178a-d** into 3-pentadecylcyclohexanone **181**, with the concomitant formation of small amounts of the hydrogenated phenol **182** (**Scheme 63**).[165] Albeit for the long chain, **181** resembles petrochemically derived cyclohexanone very closely. Since cyclohexanone is an important building block in the synthesis of several petrochemically derived compounds,[177] it may not be impossible that cardanol-derived **181** could similarly be used in synthesis.

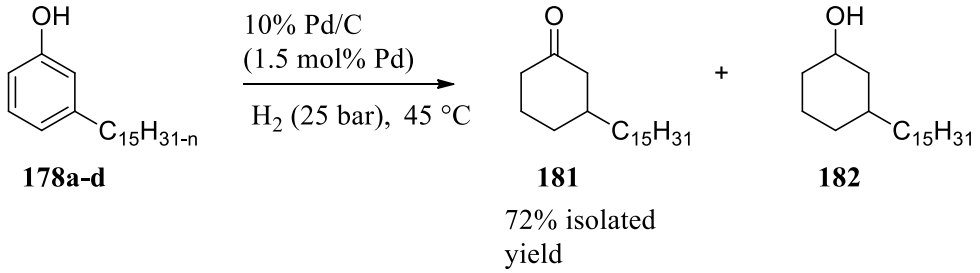

178a-d **181** 72% isolated yield **182**

Scheme 63: Direct hydrogenation of the cardanols into 3-pentadecylcyclohexanone.

Another particularly pertinent contribution was made by the group of Cole-Hamilton in their recently described synthesis of pharmaceutical drugs using the cardanols **178a-d** as the starting material (**Scheme 64**).[178] Cardanols **178a-d** were first transformed by means of an ethenolysis in the presence of catalytic amounts of the Hoveyda-Grubbs first generation catalyst **183** (HG1), generating 3-non-8-enylphenol **184** in a 96% yield. This was subsequently converted into the key intermediate 3-vinylphenol **185** in a two-step process involving, initially, a palladium-mediated isomerization of 3-non-8-enylphenol **184**, followed by a metathesis of crude **186** in the presence of a M1 catalyst **187** (see bottom of **Scheme 64**) furnishing 3-vinylphenol **185** in an overall yield of 65%. Phenol **185** thereafter served as the key precursor to two pharmaceutical drugs. A hydroxyamination on the double bond of **185** delivered the sympathomimetic drug norfenefrine **188** in a 71% yield. The antihypotensive drug etilefrine **189**, which has a similar structure to norfenefrine **188**, was formed in a single step from **188** by a selective *N*-ethylation using ethyl triflate in HFIP. The di-*N*-ethylated compound **190** was also formed as a side product in 17% yield. In addition, the Cole-Hamilton group also demonstrated the synthesis of the nonsteroidal anti-inflammatory drug fenoprofen **191** in four steps from phenyl-protected cardanol **192**, in an impressive overall yield of 48% from the cardanols **178a-d**. This use of an inedible waste bio-renewable resource to synthesize pharmaceutical drugs is an immense step forward in the replacement of the fast-depleting petrochemical industry with bio-renewable resources.

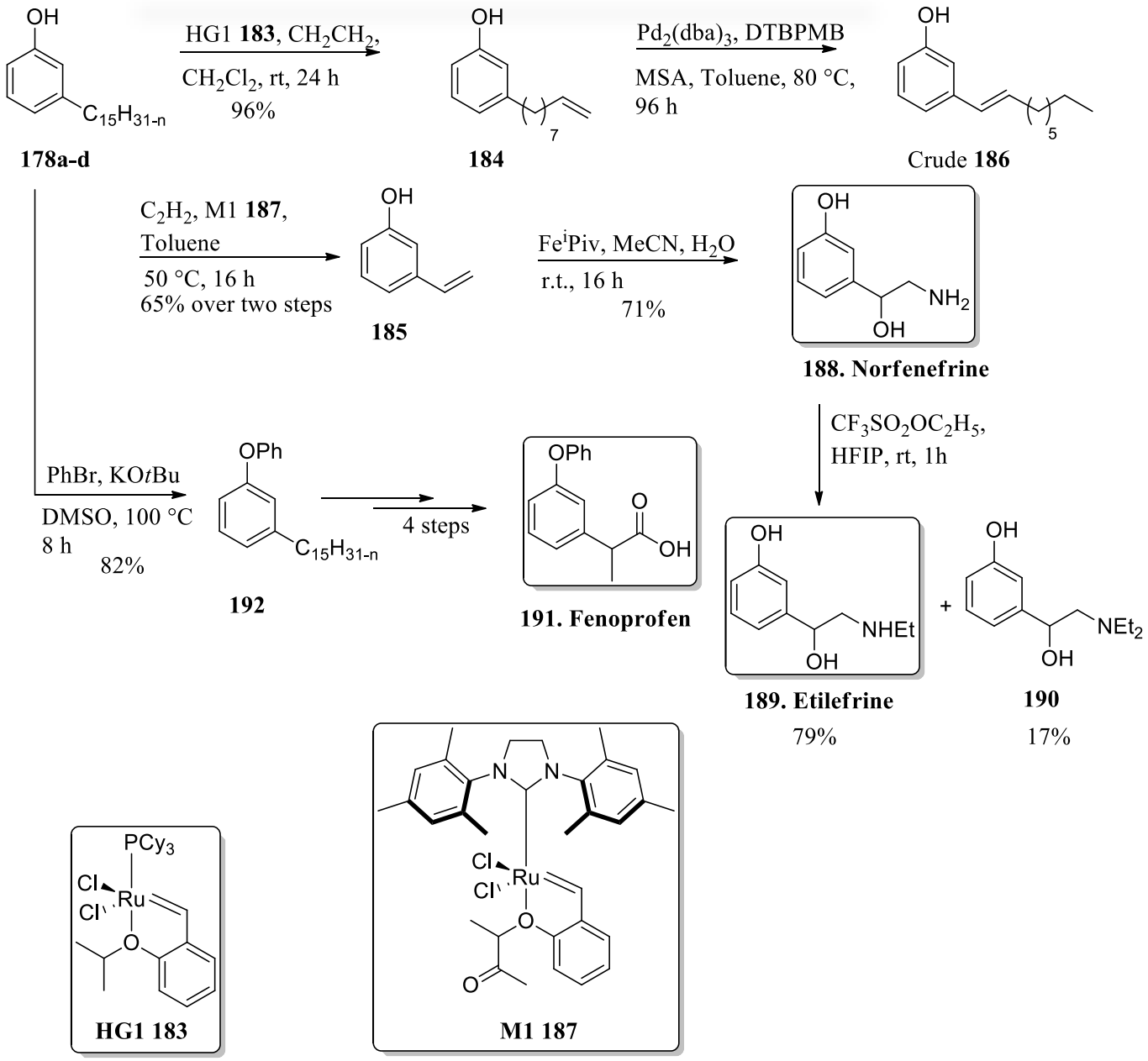

Scheme 64: Synthesis of norfenefrine, etilefrine, and fenoprofen from cardanol. * DTBPMB = 1,2-Bis(di-*tert*-butylphosphinomethyl)benzene**,** Fe^{i}Piv = Iron(II) phthalocyanine + *O*-pivaloylhydroxylammonium triflate, MSA = Methanesulfonic acid, HFIP = Hexafluoroisopropanol.

In 2019 in our laboratory, the de Koning group in collaboration with the Opatz group, demonstrated the xylochemical construction of several classes of compounds from cardanol **178a** and anacardic acid **177a** that were found to display interest UV absorption profiles.[179] Hydroxybenzophenone **193**, hydroxyflavone **194**, dihydroxyxanthone **195**, triazines **196** and

197, and oxadiazole **198** were all expediently fashioned from CNSL-derived cardanol **178a** (**Scheme 65**).[179]

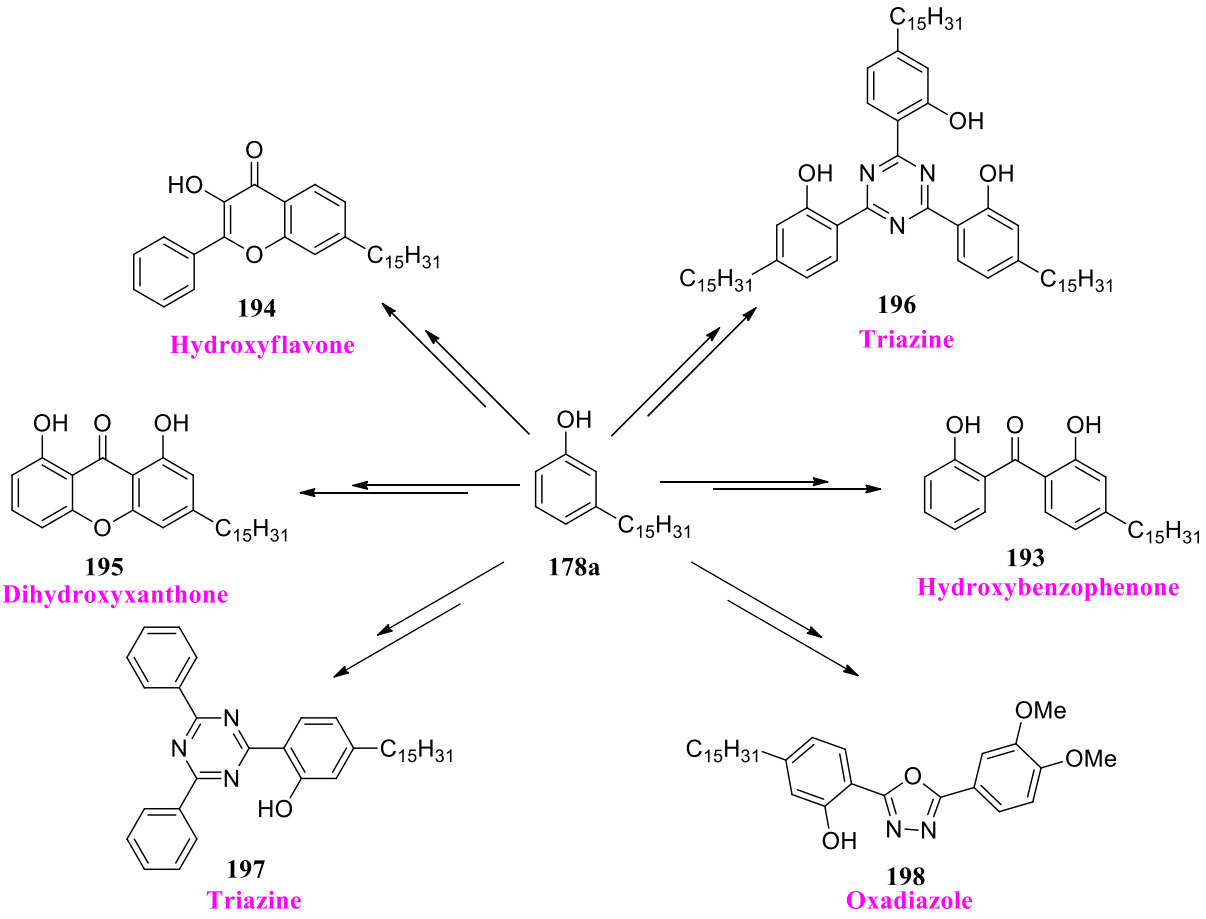

Scheme 65: Synthesis by de Koning and coworkers of several classes of heterocycles using cardanol 178a as the starting material.

These syntheses establish that biodegradable, renewable resources like cardanols **178a-d** can successfully be used to synthesize higher value added compounds that have previously only been made from petrochemically-derived starting materials. In addition, the compounds have the potential to display interesting physical as well as biological properties. Thus, eventually rendering the cardanols **178a-d** a valuable starting material in the synthesis of various structurally rich classes of compounds. One particular group of compounds that our group has been interested in are the xanthones, which shall be the focus of the next section of this chapter.

3.3 Xanthones

The term ‘xanthone’ derives from the Greek word ‘xanthos’ or rather more accurately ‘ξανθός’ meaning yellow or blond.[180] Xanthones are a group of naturally-occurring, as well as synthetic, oxygen-containing, symmetrical heterocycles that bear the framework of a 9*H*-xanthene-9-one

199 (**Figure 21**).[180-183] In Nature, xanthones occur as secondary metabolites that are found in various species of both terrestrial as well as marine plants, fungi, and lichen.[184] Naturally-occurring xanthones have been isolated from plants as early as in the 1800s, as exemplified by Claude Leconte's isolation, in 1838, of a certain yellow crystalline compound which he coined 'gentisin' **200**, a xanthone from the plant family of *Gentianaceae*.[185] Other plant families that xanthones have since been isolated from include *Guttiferae*, *Polygalaceae*, *Leguminosae*, *Lythraceae*, *Moraceae*, *Loganiaceae* and *Rhamnaceae*.[186]

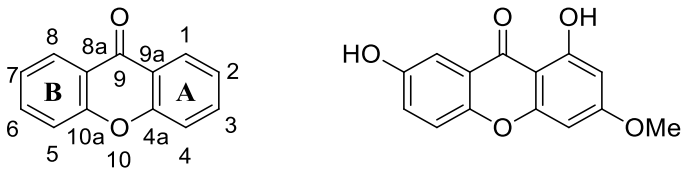

199. 9*H*-xanthene-9-one

200. Gentisin
Simple xanthone

Figure 21: Structures of xanthone core and xanthone gentisin.

As far as it is known, the xanthone core itself is not found in Nature, but was first obtained through synthesis by Kolbe and Lautermann in 1860.[181] The planar, rigid core however, is found in Nature substituted in various positions of the skeleton by a diverse array of substituents, giving rise to the various groups or classes of xanthones. Of these, there are six categories or classes, namely; simple xanthones, prenylated xanthones, xanthone glycosides, xanthonolignoids, bisxanthones and miscellaneous xanthones.[181-183]

The simple xanthones, which are found abundantly in natural products, include all those that bear simple substituents such as hydroxyl, methoxy, or methyl groups.[181, 183] Gentisin **200** (**Figure 21**), for example, belongs to this class of xanthones. The prenylated xanthones constitute the majority of naturally-occurring xanthones, and are substituted with the commonly found isoprenyl group, or the less frequent 3-hydroxy-3-methylbutyl and 1,1-dimethyl-prop-2-enyl substituents. Various modifications of these side chains, including cyclization, epoxidation, hydrogenation, among several others, have also been observed.[183] Isoemericellin **201** (**Figure 22**), as an example, is a prenylated xanthone isolated from the *Emericella variecolor* strain of fungi derived from the marine sponge *Haliclona valliculata*.[187]

Mangiferin **202** is a classical specimen of a glycosylated xanthone, isolated from the leaves and bark of *Mangifera indica*.[186] It is most likely a metabolic precursor to the pigment euxanthoic acid, also known as Indian yellow, which was originally extracted from the urine

of animals fed with mango leaves.[186] The third category of xanthones, i.e. the xanthonolignoids comprise of a phenylpropyl group that is connected to a dihydroxyxanthone core by a dioxane ring, and has only recently been identified as a separate group.[188] The first xanthonolignoid to be isolated was kielcorin **203** in 1969 from the *Kielmeyera* species (Guttiferae).[189] Bisxanthones, on the other hand, have been investigated to a lesser extent than monomeric xanthones. One such example is swertiabisxanthone-I **204** isolated from the fungi *Swertia macrosperma.*[190]

All other xanthones that do not fit these categories are classified as miscellaneous xanthones, an example being xanthofulvin **205** isolated from *penicillium sp.*[183]

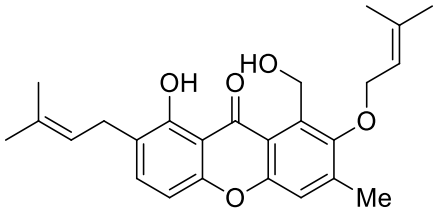

201. Isoemericellin
Prenylated Xanthone

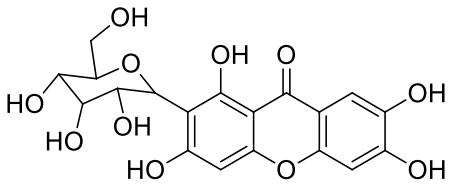

202. Mangiferin
Xanthone glycoside

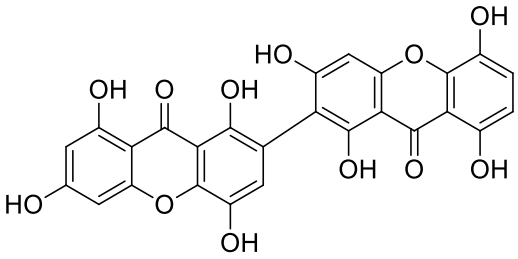

204. Swertiabisxanthone
Bisxanthone

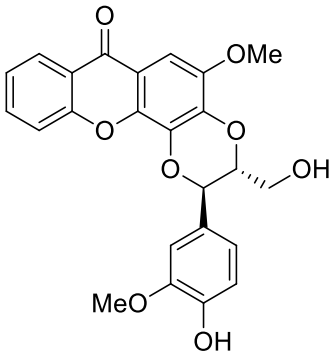

203. Kielcorin
Xanthonolignoid

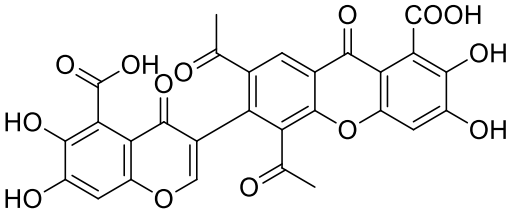

205. Xanthofulvin
Miscellaneous xanthone

Figure 22: Examples of xanthones in different classes.

3.3.1 Biological properties of the xanthones

The xanthone framework is often referred to as a 'privileged structure' owing to the diverse array of substituents which elicit a variety of biological responses due to their ability to interact with different drug targets.[181-182] In fact, the recognition of the biological significance of xanthones is not a recent development, and has been investigated since the late 1900s.[186, 191] So far, xanthones have been found to demonstrate antimicrobial,[192] anti-inflammatory,[193] antitumor,[194] and antioxidant properties.[195] The antitumor and anticancer properties of xanthones, in particular, have been critically investigated due to their ability to inhibit several stages of the carcinogenesis process.[196-197] Xanthones have been known to inhibit several molecular targets in the tumor cells, such as kinases and DNA polymerases.[196] Accordingly, the anti-tumor properties of xanthones include amongst many others, cell cycle arrest and inhibition of metastasis, induction of apoptosis, and reduction of inflammation.[196] It is intriguing to note that xanthones have also been found to exhibit anti-obesity properties, as demonstrated by mangiferin **202**.[198] Mangiferin **202** was reported to reduce free fatty acids and triglycerides in the plasma of hyperlipidaemic rats and was found to inhibit differentiation of preadipocytes, and suppressed lipid accumulation, and has been used as a supplementary food in Japan to prevent obesity and diabetes.[198]

So it is that the interest in xanthones arises primarily due to the pharmacological properties of these compounds, which in turn is brought about principally due to their structural diversity. This has, as a result, brought about an interest by organic chemists in the total synthesis of xanthones, both natural and synthetic. It is just as important to synthesize new non-natural xanthones as it is to synthesize naturally-occurring xanthones, as this can lead to the development of novel structures that could potentially serve as clinically useful drugs.

3.3.2 Chemical synthesis of xanthones

3.3.2.1 The Grover, Shah and Shah method

The first known method to synthesize hydroxyxanthones involved distilling a mixture of phenol and phenolic acid in the presence of acetic anhydride.[199-200] Even though the desired xanthones were delivered successfully, the reaction conditions were often drastic, and side reactions were eminent.[201] To overcome these limitations, a modification of this method was then developed in 1955 by Grover *et al.* which involved condensation under mild conditions of a salicylic acid derivative with a reactive phenol in the presence of phosphorus oxychloride and zinc chloride, to form a hydroxyxanthone.[201] This convenient method, which is still being

used in the synthesis of hydroxyxanthones, is commonly referred to as the Grover, Shah and Shah (GSS) method.[202] Grover *et al.* reported the use of this method to synthesize a number of hydroxyxanthones. For example, 1,3,6-trihydroxyxanthone **206** was synthesized, albeit in a poor yield of 30%, from 2,4-dihydroybenzoic acid **207** and phloroglucinol **208** using mild reaction conditions (**Scheme 66**).[201]

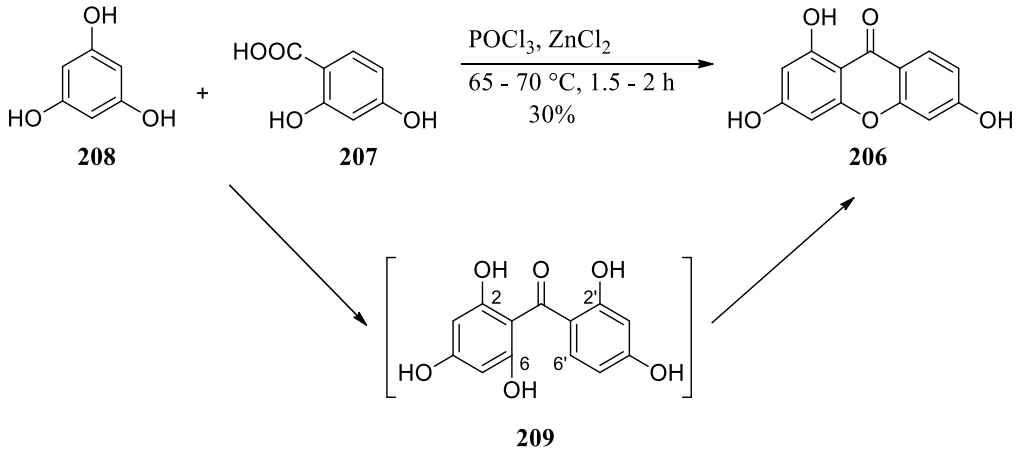

Scheme 66: GSS method for the synthesis of hydroxyxanthones.[201]

Modifications of this original method have been employed since for the construction of hydroxyxanthones;[203] however, the reaction only works if the intermediate benzophenone possesses a hydroxy group in the 6 and 2' position, or in the 2 and 6' position (refer to **209**, **Scheme 66**).[202, 204] Without such a benzophenone intermediate, an additional cyclization step would be necessary to form the xanthone. For this reason, other methodologies for the synthesis of xanthones have been developed. Two different classical and well-known synthetic routes proceed either by the initial formation of a diaryl ether **210**, or a benzophenone **211** as key intermediates, followed by the cyclization of the respective intermediate leading to the desired xanthone **212** (**Scheme 67**).[203]

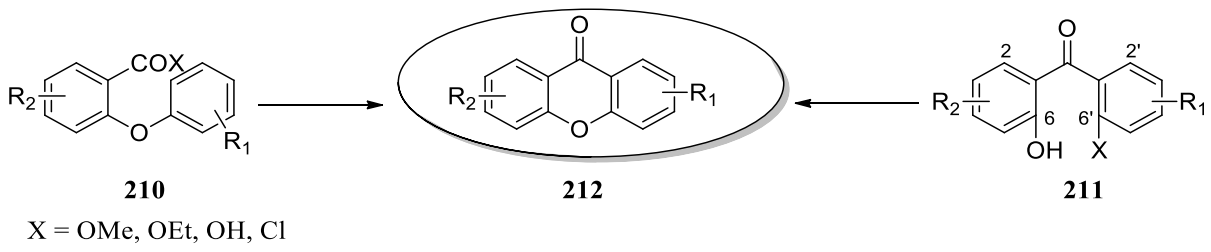

Scheme 67: Two classical synthetic routes leading to xanthones.

3.3.2.2 Synthesis of xanthones via a diaryl ether intermediate

Although several methods exist for the formation of an ether linkage between aromatic rings to form diaryl ethers, the most commonly applied strategy in the synthesis of xanthones involves the Ullmann coupling between a phenol and aryl halide, as the reaction is regiospecific and only one product is formed.[202-203] Other strategies that have been used for the formation of a diaryl ether intermediate include the [3+3] cyclocondensations between two arene moieties, which is useful for the synthesis of highly hindered xanthones,[205] as well as the intermolecular conjugate substitution of salicylate derivatives with 1,4-halobenzoquinone, which is useful for the synthesis of xanthones bearing a hydroquinone moiety.[206]

Following the construction of the diaryl ether intermediate, a cyclization must be performed to yield the desired xanthone. Depending on the nature of the substituents present on the diaryl ether intermediate, different approaches can be used, the most widely employed of which involves an acid catalyzed intramolecular electrophilic cycloaddition.[203] Goodell *et al.*[207] used this approach in the synthesis of several 3-carboxamidexanthone derivatives as part of their investigative studies into the mechanism of action of anti-herpes agents that can inhibit topoisomerase activity. The synthesis began with a modified Ullmann-Goldberg coupling reaction between phenol **213** and bromoterephthalic acid **214** in the presence of the non-nucleophilic base 1,8-diazabycyclo[5.4.0]undec-7-ene (DBU), to yield the diaryl ether intermediate **215** (**Scheme 68**). Intermediate **215** was then cyclized with concentrated sulfuric acid at 100 °C, an acid-catalyzed intramolecular electrophilic cycloaddition, to yield 3-carboxyxanthone **216** in an average yield of 55%. To form carboxamidexanthone **217**, an acid chloride intermediate of **216** was initially formed by refluxing in thionyl chloride, which was thereafter reacted with the requisite amine in CH_2Cl_2.

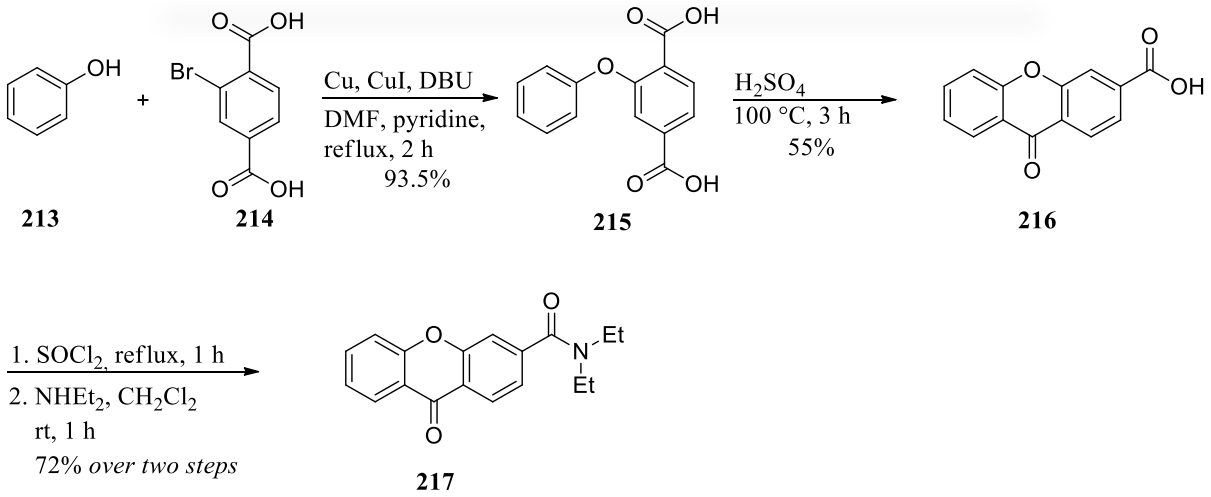

Scheme 68: Synthesis of carboxamidexanthone 217 using Ullmann coupling and intramolecular SNAr as key steps.[207]

However, the reactions used for this type of route are generally harsh due to the high temperatures needed, in addition to the often super-stoichiometric amounts of copper catalyst that are required.

In the case where the diaryl ether intermediate does not possess a carboxylic acid-derived substituent *ortho* to the ether linkage, an electrophilic aromatic substitution can be used to selectively introduce the carbonyl moiety. Granoth *et al.*[208] were the first to demonstrate this methodology, when either ether **218a or b** was treated with oxalyl chloride in the presence of aluminium chloride and carbon disulfide to yield either xanthone **219a or b** respectively in one step (**Scheme 69**).

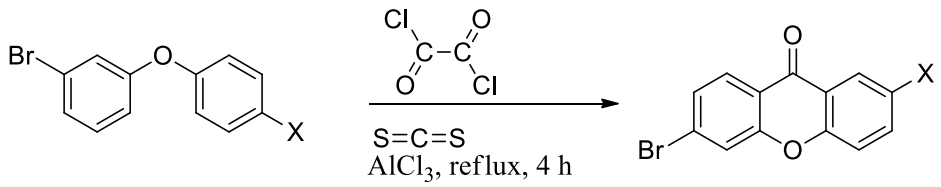

218a. X = Cl
218b. X = F

219a. X = Cl, 65% yield
219b. X = F, 83% yield

Scheme 69: Synthesis of xanthone from diaryl ether intermediate lacking a carbonyl group.

However, with this methodology, it is important that the position *para* to the ether linkage of the most nucleophilic aryl ring of the diaryl ether is substituted to avoid *para*-acylation or an electrophilic attack on a less hindered position.[203]

Methods also do exist that involve the cyclization of diaryl ethers that possess formyl groups instead of carboxylic acid derivatives. These methods for example involve an oxidative double C-H functionalization/carbonylation catalyzed by palladium,[209-210] or a rhodium-catalyzed cross-dehydrogenative coupling.[211] On the downside, however, the catalysts or ligands used are often expensive which can prove to be a hindrance.

3.3.2.3 Synthesis of xanthones via benzophenone intermediate

The synthetic approach involving benzophenones as the key intermediate to the synthesis of xanthones is often used to overcome the limitations of the previously mentioned strategies, and is most preferred due to the often high yields obtained.[202-203] This route, just as with the diaryl ether route, involves the initial synthesis of the benzophenone key intermediate, followed by a subsequent cyclization to yield the desired xanthone.

The preferred methodology for the synthesis of benzophenone intermediates, due to the high yields obtained, involves a Friedel-Crafts acylation between a phenol derivative and an acyl chloride, despite the certain limitations of this method, such as the lack of regioselectivity in terms of either *ortho* or *para* positions being acylated, in addition to the often strongly acidic conditions that are required.[184, 202-203] Another methodology that is commonly used, especially for the synthesis of highly-substituted benzophenones, is the 1,2-nucleophilic addition of an aryllithium to a carbonyl group. Where the substrate bears an ester or acyl chloride moiety, the benzophenone would be obtained in one step,[212-213] but in the case of an aldehyde-bearing substrate, the benzophenone is obtained in two steps following an oxidation of the secondary alcohol that is formed (refer to **Scheme 71**).[214] Besides these general methodologies, other less frequently used procedures do exist such as the palladium-catalyzed C-H addition of an arene to a nitrile to form a ketimine which upon hydrolysis leads to a benzophenone.[215]

Upon construction of the benzophenone intermediate, an ensuing cyclization will then lead to the formation of the xanthone core. If a hydroxyl group is substituted either on position 2 or 6 and a leaving group on position 6' of the benzophenone intermediate (**211**, **Scheme 67**), a base-catalyzed intramolecular aromatic substitution can take place to form the ether bridge linking the two aryl moieties.

Dai *et al.* applied this strategy to synthesize a number of tetraoxygenated xanthone derivatives whose cytotoxic activity against human hepatocellular carcinoma (HCC) cells was investigated.[216] Xanthone **220** was found to show the most promising result as a potential chemotherapeutic agent for the treatment of human HCC.[216] The synthesis began with 2,3,4-

trimethoxybenzoic acid **221**, which was subsequently converted into the intermediate acid chloride **222** by reaction with thionyl chloride (**Scheme 70**). This was then treated with 1,3,5-trimethoxybenzene **223** in ether in the presence of $AlCl_3$ to mediate a Friedel-Crafts acylation, which was accompanied by a selective demethylation of the methoxy group *ortho* to the carbonyl group, resulting in the benzophenone intermediate **224** in a 65% yield. The xanthone core **225** was then expediently constructed through a base-catalyzed cyclisation of **224** in an 83% yield. To furnish the desired xanthone **220**, compound **225** was initially iodinated using NIS to deliver iodo-xanthone **226**, which was thereafter subjected to a Suzuki-Miyaura coupling reaction catalyzed by tetrakis(triphenylphosphine)palladium(0).

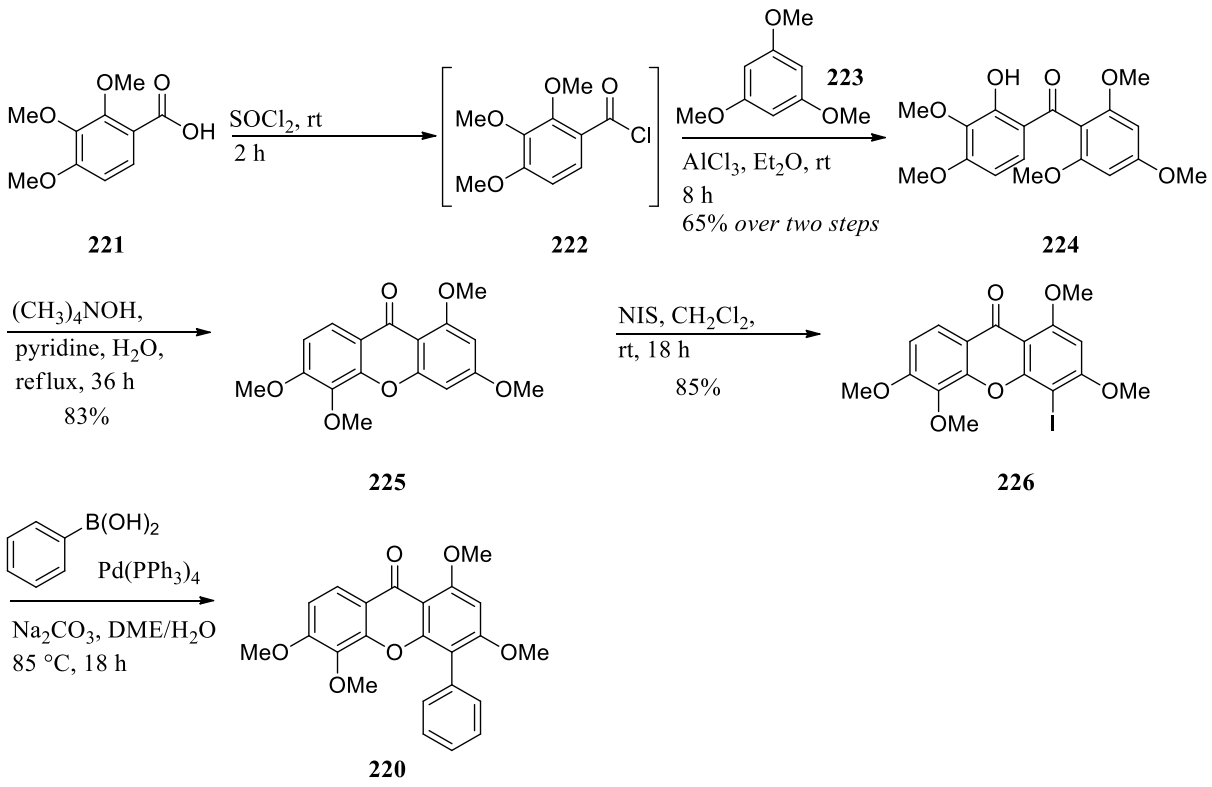

Scheme 70: Use of a Friedel-Crafts acylation and base-catalyzed intramolecular substitution as key steps for the synthesis of a xanthone.[216]

This relatively simple cyclization strategy was also showcased in the Hintermann *et al.* synthesis of the xanthone core **227** of the highly oxygenated antibiotic FD-594 (**Scheme 71**).[217] Terephthalate **228** was transformed into aldehyde **229** in a five-step process involving the initial protection of the free hydroxyl groups, followed by a semi-saponification and eventual reduction of one of the ester groups, and finally an oxidation of the resulting primary alcohol. Intermediate aryllithium **230**, which was furnished upon subjection of **231** to a solution of *n*-BuLi, then underwent a nucleophilic aromatic addition to aldehyde **229**, delivering the

secondary alcohol **232** in a good yield of 79%. Oxidation of the secondary alcohol, followed by a deprotection of the MOM group, led to the formation of key intermediate benzophenone **233**. Subsequently, a base-catalyzed nucleophilic aromatic substitution furnished the desired xanthone **227** in a yield of 83%. Due to the potential leaving group ability of the O^{i}Pr group, xanthone **234** was also formed as a side product, albeit in very low yields when DMPU was used as the solvent. When TFA, MeOH, EtOH, or formamide were used as solvent, xanthone **234** was found to be the major product, concluding from their study that the selectivity of leaving group can be controlled by solvent polarity.[217]

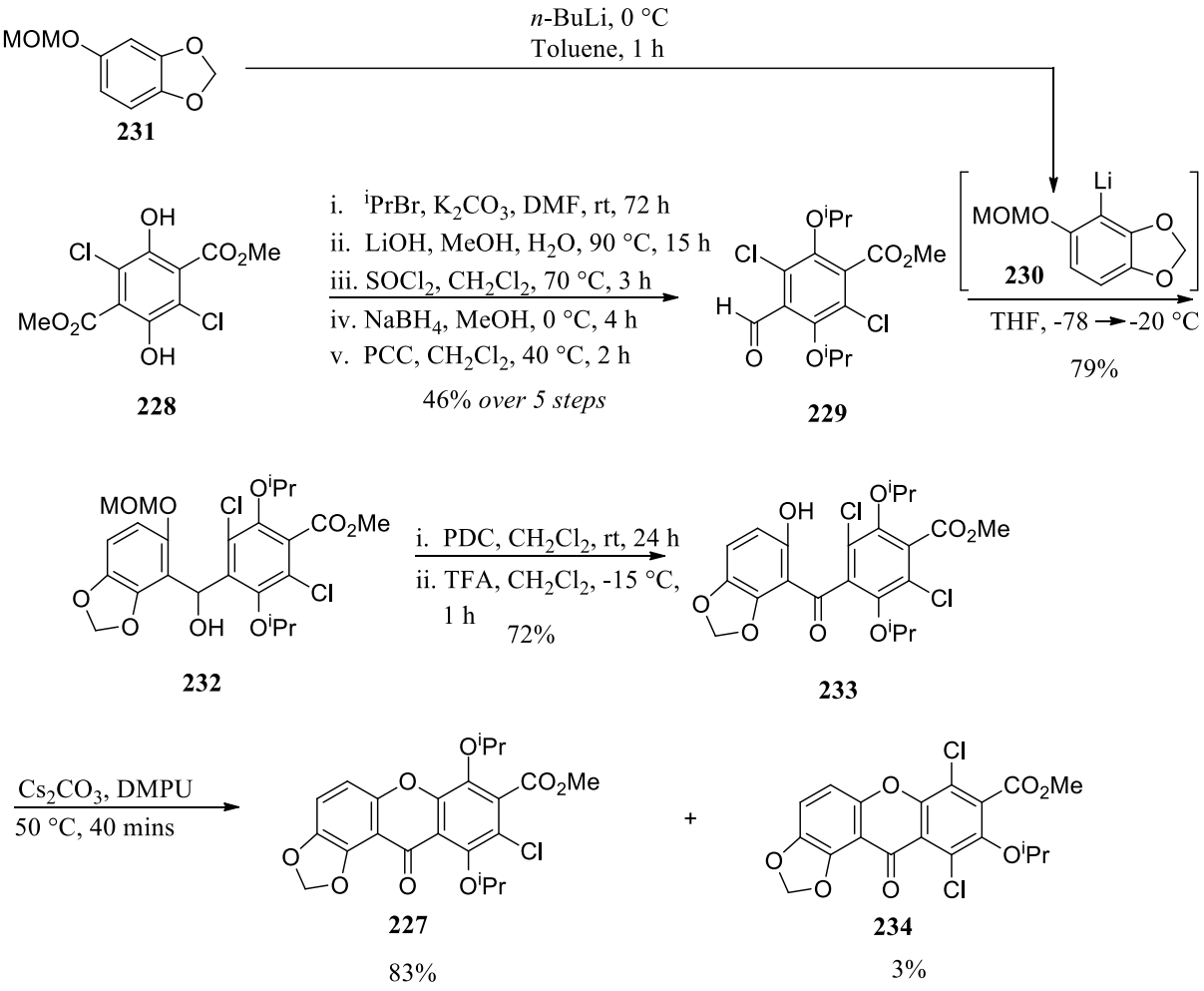

Scheme 71: Synthesis of the xanthone core of the antibiotic FD-594.[217]

Alternatively, the cyclization of benzophenone intermediates can take place *via* oxidative coupling.[203] In 2010, our research group reported on a novel cerium ammonium sulfate (CAS)-mediated oxidative coupling methodology for the synthesis of xanthones from methoxy-substituted benzophenones.[212, 218] This method allowed for the relatively facile oxidation of benzophenones possessing at least two methoxy groups, one that is *ortho* to the carbonyl bridge

of the benzophenone, and the second that is either *ortho* or *para* to the first methoxy group. A possible reaction mechanism that was proposed is shown in **Scheme 72**.[218] An initial single electron transfer of the electron-rich aromatic ring of benzophenone **235** possessing the methoxy groups could possibly lead to the radical cation **236**, which upon subsequent cyclization would result in the resonance-stabilized radical intermediate **237**. A one electron reduction of this intermediate in the presence of a proton leads to the formation of enol **238**, elimination of methanol from which subsequently results in the desired xanthone product **239**.

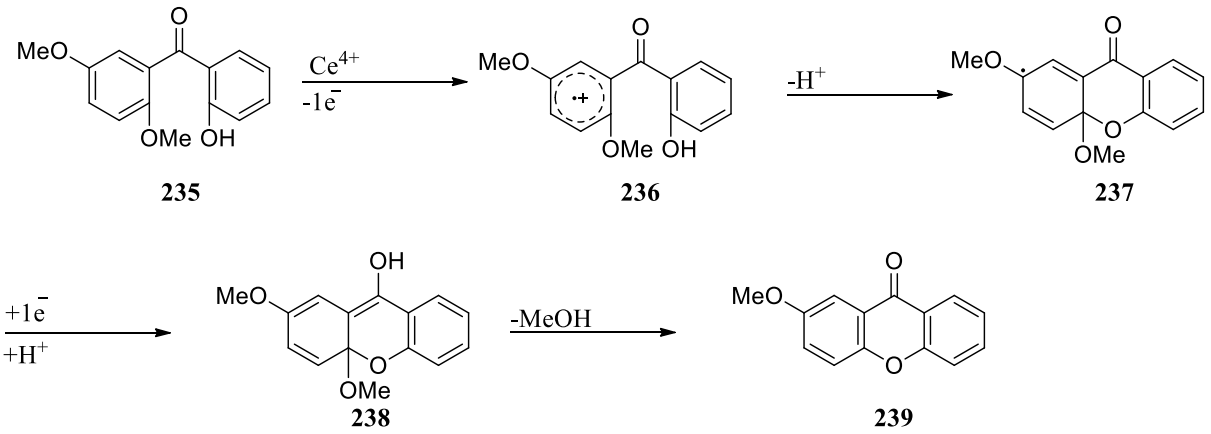

Scheme 72: A proposed reaction mechanism for the synthesis of xanthone using a CAS mediated oxidative coupling.[218]

Although the scope of this methodology in terms of methoxy groups has already been established, the scope in terms of the nature of the substrate (possession of various other functional groups) has not yet been fully recognized.

3.4 Ultraviolet radiation and absorption

The sun is often referred to as the source of life for all living organisms on the planet. Of the radiation emitted by the sun, known as solar radiation, around 92% is made up of visible light and infrared radiation.[219] The remaining 8% consists of ultraviolet (UV) radiation that is divided into three bands depending on the wavelength of radiation. UVC (200 – 290 nm) is almost completely filtered off by the ozone layer and is therefore of less biological significance than the other two types of UV radiation.[220] UVB (280 – 320 nm), which does reach the earth's surface, is primarily responsible for causing sun burns and erythema.[221] UVA (320 – 400 nm), which reaches the earth's surface in excess of UVB, is known to be largely responsible for causing photo-ageing, and, in conjunction with UVB, cause skin cancer, as well as

immunosuppression.[221-222] This indicates the pressing need for UV protectants or UV filters globally.

There exist two categories of UV filters: inorganic particulates and organic UV absorbers. Inorganic particulates absorb, scatter and reflect UVA and UVB rays, whereas organic UV absorbers filter UV rays purely by absorption of either UVA or UVB radiation, or both. Organic UV absorbers primarily comprise of at least one electron-donating group, and one electron-accepting group in either the *ortho* or *para* positions, which allow for the efficient delocalization of electrons. In addition, the presence of internal hydrogen bonding within the molecule, made possible in an *ortho*-disubstituted molecule, for example a benzophenone (see **Figure 23**), lowers the energy requirements for absorption, hence resulting in an increase in the absorption maxima wavelengths.[223]

Benzophenone

Benzophenone-
Resonance form

Figure 23: Electron delocalisation and hydrogen-bonding of a benzophenone.

3.5 Aim and objectives

The purpose of the second component of this PhD thesis is to use the CAS-mediated oxidative coupling methodology to synthesize a library of C15 side chain-substituted xanthones **240a-c**. Particular emphasis is placed on using bio-renewable cardanol **178a** as a starting material, to synthesize intermediate benzophenones **241** possessing either two or three methoxy groups in the requisite *ortho* and *para* positions (**Scheme 73**). The purpose of this is two-fold, firstly to establish the scope of the CAS methodology in terms of the nature of the substrate, and secondly to synthesize potential UV absorbers that could be used as sun protectants. This was encouraged by the promising UV absorption profiles of the compounds synthesized in our laboratory (refer to **Scheme 65**).[179] In order to accomplish the second feat, the synthesized xanthones will be subjected to late-stage oxidation protocols in order to introduce hydroxyl groups *ortho* to the carbonyl moiety, to furnish hydroxy-xanthones **242**. The ensuing internal hydrogen bonding effect is an important feature in rendering the molecule UV active.

The results of this endeavor are described in the following chapter.

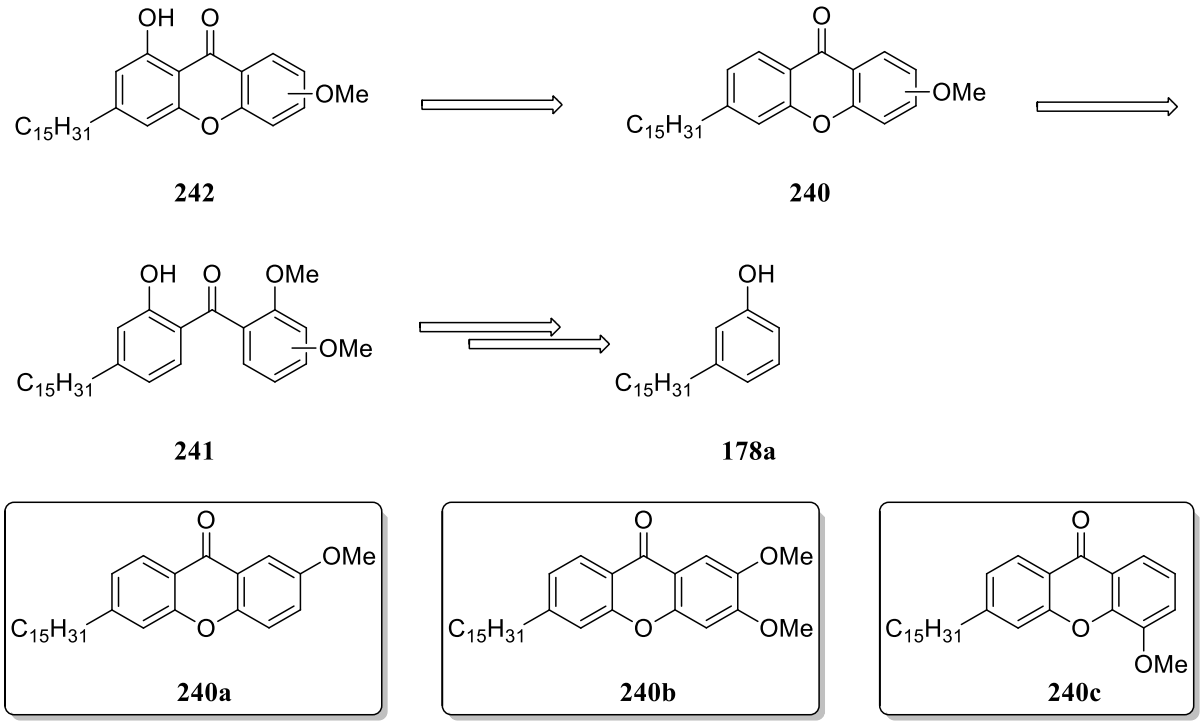

Scheme 73: Retrosynthetic scheme for the synthesis of xanthones.

CHAPTER 4

4.1 Synthesis plan

As was highlighted in Chapter 3, it was our primary aim to synthesize a library of UV absorbing compounds, specifically benzophenones and hydroxy-xanthones, using bio-renewable cardanol **178a** as a starting material. Our retrosynthetic plan entailed the use of the carbonyl-directed late-stage oxidation protocol described in Chapter 2 to assemble, for example, hydroxy-xanthone **242a** from xanthone **240a** (**Scheme 74**). We envisaged that the construction of xanthone **240a** could in turn be accomplished from benzophenone **241a** by exploiting the CAS oxidation procedure developed in our laboratory,[218] and this would also serve the purpose of enabling us to further ascertain the reproducibility and generality of this reaction. In our initial undertaking of the assembly of benzophenone **241a**, we envisioned using the Grignard reaction to couple formylated cardanol **243** with methoxy-substituted bromobenzene **244a**. The resulting secondary alcohol **245a** would be subjected to oxidation conditions to eventually lead to the desired benzophenone **241a**. The same retrosynthetic scheme applies for hydroxy-xanthones **242b** and **242c**, which we proposed to synthesize using bromobenzene **244b** and **244c** respectively. These specific bromobenzenes **244a-c** were chosen due to their methoxy-substitution patterns; i.e. two or more methoxy groups are present which are either *ortho* or *para* to each other, as this is a pre-requisite for the CAS oxidation reaction.[218]

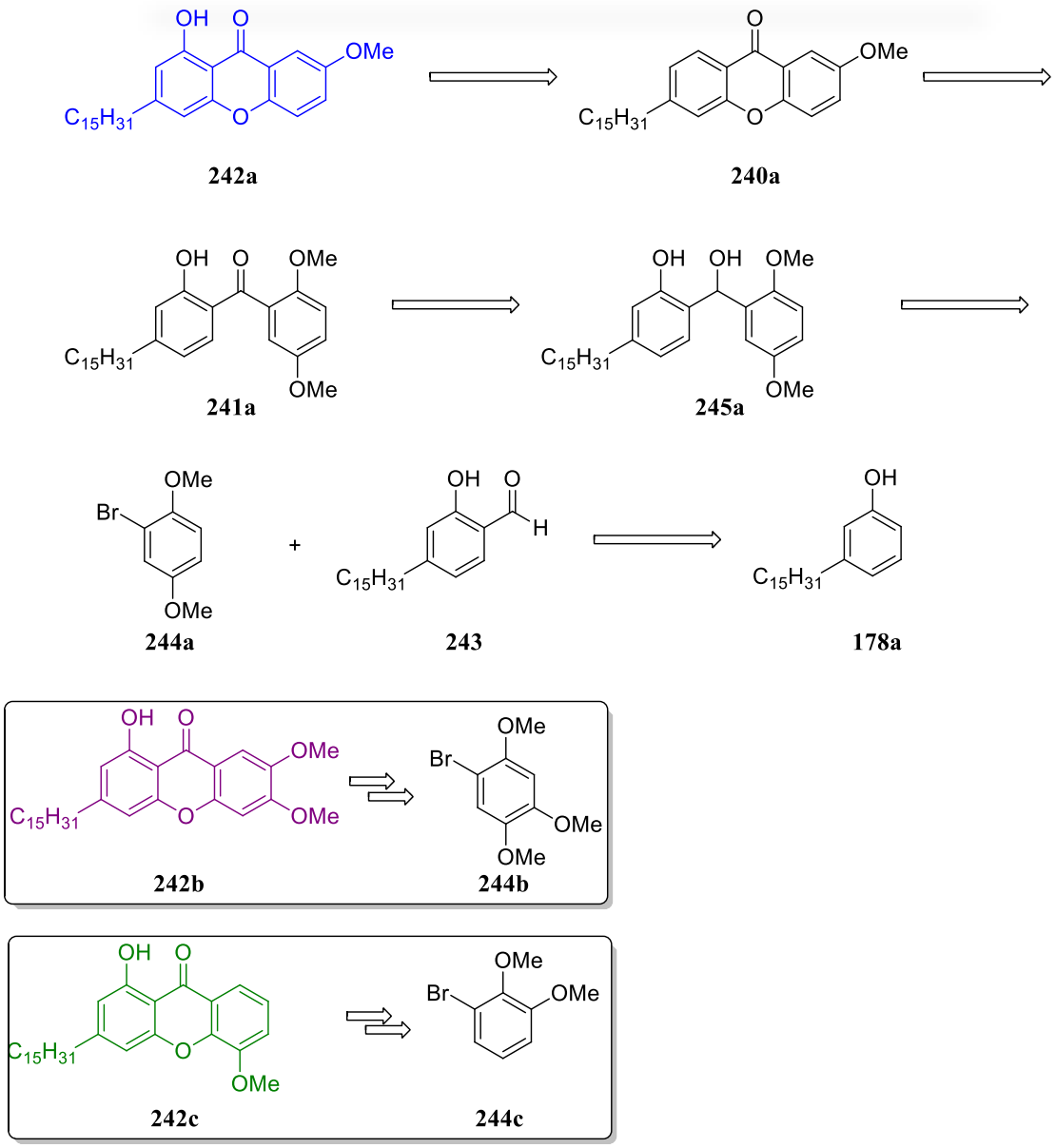

Scheme 74: Initial retrosynthetic plan for the synthesis of hydroxy-xanthones 242a-c.

Discussed in this chapter is our journey towards the synthesis of hydroxy-xanthones **242a-c**. Also presented are the results of the UV-absorbing properties of the synthesized benzophenones and hydroxy-xanthones.

4.2 Formylation of cardanol

The synthesis began with the formylation of cardanol **178a** to introduce an aldehyde moiety in the least sterically hindered position *ortho* to the phenol substituent (**Scheme 75**). This was achieved using the protocol developed by Casiraghi *et al.*[224] using *para*-formaldehyde as the formylating agent, triethylamine as the base, and tin(IV) chloride as the Lewis acid. The reaction mixture was then heated to 100 °C and stirred for 8 hours. Purification by column

chromatography furnished formylated cardanol **243**, the identity of which was confirmed by NMR spectral analysis, as a white solid in a decent yield of 67%. The presence of the aldehyde moiety was established in the ^{1}H NMR spectrum by the diagnostic peak at δ 9.84 ppm. This was further confirmed by the ^{13}C NMR spectrum which showed the appearance of a carbonyl peak at δ 195.7 ppm. The fact that the aldehyde moiety was *ortho* to the phenol group was verified by the strongly deshielded peak at δ 11.04 ppm, representing a hydrogen bonded phenol proton. The presence of a doublet signal at 7.41 ppm was representative of H-6 which couples only with H-5 (J = 7.8 Hz), confirming the identity of the desired formylated compound as opposed to the other *ortho*-regioisomer.

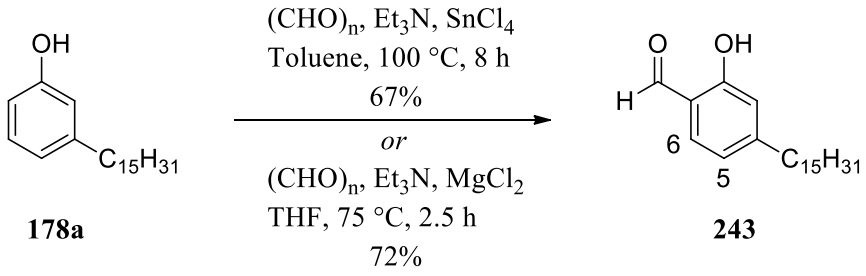

Scheme 75: Formylation of cardanol.

Although this reaction proceeded smoothly, the use of $SnCl_4$ is problematic as it is not the most pleasant Lewis acid to work with, especially on a large scale. We then decided to attempt the reaction using anhydrous $MgCl_2$ as the Lewis acid instead, and THF as the solvent. The reaction mixture was heated at 75 °C for 2.5 hours, after which, following an acidic work up, formylated cardanol **243** was readily isolated by recrystallization from methanol in a better yield of 72%.

4.3 Synthesis of benzophenone *via* Grignard and oxidation reactions

4.3.1 Grignard reaction

With the requisite aldehyde functionality in place, the next step was to bring about the union of **243** with methoxy-substituted bromobenzenes **244a-c** *via* the renowned Grignard reaction. We selected 2-bromo-1,4-dimethoxybenzene **244a** as our initial coupling partner, which was synthesized following literature precedent.[212] To form the Grignard reagent, bromobenzene **244a** in dry diethyl ether was treated with magnesium turnings. A granule of iodine was also added to activate the surface of magnesium. We observed that the mixture had to be gently heated to reflux for 4 hours, with repeated scratching of the surfaces of magnesium turnings, before the solution eventually turned white and cloudy, indicating the formation of the Grignard reagent. Thereafter, formylated cardanol **243** in dry THF was added *via* syringe and

then stirred for 18 hours at room temperature. The decision not to protect the phenol group of formylated cardanol **243** was undertaken primarily to maintain atom economy, as well as step-wise economy, as the use of protecting agents is certainly not in line with Green Chemistry principles.[17, 150] It should be noted however, that four equivalents of Grignard reagent had to be used to account for the free hydroxyl group. Although this contradicts with the Green Chemistry theme, 1,4-dimethoxybenzene was recovered to account for the wastage.

Much to our delight, the reaction was successful and purification by column chromatography led to the isolation of secondary alcohol **245a** as a cream-colored solid in a good yield of 78% (**Scheme 76**). This was ascertained by ^{1}H NMR spectral analysis by the presence of a doublet signal at δ 4.14 ppm representing methine H-1″, which couples (J = 4.5 Hz) with the secondary OH proton at δ 6.12 ppm, as anticipated. The aromatic phenol proton no longer appears in the strongly deshielded region, which is to be expected due to the absence of the aldehyde group and therefore the lack of a strong hydrogen bonding effect. This was further established by the ^{13}C NMR spectrum which lacks a carbonyl signal, and shows the appearance of a peak at δ 72.8 ppm representing C-1″.

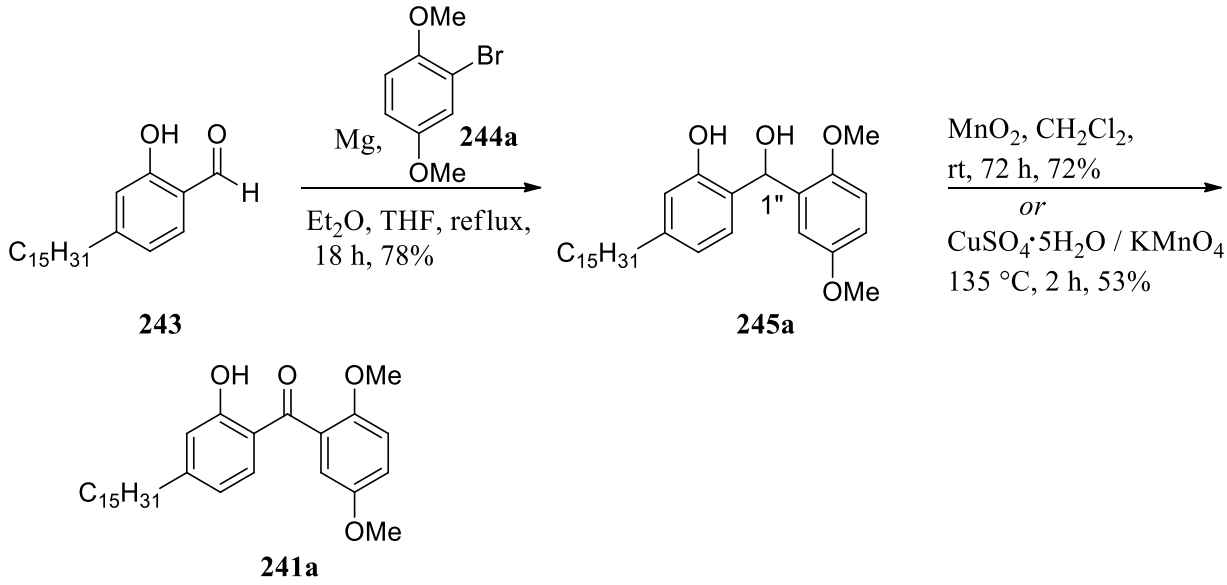

Scheme 76: Synthesis of benzophenone 241a.

4.3.2 Oxidation

To access the benzophenone intermediate **241a**, secondary alcohol **245a** was subjected to oxidizing conditions. This was initially achieved using the oxidant MnO_2 delivering benzophenone **241a** in a decent yield of 72%; however, the reaction took long periods to go to completion (**Scheme 76**). In an attempt to improve the conditions, the oxidation was repeated

using the $KMnO_4$ and $CuSO_4 \cdot 5H_2O$ solvent-free protocol as described in Chapter 2, heating the mixture at 135 °C. The reaction, which took only 2 hours to go to completion, was a success, albeit furnishing benzophenone **241a** in a lower yield of 53% following column chromatographic purification. ^{1}H NMR spectral analysis was used to verify the identity of the product. The appearance of a signal at δ 12.16 ppm was indicative of a strongly hydrogen bonded phenol proton. In addition, the disappearance of the peak at δ 4.14 ppm pointed towards the successful oxidation of the secondary alcohol. The signal at δ 200.9 ppm in the ^{13}C NMR spectrum confirmed the presence of a carbonyl functionality.

It was then that we inopportunely were met with a stumbling block, as reproducing the Grignard reaction proved to be problematic, even when attempted on the same scale as previously. All our attempts resulted only in the isolation of formylated cardanol **243**, despite the successful formation of Grignard reagent. It is quite possible that the free hydroxyl group of **243** was the reason behind the irreproducibility of the Grignard reaction. The decision to abandon this reaction was further strengthened when the same result was attained even with bromobenzenes **244b** and **244c** as substrates.

The time had inevitably come to get back to the drawing board.

4.4 An alternative route

4.4.1 Metal-mediated coupling and Friedel-Crafts acylation

Rather than undertaking the Grignard reaction on protected formylated cardanol, we chose to search for a more atom economical route. Naturally, the first to come to mind was C-H bond activation, in the anticipation of synthesizing the desired hydroxy-benzophenones in one step from formylated cardanol **243** (**Scheme 77**). Following literature precedent,[225-226] the palladium-mediated direct coupling of **243** with dimethoxybenzene **244a** was attempted. All our efforts at this rather ambitious endeavor, however, were met with failure, recovering only starting material in all cases.

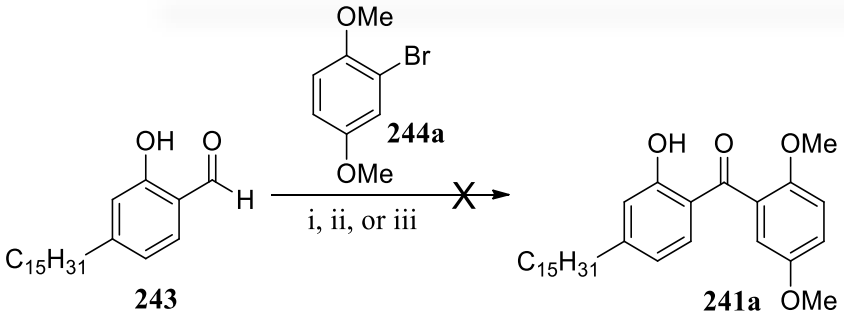

Scheme 77: Direct coupling of formylated cardanol 243 with bromobenzene 244a. ***Condition i***: *N*-cyclohexylpicolinamide, $Pd(OAc)_2$, $KHCO_3$, *Tert*-Amyl alcohol, sealed tube, 150 °C, 24 h. ***ii***: *N*-cyclopentylpicolinamide, $Pd(OAc)_2$, $KHCO_3$, *Tert*-Amyl alcohol, sealed tube, 150 °C, 24 h. ***iii***: TBABr, $PdCl_2$, NaOH (aq), 100 °C.

Consequently, we turned our attention to attempting Friedel-Crafts acylation instead, and various conditions were used to facilitate the acylation of cardanol **178a** with the acid chloride **246**, with the hope of achieving a one-step formation of benzophenone. This was sadly also met with failure. The only reaction condition that resulted in some acylation was the solvent-free, $TiCl_4$ mediated *ortho*-acylation protocol[126] (**Scheme 78**). This resulted in negligible amounts of crude **247** which was identified by the presence of two strongly hydrogen bonded phenol protons, and the absence of methoxy groups. Since very small amounts were formed, no effort was made to isolate the compound from the crude mixture.

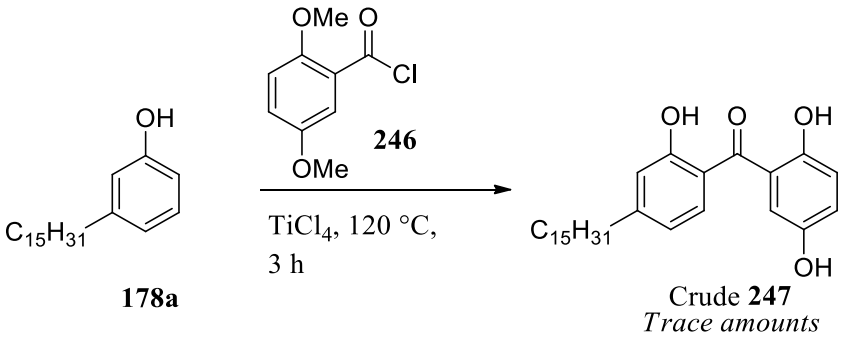

Scheme 78: Attempted Friedel-Crafts acylation of cardanol.

Not yet willing to give up, we then resolved to try treating the commercially available acid **248a** with TFAA to form the respective anhydride, which we anticipated, would serve as a good acylating agent. Due to the free hydroxy group, we reasoned that it was also possible that the reaction would result in the formation of an ester. Acid **248a** was stirred with TFAA for 10 minutes and thereafter, cardanol **178a** dissolved in CH_2Cl_2 was added and the mixture stirred

at room temperature for 8 hours. TLC analysis showed the complete consumption of starting material, and only one spot was observed on the TLC; normally a good sign.

Purification by column chromatography led not to the isolation of the desired benzophenone **241a**, but rather, and not unexpectedly, to the isolation of ester **249a** in near quantitative yields (**Scheme 79**) as a pale yellow low melting solid, whose identity was elucidated by NMR spectral analysis. It was immediately clear that a Friedel-Crafts acylation had not taken place, due to the absence of any strongly deshielded signals representing a hydrogen-bonded phenol proton. A total number of seven aromatic protons were observed, pointing towards an ester. This was verified by the ^{13}C NMR spectrum which showed the presence of an ester carbonyl peak at δ 164.3 ppm. To further establish that an ester had indeed formed, an HRMS of the sample was run, which gave a mass of 469.3299, agreeing well with the calculated mass $[M + H]^+$ of 469.3318.

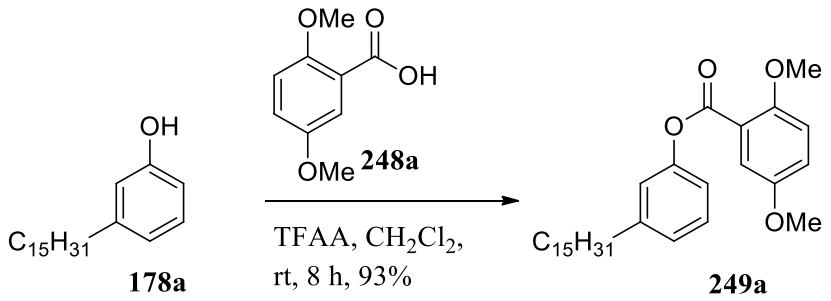

Scheme 79: Synthesis of ester 249a from cardanol.

4.4.2 Esterification and Fries rearrangement

Excited about the ease with which the ester formed, and not to mention the excellent yields, we chose to try these reaction conditions to form esters **249b** and **249c** from the commercially available acids **248b** and **248c** respectively with cardanol **178a** (**Scheme 80**). We envisioned that the desired hydroxy-benzophenones **241a-c** could then be formed *via* Fries rearrangement of the corresponding esters **249a-c**. This rather more elegant sequence would not only be more atom economical than performing a Grignard reaction, but would also result in a more step-wise economical synthesis.

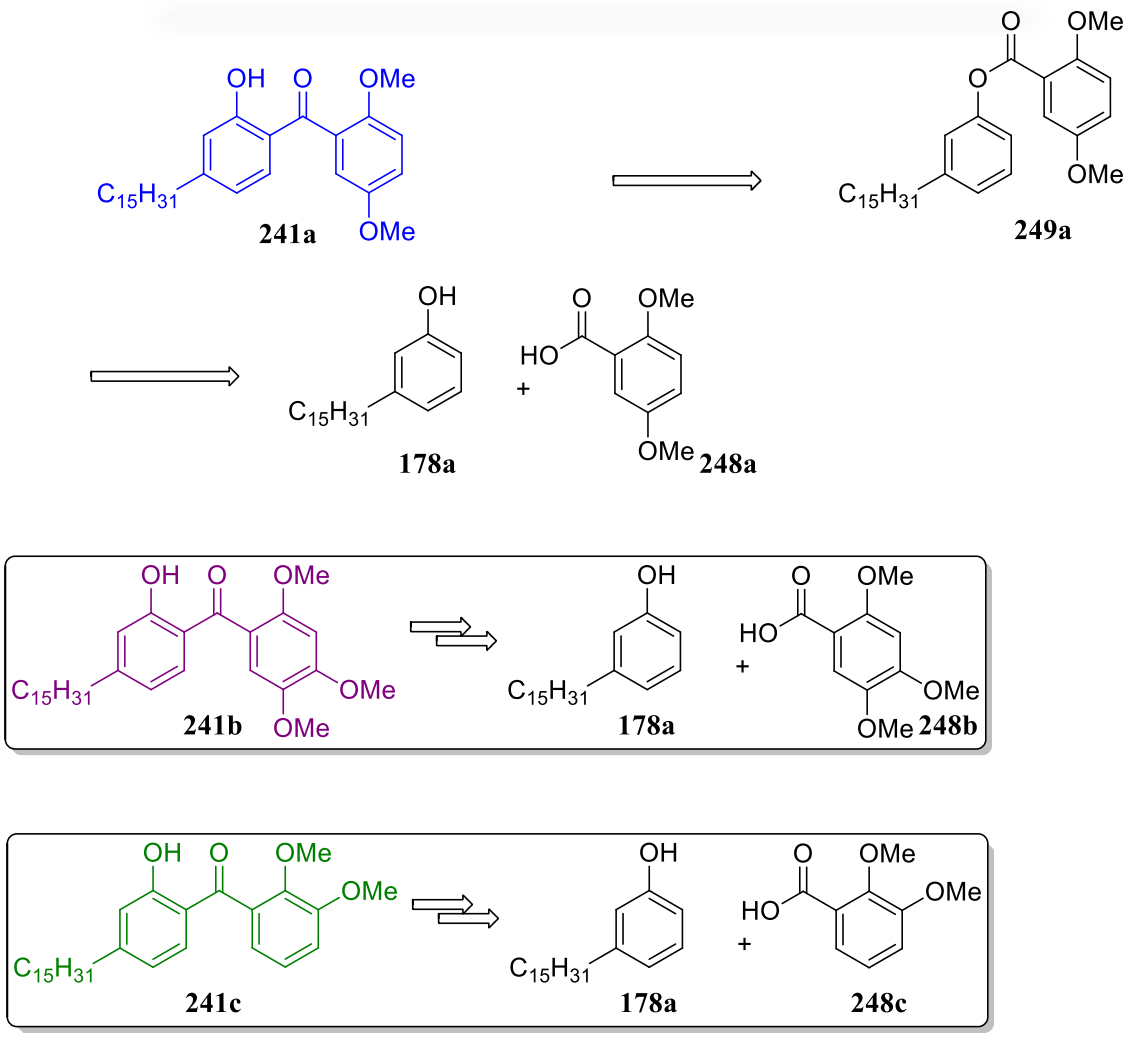

Scheme 80: Alternative retrosynthetic plan towards the synthesis of benzophenones 241a-c.

4.4.2.1 Esterification

Esters **249b** and **249c** were readily synthesized from acids **248b** and **248c** respectively, using the same procedure as described for the formation of ester **249a**. The reaction worked very well for both substrates, furnishing ester **249b** as a white solid in 94% yield, and ester **249c** as a white solid in 96% yield (**Scheme 81**). Similar NMR spectra were obtained for both esters as that for ester **249a**, with the requisite number of six and seven aromatic protons being observed for **249b** and **249c** respectively. Three sets of methoxy group protons at δ 3.97, 3.93, and 3.90 ppm were observed for ester **249b**, and two sets for ester **249c** at δ 3.96, and 3.92 ppm as expected. Furthermore, a signal representing the ester carbonyl functionality was observed for both esters in the region δ 165 – 163 ppm of the ^{13}C NMR spectra.

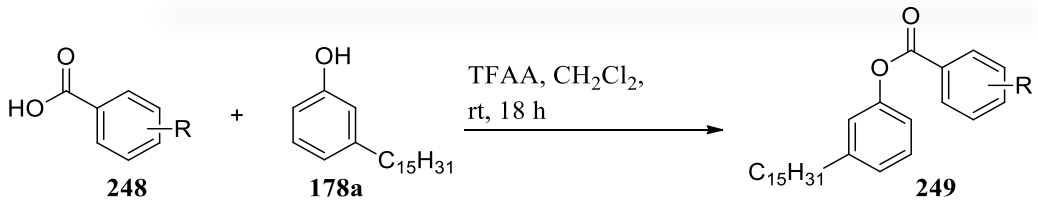

Substrate	Product	Yield (%)
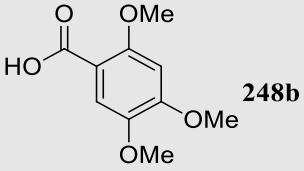 **248b**	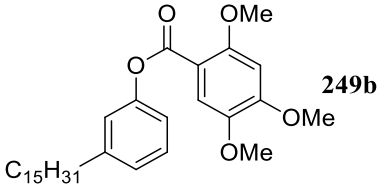 **249b**	94
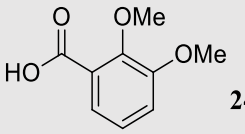 **248c**	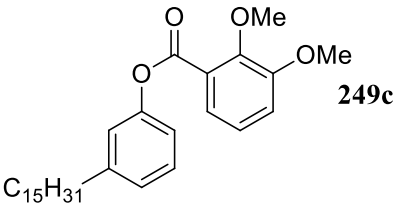 **249c**	96

Scheme 81: Formation of esters 249b-c.

It was clear that the reaction conditions resulted in excellent yields of esters; however, in trying to keep in line with the Green Chemistry theme as much as possible, it was unavoidable that we investigate if this reaction could proceed in a non-chlorinated solvent. Initially, we chose to screen the polar solvents acetonitrile and 2-methyltetrahydrofuran. Using acetonitrile resulted solely in the recovery of cardanol **178a** for esters **249a** and **249c**, whereas ester **249b** was formed in a poor yield of 40%. Replacing CH_2Cl_2 with 2-methyltetrahydrofuran led to the formation of ester **249a** in a poor yield of 38% upon refluxing, and only cardanol **178a** was recovered for esters **249b-c**.

Interestingly, when the non-polar solvent toluene was used instead, the esterification proceeded smoothly for all three substrates (**Scheme 82**). It is possible that this is as a result of the better solubility of cardanol-based substrates in toluene, owing to the long hydrocarbon chain. Nevertheless, with toluene being a bio-renewable solvent,[227] this was indeed an exciting result.

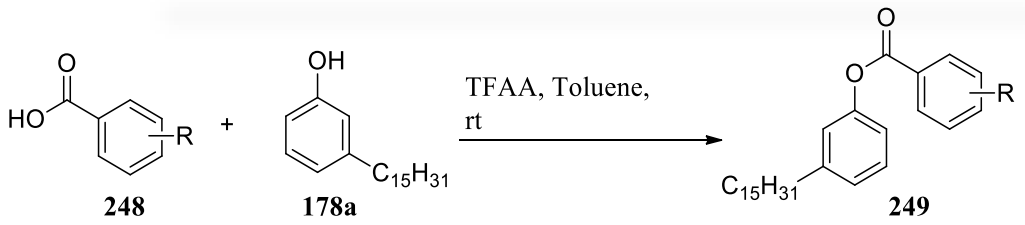

248 178a 249

Substrate	Time (h)	Product	Yield (%)
248a	3	**249a**	95
248b	18	**249b**	78
248c	18	**249c**	83

Scheme 82: Synthesis of esters 249a-c using toluene as solvent.

4.4.2.2 Fries rearrangement

This early success was morale boosting, and, armed with the requisite esters, we proceeded to attempt the *ortho*-Fries rearrangement as planned, to deliver the desired hydroxy-benzophenones **241a-c**. It was, however, not long before we realized that this seemingly easy task would prove to be more difficult than first presumed. Various conditions were tried with either no success or with very little success. Beginning with ester **249a**, traditional methods involving heating with Lewis acids such as $AlCl_3$ only led to decomposition, whereas photochemical conditions disappointingly resulted in mixtures of the *ortho* and *para* regioisomers in very low yields. Anionic Fries rearrangement conditions were also attempted, albeit with no success. Eventually electing to use Eaton's reagent,[228] that has often been met with success in mediating Fries rearrangements, the reaction mixture was heated in an oil bath to 100 °C. This led to the isolation of cardanol **178a**, indicating that dissociation of the ester-acid complex did take place; however nucleophilic attack of the aromatic ring with the acylium ion failed to occur. Not discouraged, the reaction was attempted again, this time in the microwave. Phosphorous pentoxide (7.7% of the weight of methanesulfonic acid) was carefully added to a microwave tube, although care had to be taken to minimize exposure to air. Thereafter, methanesulfonic acid and ester **249a** were added, and the mixture was heated under microwave irradation at 80 W for 30 minutes at 100 °C. To our satisfaction, it was observed, following purification by column chromatography, that small amounts of the *ortho* hydroxy-benzophenone **241a** were generated. A series of optimization studies ensued immediately after, with the best yield of 50% being obtained when nine equivalents of methanesulfonic acid were used, 7.7% of phosphorous pentoxide, at 50 W, and a temperature of 80 °C for 15 minutes (**Scheme 83**). Some starting material was recovered (20%), which could be recycled.

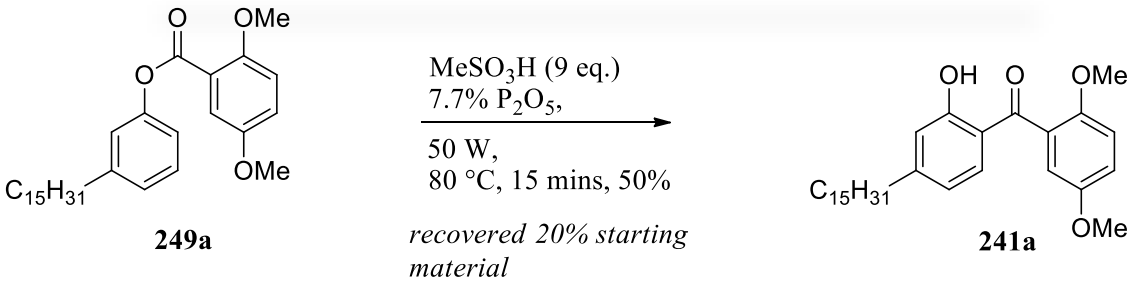

Scheme 83: Fries rearrangement of ester 249a.

The identity of the product was established by NMR spectral analysis. The characteristic hydrogen-bonded phenol proton was represented in the ^{1}H NMR spectrum by the signal at δ 12.16 ppm, confirming that an *ortho*-Fries rearrangement had taken place. The two methoxy group protons at δ 3.77 and 3.72 ppm were also present, as were six aromatic protons. The success of the reaction was further pronounced by the ^{13}C NMR spectrum by the shift in the carbonyl peak from δ 164.3 ppm to δ 200.9 ppm, confirming the presence of a ketone. In addition, the signal at δ 163.1 ppm was representative of the aromatic carbon bearing the hydroxyl substituent.

When these conditions were tried on esters **249b-c**, rearrangement disappointingly failed to occur. It seemed like it was back to square one, having to try various conditions to get the rearrangement to occur. The only Lewis acid that seemed to show promising results for both esters **249b-c** was trifluoromethanesulfonic acid (CF_3SO_3H). After the screening of various solvents, it was observed that the Fries rearrangement of ester **249b** would only proceed by heating in acetonitrile, albeit forming benzophenone **241b** as a white solid in a low yield of 20% (**Scheme 84**). All attempts at improving this yield failed.

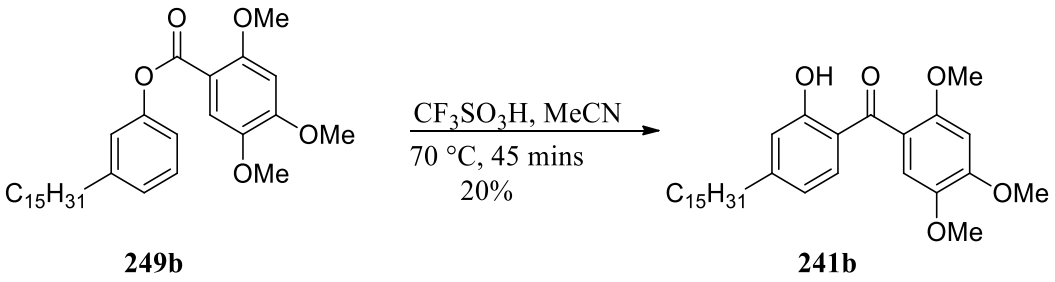

Scheme 84: Fries rearrangement-mediated synthesis of benzophenone 241b.

Analysis of the ^{1}H NMR spectrum of compound **241b** confirmed the presence of the hydrogen-bonded phenol proton by the strongly deshielded signal at δ 12.25 ppm. This was accompanied by three singlets representing the methoxy group protons at δ 3.97, 3.84 and 3.76 ppm, as well

as five aromatic protons. A ketone carbonyl signal was observed at δ 200.4 ppm in the ^{13}C NMR spectrum, and the aromatic carbon bearing the hydroxyl substituent at δ 163.0 ppm.

Whereas the Fries rearrangement of ester **249c** proceeded to give a good yield (63%) of benzophenone **241c**, as a clear, low melting solid, with CF_3SO_3H in toluene (**Scheme 85**). Similar to the NMR spectra of benzophenones **241a** and **241b**, the OH proton was observed at δ 12.20 ppm, two methoxy group protons were observed at δ 3.91 and 3.79 ppm, and six aromatic protons were observed. The ^{13}C NMR spectrum displayed a ketone carbonyl peak at δ 201.0 ppm, and the carbon bearing the hydroxyl substituent at δ 163.1 ppm.

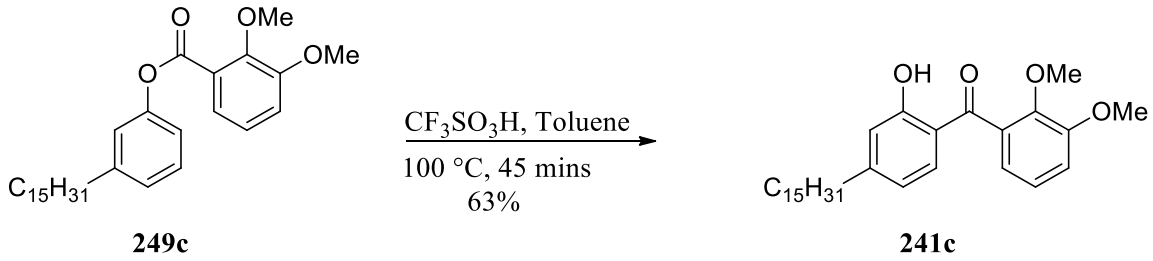

249c **241c**

Scheme 85: Fries rearrangement-mediated synthesis of benzophenone 241c.

4.5 Synthesis of xanthones

Having secured the hydroxy-benzophenone moieties **241a-c**, the subsequent step involved generating the corresponding methoxy-substituted xanthones. We anticipated achieving this using CAS-mediated oxidation reaction conditions.[218] To this end, the benzophenone substrate was dissolved in a mixture of acetonitrile and a small amount of $CHCl_3$ in a ratio of 1:0.25. Water was then added to form a suspension, to which CAS was added. For all three substrates **241a-c**, the reaction mixture had to be heated to 70 °C, in contrast to the original procedure done at room temperature, to attain complete consumption of starting material. Much to our delight, the reactions proceeded smoothly and efficiently, and following purification by column chromatography, the resulting xanthones were isolated with generally good yields as white solids (**Scheme 86**).

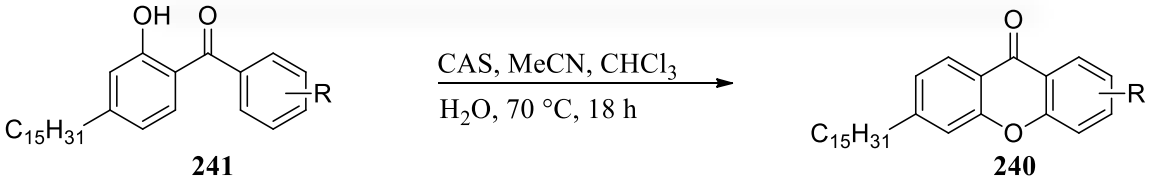

Substrate	Product	Yield (%)
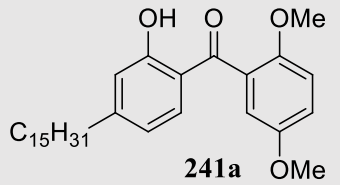 **241a**	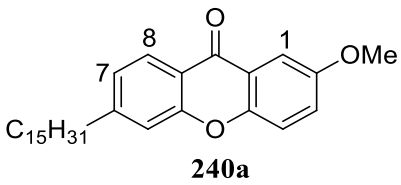 **240a**	70
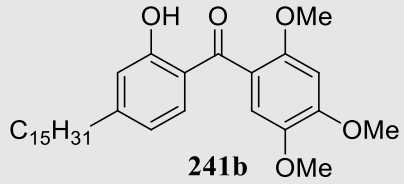 **241b**	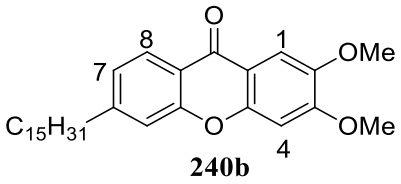 **240b**	74
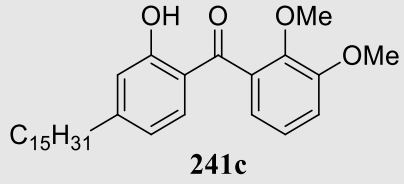 **241c**	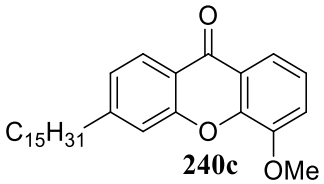 **240c**	57

Scheme 86: Synthesis of xanthones 240a-c *via* CAS oxidation.

The identity of xanthone **240a**, which was furnished with a yield of 70%, was ascertained by NMR spectral analysis. It was evident from the ^{1}H NMR spectrum that the hydrogen bonded OH proton was absent. In addition, only one set of methoxy group protons were present, represented by the signal at δ 3.92 ppm. H-8 and H-7 appeared at δ 8.24 and 7.20 ppm respectively, coupling with each other (J = 8.2 Hz). H-1 appeared as a singlet at δ 7.71 ppm. The ^{13}C NMR spectrum showed the presence of a carbonyl group at δ 177.9 ppm, and a methoxy carbon at δ 55.9 ppm. To further establish that the xanthone had indeed formed, an HRMS of the sample was obtained, and a mass of 437.3024 was found which agrees well with the calculated mass of $[M + H]^{+}$ of 437.3056.

Similarly, the identities of xanthones **240b** and **240c** were established by NMR spectral analysis. For xanthone **240b**, two methoxy groups were present as expected at δ 4.02 and 4.00 ppm. H-1 and H-4 appeared as singlets, as was anticipated, at δ 7.67 and 6.90 ppm, and H-8 appeared as a doublet at δ 8.24 ppm, coupling with H-7 at δ 7.20 ppm (J = 8.2 Hz). The ^{1}H NMR spectrum of xanthone **240c** displayed a signal for one set of methoxy group protons at δ 4.05 ppm. For both xanthones **240b** and **240c**, the carbonyl signal appeared in the ^{13}C NMR

spectrum in the range of δ 176 – 177 ppm. The HRMS mass found for xanthone **240b** was 467.3145 which is in concurrence with the calculated mass $[M + H]^+$ of 467.3161, and the mass found for xanthone **240c** was 437.3050 which is in excellent agreement with the calculated mass $[M + H]^+$ of 437.3056.

Satisfied that the modified CAS oxidation protocol for the synthesis of xanthones works even for compounds possessing long chains, i.e. derived from CNSL, we could happily move on to the consequent and final step of our synthesis.

4.6 Synthesis of hydrogen-bonded xanthones

As the aim was to synthesize UV absorbers, a hydroxyl functionality was to be appended onto the xanthone moiety, which we anticipated would serve the purpose of rendering aromatic compounds with good UV-absorbing properties. We envisaged achieving this in an atom economical way by means of the carbonyl-directed late-stage OH functionalization reaction.[141-142, 144] Since our requirement was only for a hydrogen-bonded hydroxyl group, whether the hydroxyl group was directed to the cardanol half of the xanthone, or the aromatic methoxy-substituted half of the xanthone was of irrelevance for our purposes. However, based on literature, the carbonyl-directed hydroxyl functionalization is influenced primarily by electronic and steric effects.[144]

The reaction was set up in a similar manner as was described in chapter 2. Xanthone **240a** was placed in a 2.5 ml sealed tube, to which was added PIFA, $Ru[(p\text{-cymene})Cl_2]_2$, and TFAA and TFA in a ratio of 1:0.02 ml. The tube was sealed and placed in an oil bath heated to 80 °C for 18 hours. Following an acidic work up, purification by column chromatography led, much to our delight, to the isolation of hydroxy-xanthone **242a** as a pale-yellow solid, albeit in a poor yield of 38% (**Scheme 87**). It should be noted that, in an attempt at improving the yield, the reaction was repeated again using PIDA as the oxidant; however, this disappointingly led to a decreased yield of 10%. When $K_2S_2O_8$ was used as the oxidant, a yield of 20% was obtained.

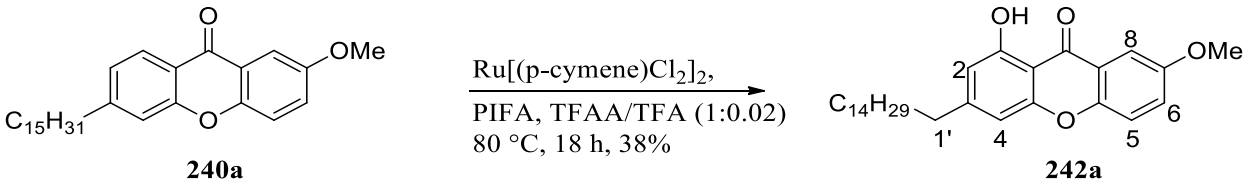

Scheme 87: Hydroxy functionalization of xanthone 240a

The hydrogen-bonded hydroxyl group was clearly visible in the ^{1}H NMR spectrum at δ 12.57 ppm. H-2 and H-4 appeared as singlets at δ 6.64 and 6.76 ppm respectively. H-8 appeared as a doublet at δ 7.62 ppm, coupling with H-6 at δ 7.33 ppm (J = 2.9 Hz), confirming that the hydroxyl group had appended to the cardanol half of the molecule, *ortho* to the carbonyl group. This was also established using the COSY spectrum, which showed a positive correlation between the hydroxyl group proton and H-1′ of the chain. H-5 was observed at δ 7.40 ppm as a doublet, also coupling with H-6 (J = 9.1 Hz). The carbonyl peak was observed at δ 181.6 ppm, and the carbon bearing the hydroxyl group at δ 161.5 ppm. Furthermore, an HRMS of the sample was obtained, and a mass of 453.2978 was found, which corresponds to the calculated mass $[M + H]^+$ of 453.3005.

The execution of the reactions for the synthesis of hydroxy-xanthones **242b** and **242c** was done in a similar manner to that for the synthesis of hydroxy-xanthone **242a**. An optimized yield of 43% for the synthesis of hydroxy-xanthone **242b** was obtained when $K_2S_2O_8$ was used as the oxidant, in conjunction with an optimized ratio of TFA:TFAA of 1:0.05 ml (**Scheme 88**). The hydroxyl group was observed at δ 12.72 ppm as a singlet signal. Just as was anticipated, H-8 and H-5 appeared as singlet signals at δ 7.57 and 6.88 ppm respectively. H-4 and H-2 also appeared as singlet signals at δ 6.73 and 6.63 ppm respectively. The carbonyl peak was observed at δ 180.6 ppm and the hydroxyl carbon at δ 161.3 ppm.

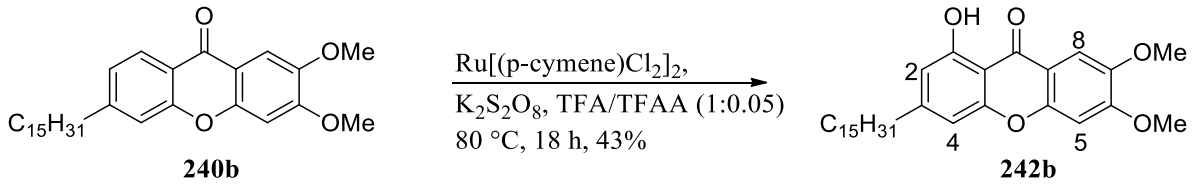

Scheme 88: Hydroxy functionalization of xanthone 240b.

Hydroxy-xanthone **242c** was prepared using PIFA as the oxidant, and a TFAA:TFA ratio of 1: 0.02 ml, albeit isolated in a poor yield of 26%, as a yellow solid (**Scheme 89**). It was clear, from NMR spectral analysis, that the hydroxyl group had been directed to the aromatic methoxy-substituted half of the xanthone, in contrast to xanthones **242a-b**. The hydroxyl group was certainly *ortho* to the carbonyl group, as was evidenced by the deshielded signal at δ 12.09 ppm due to hydrogen-bonding. However, a doublet signal was seen at δ 8.11 ppm representing H-8, coupling with H-7 at δ 7.21–7.14 ppm (J = 8.1 Hz). H-5 was seen at δ 7.34 ppm as a singlet, and H-3 as a doublet at δ 6.66 coupling with H-2 at δ 7.21–7.14 ppm (J = 8.7 Hz). Furthermore, an analysis of the COSY spectrum showed a lack of correlation of the hydroxyl

group with the chain, unlike that which was observed with xanthones **242a** and **242b**. HRMS data of hydroxy-xanthones **242b** and **242c** displayed signals at 483.3098 and 453.2995 respectively, concurring well with the calculated masses $[M + H]^+$ of 483.3110 and 453.3005 respectively.

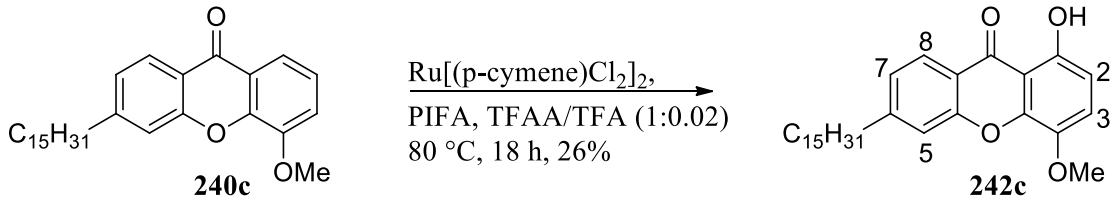

Scheme 89: Hydroxy functionalization of xanthone 240c.

With the desired hydrogen-bonded xanthones thus prepared successfully, what remained now was to analyze the compounds for their UV absorbing capabilities.

4.7 UV absorption analysis

Consequently, the UV spectral behaviour of the benzophenones **241a-c** and hydroxy-xanthones **242a-c** in relation to their UV absorption maxima in the range of 250 – 400 nm were analyzed, and the corresponding molar absorption coefficients (ε) were determined.

All three benzophenones were found to absorb in the UVA region of the UV spectrum, and a comparison of the molar absorption coefficients of benzophenones **241a-c** is shown in **Figure 23**. Benzophenone **241a** was found to show a good UV absorption profile in the UVA region at 338 nm (ε = 9045 L mol^{-1} cm^{-1}), whereas benzophenone **241b** showed excellent UV absorbance, also in the UVA region at 345 nm (ε = 13016 L mol^{-1} cm^{-1}). This value compares agreeably to that of the previously synthesized benzophenone derived from cardanol.[179] Benzophenone **241c** showed equally good UV absorption properties in a similar region of the UV spectrum, with a molar absorption coefficient of 10311 L mol^{-1} cm^{-1} at 334 nm. It was also observed that all three benzophenones displayed excellent UV absorption towards the end of the UVC region (**Figure 23**), however this is of less relevance to their potential use in sunscreens, or for the protection of materials on exposure to the sun.

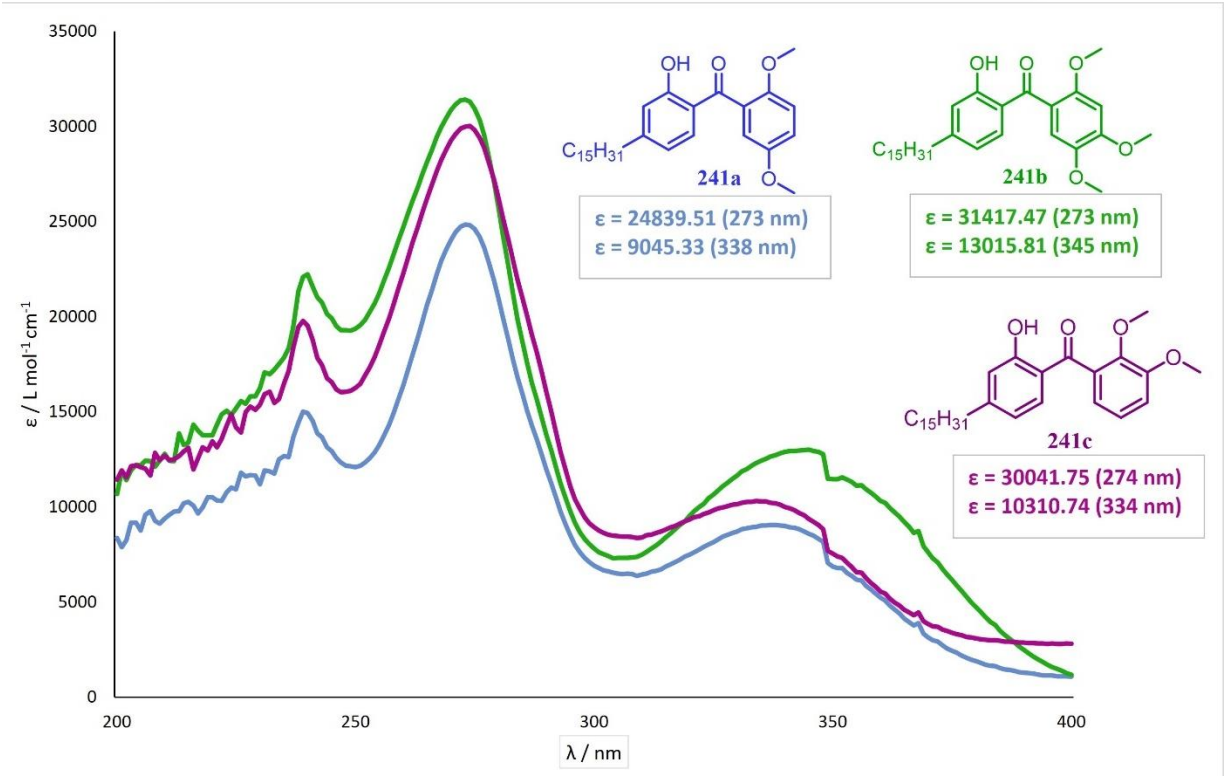

Figure 24: Molar absorption coefficients of the benzophenones 241a-c

While the hydroxy-xanthones **242a-c** generally were found to absorb in both the UVA and UVB regions. The comparison of their molar absorption coefficients is displayed in **Figure 24**. Hydroxy-xanthone **242a** displayed excellent UVB absorption properties, with a maximum absorption at 290 nm (ε = 12628 L mol^{-1} cm^{-1}). An absorbance was also observed in the UVA region, with a maximum absorption at 384 nm and a molar absorption coefficient of 6654 L mol^{-1} cm^{-1}, qualifying it as broad-spectrum UV absorbing agent. In contrast, hydroxy-xanthone **242c** was found to absorb in the UVA region only, albeit with lower molar absorption coefficients, with absorption maxima at 348 nm (ε = 2897 L mol^{-1} cm^{-1}), and at 384 nm (ε = 4119 L mol^{-1} cm^{-1}) being observed. Hydroxy-xanthone **242b**, much to our delight, was found to show the best UV absorption profile in the UVB region, with a molar absorption coefficient of 20320 L mol^{-1} cm^{-1} at 290 nm, as well as in the UVA region with a molar absorption coefficient of 13949 L mol^{-1} cm^{-1} at 368 nm. The hydroxy-xanthones, similarly to the benzophenones, all display excellent UV absorption in the UVC region (**Figure 24**).

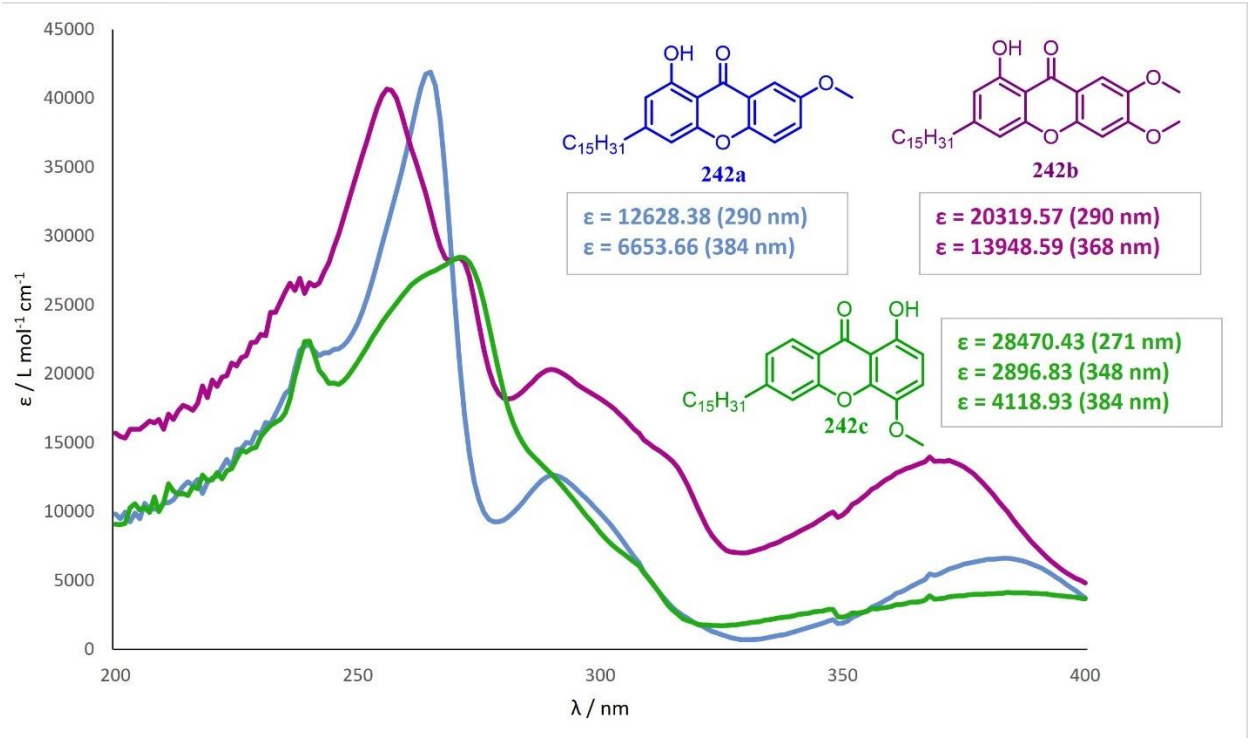

Figure 25: Molar absorption coefficients for hydroxy-xanthones 242a-c.

In comparison, the commercially available UV absorbing agent oxybenzone (OB, now banned in some areas of the world as a sunscreen)[229] has a molar absorptivity coefficient of 15150 L mol^{-1} cm^{-1} at 287 nm, in the UVB region. Hydroxy-xanthone **242a** compares agreeably with this, while hydroxy-xanthone **242b** far surpasses this absorption in the UVB region. The sun protectants 2-ethyl hexyl 4-methoxycinnamate (OMC), and avobenzone on the other hand have large molar absorption coefficients in the UVA region of 39470 L mol^{-1} cm^{-1} at 356 nm, and 31670 L mol^{-1} cm^{-1} at 310 nm respectively.[230] Although our synthesized benzophenones and hydroxy-xanthones do not compare to these values, they have the advantage of being derived, at least partially, from a bio-renewable source. Furthermore, since hydroxy-xanthones **242a** and **242b** were found to absorb in both the UVA and UVB regions, they can be classified as broad-spectrum UV protectants.

4.8 Conclusion

The use of bio-renewable feedstock in the form of cardanol **178a** derived from CNSL has been successfully demonstrated in the four-step synthesis of hydroxy-xanthones. Fries rearrangement-mediated benzophenone intermediates possessing two or more methoxy groups either *ortho* or *para* to each other were synthesized, and served as precursors to the key CAS-mediated oxidation protocol for the synthesis of xanthones. The reaction proceeded to smoothly

and efficiently deliver the desired xanthones in good yields, under optimized conditions. Finally, in order to introduce a hydroxyl group *ortho* to the carbonyl functionality of the xanthones, ruthenium-catalyzed late-stage oxidation conditions were implemented. Hydroxy-xanthone **242a** was formed in an overall yield of 13%, hydroxy-xanthone **242b** in an overall yield of 5%, and hydroxy-xanthone **242c** in an overall yield of 8% based on cardanol as the starting material. The benzophenones and hydroxy-xanthones were thereafter analyzed for their UV absorption properties. Benzophenone **241b** displayed excellent UV absorption in the UVA region with a molar absorption coefficient of 13016 L mol^{-1} cm^{-1} at 345 nm, and hydroxy-xanthone **242b** was found to absorb brilliantly in both the UVA and UVB regions with molar absorption coefficients of 20320 L mol^{-1} cm^{-1} at 290 nm, and 13949 L mol^{-1} cm^{-1} at 368 nm, qualifying it for a broad-spectrum UV protectant.

This work was peer-reviewed and has been accepted for publication.[231]

4.9 Future work

In keeping in line with the Green Chemistry theme, the synthesis of the hydroxy-xanthones should be attempted again so that all atoms of the final products are derived from a bio-renewable source. Asaronic acid from asarone, as well as catechol and hydroquinone are potential examples of bio-renewable starting materials that could be used for the syntheses of acids **248a-c**. Furthermore, with the CAS oxidation being the only step in the synthesis that makes use of a chlorinated solvent, the conditions must be revisited so as to replace the chloroform with an alternative solvent. 2-Methyltetrahydrofuran is a green solvent alternative that will be considered. This will allow for a completely sustainable synthesis of these UV-absorbing compounds.

Since hydroxy-xanthone **242b** displays the most promising properties in terms of UV-absorption due to an excellent broad-spectral absorption profile, it could serve as the main UV-absorbing active ingredient for sunscreens, or for protecting materials against the damaging effects of UV radiation. In addition, the lipophilic nature of **242b** will make it easily spreadable on skin when used in sunscreen formulations, and, as a result of its high molecular weight, penetration through the dermis should be minimal. Photostability studies, however, must first be conducted to ensure that the compound does not degrade upon exposure to UVB and UVA light. Additionally, cytotoxicity studies have to be thoroughly conducted before any conclusions regarding the application of the hydroxy-xanthone **242b** in sunscreen formulations can be made.

CHAPTER 5

5.1 General experimental procedures

5.1.1 Laboratory solvents and reagents

All reagents used during the course of this project were purchased from ACE Chemicals or Sigma-Aldrich, and were used without purification unless otherwise stated. All solvents (except 1,2-dimethoxyethane, and 1,2-dichloroethane) used were distilled under a nitrogen atmosphere prior to use. Dichloromethane (CH_2Cl_2) and acetonitrile (MeCN) were distilled over calcium hydride. Tetrahydrofuran (THF) and diethyl ether (Et_2O) were distilled over sodium wire in the presence of benzophenone as indicator. Toluene was distilled over sodium metal.

All reactions were performed under nitrogen gas, unless otherwise stated.

5.1.2 Chromatographic separation

Reactions were monitored using thin layer chromatography (TLC) which was performed on Macherey-Nagel Alugram Sil G/UV254 plates pre-coated with 0.25 mm silica gel 60. The TLC plates were viewed under UV light (254 nm and 366 nm). Purification of products from reactions was achieved using either normal column chromatography on silica gel 60 (70 – 230 mesh) or flash column chromatography on silica gel 60 (230 – 400 mesh).

5.1.3 Spectroscopic analysis and physical data

^{1}H and ^{13}C NMR spectra were recorded on Bruker Advance-300, Bruker Advance-400, and Bruker Advance-500 instruments operating at 300, 400 or 500 MHz respectively for ^{1}H NMR, and 75.47, 101 and 125 MHz respectively for ^{13}C NMR. All spectra were recorded using deuterated chloroform ($CDCl_3$) as solvent, and all chemical shift values are reported in parts per million (ppm), referenced against tetramethylsilane (TMS) as an internal standard (0.00 ppm). All coupling constants (*J*) are reported in Hertz (Hz). Commonly used abbreviations in assignments include s = singlet, d = doublet, t = triplet, q = quartet, p = pentet, h = heptet, m = multiplet, and app. = apparent. *Infrared spectra* were recorded on a Bruker Tensor 27 spectrophotometer, and all samples were loaded directly onto a diamond cell. All measurements are reported on the wavenumber scale ($/cm^{-1}$). *High resolution mass spectra*

(HRMS) were recorded on a Bruker Compact Q-TOF High Resolution Mass Spectrometer. The ionization mode used was electrospray positive (ESI+). All *melting points* were obtained using a Stuart SMP10 melting point apparatus. *UV absorption analysis*: to prepare the benzophenones and hydroxy-xanthones for UV absorption analysis, each compound was dissolved in 1 ml of chloroform to obtain a stock solution of 1 mg ml^{-1}. The stock solution was then appropriately diluted down to obtain a concentration of 10 ppm. All samples were thus analyzed for their UV absorption properties at a concentration of 10 ppm. UV spectra were recorded using an Agilent Cary 100 UV-vis spectrophotometer, using quartz cuvettes of 1 cm path length (*l*). The data was collected over the wavelength (λ) range of 200 – 800 nm at a scan rate of 600 nm min^{-1}, and at data intervals of 1.0 nm. The data was processed using Agilent Cary WinUV software version 12.00, and a plot of Absorption (A) versus λ was obtained. The molar absorption coefficient (ε) at each λ_{max} was determined using the formula $A = \varepsilon * l * M$ where M = Molarity.

5.2 Experimental procedures for Chapter 2

5.2.1 Preparation of 2-bromo-1,4-naphthoquinone 131[113]

To a solution of *N*-bromosuccinimide (14.95 g, 84.00 mmol, 4.0 eq) in AcOH (200 ml) and water (400 ml) at 45 - 55 °C, was added, dropwise, a solution of 1-naphthol (3.03 g, 21.0 mmol, 1.0 eq) in warm AcOH (150 ml) using a dropping funnel. The mixture was stirred at this temperature for 1 h. After cooling to room temperature, the reaction was quenched with water (100 ml) and extracted into CH_2Cl_2 (3 × 100 ml). The combined organic layers were washed sequentially with an aqueous solution of saturated $NaHCO_3$ (100 ml), water (100 ml), and brine (100 ml). The organic extract was dried over $MgSO_4$, filtered and concentrated *in vacuo*. The crude product was purified by silica gel column chromatography (5% EtOAc/ Hexane) to yield 2-bromo-1,4-naphthoquinone **131** as a bright yellow solid (4.28 g, 86%), the spectra of which compared well to that found in literature.[113]

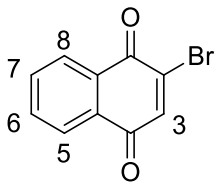

^{1}H NMR (300 MHz, $CDCl_3$) δ 8.15 – 8.10 (m, 1H, ArH-5 or ArH-8), 8.07 – 8.02 (m, 1H, ArH-5 or ArH-8), 7.82 – 7.74 (m, 2H, ArH-6, 7), 7.49 (s, 1H, ArH-3); **^{13}C NMR (75 MHz, $CDCl_3$)** δ 182.2 (ArC=O), 177.6 (ArC=O), 140.2, 140.0, 134.3, 134.0, 131.5, 130.7, 127.6, 126.7.

5.2.2 Preparation of 3-allyl-2-bromo-1,4-naphthoquinone 132[110]

In a round bottom flask containing 2-bromo-1,4-naphthoquinone **131** (3.04 g, 12.8 mmol, 1.0 eq) in MeCN (200 ml), $AgNO_3$ (1.09 g, 6.40 mmol, 0.5 eq) and 3-butenoic acid (1.76 g, 20.5 mmol, 1.6 eq) were added. The reaction mixture was heated to 65 °C. Ammonium persulphate

(5.84 g, 25.6 mmol, 2.0 eq) dissolved in water (100 ml) was then added dropwise. The reaction was maintained at 65 °C and stirred until all starting material was consumed (3 h). The reaction was allowed to cool to room temperature and thereafter quenched with water (100 ml), and extracted into EtOAc (3 × 100 ml). The combined organic layers were washed sequentially with an aqueous solution of saturated $NaHCO_3$ (100 ml), water (100 ml), and brine (100 ml). The organic extract was dried over $MgSO_4$, filtered and concentrated *in vacuo*. The crude product was purified using silica gel column chromatography (5% EtOAc/ Hexane) to yield 3-allyl-2-bromo-1,4-naphthoquinone **132** as a fluffy yellow solid (2.48 g, 70%), the spectra of which compared well with that found in literature.[110]

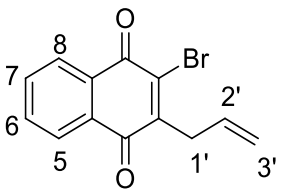

^{1}H NMR (300 MHz, $CDCl_3$) δ 8.15 – 8.09 (m, 2H, ArH-5, 8), 7.78 – 7.71 (m, 2H, ArH-6, 7), 5.85 (ddt, *J* = 16.6, 10.0, 6.6, 1H, H-2′), 5.29 – 5.22 (m, 1H, H-3′), 5.17 – 5.12 (m,1H, H-3′), 3.61 (dt, *J* = 6.6, 1.4, 2H, H-1′); **^{13}C NMR (75 MHz, $CDCl_3$)** δ 181.3 (ArC=O), 177.6 (ArC=O), 148.9, 139.3, 134.1, 133.9, 131.4, 131.3, 131.0, 127.4, 127.1, 118.2, 35.4 (C-1′).

5.2.3 Preparation of 3-allyl-2-bromo-1,4-dimethoxynaphthalene 118[110]

In a 500 ml round bottom flask, 3-allyl-2-bromo-1,4-naphthoquinone **132** (2.30 g, 8.30 mmol, 1.0 eq) was dissolved in THF (130 ml). A solution of $Na_2S_2O_4$ (7.23 g, 41.5 mmol, 5.0 eq) in water (45 ml) was then added, followed by TBAI (0.31 g, 0.83 mmol, 10 mol%). The mixture was stirred for 30 mins at room temperature under an inert atmosphere. A solution of KOH (4.66 g, 83.0 mmol, 10.0 eq) in water (180 ml) was then added and stirred for a further 1 h before adding Me_2SO_4 (10.47 g, 83.00 mmol, 10.0 eq). The reaction mixture was stirred for 18 h and then quenched with an aqueous solution of NH_4OH (25%, 100 ml). The organic phase was extracted into EtOAc (3 × 100 ml), and sequentially washed with HCl solution (10%, 100 ml), water (100 ml), and brine (100 ml). This was then dried over $MgSO_4$, filtered, and concentrated *in vacuo*. The crude product was purified using silica gel column chromatography (20% EtOAc/Hexane) to yield 3-allyl-2-bromo-1,4-dimethoxynaphthalene **118** as a white low melting solid (2.22 g, 87%), the spectra of which compared well with that found in literature.[110]

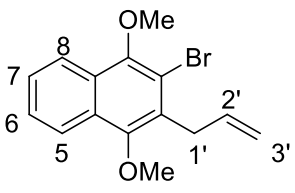

^{1}H NMR (300 MHz, $CDCl_3$) δ 8.18 – 8.10 (m, 2H, ArH-5, 8), 7.60 – 7.51 (m, 2H, ArH-6, 7), 6.15 (ddt, *J* = 17.1, 10.2, 5.8, 1H, H-2′), 5.19 – 5.09 (m, 2H, H-3′), 4.02 (s, 3H, OMe), 3.96 (s, 3H, OMe), 3.86 (dt, *J* = 5.8, 1.8, 2H, H-1′); **^{13}C NMR (75 MHz, $CDCl_3$)** δ 150.9

(ArC-OMe), 150.1 (ArC-OMe), 135.7, 128.7, 128.0, 127.8, 126.5, 126.4, 122.5, 122.4, 116.6, 115.8, 62.5 (OMe), 61.1 (OMe), 34.3 (C-1′).

5.2.4 Preparation of 2-(3-allyl-1,4-dimethoxynaphthalen-2-yl)-5-methoxybenzaldehyde 120b[110]

To a three-necked round bottom flask purged with nitrogen gas was added dimethoxynaphthalene **118** (1.19 g, 3.89 mmol, 1.0 eq), 2-formyl-4-methoxyphenyl boronic acid **119b** (1.05 g, 5.83 mmol, 1.5 eq), and catalytic $Pd(PPh_3)_4$ (0.45 g, 0.39 mmol, 10 mol%). Deoxygenated solutions of DME (47 ml) and aqueous Na_2CO_3 (2M, 8 ml, 4.0 eq) were then added in succession and the mixture was stirred under reflux, under inert gas, for 18 h. After cooling the reaction mixture, water (40 ml) was added to quench the reaction and EtOAc (3 × 50 ml) was used for extraction. The combined organic layers were washed with water (50 ml) and brine (50 ml), then dried over $MgSO_4$, filtered, and concentrated *in vacuo*. The crude product was purified using silica gel column chromatography (5% EtOAc/Hexane) to yield biaryl compound **120b** as a cream solid (1.40 g, 60%), the spectra of which compared well with that found in literature.[110]

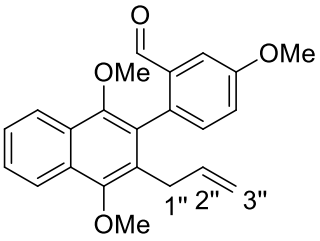

R_f (20% EtOAc/ Hexane): 0.59. **^{1}H NMR (400 MHz, $CDCl_3$)** δ 9.58 (s, 1H, CHO), 8.07 – 8.02 (m, 2H, ArH), 7.53 – 7.42 (m, 3H, ArH), 7.22 – 7.14 (m, 2H, ArH), 5.67 – 5.55 (m, 1H, H-2″), 4.76 – 4.74 (m, 1H, H-3″), 4.51 (dd, *J* = 17.1, 1.6, 1H, H-3″), 3.89 (s, 3H, OMe), 3.86 (s, 3H, OMe), 3.37 (s, 3H, OMe), 3.32 (d, *J* = 5.8, 2H, H-1″). **^{13}C NMR (101 MHz, $CDCl_3$)** δ 192.1 (C=O), 159.3 (ArC-OMe), 150.7 (ArC-OMe), 150.4 (ArC-OMe), 136.1, 135.2, 132.8, 132.8, 128.8, 127.9, 127.8, 127.5, 126.7, 126.2, 122.8, 122.5, 121.0, 115.7, 109.5, 62.4 (OMe), 61.1 (OMe), 55.5 (OMe), 31.8 (C-1″).

5.2.5 Preparation of 2-bromo-1,4-dimethoxy-3-((*E*)-prop-1-en-1-yl) naphthalene 133

To a round bottom flask was added 3-allyl-2-bromo-1,4-dimethoxynaphthalene **118** (3.32 g, 10.8 mmol, 1.0 eq), and this was dissolved in dry THF (100 ml) under inert gas. In a separate round bottom flask, KO*t*Bu (4.85 g, 43.2 mmol, 4.0 eq) was dissolved in dry THF (100 ml) and thereafter delivered portionwise to the solution of dimethoxynaphthalene **118** in THF. The reaction mixture was stirred for 4 h at room temperature, then quenched with an aqueous solution of saturated NH_4Cl (100 ml), and extracted into EtOAc (3 × 100 ml). The combined organic layers were washed sequentially with water (100 ml), followed by brine (100 ml), then dried over $MgSO_4$, filtered, and concentrated *in vacuo*. The crude product was purified using

silica gel column chromatography (15% EtOAc/Hexane) to yield the isomerized dimethoxynaphthalene **133** as a cream solid (2.90 g, 87%).

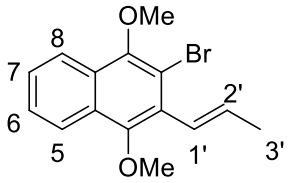

R_f (20% EtOAc/ Hexane): 0.82. **^{1}H NMR (400 MHz, $CDCl_3$)** δ 8.02 – 7.96 (m, 2H, ArH-5, 8), 7.45 – 7.38 (m, 2H, ArH-6, 7), 6.50 (d, *J* = 16.1, 1H, H-1′), 6.44 – 6.33 (m, 1H, H-2′), 3.87 (s, 3H, OMe), 3.70 (s, 3H, OMe), 1.92 (d, *J* = 6.4, 3H, H-3′). **^{13}C NMR (101 MHz, $CDCl_3$)** δ 150.6 (ArC-OMe), 149.7 (ArC-OMe), 133.3 (C-2′), 128.3, 127.6, 127.3, 126.6, 126.6, 125.7 (C-1′), 122.8, 122.3, 115.7, 61.2 (OMe), 60.5 (OMe), 19.5 (C-3′). **M.p**. 76 – 79 °C. **FTIR**: **$\tilde{\nu}$ =** 2959 (C-H), 2851 (C-H), 1638 (C=C), 1348 (C-O) cm^{-1}. **HRMS** (ESI^+): calcd for $C_{15}H_{16}{}^{79}BrO_2$ $[M + H]^+$ 307.0334; found $[M + H]^+$ 307.0291; *m/z* (%) = 307.0291 (100) $[M + H]^+$, 308.0317 (12), 309.0271 (97), 310.0302 (10).

5.2.6 Preparation of (*E*)-2-[1,4-dimethoxy-3-(prop-1-en-1-yl)naphthalen-2-yl]benzaldehyde 134

To a three-necked round bottom flask purged with nitrogen gas was added dimethoxynaphthalene **133** (1.91 g, 6.22 mmol, 1.0 eq), 2-formyl phenyl boronic acid **119a** (1.40 g, 9.33 mmol, 1.5 eq), and catalytic $Pd(PPh_3)_4$ (0.72 g, 0.62 mmol, 10 mol%). Deoxygenated solutions of DME (75 ml) and aqueous Na_2CO_3 (2M, 12 ml, 4.0 eq) were then added in succession and the mixture was stirred under reflux, under nitrogen, for 18 h. After cooling the reaction mixture, water (40 ml) was added to quench the reaction and EtOAc (3 × 50 ml) was used for extraction. The combined organic layers were washed with water (50 ml) and brine (50 ml), then dried over $MgSO_4$, filtered, and concentrated *in vacuo*. The crude product was purified using silica gel column chromatography (5% EtOAc/Hexane) to yield biaryl compound **134** as a pale yellow solid (1.46 g, 71%).

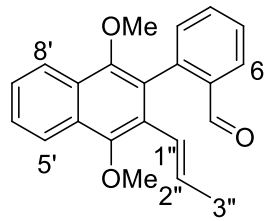

R_f (20% EtOAc/ Hexane): 0.67. **^{1}H NMR (300 MHz, $CDCl_3$)** δ 9.80 (s, 1H, CHO), 8.19 (d, *J* = 8.5, 1H, ArH-5′ or 8′), 8.13 – 8.05 (m, 2H, ArH-5′ or 8′ and ArH-6), 7.71 – 7.49 (m, 4H, ArH), 7.37 (d, *J* = 7.6, 1H, ArH), 6.13 (d, *J* = 15.9, 1H, H-1″), 5.90 (dq, *J* = 15.9, 6.5, 1H, H-2″), 3.86 (s, 3H, OMe), 3.41 (s, 3H, OMe), 1.68 (d, *J* = 6.5, 3H, H-3″); **^{13}C NMR (75 MHz, $CDCl_3$)** δ 192.2 (C=O), 150.2 (ArC-OMe), 149.8 (ArC-OMe), 140.8, 134.3, 133.2 (C-2″), 132.4, 129.3, 127.9, 127.5, 126.9, 126.8, 126.7, 126.4, 124.6 (C-1″), 122.7, 122.7, 60.9 (OMe), 60.8 (OMe), 19.5 (C-3″). **M.p**. 94 – 95 °C. **FTIR**: **$\tilde{\nu}$** = 3006 (C-H), 2930 (C-H), 1688 (C=O), 1596 (C=C), 1275 (C-O) cm^{-1}. **HRMS** (ESI^+): calcd for $C_{22}H_{21}O_3$ [M +

$H]^+$ 333.1491; found $[M + H]^+$ 333.1458; *m/z* (%) = 333.1458 (100) $[M + H]^+$, 334.1573 (97), 335.1400 (60).

5.2.7 Preparation of 3-bromo-1,4-dimethoxy-2-naphthaldehyde 139

In a round bottom flask, dimethoxynaphthalene **133** (1.89 g, 6.15 mmol, 1.0 eq) was dissolved in CH_2Cl_2 (47 ml). Ozone was bubbled through the solution, with stirring, for 7 mins at –78 °C. The solution was then immediately purged with nitrogen gas for 5 mins, after which Me_2S (1.15 g, 18.5 mmol, 1.40 ml, 3.0 eq) was added to the reaction, and left to warm to room temperature with stirring for 18 h. CH_2Cl_2 and excess Me_2S were removed *in vacuo*. The crude product was purified by silica gel column chromatography (10% EtOAc/Hexane) to yield 3-bromo-1,4-dimethoxy-2-naphthaldehyde **139** as a pale yellow solid (1.25 g, 65%).

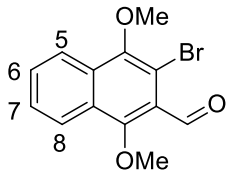

R_f (20% EtOAc/ Hexane): 0.56. **^{1}H NMR (300 MHz, $CDCl_3$)** δ 10.52 (s, 1H, CHO), 8.22 (d, *J* = 8.2, 1H, ArH-5 or 8), 8.10 (d, *J* = 8.2, 1H, ArH-5 or 8), 7.70 – 7.57 (m, 2H, ArH-6, 7), 4.05 (s, 3H, OMe), 3.98 (s, 3H, OMe); **^{13}C NMR (75 MHz, $CDCl_3$)** δ 190.5 (C=O), 157.1 (ArC-OMe), 150.4 (ArC-OMe), 131.4, 129.9, 128.2, 127.4, 124.1, 123.3, 122.6, 111.6, 65.0 (OMe), 61.4 (OMe). **M.p**. 96 – 98 °C. **FTIR: $\tilde{\nu}$ =** 2937 (C-H), 2848 (C-H), 1639 (C=O), 1551 (C=C), 1350 (C-O), 718 (C-Br) cm^{-1}. **HRMS** (ESI^+): calcd for $C_{13}H_{12}O_3{}^{79}Br$ $[M + H]^+$ 294.9970; found $[M + H]^+$ 294.9977; *m/z* (%) = 294.9977 (100) $[M + H]^+$, 296.9960 (97), 296.0010 (13).

5.2.8 Preparation of isopropyl triphenylphosphonium bromide 140[121]

Triphenylphosphine (10.6 g, 40.6 mmol, 1.0 eq) and 2-bromopropane (5.00 g, 40.6 mmol, 3.80 ml, 1.0 eq) were added to an autoclave glass sealed tube and heated in the autoclave at 150 °C for 48 h under pressure. After cooling to room temperature, the resulting salt was recrystallized from ethanol and then dried *in vacuo*. The salt (6.00 g, 45%) was used in the next step without characterization.

5.2.9 Preparation of 2-bromo-1,4-dimethoxy-3-(2-methylprop-1-en-1-yl)naphthalene 138

n-BuLi (1.2 M, 1.7 mmol, 1.4 ml, 2.5 eq) was added dropwise at room temperature to a suspension of isopropyl triphenylphosphonium bromide **140** (655 mg, 1.72 mmol, 2.5 eq) in dry THF (10 ml). The resulting orange solution was stirred for 30 mins before being cooled to 0 °C using an ice bath. To the resulting ylide, was added dropwise at 0 °C, the naphthaldehyde **139** (203 mg, 0.690 mmol, 1.0 eq) in dry THF (5 ml). The reaction was then allowed to warm to room temperature and stirred for 18 h. The reaction was quenched with water (20 ml) and

extracted using EtOAc (3 × 20 ml). The combined organic extracts were washed with water (20 ml) and brine (20 ml), dried over $MgSO_4$, filtered and concentrated *in vacuo*. The crude product was purified using silica gel column chromatography (15% EtOAc/Hexane) to yield substituted naphthalene **138** as a yellow oil (134 mg, 60%).

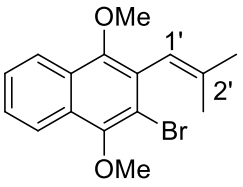

R_f (20% EtOAc/ Hexane): 0.82. **^{1}H NMR (300 MHz, $CDCl_3$)** δ 8.15 – 8.07 (m, 2H, ArH), 7.54 – 7.51 (m, 2H, ArH), 6.18 (app. sept, *J* = 1.4, 1H, H-1′), 3.98 (s, 3H, OMe), 3.77 (s, 3H, OMe), 2.01 (d, *J* = 1.4, 3H, CH_3), 1.59 (d, *J* = 1.4, 3H, CH_3); **^{13}C NMR (75 MHz, $CDCl_3$)** δ 150.4 (ArC-OMe), 149.4 (ArC-OMe), 138.5 (C-2′), 128.2, 128.1, 126.5, 126.3, 122.8, 122.2, 120.1 (C-1′), 116.4, 99.9, 61.2 (OMe), 60.9 (OMe), 25.4 (CH_3), 20.1 (CH_3). **HRMS** (ESI^+): calcd for $C_{16}H_{18}O_2{}^{79}Br$ $[M + H]^+$ 321.0490; found $[M + H]^+$ 321.0465; *m/z* (%) =321.0465 (100) $[M +H]^+$, 322.0491 (20), 323.0446 (97), 324.0474 (15).

5.2.10 Preparation of 2-[1,4-dimethoxy-3-(2-methylprop-1-en-1-yl)naphthalen-2-yl]benzaldehyde 137

To a three-necked round bottom flask purged with nitrogen gas, were added substituted naphthalene **138** (99 mg, 0.31 mmol, 1.0 eq), 2-formyl-phenyl boronic acid **119a** (70 mg, 0.47 mmol, 1.5 eq), and catalytic $Pd(PPh_3)_4$ (36 mg, 0.031 mmol, 10 mol%). Deoxygenated solutions of DME (3 ml) and aqueous Na_2CO_3 (2M, 0.6 ml, 4.0 eq) were then added in succession and the mixture was stirred under reflux, under nitrogen, for 18 h. After cooling the reaction mixture, water (10 ml) was added, and the reaction was extracted into EtOAc (3 × 20 ml). The combined organic layers were washed with water (20 ml) and brine (20 ml), then dried over $MgSO_4$, filtered, and concentrated *in vacuo*. The crude product was purified using silica gel column chromatography (5% EtOAc/Hexane) to yield biaryl compound **137** as a yellow solid (50 mg, 47%).

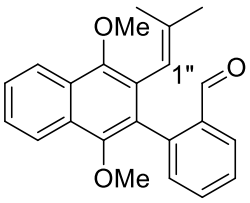

R_f (20% EtOAc/ Hexane): 0.69. **^{1}H NMR (300 MHz, $CDCl_3$)** δ 9.75 (s, 1H, CHO), 8.24 – 8.21 (m, 1H, ArH), 8.16 – 8.13 (m, 1H, ArH), 8.06 – 8.03 (dd, *J* = 7.8, 1.4, 1H, ArH), 7.66 – 7.47 (m, 4H, ArH), 7.36 – 7.33 (dd, *J* = 7.8, 1.4, 1H, ArH), 5.75 (app. sept, *J* = 1.4, 1H, H-1″), 3.79 (s, 3H, OMe), 3.43 (s, 3H, OMe), 1.67 (d, *J* = 1.4, 3H, CH_3), 1.46 (d, *J* = 1.4, 3H, CH_3); **^{13}C NMR (75 MHz, $CDCl_3$)** δ 192.0 (C=O), 150.0 (ArC-OMe), 149.4 (ArC-OMe), 140.6, 138.4, 134.1, 132.9, 132.2, 129.1, 127.8, 127.7, 127.5, 127.4, 126.7, 126.6, 126.3, 122.7, 122.6, 119.6, 60.9 (OMe), 25.3 (CH_3), 20.0 (CH_3). **M.p.** 122 – 123 °C. **FTIR**: **$\tilde{\nu}$ =** 2956 (C-H), 2931 (C-H), 2847

(C-H), 1695 (C=O), 1597 (C=C), 1352 (C-O) cm^{-1}. **HRMS** (ESI^+): calcd for $C_{23}H_{23}O_3$ $[M + H]^+$ 347.1647; found $[M + H]^+$ 347.1638; *m/z* (%) = 347.1638 (100) $[M + H]^+$, 348.1671 (30), 349.1714 (10).

5.2.11 General method for carbonyl-olefin metathesis

Into a round bottom flask was weighed out directly $FeCl_3$ avoiding as much exposure to air as possible. This was dissolved in anhydrous DCE and stirred under inert gas for 5 mins. In a separate flask under inert gas, was added biaryl compound which was dissolved in anhydrous DCE and added *via* syringe to the $FeCl_3$ solution. The reaction was stirred at room temperature until all starting material was consumed before being passed through a short silica plug, eluting with CH_2Cl_2 (15 ml). This was concentrated *in vacuo*, and purified using silica gel column chromatography.

*5.2.11.1 Synthesis of 7,12-dimethoxytetraphene **135***

Trial 1: Using biaryl compound **134** (105 mg, 0.320 mmol, 1.0 eq), $FeCl_3$ (10 mg, 0.060 mmol, 20 mol%), anhydrous DCE (2.7 ml and 2.7 ml), 50 °C for 8 h. The crude product was purified using silica gel column chromatography (10% EtOAc/Hexane) to yield tetracycle **135** as a yellow solid (48 mg, 28%). Following the same procedure but using $FeCl_3$ (49 mg, 0.30 mmol, 100 mol%) led to the isolation of **135**[120] (5 mg, 6% yield), and quinone **136**[120] (6 mg, 7% yield).

Trial 2: Using biaryl compound **137** (48 mg, 0.14 mmol, 1.0 eq), $FeCl_3$ (4.5 mg, 0.028 mmol, 20 mol%), anhydrous DCE (1.5 ml and 1.5 ml), 50 °C for 8 h. The crude product was purified using silica gel column chromatography (10% EtOAc/Hexane) to yield tetracycle **135** as a yellow solid (23.8 mg, 60%).

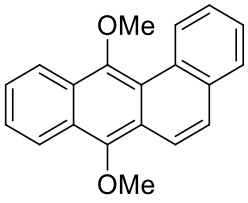

R_f (20% EtOAc/ Hexane): 0.75. **^{1}H NMR (300 MHz, $CDCl_3$)** δ 9.67 (d, *J* = 8.3, 1H, ArH), 8.48 – 8.44 (m, 1H, ArH), 8.35 – 8.32 (m, 1H, ArH), 8.14 (d, *J* = 9.3, 1H, ArH), 7.84 (d, *J* = 7.5, 1H, ArH), 7.71 – 7.58 (m, 5H, ArH), 4.11 (s, 3H, OMe), 3.97 (s, 3H, OMe); **^{13}C NMR (75 MHz, $CDCl_3$)** δ 151.1 (ArC-OMe), 148.6 (ArC-OMe), 132.6, 129.9, 128.4, 128.2, 127.6, 127.3, 127.2, 127.0, 126.0, 126.0, 125.9, 124.2, 123.1, 122.2, 121.0, 120.7, 63.1 (OMe), 60.8 (OMe). **M.p**. 131 – 132 °C. **FTIR**: **$\tilde{\nu}$ =** 3012 (C-H), 1598 (C=C), 1277 (C-O) cm^{-1}. **HRMS** (ESI^+): calcd for $C_{20}H_{17}O_2$ $[M + H]^+$ 289.1229; found $[M + H]^+$ 289.1246; *m/z* (%) = 288.1166 (14) $[M]^+$, 289.1246 (100) $[M + H]^+$, 290.1280 (20).

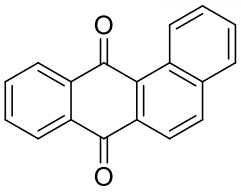

R_f (20% EtOAc/ Hexane): 0.65. **^{1}H NMR (400 MHz, $CDCl_3$)** δ 9.57 (d, *J* = 8.7, 1H, ArH), 8.26 – 8.12 (m, 3H, ArH), 8.06 (d, *J* = 8.6, 1H, ArH), 7.79 (d, *J* = 8.1, 1H, ArH), 7.75 – 7.61 (m, 3H, ArH), 7.55 (app. t, dd, *J* = 7.4, 7.4, 1H, ArH). **^{13}C NMR (101 MHz, $CDCl_3$)** δ 185.8 (C=O), 183.7 (C=O), 136.5, 135.1, 134.8, 134.1, 133.8, 133.3, 132.0, 130.3, 129.8, 129.0, 128.6, 128.6, 127.1, 126.3, 122.3.

5.2.12 Preparation of 4-methoxynaphthalene-1-ol 146[127]

A solution of 1,4-naphthoquinone (400 mg, 2.52 mmol, 1.0 eq) in Et_2O (22 ml) and water (22 ml) were deoxygenated for 10 mins. Sodium dithionite (2.20 g, 12.6 mmol, 5.0 eq) was then added and the reaction mixture was stirred under inert atmosphere, at room temperature, for 1 h. The reaction mixture was then quickly transferred to a separating funnel, minimizing exposure to air, and the aqueous layer was run off. The organic layer was then immediately transferred to a round bottom flask, and KOH (283 mg, 5.04 mmol, 2.0 eq) was added. The reaction was stirred under inert gas for 30 mins. Me_2SO_4 (350 mg, 2.8 mmol, 0.26 ml, 1.1 eq) was then added dropwise, and the reaction was stirred for another 1 h at room temperature. The reaction was quenched with water (20 ml) and extracted with EtOAc (3 × 20 ml). The combined organic layers were washed sequentially with water (20 ml) and brine (20 ml), dried over $MgSO_4$, filtered and concentrated *in vacuo*. The crude product was purified using silica gel column chromatography (20% EtOAc/Hexane) to yield 4-methoxynaphthalene-1-ol **146** as a white solid with a slight purple tinge (332 mg, 76% yield), the spectra of which compared well with that found in literature.[127]

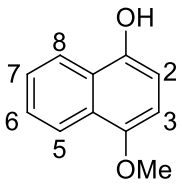

R_f (20% EtOAc/ Hexane): 0.35. **^{1}H NMR (300 MHz, $CDCl_3$)** δ 8.29 – 8.15 (m, 2H, ArH-5, 8), 7.59 – 7.53 (m, 2H, ArH-6, 7), 6.77 (d, *J* = 8.1, 1H, ArH-3), 6.68 (d, *J* = 8.1, 1H, ArH-2), 5.01 (s, 1H, OH), 4.00 (s, 3H, OMe). **^{13}C NMR (75 MHz, $CDCl_3$)** δ 150.1 (ArC-OMe), 145.3 (ArC-OH), 126.7, 126.2, 126.1, 125.6, 122.3, 121.7, 108.2 (ArC-3), 103.8 (ArC-2), 56.1 (OMe). **M.p.** 128 – 129 °C. **FTIR**: **$\tilde{\nu}$ =** 3250 (O-H), 3010 (C-H), 2954 (C-H), 1597 (C=C), 1375 (O-H bend), 1311 (C-O), 1265 (C-O) cm^{-1}. **HRMS** (ESI^+): calcd for $C_{11}H_{11}O_2$ $[M + H]^+$ 175.0759; found $[M + H]^+$ 175.0749; *m/z* (%) = 175.0749 (100) $[M + H]^+$.

5.2.13 Synthesis of isobutyryl chloride 148[232]

Isobutyric acid (3.05 g, 34.7 mmol, 3.20 ml, 1.0 eq) was dissolved in CH_2Cl_2 (10 ml) and cooled to 0 °C using an ice bath. Thionyl chloride (49.5 mmol, 3.60 ml, 1.4 eq) was then added dropwise *via* syringe. After complete addition, the temperature was raised to 40 °C and the reaction mixture was stirred for 3 h. Excess solvent and thionyl chloride were removed *in vacuo* to yield the acyl chloride **148** as an oil (963 mg, 26%) which was used immediately in the next step.

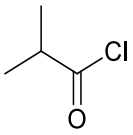

^{1}H NMR (300 MHz, $CDCl_3$) δ 2.59 (m, 1H, CH), 1.20 (d, *J* = 7.0, 6H, CH_3); **^{13}C NMR (75 MHz, $CDCl_3$)** δ 183.8 (C=O), 33.8 (CH), 18.7 (CH_3).

5.2.14 Preparation of 1-(1-hydroxy-4-methoxynaphthalen-2-yl)-2-methylpropan-1-one 149

To a two-necked round bottom flask under inert gas was added 4-methoxy-naphthol **146** (231 mg, 1.33 mmol, 1.0 eq). $TiCl_4$ (277 mg, 1.46 mmol, 0.16 ml, 1.1 eq) was added dropwise *via* syringe at room temperature. Once gas evolution had ceased, isobutyryl chloride **148** (213 mg, 2.00 mmol, 1.5 eq) was added, and the temperature of the reaction mixture was increased to 120 °C. The resulting paste was left at this temperature for 8 h. The reaction was then allowed to cool to room temperature, and CH_2Cl_2 (30 ml), water (10 ml) and aqueous HCl solution (10%, 10 ml) were added to the reaction flask. The organic extract was washed sequentially with water (10 ml), followed by brine (10 ml), and dried over $MgSO_4$, filtered and concentrated *in vacuo*. The crude product was purified using silica gel column chromatography (15% EtOAc/Hexane) to yield substituted hydroxy-naphthalene **149** as a yellow solid (170 mg, 52% yield).

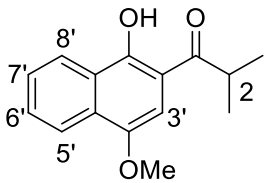

R_f (20% EtOAc/ Hexane): 0.71. **^{1}H NMR (300 MHz, $CDCl_3$)** δ 14.09 (s, 1H, OH), 8.49 (d, *J* = 8.3, 1H, ArH-8′), 8.22 (d, *J* = 8.3, 1H, ArH-5′), 7.72 – 7.58 (m, 2H, ArH-6′, 7′), 6.95 (s, 1H, ArH-3′), 4.02 (s, 3H, OMe), 3.65 (h, *J* = 6.8, 1H, H-2), 1.35 (d, *J* = 6.8, 6H, CH_3). **^{13}C NMR (75 MHz, $CDCl_3$)** δ 210.2 (C=O), 158.5 (ArC-OH), 147.7 (ArC-OMe), 130.5, 130.0, 126.8, 126.6, 124.7 (ArC-8′), 122.1 (ArC-5′), 110.8, 100.7 (ArC-3′), 56.0 (OMe), 35.5 (C-2), 19.5 (CH_3). **M.p.** 92 – 93 °C. **FTIR**: $\tilde{\nu}$ = 2980 (O-H), 2932 (C-H), 1618 (C=O), 1507 (C=C), 1304 (C-O), 1278 (C-O) cm^{-1}. **HRMS** (ESI^+): calcd for $C_{15}H_{17}O_3$ $[M + H]^+$ 245.1178; found $[M + H]^+$ 245.1171; *m/z* (%) = 244.1364 (15) $[M]^+$, 245.1175 (100) $[M + H]^+$, 246.1600 (25).

5.2.15 Preparation of 1-(1,4-dimethoxynaphthalen-2-yl)-2-methylpropan-1-one 150

Method 1: To a solution of substituted naphthol **149** (110 mg, 0.45 mmol, 1.0 eq) in THF (6 ml), was added KOH (126 mg, 2.25 mmol, 5.0 eq) dissolved in water (4 ml). After stirring at room temperature for 1 h, Me_2SO_4 (284 mg, 2.25 mmol, 0.210 ml, 5.0 eq) was added dropwise *via* syringe, and the reaction was stirred under reflux for 18 h. Upon completion, the reaction was quenched with aqueous NH_4OH solution (25%, 2 ml), and extracted with EtOAc (3 × 10 ml). The combined organic layers were washed sequentially with a 10% aqueous solution of HCl (5 ml), and water (10 ml), followed by brine (10 ml). The organic layer was dried over $MgSO_4$, filtered, concentrated *in vacuo*, and purified using silica gel column chromatography (10% EtOAc/Hexane) to yield dimethoxynaphthalene **150** as a yellow oil (96 mg, 83% yield).

Method 2: To 1,4-dimethoxynaphthalene **152** (100 mg, 0.53 mmol, 1.0 eq) in a round bottom flask, was added TFAA (168 mg, 0.800 mmol, 0.110 ml, 1.5 eq) and isobutyric acid (56 mg, 0.64 mmol, 0.060 ml, 1.2 eq). TFA (0.6 ml) was then added, and the reaction mixture was stirred at 70 °C for 24 h. A saturated aqueous solution of $NaHCO_3$ (10 ml) was added to quench the reaction, and the product was extracted using EtOAc (3 × 10 ml). The combined organic extracts were washed sequentially with water (10 ml) and brine (10 ml) and dried over $MgSO_4$, filtered and concentrated *in vacuo*. The crude product was purified using silica gel column chromatography (10% EtOAc/ Hexane) to yield dimethoxynaphthalene **150** as a yellow oil (32 mg, 23%).

Method 3: To a sealed tube were added isobutyric acid (140 mg, 1.59 mmol, 0.140 ml, 1.5 eq) and TFAA (334 mg, 1.59 mmol, 0.220 ml, 1.5 eq). The solution was allowed to stir for 15 mins before a solution of 1,4-dimethoxynaphthalene **152** (200 mg, 1.06 mmol, 1.0 eq) in TFA (1.2 ml) was added. The reaction mixture was stirred at 80 °C for 18 h. Upon cooling, the reaction was quenched with a saturated aqueous solution of $NaHCO_3$ (10 ml) and extracted with EtOAc (3× 10 ml). The combined organic layers were washed with water (10 ml) and brine (10 ml), and concentrated *in vacuo.* Purification of the crude product was achieved using silica gel column chromatography (10% EtOAc/Hexane) to yield dimethoxynaphthalene **150** as a yellow oil (100 mg, 37%).

Method 4: To a two-necked round bottom flask under a nitrogen atmosphere were added isobutyric acid (70 mg, 0.80 mmol, 0.07 ml, 1.5 eq) and TFAA (168 mg, 0.800 mmol, 0.110 ml, 1.5 eq). The solution was allowed to stir for 15 mins before a solution of 1,4-dimethoxynaphthalene **152** (100 mg, 0.53 mmol, 1.0 eq) in triflic acid (0.6 ml) was added. The

reaction mixture was stirred at room temperature for 6 h. Upon completion, the reaction was quenched with a saturated aqueous solution of $NaHCO_3$ (10 ml), and extracted with EtOAc (3 × 10 ml). The combined organic layers were washed with water (10 ml) and brine (10 ml), and concentrated *in vacuo.* Purification was achieved using silica gel column chromatography (10% EtOAc/Hexane) to yield dimethoxynaphthalene **150** as a yellow oil (90 mg, 66%).

Method 5: To a two-necked flask under a nitrogen atmosphere were added isobutyric acid (1.40 g, 15.9 mmol, 1.50 ml, 1.5 eq) and TFAA (3.34 g, 15.9 mmol, 2.20 ml, 1.5 eq). The solution was allowed to stir for 15-20 mins, and thereafter 1,4-dimethoxynaphthalene (2.00 g, 10.6 mmol, 1.0 eq) and methanesulfonic acid (20 ml) were sequentially added. The reaction mixture was stirred at room temperature for 18 h. Upon completion, the reaction was poured into ice, and extracted with EtOAc (3 × 75 ml). The combined organic layers were washed sequentially with a saturated aqueous solution of $NaHCO_3$ (75 ml), water (50 ml) and brine (50 ml). The organic layer was then dried over $MgSO_4$, filtered, and concentrated *in vacuo.* Purification of the crude product was achieved using silica gel column chromatography (5% EtOAc/Hexane) to yield dimethoxynaphthalene **150** as a yellow oil (2.26 g, 84%).

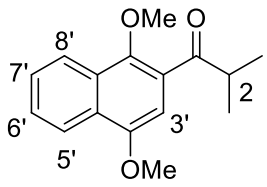

R_f (20% EtOAc/ Hexane): 0.72. **^{1}H NMR (400 MHz, $CDCl_3$)** δ 8.26 – 8.23 (m, 1H, ArH-5′ or 8′), 8.14 – 8.12 (m, 1H, ArH-5′ or 8′), 7.59 – 7.52 (m, 2H, ArH-6′, 7′), 6.85 (s, 1H, ArH-3′), 3.99 (s, 3H, OMe), 3.90 (s, 3H, OMe), 3.71 (h, *J* = 7.0, 1H, H-2), 1.22 (d, *J* = 7.0, 6H, CH_3). **^{13}C NMR (101 MHz, $CDCl_3$)** δ 208.7 (C=O), 151.9 (ArC-OMe), 149.4 (ArC-OMe), 128.6, 128.3, 127.8, 127.2, 127.1, 122.9, 122.5, 102.6 (ArC-3′), 64.1 (OMe), 55.7 (OMe), 39.9 (C-2), 18.9 (CH_3). **FTIR**: $\tilde{\nu}$ = 2967 (C-H), 2935 (C-H), 1673 (C=O), 1592 (C=C), 1365 (C-O) cm^{-1}. **HRMS** (ESI^+): calcd for $C_{16}H_{19}O_3$ $[M + H]^+$ 259.1334; found $[M + H]^+$ 259.1339; *m/z* (%) = 259.1339 (100) $[M + H]^+$, 260.1371 (20).

5.2.16 Preparation of 2-bromo-1-(1,4-dimethoxynaphthalen-2-yl)-2-methylpropan-1-one 154

To a solution of dimethoxynaphthalene **150** (251 mg, 0.97 mmol, 1.0 eq) in dry CH_2Cl_2 (20 ml), was added recrystallized NBS (190 mg, 1.07 mmol, 1.1 eq) and the solution was heated at reflux for 2 h. The reaction was quenched with a saturated aqueous solution of $Na_2S_2O_3$ (10 ml), and extracted with CH_2Cl_2 (3 × 10 ml). The combined organic layers were washed with brine (10 ml) and dried over $MgSO_4$, filtered, and concentrated *in vacuo*. The crude product

was purified using silica gel column chromatography (10% EtOAc/Hexane) to yield bromo-naphthalene **154** as a yellow solid (266 mg, 79% yield).

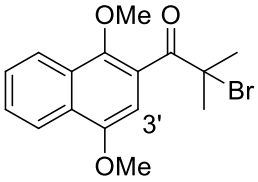

R_f (20% EtOAc/ Hexane): 0.78. **^{1}H NMR (300 MHz, $CDCl_3$):** δ 8.27 (dd, *J* = 8.1, 1.7, 1H, ArH), 8.04 (dd, *J* = 8.1, 1.7, 1H, ArH), 7.61 – 7.52 (m, 2H, ArH), 6.96 (s, 1H, ArH-3′), 4.01 (s, 3H, OMe), 3.86 (s, 3H, OMe), 2.00 (s, 6H, CH_3). **^{13}C NMR (101 MHz, $CDCl_3$)** δ 201.9 (C=O), 151.6 (ArC-OMe), 145.9 (ArC-OMe), 128.0, 127.8, 127.1, 127.0, 126.5, 122.7, 122.1, 103.1, 63.8, 63.4, 55.8, 29.9 (CH_3). **M.p.** 96 – 98 °C. **FTIR**: $\tilde{\nu}$ = 2968 (C-H), 2849 (C-H), 1690 (C=O), 1589 (C=C), 1356 (C-O), 1102 (C-O), 775 (C-Br) cm^{-1}. **HRMS** (ESI^+): calcd for $C_{16}H_{18}{}^{79}BrO_3$ $[M + H]^+$ 337.0439; found $[M + H]^+$ 337.0402; *m/z* (%) = 337.0402 (100) $[M + H]^+$, 338.0428 (15), 339.0387 (97), 340.0417 (15).

5.2.17 Preparation of 2-bromo-1-(3-bromo-1,4-dimethoxynaphthalen-2-yl)-2-methylpropan-1-one 155

Molecular bromine (67 mg, 0.42 mmol, 0.020 ml, 2.2 eq) dissolved in CH_2Cl_2 (1 ml) was added dropwise, very slowly, to a solution of dimethoxynaphthalene **150** (50 mg, 0.19 mmol, 1.0 eq) in CH_2Cl_2 (1 ml) at room temperature. After complete addition of Br_2 solution, the reaction was heated at reflux for 2 h, after which another equivalent of Br_2 (30 mg, 0.19 mmol, 0.010 ml, 1.0 eq) in acetic acid (2 ml) was added and further heated under reflux for 3 h. Upon completion, the reaction was quenched with a saturated aqueous solution of $Na_2S_2O_3$ (5 ml), and extracted with CH_2Cl_2 (3 × 10 ml). The combined organic layers were washed with water (10 ml), followed by brine (10 ml), dried over Na_2SO_4, and concentrated under reduced pressure. Purification of the crude product was achieved using silica gel column chromatography (10% EtOAc/ Hexane) to yield dibromo-naphthalene **155** as a yellow solid (55 mg, 70%).

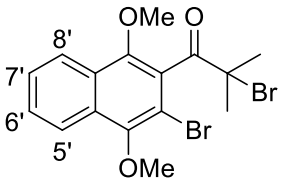

R_f (20% EtOAc/ Hexane): 0.72. **^{1}H NMR (400 MHz, $CDCl_3$)** δ 8.16 – 8.12 (m, 1H, ArH-5′or 8′), 8.09 – 8.05 (m, 1H, ArH-5′ or 8′), 7.62 – 7.59 (m, 2H, ArH-6′, 7′), 3.99 (s, 3H, OMe), 3.88 (s, 3H, OMe), 2.08 (s, 6H, CH_3). **^{13}C NMR (101 MHz, $CDCl_3$)** δ 203.2 (C=O), 150.5 (ArC-OMe), 148.5 (ArC-OMe), 132.0, 129.4, 127.9, 127.7, 127.2, 122.9, 122.8, 107.7 (ArC-Br), 63.6 (C-Br), 63.5 (OMe), 61.7 (OMe), 31.9 (CH_3), 31.8 (CH_3). **M.p.** 102 – 104 °C. **FTIR**: $\tilde{\nu}$ = 2962 (C-H), 2847 (C-H), 1696 (C=O), 1580 (C=C), 1355 (C-O), 731 (C-Br) cm^{-1}. **HRMS**

(ESI$^+$): calcd for $C_{16}H_{17}{}^{79}Br_2O_3$ $[M + H]^+$ 414.9544; found $[M + H]^+$ 414.9514; *m/z* (%) = 414.9514 (50) $[M + H]^+$, 416.9496 (100).

5.2.18 Preparation of 1-(1,4-dimethoxynaphthalen-2-yl)-2-methylpropan-1-ol 158

To a two-necked round bottom flask was added dimethoxynaphthalene **150** (1.00 g, 3.87 mmol, 1.0 eq). This was dissolved in THF (15 ml), and MeOH (3 ml). Thereafter, $NaBH_4$ (732 mg, 19.4 mmol, 5.0 eq) was carefully added at 0 °C, and the reaction was stirred at this temperature for 2 h before warming to room temperature and stirring for 8 h. Upon completion, water (20 ml), followed by the careful addition of a 10% aqueous solution of HCl (15 ml) were added. The reaction was extracted with EtOAc (3 × 50 ml), and the combined organic layers were washed with water (40 ml), followed by brine (40 ml). The organic layer was dried over $MgSO_4$, filtered, and concentrated *in vacuo*. The crude product was purified using silica gel column chromatography (20% EtOAc/Hexane), to yield alcohol **158** as a low melting yellow solid (1.0 g, Quantitative).

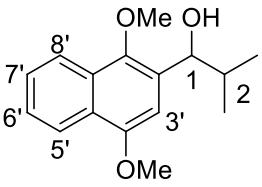

R_f (20% EtOAc/ Hexane): 0.42. **^{1}H NMR (300 MHz, $CDCl_3$)** δ 8.25 – 8.24 (m, 1H, ArH-5′ or 8′), 8.02 – 7.98 (m, 1H, ArH-5′ or 8′), 7.55 – 7.44 (m, 2H, ArH-6′ or 7′), 6.82 (s, 1H, ArH-3′), 4.87 (d, *J* = 8.1, 1H, H-1), 3.97 (s, 3H, OMe), 3.88 (s, 3H, OMe), 2.74 (s, 1H, OH), 2.17 – 2.01 (m, 1H, H-2), 1.16 (d, *J* = 6.6, 3H, CH_3), 0.82 (d, *J* = 6.8, 3H, CH_3). **^{13}C NMR (75 MHz, $CDCl_3$)** δ 152.2 (ArC-OMe), 146.5 (ArC-OMe), 131.3, 128.2, 126.6, 126.2, 125.4, 122.4, 122.0, 101.8 (ArC-3′), 74.2 (C-1), 62.7 (OMe), 55.6 (OMe), 34.8 (C-2), 19.4 (CH_3), 18.9 (CH_3). **M.p** 66 – 67 °C. **FTIR**: **$\tilde{\nu}$** = 3316 (O-H), 2943 (C-H), 2871 (C-H), 1595 (C=C), 1367 (C-O), 1236 (C-O), 1087 (C-O) cm^{-1}. **HRMS** (ESI$^+$): calcd for $C_{16}H_{19}O_2$ $[M - H_2O + H]^+$ 243.1385; found $[M - H_2O + H]^+$ 243.1389; *m/z* (%) = 243.1389 (100) $[M - H_2O + H]^+$, 244.1485 (20).

5.2.19 Preparation of 1-(3-iodo-1,4-dimethoxynaphthalen-2-yl)-2-methylpropan-1-ol 157

To a two-necked round bottom flask under an inert atmosphere was added alcohol **158** (4.78 g, 18.4 mmol, 1.0 eq)**.** This was dissolved in dry Et_2O (70 ml), and the reaction was cooled to –78 °C. A solution of *n*-BuLi (1.6 M, 46 mmol, 29 ml, 2.5 eq) was then added dropwise. After complete addition, the reaction was allowed to slowly warm to room temperature, and then stirred for a further 4 h. Thereafter, the reaction was cooled to 0 °C and dry THF (35 ml) was added. The reaction was stirred at 0 °C for 1 h, before a solution of iodine (5.6 g, 22 mmol, 1.2

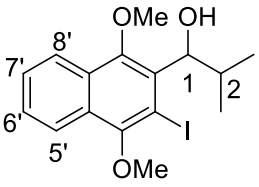

eq) in dry THF (35 ml) was added slowly using a dropping funnel at 0 °C. The reaction was left to stir for 30 mins before being allowed to warm to room temperature, and then stirred for 18 h. The reaction was quenched with a saturated aqueous solution of $Na_2S_2O_3$ (100 ml), and extracted with EtOAc (3 × 100 ml). The combined organic layers were washed with water (100 ml), followed by brine (100 ml). The organic layer was dried over $MgSO_4$, filtered, and concentrated *in vacuo*. The crude product was purified using silica gel column chromatography (10-30% EtOAc/Hexane), to yield iodinated-naphthalene **157** as a yellow oil (3.21 g, 45% yield; Recovered 1.9 g starting material **158**, therefore 77% yield based on recovered starting material).

R_f (20% EtOAc/ Hexane): 0.50. **^{1}H NMR (500 MHz, $CDCl_3$)** δ 8.07 (dd, *J* = 8.1, 1.4, 1H, ArH-5′ or 8′), 8.03 (dd, *J* = 8.1, 1.3, 1H, ArH-5′ or 8′), 7.57 – 7.50 (m, 2H, ArH-6′, 7′), 4.96 (app. t, dd, *J* = 8.6, 8.6, 1H, H-1), 4.02 (s, 3H, OMe), 3.93 (s, 3H, OMe), 3.49 (d, *J* = 9.3, 1H, OH), 2.40 (app. h, dd, *J* = 7.0, 7.0, 1H, H-2), 1.20 (d, *J* = 6.6, 3H, CH_3), 0.86 (d, *J* = 6.9, 3H, CH_3). **^{13}C NMR (126 MHz, $CDCl_3$)** δ 153.2 (ArC-OMe), 150.7 (ArC-OMe), 133.1, 128.7, 127.4, 126.9, 123.2, 122.8, 93.7 (C-I), 83.3 (C-1), 63.7 (OMe), 61.6 (OMe), 34.9 (C-2), 19.6 (CH_3), 19.4 (CH_3). **FTIR**: **$\tilde{\nu}$** = 3501 (O-H), 2958 (C-H), 2868 (C-H), 1560 (C=C), 1352 (C-O), 1099 (C-O), 773 (C-I) cm^{-1}. **HRMS** (ESI^+): calcd for $C_{16}H_{18}O_2I$ $[M - H_2O + H]^+$ 369.0352; found $[M - H_2O + H]^+$ 369.0330; *m/z* (%) = 369.0330 (100) $[M - H_2O + H]^+$.

5.2.20 Preparation of 1-(3,8-diiodo-1,4-dimethoxynaphthalen-2-yl)-2-methylpropan-1-ol 159

To a two-necked round bottom flask under an inert atmosphere was added alcohol **158** (1.57 g, 6.03 mmol, 1.0 eq). This was dissolved in dry Et_2O (40 ml), and the reaction was cooled to –78 °C. TMEDA (2.10 g, 18.1 mmol, 2.70 ml, 3.0 eq) was then added to the solution, followed by the dropwise addition, *via* syringe, of a solution of *n*-BuLi (1.1 M, 18 mmol, 17 ml, 3.0 eq). After complete addition, the reaction was allowed to slowly warm to room temperature, and then stirred for a further 4 h. Thereafter, the reaction was cooled to 0 °C and dry THF (20 ml) was added. The reaction was stirred at 0 °C for 1 h, before a solution of iodine (2.3 g, 9.1 mmol, 1.5 eq) in dry THF (20 ml) was added slowly using a dropping funnel at 0 °C. The reaction was left to stir for 30 mins before being allowed to warm to room temperature, and then stirred for 48 h. The reaction was quenched with a saturated aqueous solution of $Na_2S_2O_3$ (50 ml), and extracted with EtOAc (3 × 50 ml). The combined organic layers were washed with water (50 ml), followed by brine (50 ml). The organic layer was dried over $MgSO_4$, filtered, and

concentrated under reduced pressure. The crude product was purified using silica gel column chromatography (10-30% EtOAc/ Hexane), to yield diiodo-naphthalene **159** as a yellow oil (1.1 g, 36% yield). Also isolated 220 mg (10%) of **157**.

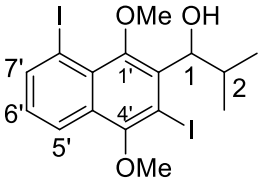

^{1}H NMR (300 MHz, $CDCl_3$) δ 8.25 (dd, *J* = 7.3, 1.2, 1H, H-7′), 8.11 (dd, *J* = 8.4, 1.2, 1H, H-5′), 7.12 (dd, *J* = 8.4, 7.3, 1H, H-6′), 4.98 (dd, *J* = 10.6, 9.0, 1H, H-1), 3.91 (s, 3H, OMe), 3.78 (s, 3H, OMe), 3.41 (d, *J* = 10.6, 1H, OH), 2.49 – 2.42 (m, 1H, H-2), 1.23 (d, *J* = 6.5, 3H, CH_3), 0.83 (d, *J* = 6.9, 3H, CH_3). **^{13}C NMR (75 MHz, $CDCl_3$)** δ 152.9 (ArC-4′), 150.3 (ArC-1′), 142.6, 134.9, 129.1, 128.1, 127.6, 126.9, 123.8, 86.2 (C-1), 65.1 (OMe), 61.7 (OMe), 34.6 (C-2), 19.6 (CH_3). **HRMS** (ESI^+): calcd for $C_{16}H_{17}O_2I_2$ $[M - H_2O + H]^+$ 494.9318; found $[M - H_2O + H]^+$ 494.9390; *m/z* (%) = 494.9390 (70) $[M - H_2O + H]^+$, 534.9324 (100), 535.9371 (15).

5.2.21 Preparation of 2-iodo-1,4-dimethoxy-3-(2-methylprop-1-en-1-yl)naphthalene 156

Iodo-naphthalene **157** (2.75 g, 7.12 mmol, 1.0 eq) was added to a round bottom flask and dissolved in dry toluene (160 ml). *Para*-toluenesulfonic acid (101 mg, 0.58 mmol, 30 mol%) was then added to the solution and heated to 110 °C for 18 h using a Dean-Stark apparatus. After cooling, the reaction was quenched with a saturated aqueous solution of $NaHCO_3$ (100 ml), and extracted with EtOAc (3 × 100 ml). The combined organic layers were washed with water (100 ml), followed by brine (100 ml) and dried over $MgSO_4$. After filtering, the organic layer was concentrated *in vacuo*. The crude product was purified using silica gel column chromatography (5% EtOAc/ Hexane), to yield isoprenyl-naphthalene **156** as a yellow low melting solid (2.03 g, 78% yield).

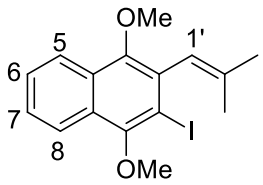

R_f (20% EtOAc/ Hexane): 0.84. **^{1}H NMR (500 MHz, $CDCl_3$)** δ 8.01 (dd, *J* = 7.9, 1.4, 1H, ArH-5 or 8), 7.94 (dd, *J* = 7.9, 1.4, 1H, ArH-5 or 8), 7.42 – 7.33 (m, 2H, ArH-6, 7), 6.03 (s, 1H, H-1′), 3.82 (s, 3H, OMe), 3.63 (s, 3H, OMe), 1.89 (s, 3H, CH_3), 1.44 (s, 3H, CH_3). **^{13}C NMR (126 MHz, $CDCl_3$)** δ 152.7 (ArC-OMe), 149.9 (ArC-OMe), 138.1, 130.9, 129.0, 127.3, 126.7, 126.6, 124.7 (C-1′), 123.1, 122.7, 95.9 (C-I), 61.5 (OMe), 61.0 (OMe), 25.4 (CH_3), 20.2 (CH_3). **FTIR**: $\tilde{\nu}$ = 2928 (C-H), 2842 (C-H), 1559 (C=C), 1348 (C-O), 1222 (C-O), 771 (C-I) cm^{-1}. **HRMS** (ESI^+): calcd for $C_{16}H_{18}O_2I$ $[M + H]^+$ 369.0352; found $[M + H]^+$ 369.0315; *m/z* (%) = 369.0315 (100) $[M + H]^+$, 370.0349 (5).

5.2.22 Preparation of (2-bromo-5-methoxy-3-methylphenyl)methanol 161[111]

Step i). To a solution of 3,5-dimethylanisole (2.00 g, 14.7 mmol, 1.0 eq) in CCl_4 (30 ml), were added NBS (6.27 g, 35.2 mmol, 2.4 eq), and benzoyl peroxide (356 mg, 1.47 mmol, 10 mol%). The reaction mixture was stirred at 80 °C for 4 h. After cooling, the CCl_4 was evaporated *in vacuo* and recycled, and water (50 ml) was added to the residue. The mixture was extracted with EtOAc (3 × 50 ml), and the organic layer was washed sequentially with a 10% aqueous HCl solution (50 ml), followed by a saturated aqueous solution of $NaHCO_3$ (50 ml), and brine (100 ml). After drying over $MgSO_4$, and filtering, the solution was concentrated *in vacuo* to yield crude product (3.76 g) which was used in the next step without purification.

Step ii). The crude product (3.76 g) was dissolved in 1,4-dioxane (30 ml). To this solution was added water (30 ml), and $CaCO_3$ (2.56 g, 25.6 mmol, 2.0 eq) under inert atmosphere. The mixture was heated under reflux and stirred for 12 h. After cooling, water was added, and the solution was extracted with EtOAc (3 × 50 ml). The combined organic layers were washed with brine (50 ml). After drying over $MgSO_4$, and filtering, the solution was concentrated *in vacuo* and purified using silica gel column chromatography (10-30% EtOAc/ Hexane) to yield bromo-anisole **161** as a white low melting solid (2.05 g, 37% over two steps), the spectra of which compared agreeably to that found in literature.[111]

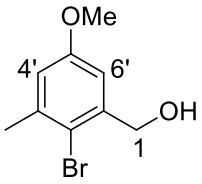

R_f (20% EtOAc/ Hexane): 0.40. **^{1}H NMR (400 MHz, $CDCl_3$)** δ 6.90 (d, *J* = 3.0, 1H, ArH-6′), 6.74 (d, *J* = 3.0, 1H, ArH-4′), 4.71 (d, *J* = 5.4, 2H, H-1), 3.79 (s, 3H, OMe), 2.39 (s, 3H, CH_3), 2.15 – 2.07 (m, 1H, OH). **^{13}C NMR (101 MHz, $CDCl_3$)** δ 158.7 (ArC-OMe), 140.9 (C-6′), 139.3 (C-4′), 115.6, 115.2, 111.6, 65.6 (C-1), 55.4 (OMe), 23.4 (CH_3). **FTIR**: **$\tilde{\nu}$** = 3278 (O-H), 2994 (C-H), 2933 (C-H), 2832 (C-H), 1583 (C=C), 1307 (C-O), 1157 (C-O), 592 (C-Br) cm^{-1}.

5.2.23 Preparation of (3-methoxy-5-methylphenyl)methanol 162[111]

Method 1: To a two-necked round bottom flask under inert gas was added bromo-anisole **161** (1.02 g, 4.41 mmol, 1.0 eq). This was dissolved in dry THF (20 ml), and a solution of *n*-BuLi (0.77 M, 6.6 mmol, 8.6 ml, 1.5 eq) was then added dropwise *via* syringe at –78 °C. The mixture was stirred at –78 °C for 2 h, and thereafter warmed to room temperature. The reaction mixture was quenched with water (50 ml), extracted with EtOAc (3 × 50 ml), and the combined organic layers were washed with brine (50 ml). After drying over $MgSO_4$, and filtering, the solution was concentrated *in vacuo*. The crude product was purified using silica gel column

chromatography (30% EtOAc/ Hexane) to yield alcohol **162** as a yellow oil (651 mg, 97% yield).

Method 2: To a solution of aldehyde **164** (150 mg, 1.00 mmol, 1.0 eq) in THF (5 ml) and MeOH (1 ml) was added $NaBH_4$ (189 mg, 5.00 mmol, 5.0 eq) at 0 °C. The reaction mixture was stirred at 0 °C for 1 h before being allowed to warm to room temperature, and then stirred for 12 h. The reaction was carefully quenched with a 10% aqueous solution of HCl (2 ml) and water (2 ml), and then extracted into EtOAc (3 × 5 ml). The combined organic layers were washed with water (2 ml), followed by brine (2 ml), and dried over $MgSO_4$. After filtering, the solution was concentrated *in vacuo*. The crude product was purified using silica gel column chromatography (30% EtOAc/ Hexane) to yield alcohol **162** as a yellow oil (130 mg, 85% yield), the spectra of which compared well with that found in literature.[111]

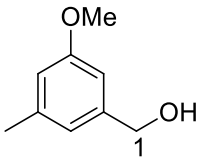

R_f (20% EtOAc/ Hexane): 0.26. **^{1}H NMR (400 MHz, $CDCl_3$)** δ 6.73 (s, 1H, ArH), 6.70 (s, 1H, ArH), 6.63 (s, 1H, ArH), 4.58 (s, 2H, H-1), 3.77 (s, 3H, OMe), 2.31 (s, 3H, CH_3), 2.27 – 2.13 (m, 1H, OH). **^{13}C NMR (101 MHz, $CDCl_3$)** δ 159.8 (ArC-OMe), 142.3, 139.6, 120.0, 114.0, 109.2, 65.1 (C-1), 55.1 (OMe), 21.4 (CH_3). **FTIR**: **$\tilde{\nu}$** = 3340 (O-H), 2937 (C-H), 2838 (C-H), 1597 (C=C), 1295 (C-O), 1151 (C-O), 1067 (C-O) cm^{-1}.

5.2.24 Preparation of (2-iodo-3-methoxy-5-methylphenyl)methanol 163[111]

To a two-necked round bottom flask under inert gas was added alcohol **162** (642 mg, 4.22 mmol, 1.0 eq). This was dissolved in dry Et_2O (10 ml), and cooled to –78 °C. A solution of *n*-BuLi (1.50 M, 10.6 mmol, 7 ml, 2.5 eq) was then added dropwise *via* syringe. After complete addition, the solution was allowed to warm to room temperature, and stirred for 4 h before being cooled to 0 °C. Dry THF (5 ml) was then added to the reaction mixture, which was then stirred at 0 °C for a further 1 h. A solution of iodine (1.28 g, 5.06 mmol, 1.2 eq) in dry THF (5 ml) was thereafter added dropwise. After complete addition, the reaction mixture was allowed to stir at 0 °C for 30 mins before being quenched with a saturated aqueous solution of $Na_2S_2O_3$ (10 ml). The organic layer was extracted with EtOAc (3 × 20 ml). The combined organic layers were washed with water (10 ml), followed by brine (10 ml). The organic layer was dried over $MgSO_4$, filtered, and concentrated *in vacuo.* The crude product was purified using silica gel column chromatography (10-30% EtOAc/ Hexane), to yield iodo-alcohol **163** as a cream solid (600 mg, 51% yield), the spectra of which compared agreeably to that found in literature.[111]

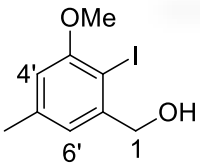

R_f (20% EtOAc/ Hexane): 0.40. **^{1}H NMR (400 MHz, $CDCl_3$)** δ 6.92 (d, *J* = 1.8, 1H, H-6′), 6.59 (d, *J* = 1.8, 1H, H-4′), 4.67 (d, *J* = 3.5, 2H, H-1), 3.88 (s, 3H, OMe), 2.35 (s, 3H, CH_3), 2.10 (s, 1H, OH). **^{13}C NMR (101 MHz, $CDCl_3$)** δ 157.8 (ArC-OMe), 144.0, 139.7, 121.9 (C-6′), 111.2 (C-4′), 85.4 (C-I), 69.6 (C-1), 56.5 (OMe), 21.3 (CH_3). **FTIR**: **$\tilde{\nu}$** = 3266 (O-H), 2902 (C-H), 2841 (C-H), 1574 (C=C), 1305 (C-O), 1167 (C-O), 1038 (C-O), 582 (C-I) cm^{-1}.

5.2.25 Preparation of 2-iodo-3-methoxy-5-methylbenzaldehyde 145[111]

A pestle and mortar were used to grind together $KMnO_4$ (142 mg, 0.900 mmol, 2.5 eq), $CuSO_4 \cdot 5H_2O$ (225 mg, 0.900 mmol, 2.5 eq), and iodo-alcohol **163** (100 mg, 0.4 mmol, 1.0 eq) until a completely homogenous mixture was formed. This homogenous mixture was then transferred to a round bottom flask and heated to 120 °C for 3 h. After cooling, the reaction mixture was diluted with EtOAc (20 ml) and water (10 ml). The organic layer was washed with brine (10 ml), and dried over $MgSO_4$. After filtering, the solution was concentrated *in vacuo*. The crude product was purified using silica gel column chromatography (10% EtOAc/ Hexane) to yield iodo-aldehyde **145** as a white fluffy solid (54 mg, 54% yield), the spectra of which compared agreeably to that found in literature.[111]

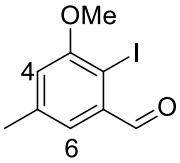

R_f (20% EtOAc/ Hexane): 0.69. **^{1}H NMR (400 MHz, $CDCl_3$)** δ 10.14 (s, 1H, CHO), 7.30 (d, *J* = 1.9, 1H, ArH-6), 6.87 (d, *J* = 1.9, 1H, ArH-4), 3.92 (s, 3H, OMe), 2.37 (s, 3H, CH_3). **^{13}C NMR (101 MHz, $CDCl_3$)** δ 196.4 (C=O), 158.1 (ArC-OMe), 139.9, 136.1, 122.8, 117.1, 90.0 (C-I), 56.7 (OMe), 21.1 (CH_3). **FTIR**: **$\tilde{\nu}$** = 2958 (C-H), 2848 (C-H), 2741 (C-H), 1686 (C=O), 1568 (C=C), 1285 (C-O), 1163 (C-O), 854 (C-I) cm^{-1}.

5.2.26 Preparation of 3-methoxy-5-methylbenzaldehyde 164[233]

To a sealed pressure tube were added 3,5-dimethylanisole (5.00 g, 36.7 mmol, 1.0 eq), *N*-hydroxyphthalimide (599 mg, 3.67 mmol, 10 mol%), $Co(OAc)_2 \cdot 4H_2O$ (183 mg, 0.730 mmol, 2 mol%), $K_2S_2O_8$ (2.48 g, 9.17 mmol, 25 mol%), and AcOH (50 ml). The solution was bubbled with oxygen gas for a minimum of 10 mins, and was immediately after sealed with a Teflon lined cap. The sealed tube was placed in an oil bath heated to 105 °C and stirred. Oxygen gas was bubbled through the solution every 10 h. After stirring for 24 h, another portion of $K_2S_2O_8$ (2.48 g, 9.17 mmol, 25 mol%) was added, and thereafter stirred for another 48 h, with oxygen gas being bubbled through every 10 h for a minimum of 10 mins. After cooling, the reaction was quenched with solid $NaHCO_3$ (10 g), and then extracted into EtOAc (3 × 100 ml). The

combined organic layers were washed with water (100 ml), followed by brine (100 ml) and dried over $MgSO_4$. After filtering, the solution was concentrated *in vacuo* and purified using silica gel column chromatography (20% EtOAc/ Hexane) to yield aldehyde **164** as a yellow oil, the spectra of which compared well with that found in literature[233] (1.1 g, 20% yield. Recovered 3.4 g starting material, accordingly, 56% yield based on recovered starting material).

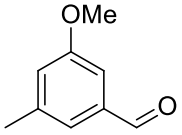

R_f (20% EtOAc/ Hexane): 0.59. **^{1}H NMR (300 MHz, $CDCl_3$)** δ 9.93 (s, 1H, CHO), 7.27 (s, 1H, ArH), 7.20 (s, 1H, ArH), 6.99 (s, 1H, ArH), 3.85 (s, 3H, OMe), 2.40 (s, 3H, CH_3). **^{13}C NMR (75 MHz, $CDCl_3$)** δ 192.3 (CHO), 160.1 (ArC-OMe), 140.3, 137.7, 124.3, 122.1, 109.4, 55.4 (OMe), 21.2 (CH_3). **FTIR**: **ṽ** = 2949 (C-H), 2839 (C-H), 1717 (C=O), 1587 (C=C), 1138 (C-O), 1094 (C-O) cm^{-1}.

5.2.27 Preparation of 2-[1,4-dimethoxy-3-(2-methylprop-1-en-1-yl)naphthalen-2-yl]-4,4,5,5-tetramethyl-1,3,2-dioxaborolane 166

To a three-necked round bottom flask equipped with a condenser and flushed with inert gas, were added iodo-naphthalene **156** (400 mg, 1.09 mmol, 1.0 eq), bis(pinacolato)diboron (415 mg, 1.64 mmol, 1.5 eq), dry KOAc (641 mg, 6.54 mmol, 5.0 eq), and $Pd(PPh_3)_4$ (126 mg, 0.110 mmol, 10 mol%). After de-oxygenating with nitrogen gas for 10 mins, DMSO (16 ml) was added to the mixture of solids, and the solution was heated to 90 °C and stirred for 20 h. After cooling, water (160 ml) was added to the reaction, and extracted with EtOAc (3 × 50 ml). The combined organic layers were washed with water (50 ml), followed by brine (50 ml) and dried over $MgSO_4$. After filtering, the organic layer was concentrated *in vacuo*. The crude product was purified using silica gel column chromatography (5% EtOAc/Hexane), to yield the boronic ester **166** as a yellow oil (260 mg, 65% yield).

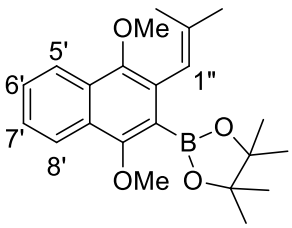

R_f (20% EtOAc/ Hexane): 0.81. **^{1}H NMR (400 MHz, $CDCl_3$)** δ 8.12 – 8.10 (m, 1H, ArH-5′ or 8′), 8.05 – 8.03 (m, 1H, ArH-5′ or 8′), 7.51 – 7.43 (m, 2H, ArH-6′, 7′), 6.39 (s, 1H, H-1″), 3.97 (s, 3H, OMe), 3.77 (s, 3H, OMe), 1.91 (s, 3H, CH_3), 1.59 (s, 3H, CH_3), 1.38 (s, 12H, CH_3). **^{13}C NMR (75 MHz, $CDCl_3$)** δ 155.6 (ArC-OMe), 149.2 (ArC-OMe), 137.4, 129.9, 127.4, 126.3, 125.4, 122.6, 122.3, 121.7, 83.9, 63.4, 60.9, 25.5, 24.8, 20.0. **FTIR**: **ṽ** = 2977 (C-H), 2840 (C-H), 1593 (C=C), 1346 (C-O), 1222 (C-O) cm^{-1}. **HRMS** (ESI^+): calcd for $C_{22}H_{30}O_4B$ $[M + H]^+$ 369.2237; found $[M + H]^+$ 369.2241; *m/z* (%) = 368.2316 (30) $[M]^+$, 369.2241 (100) $[M + H]^+$, 370.2273 (25), 371.1106 (85).

5.2.28 Preparation of 2-[1,4-dimethoxy-3-(2-methylprop-1-en-1-yl)naphthalen-2-yl]-3-methoxy-5-methylbenzaldehyde 143

To a three-necked round bottom flask equipped with a condenser and flushed with inert gas, were added iodo-anisole **145** (187 mg, 0.680 mmol, 1.0 eq), tri(*o*-tolyl)-phosphine (62 mg, 0.20 mmol, 30 mol%), $Pd_2(dba)_3$ (62 mg, 0.068 mmol, 10 mol%), and K_2CO_3 (217 mg, 1.02 mmol, 1.5 eq). In a separate 25 ml conical flask was added boronic ester **166** (300 mg, 0.8 mmol, 1.2 eq) dissolved in DMF (10 ml), and this was de-oxygenated with nitrogen gas for 10 mins before being added to the mixture of solids. The reaction mixture was heated to 100 °C and stirred for 20 h. After cooling, water (100 ml) was added to the reaction, and extracted with EtOAc (3 × 50 ml). The combined organic layers were washed with water (50 ml), followed by brine (50 ml) and dried over $MgSO_4$. After filtering, the organic layer was concentrated *in vacuo*. The crude product was purified using silica gel column chromatography (1-5% EtOAc/ Hexane), to yield biaryl compound **143** as a yellow sticky oil (162 mg – 170 mg, 61 -64% yield).

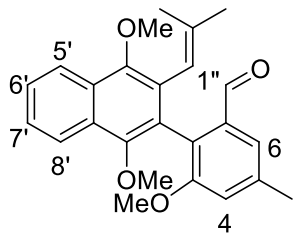

R_f (20% EtOAc/ Hexane): 0.58. **^{1}H NMR (400 MHz, $CDCl_3$)** δ 9.64 (s, 1H, CHO), 8.23 – 8.20 (m, 1H, ArH-5′ or 8′), 8.13 – 8.09 (m, 1H, ArH-5′ or 8′), 7.57 – 7.50 (m, 2H, ArH-6′, 7′), 7.47 (s, 1H, ArH-6), 7.01 (s, 1H, ArH-4), 5.74 (s, 1H, H-1″), 3.79 (s, 3H, OMe), 3.73 (s, 3H, OMe), 3.47 (s, 3H, OMe), 2.48 (s, 3H, CH_3), 1.66 (s, 3H, CH_3), 1.44 (s, 3H, CH_3). **^{13}C NMR (101 MHz, $CDCl_3$)** δ 192.8 (C=O), 157.1 (ArC-OMe), 149.9 (ArC-OMe), 149.6 (ArC-OMe), 139.0, 137.4, 134.6, 129.2, 128.4, 127.7, 127.5, 126.4, 125.9, 123.8, 122.7, 122.6, 119.2, 119.1, 116.8, 60.9 (OMe), 60.8 (OMe), 55.7 (OMe), 25.4 (CH_3), 21.7 (CH_3), 19.9 (CH_3). **FTIR**: **$\tilde{\nu}$** = 2930 (C-H), 2840 (C-H), 1692 (C=O), 1605 (C=C), 1350 (C-O), 1309 (C-O), 1280 (C-O) cm^{-1}. **HRMS** (ESI^+): calcd for $C_{25}H_{27}O_4$ $[M + H]^+$ 391.1909; found $[M + H]^+$ 391.1912; *m/z* (%) = 391.1912 (100) $[M + H]^+$, 392.1954 (30).

5.2.29 Preparation of 1,7,12-trimethoxy-3-methyltetraphene 142

Into a round bottom flask was weighed out directly $FeCl_3$ (33 mg, 0.20 mmol, 27 mol%), avoiding as much exposure to air as possible. This was dissolved in anhydrous DCE (50 ml) and stirred under inert gas for 5 mins. In a separate flask under inert gas, was added biaryl compound **143** (300 mg, 0.8 mmol, 1.0 eq) which was dissolved in anhydrous DCE (52 ml) and added *via* syringe to the $FeCl_3$ solution. The reaction was stirred at room temperature for 4.5 h before being passed through a short silica plug, eluting with CH_2Cl_2 (20 ml). This was concentrated under reduced pressure, and purified using silica gel column chromatography

(10% EtOAc/Hexane) to yield tetracycle **142** as a yellow solid (170 mg, 67% yield). Also isolated quinone **141** (40 mg, 17%).

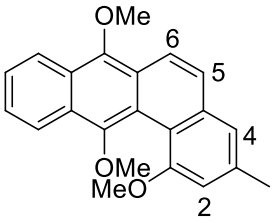

R_f (20% EtOAc/ Hexane): 0.66. **^{1}H NMR (400 MHz, $CDCl_3$)** δ 8.56 – 8.54 (m, 1H, ArH), 8.33 – 8.31 (m, 1H, ArH), 7.99 (d, *J* = 9.1, 1H, ArH-6), 7.63 – 7.58 (m, 2H, ArH), 7.41 (d, *J* = 9.1, 1H, ArH-5), 7.21 (s, 1H, ArH-4), 6.99 (s, 1H, ArH-2), 4.12 (s, 3H, OMe), 4.04 (s, 3H, OMe), 3.58 (s, 3H, OMe), 2.58 (s, 3H, CH_3). **^{13}C NMR (101 MHz, $CDCl_3$)** δ 157.9 (ArC-OMe), 151.4 (ArC-OMe), 146.7 (ArC-OMe), 138.0, 134.3, 127.6, 126.5, 125.9, 125.8, 125.5, 124.2, 123.5, 122.0, 121.7, 119.8, 116.8, 116.8, 110.9, 63.3 (OMe), 60.5 (OMe), 56.2 (OMe), 21.7 (CH_3). **M.p** 119 – 120 °C. **FTIR**: **$\tilde{\nu}$** = 2926 (C-H), 1537 (C=C), 1394 (C-O), 1281 (C-O) cm^{-1}. **HRMS** (ESI^+): calcd for $C_{22}H_{21}O_3$ $[M + H]^+$ 333.1491; found $[M + H]^+$ 333.1488; *m/z* (%) = 332.1428 (90) $[M]^+$, 333.1488 (100) $[M + H]^+$, 334.1565 (25).

5.2.30 Preparation of 1-methoxy-3-methyltetraphene-7,12-dione 141

To a solution of tetracycle **142** (110 mg, 0.33 mmol, 1.0 eq) in MeCN (15 ml) was added a solution of CAN (544 mg, 0.990 mmol, 3.0 eq) in water (5 ml) at room temperature. The reaction was allowed to stir for 1.5 h before being poured into water (5 ml) and extracted with EtOAc (3 × 20 ml). The combined organic layers were washed with water (25 ml), followed by brine (25 ml) and dried over $MgSO_4$. After filtering, and concentrating *in vacuo*, the crude product was purified by silica gel column chromatography (20% EtOAc/ Hexane) to generate quinone **141** as an orange solid (89 mg, 89% yield).

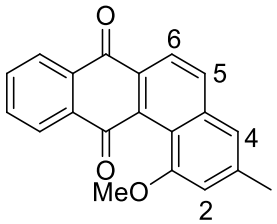

R_f (20% EtOAc/ Hexane): 0.47. **^{1}H NMR (400 MHz, $CDCl_3$)** δ 8.23 (d, *J* = 8.5, 1H, ArH-6), 8.20 (d, *J* = 6.4, 1H, ArH), 8.09 (d, *J* = 7.7, 1H, ArH), 7.94 (d, *J* = 8.5, 1H, ArH-5), 7.80 – 7.69 (m, 2H, ArH), 7.28 (s, 1H, ArH-4), 6.91 (s, 1H, ArH-2), 3.99 (s, 3H, OMe), 2.55 (s, 3H, CH_3). **^{13}C NMR (126 MHz, $CDCl_3$)** δ 186.1 (C=O), 183.1 (C=O), 157.2 (ArC-OMe), 140.6, 138.2, 137.0, 136.5, 133.9, 132.8, 132.6, 132.5, 132.4, 126.4, 126.1, 122.5, 120.0, 119.6, 111.3, 56.0 (OMe), 22.1 (CH_3). **M.p** 162 – 164 °C. **HRMS** (ESI^+): calcd for $C_{20}H_{15}O_3$ $[M + H]^+$ 303.1021; found $[M + H]^+$ 303.1017; *m/z* (%) = 303.1017 (100) $[M + H]^+$, 304.1167 (25), 305.1319 (5).

5.2.31 Synthesis of 2,4-dichloro-11-hydroxy-1-methoxy-3-methyltetraphene-7,12-dione 169 and 2,4-dichloro-6-hydroxy-1-methoxy-3-methyltetraphene-7,12-dione 170

To a 2 ml sealed pressure tube equipped with a stirrer bar, were added, quinone **141** (40 mg, 0.13 mmol, 1.0 eq), $Ru[Cl_2(p\text{-cymene})]_2$ (16 mg, 0.026 mmol, 20 mol%), PIFA (168 mg, 0.39 mmol, 3.0 eq), TFAA (0.4 ml), TFA (0.008 ml), and CH_2Cl_2 (0.4 ml). The tube was sealed with a Teflon lined cap and placed in an oil bath heated to 100 °C. The solution was stirred for 18 h. After cooling to room temperature, the reaction mixture was poured into CH_2Cl_2 (2 ml), and water (2 ml), followed by an aqueous solution of HCl (10%, 2 ml), were added. The reaction mixture was stirred for 5 mins before being transferred to a separating funnel. The organic layer was extracted into CH_2Cl_2 (3 × 5 ml), and the combined organic layers were washed with brine (5 ml) and dried over $MgSO_4$. After filtering, the solution was concentrated *in vacuo*, and the crude product was purified using silica gel column chromatography (1-5% EtOAC/Hexane) to yield **169** as a yellow solid (4.5 mg, 9% yield).

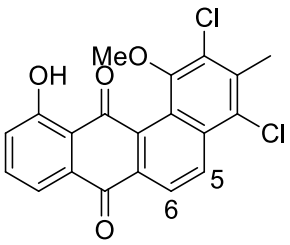

169

R_f (20% EtOAc/ Hexane): 0.68; **^{1}H NMR (500 MHz, $CDCl_3$)** δ 11.51 (s, 1H, OH), 8.65 (d, *J* = 8.8, 1H, ArH-5 or 6), 8.35 (d, *J* = 8.8, 1H, ArH-5 or 6), 7.81 (d, *J* = 7.5, 1H, ArH), 7.67 (app.t, dd, *J* = 7.9, 7.9, 1H, ArH), 7.35 (d, *J* = 8.4, 1H, ArH), 3.75 (s, 3H, OMe), 2.76 (s, 3H, CH_3). **^{13}C NMR (126 MHz, $CDCl_3$)** δ 187.4 (C=O), 182.3 (C=O), 160.3 (ArC-OH), 152.9 (ArC-OMe), 137.6, 135.7, 134.5, 133.7, 133.0, 132.2, 131.5, 130.2, 127.7, 124.4, 123.5, 123.2, 119.1, 117.4, 61.5 (OMe), 19.3 (CH_3). **HRMS** (ESI^+): calcd for $C_{20}H_{13}O_4{}^{35}Cl_2$ $[M + H]^+$ 387.0191; found $[M + H]^+$ 387.0111; *m/z* (%) = 387.0111 (30) $[M + H]^+$, 388.3860 (100), 389.3879 (30), 391.1892 (5).

170 was isolated as a dark red solid (10 mg, 20% yield).

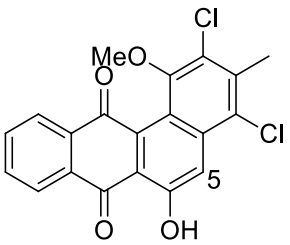

170

R_f (20% EtOAc/ Hexane): 0.62; **^{1}H NMR (500 MHz, $CDCl_3$)** δ 12.07 (s, 1H, OH), 8.26 – 8.24 (m, 1H, ArH), 8.12 (dd, *J* = 7.5, 1.3, 1H, ArH), 8.02 (s, 1H, ArH-5), 7.86 – 7.78 (m, 2H, ArH), 3.81 (s, 3H, OMe), 2.70 (s, 3H, CH_3). **^{13}C NMR (126 MHz, $CDCl_3$)** δ 188.9 (C=O), 184.9 (C=O), 157.6 (ArC-OH), 152.7 (ArC-OMe), 138.2, 137.0, 136.5, 136.1, 135.2, 133.3, 132.0, 126.7, 126.3, 126.2, 125.6, 119.8, 119.5, 115.6, 61.6 (OMe), 19.4 (CH_3). **HRMS** (ESI^+): calcd for $C_{20}H_{13}O_4{}^{35}Cl_2$ $[M + H]^+$ 387.0191; found $[M + H]^+$ 387.0158; *m/z* (%) = 387.0158 (100) $[M + H]^+$, 388.0193 (5), 389.0134 (60), 390.0162 (3), 391.1875 (10).

5.3 Experimental procedures for Chapter 4

5.3.1 Preparation of 2-hydroxy-4-pentadecylbenzaldehyde 243[179]

Method 1: To a solution of cardanol **178a** (10.0 g, 32.8 mmol, 1.0 eq, sourced from Sigma-Aldrich and used without purification) in dry toluene (125 ml), were added $SnCl_4$ (0.854 g, 3.28 mmol, 0.4 ml, 0.1 eq) and Et_3N (7 ml, 0.4 M) under an inert atmosphere. The mixture was stirred at room temperature for 30 mins. Paraformaldehyde (2.17 g, 72.2 mmol, 2.2 eq) was then added, and the reaction mixture stirred for another 30 mins at room temperature, before being heated to 100 °C. The reaction mixture was stirred for 8 h and then quenched with aqueous 1 M HCl solution (100 ml). The mixture was extracted with EtOAc (3 × 100 ml), and the combined organic layers were washed with water (100 ml), followed by brine (100 ml), dried over $MgSO_4$, and concentrated *in vacuo*. The crude compound was purified using silica gel column chromatography (5% EtOAc/Hexane) to yield formylated cardanol **243** as a white solid (7.4 g, 67%).

Method 2: To a flask purged with inert gas, was added paraformaldehyde (296 mg, 9.84 mmol, 3.0 eq) and anhydrous $MgCl_2$ (625 mg, 6.56 mmol, 2.0 eq) in a glovebox. Dry THF (20 ml) was then added and the reaction stirred at room temperature. Triethylamine (664 mg, 6.56 mmol, 0.9 ml, 2.0 eq) was added dropwise *via* syringe and the mixture was stirred for 10 mins. Cardanol **178a** (1.00 g, 3.28 mmol, 1.0 eq) was then added portion-wise and heated to 75 °C. The reaction was stirred for 2.5 h. Upon completion, the reaction was quenched with aqueous 1 M HCl (10 ml) and extracted with EtOAc (3 × 50 ml). The organic layers were washed with water (50 ml) and brine (50 ml), dried over $MgSO_4$, and concentrated *in vacuo*. The crude compound was purified by recrystallization from methanol to yield formylated cardanol **243** as a white solid (740 mg, 72%), the spectra of which compared well with that found in literature.[179]

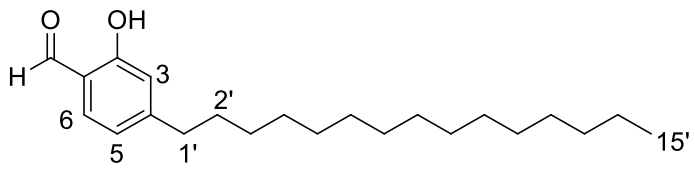

R_f (20% EtOAc/Hexane) = 0.86. **^{1}H NMR (300 MHz, $CDCl_3$)** δ 11.04 (s, 1H, OH), 9.80 (s, 1H, CHO), 7.41 (d, *J* = 7.8, 1H, ArH-6), 6.83–6.77 (m, 2H, ArH-3, 5), 2.60 (t, *J* = 7.7, 2H, H-1′), 1.61 (app. p, *J* = 6.9, 2H, H-2′), 1.33 – 1.25 (m, 24H), 0.88 (t, *J* = 6.4, 3H, H-15′); **^{13}C NMR (75 MHz, $CDCl_3$**, not all aliphatic signals were observable as individual signals in this, and subsequent spectra**)** δ 195.7 (C=O), 161.8 (ArC-OH), 153.8, 133.6, 120.5, 118.9, 117.1, 36.5, 32.0, 30.7, 29.8, 29.3, 22.8, 14.2.

5.3.2 Preparation of 2-bromo-1,4-dimethoxybenzene 244a[212]

To a solution of 1,4-dimethoxybenzene (5.00 g, 36.2 mmol, 1.0 eq) in dry CH_2Cl_2 (80 ml) was added NBS (7.00 g, 39.8 mmol, 1.1 eq). The reaction mixture was stirred under reflux for 72 h. After cooling, the reaction was quenched with a saturated aqueous solution of Na_2SO_3 (40 ml) and extracted with CH_2Cl_2 (3 × 40 ml). The organic layers were washed sequentially with water (50 ml) and brine (50 ml), dried over $MgSO_4$, and concentrated *in vacuo.* The crude product was purified using silica gel column chromatography (20% EtOAc/ Hexane) to yield 2-bromo-1,4-dimethoxybenzene **244a** as a yellow oil (5.6 g, 72% yield), the spectra of which compared well with that found in literature.[212]

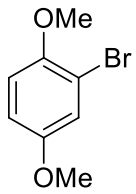

R_f (20% EtOAc/Hexane) = 0.76. **^{1}H NMR (300 MHz, $CDCl_3$)** δ 7.08 (dd, *J* = 2.1, 1.3, 1H, ArH), 6.75 – 6.74 (m, 2H, ArH), 3.76 (s, 3H, OMe), 3.68 (s, 3H, OMe); **^{13}C NMR (75 MHz, $CDCl_3$)** δ 153.9 (ArC-OMe), 150.2 (ArC-OMe), 119.0, 113.4, 112.8, 111.8, 56.6 (OMe), 55.7 (OMe).

5.3.3 Preparation of 2-[(2,5-dimethoxyphenyl)(hydroxy)methyl]-5-pentadecylphenol 245a

All glassware was oven dried for a minimum of 2 h before setting up this reaction. In an oven dried, three-necked round bottom flask, Mg turnings (58 mg, 2.4 mmol, 4.0 eq) and a granule of I_2 were dissolved in dry Et_2O (5 ml). To this suspension was added dropwise a solution of 2-bromo-1,4-dimethoxybenzene **244a** (521 mg, 2.40 mmol, 4.0 eq) in dry Et_2O (1.5 ml). The reaction was gently heated for 4 h, and the surfaces of Mg turnings were repeatedly scratched until the first signs of Grignard reagent formation were observed. After complete formation of Grignard reagent, the reaction was cooled to 0 °C and a solution of 2-hydroxy-4-pentadecylbenzaldehyde **243** (200 mg, 0.6 mmol, 1.0 eq) in dry THF (1.5 ml) was added dropwise to the Grignard reagent. This was refluxed for 90 mins, and thereafter stirred for 18 h at room temperature. Upon completion, the reaction was cooled to 0 °C. A saturated aqueous solution of NH_4Cl (20 ml) was added to quench the reaction, and thereafter the organic material was extracted using EtOAc (3 × 50 ml). The combined organic layers were washed with water (50 ml) followed by brine (50 ml), dried over $MgSO_4$ and concentrated *in vacuo.* The crude product was purified using silica gel column chromatography (10% EtOAc/ Hexane) to yield the secondary alcohol **245a** as a cream solid (220 mg, 78% yield).

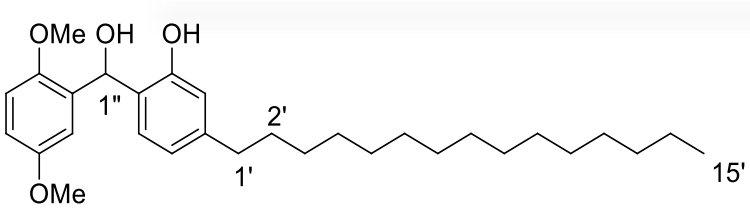

R_f (20% EtOAc/Hexane) = 0.49. **^{1}H NMR (300 MHz, $CDCl_3$)** δ 8.20 (s, 1H, ArOH), 6.85 - 6.55 (m, 6H, ArH), 6.12 (d, *J* = 4.6, 1H, C-OH), 4.14 (d, *J* = 4.6, 1H, H-1″), 3.76 (s, 3H, OMe), 3.65 (s, 3H, OMe), 2.52 (t, *J* = 7.7, 2H, H-1′), 1.55 (app. p, *J* = 7.0, 2H, H-2′), 1.28 – 1.20 (m, 24H), 0.88 (t, *J* = 6.5, 3H, H-15′). **^{13}C NMR (75 MHz, $CDCl_3$)** δ 155.9, 153.9, 150.9, 144.4, 130.8, 127.6, 122.8, 119.9, 116.9, 114.6, 113.3, 111.7, 72.8 (C-1″), 55.9 (OMe), 55.5 (OMe), 35.6, 32.0, 31.2, 29.4, 22.7. **M.p.** 78 – 79 °C. **FTIR**: **$\tilde{\nu}$ =** 3352 (O-H), 3185 (O-H), 1501 (C=C), 1252 (C-O), 1225 (C-O) cm^{-1}. **HRMS** (ESI^+): calcd for $C_{30}H_{45}O_3$ $[M - H_2O + H]^+$ 453.3367; found $[M - H_2O + H]^+$ 453.3340; *m/z* (%) = 453.3340 (100) $[M - H_2O + H]^+$, 454.3375 (30).

5.3.4 General procedure for the synthesis of benzoate esters.

Method 1: To a two-necked flask containing acid (1.1 eq), was added TFAA (4.0 eq) under a nitrogen atmosphere, and the solution was stirred for 15 mins at room temperature. Then cardanol **178a** (1.0 eq) dissolved in dry CH_2Cl_2 (20 ml) was added to the mixture and stirred at room temperature until complete consumption of starting material. The reaction was quenched with a saturated aqueous solution of $NaHCO_3$ (20 ml) and extracted with CH_2Cl_2 (3 × 20 ml). The combined organic layers were washed with water (50 ml) followed by brine (50 ml), and dried over $MgSO_4$, before being concentrated *in vacuo.* The product was purified using silica gel column chromatography (20% EtOAc/Hexane) to yield benzoate ester.

Method 2: To a two-necked flask containing acid (1.2 eq), was added TFAA (7.0 eq) under a nitrogen atmosphere, and the solution was stirred for 15 mins at room temperature. Then cardanol **178a** (1.0 eq) dissolved in dry toluene (3 ml) was added to the mixture and stirred at room temperature until complete consumption of starting material. The reaction was quenched with a saturated aqueous solution of $NaHCO_3$ (5 ml) and extracted with EtOAc (3 × 20 ml). The combined organic layer was washed with water (10 ml) followed by brine (10 ml), and dried over $MgSO_4$, before being concentrated *in vacuo.* The product was purified using silica gel column chromatography (20% EtOAc/Hexane) to yield benzoate ester.

*5.3.4.1 3-Pentadecylphenyl 2,5-dimethoxybenzoate **249a***

Method 1: Synthesized using 2,5-dimethoxybenzoic acid **248a** (657 mg, 3.61 mmol), TFAA (1.80 ml, 13.1 mmol), and cardanol **178a** (1.00 g, 3.28 mmol). Stirred for 8 h. Benzoate ester **249a** was isolated as a pale-yellow low melting solid (1.4 g, 93%).

Method 2: Synthesized using 2,5-dimethoxybenzoic acid **248a** (40 mg, 0.22 mmol), TFAA (0.18 ml, 1.3 mmol), and cardanol **178a** (55 mg, 0.18 mmol). Stirred for 3 h. Benzoate ester **249a** was isolated as a pale-yellow low melting solid (80 mg, 95%).

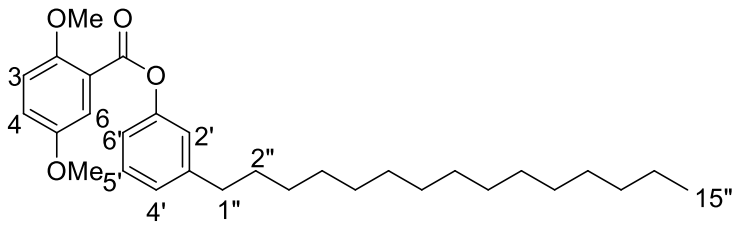

R_f (20% EtOAc/Hexane) = 0.60; **^{1}H NMR (300 MHz, $CDCl_3$)** δ 7.54 (d, *J* = 3.2, 1H, ArH-6), 7.33–7.26 (m, 1H, ArH-5′), 7.09 (dd, *J* = 9.0, 3.1, 2H, ArH-4, 2′), 7.03 (dd, *J* = 7.8, 1.6, 2H, ArH-6′, 4′), 6.96 (d, *J* = 9.0, 1H, ArH-3), 3.88 (s, 3H, OMe), 3.81 (s, 3H, OMe), 2.62 (dd, *J* = 8.8, 6.7, 2H, H-1″), 1.62 (app. p, *J* = 7.3, 2H, H-2″), 1.36 – 1.31 (m, 24H), 0.93 (t, *J* = 6.8, 3H, H-15″). **^{13}C NMR (75 MHz, $CDCl_3$)** δ 164.3 (C=O), 154.3, 153.1, 151.0, 144.6, 129.1, 125.9, 121.7, 120.3, 119.7, 119.0, 116.3, 114.1, 56.8 (OMe), 55.9 (OMe), 35.8, 32.0, 31.3, 29.7, 29.7, 29.6, 29.5, 29.4, 29.4, 22.7, 14.2. **M.p** 43 – 44.5 °C. **FTIR: $\tilde{\nu}$** = 2917 (C-H), 2850 (C-H), 1715 (C=O), 1584 (C=C), 1286 (C-O), 1232 (C-O) cm^{-1}. **HRMS:** (ESI^+): calcd for $C_{30}H_{45}O_4$ $[M + H]^+$ 469.3318; found $[M + H]^+$ 469.3299; *m/z* (%) = 469.3299 (100) $[M + H]^+$, 470.3334 (30), 471.3362 (5).

*5.3.4.2 3-Pentadecylphenyl 2,4,5-trimethoxybenzoate **249b***

Method 1: Synthesized using 2,4,5-trimethoxybenzoic acid **248b** (1.15 g, 5.41 mmol), TFAA (2.74 ml, 19.7 mmol), and cardanol **178a** (1.50 g, 4.92 mmol). Stirred for 18 h. Benzoate ester **249b** was isolated as a white solid (2.3 g, 94%).

Method 2: Synthesized using 2,4,5-trimethoxybenzoic acid **248b** (47 mg, 0.22 mmol), TFAA (0.18 ml, 1.3 mmol), and cardanol **178a** (55 mg, 0.18 mmol). Stirred for 18 h. Benzoate ester **249b** was isolated as a white solid (70 mg, 78%).

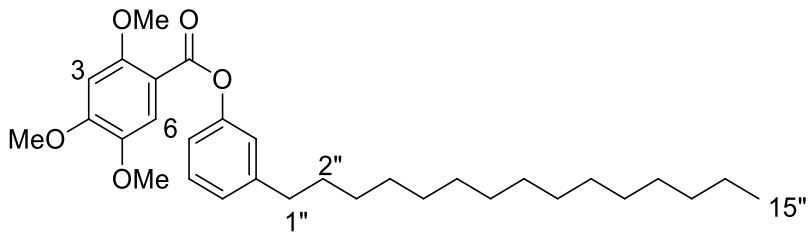

R_f (20% EtOAc/Hexane) = 0.24. **^{1}H NMR (400 MHz, $CDCl_3$)** δ 7.59 (s, 1H, ArH-6), 7.32-7.26 (m, 1H, ArH), 7.08–6.99 (m, 3H, ArH), 6.58 (s, 1H, ArH-3), 3.97 (s, 3H, OMe), 3.93 (s, 3H, OMe), 3.90 (s, 3H, OMe), 2.62 (t, *J* = 7.7, 2H, H-1″), 1.62 (app. p, *J* = 8.7, 3H, H-2″), 1.31-1.26 (m, 24H), 0.88 (t, *J* = 6.8, 3H, H-15″). **^{13}C NMR (75 MHz, $CDCl_3$)** δ 163.9 (C=O), 156.6 (ArC-OMe), 154.2 (ArC-OMe), 151.0, 144.6, 142.6 (ArC-OMe), 129.0, 125.7, 121.8, 119.1, 114.6, 109.8, 97.8, 57.1 (OMe), 56.5

(OMe), 56.1 (OMe), 35.8, 31.9, 31.3, 29.7, 29.7, 29.6, 29.5, 29.4, 22.7, 14.1. **M.p**. 62.3-62.6°C. **FTIR**: **ṽ** = 2919 (C-H), 2850 (C-H), 1707 (C=O), 1578 (C=C), 1268 (C-O), 1238 (C-O), 1205 (C-O) cm^{-1}. **HRMS:** (ESI^+): calcd for $C_{31}H_{47}O_5$ $[M + H]^+$ 499.3423; found $[M + H]^+$ 499.3406; *m/z* (%) = 499.3406 (100) $[M + H]^+$, 500.3434 (30)**.**

*5.3.4.3 3-Pentadecylphenyl 2,3-dimethoxybenzoate **249c***

Method 1: Synthesized using 2,3-dimethoxybenzoic acid **248c** (987 mg, 5.41 mmol), TFAA (2.74 ml, 19.7 mmol), and cardanol **178a** (1.50 g, 4.92 mmol). Stirred for 18 h. Benzoate ester **249c** was isolated as a white solid (2.2 g, 96%).

Method 2: Synthesized using 2,3-dimethoxybenzoic acid **248c** (40 mg, 0.22 mmol), TFAA (0.18 ml, 1.3 mmol), and cardanol **178a** (55 mg, 0.18 mmol). Stirred for 18 h. Benzoate ester **249c** was isolated as a white solid (70 mg, 83%).

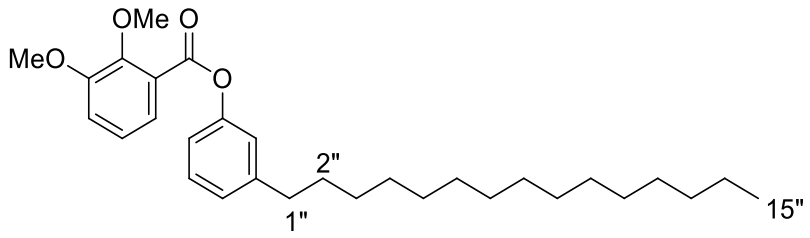

R_f (20% EtOAc/Hexane) = 0.64. **^{1}H NMR (300 MHz, $CDCl_3$)** δ 7.52 (dd, *J* = 6.9, 2.5, 1H, ArH), 7.35–7.28 (m, 1H, ArH), 7.19–7.11 (m, 2H, ArH), 7.10–7.02 (m, 3H, ArH), 3.96 (s, 3H, OMe), 3.92 (s, 3H, OMe), 2.62 (t, *J* = 7.7, 2H, H-1″), 1.62 (app. p, *J* = 8.7, 3H, H-2″), 1.31-1.25 (m, 24H), 0.88 (t, *J* = 6.8, 3H, H-15″). **^{13}C NMR (75 MHz, $CDCl_3$)** δ 164.6 (C=O), 153.7, 150.9, 149.7, 144.8, 129.1, 126.0, 125.5, 123.9, 122.6, 121.6, 118.9, 116.4, 61.6 (OMe), 56.1 (OMe), 35.8, 31.9, 31.3, 30.9, 29.7, 29.7, 29.6, 29.5, 29.4, 29.3, 22.7, 14.1. **M.p.** 65.6 – 66.4 °C. **FTIR**: **ṽ** = 2921 (C-H), 1731 (C=O), 1583 (C=C), 1307 (C-O), 1251 (C-O), 1210 (C-O), 1096 (C-O) cm^{-1}. **HRMS:** (ESI^+): calcd for $C_{30}H_{45}O_4$ $[M + H]^+$ 469.3318; found $[M + H]^+$ 469.3304; *m/z* (%) = 469.3304 (100) $[M + H]^+$, 470.3339 (30), 471.3369 (5).

5.3.5 Synthesis of (2,5-dimethoxyphenyl)(2-hydroxy-4-pentadecylphenyl)methanone 241a

Method 1 (oxidation using MnO_2): To a solution of secondary alcohol **245a** (200 mg, 0.44 mmol, 1.0 eq) dissolved in CH_2Cl_2 (10 ml), was added activated MnO_2 (306 mg, 3.50 mmol, 8.0 eq). The reaction mixture was stirred for 72 h at room temperature. Upon completion, the reaction was filtered through Celite, concentrated *in vacuo*, and purified using silica gel column

chromatography (15% EtOAc/ Hexane) to yield benzophenone **241a** as a white solid (145 mg, 72%).

Method 2 (solvent free oxidation): Using a pestle and mortar, secondary alcohol **245a** (200mg, 0.44 mmol, 1.0 eq) was ground to a fine powder, and transferred to a round bottom flask. Using the same pestle and mortar, $KMnO_4$ (243 mg, 1.54 mmol, 3.5 eq) and $CuSO_4 \cdot 5H_2O$ (385 mg, 1.54 mmol, 3.5 eq) were ground together until they formed a fine homogeneous powder. This was then added to the round bottom flask containing ground compound **245a** and stirred through until homogeneous. The mixture was heated to 135 °C for 2 h. Upon cooling, EtOAc (20 ml) was added, and the reaction was quenched with a saturated aqueous solution of $Na_2S_2O_3$ (10 ml). The organic material was extracted with EtOAc (3 × 20 ml), and the combined organic layers were washed sequentially with water (20 ml) and brine (20 ml), dried over $MgSO_4$, and concentrated *in vacuo*. The crude product was purified using silica gel column chromatography (15% EtOAc/ Hexane) to yield benzophenone **241a** as a white solid (110 mg, 53%).

Method 3 (Fries rearrangement): In a microwave tube was added P_2O_5 (65 mg, 0.46 mmol, 7.7% of $MeSO_3H$), being careful to minimize exposure to the atmosphere. This was quickly followed by the addition of $MeSO_3H$ (573 mg, 5.96 mmol, 9.2 eq), and benzoate ester **249a** (305 mg, 0.65 mmol, 1.0 eq). The reaction was placed in the microwave, at 50 W, and 80 °C for 15 mins. The reaction was quenched with water (10 ml), and extracted with EtOAc (3 × 20 ml). The combined organic layers were washed sequentially with a saturated aqueous solution of $NaHCO_3$ (20 ml), water (20 ml) and brine (20 ml), and dried over $MgSO_4$. After concentrating *in vacuo*, the product was purified using silica gel column chromatography (5% EtOAc/ Hexane) to yield benzophenone **241a** as a white solid (153 mg, 50%, and 63% yield based on recovered starting material).

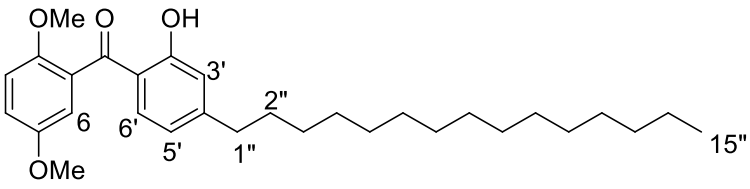

R_f (20% EtOAc/Hexane) = 0.66. **^{1}H NMR (400 MHz, $CDCl_3$)** δ 12.16 (s, 1H, OH), 7.24 (d, *J* = 8.3, 1H, ArH-6′), 7.01–6.97 (m, 1H, ArH), 6.95–6.91 (m, 1H, ArH), 6.83 (s, 2H, ArH-3′, 6), 6.62 (d, *J* = 8.2, 1H, ArH-5′), 3.77 (s, 3H, OMe), 3.72 (s, 3H, OMe), 2.58 (t, *J* = 7.7, 2H, H-1″), 1.61 (app. p, *J* = 7.2, 2H, H-2″), 1.39-1.30 (m, 24H), 0.88 (t, *J* = 6.6, 3H, H-15″). **^{13}C NMR (101 MHz, $CDCl_3$)** δ 200.9 (C=O), 163.1 (ArC-OH), 153.1 (ArC-OMe), 153.3, 150.5 (ArC-OMe), 133.7, 128.1, 119.4, 118.0,

117.4, 116.9, 113.9, 113.0, 56.4 (OMe), 55.9 (OMe), 36.3, 31.9, 30.1, 29.7, 29.6, 29.5, 29.4, 29.3, 22.7, 14.1 **M.p.** 61 – 62 °C. **FTIR**: **ṽ** = 3001 (O-H), 2914 (C-H), 2849 (C-H), 1632 (C=O), 1574 (C=C), 1307 (C-O), 1229 (C-O), 1099 (C-O) cm^{-1}. **HRMS** (ESI^+): calcd for $C_{30}H_{45}O_4$ $[M + H]^+$ 469.3318; found $[M + H]^+$ 469.3311; *m/z* (%) = 469.3311 (100) $[M + H]^+$, 470.3355 (35), 471.3368 (5).

5.3.6 Synthesis of (2-hydroxy-4-pentadecylphenyl)(2,4,5-trimethoxyphenyl)methanone 241b

To a small reaction tube was added benzoate ester **249b** (300 mg, 0.6 mmol). This was dissolved in dry MeCN (2.5 ml), and stirred until completely dissolved at 70 °C, after which triflic acid (0.09 ml) was added. The reaction mixture was stirred for 45 mins at 70 °C. The reaction was then quenched with water (5 ml), followed by a saturated aqueous solution of $NaHCO_3$ (5 ml), and extracted with EtOAc (3 × 15 ml). The combined organic layers were washed with water (5 ml) followed by brine (5 ml), and dried over $MgSO_4$, before being concentrated *in vacuo*. The crude product was purified using silica gel column chromatography (20% EtOAc/ Hexane) to yield benzophenone **241b** as a white solid (60 mg, 20%).

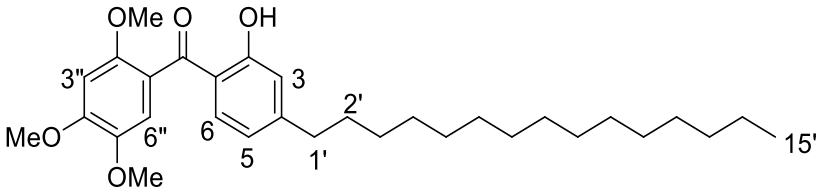

R_f (20% EtOAc/Hexane) = 0.36; **^{1}H NMR (400 MHz, $CDCl_3$)** δ 12.25 (s, 1H, OH), 7.31 (d, *J* = 8.3, 1H, ArH-6), 6.87 (s, 1H, ArH-6″), 6.84 (s, 1H, ArH-3), 6.63 (d, *J* = 8.3, 1H, ArH-5), 6.59 (s, 1H, ArH-3″), 3.97 (s, 3H, OMe), 3.84 (s, 3H, OMe), 3.76 (s, 3H, OMe), 2.59 (t, *J* = 7.8, 2H, H-1′), 1.63-1.61 (m, 2H, H-2′), 1.30-1.25 (m, 24H), 0.88 (t, *J* = 6.6, 3H, H-15′). **^{13}C NMR (101 MHz, $CDCl_3$)** δ 200.4 (C=O), 163.0 (ArC-OH), 152.9 (ArC-OMe), 151.9 (ArC-OMe), 151.8 (ArC-OMe), 143.0, 133.7, 119.3, 118.3, 117.4 (C-3), 112.6 (C-6″), 97.5 (C-3″), 56.7 (OMe), 56.5 (OMe), 56.2 (OMe), 36.3, 31.9, 31.0, 30.6, 29.7, 29.7, 29.6, 29.5, 29.4, 29.3, 22.7, 14.1. **M.p.** 62.8 – 63.8 °C. **FTIR**: **ṽ** = 2915 (C-H), 2849 (C-H), 1662 (C=O), 1508 (C=C), 1307 (C-O), 1263 (C-O), 1218 (C-O), 1097 (C-O) cm^{-1}. **HRMS:** (ESI^+): calcd for $C_{31}H_{47}O_5$ $[M + H]^+$ 499.3423; found $[M + H]^+$ 499.3412; *m/z* (%) = 499.3412 (100) $[M + H]^+$, 500.3445 (30), 501.3470 (5).

5.3.7 Preparation of (2,3-dimethoxyphenyl)(2-hydroxy-4-pentadecylphenyl)methanone 241c

To a one-necked round bottom flask was added benzoate ester **249c** (1.00 g, 2.13 mmol, 1.0 eq). This was dissolved in dry toluene (8.5 ml), and placed in an oil bath heated to 100 °C. After stirring for 5 mins, triflic acid (0.32 ml) was added and the mixture was stirred at 100 °C for 45 mins. The reaction was quenched with water (10 ml) followed by a saturated aqueous solution of $NaHCO_3$ (10 ml), and then extracted with EtOAc (3 × 20 ml). The combined organic layers were washed with water (15 ml) and brine (15 ml) and dried over $MgSO_4$. After concentration *in vacuo*, the crude product was purified using silica gel column chromatography (5% EtOAc/ Hexane) to yield benzophenone **241c** as a clear low melting solid (630 mg, 63%).

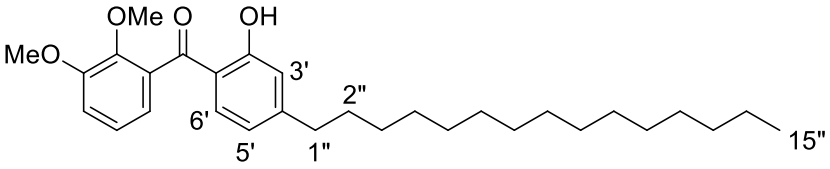

R_f (20% EtOAc/Hexane) = 0.70. **^{1}H NMR (400 MHz, $CDCl_3$)** δ 12.20 (s, 1H, OH), 7.23 (d, *J* = 8.3, 1H, ArH-6′), 7.15-7.11 (m, 1H, ArH), 7.04 (d, *J* = 8.2, 1H, ArH), 6.86 (s, 1H, ArH), 6.84 (s, 1H, ArH-3′), 6.61 (d, *J* = 8.3, 1H, ArH-5′), 3.91 (s, 3H, OMe), 3.79 (s, 3H, OMe), 2.58 (t, *J* = 7.8, 2H, H-1″), 1.60 (app. p, *J* = 7.7, 2H, H-2″), 1.29-1.25 (m, 24H), 0.87 (t, *J* = 7.1, 3H, H-15″). **^{13}C NMR (101 MHz, $CDCl_3$)** δ 201.0 (C=O), 163.1 (ArC-OH), 153.4 (ArC-OMe), 152.8 (ArC-OMe), 146.2, 133.8 (ArC-6′), 133.3, 124.0, 119.9, 119.5, 118.1, 117.4, 114.1, 61.8 (OMe), 55.9 (OMe), 36.3, 32.0, 30.6, 29.7, 29.6, 29.5, 29.4, 29.3, 22.7, 14.2. **M.p.** 38 – 39 °C. **FTIR**: **$\tilde{\nu}$** = 2917 (C-H), 2849 (C-H), 1634 (C=O), 1580 (C=C), 1364 (C-O), 1269 (C-O), 1229 (C-O), 1075 (C-O) cm^{-1}. **HRMS**: (ESI$^+$): calcd for $C_{30}H_{45}O_4$ $[M + H]^+$ 469.3318; found $[M + H]^+$ 469.3292; *m/z* (%) = 469.3292 (100) $[M + H]^+$, 470.3327 (30), 471.3355 (5).

5.3.8 General procedure for the synthesis of xanthones.

In a round bottom flask, $CHCl_3$ and MeCN were used to dissolve the benzophenone (1.0 eq). Water was then added and a suspension formed to which CAS (4.0 eq) was added in portions. The reaction was heated to 70 °C and stirred for 18 h. Upon completion, the reaction was transferred to a separating funnel, and EtOAc (50 ml) and water (20 ml) were added. The aqueous layer was run off and the organic layer was washed with a saturated aqueous solution of $NaHCO_3$ (20 ml), followed by brine (20 ml). The organic layer was dried over $MgSO_4$ and concentrated *in vacuo*. The crude product was purified using silica gel column chromatography (10% EtOAc/Hexane) to yield xanthone.

*5.3.8.1 2-Methoxy-6-pentadecyl-9H-xanthen-9-one **240a***

Synthesized using benzophenone **241a** (145 mg, 0.320 mmol), $CHCl_3$ (3 ml), MeCN (12 ml), H_2O (6 ml), CAS (810 mg, 1.28 mmol). Xanthone **240a** was isolated as a white solid (98 mg, 70%).

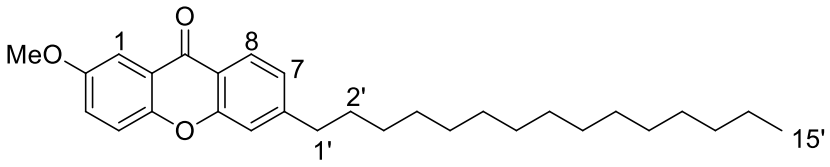

R_f (20% EtOAc/Hexane) = 0.71. **^{1}H NMR (400 MHz, $CDCl_3$)** δ 8.24 (d, *J* = 8.2, 1H, ArH-8), 7.71 (s, 1H, ArH-1), 7.42 (d, *J* = 9.2, 1H, ArH), 7.33–7.25 (m, 2H, ArH), 7.20 (d, *J* = 8.2, 1H, ArH-7), 3.92 (s, 3H, OMe), 2.75 (t, *J* = 7.8, 2H, H-1′), 1.69 (app. p, *J* = 7.4, 2H, H-2′), 1.36-1.25 (m, 24H), 0.88 (t, *J* = 6.6, 3H, H-15′). **^{13}C NMR (101 MHz, $CDCl_3$)** δ 177.9 (C=O), 156.3, 155.9, 151.0, 151.0, 126.5, 124.6, 124.6, 122.2, 119.3, 119.2, 117.0, 105.9, 55.9 (OMe), 36.2, 31.9, 30.9, 29.7, 29.7, 29.5, 29.4, 29.4, 29.2, 22.7, 14.1. **M.p.** 94 – 95 °C. **FTIR: ṽ** = 2920 (C-H), 2848 (C-H), 1651 (C=O), 1483 (C=C), 1346 (C-O), 1315, 1226 (C-O) cm^{-1}. **HRMS** (ESI^+): calcd for $C_{29}H_{41}O_3$ $[M + H]^+$ 437.3056; found $[M + H]^+$ 437.3024; *m/z* (%) = 437.3024 (100) $[M + H]^+$, 438.3057 (30), 439.3085 (5).

*5.3.8.2 2,3-Dimethoxy-6-pentadecyl-9H-xanthen-9-one **240b***

Synthesized using benzophenone **241b** (159 mg, 0.320 mmol), $CHCl_3$ (3 ml), MeCN (12 ml), H_2O (6 ml), CAS (810 mg, 1.28 mmol). Xanthone **240b** was isolated as a white solid (110 mg, 74%).

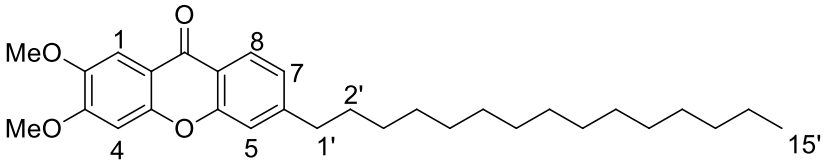

R_f (20% EtOAc/Hexane) = 0.33; **^{1}H NMR (400 MHz, $CDCl_3$)** δ 8.24 (d, *J* = 8.1, 1H, ArH-8), 7.67 (s, 1H, ArH-1), 7.26 (d, *J* = 7.3, 1H, ArH-5), 7.20 (d, *J* = 8.1, 1H, ArH-7), 6.90 (s, 1H, ArH-4), 4.02 (s, 3H, OMe), 4.00 (s, 3H, OMe), 2.75 (t, *J* = 7.7, 2H, H-1′), 1.69 (app. p, *J* = 7.5, 2H, H-2′), 1.35-1.25 (m, 24H), 0.88 (t, *J* = 6.6, 3H, H-15′). **^{13}C NMR (101 MHz, $CDCl_3$)** δ 176.0 (C=O), 156.2, 155.2 (ArC-OMe), 152.4, 150.4, 146.6 (ArC-OMe), 126.3, 124.7, 119.5, 116.8, 115.0, 105.4, 99.6, 56.5 (OMe), 56.3 (OMe), 36.2, 31.9, 31.0, 29.7, 29.7, 29.6, 29.5, 29.4, 29.3, 22.7, 14.1. **M.p.** 96.5 – 97.7 °C. **FTIR**: **ṽ** = 2916 (C-H), 2849 (C-H), 1646 (C=O), 1508 (C=C), 1270 (C-O), 1208 (C-O), 1170 (C-O) cm^{-1}. **HRMS** (ESI^+): calcd for $C_{30}H_{43}O_4$ $[M + H]^+$ 467.3161; found $[M + H]^+$ 467.3145; *m/z* (%) = 467.3145 (100) $[M + H]^+$, 468.3178 (30), 469.3209 (5).

*5.3.8.3 5-Methoxy-3-pentadecyl-9H-xanthen-9-one **240c***

Synthesized using benzophenone **241c** (113 mg, 0.240 mmol), $CHCl_3$ (2.5 ml), MeCN (10 ml), H_2O (5 ml), CAS (607 mg, 0.960 mmol). Xanthone **240c** was isolated as a white solid (60 mg, 57%).

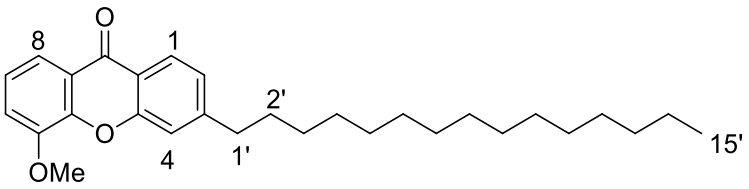

R_f (20% EtOAc/Hexane) = 0.52; **^{1}H NMR (400 MHz, $CDCl_3$)** δ 8.24 (d, *J* = 8.2, 1H, ArH-1), 7.91 (d, *J* = 7.9, 1H, ArH-8), 7.44 (s, 1H, ArH-4), 7.32–7.18 (m, 3H, ArH), 4.05 (s, 3H, OMe), 2.75 (t, *J* = 7.7, 2H, H-1′), 1.69 (app. p, *J* = 7.6, 2H, H-2′), 1.30-1.25 (m, 24H), 0.90–0.84 (m, 3H, H-15′). **^{13}C NMR (101 MHz, $CDCl_3$)** δ 177.0 (C=O), 156.1, 151.3, 148.6 (ArC-OMe), 146.5, 126.4, 125.1, 123.3, 122.8, 119.6, 117.7, 117.4, 115.1, 56.4 (OMe), 36.2, 31.9, 30.8, 29.7, 29.7, 29.6, 29.5, 29.4, 29.2, 22.7, 14.2. **M.p.** 103 – 104.8 °C. **FTIR**: **$\tilde{\nu}$** = 2916 (C-H), 2849 (C-H), 1661 (C=O), 1508 (C=C), 1270 (C-O), 1198 (C-O), 1110 (C-O) cm^{-1}. **HRMS** (ESI^+): calcd for $C_{29}H_{41}O_3$ $[M + H]^+$ 437.3056; found $[M + H]^+$ 437.3051; *m/z* (%) = 437.3051 (100) $[M + H]^+$, 438.3073 (30).

5.3.9 Preparation of 1-hydroxy-7-methoxy-3-pentadecyl-9*H*-xanthen-9-one 242a

To a sealed tube were added xanthone **240a** (30 mg, 0.069 mmol, 1.0 eq), PIFA (36 mg, 0.084 mmol, 1.2 eq), $Ru[(p\text{-cymene})Cl_2]_2$ (4 mg, 0.007 mmol, 10 mol%), TFAA (0.18 ml), and TFA (0.004 ml). The tube was sealed and heated to 80 °C for 18 h. After cooling, the reaction mixture was added to a saturated aqueous solution of $NaHCO_3$ (10 ml) and then extracted with EtOAc (3 × 15 ml). The combined organic layers were washed with water (10 ml) followed by brine (10 ml), dried over $MgSO_4$, and concentrated *in vacuo*. The crude product was purified using silica gel column chromatography (5% EtOAc/Hexane) to yield hydroxy-xanthone **242a** as a pale-yellow solid (12 mg, 38%).

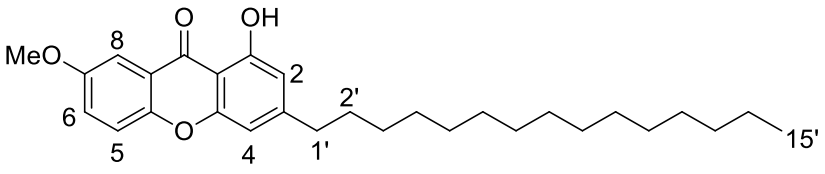

R_f (20% EtOAc/Hexane) = 0.86; **^{1}H NMR (400 MHz, $CDCl_3$)** δ 12.57 (s, 1H, OH), 7.62 (d, *J* = 2.9, 1H, ArH-8), 7.40 (d, *J* = 9.1, 1H, ArH-5), 7.33 (dd, *J* = 9.1, 2.9, 1H, ArH-6), 6.76 (s, 1H, ArH-4), 6.64 (s, 1H, ArH-2), 3.92 (s, 3H, OMe), 2.66 (t, *J* = 7.7, 2H, H-1′), 1.66 (app. p, *J* = 7.4, 2H, H-2′), 1.30-1.26 (m, 24H), 0.88 (t, *J* = 6.7, 3H, H-15′). **^{13}C NMR (101 MHz, $CDCl_3$)** δ 181.6 (C=O), 161.5 (ArC-OH), 156.3, 156.0, 153.7, 151.0, 125.4, 120.9, 119.2, 110.3, 106.9, 106.8,

105.1, 55.9 (OMe), 36.8, 31.9, 30.6, 29.7, 29.7, 29.5, 29.5, 29.4, 29.2, 22.7, 14.1. **M.p** 98 – 99 °C. **FTIR**: **ṽ** = 3080 (O-H), 2918 (C-H), 2849 (C-H), 1652 (C=O), 1484 (C=C), 1277 (C-O), 1207 (C-O) cm^{-1}. **HRMS:** (ESI^+): calcd for $C_{29}H_{41}O_4$ $[M + H]^+$ 453.3005; found $[M + H]^+$ 453.2978; *m/z* (%) = 453.2978 (100) $[M + H]^+$, 454.3009 (30), 455.3047 (5).

5.3.10 Preparation of 1-hydroxy-6,7-dimethoxy-3-pentadecyl-9*H*-xanthen-9-one 242b

To a sealed tube were added xanthone **240b** (45 mg, 0.096 mmol, 1.0 eq), $K_2S_2O_8$ (52 mg, 0.19 mmol, 2.0 eq), $Ru[(p\text{-cymene})Cl_2]_2$ (6 mg, 0.01 mmol, 10 mol%), TFA (1 ml), and TFAA (0.05 ml). The tube was sealed and heated to 80 °C for 18 h. After cooling, the reaction mixture was added to a saturated aqueous solution of $NaHCO_3$ (10 ml) and extracted with EtOAc (3 × 10 ml). The combined organic layers were washed with water (10 ml) followed by brine (10 ml), dried over $MgSO_4$, and concentrated *in vacuo*. The crude product was purified using silica gel column chromatography (5% EtOAc/Hexane) to yield hydroxy-xanthone **242b** as a pale-yellow solid (20 mg, 43%).

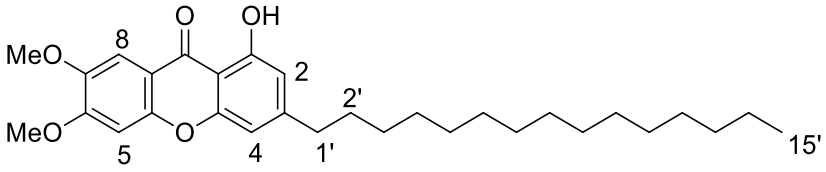

R_f (20% EtOAc/Hexane) = 0.45; **^{1}H NMR (400 MHz, $CDCl_3$)** δ 12.72 (s, 1H, OH), 7.57 (s, 1H, ArH-8), 6.88 (s, 1H, ArH-5), 6.73 (s, 1H, ArH-4), 6.63 (s, 1H, ArH-2), 4.02 (s, 3H, OMe), 4.00 (s, 3H, OMe), 2.66 (t, *J* = 7.7, 2H, H-1′), 1.66 (app. p, *J* = 7.7, 2H, H-2′), 1.32-1.25 (m, 24H), 0.88 (t, *J* = 6.7, 3H, H-15′). **^{13}C NMR (101 MHz, $CDCl_3$)** δ 180.6 (C=O), 161.3 (ArC-OH), 156.2, 155.9 (ArC-OMe), 152.9, 152.6, 146.8 (ArC-OMe), 113.5, 110.4, 106.8, 106.6, 104.5, 99.5, 56.6 (OMe), 56.4 (OMe), 36.7, 31.9, 30.7, 29.7, 29.7, 29.6, 29.5, 29.4, 29.2, 22.7, 14.1. **M.p.** 104 – 105.8 °C. **FTIR**: **ṽ** = 2918 (C-H), 2851 (C-H), 1645 (C=O), 1510 (C=C), 1272 (C-O), 1172 (C-O) cm^{-1}. **HRMS:** (ESI^+): calcd for $C_{30}H_{43}O_5$ $[M + H]^+$ 483.3110; found $[M + H]^+$ 483.3098; *m/z* (%) = 483.3098 (100) $[M + H]^+$, 484.3128 (30).

5.3.11 Preparation of 1-hydroxy-4-methoxy-6-pentadecyl-9*H*-xanthen-9-one 242c

To a sealed tube were added xanthone **240c** (50 mg, 0.11 mmol, 1.0 eq), PIFA (57 mg, 0.13 mmol, 1.2 eq), $Ru[(p\text{-cymene})Cl_2]_2$ (7 mg, 0.01 mmol, 10 mol%), TFAA (1 ml), and TFA (0.02 ml). The tube was sealed and heated to 80 °C for 18 h. After cooling, the reaction mixture was added to a saturated aqueous solution of $NaHCO_3$ (10 ml) and extracted with EtOAc (3 × 20 ml). The combined organic layers were washed with water (10 ml) followed by brine (10 ml), dried over $MgSO_4$, and concentrated *in vacuo*. The crude product was purified using silica gel

column chromatography (5% EtOAc/Hexane) to yield hydroxy-xanthone **242c** as a yellow solid (13 mg, 26%).

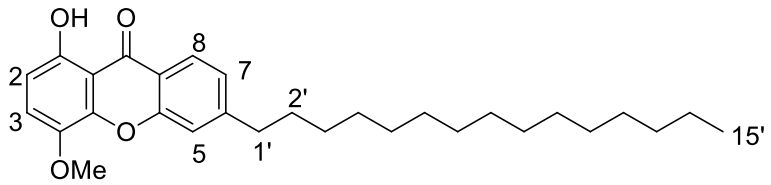

R_f (20% EtOAc/Hexane) = 0.73; **^{1}H NMR (400 MHz, $CDCl_3$)** δ 12.09 (s, 1H, OH), 8.11 (d, *J* = 8.1, 1H, ArH-8), 7.34 (s, 1H, ArH-5), 7.21–7.14 (m, 2H, ArH-2, 7), 6.66 (d, *J* = 8.7, 1H, ArH-3), 3.90 (s, 3H, OMe), 2.69 (t, *J* = 7.9, 2H, H-1′), 1.63-1.57 (m, 2H, H-2′), 1.28-1.18 (m, 24H), 0.82-0.79 (m, 3H, H-15′). **^{13}C NMR (101 MHz, $CDCl_3$)** δ 182.3 (C=O), 156.2, 154.6 (ArC-OH), 152.4, 145.9, 140.0 (ArC-OMe), 125.7, 125.3, 120.2, 118.5, 117.3, 109.5, 108.7, 57.5 (OMe), 36.3, 31.9, 30.9, 30.7, 29.6, 29.5, 29.4, 29.4, 29.2, 22.7, 14.1. **M.p.** 81 – 83 °C. **FTIR**: **$\tilde{\nu}$** = 2919 (C-H), 2852 (C-H), 1625 (C=O), 1511 (C=C), 1273 (C-O), 1120 (C-O) cm^{-1}. **HRMS** (ESI^+): calcd for $C_{29}H_{41}O_4$ $[M + H]^+$ 453.3005; found $[M + H]^+$ 453.3000; *m/z* (%) = 453.3000 (100) $[M + H]^+$, 454.3022 (30).

APPENDICES

A.1 – ^{1}H and ^{13}C NMR spectra for all compounds

A.2 – Crystallography data for compounds **142**, **169**, and **170**

Compound 131

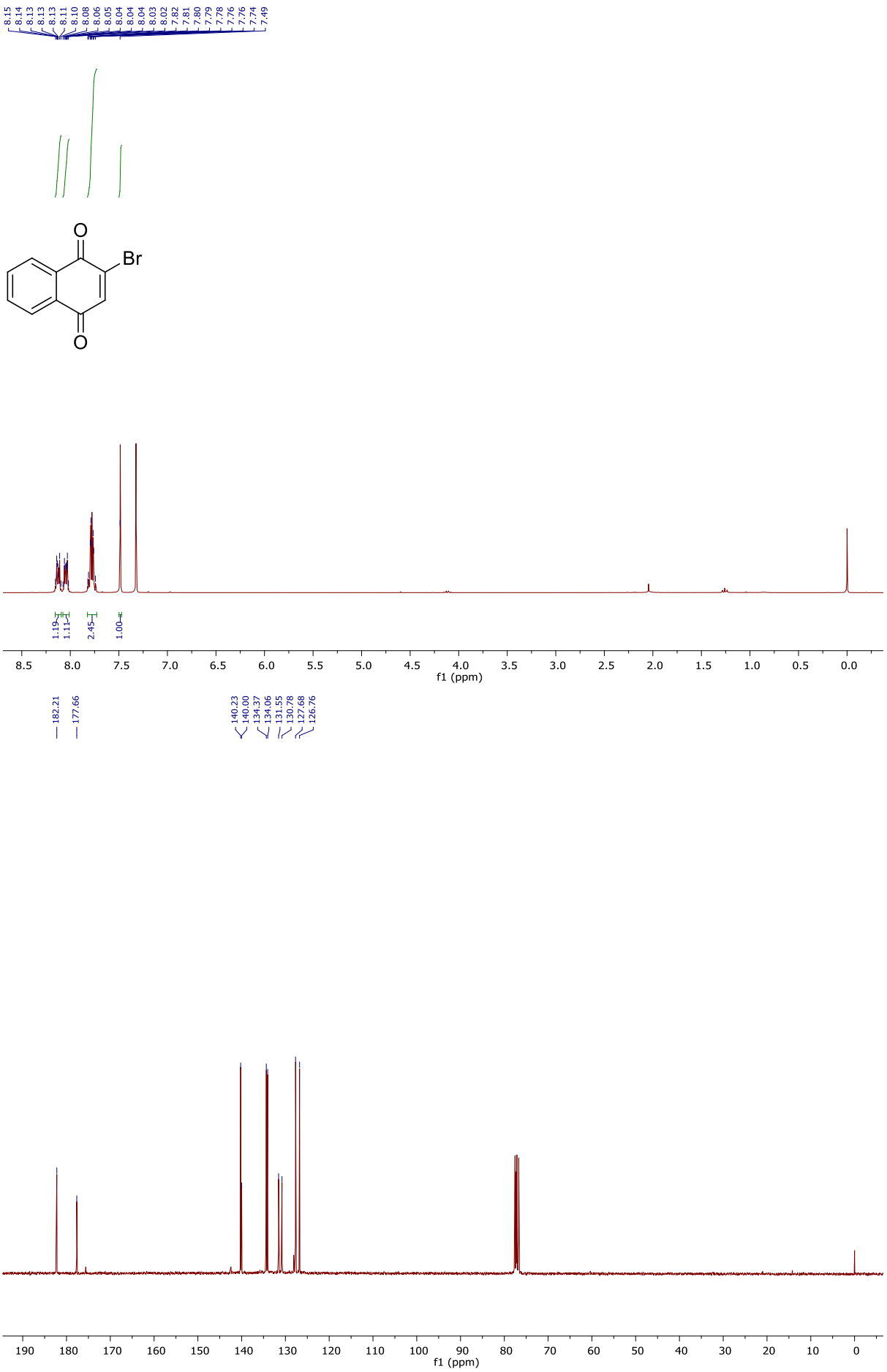

Compound 132

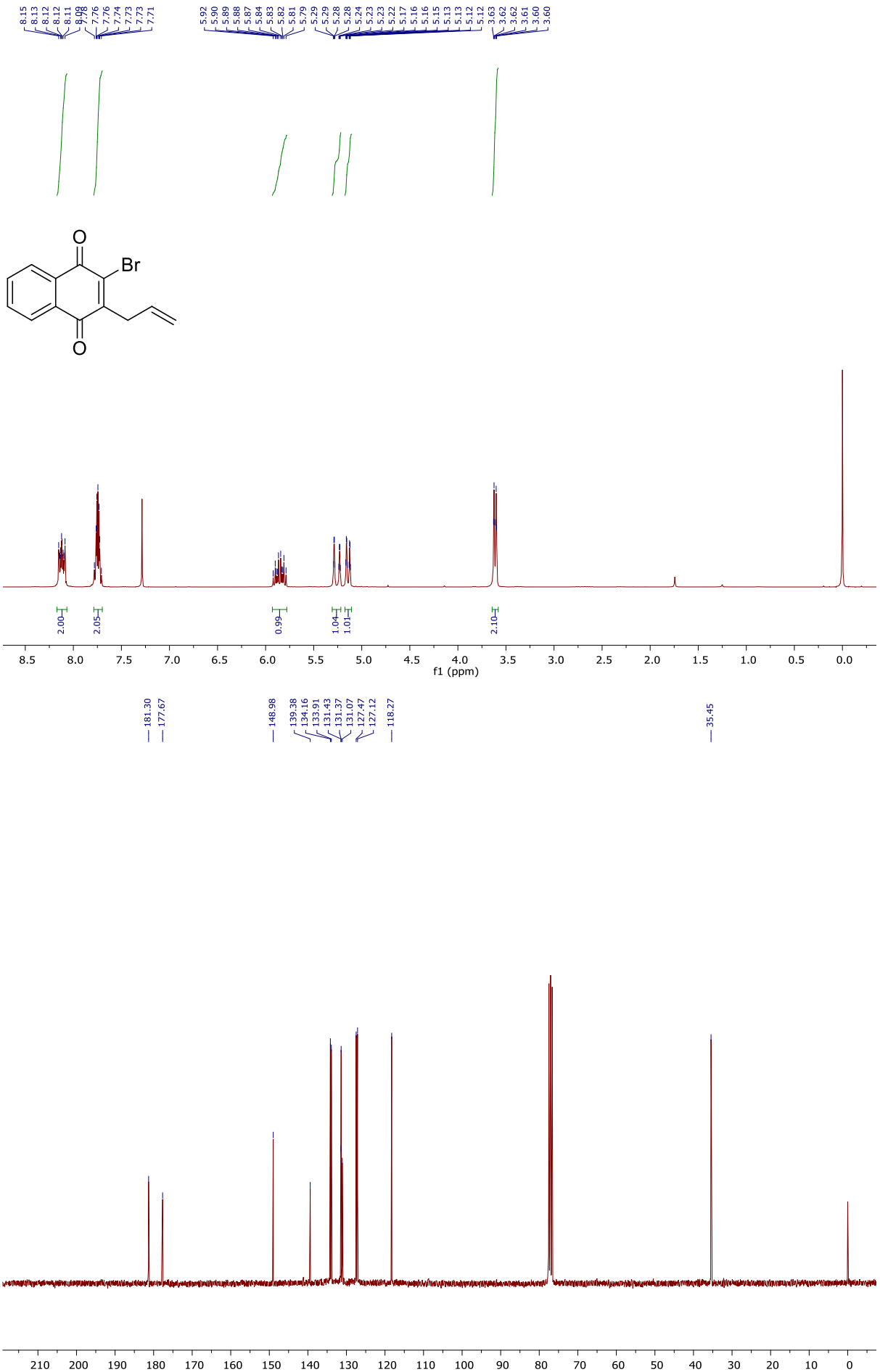

Compound 118

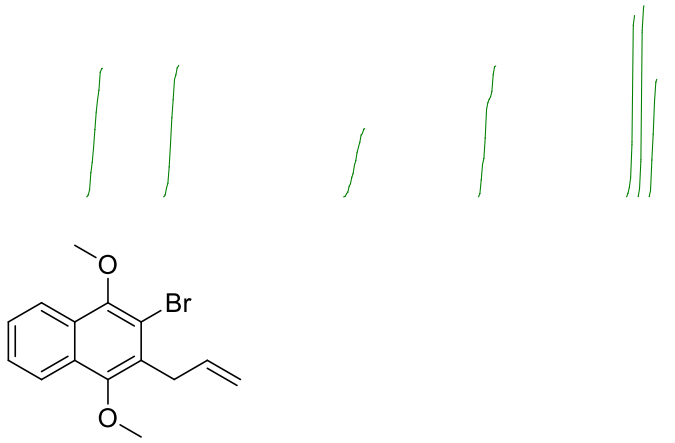

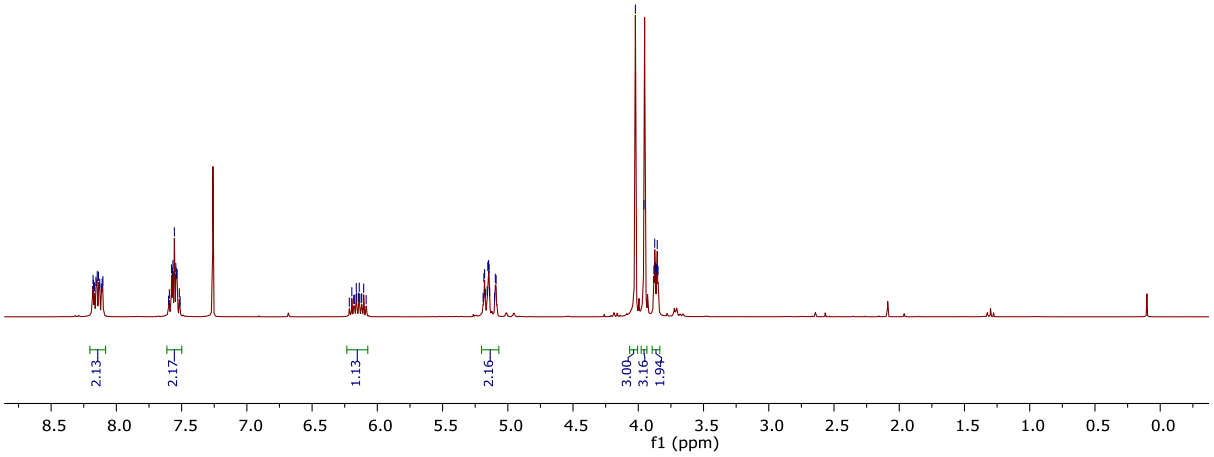

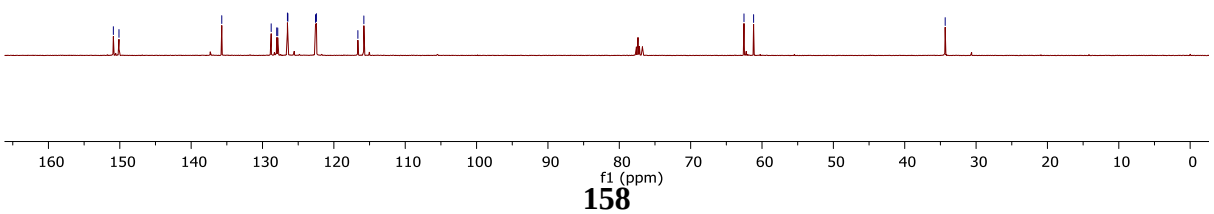

Compound 120b

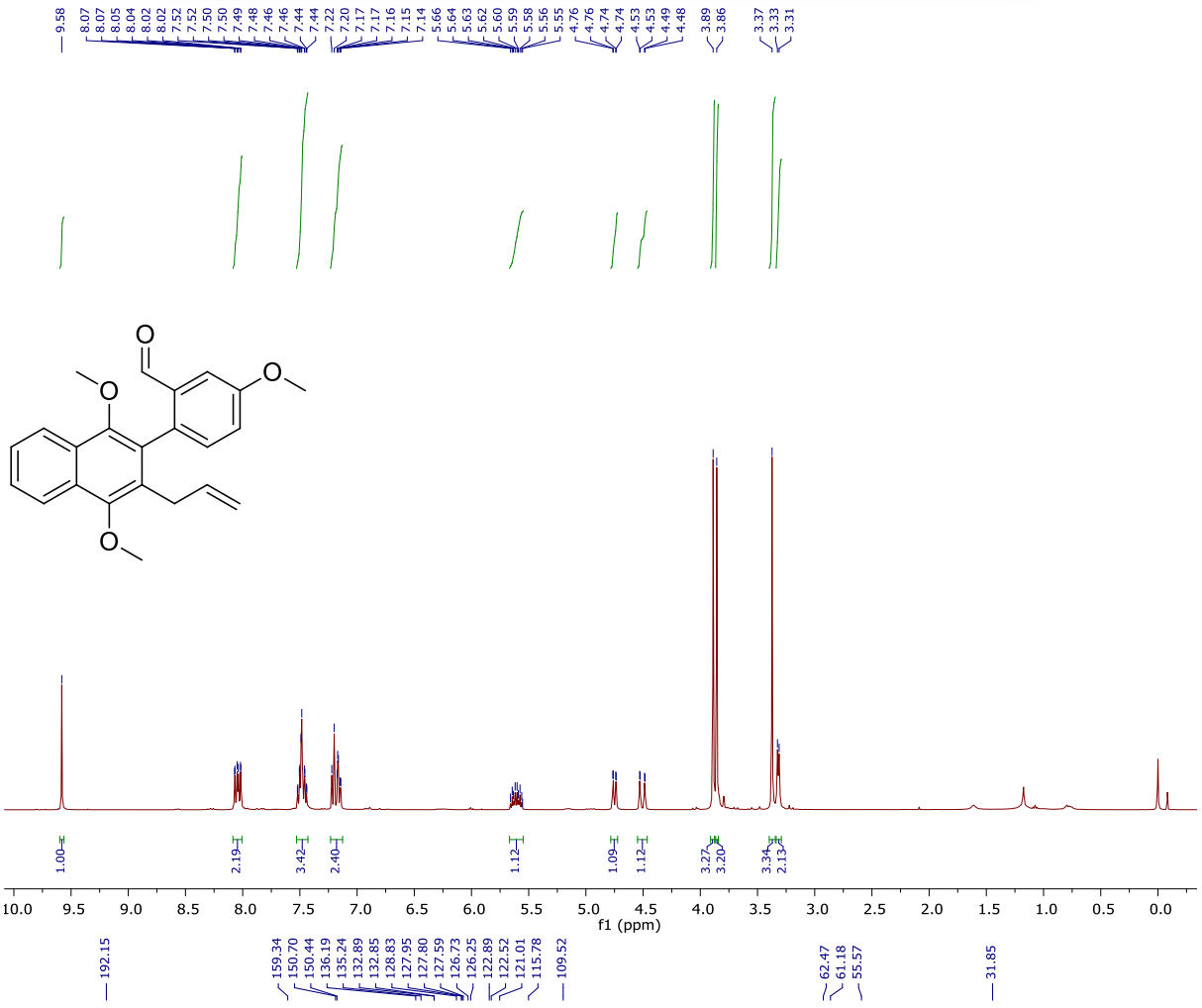

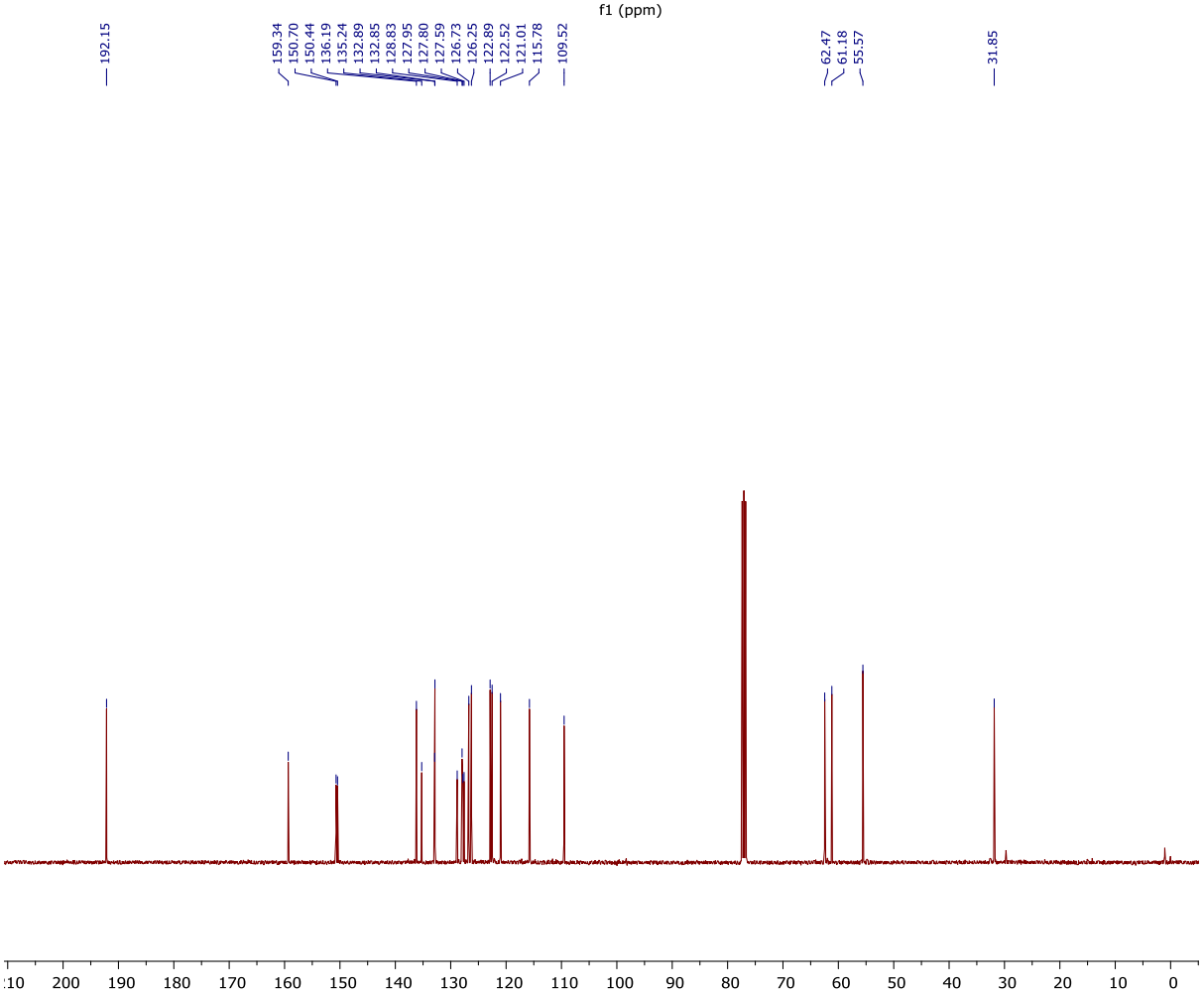

Compound 113

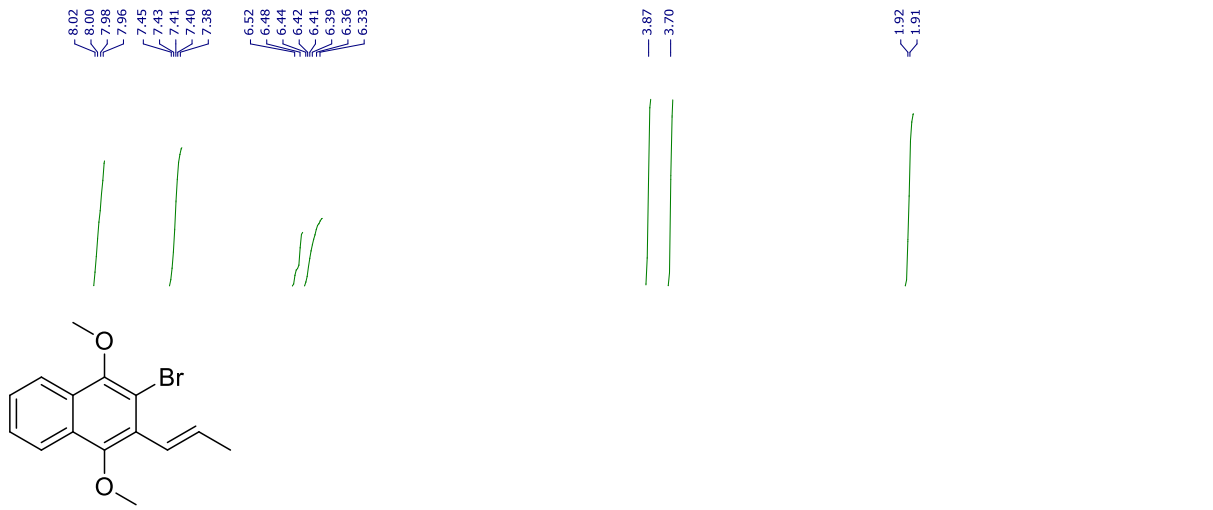

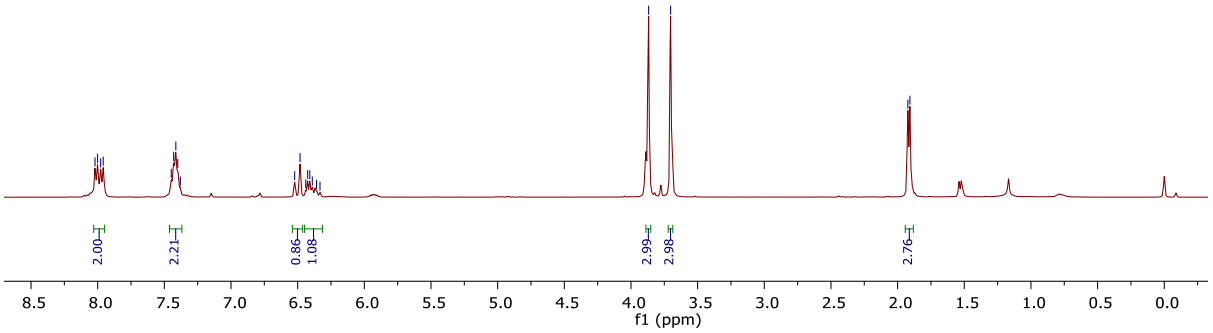

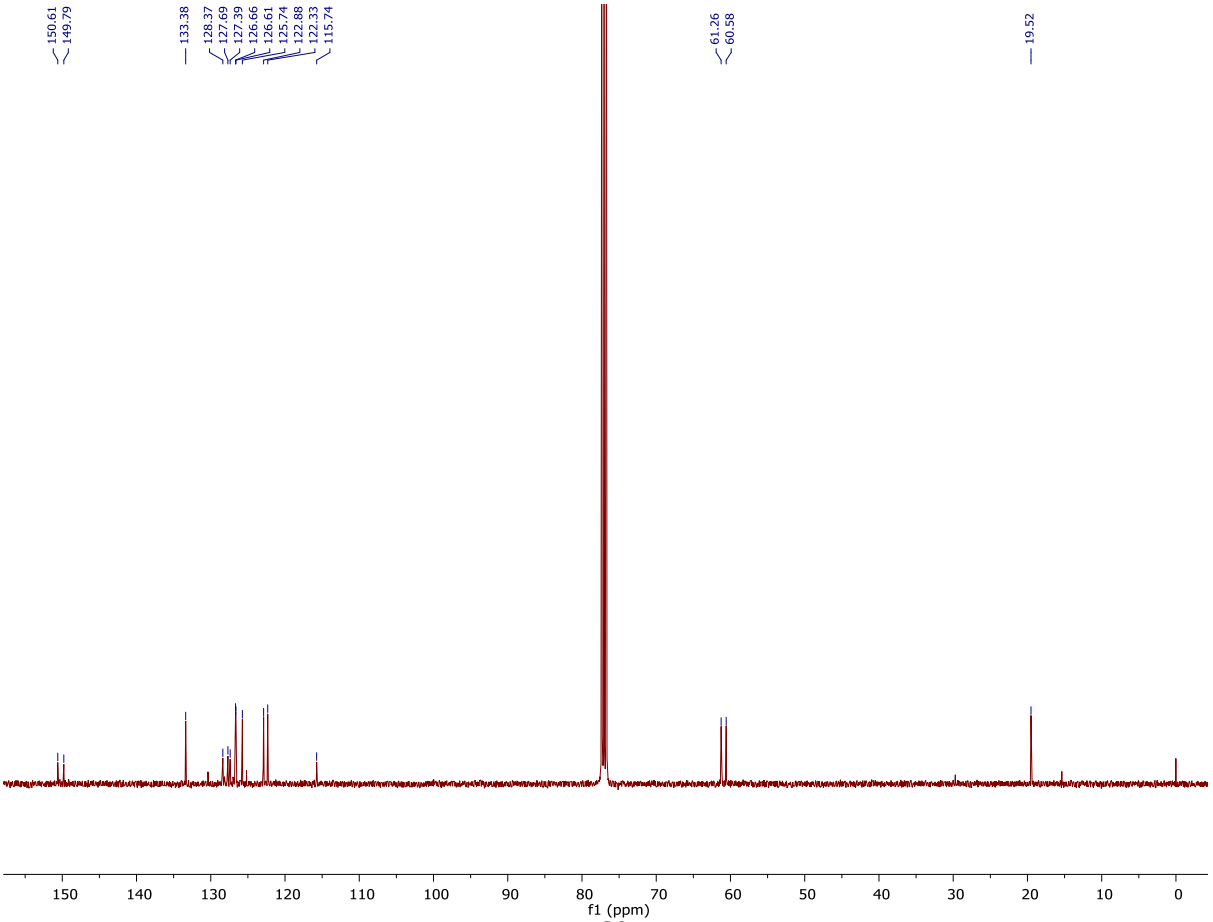

Compound 134

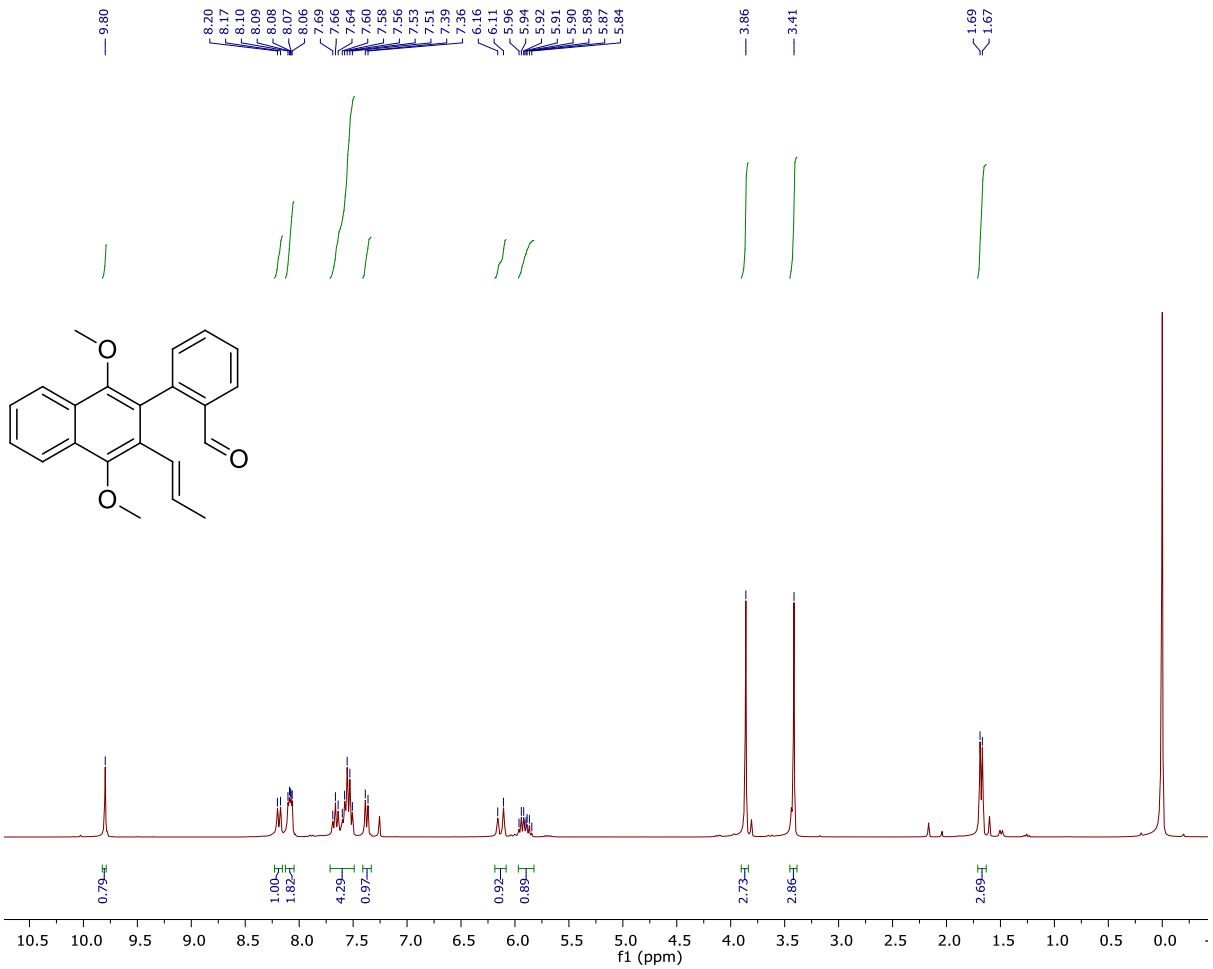

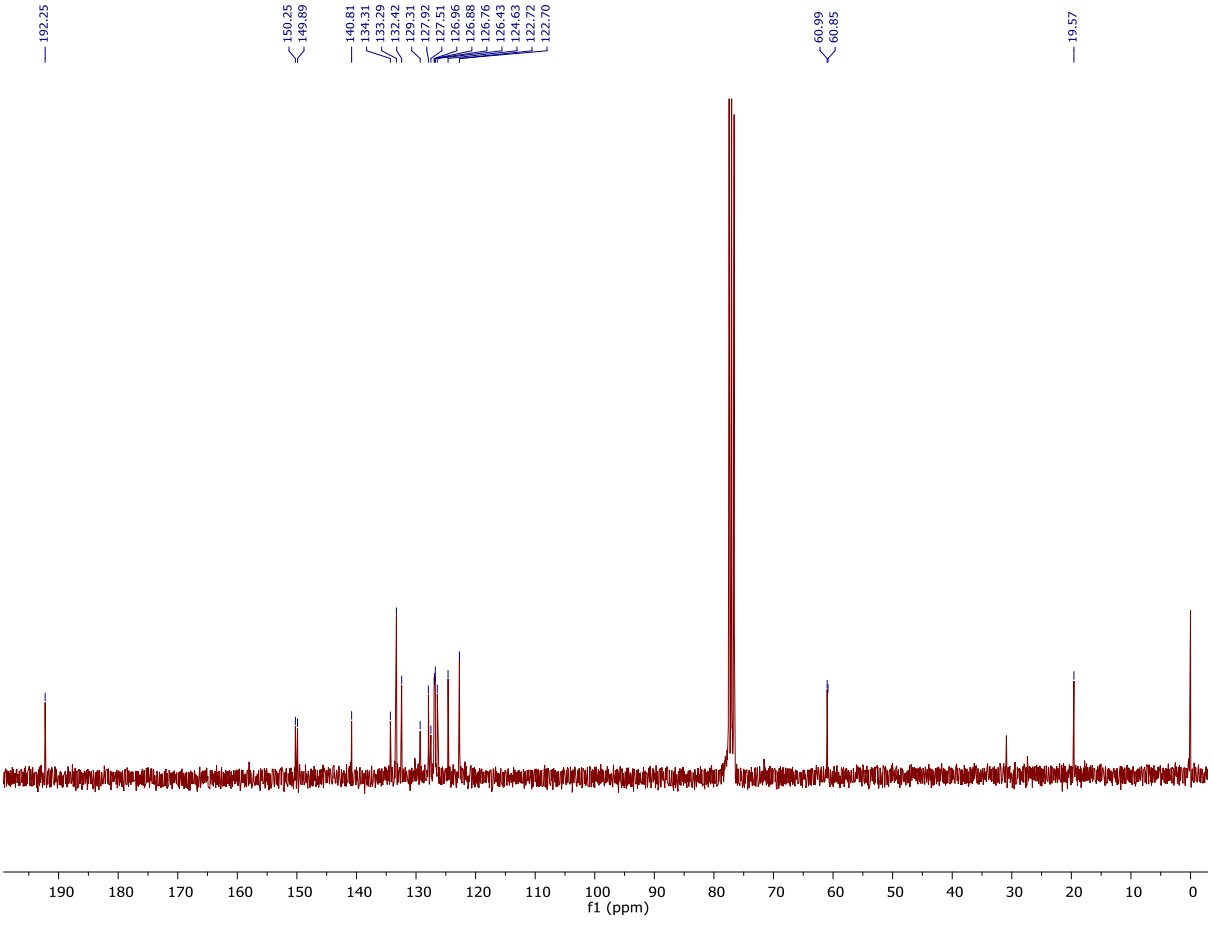

Compound 139

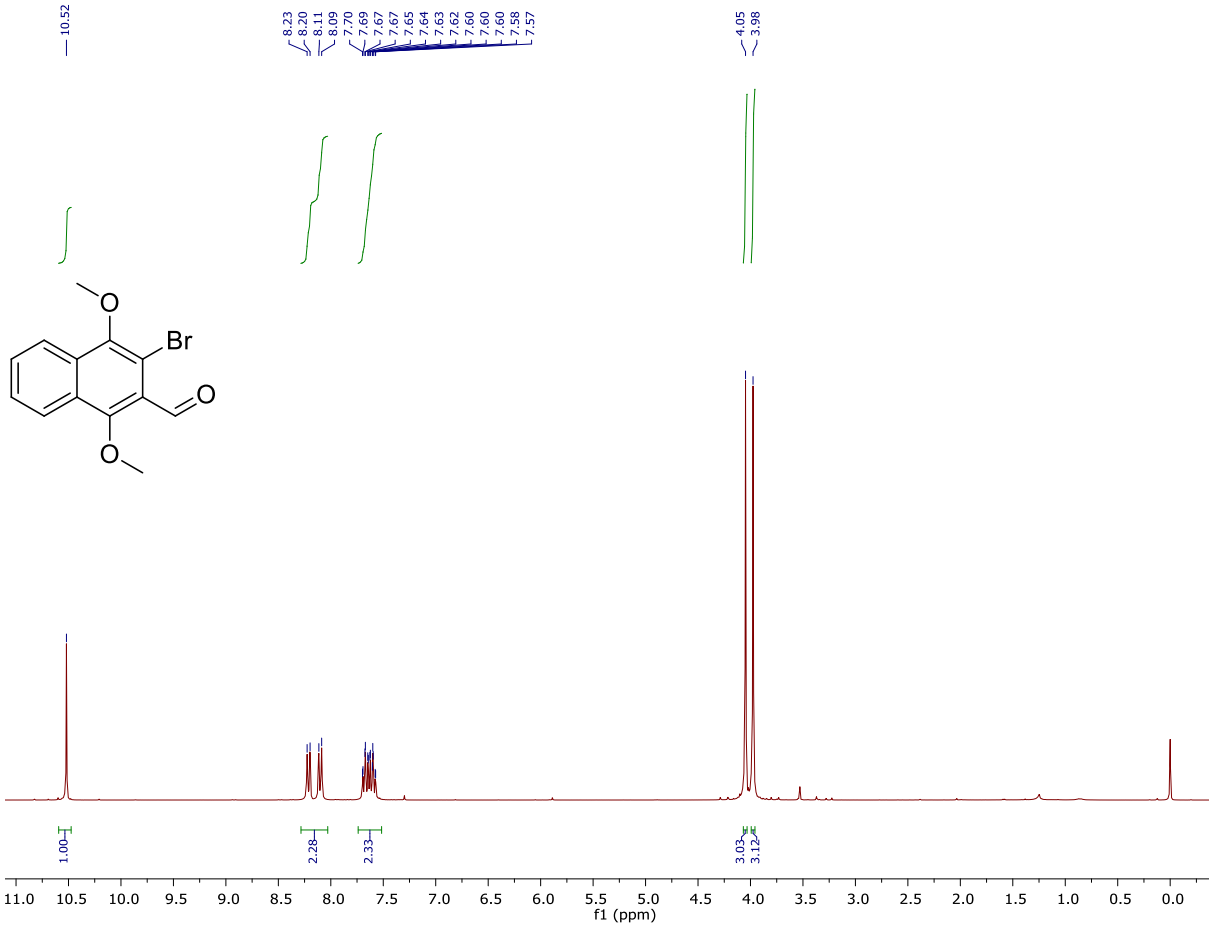

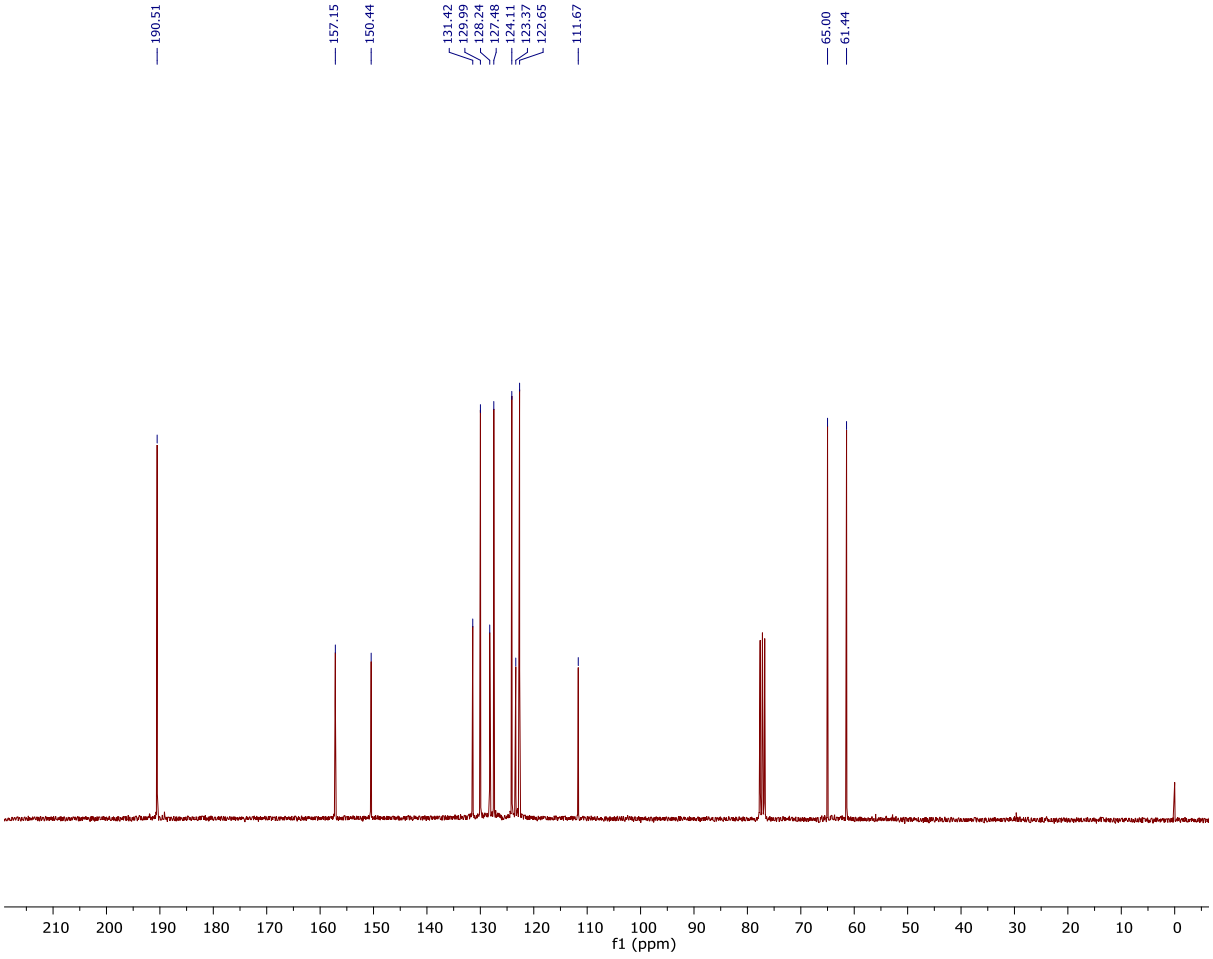

Compound 138

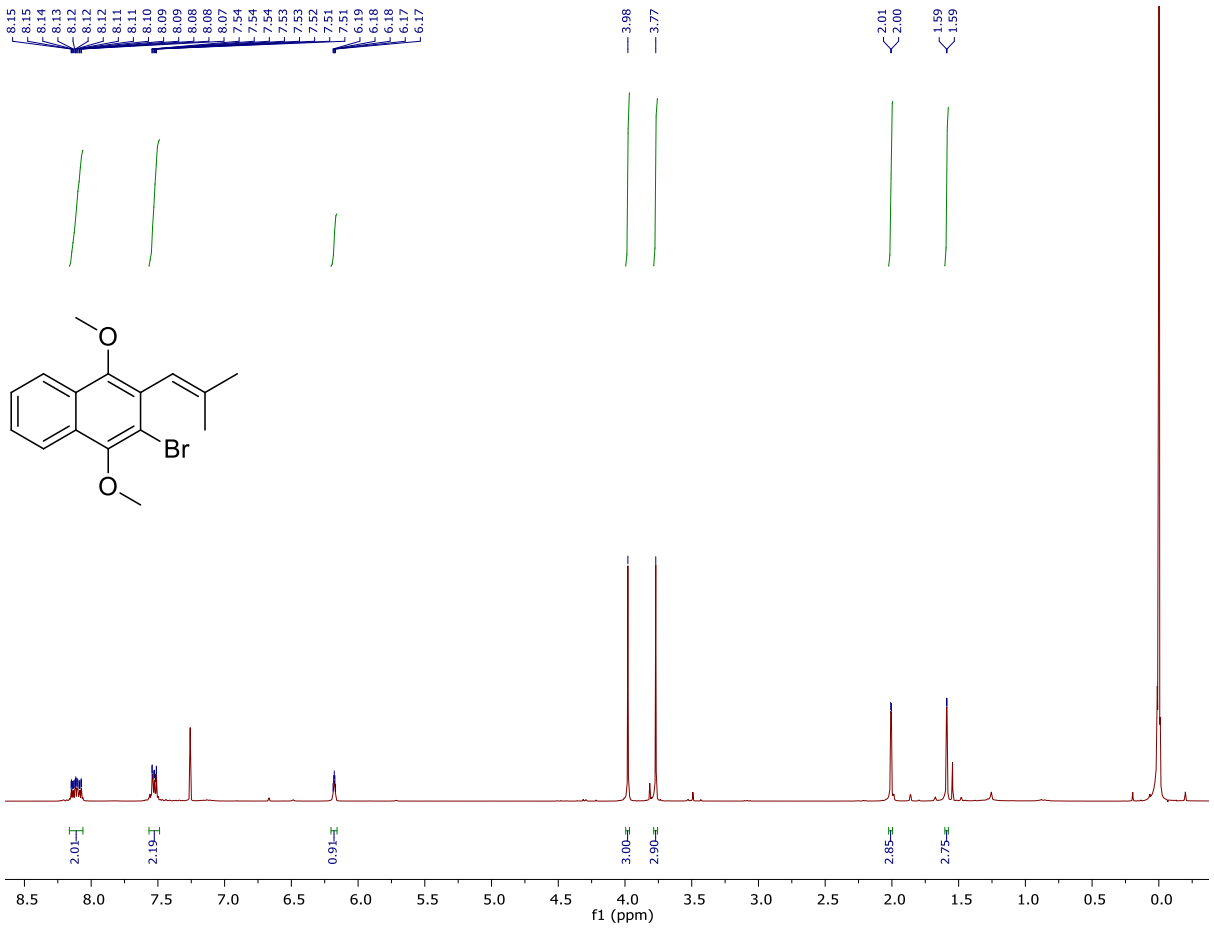

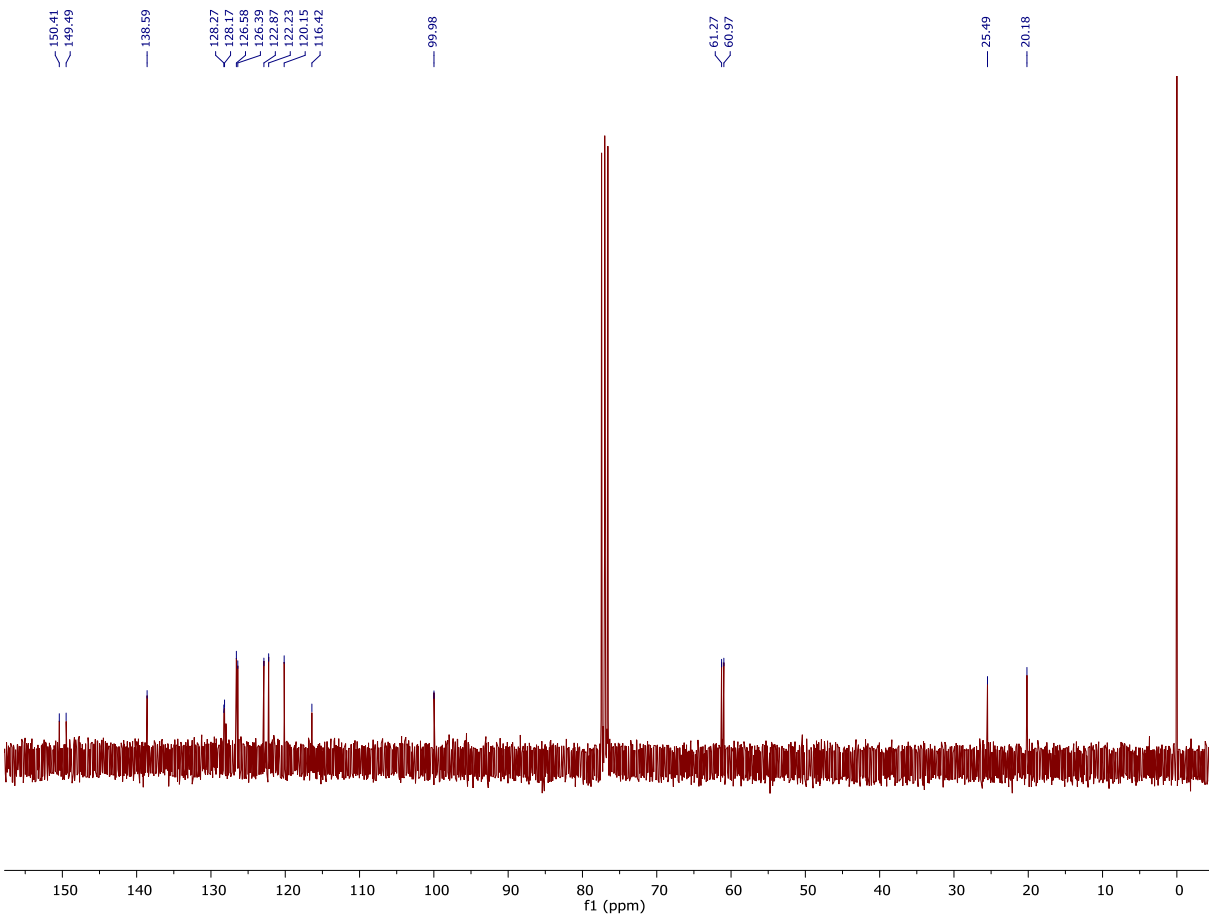

Compound 137

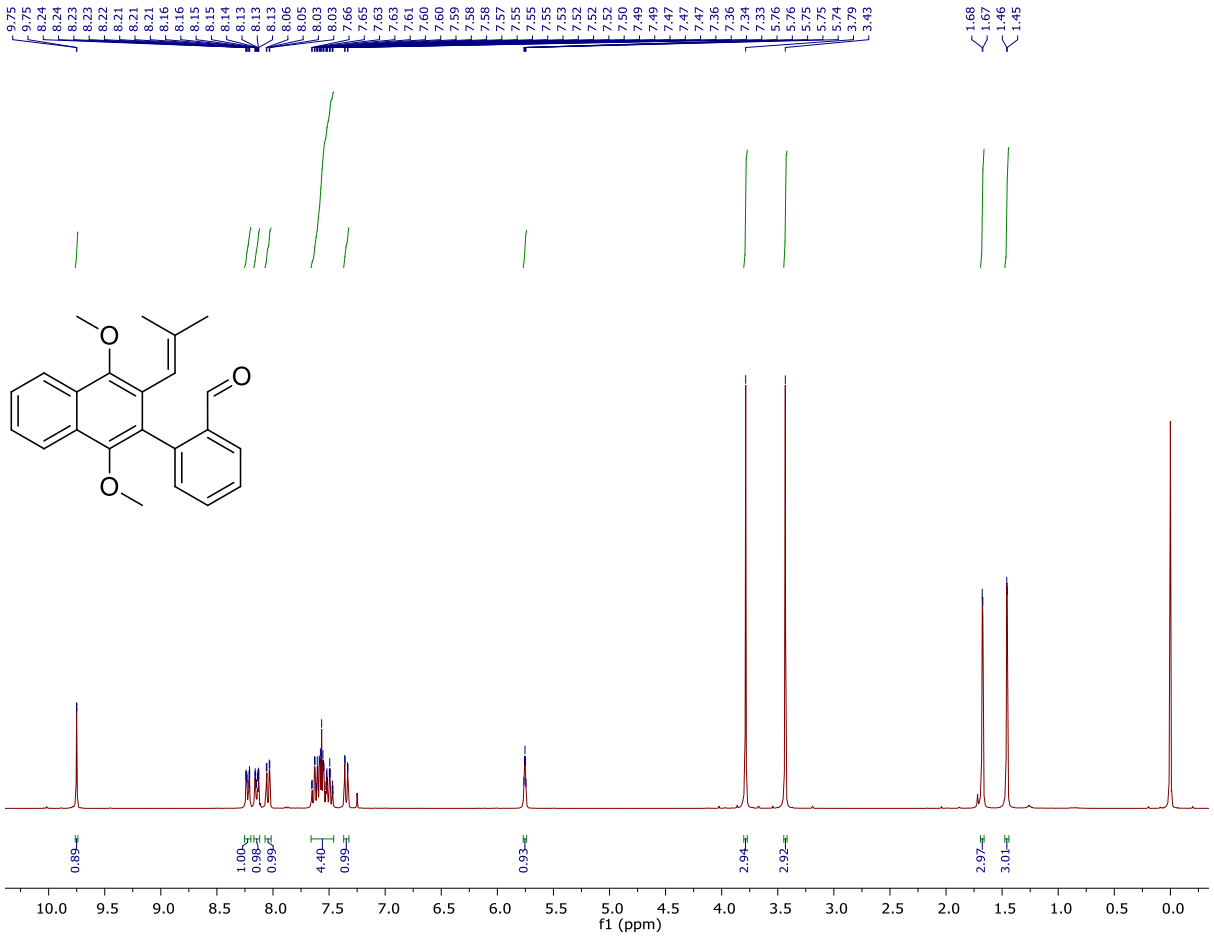

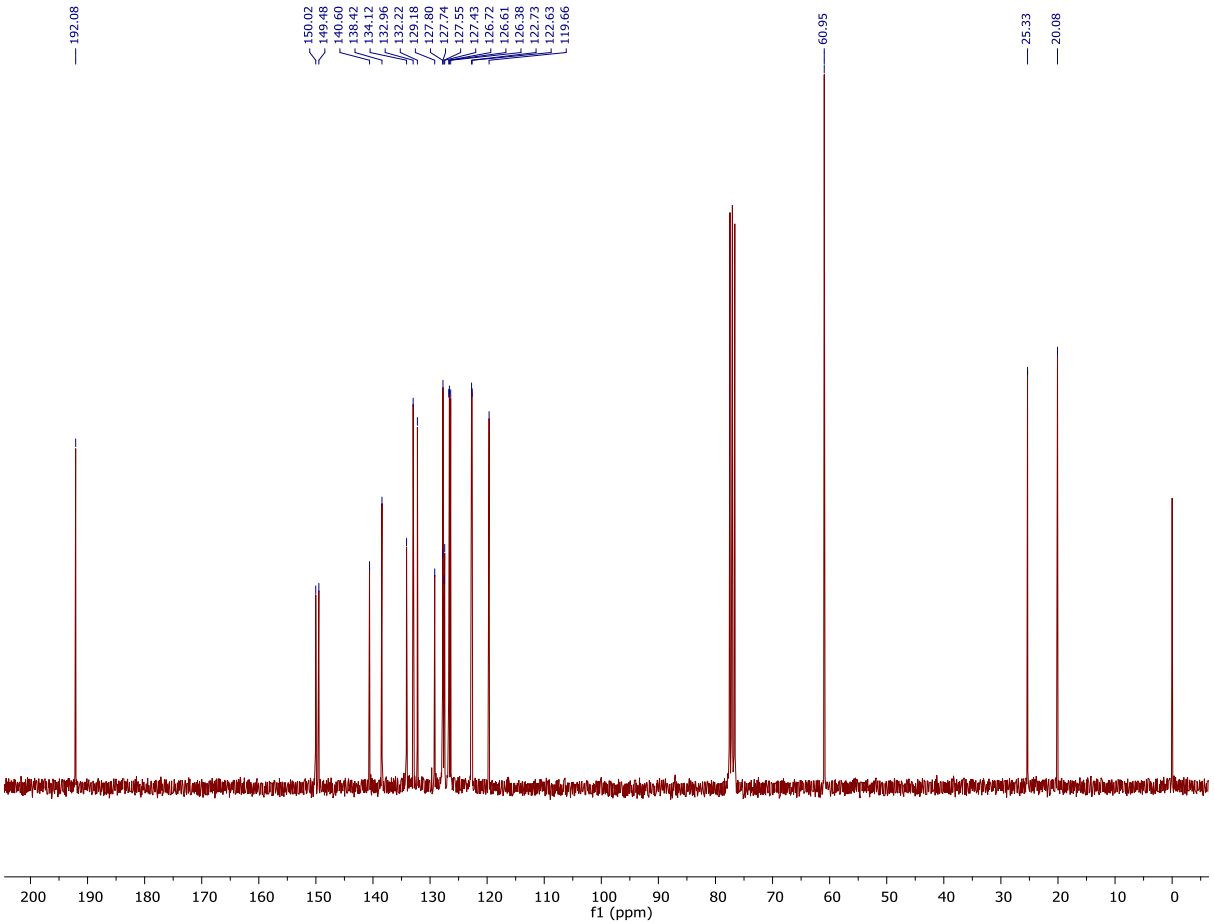

Compound 136

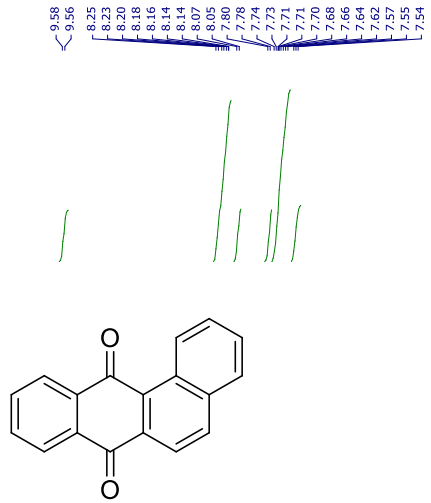

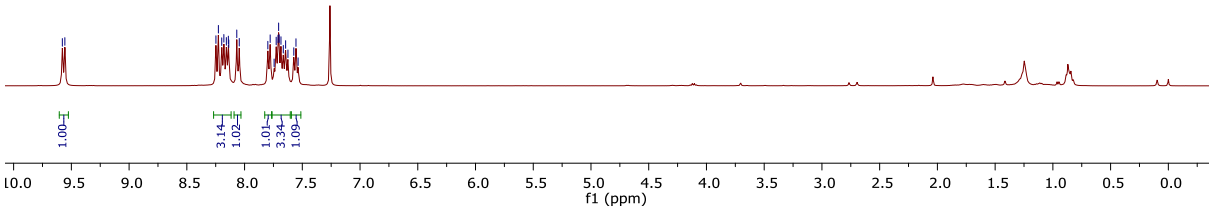

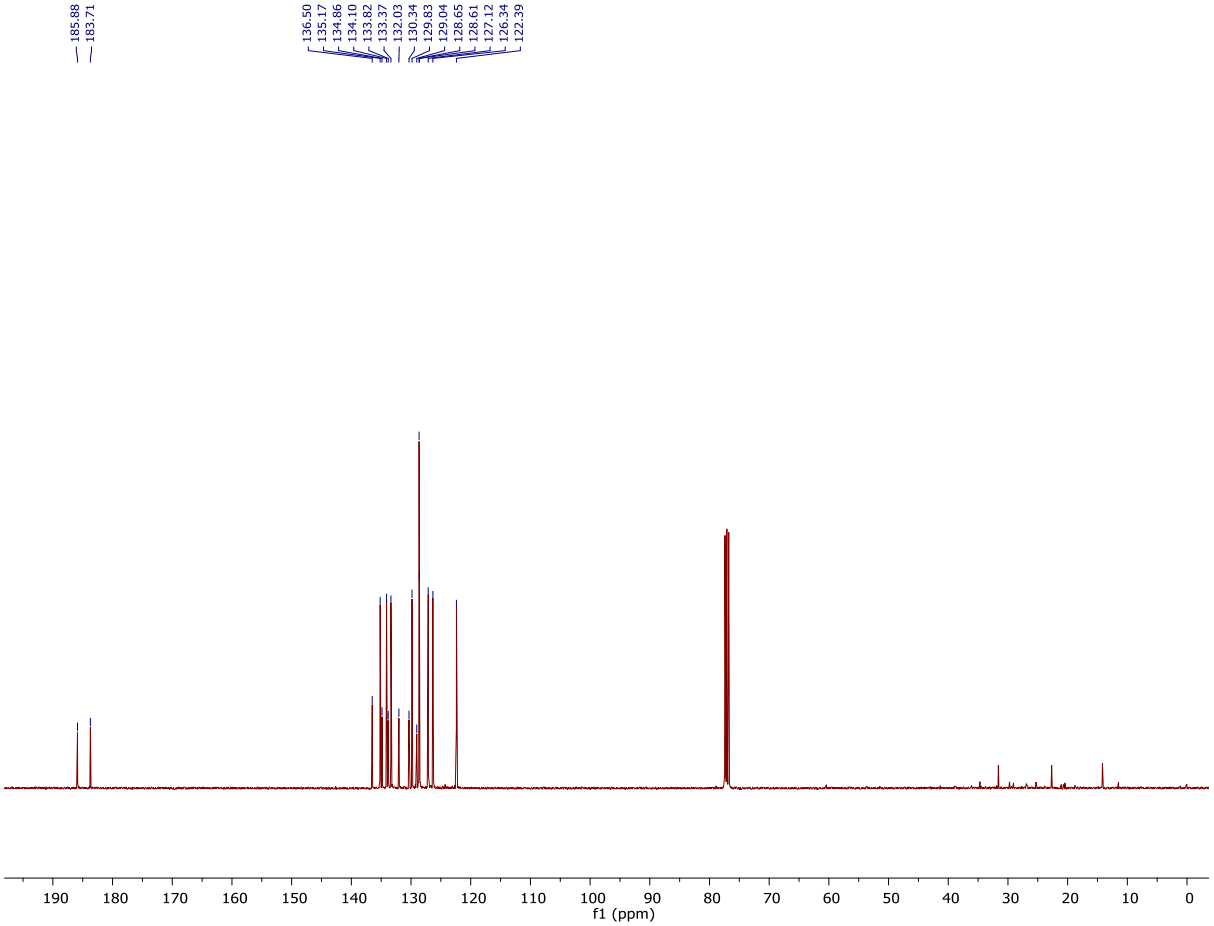

Compound 135

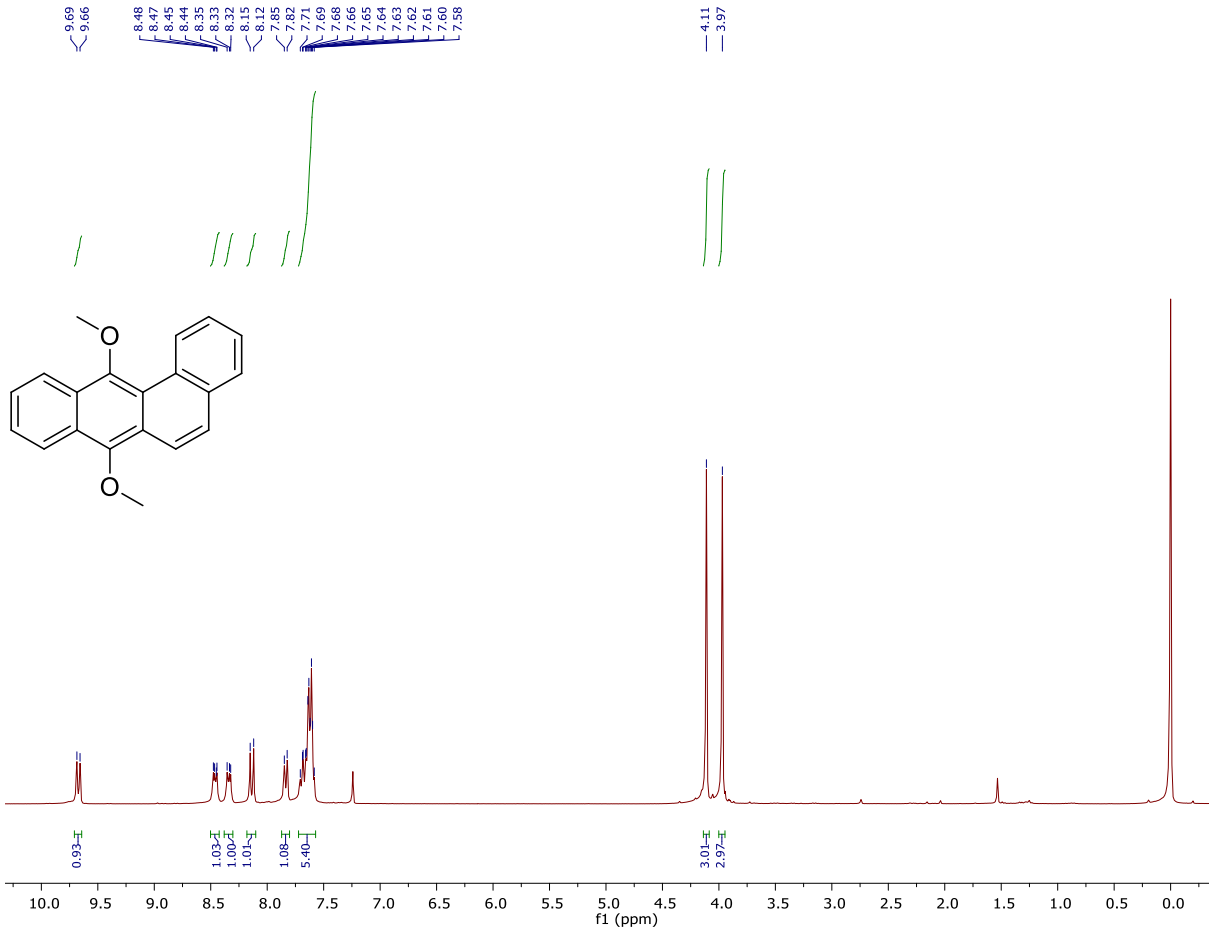

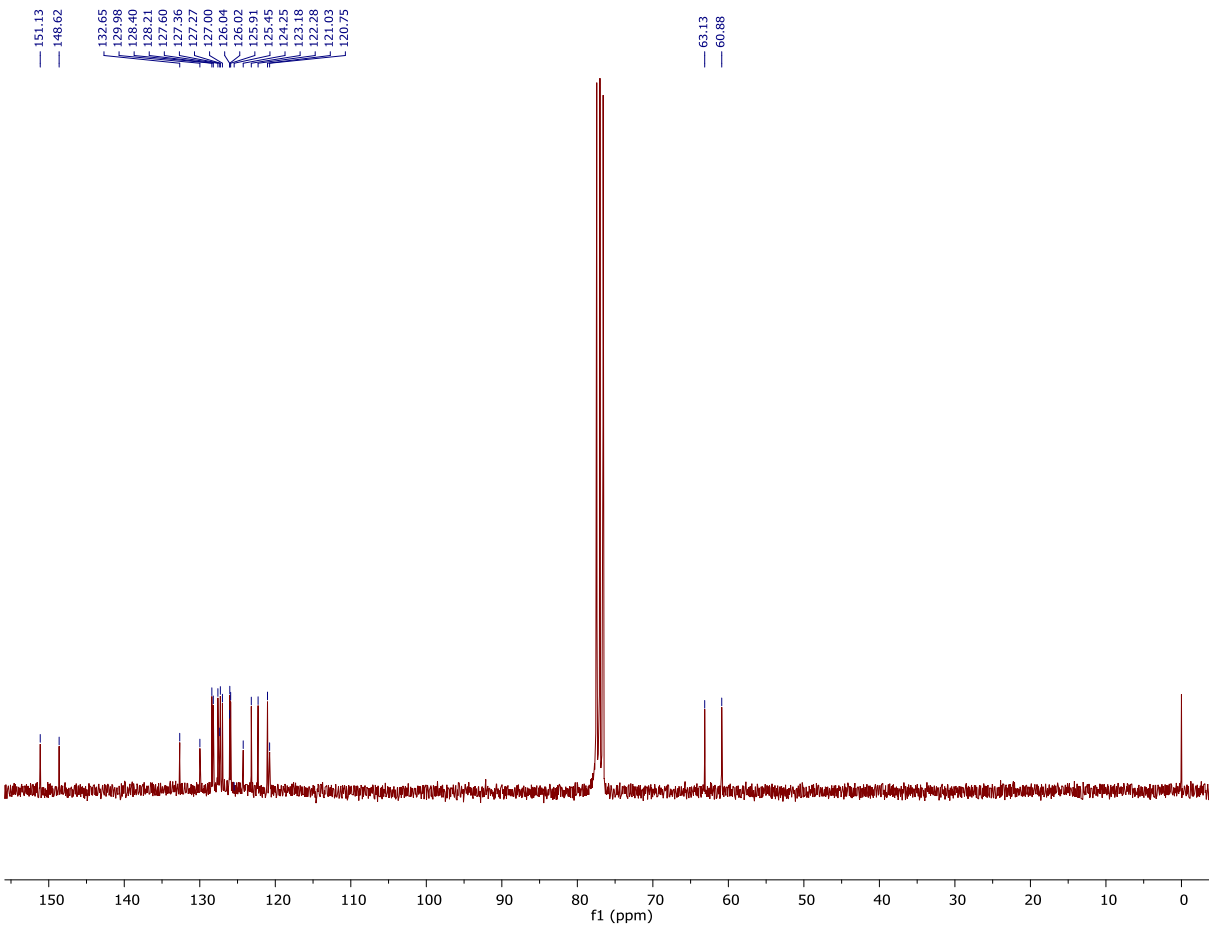

Compound 146

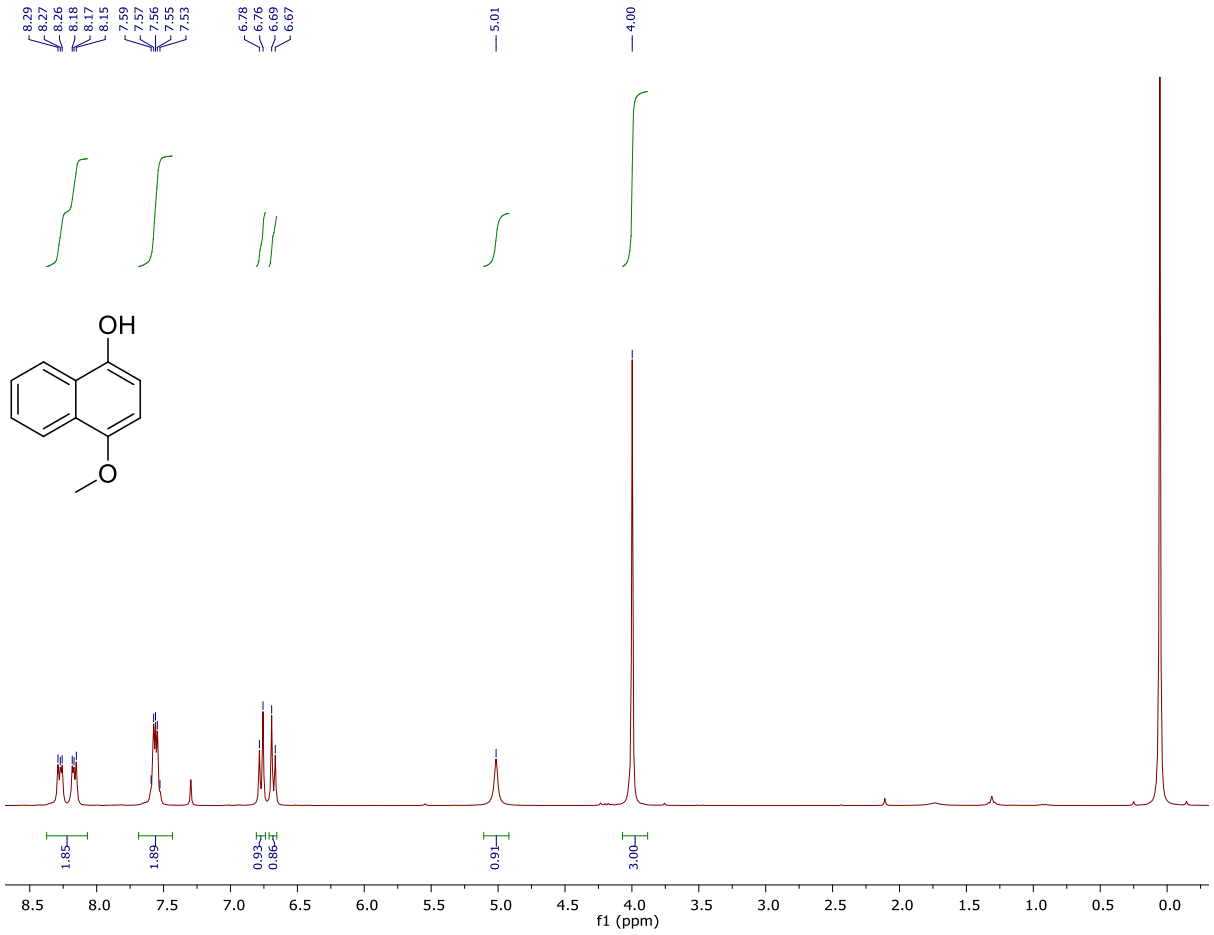

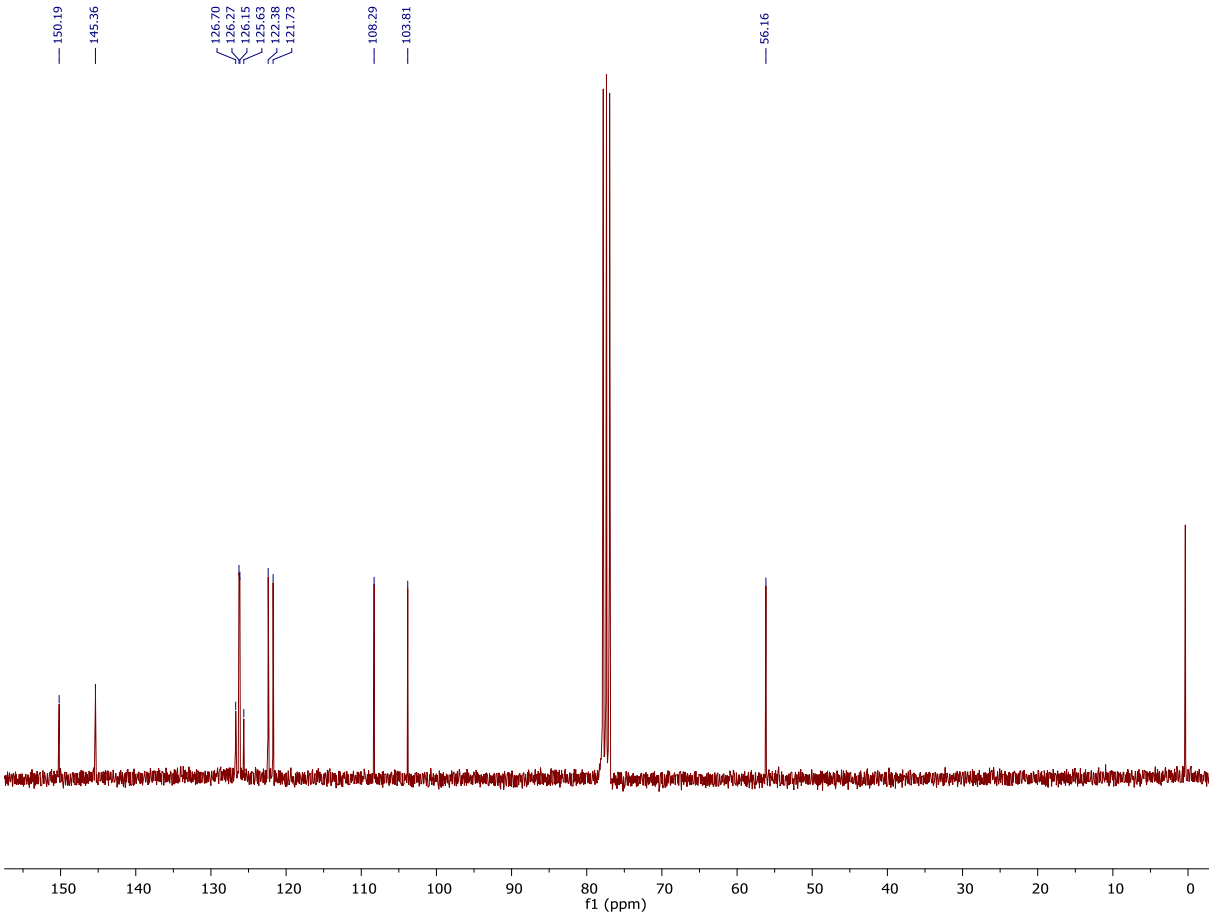

Compound 148

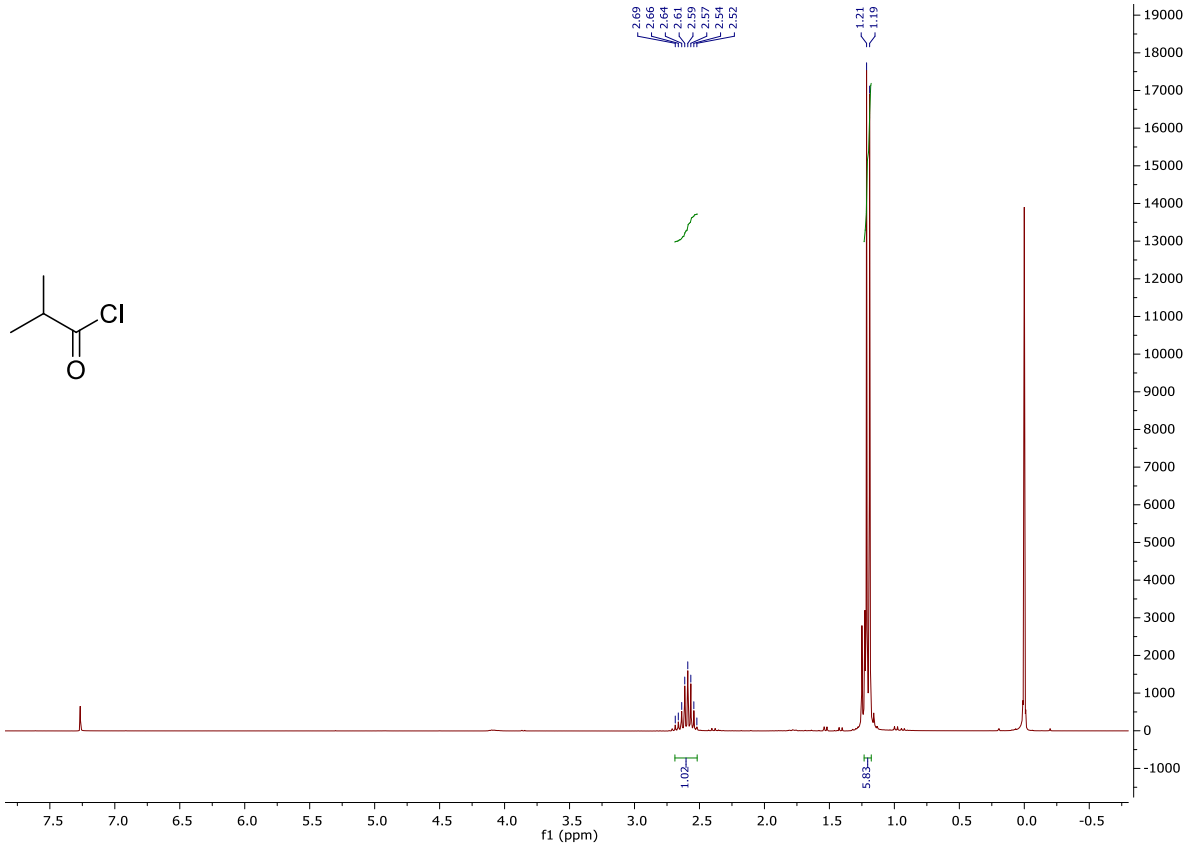

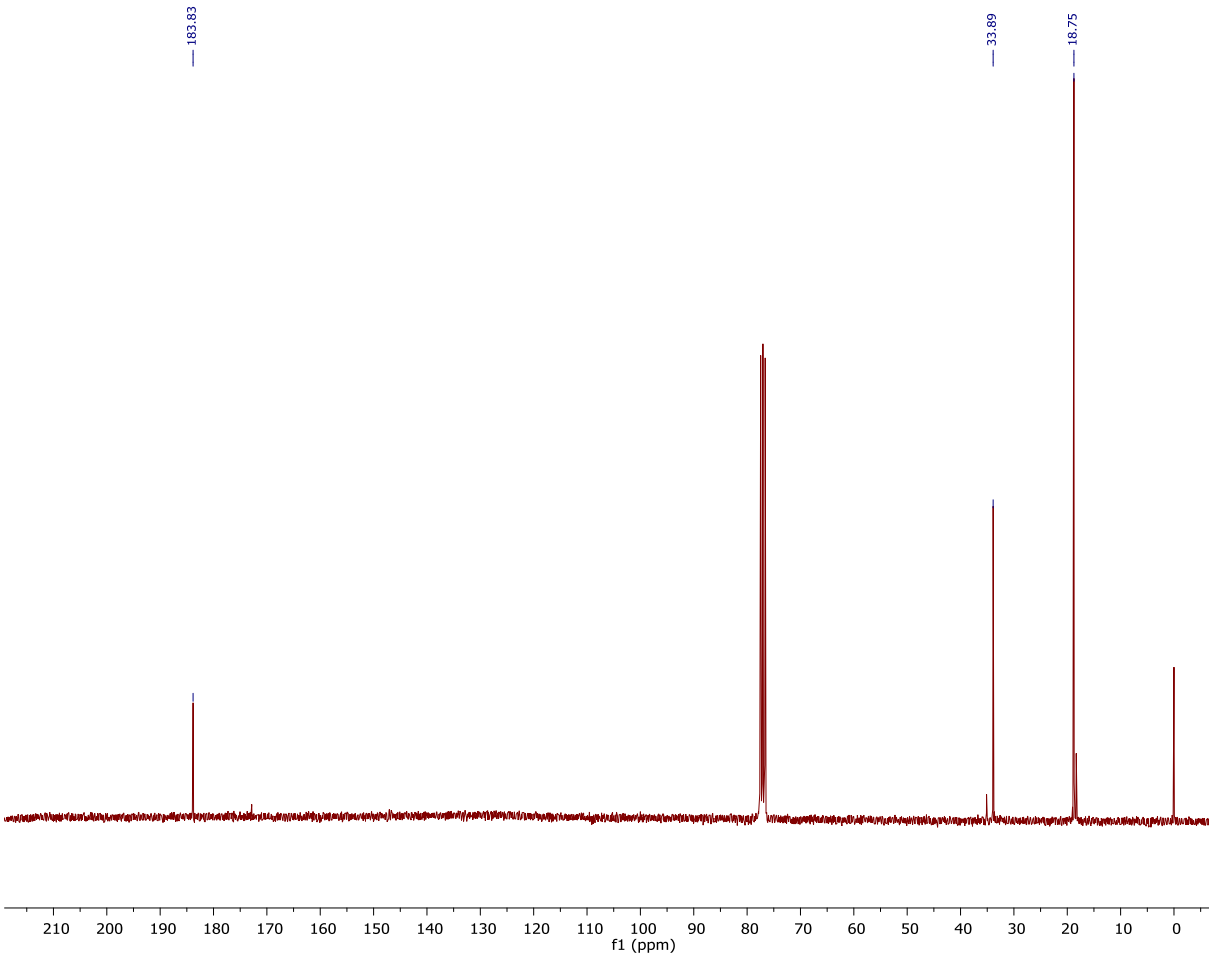

Compound 149

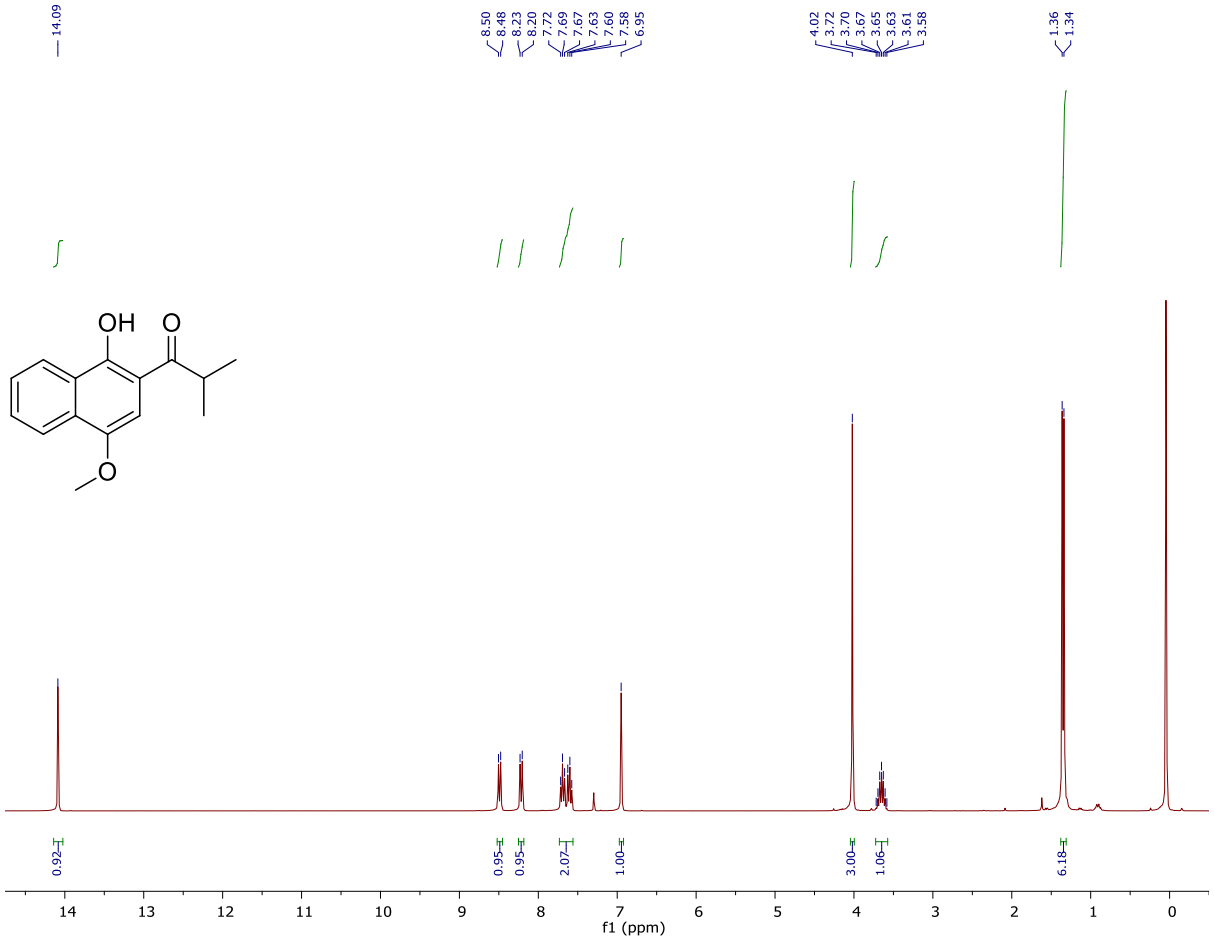

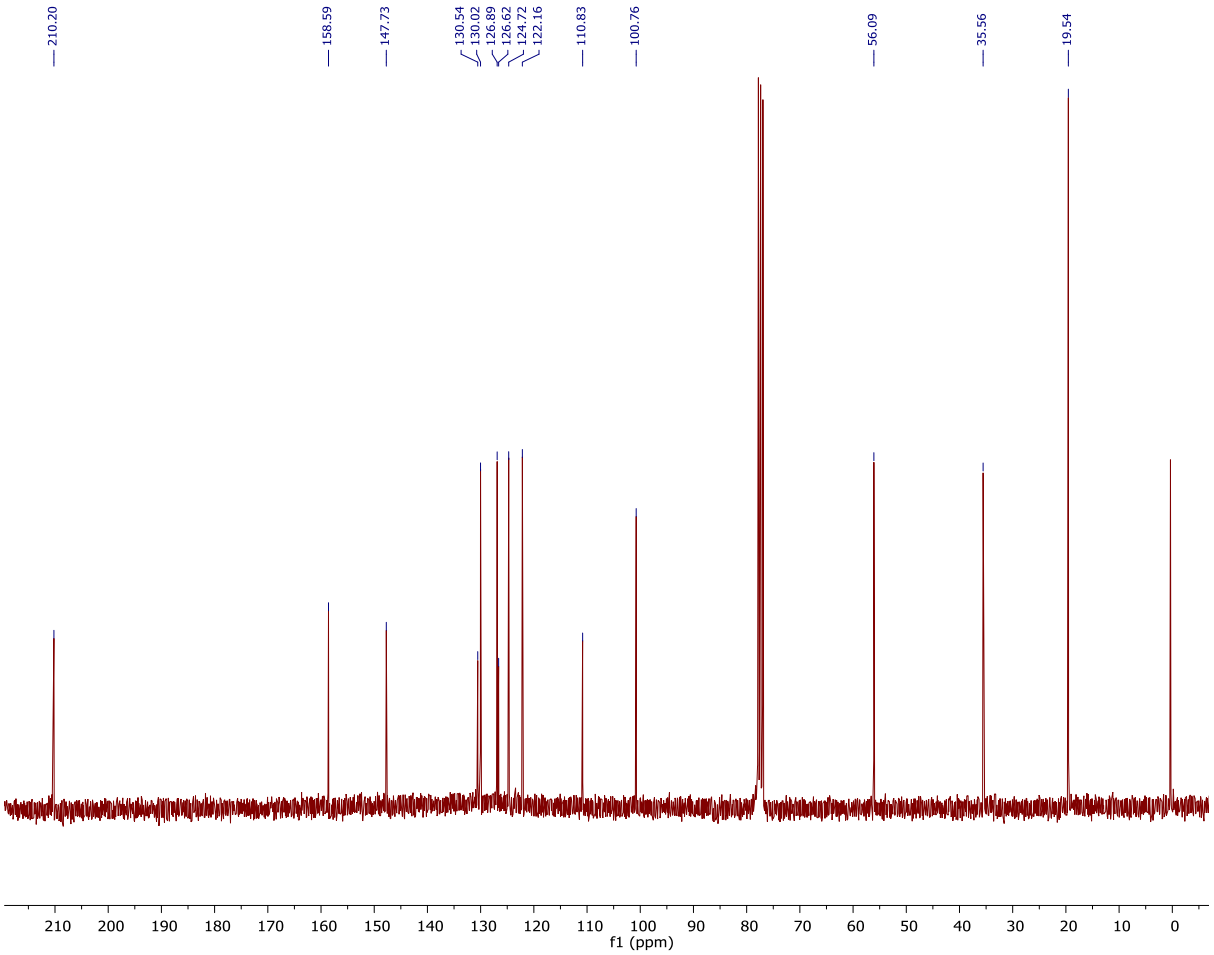

Compound 150

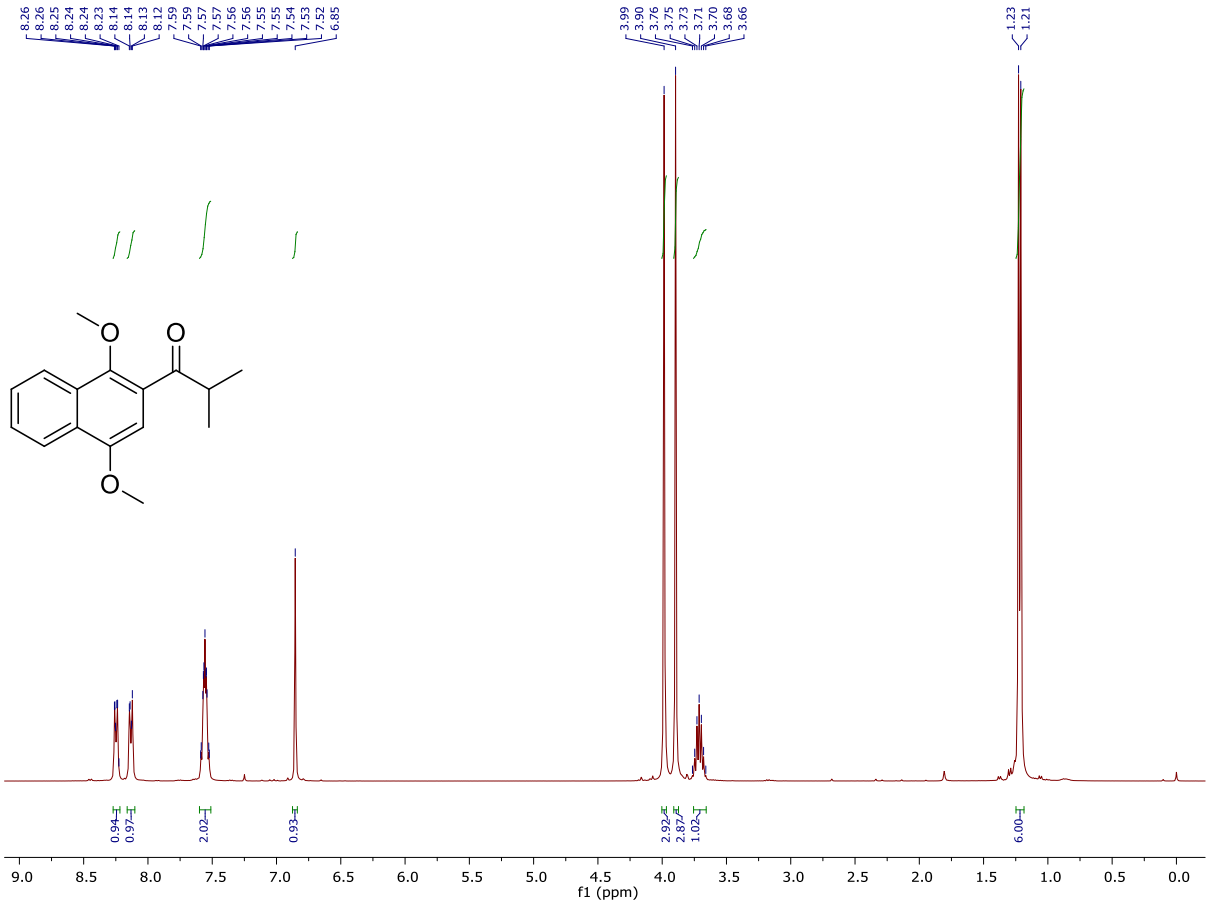

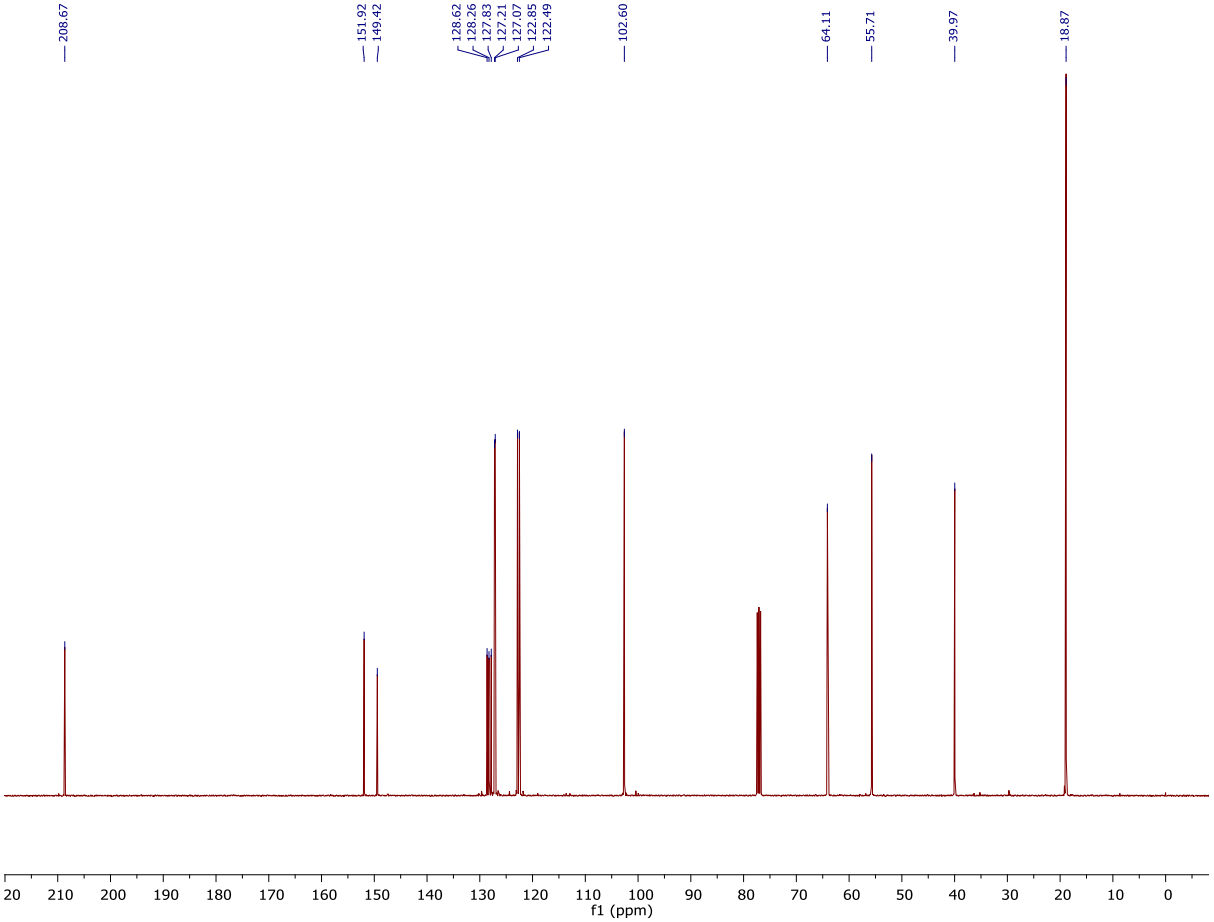

Compound 151

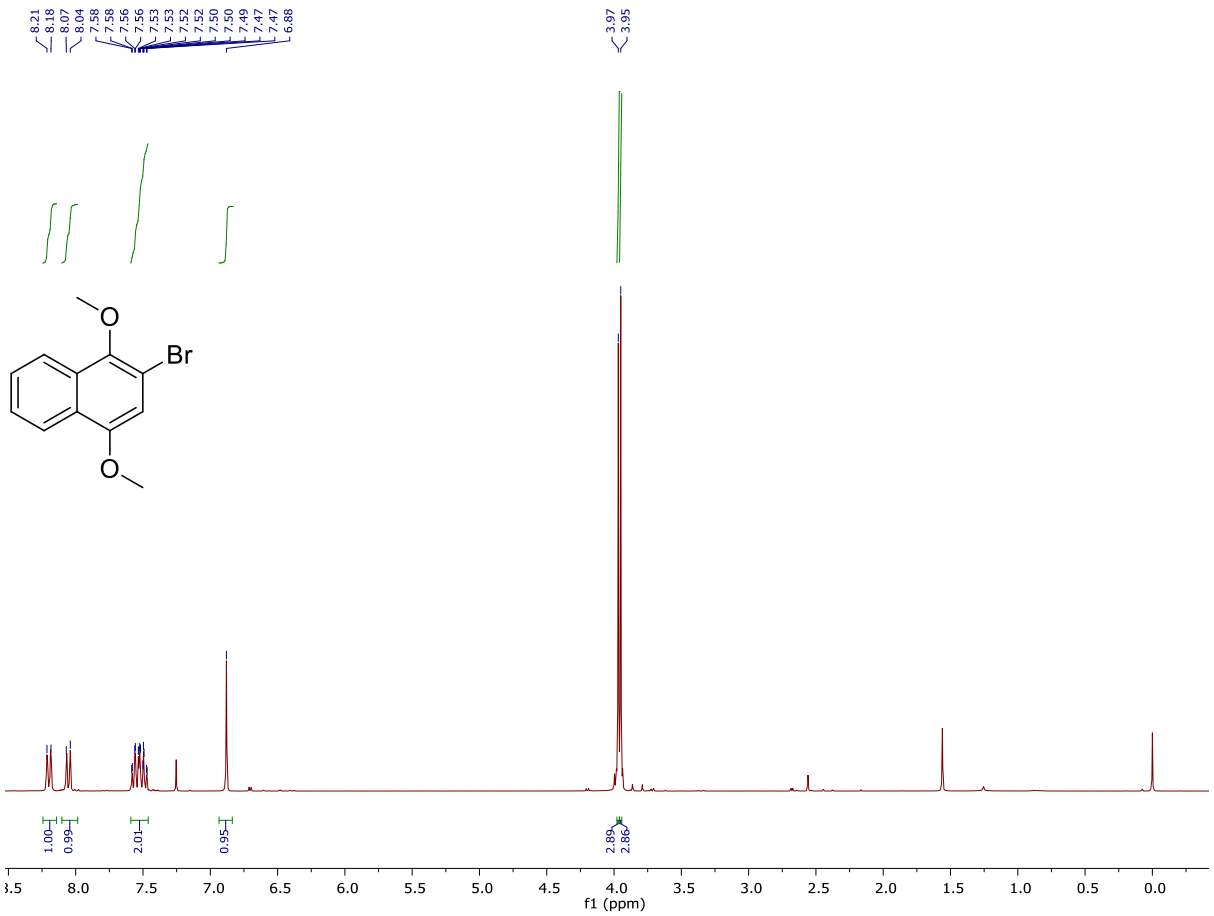

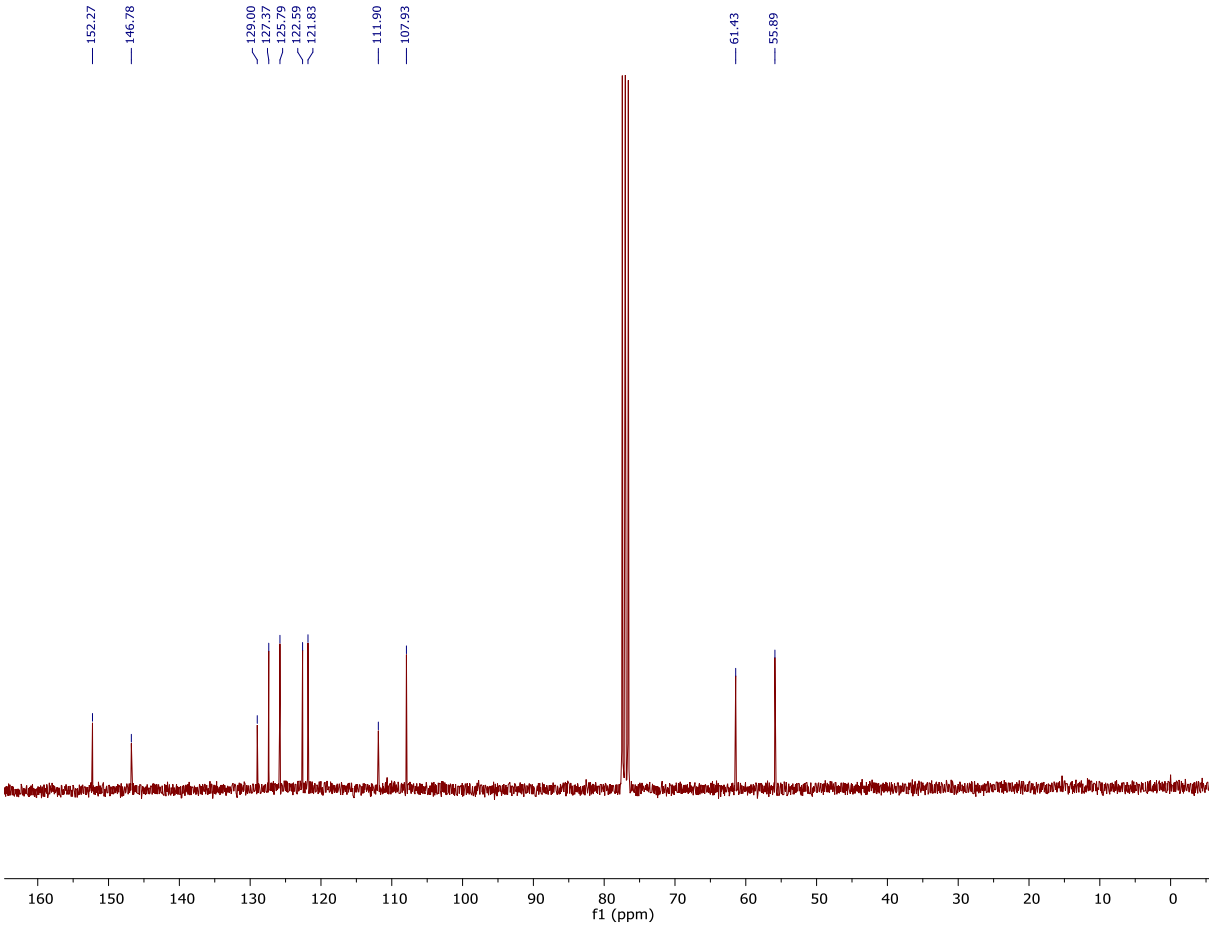

Compound 152

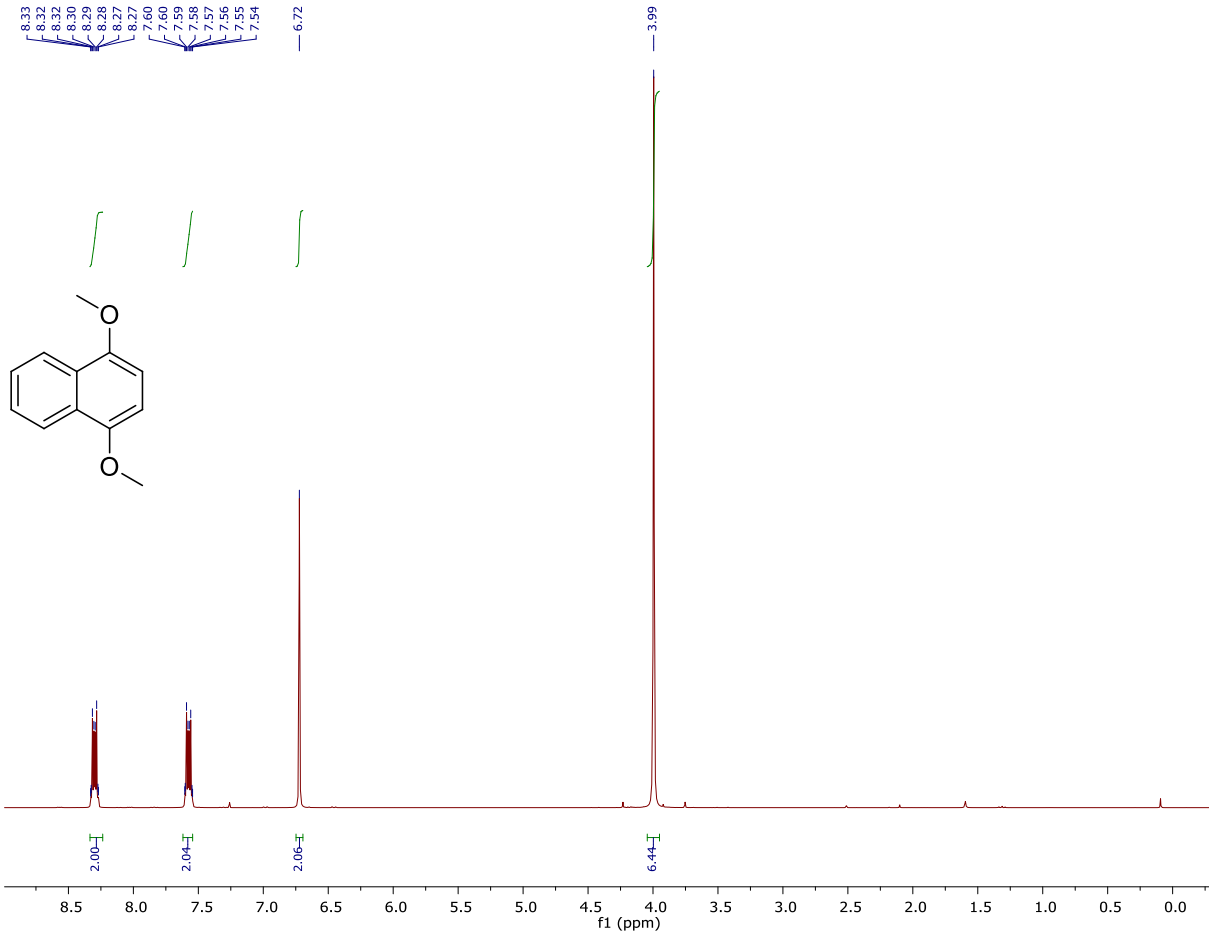

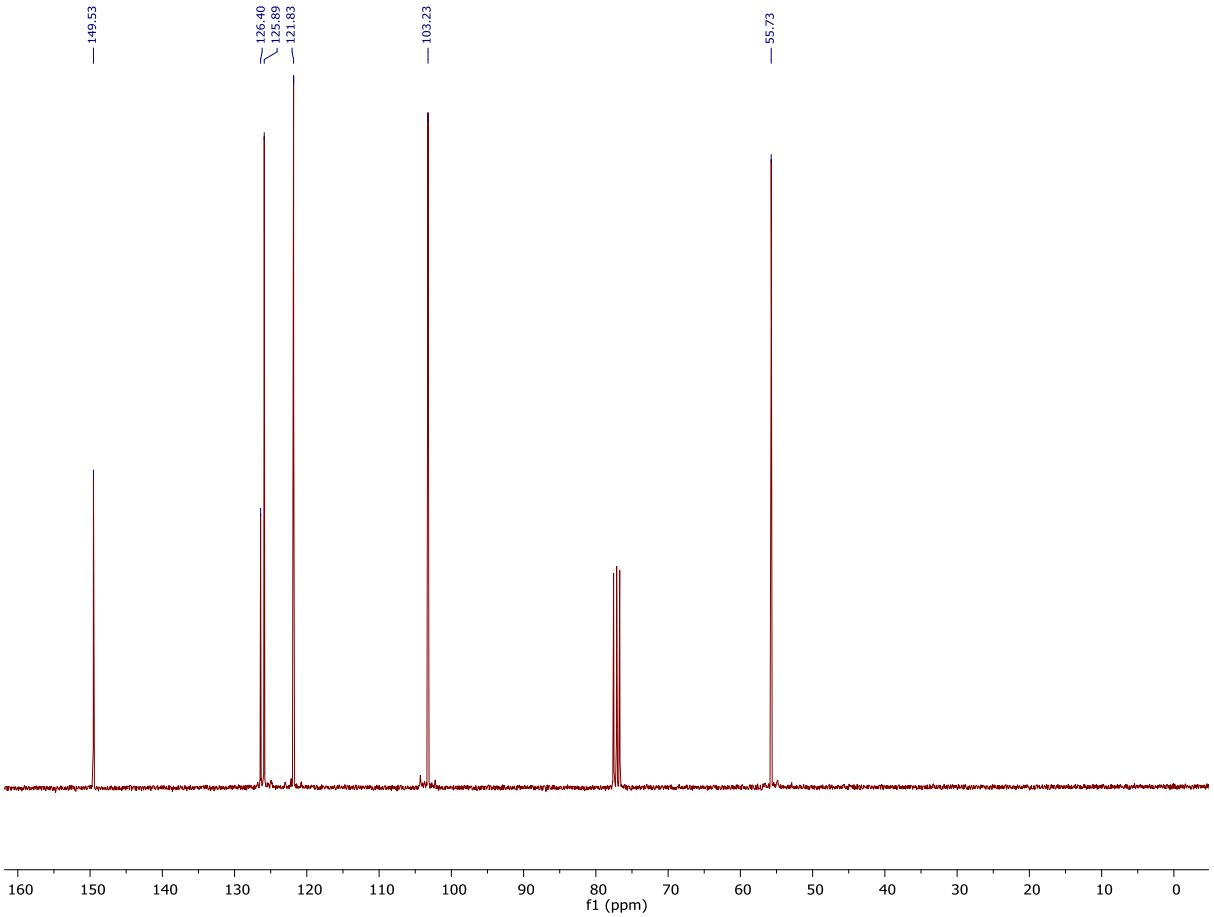

Compound 154

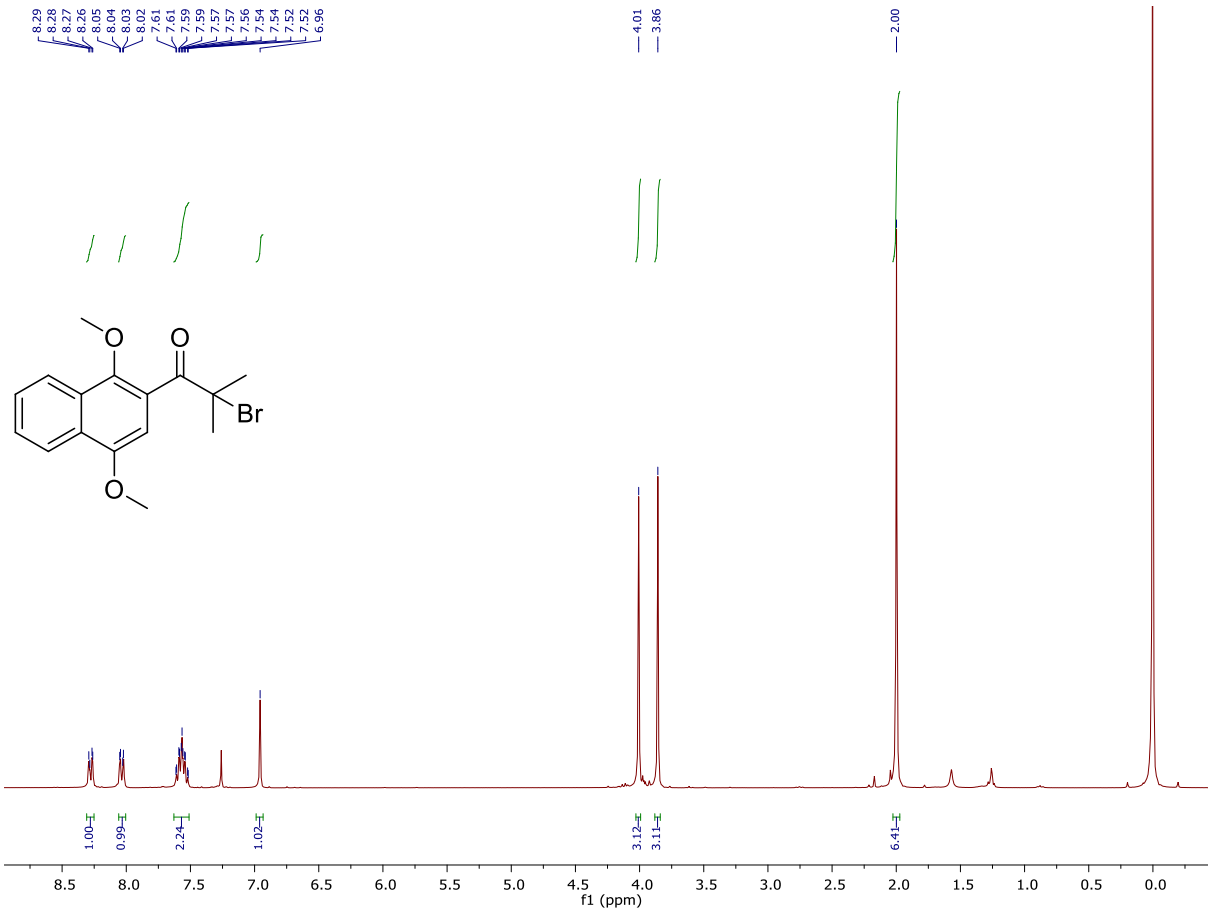

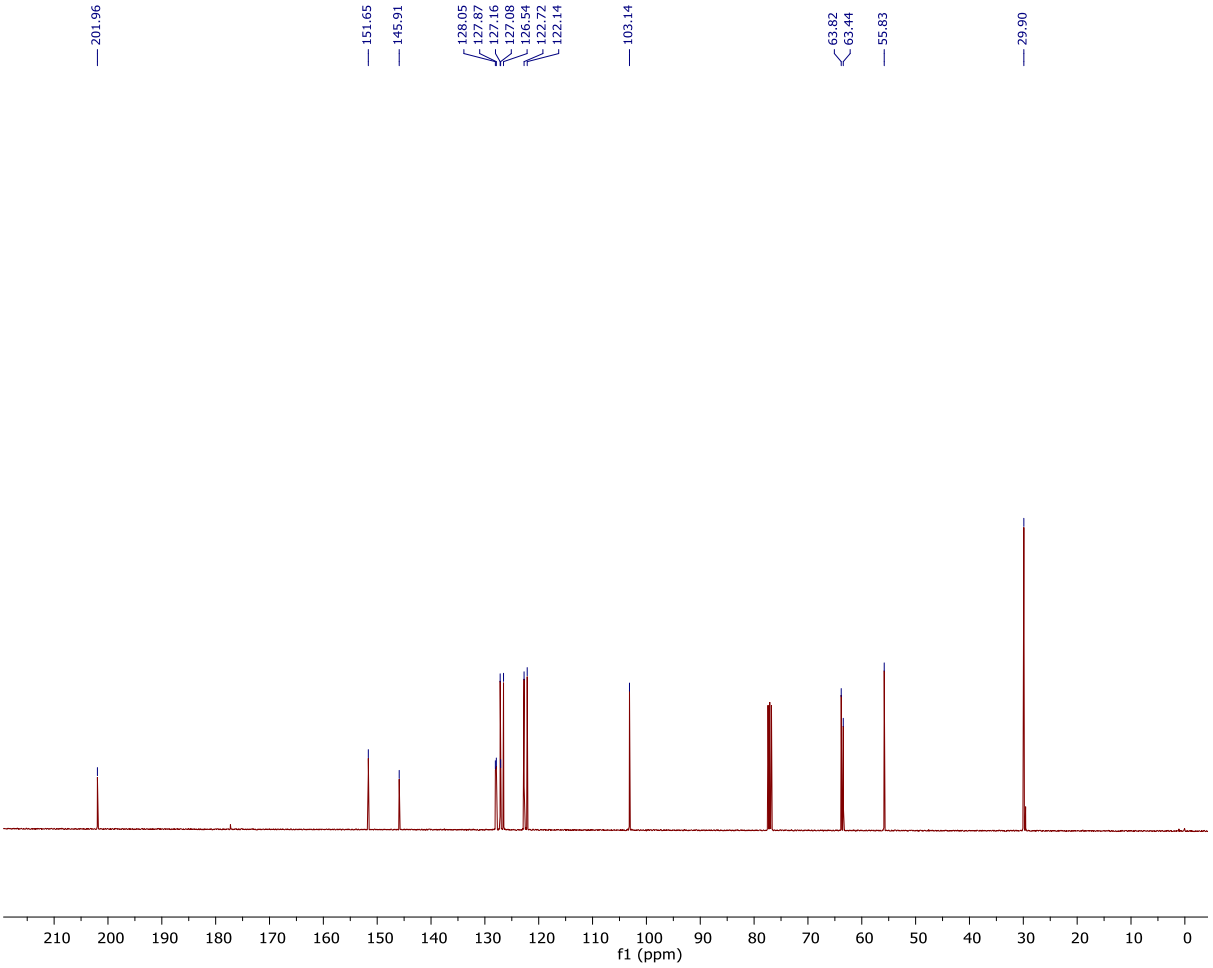

Compound 155

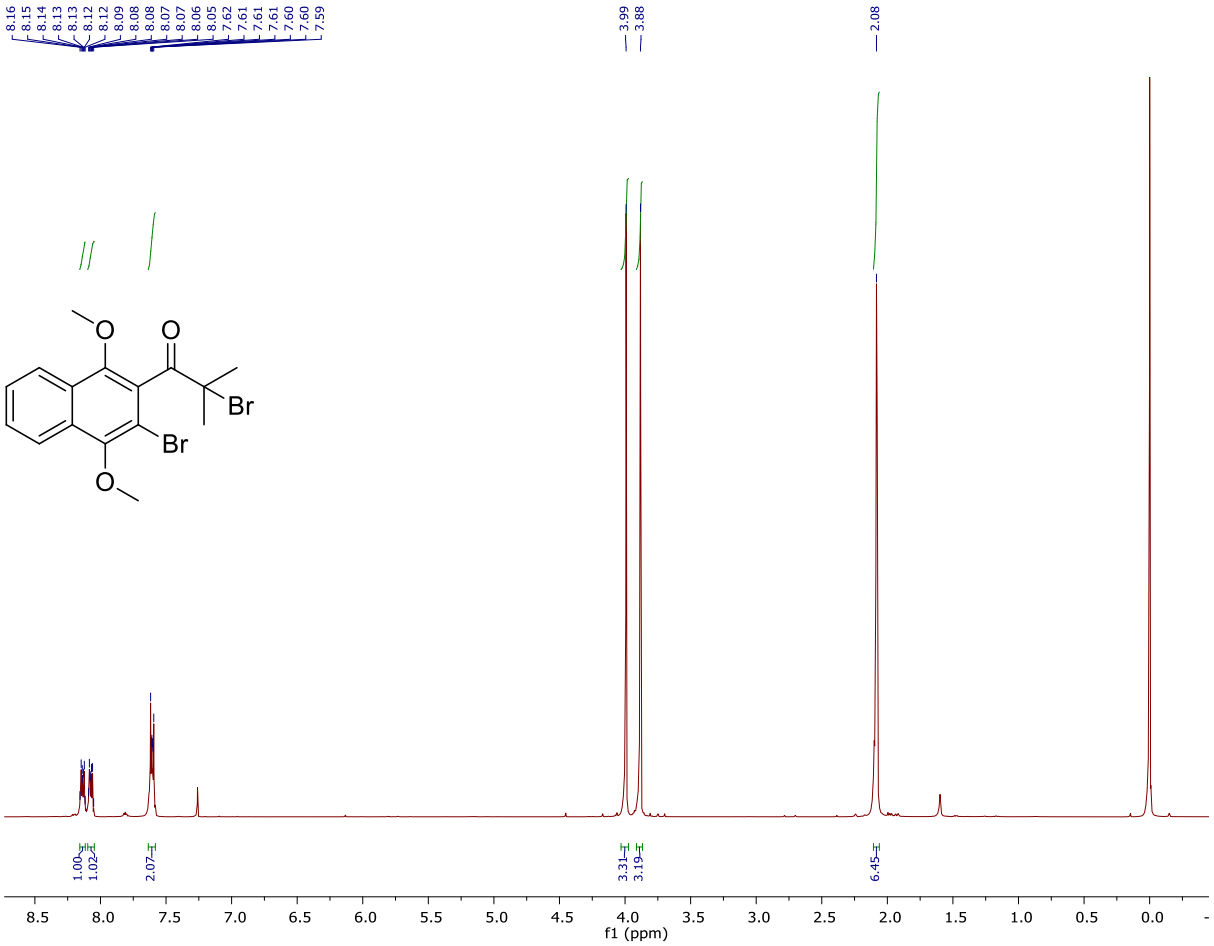

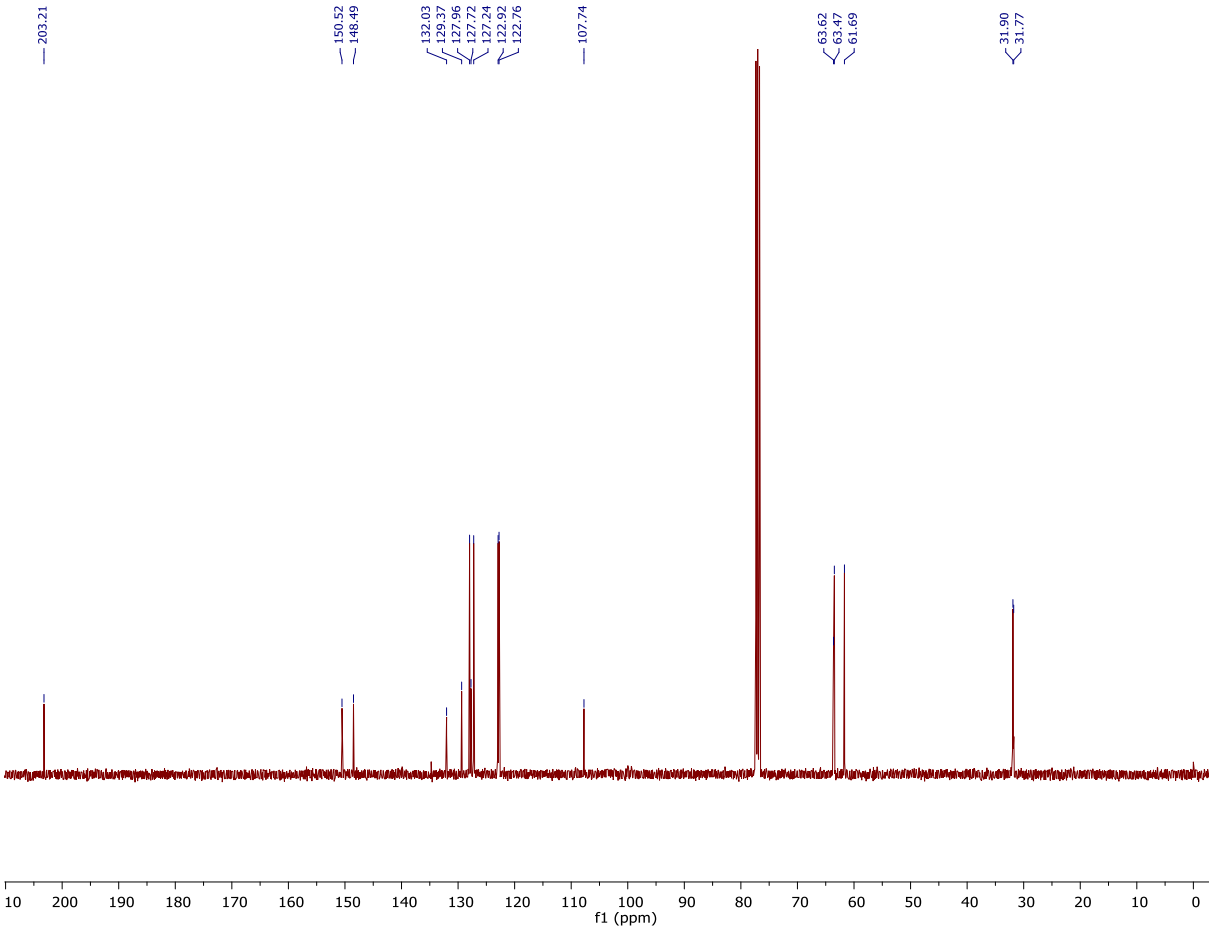

Compound 158

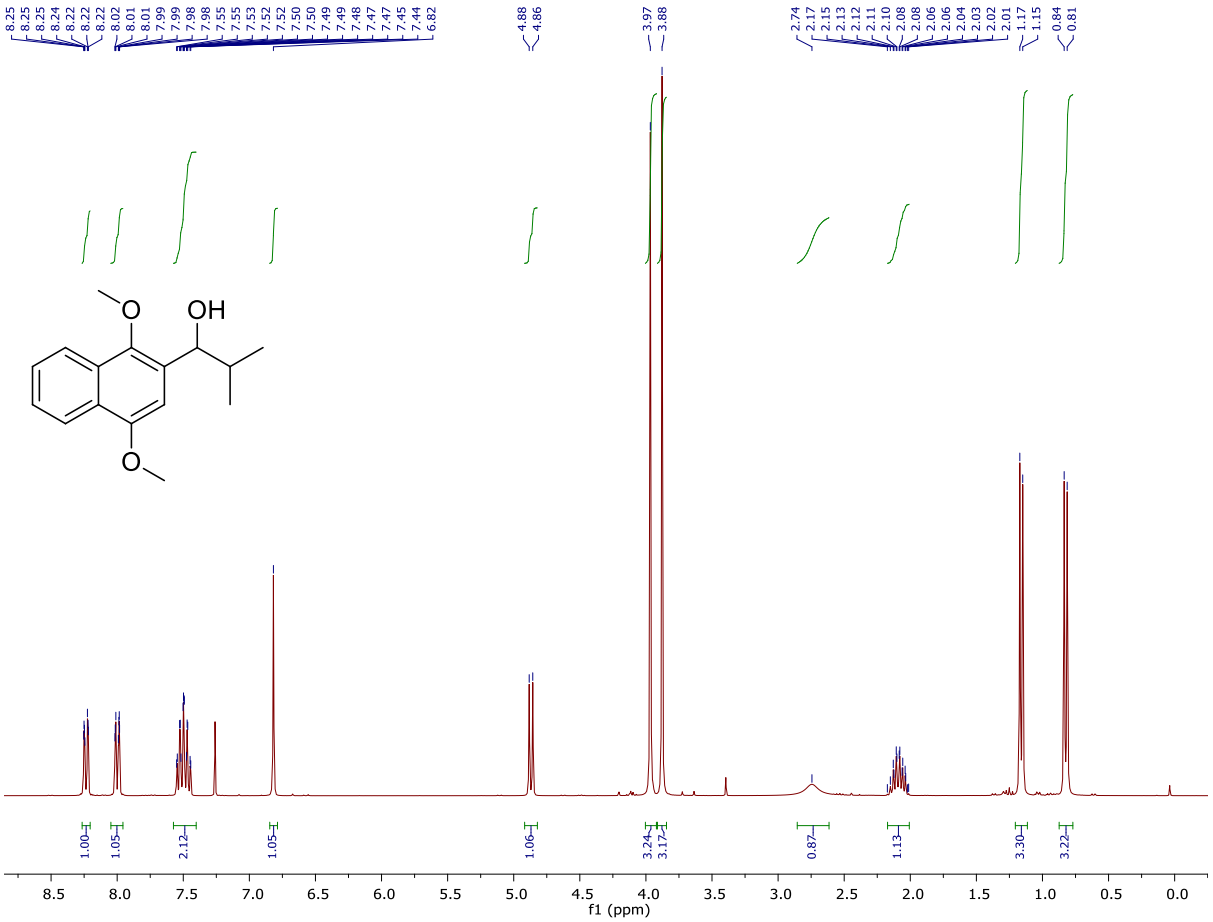

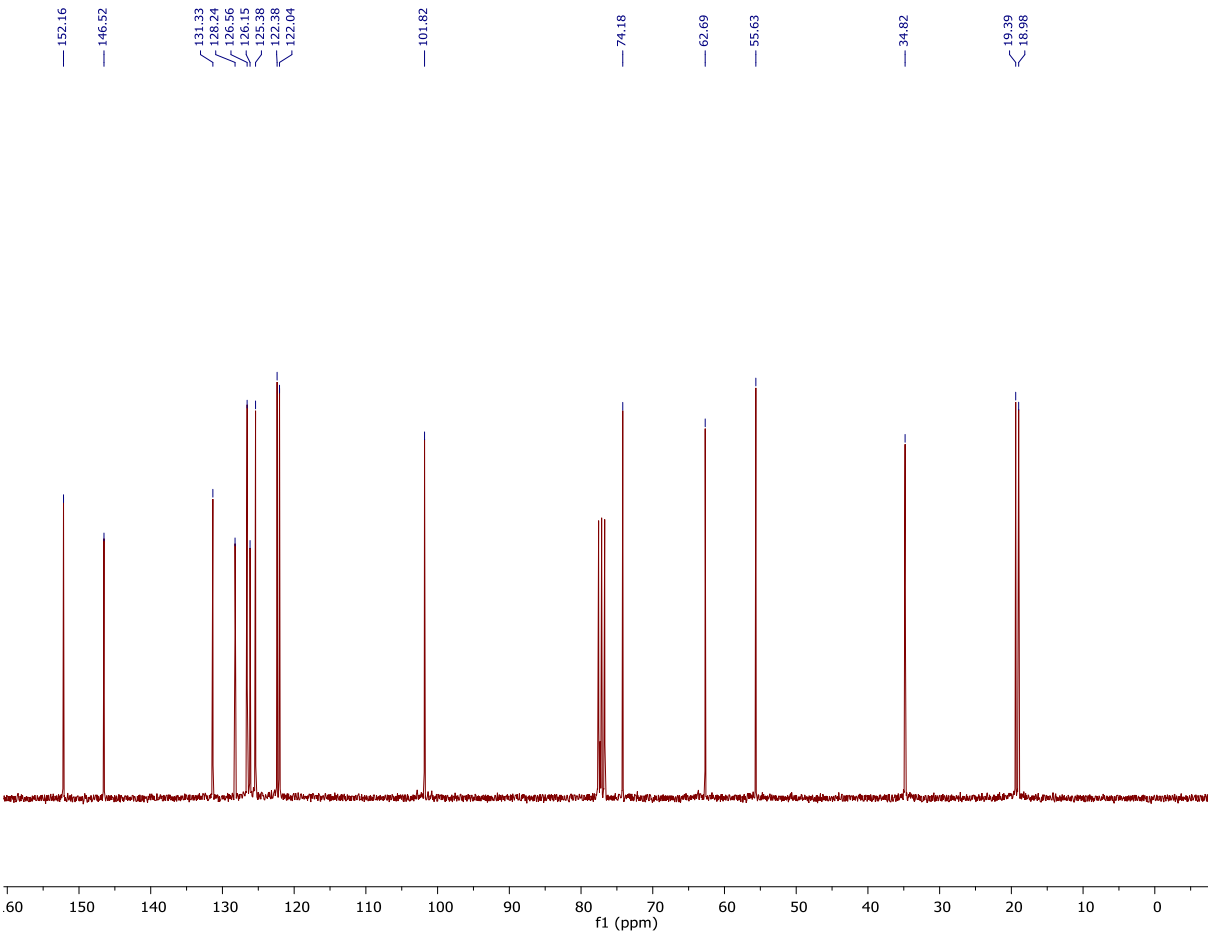

Compound 157

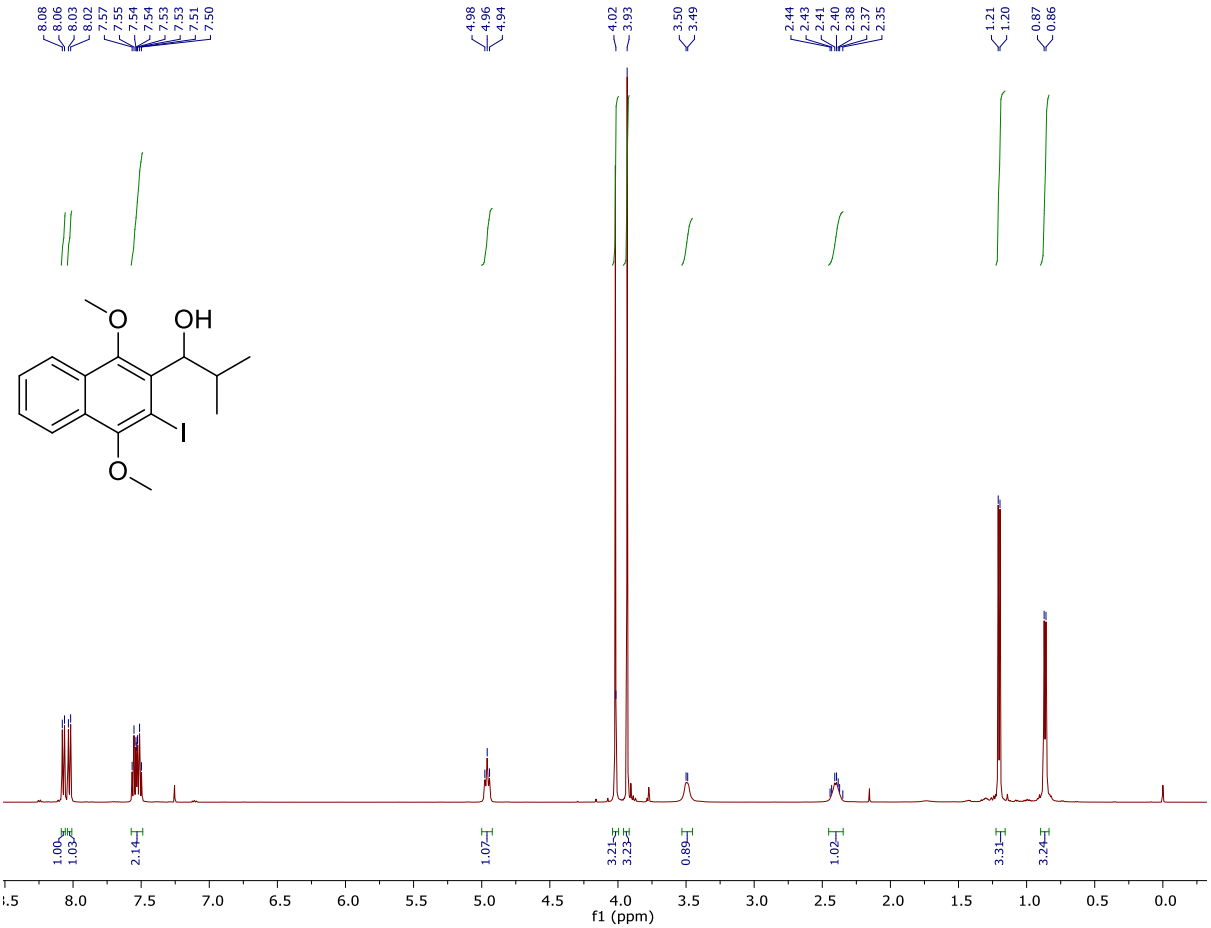

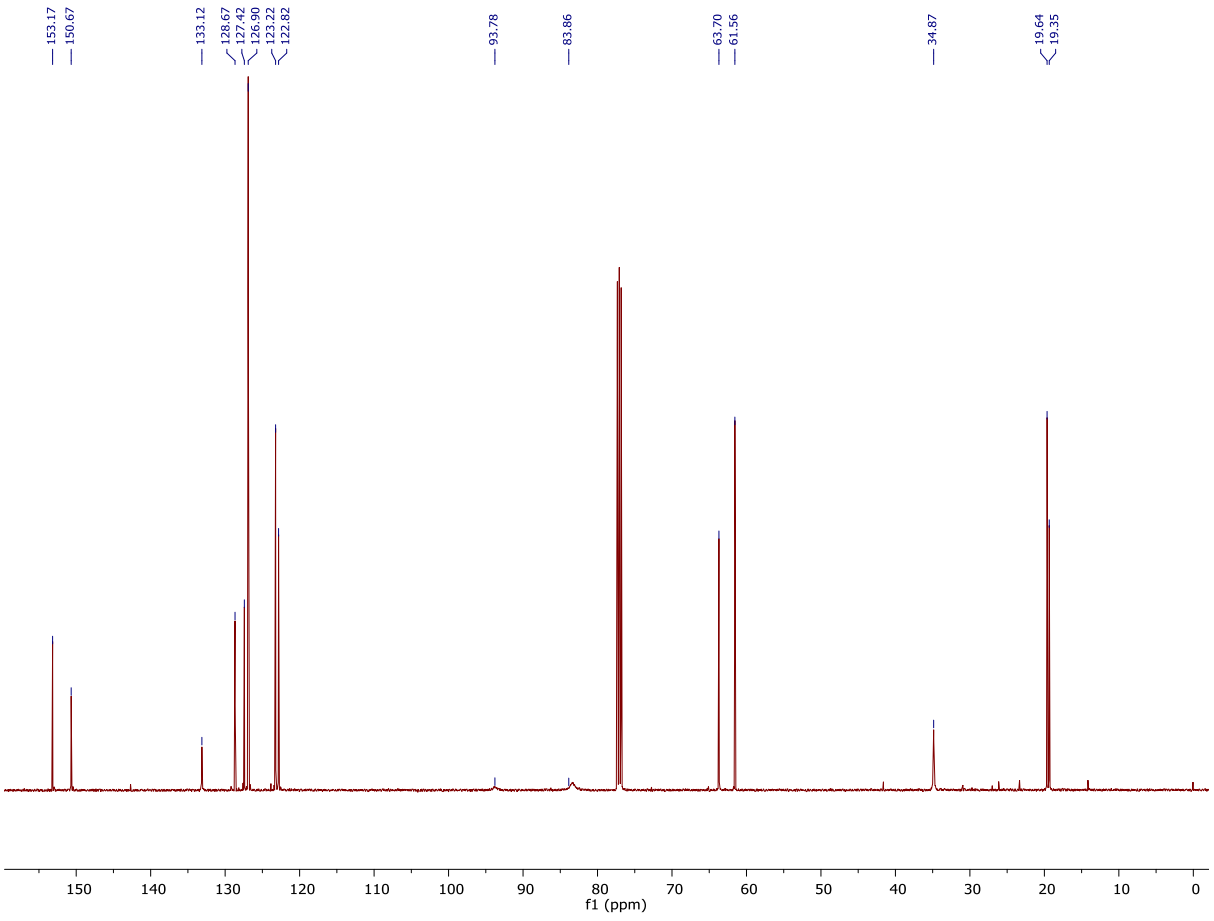

Compound 159

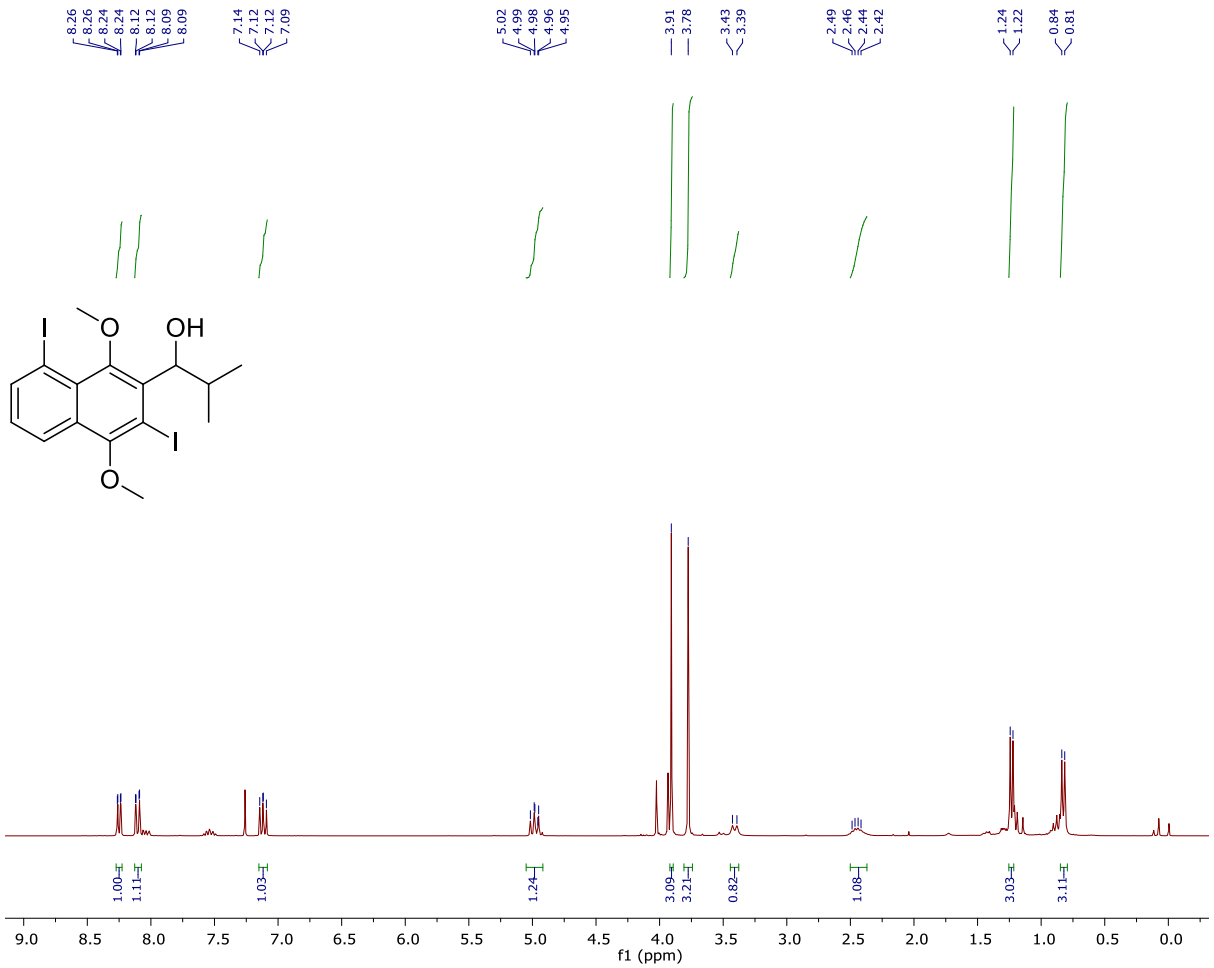

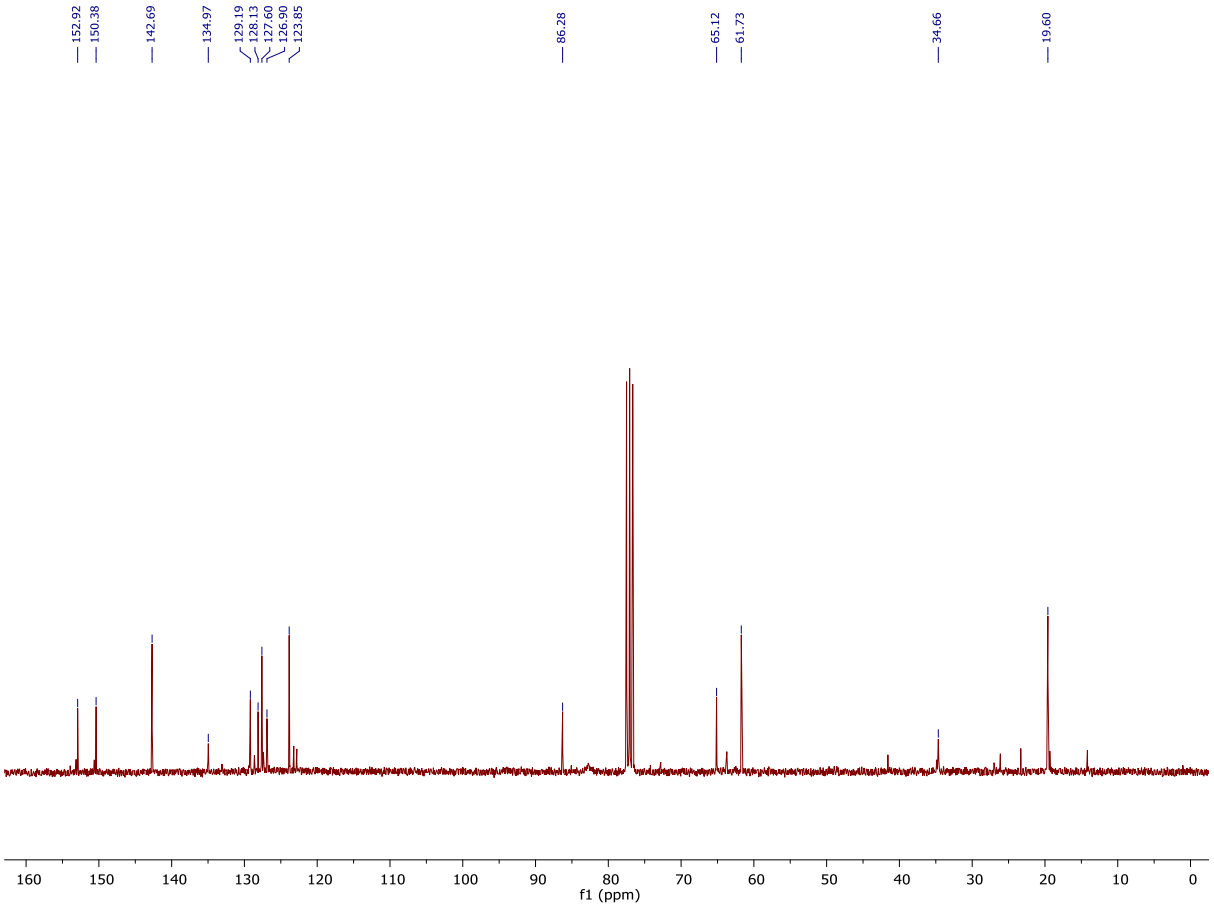

Compound 156

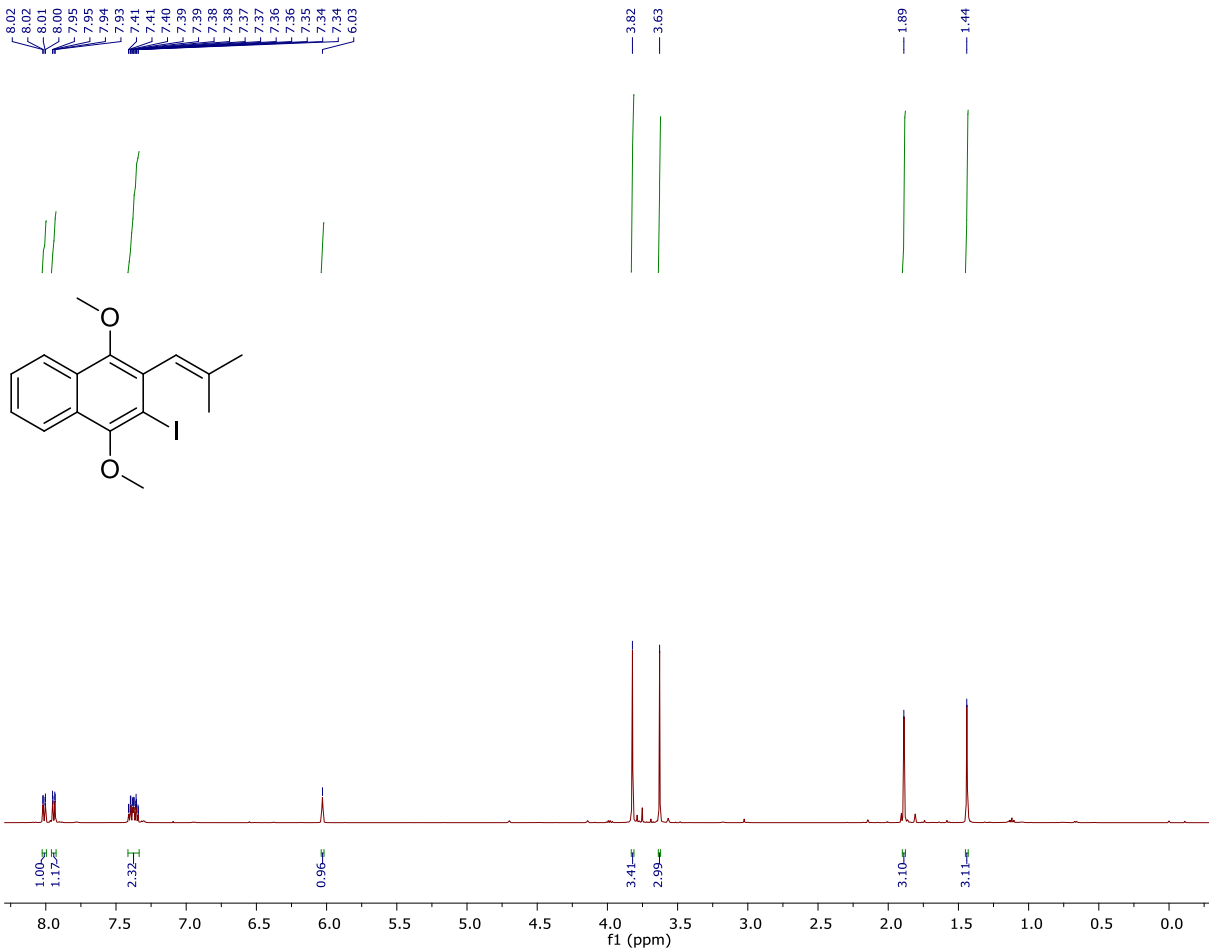

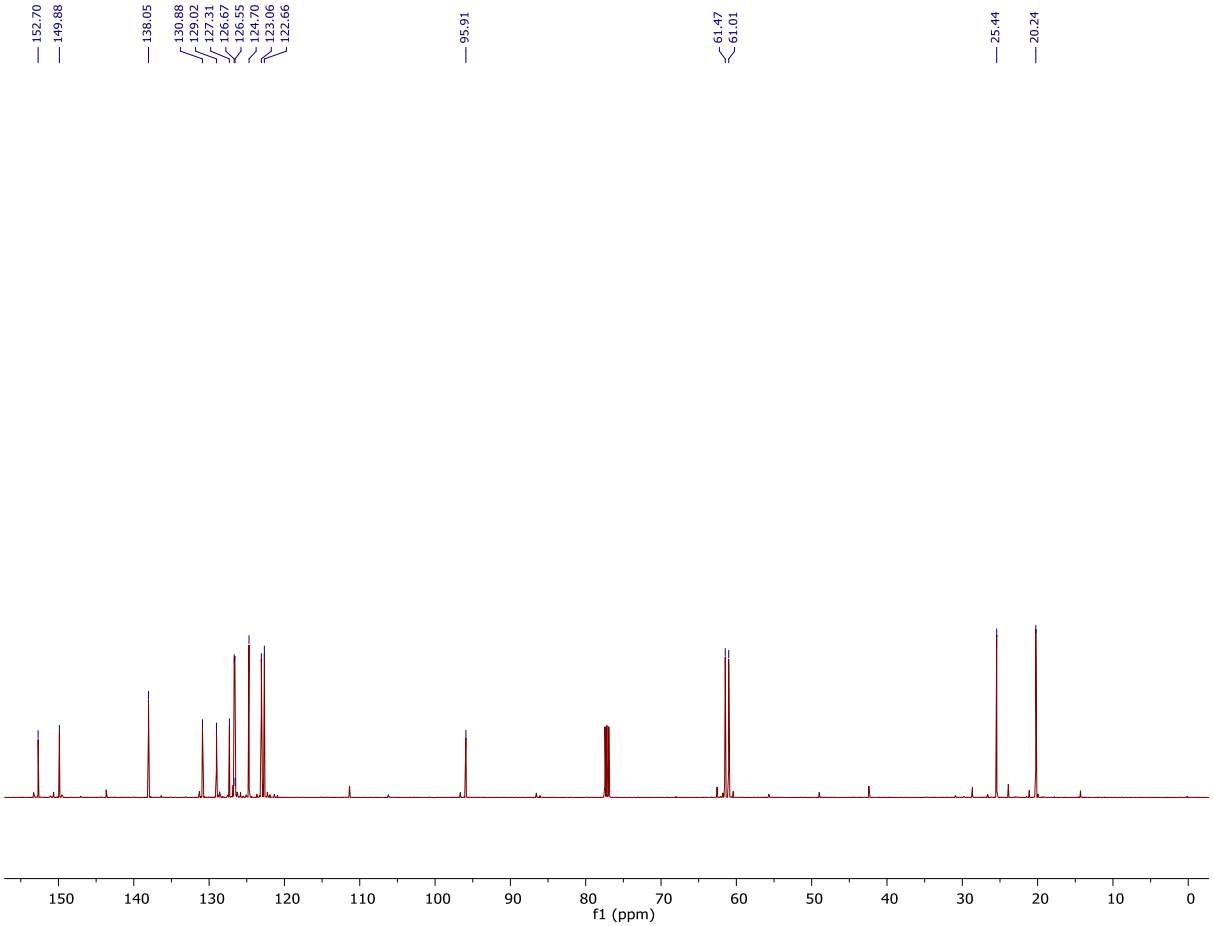

Compound 161

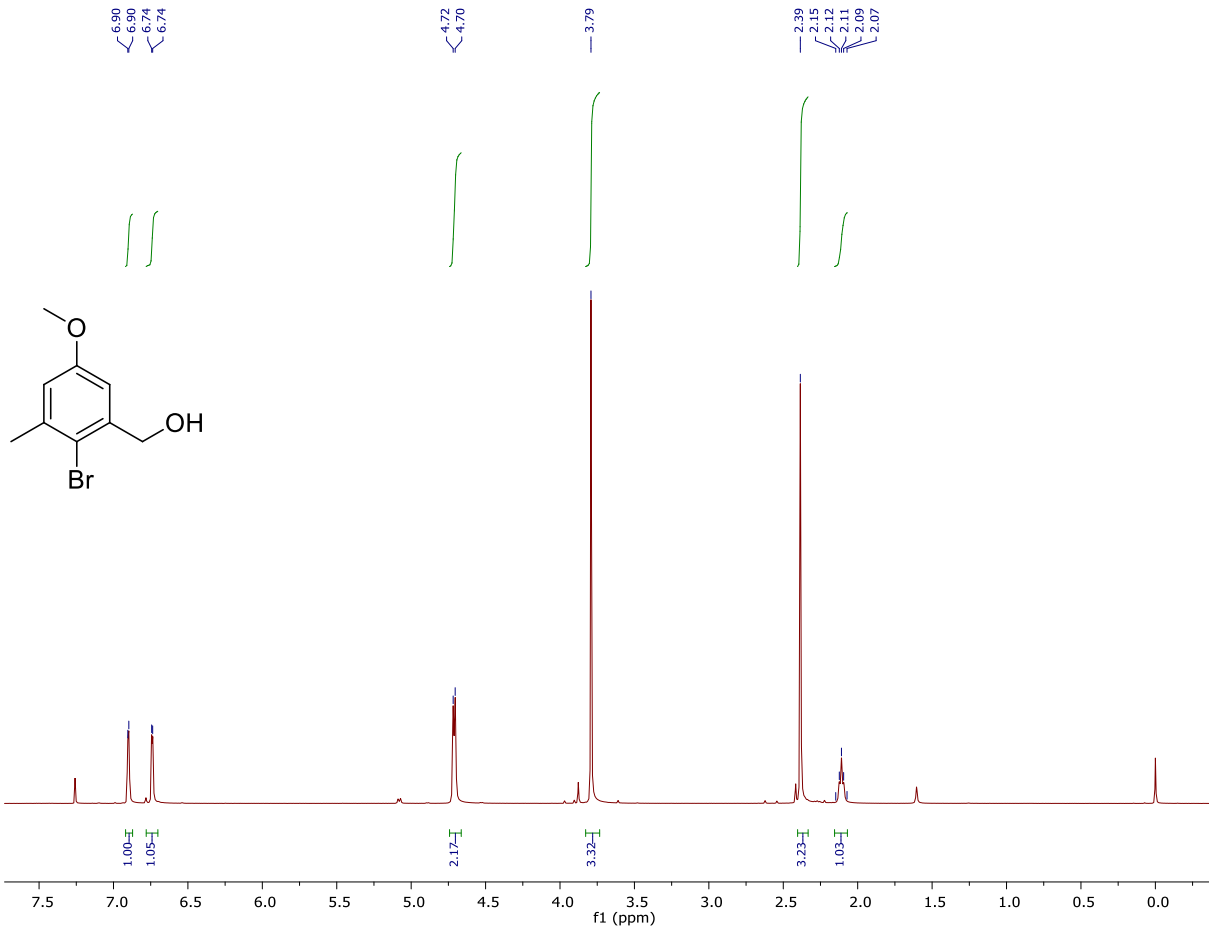

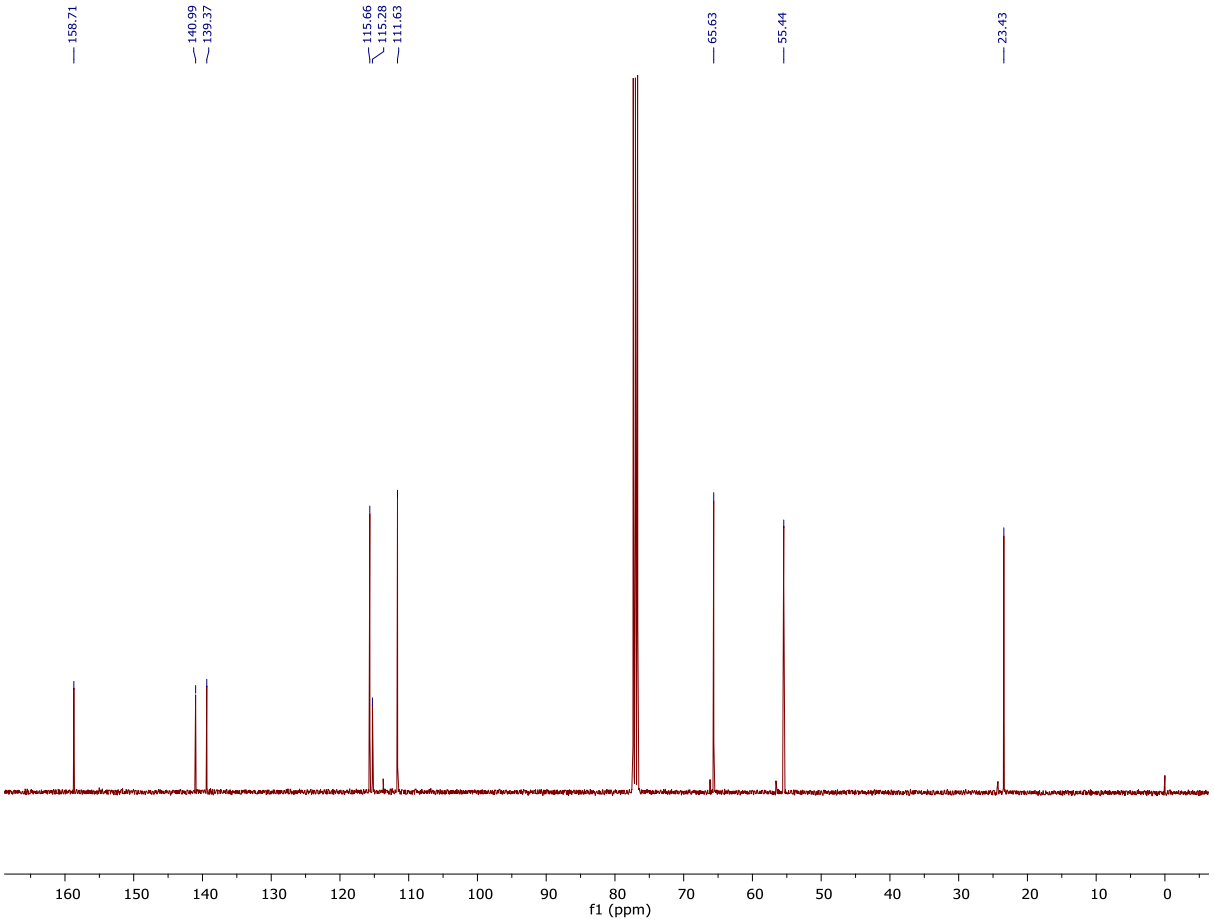

Compound 162

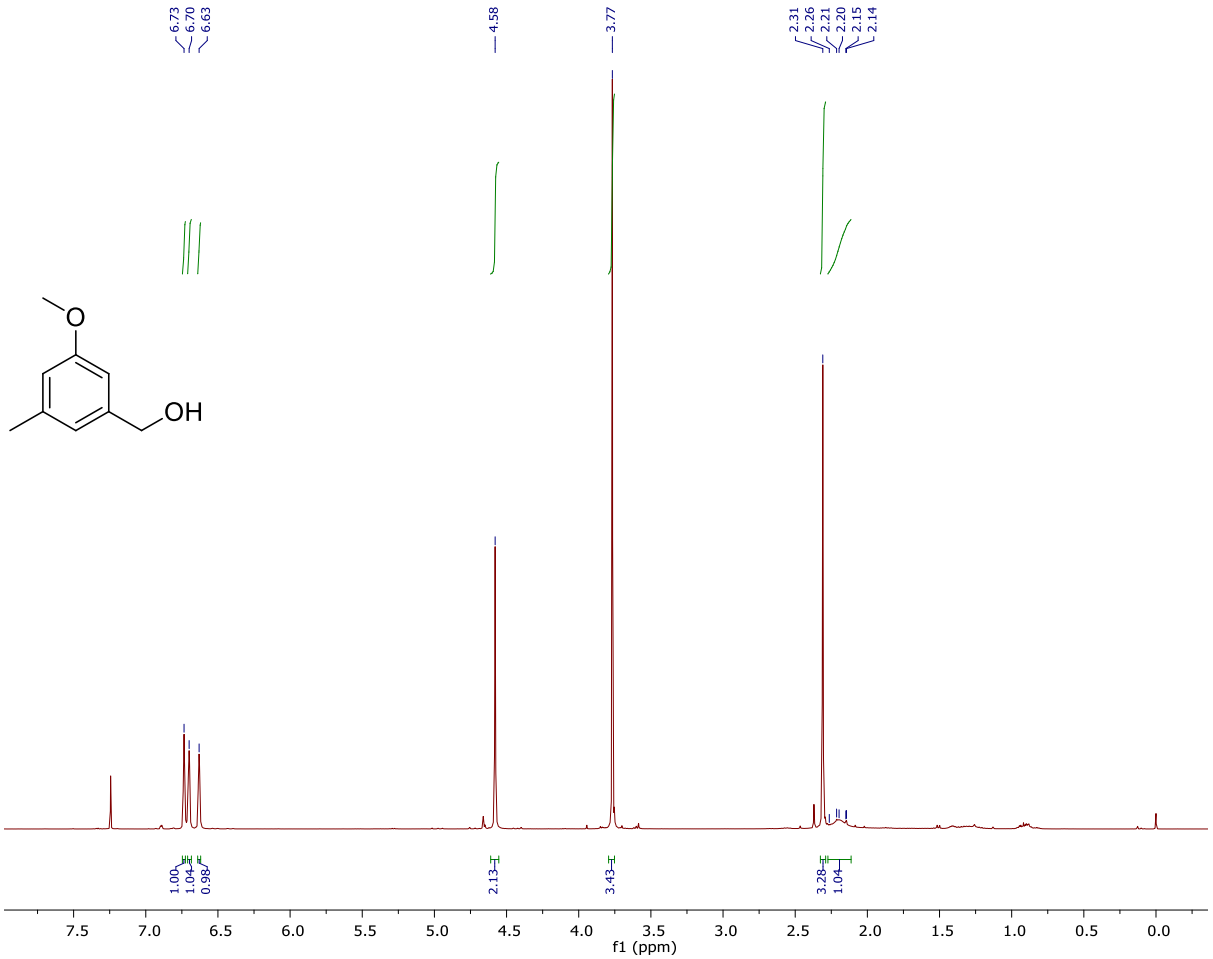

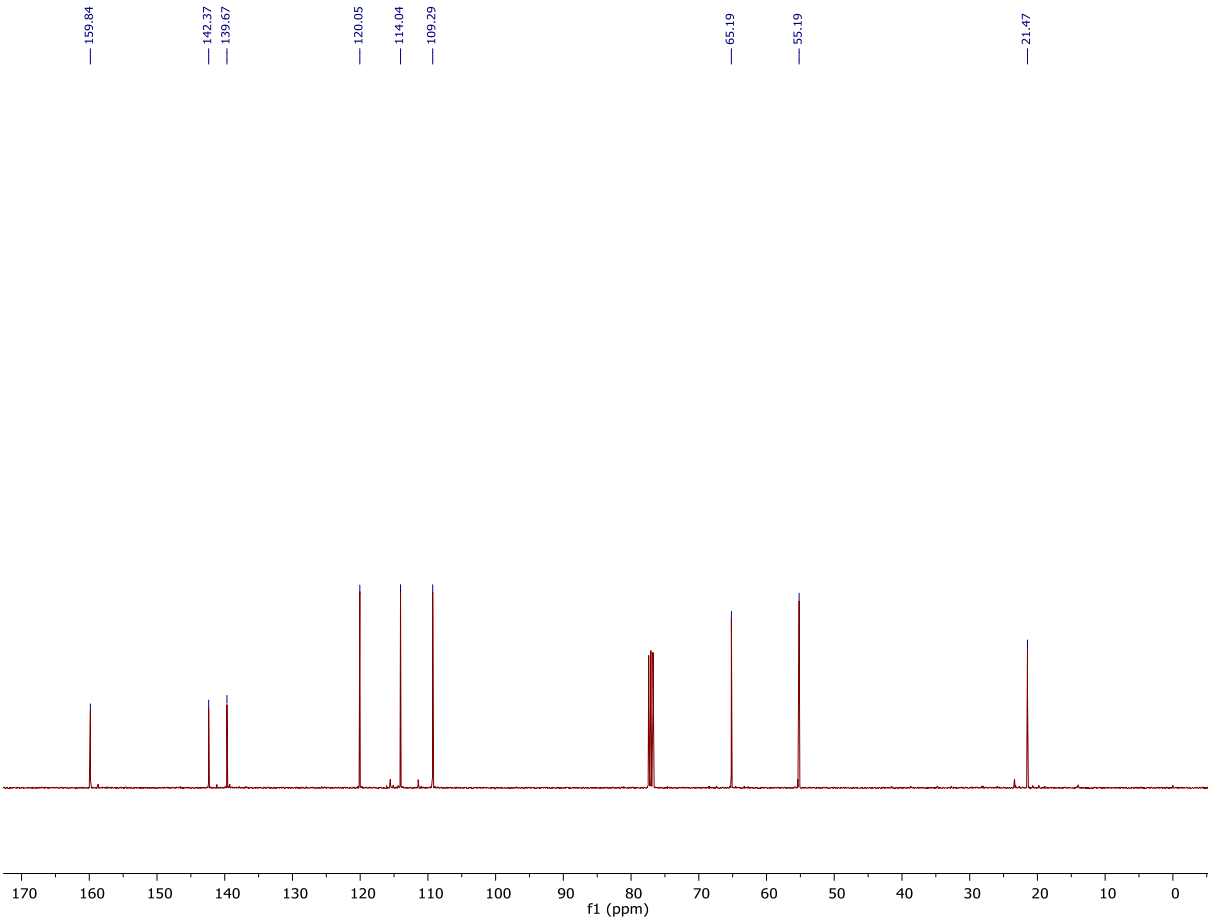

Compound 163

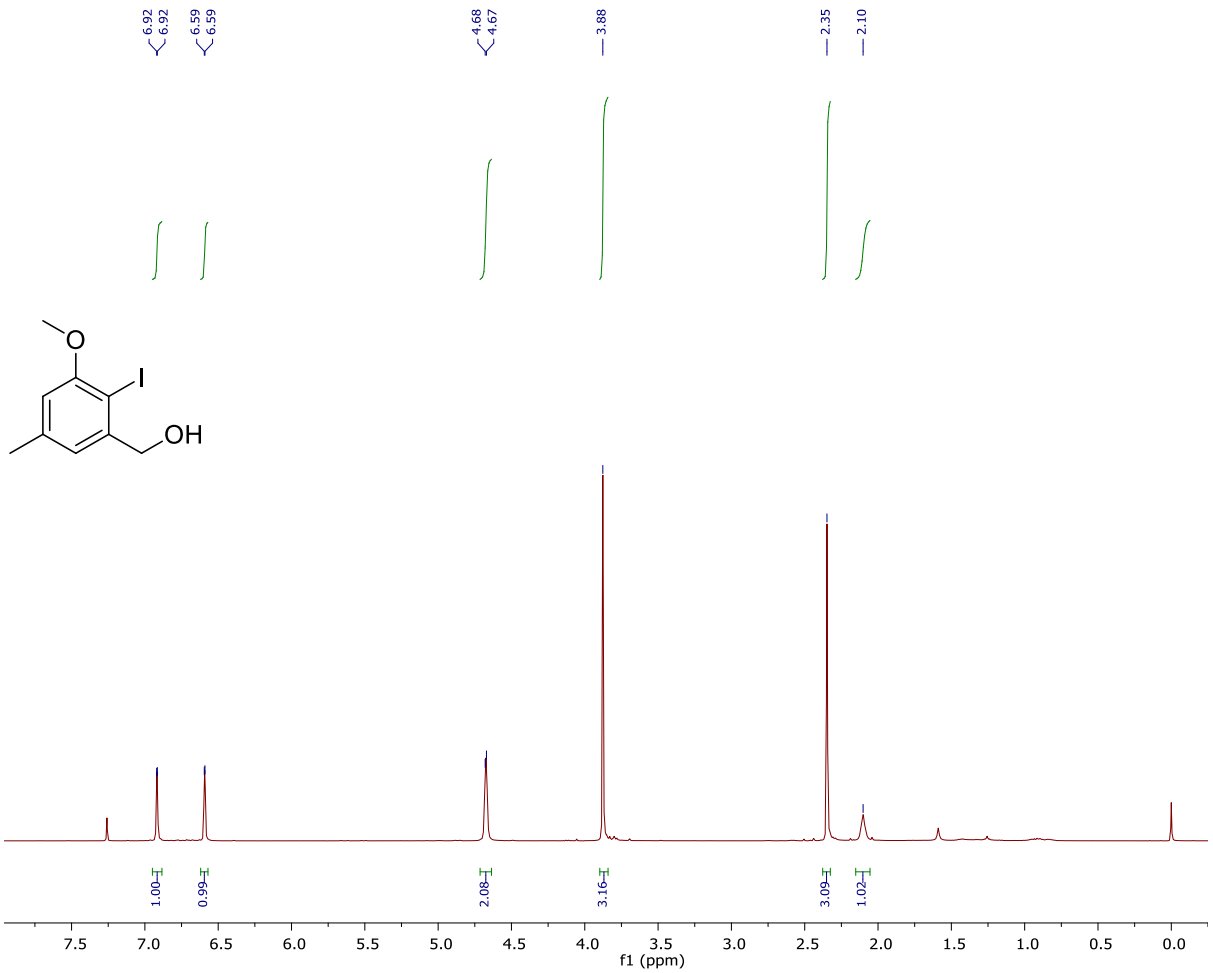

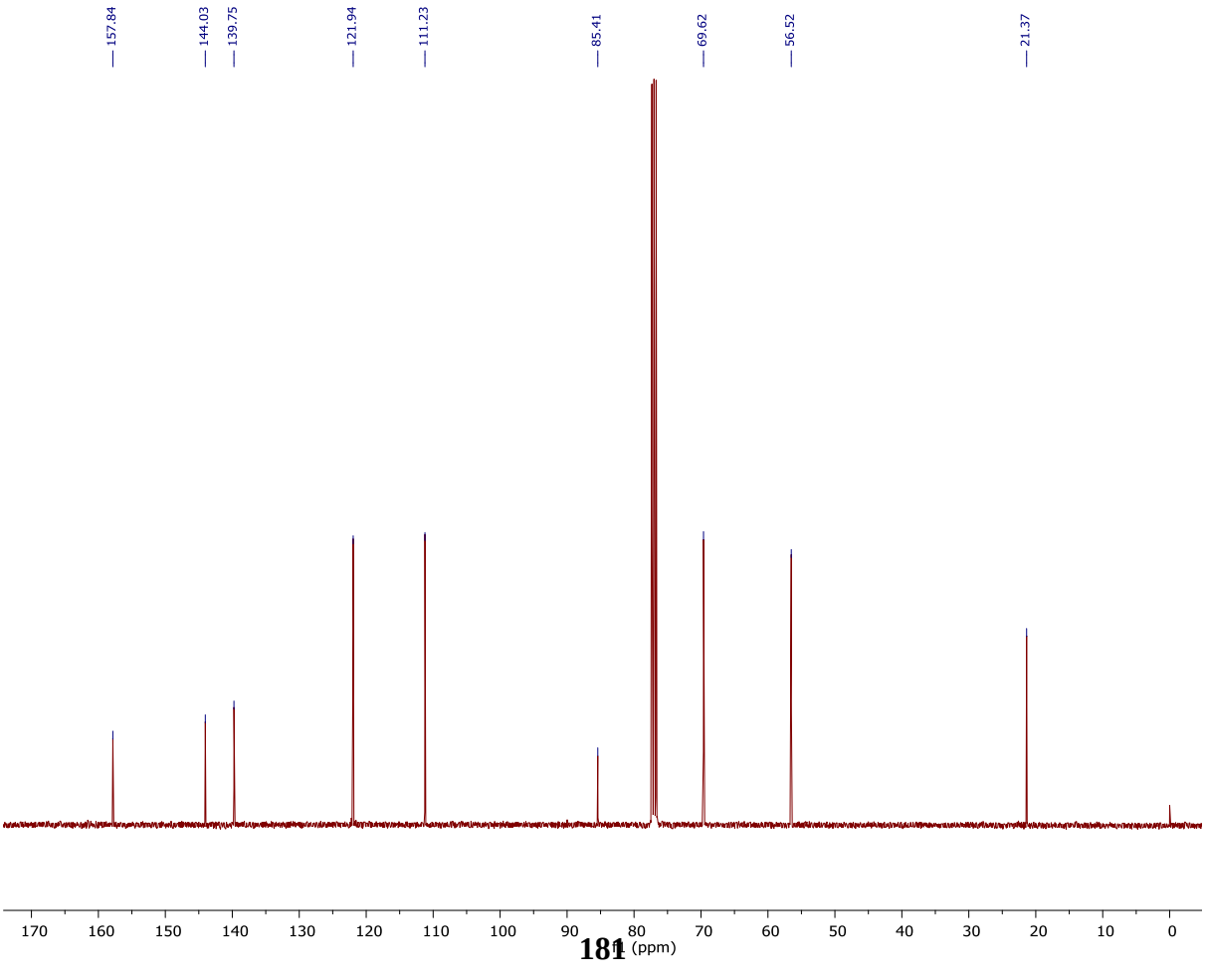

Compound 145

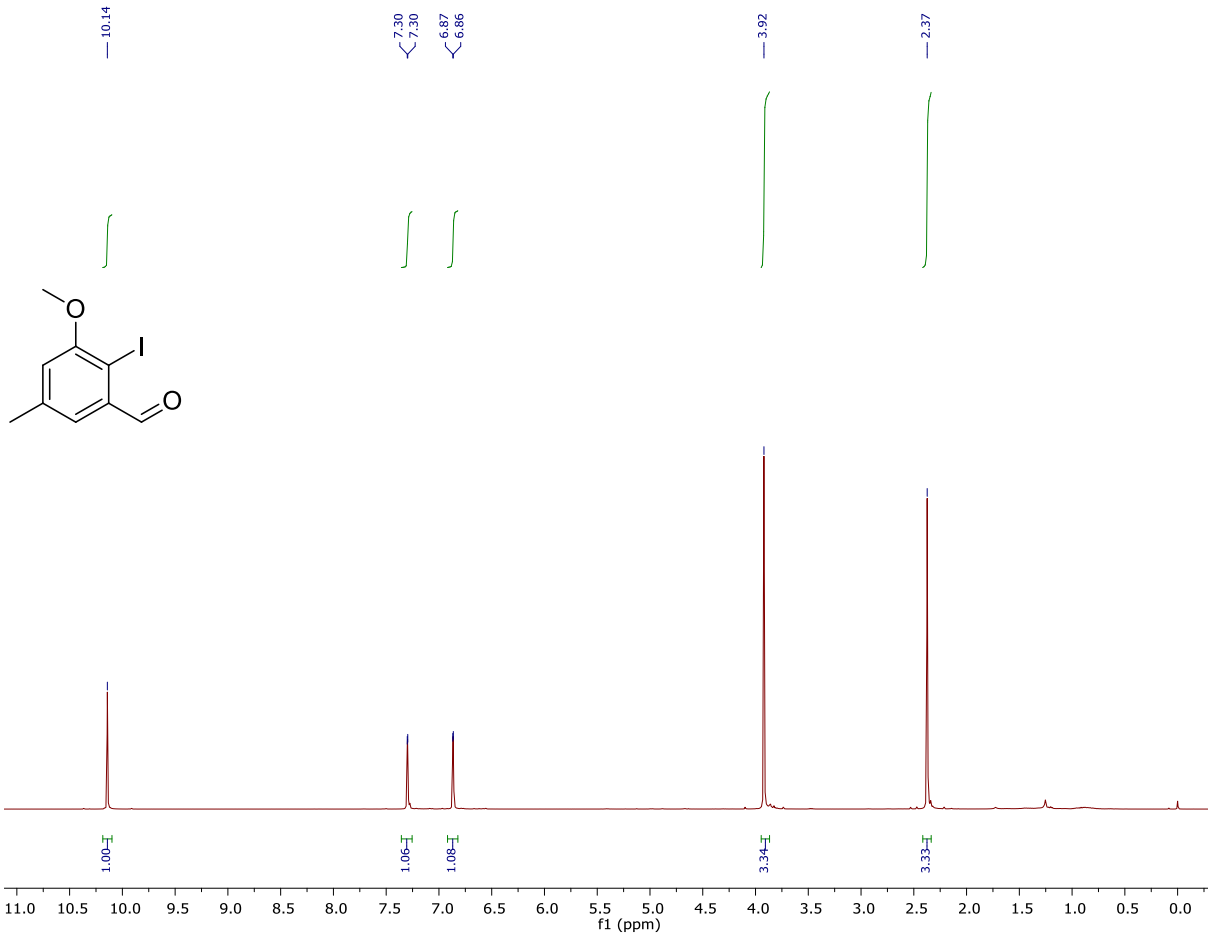

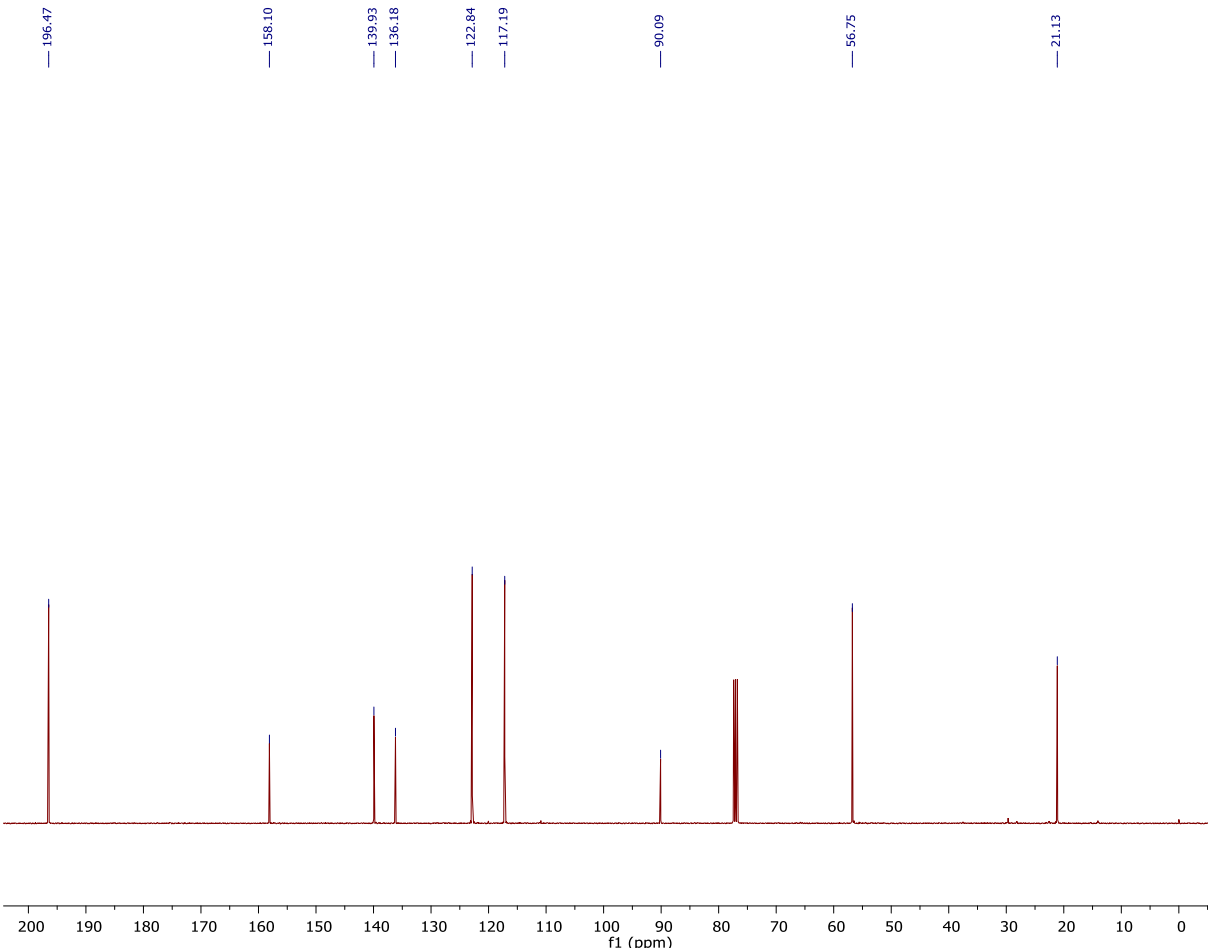

Compound 164

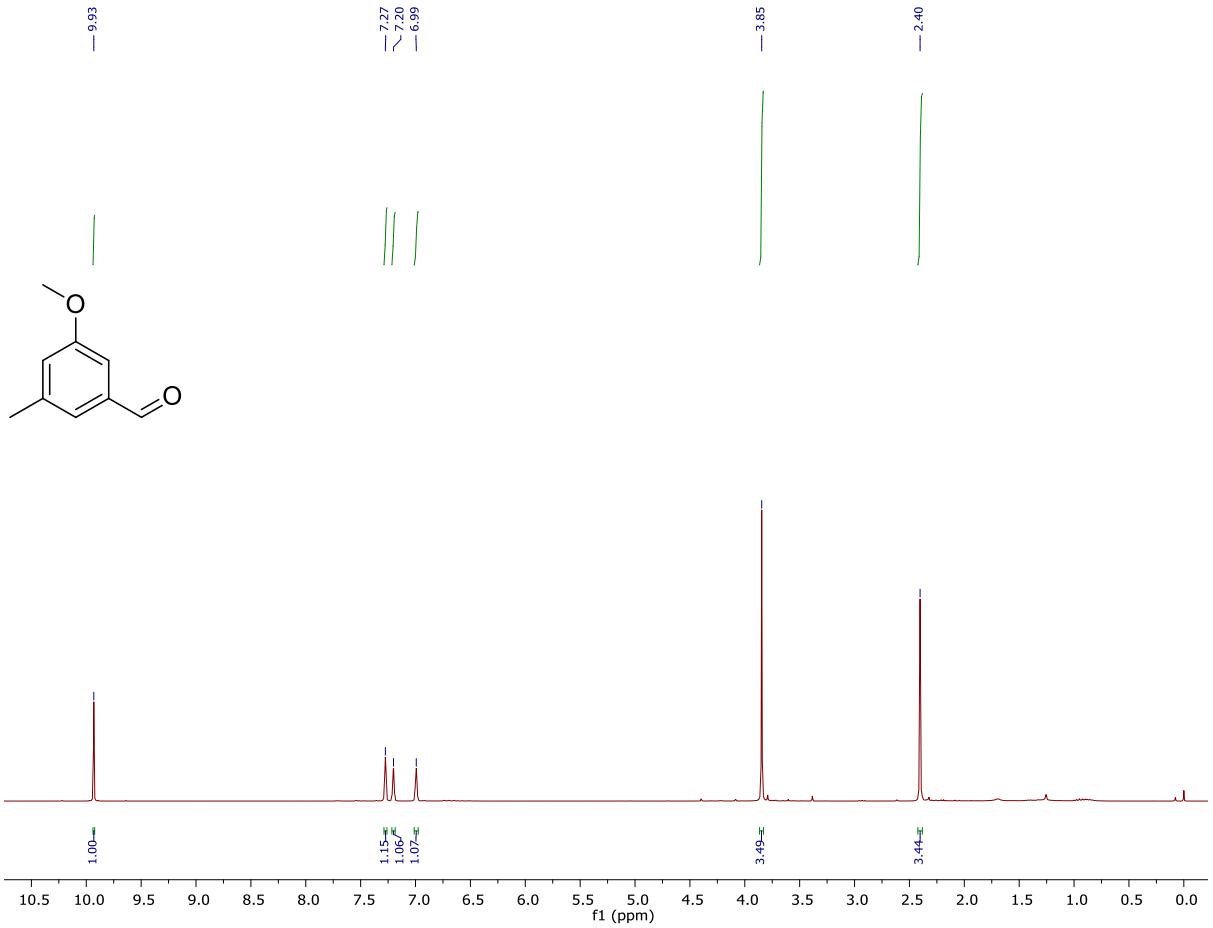

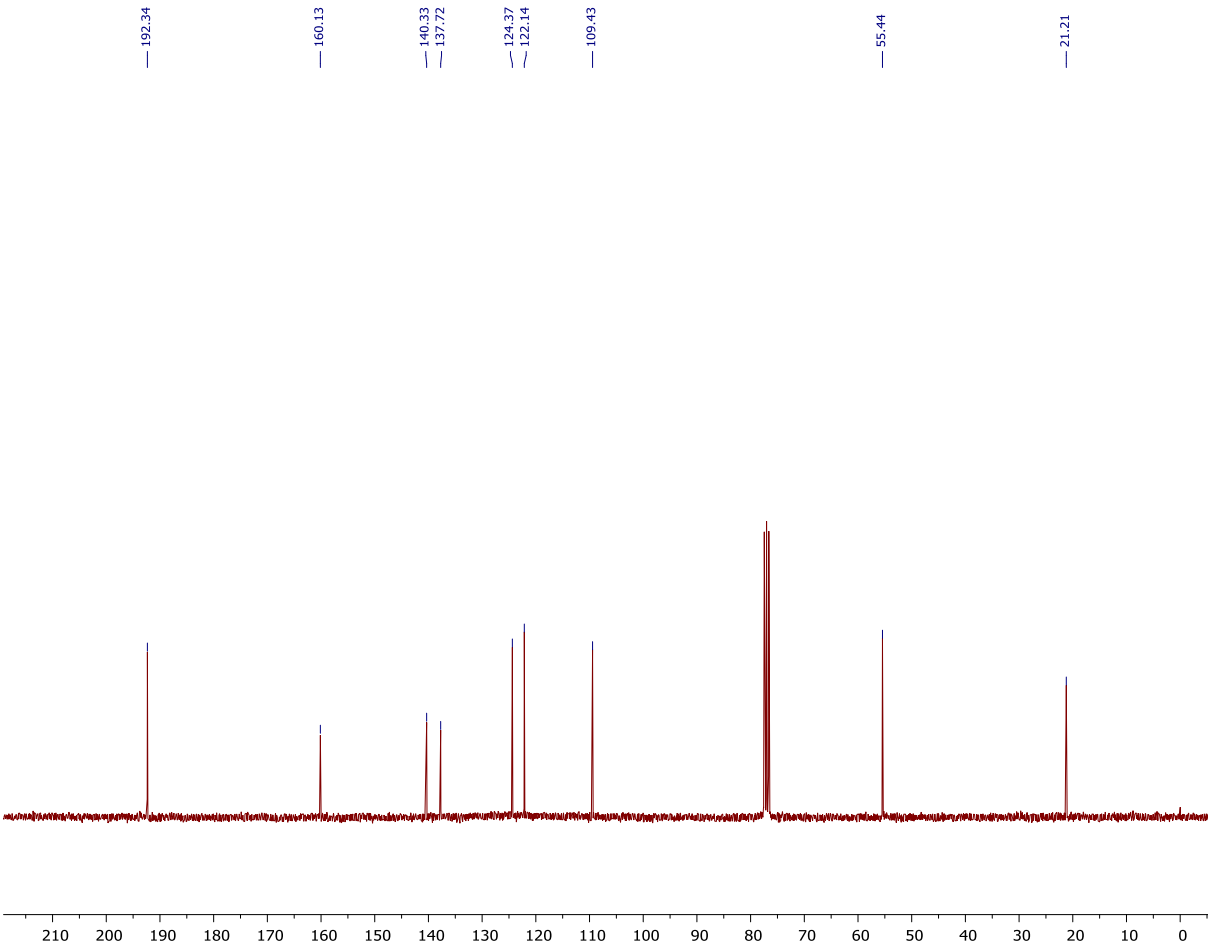

Compound 166

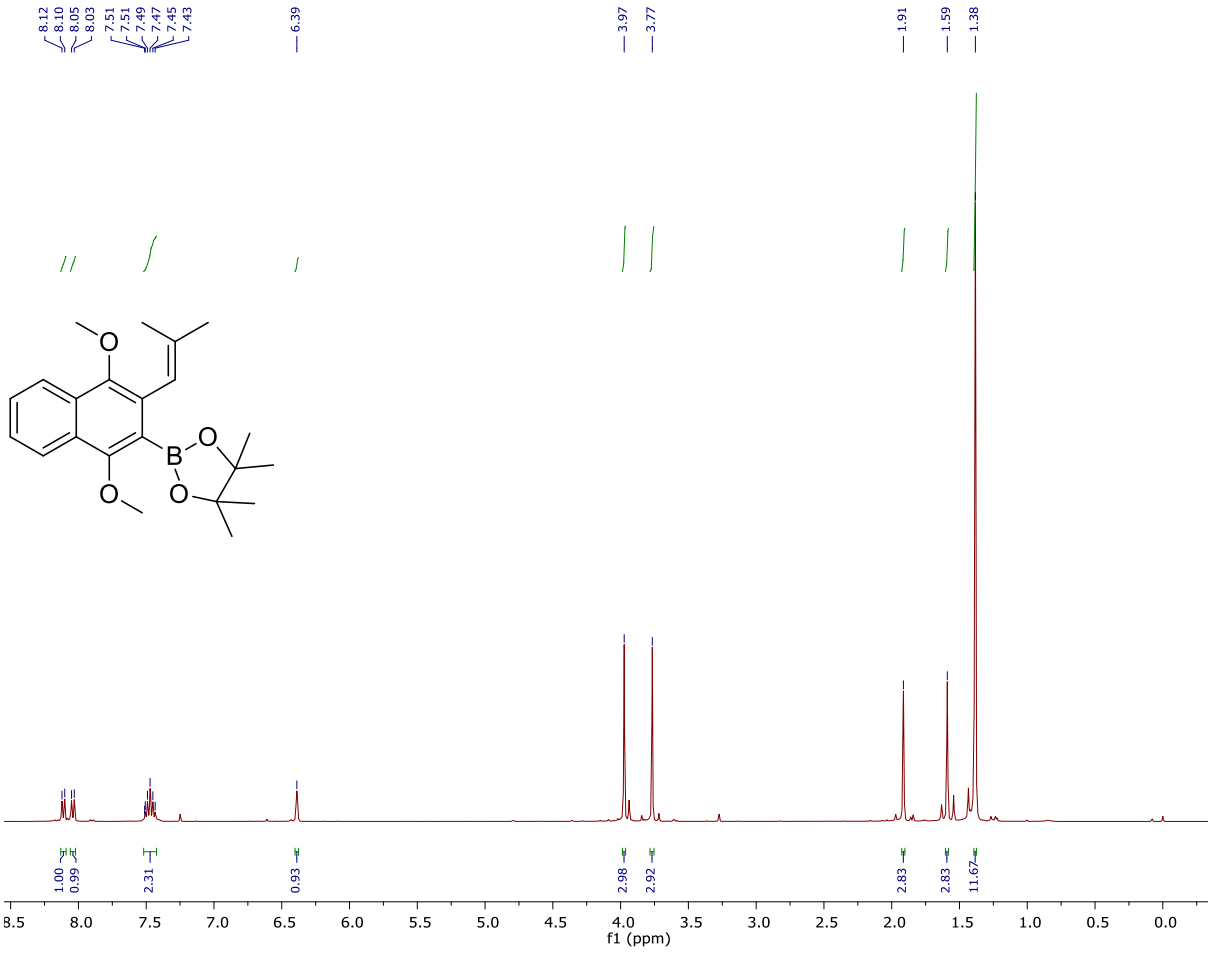

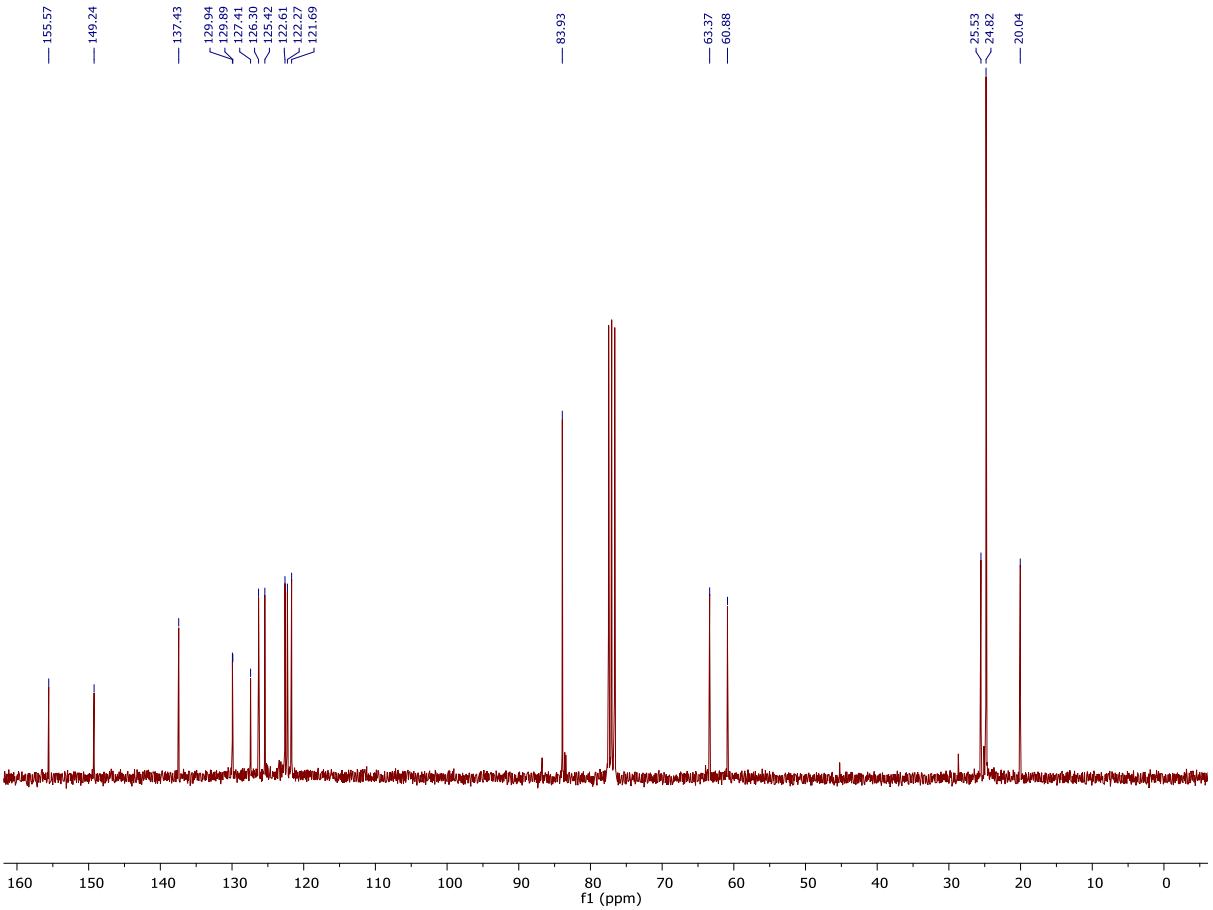

Compound 143

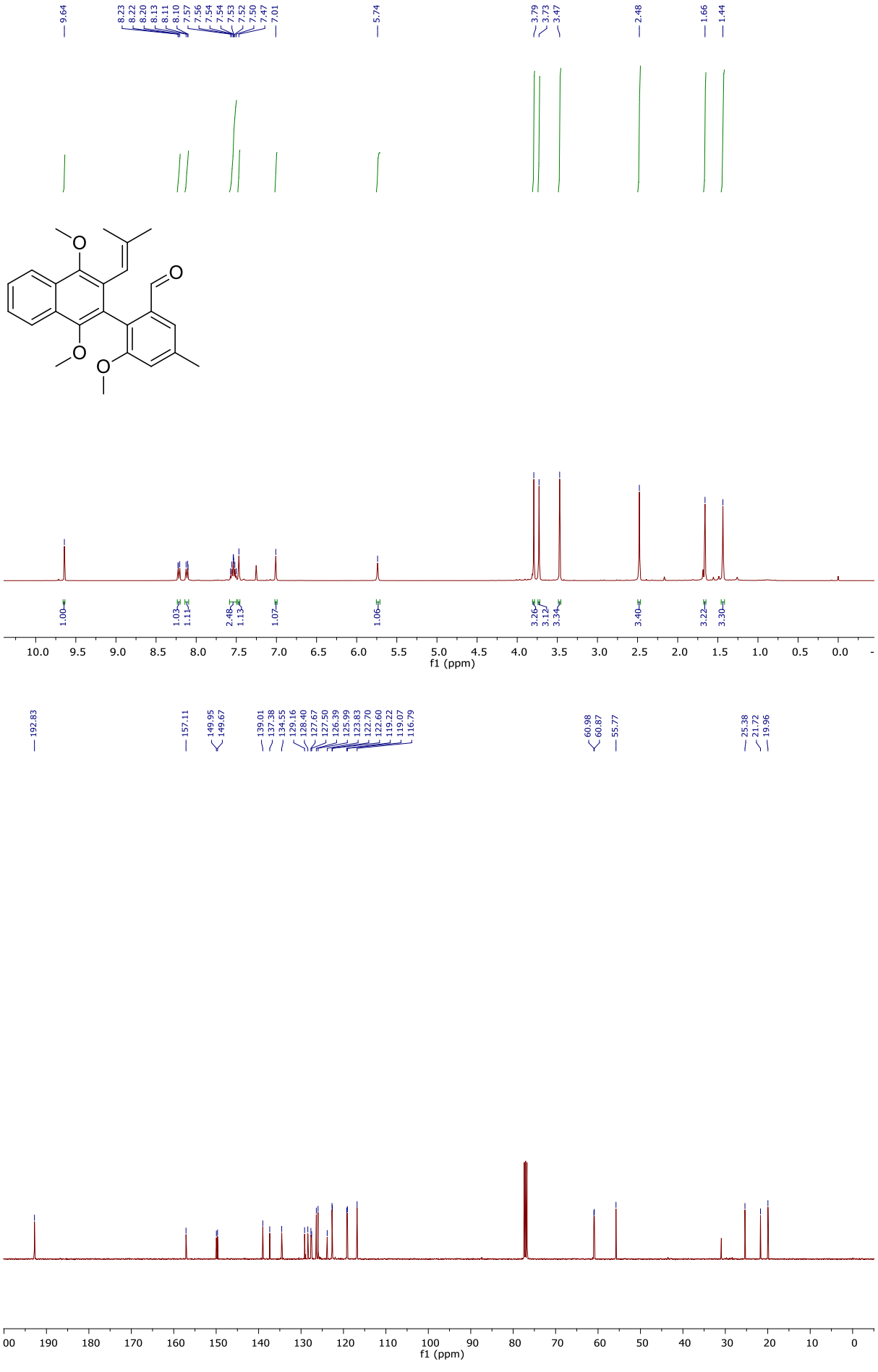

Compound 142

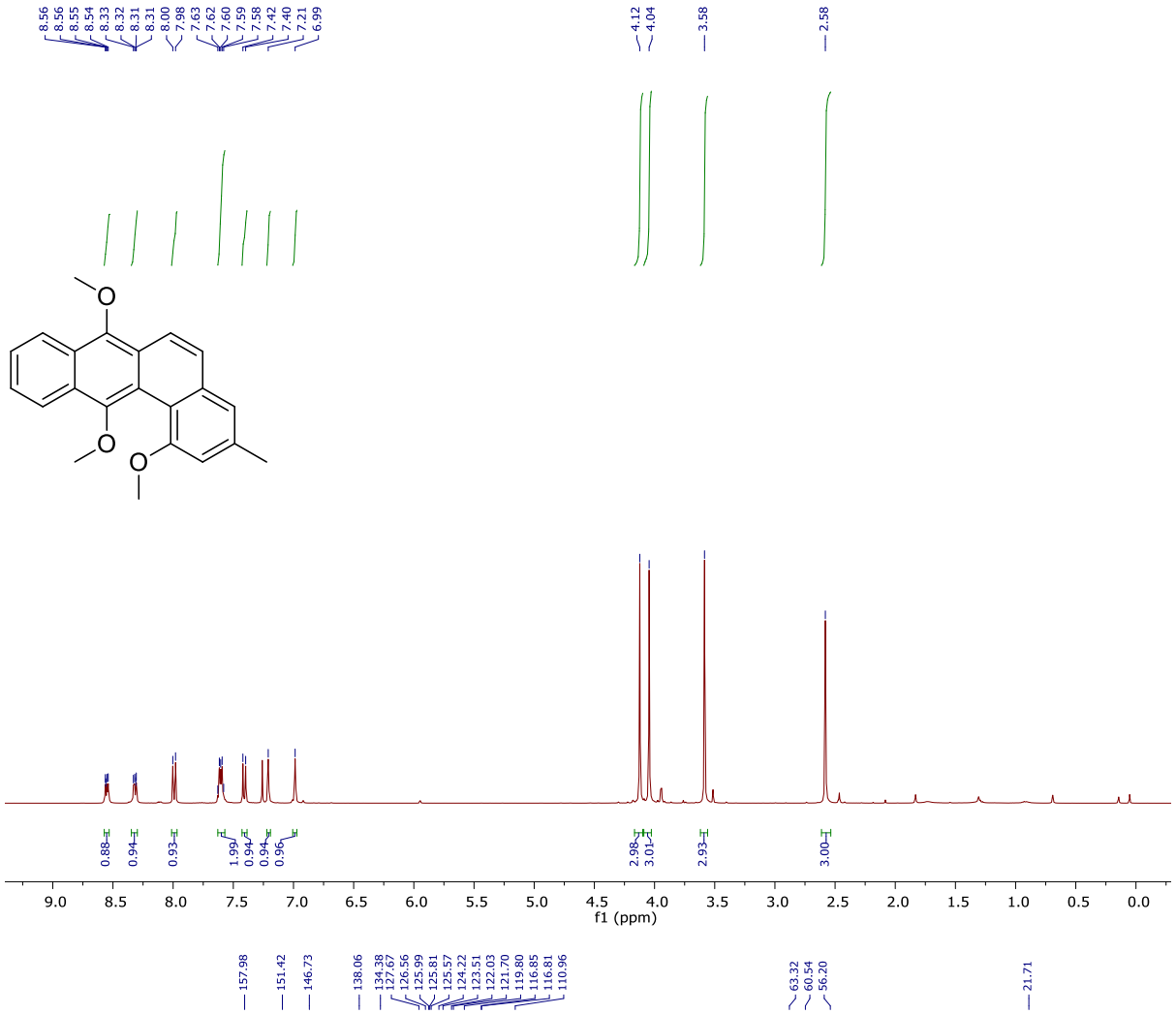

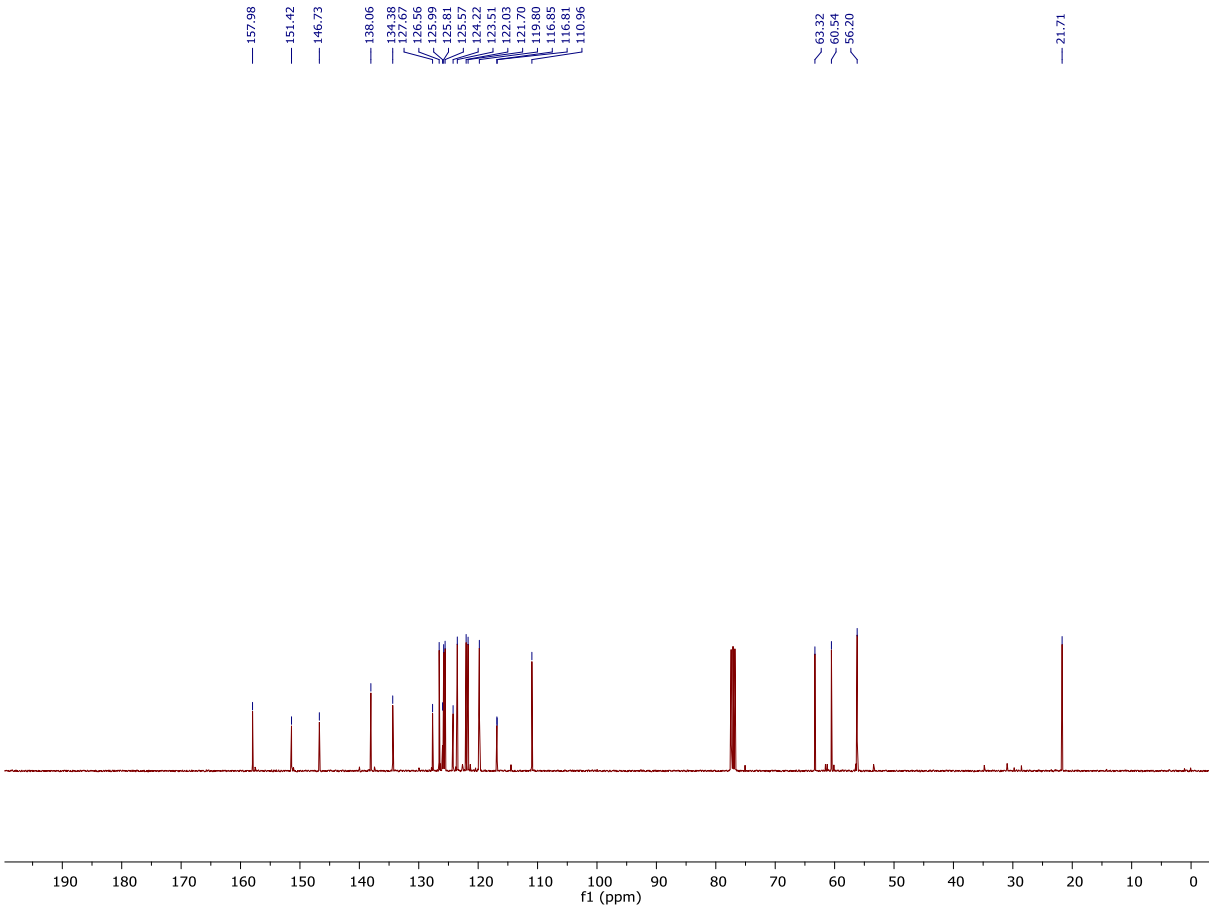

Compound 141

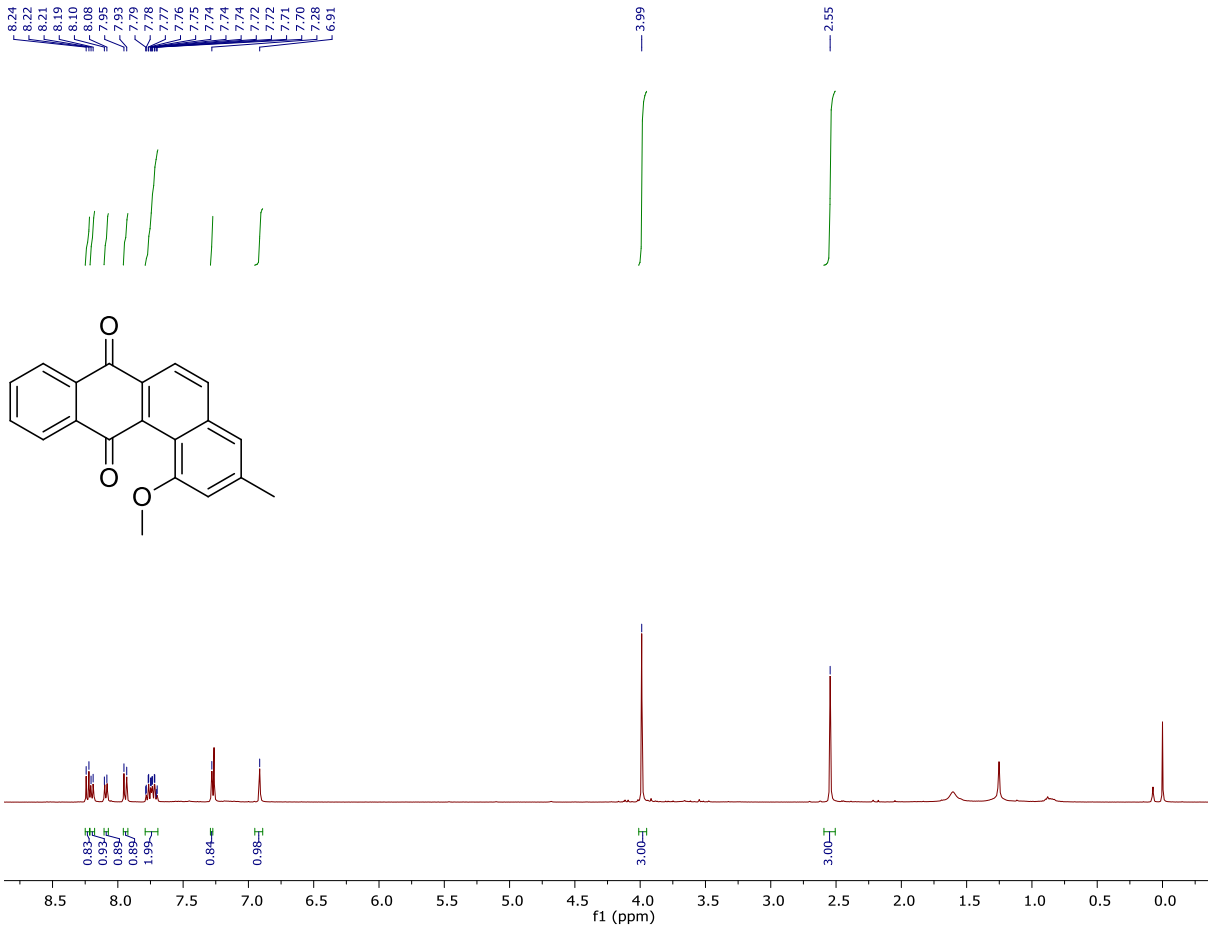

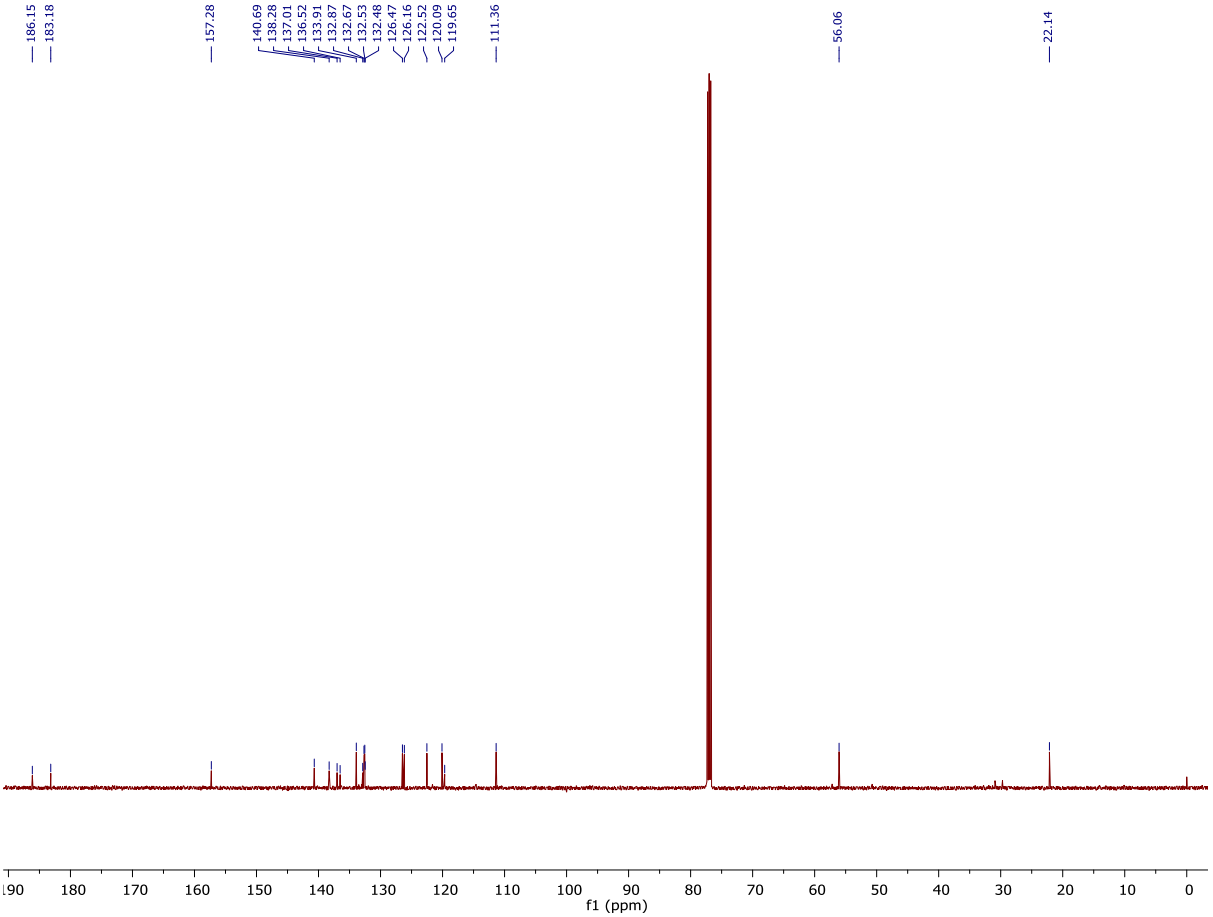

Compound 169

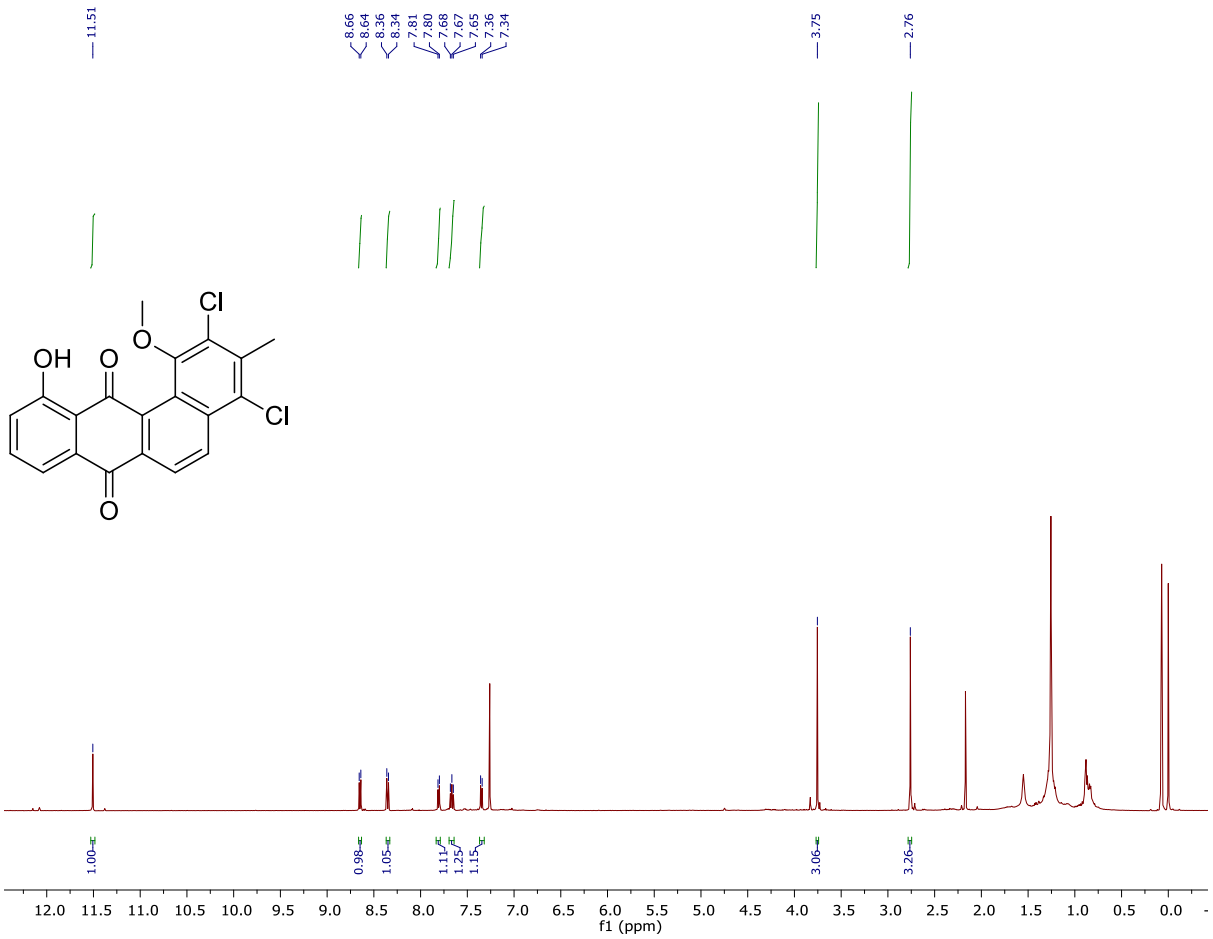

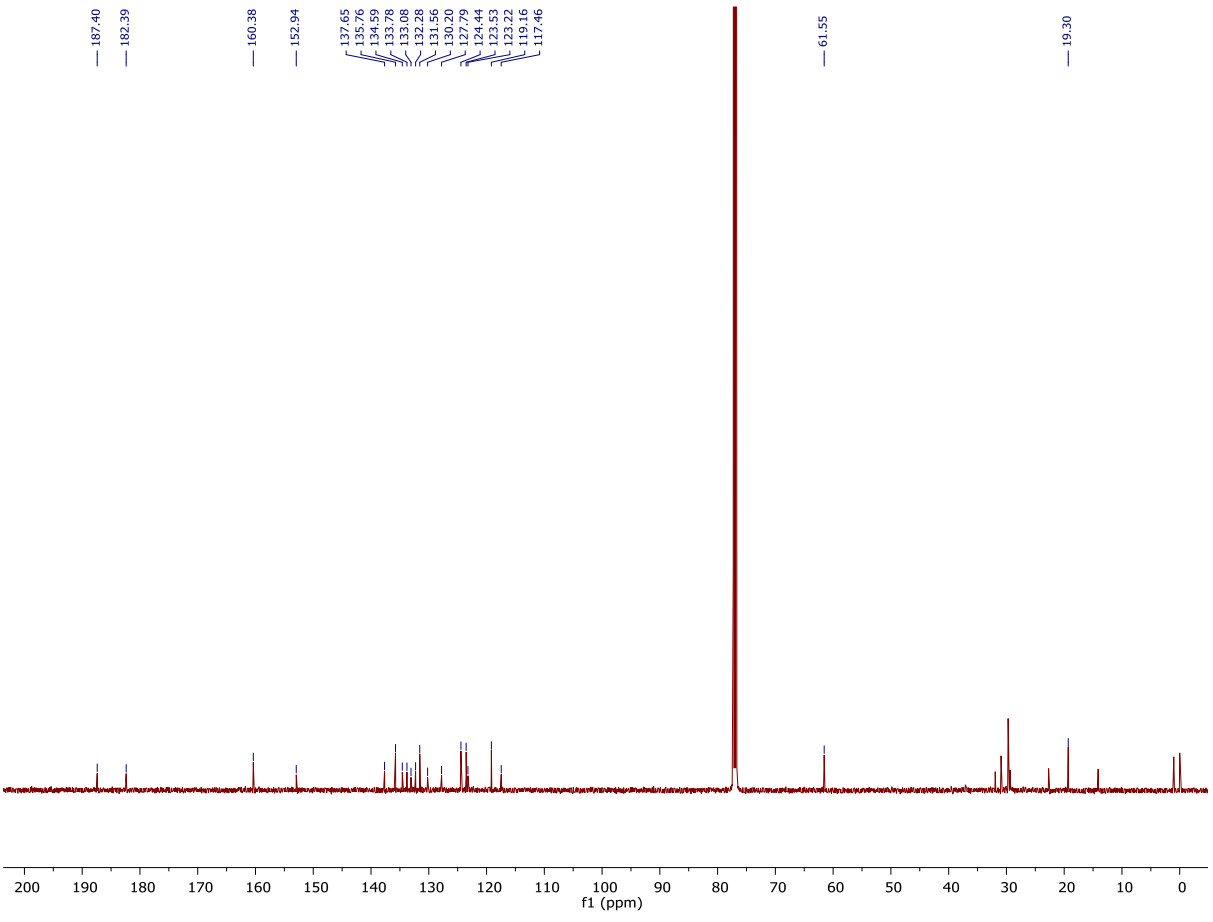

Compound 170

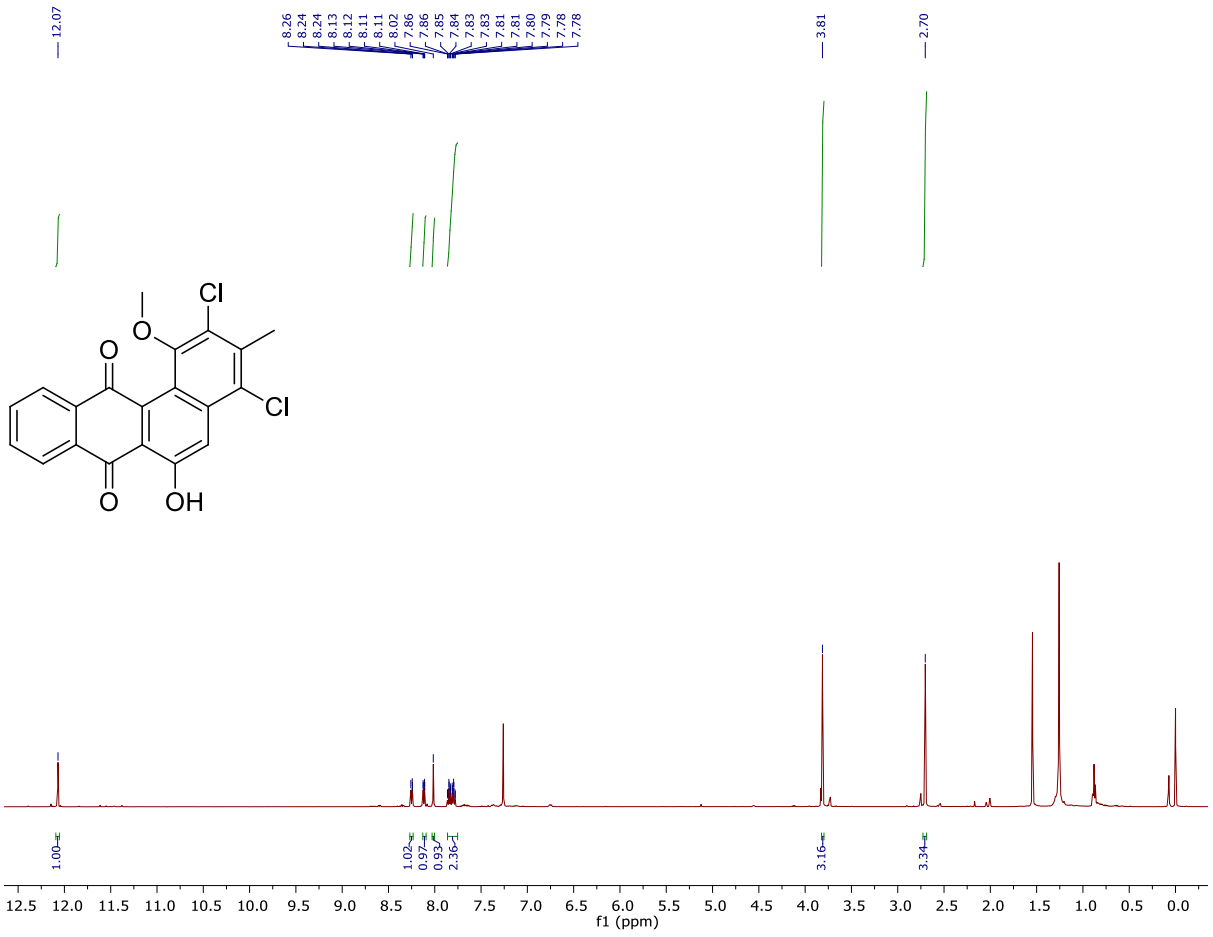

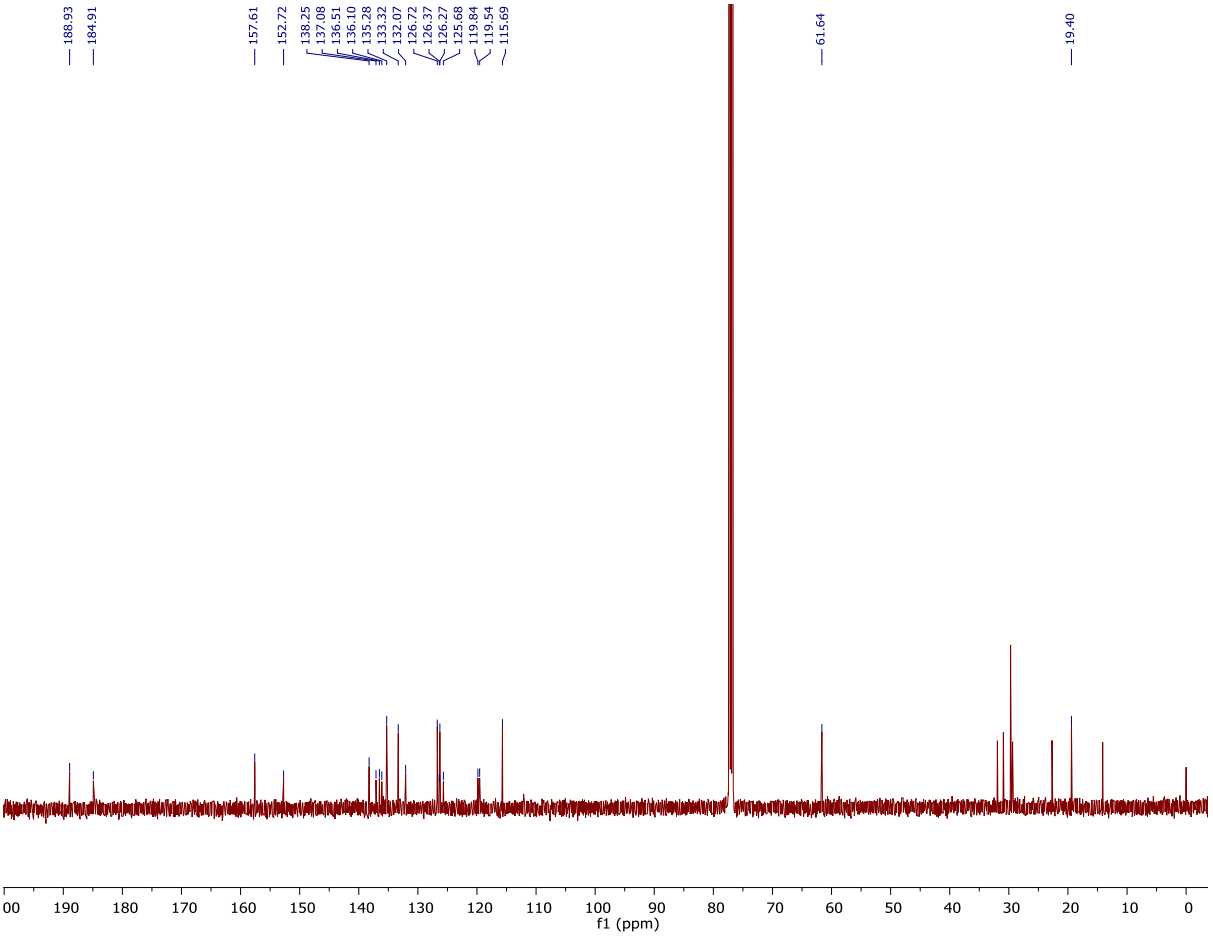

Compound 243

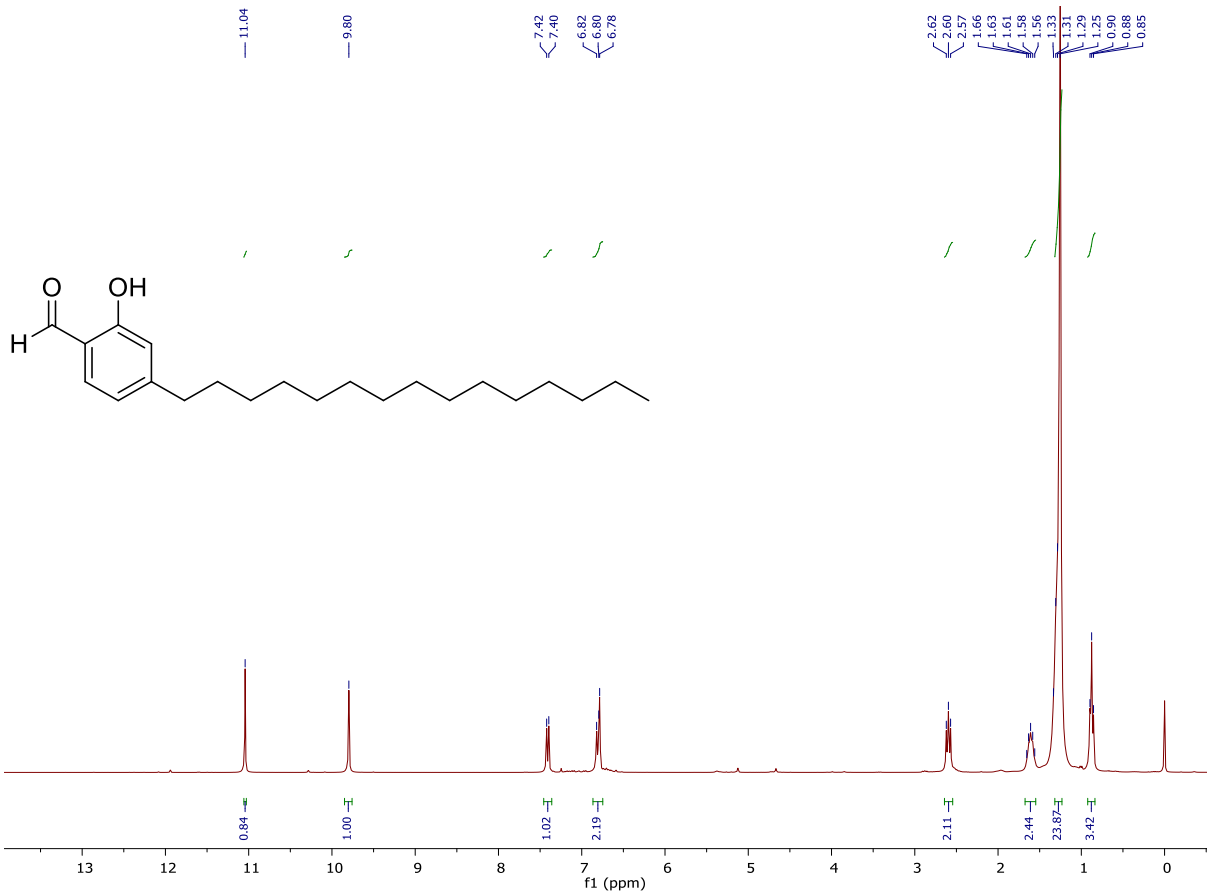

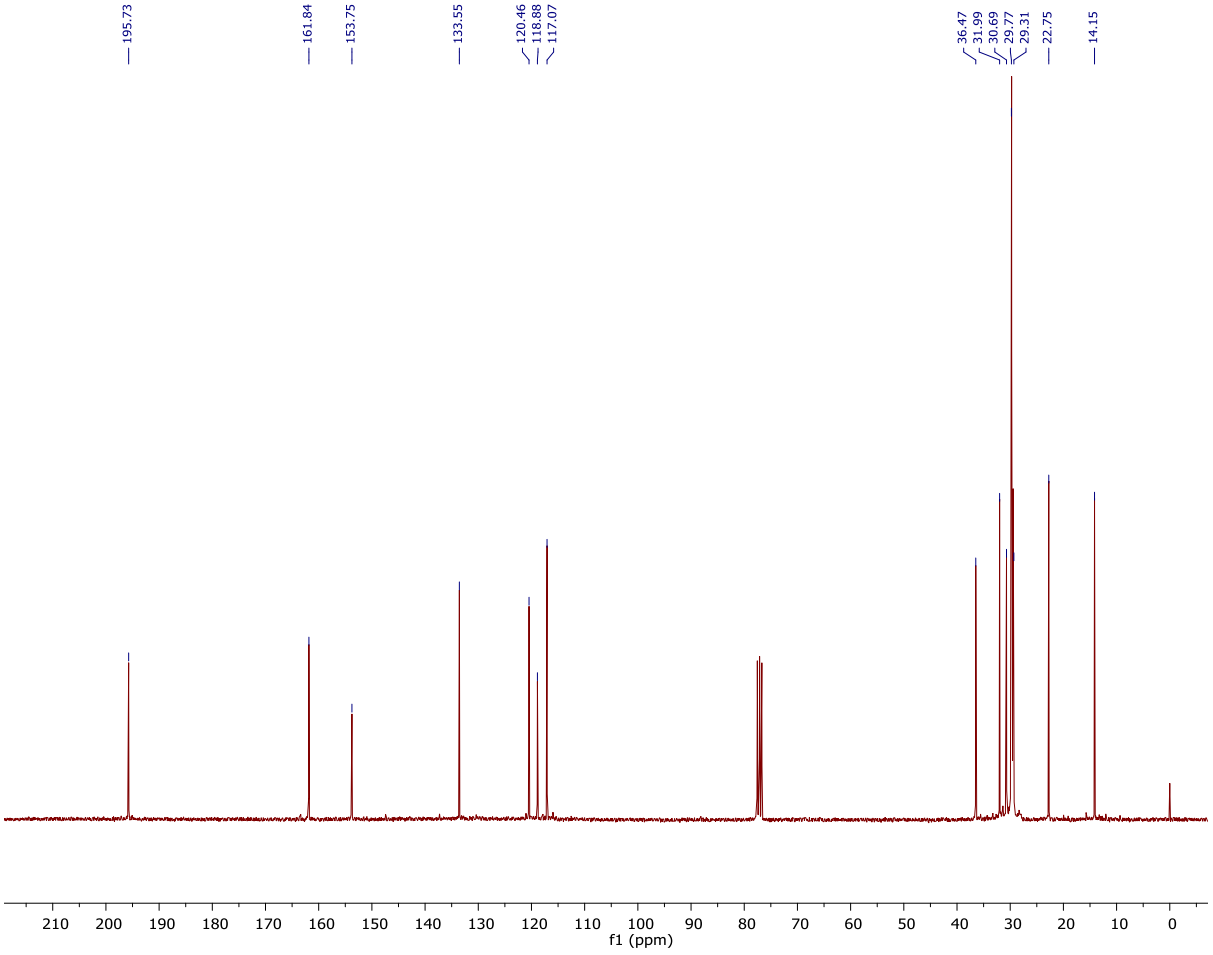

Compound 244a

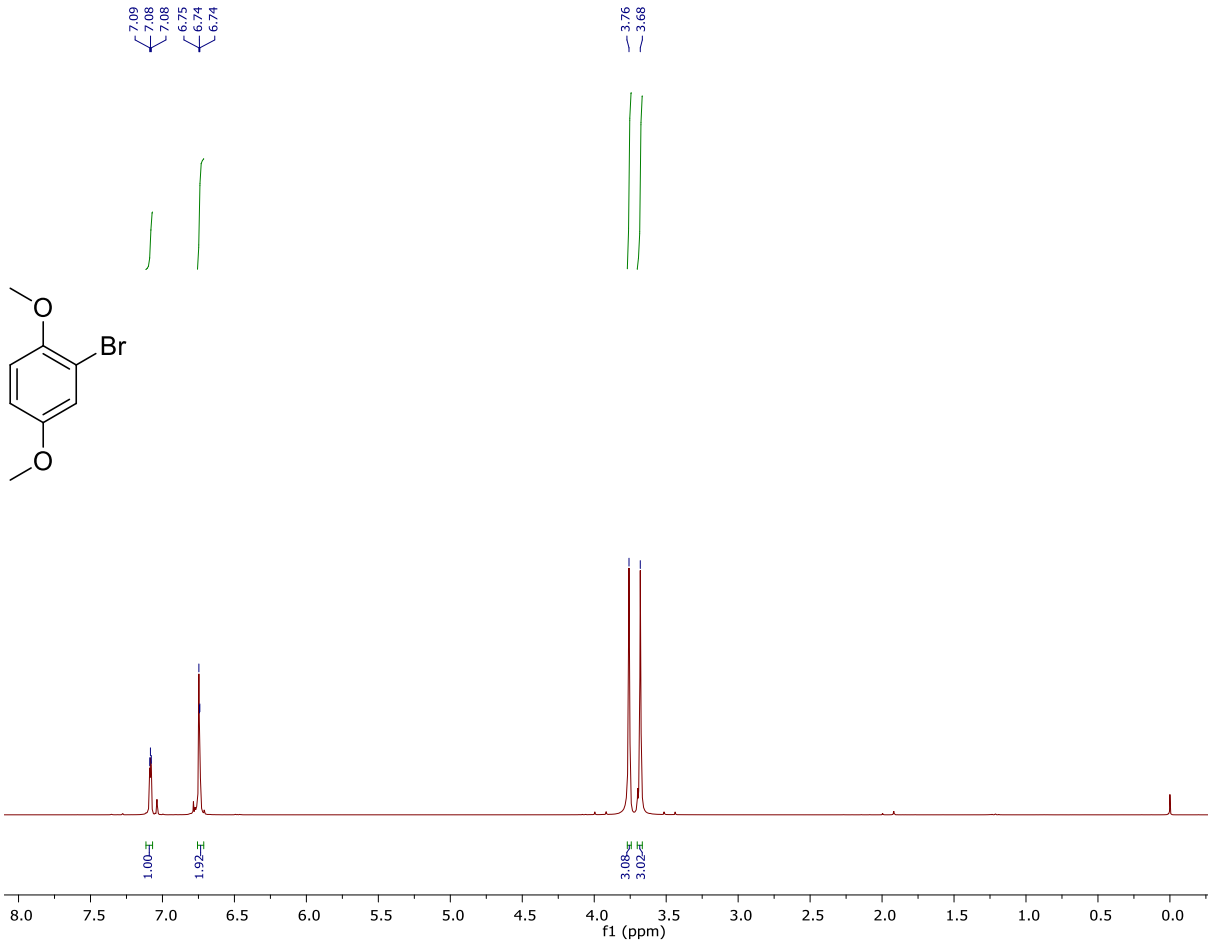

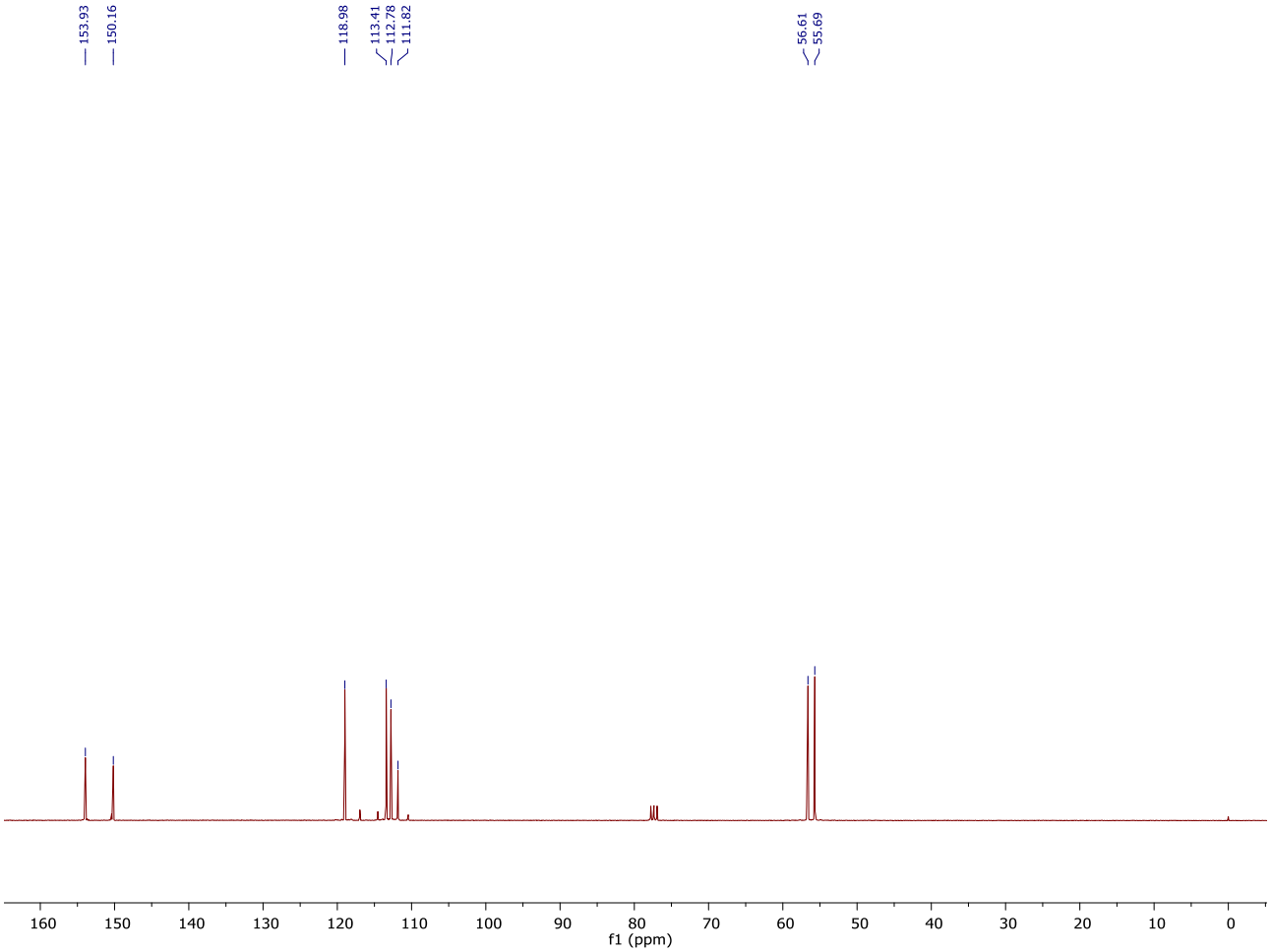

Compound 245a

Compound 249a

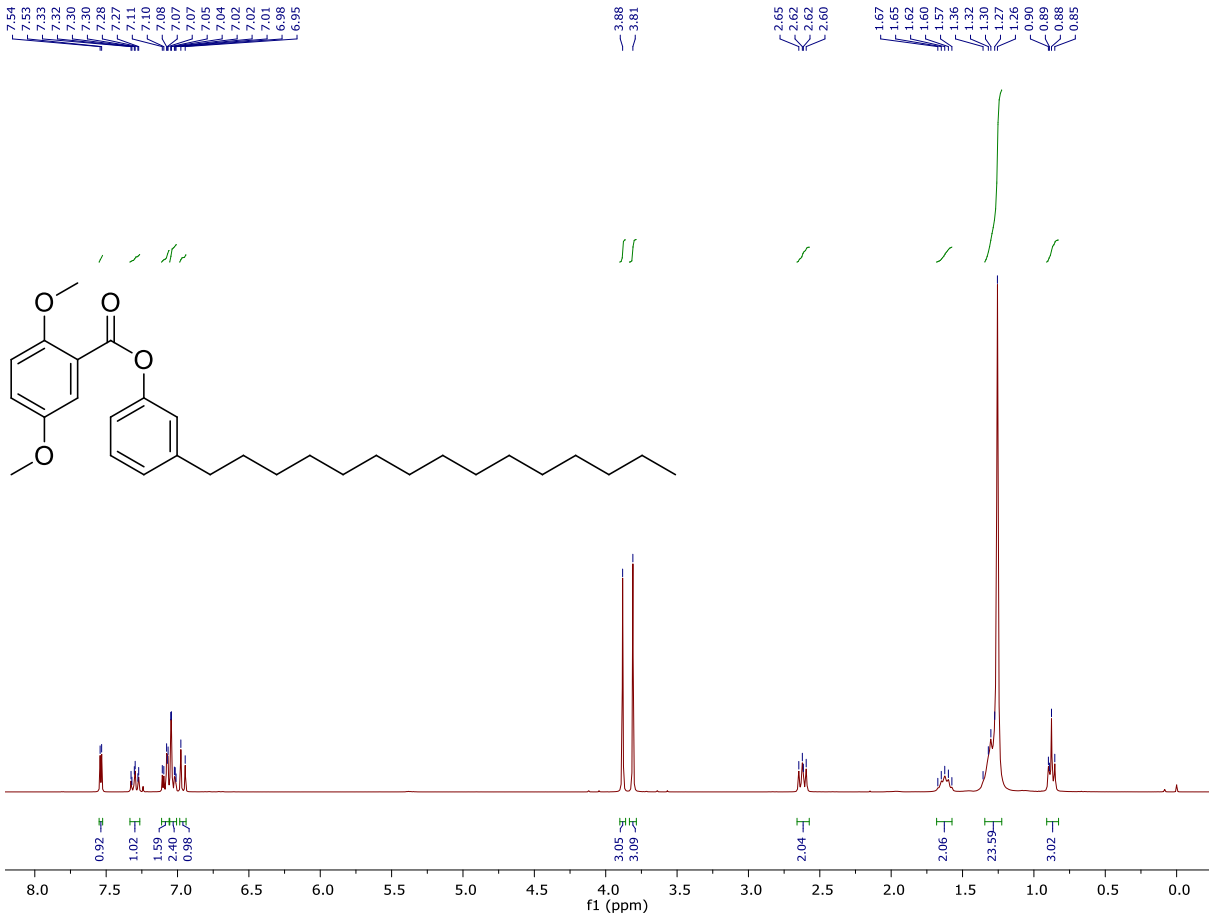

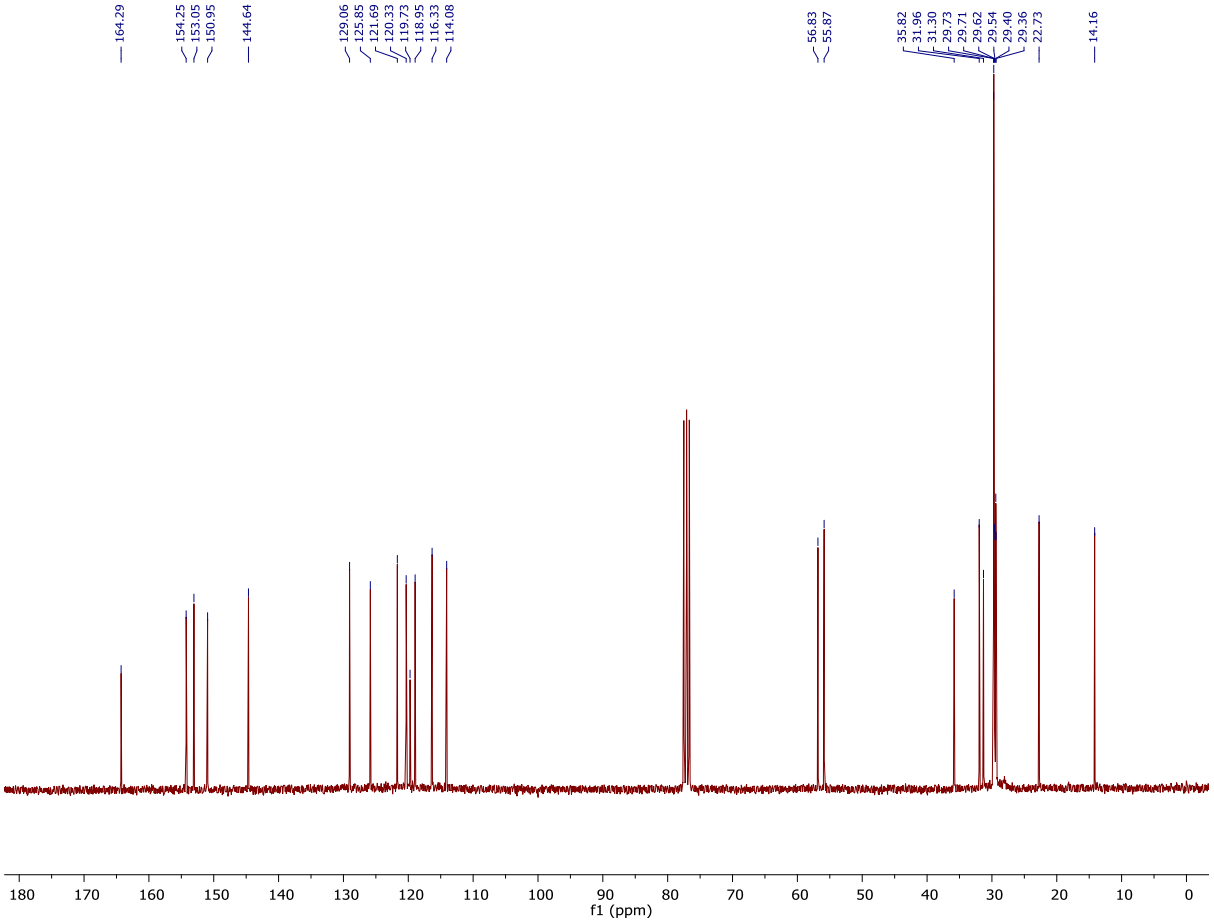

Compound 249b

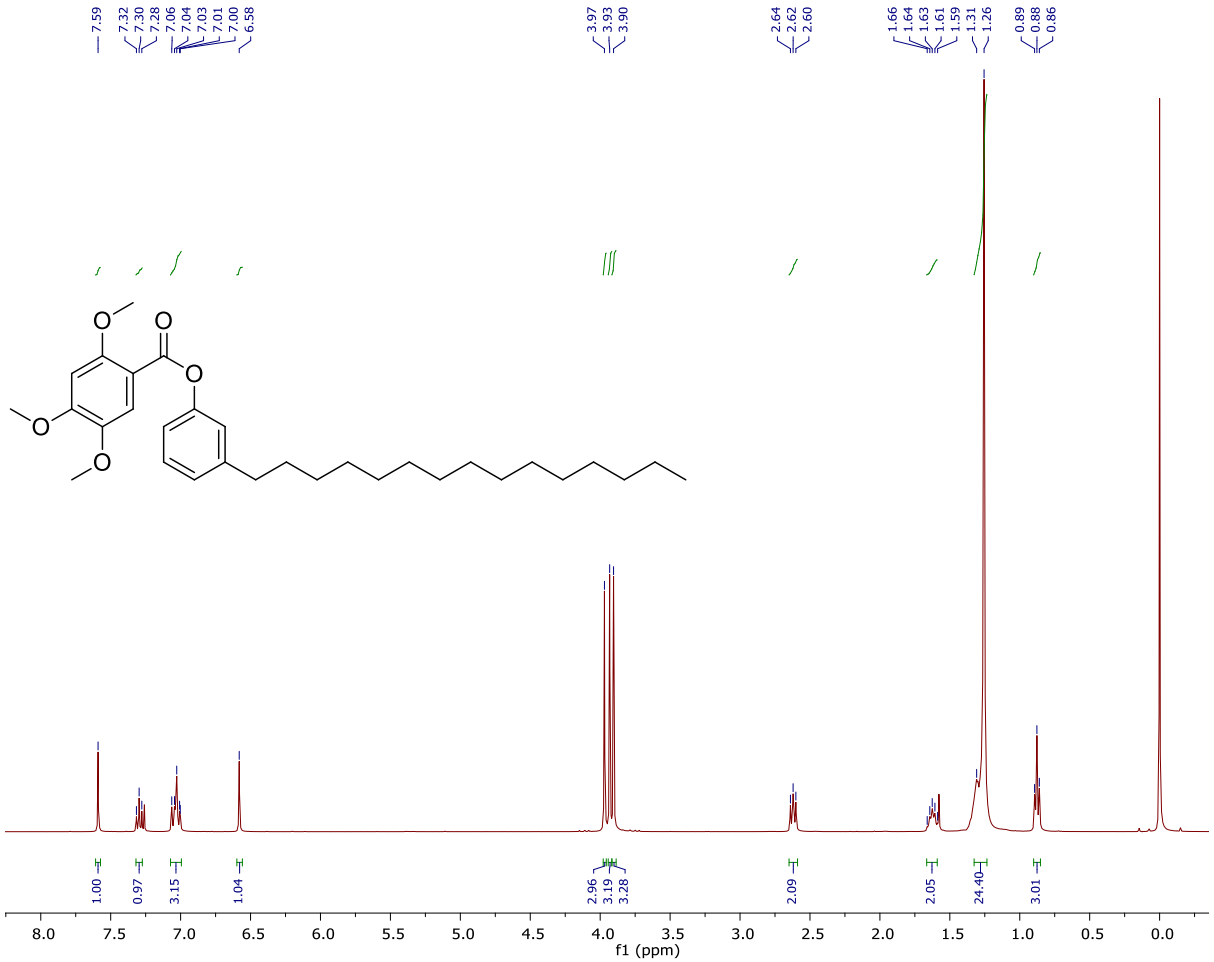

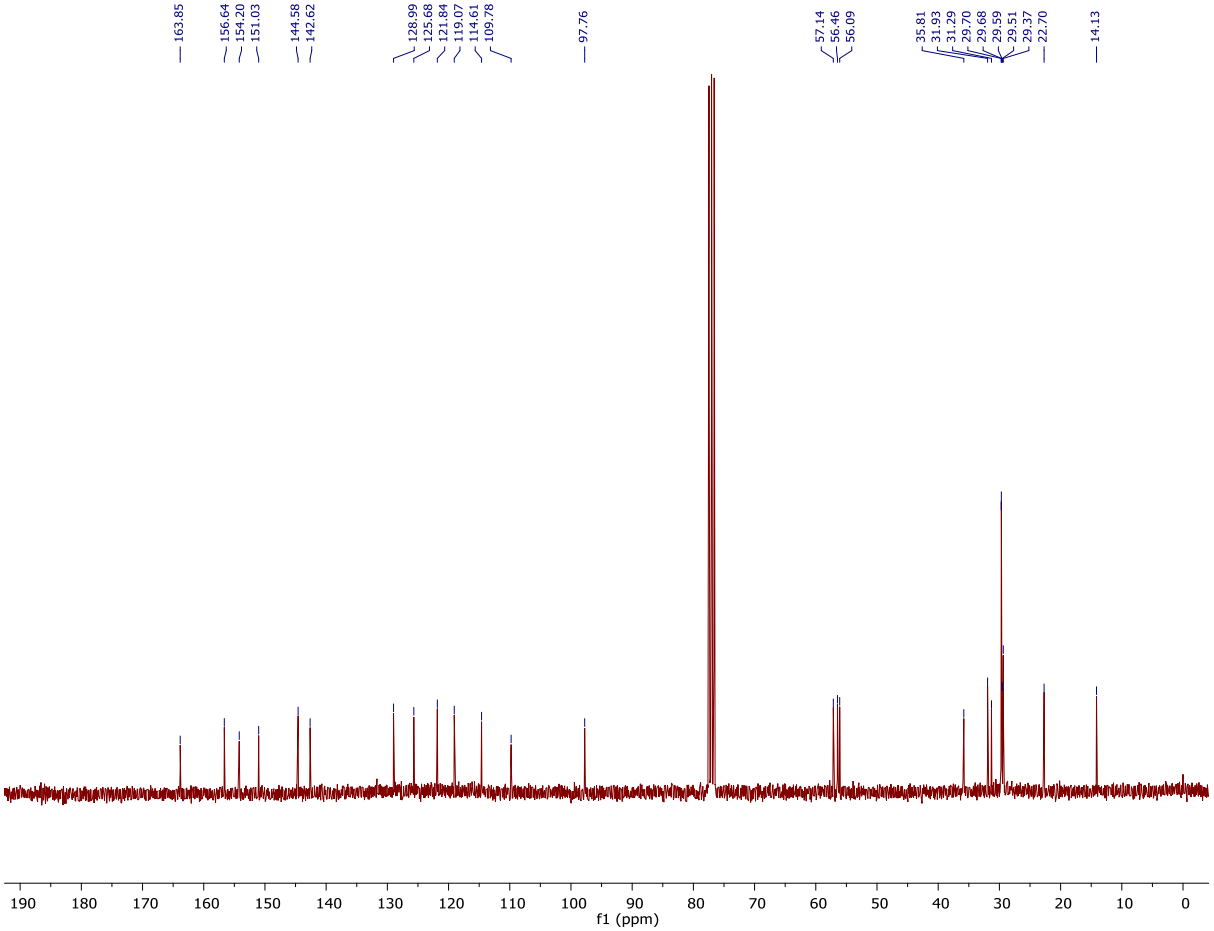

Compound 249c

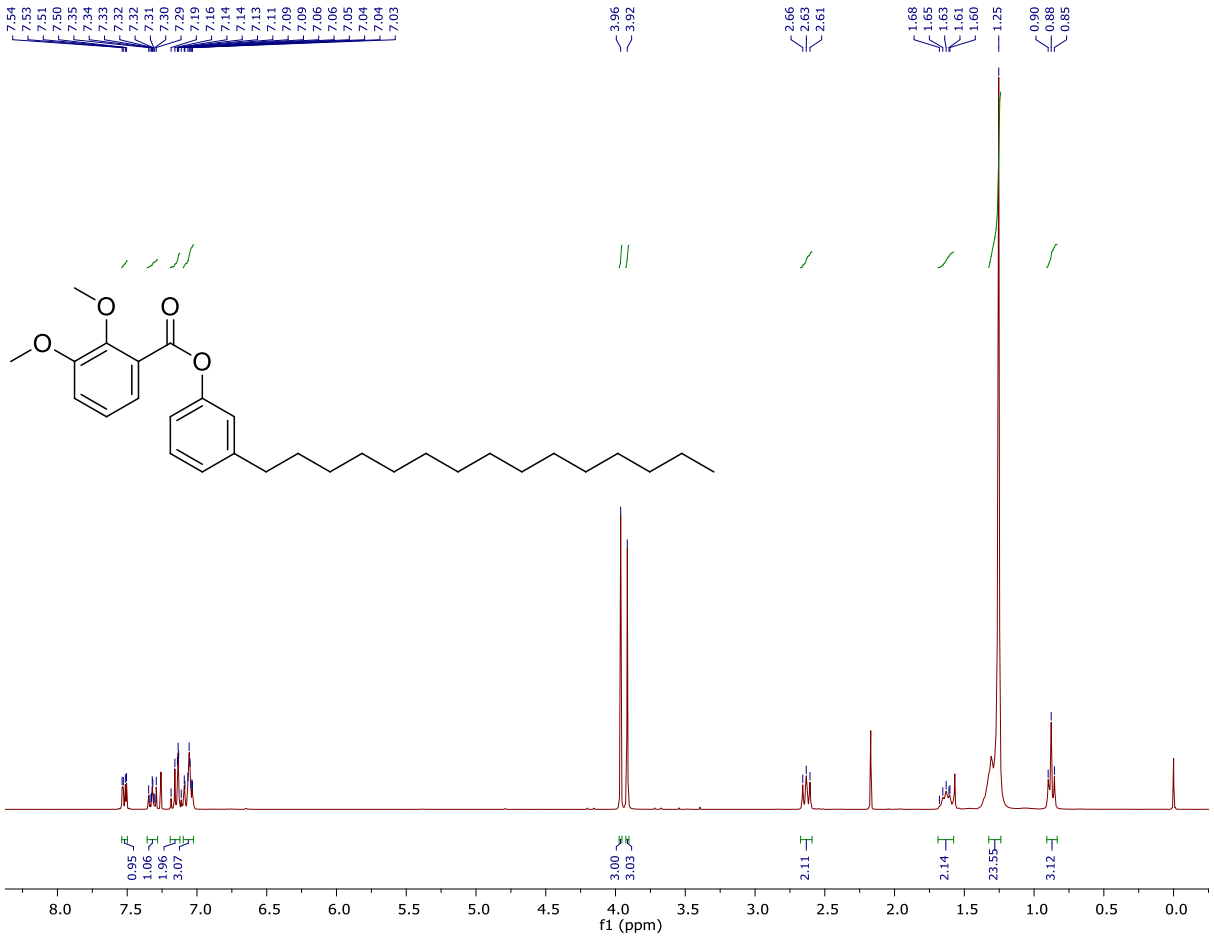

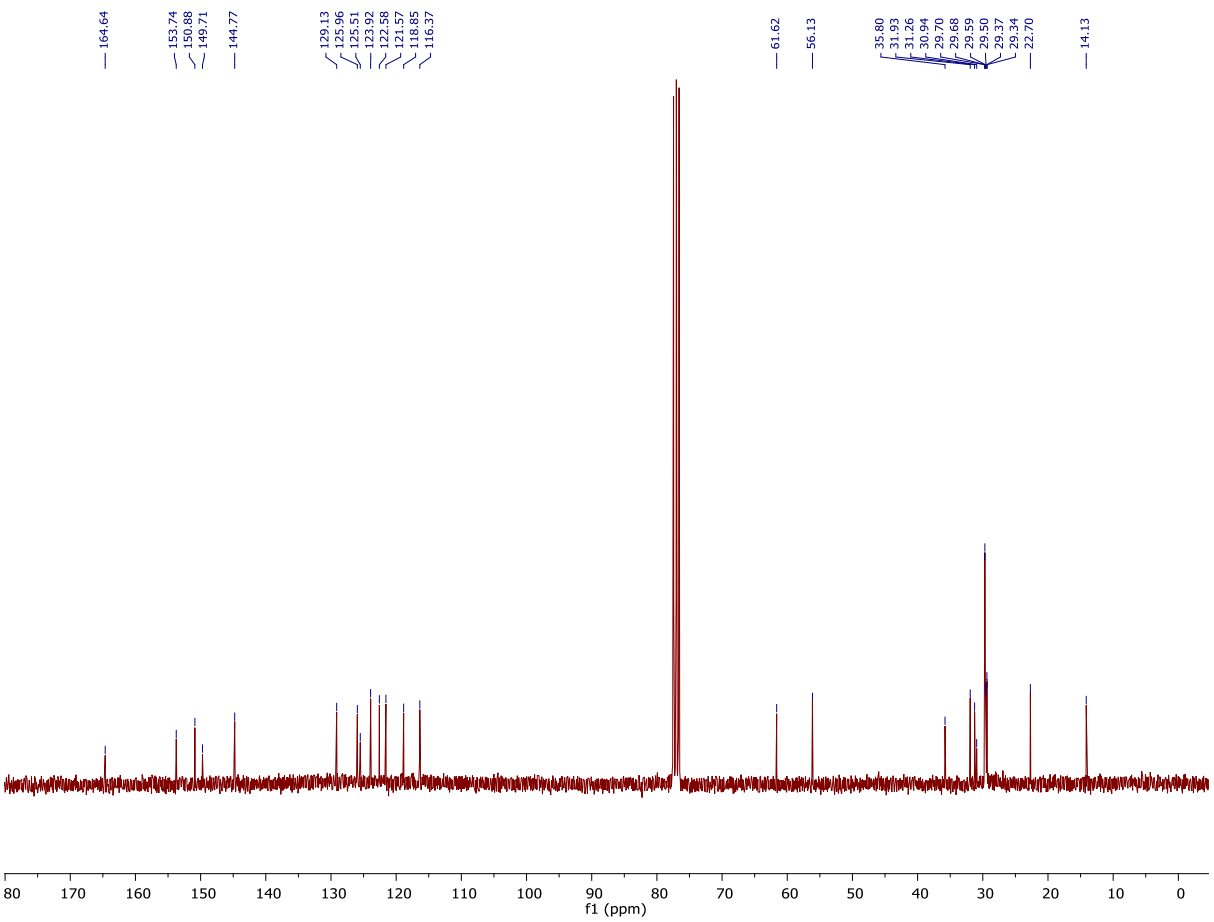

Compound 241a

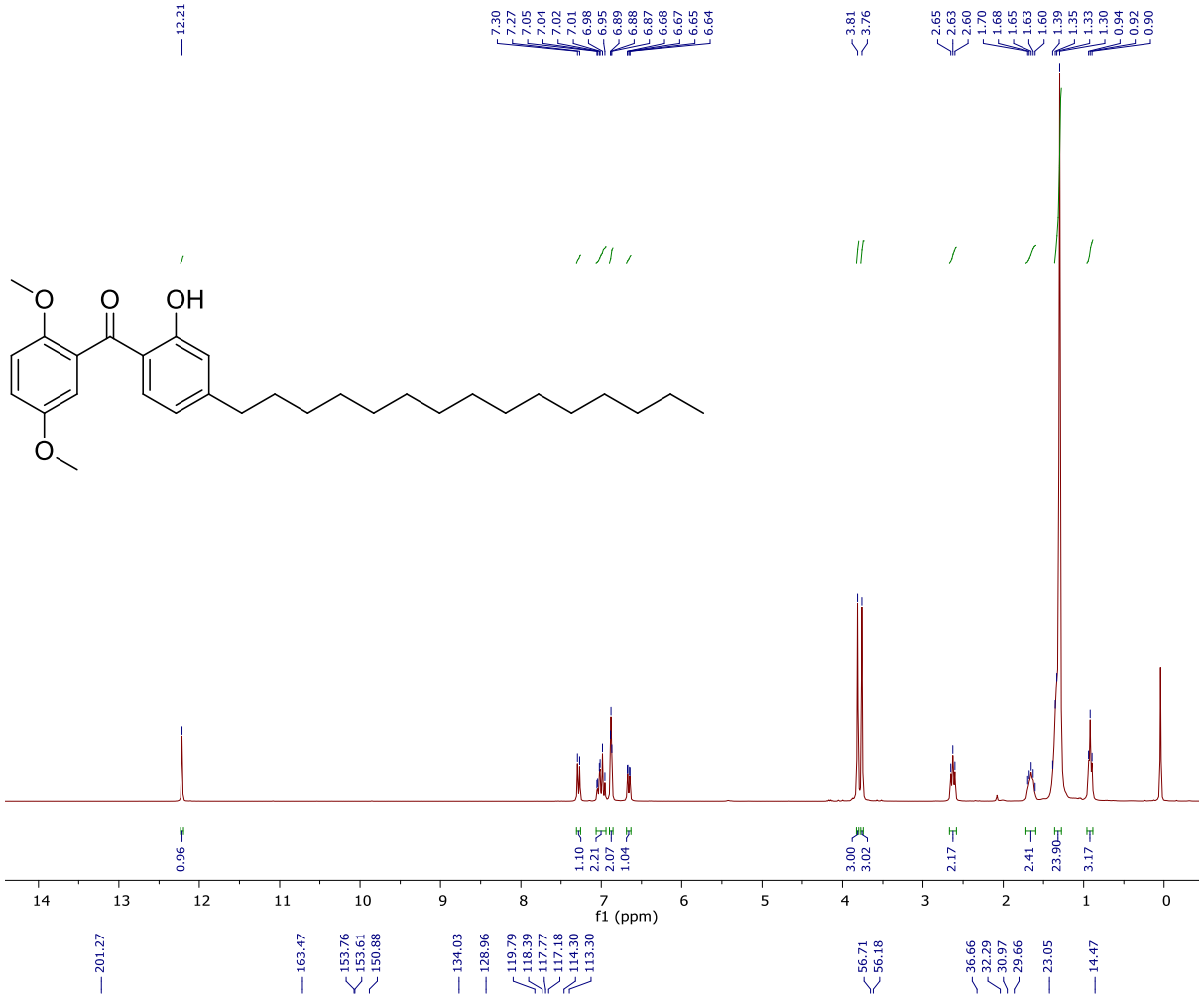

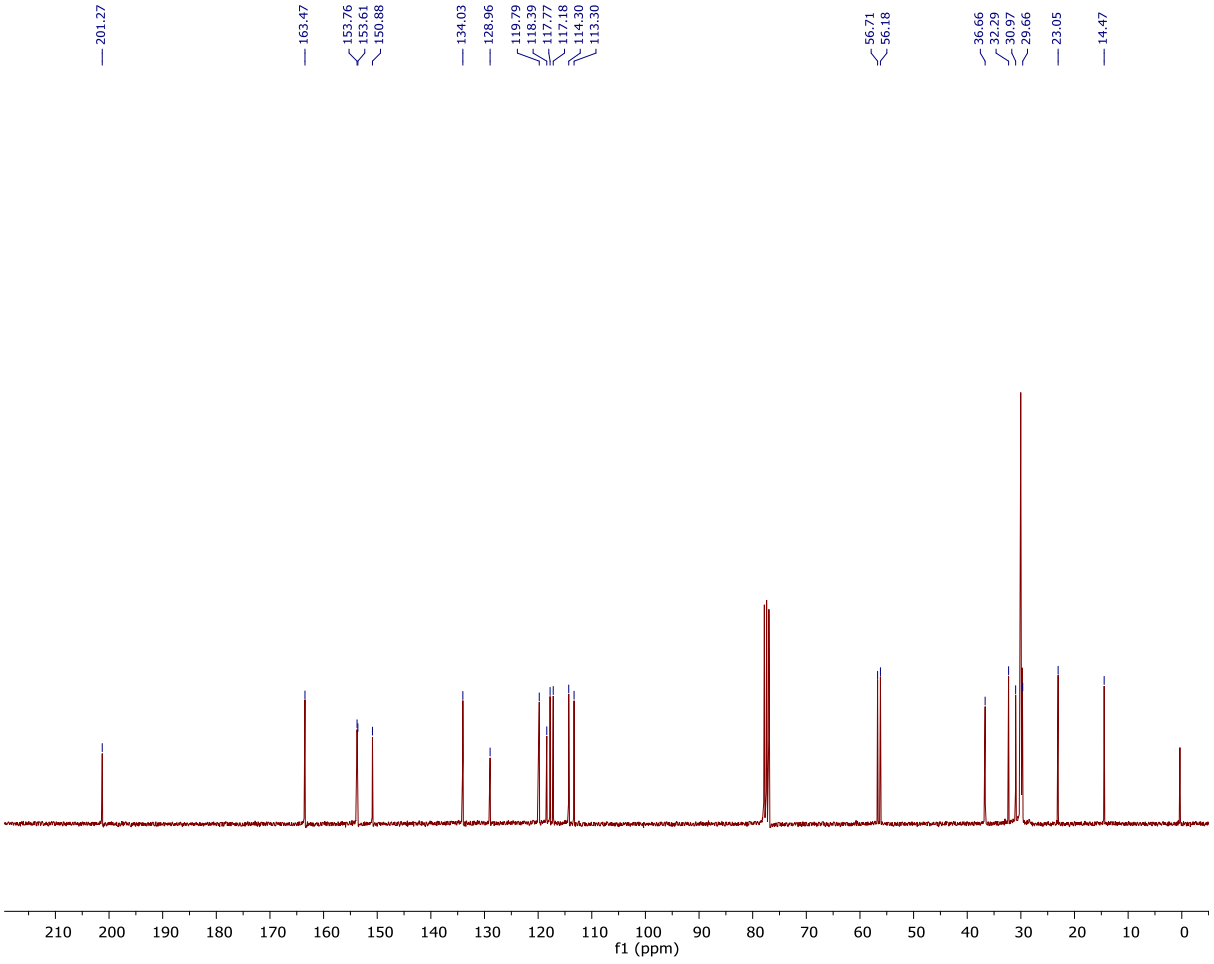

Compound 241b

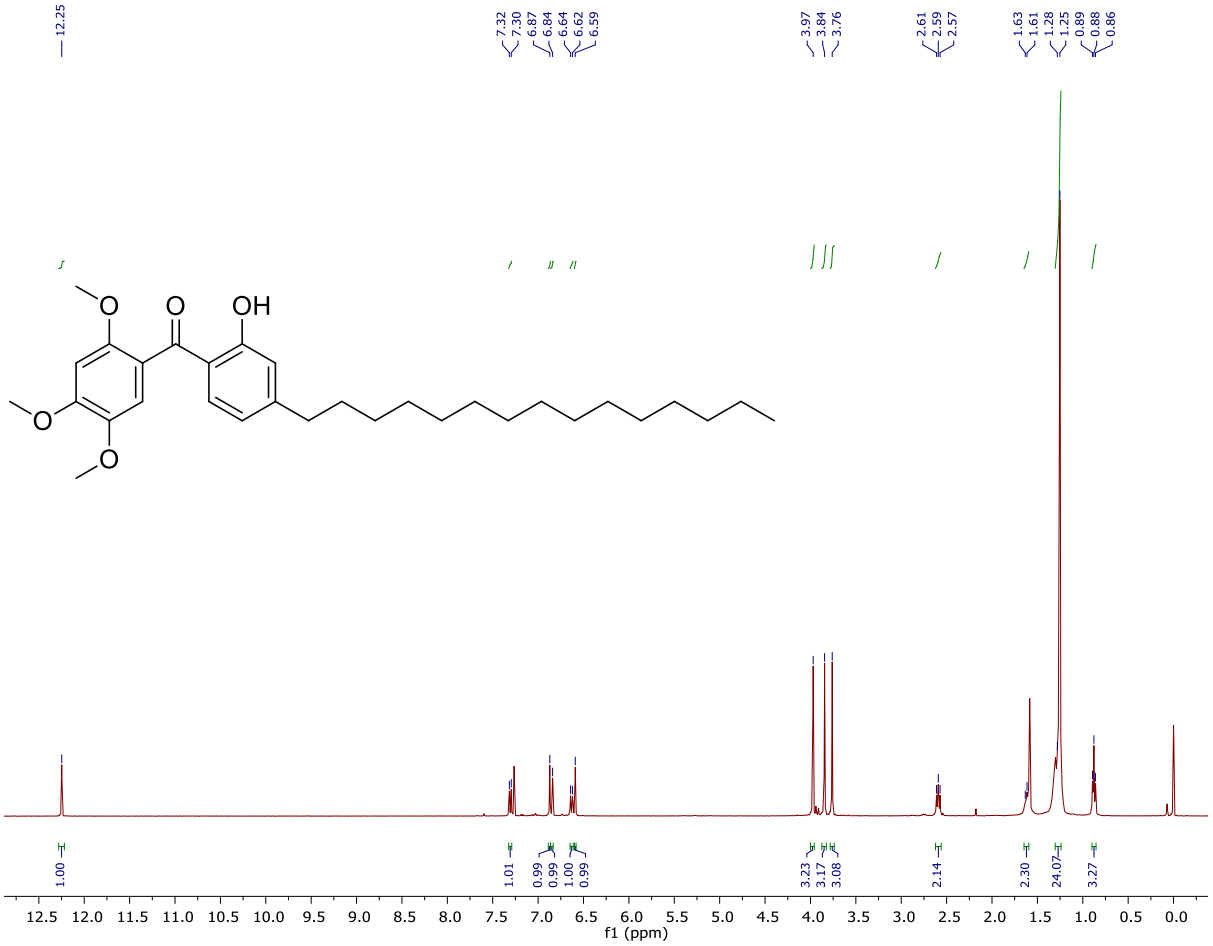

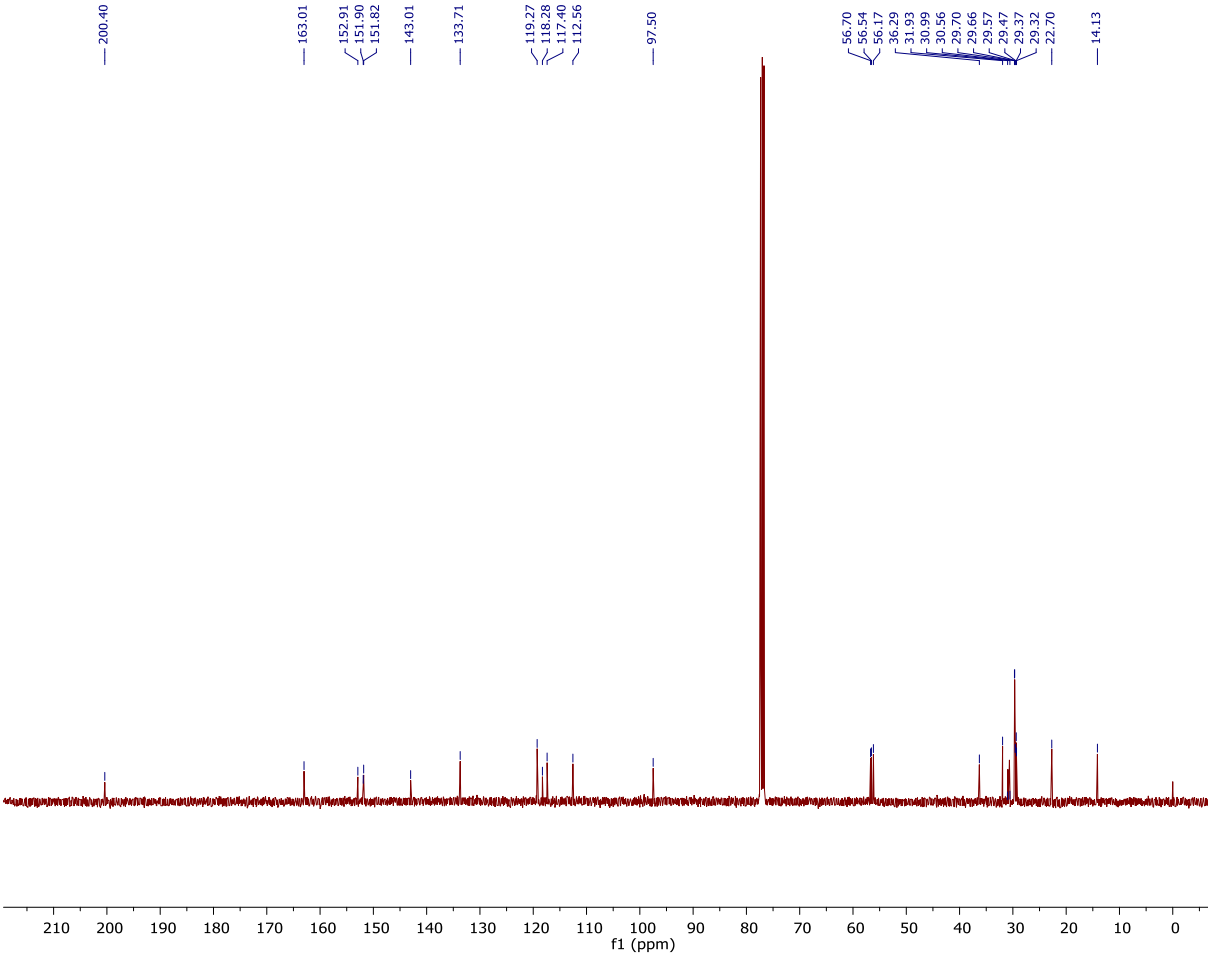

Compound 241c

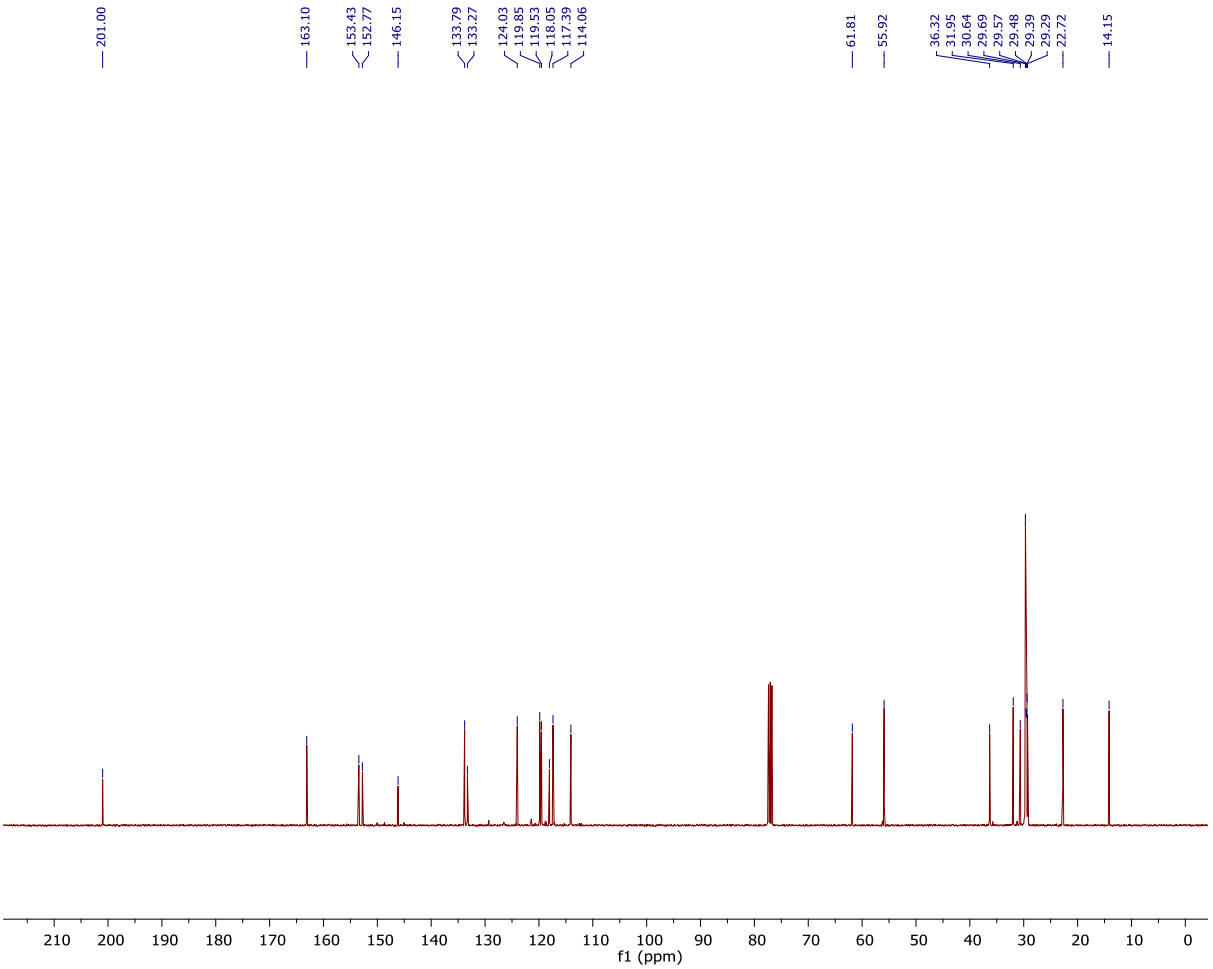

Compound 240a

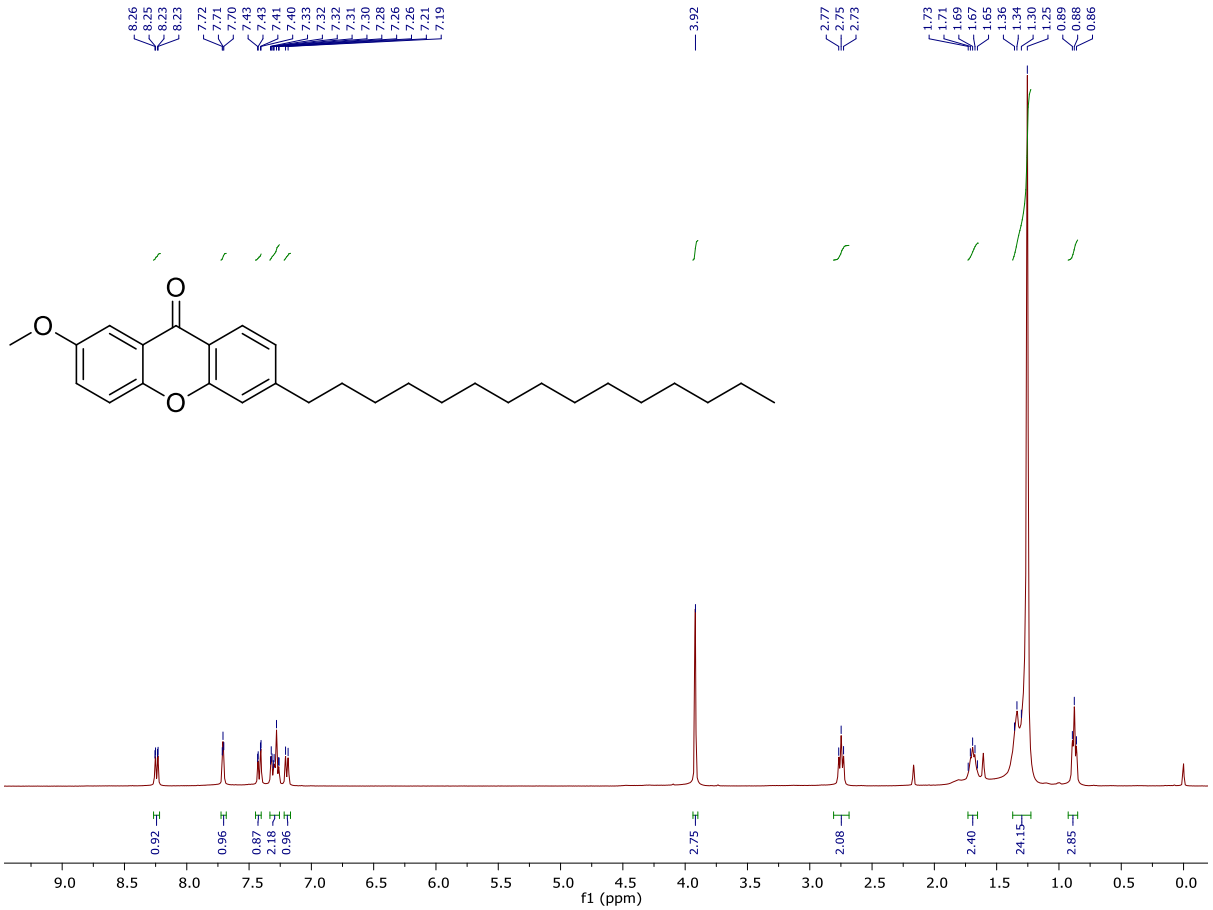

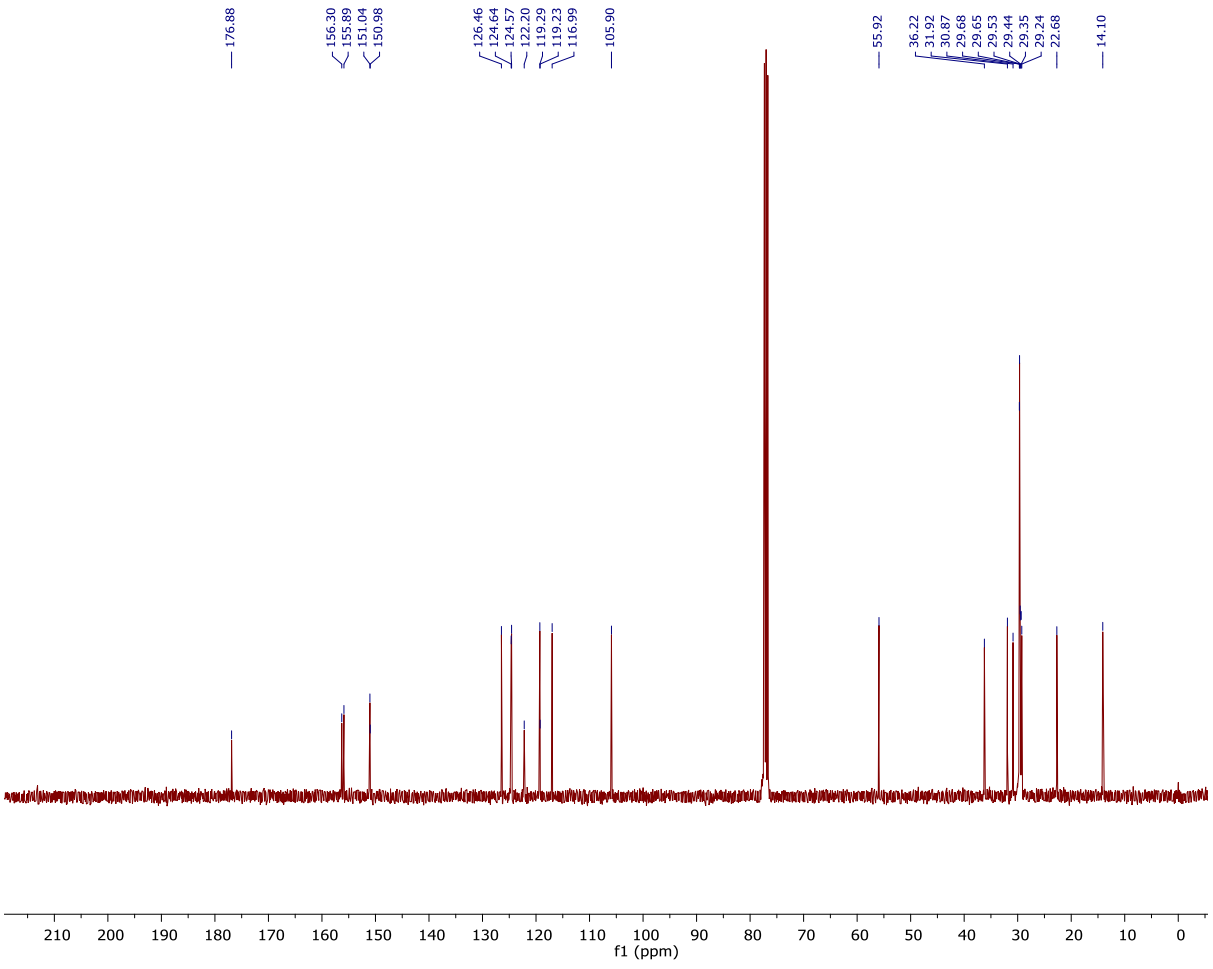

Compound 240b

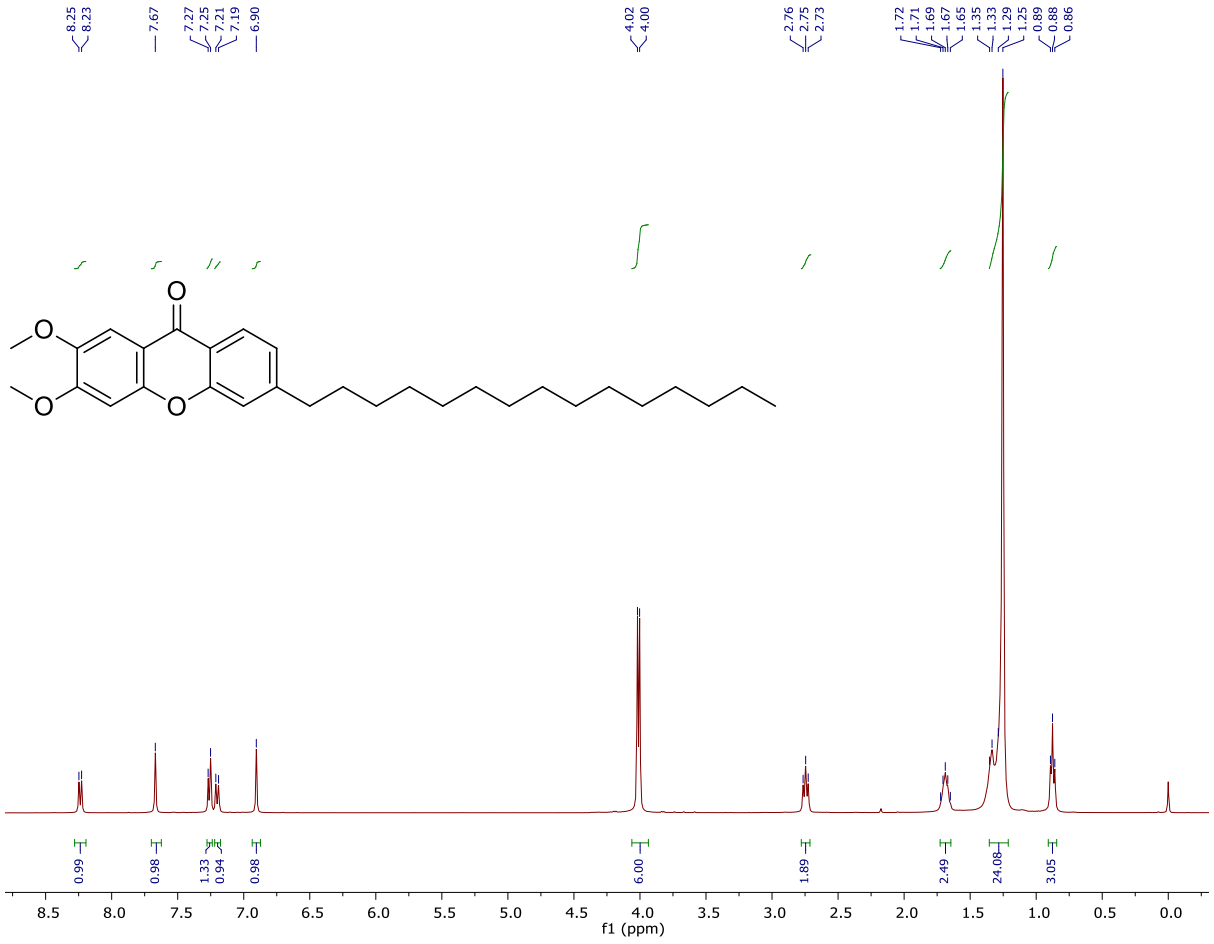

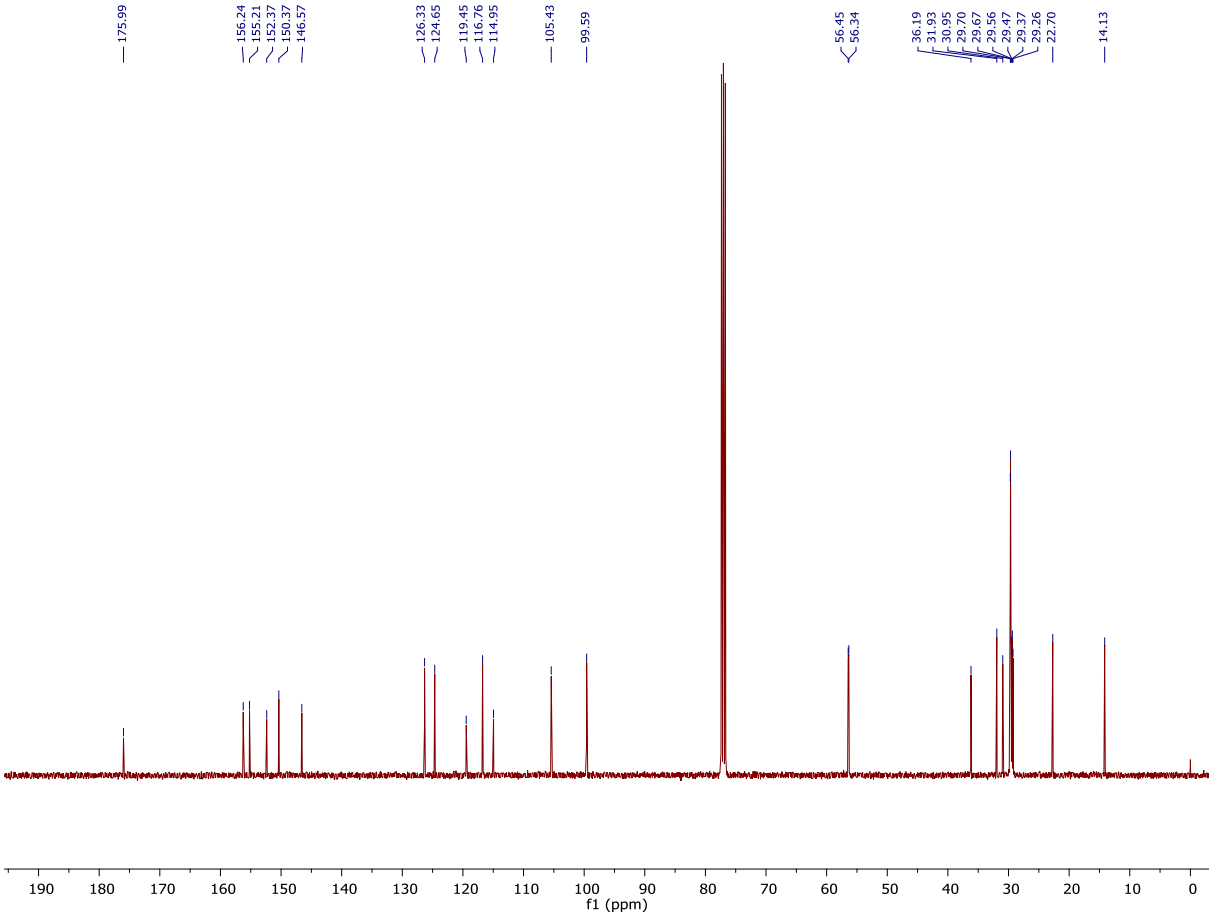

Compound 240c

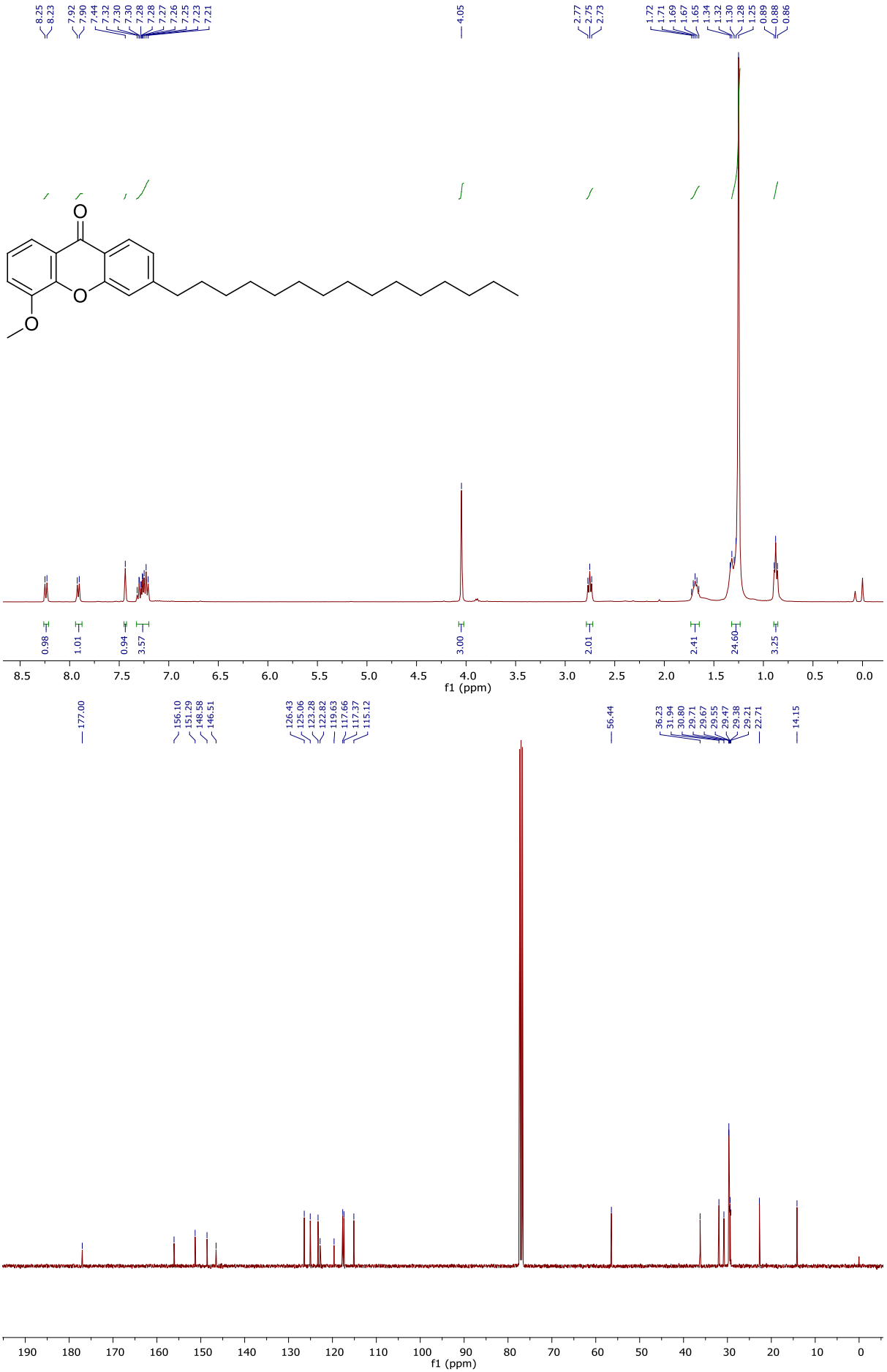

Compound 242a

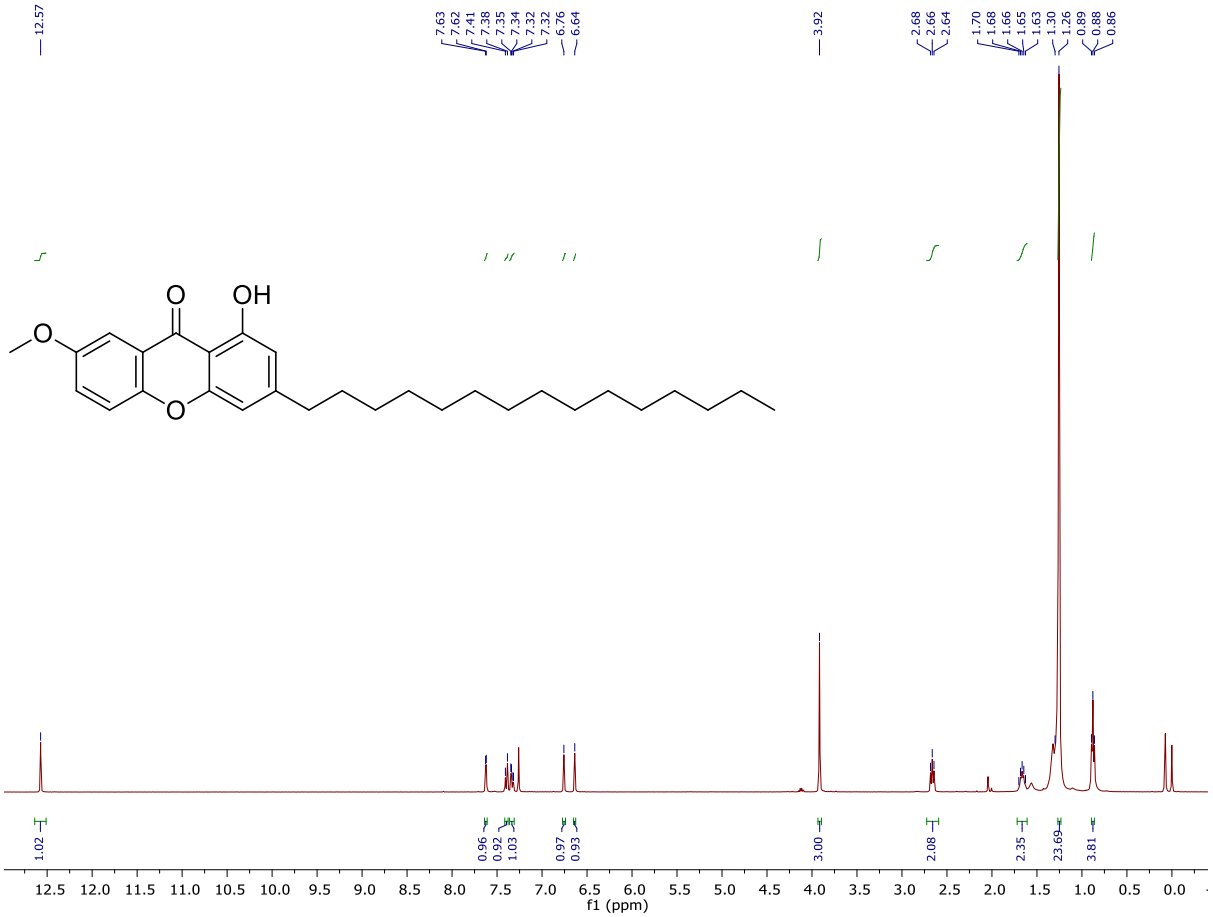

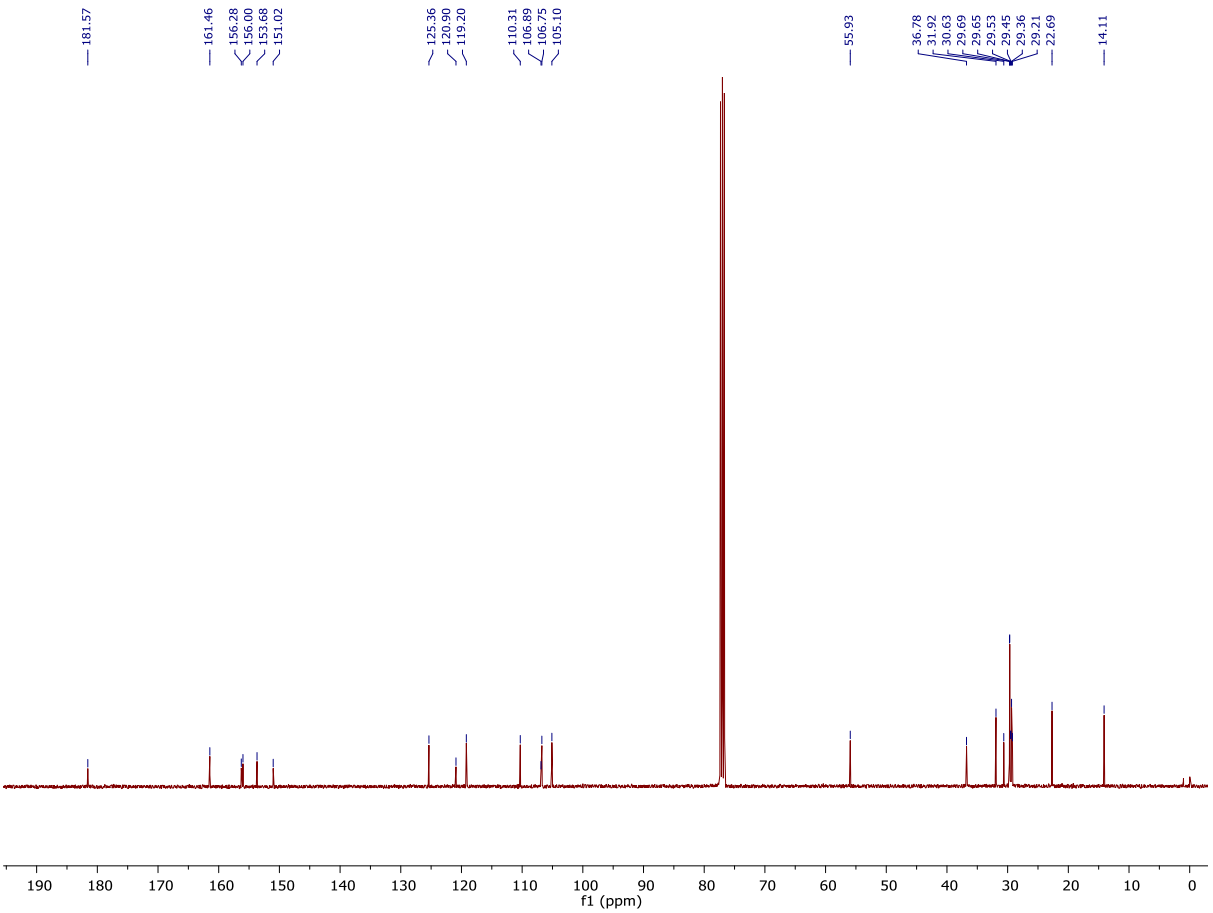

Compound 242b

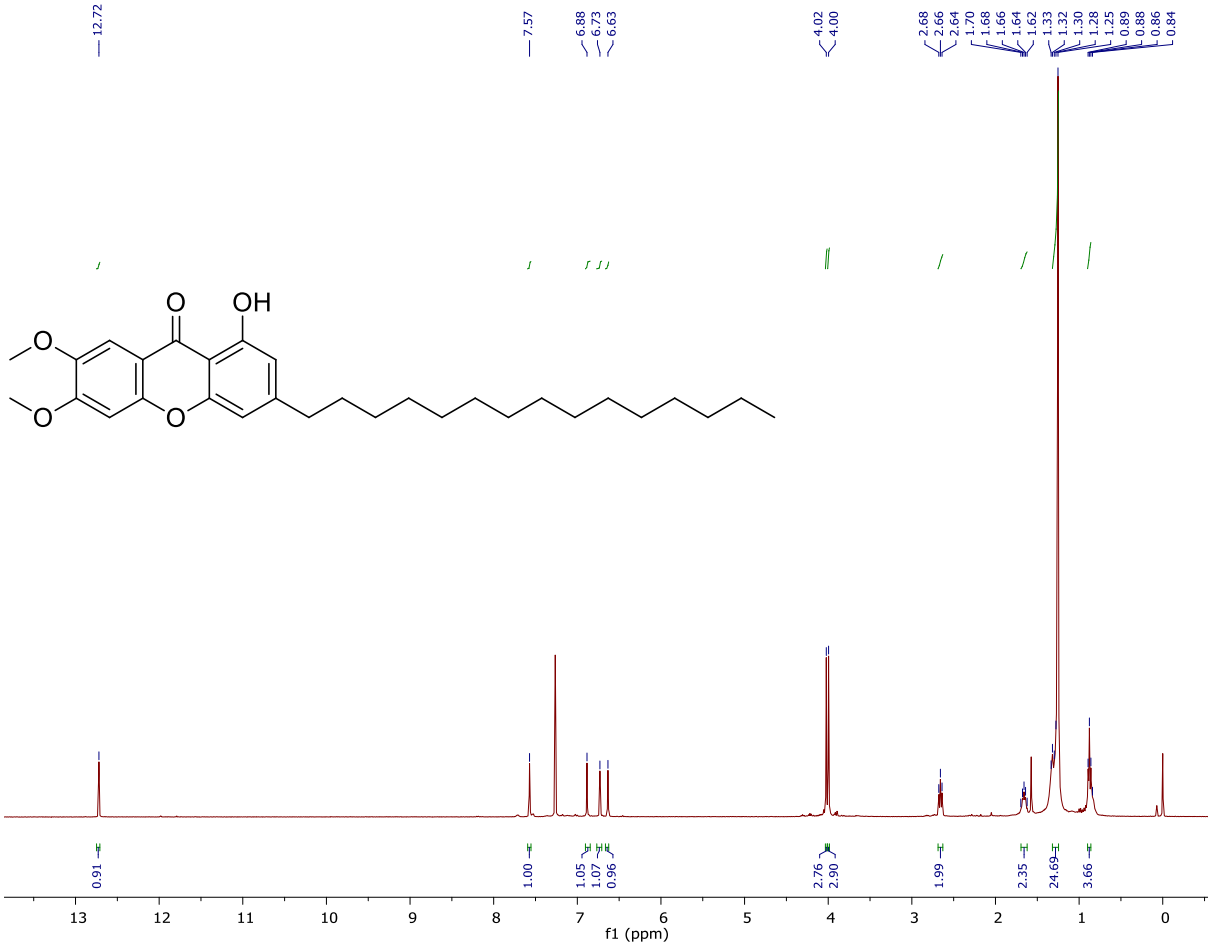

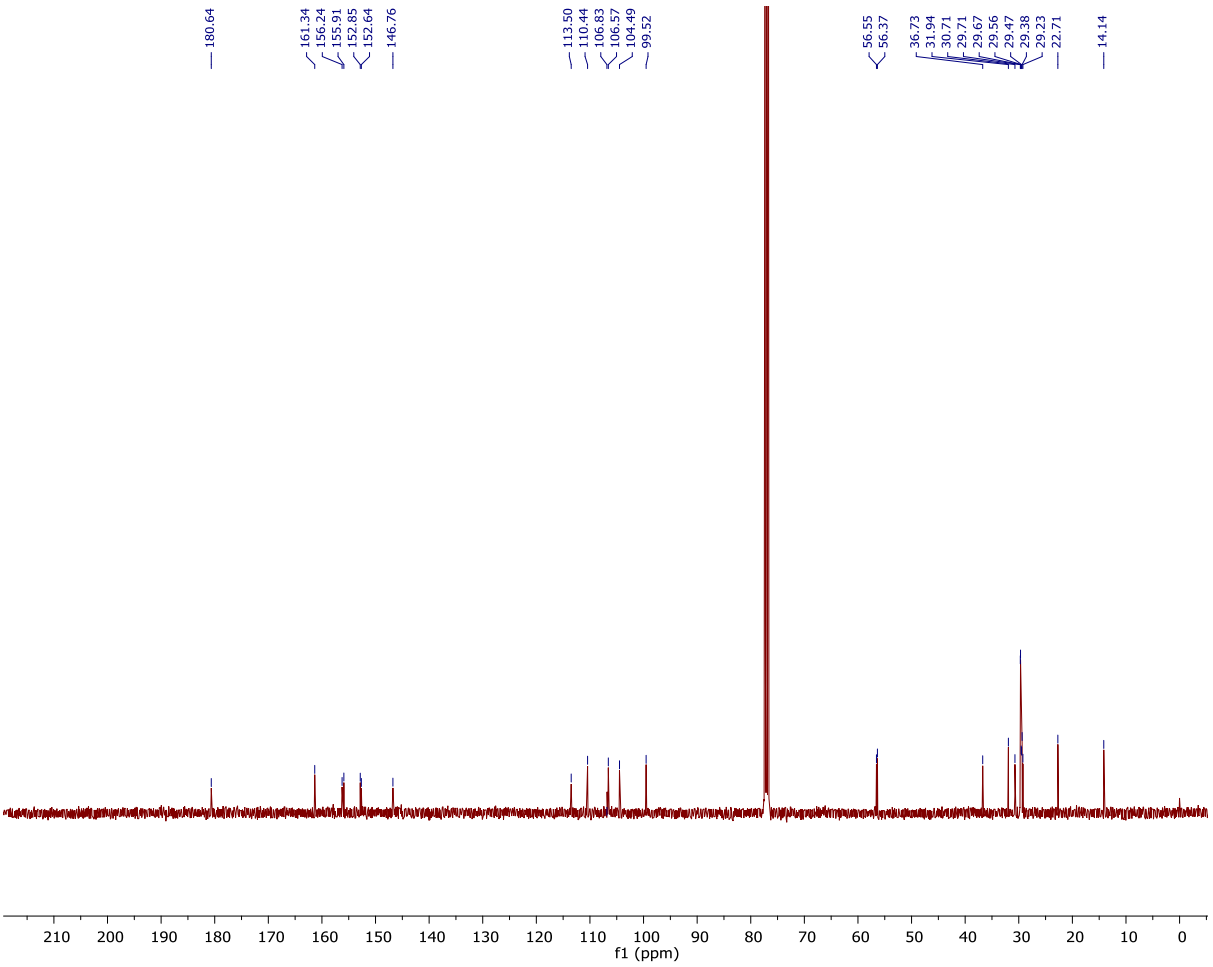

Compound 242c

Crystal structure for compound 142

b"\n \n 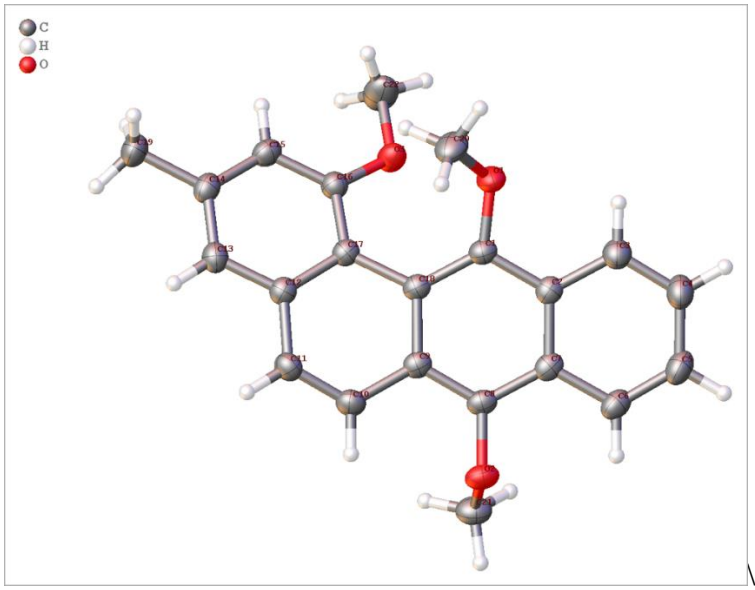

\n "

Table 1 Crystal data and structure refinement for 21mb_Fatema_Jagot1_0f_sq.

Identification code	21mb_Fatema_Jagot1_0f_sq
Empirical formula	$C_{22}H_{20}O_3$
Formula weight	332.38
Temperature/K	173.00
Crystal system	orthorhombic
Space group	Pccn
a/Å	11.4925(6)
b/Å	36.9186(17)
c/Å	8.6409(4)
α/°	90
β/°	90
γ/°	90
Volume/Å^3	3666.2(3)
Z	8
ρ_{calc}g/cm^3	1.204
μ/mm^{-1}	0.079
F(000)	1408.0

Crystal size/mm^3	0.314 × 0.219 × 0.052
Radiation	MoKα (λ = 0.71073)
2Θ range for data collection/°	3.712 to 56.464
Index ranges	-15 ≤ h ≤ 15, -49 ≤ k ≤ 49, -11 ≤ l ≤ 11
Reflections collected	80805
Independent reflections	4527 [R_{int} = 0.0591, R_{sigma} = 0.0307]
Data/restraints/parameters	4527/0/230
Goodness-of-fit on F^2	1.112
Final R indexes [I>=2σ (I)]	R_1 = 0.0573, wR_2 = 0.1258
Final R indexes [all data]	R_1 = 0.0702, wR_2 = 0.1316
Largest diff. peak/hole / e Å^{-3}	0.26/-0.19

Table 2 Fractional Atomic Coordinates (×10^4) and Equivalent Isotropic Displacement Parameters (Å^2×10^3) for 21mb_Fatema_Jagot1_0f_sq. U_{eq} is defined as 1/3 of the trace of the orthogonalised U_{IJ} tensor.

Atom	*x*	*y*	*z*	U(eq)
O1	5130.3(11)	6741.2(3)	3183.3(13)	34.5(3)
O2	3126.3(10)	5924.9(3)	7836.7(13)	33.0(3)
O3	6985.2(10)	6346.9(3)	2876.3(14)	34.3(3)
C1	4767.5(14)	6514.7(4)	4341.8(18)	26.1(3)
C2	4289.5(14)	6698.8(4)	5639.2(18)	26.2(3)
C3	4294.4(16)	7083.4(4)	5746(2)	33.6(4)
C4	3843.7(17)	7253.2(5)	7014(2)	39.2(4)
C5	3347.9(17)	7052.7(5)	8226(2)	38.3(4)
C6	3309.7(15)	6684.9(5)	8162.1(19)	32.4(4)
C7	3784.8(13)	6496.5(4)	6869.6(18)	26.8(3)
C8	3725.8(13)	6117.9(4)	6717.7(18)	26.8(3)
C9	4201.3(13)	5939.7(4)	5459.7(18)	26.2(3)
C10	3982.1(14)	5558.9(4)	5237.5(19)	29.4(3)

Table 2 Fractional Atomic Coordinates (×10^4) and Equivalent Isotropic Displacement Parameters (Å^2×10^3) for 21mb_Fatema_Jagot1_0f_sq. U_{eq} is defined as 1/3 of the trace of the orthogonalised U_{IJ} tensor.

Atom	*x*	*y*	*z*	U(eq)
C11	4342.9(14)	5388.1(4)	3950.1(19)	30.4(4)
C12	5123.4(14)	5559.1(4)	2874.0(18)	26.9(3)
C13	5626.1(14)	5354.7(4)	1677.1(19)	30.1(4)
C14	6502.0(15)	5494.1(4)	772.1(19)	30.0(4)
C15	6949.6(15)	5835.0(4)	1144.7(19)	30.9(4)
C16	6478.5(14)	6039.0(4)	2339.8(19)	28.0(3)
C17	5465.7(13)	5922.0(4)	3133.2(18)	25.7(3)
C18	4841.2(13)	6137.7(4)	4296.1(18)	25.4(3)
C19	7014.4(17)	5282.1(5)	-554(2)	39.2(4)
C20	4694.9(19)	6669.9(5)	1664(2)	41.9(4)
C21	3871.4(17)	5783.5(5)	9017(2)	39.4(4)
C22	8061.0(18)	6456.9(6)	2198(3)	51.2(5)

Table 3 Anisotropic Displacement Parameters (Å^2×10^3) for 21mb_Fatema_Jagot1_0f_sq. The Anisotropic displacement factor exponent takes the form: -2π^2[h^{2}a*^{2}U$_{11}$+2hka*b*U$_{12}$+…].

Atom	U_{11}	U_{22}	U_{33}	U_{23}	U_{13}	U_{12}
O1	46.9(7)	31.3(6)	25.3(6)	1.9(5)	5.0(5)	-1.6(5)
O2	27.4(6)	41.9(7)	29.7(6)	6.1(5)	4.6(5)	-2.7(5)
O3	30.2(6)	35.9(6)	36.9(7)	-6.9(5)	7.4(5)	-8.2(5)
C1	24.3(8)	30.2(8)	23.7(8)	1.9(6)	-0.1(6)	-1.0(6)
C2	23.2(8)	30.3(8)	25.1(8)	-0.7(6)	-3.2(6)	2.5(6)
C3	38.3(10)	32.1(8)	30.4(9)	0.2(7)	-1.3(7)	2.7(7)
C4	50.1(11)	31.9(9)	35.7(10)	-4.9(7)	-1.4(8)	5.7(8)
C5	41.2(10)	42.3(10)	31.3(9)	-7.3(8)	2.1(8)	9.7(8)
C6	29.1(9)	41.1(9)	26.9(8)	-0.5(7)	1.7(7)	7.1(7)

Table 3 Anisotropic Displacement Parameters ($Å^2×10^3$) for 21mb_Fatema_Jagot1_0f_sq. The Anisotropic displacement factor exponent takes the form: $-2\pi^2[h^2a^{*2}U_{11}+2hka^*b^*U_{12}+\ldots]$.

Atom	U_{11}	U_{22}	U_{33}	U_{23}	U_{13}	U_{12}
C7	20.6(7)	35.1(8)	24.8(8)	-0.4(6)	-1.9(6)	3.3(6)
C8	20.3(7)	34.7(8)	25.5(8)	2.4(6)	0.1(6)	-2.0(6)
C9	20.4(7)	31.6(8)	26.6(8)	0.6(6)	-1.2(6)	-0.7(6)
C10	26.1(8)	30.8(8)	31.4(8)	1.9(7)	0.8(7)	-4.0(6)
C11	30.4(9)	27.0(8)	33.9(9)	-0.1(7)	-0.3(7)	-3.6(6)
C12	24.6(8)	29.2(8)	27.0(8)	-0.6(6)	-2.0(6)	1.1(6)
C13	30.8(9)	28.0(8)	31.4(8)	-3.3(6)	-2.7(7)	2.1(6)
C14	29.9(8)	33.0(8)	27.0(8)	-2.2(6)	-0.3(7)	6.2(7)
C15	27.3(8)	35.9(8)	29.5(8)	0.7(7)	4.2(7)	2.1(7)
C16	28.0(8)	27.9(8)	28.0(8)	-1.0(6)	-0.1(7)	-0.9(6)
C17	22.9(7)	29.3(7)	24.9(8)	-0.2(6)	-1.2(6)	1.1(6)
C18	22.4(8)	30.0(8)	23.9(8)	0.2(6)	-1.2(6)	-0.9(6)
C19	42.4(10)	37.4(9)	37.8(10)	-7.0(8)	8.9(8)	4.1(8)
C20	54.5(12)	45.8(10)	25.3(9)	4.7(7)	0.3(8)	9.0(9)
C21	40.8(10)	44.0(10)	33.3(9)	9.5(8)	-0.2(8)	-0.5(8)
C22	38.4(11)	52.3(12)	63.0(14)	-14.0(10)	16.6(10)	-17.5(9)

Table 4 Bond Lengths for 21mb_Fatema_Jagot1_0f_sq.

Atom	Atom	Length/Å	Atom	Atom	Length/Å
O1	C1	1.3693(18)	C7	C8	1.406(2)
O1	C20	1.429(2)	C8	C9	1.383(2)
O2	C8	1.3846(19)	C9	C10	1.441(2)
O2	C21	1.430(2)	C9	C18	1.444(2)
O3	C16	1.3587(19)	C10	C11	1.344(2)
O3	C22	1.427(2)	C11	C12	1.438(2)

Table 4 Bond Lengths for 21mb_Fatema_Jagot1_0f_sq.

Atom	Atom	Length/Å	Atom	Atom	Length/Å
C1	C2	1.422(2)	C12	C13	1.405(2)
C1	C18	1.395(2)	C12	C17	1.414(2)
C2	C3	1.423(2)	C13	C14	1.375(2)
C2	C7	1.423(2)	C14	C15	1.397(2)
C3	C4	1.364(2)	C14	C19	1.508(2)
C4	C5	1.403(3)	C15	C16	1.388(2)
C5	C6	1.360(2)	C16	C17	1.418(2)
C6	C7	1.425(2)	C17	C18	1.469(2)

Table 5 Bond Angles for 21mb_Fatema_Jagot1_0f_sq.

Atom	Atom	Atom	Angle/°	Atom	Atom	Atom	Angle/°
C1	O1	C20	116.89(13)	C10	C9	C18	119.34(14)
C8	O2	C21	112.82(13)	C11	C10	C9	120.93(15)
C16	O3	C22	117.99(14)	C10	C11	C12	121.44(15)
O1	C1	C2	113.71(13)	C13	C12	C11	119.80(14)
O1	C1	C18	124.76(14)	C13	C12	C17	120.74(15)
C18	C1	C2	121.53(14)	C17	C12	C11	119.14(14)
C1	C2	C3	121.78(15)	C14	C13	C12	121.26(15)
C1	C2	C7	119.73(14)	C13	C14	C15	118.41(15)
C7	C2	C3	118.49(14)	C13	C14	C19	121.60(15)
C4	C3	C2	120.59(16)	C15	C14	C19	119.94(15)
C3	C4	C5	120.74(16)	C16	C15	C14	121.10(15)
C6	C5	C4	120.64(16)	O3	C16	C15	122.73(15)
C5	C6	C7	120.46(16)	O3	C16	C17	116.21(14)
C2	C7	C6	119.06(15)	C15	C16	C17	120.96(14)
C8	C7	C2	118.15(14)	C12	C17	C16	116.13(14)

Table 5 Bond Angles for 21mb_Fatema_Jagot1_0f_sq.

Atom	Atom	Atom	Angle/°	Atom	Atom	Atom	Angle/°
C8	C7	C6	122.71(15)	C12	C17	C18	119.06(14)
O2	C8	C7	118.06(14)	C16	C17	C18	124.50(14)
C9	C8	O2	120.04(14)	C1	C18	C9	117.02(14)
C9	C8	C7	121.83(14)	C1	C18	C17	126.14(14)
C8	C9	C10	119.98(14)	C9	C18	C17	116.78(13)
C8	C9	C18	120.50(14)				

Table 6 Torsion Angles for 21mb_Fatema_Jagot1_0f_sq.

A	B	C	D	Angle/°	A	B	C	D	Angle/°
O1	C1	C2	C3	-5.2(2)	C10	C9	C18	C1	163.32(14)
O1	C1	C2	C7	174.52(14)	C10	C9	C18	C17	-14.0(2)
O1	C1	C18	C9	-167.29(14)	C10	C11	C12	C13	169.95(16)
O1	C1	C18	C17	9.7(3)	C10	C11	C12	C17	-3.6(2)
O2	C8	C9	C10	5.7(2)	C11	C12	C13	C14	-170.28(15)
O2	C8	C9	C18	-179.20(13)	C11	C12	C17	C16	161.54(15)
O3	C16	C17	C12	-163.25(14)	C11	C12	C17	C18	-12.4(2)
O3	C16	C17	C18	10.3(2)	C12	C13	C14	C15	5.0(2)
C1	C2	C3	C4	-179.12(16)	C12	C13	C14	C19	-177.59(16)
C1	C2	C7	C6	179.98(14)	C12	C17	C18	C1	-156.30(15)
C1	C2	C7	C8	-3.1(2)	C12	C17	C18	C9	20.7(2)
C2	C1	C18	C9	12.5(2)	C13	C12	C17	C16	-12.0(2)
C2	C1	C18	C17	-170.48(15)	C13	C12	C17	C18	174.13(14)
C2	C3	C4	C5	-1.1(3)	C13	C14	C15	C16	-3.8(2)
C2	C7	C8	O2	-173.31(14)	C14	C15	C16	O3	170.63(15)
C2	C7	C8	C9	3.8(2)	C14	C15	C16	C17	-5.5(3)
C3	C2	C7	C6	-0.3(2)	C15	C16	C17	C12	13.1(2)

Table 6 Torsion Angles for 21mb_Fatema_Jagot1_0f_sq.

A	B	C	D	Angle/°	A	B	C	D	Angle/°
C3	C2	C7	C8	176.58(15)	C15	C16	C17	C18	-173.36(15)
C3	C4	C5	C6	0.2(3)	C16	C17	C18	C1	30.3(2)
C4	C5	C6	C7	0.7(3)	C16	C17	C18	C9	-152.63(15)
C5	C6	C7	C2	-0.6(2)	C17	C12	C13	C14	3.2(2)
C5	C6	C7	C8	-177.36(16)	C18	C1	C2	C3	175.01(15)
C6	C7	C8	O2	3.5(2)	C18	C1	C2	C7	-5.3(2)
C6	C7	C8	C9	-179.45(15)	C18	C9	C10	C11	-1.4(2)
C7	C2	C3	C4	1.2(2)	C19	C14	C15	C16	178.68(16)
C7	C8	C9	C10	-171.30(15)	C20	O1	C1	C2	-127.33(16)
C7	C8	C9	C18	3.8(2)	C20	O1	C1	C18	52.5(2)
C8	C9	C10	C11	173.69(16)	C21	O2	C8	C7	-96.00(17)
C8	C9	C18	C1	-11.8(2)	C21	O2	C8	C9	86.85(18)
C8	C9	C18	C17	170.91(14)	C22	O3	C16	C15	-1.6(2)
C9	C10	C11	C12	10.7(3)	C22	O3	C16	C17	174.67(16)

Table 7 Hydrogen Atom Coordinates (Å×10^4) and Isotropic Displacement Parameters (Å^2×10^3) for 21mb_Fatema_Jagot1_0f_sq.

Atom	*x*	*y*	*z*	U(eq)
H3	4614.51	7223.22	4926.89	40
H4	3865.65	7509.99	7076.68	47
H5	3035.95	7175.13	9099.29	46
H6	2963.68	6552.68	8985.31	39
H10	3577	5426.75	6011.7	35
H11	4076.28	5149.24	3746.73	36
H13	5355.71	5115.54	1489.34	36
H15	7586.96	5928.79	570.47	37
H19A	6792.09	5026.84	-458.68	59

Table 7 Hydrogen Atom Coordinates (Å×10^4) and Isotropic Displacement Parameters (Å^2×10^3) for 21mb_Fatema_Jagot1_0f_sq.

Atom	*x*	*y*	*z*	U(eq)
H19B	7864.35	5302.88	-531.37	59
H19C	6719.85	5378.86	-1535.15	59
H20A	4579.48	6899.26	1114.6	63
H20B	3951.26	6541.16	1739.95	63
H20C	5255.35	6520.29	1096.67	63
H21A	4376.35	5596.4	8574.26	59
H21B	3397.67	5677.82	9845	59
H21C	4350.52	5979.43	9440.72	59
H22A	7939.9	6512.22	1100.97	77
H22B	8631.27	6260.95	2297.61	77
H22C	8350.73	6673.22	2731.43	77

Table 8 Solvent masks information for 21mb_Fatema_Jagot1_0f_sq.

Number	X	Y	Z	Volume	Electron count	Content
1	0.250	0.250	-0.043	199	61	
2	0.750	0.750	-0.018	199	61	

Experimental

Single crystals of $C_{22}H_{20}O_3$ **[21mb_Fatema_Jagot1_0f_sq]** were **[]**. A suitable crystal was selected and **[]** on a **Bruker APEX-II CCD** diffractometer. The crystal was kept at 173.00 K during data collection. Using Olex2 [1], the structure was solved with the SHELXT [2] structure solution program using Intrinsic Phasing and refined with the SHELXL [3] refinement package using Least Squares minimisation.

1. Dolomanov, O.V., Bourhis, L.J., Gildea, R.J, Howard, J.A.K. & Puschmann, H. (2009), J. Appl. Cryst. 42, 339-341.
2. Sheldrick, G.M. (2015). Acta Cryst. A71, 3-8.
3. Sheldrick, G.M. (2015). Acta Cryst. C71, 3-8.

Crystal structure determination of [21mb_Fatema_Jagot1_0f_sq]

Crystal Data for $C_{22}H_{20}O_3$ (*M* =332.38 g/mol): orthorhombic, space group Pccn (no. 56), *a* = 11.4925(6) Å, *b* = 36.9186(17) Å, *c* = 8.6409(4) Å, *V* = 3666.2(3) Å^3, *Z* = 8, *T* = 173.00 K, μ(MoKα) = 0.079 mm^{-1}, *Dcalc* = 1.204 g/cm^3, 80805 reflections measured (3.712° ≤ 2Θ ≤ 56.464°), 4527 unique (R_{int} = 0.0591, R_{sigma} = 0.0307) which were used in all calculations. The final R_1 was 0.0573 (I > 2σ(I)) and wR_2 was 0.1316 (all data).

Refinement model description

Number of restraints - 0, number of constraints - unknown.

Details:

1. Fixed Uiso at 1.2 times of all C(H) groups and at 1.5 times of all C(H,H,H) groups
2a. Aromatic/amide H refined with riding coordinates:
C3(H3), C4(H4), C5(H5), C6(H6), C10(H10), C11(H11), C13(H13), C15(H15)
2b. Idealised Me refined as rotating group:
C19(H19A,H19B,H19C), C20(H20A,H20B,H20C), C21(H21A,H21B,H21C), C22(H22A,H22B,H22C)

Crystal structure for compound 169

b"\n \n 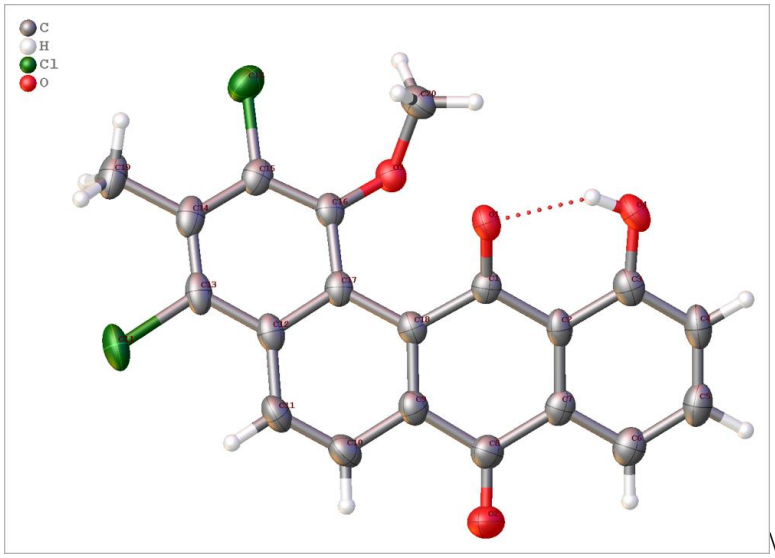

\n "

Table 1 Crystal data and structure refinement for 21mb_cdk6_FJN288B1_xtal3_0f.

Identification code	21mb_cdk6_FJN288B1_xtal3_0f
Empirical formula	$C_{20}H_{12}Cl_2O_4$
Formula weight	387.20
Temperature/K	123.00
Crystal system	monoclinic
Space group	$P2_1/c$
a/Å	16.284(3)

b/Å	3.8310(7)
c/Å	26.131(4)
α/°	90
β/°	105.538(5)
γ/°	90
Volume/Å^3	1570.6(5)
Z	4
ρ_{calc}g/cm^3	1.637
μ/mm^{-1}	0.439
F(000)	792.0
Crystal size/mm^3	0.406 × 0.034 × 0.031
Radiation	MoKα (λ = 0.71073)
2Θ range for data collection/°	4.66 to 51.998
Index ranges	-20 ≤ h ≤ 20, -4 ≤ k ≤ 4, -32 ≤ l ≤ 32
Reflections collected	22112
Independent reflections	3094 [R_{int} = 0.0917, R_{sigma} = 0.0945]
Data/restraints/parameters	3094/0/238
Goodness-of-fit on F^2	1.045
Final R indexes [I>=2σ (I)]	R_1 = 0.0700, wR_2 = 0.1752
Final R indexes [all data]	R_1 = 0.0908, wR_2 = 0.1910
Largest diff. peak/hole / e Å^{-3}	0.88/-0.33

Table 2 Fractional Atomic Coordinates (×10^4) and Equivalent Isotropic Displacement Parameters (Å^2×10^3) for 21mb_cdk6_FJN288B1_xtal3_0f. U_{eq} is defined as 1/3 of the trace of the orthogonalised U_{IJ} tensor.

Atom	*x*	*y*	*z*	U(eq)
Cl1	6501.5(8)	9778(3)	4524.8(4)	46.7(3)
Cl2	9657.9(7)	5868(3)	5593.9(4)	46.2(3)
O1	8273.8(17)	6988(7)	7135.8(10)	33.6(6)

Table 2 Fractional Atomic Coordinates ($\times 10^4$) and Equivalent Isotropic Displacement Parameters ($Å^2 \times 10^3$) for 21mb_cdk6_FJN288B1_xtal3_0f. U_{eq} is defined as 1/3 of the trace of the orthogonalised U_{IJ} tensor.

Atom	*x*	*y*	*z*	U(eq)
O2	5115.5(18)	2126(10)	6637.7(12)	50.1(8)
O3	8828.9(16)	3623(7)	6419.5(10)	32.1(6)
O4	8592.6(18)	4248(8)	8083.0(11)	40.5(7)
C1	7620(2)	5172(10)	7005.1(14)	28.8(8)
C2	7282(3)	3469(10)	7408.4(14)	31.3(9)
C3	7802(3)	3084(11)	7922.9(15)	35.9(9)
C4	7473(3)	1375(11)	8299.9(16)	41.1(10)
C5	6649(3)	248(12)	8173.7(17)	42.4(10)
C6	6112(3)	716(11)	7668.7(17)	38.9(10)
C7	6435(2)	2300(10)	7284.1(15)	31.4(8)
C8	5866(3)	2961(11)	6752.7(15)	35.9(9)
C9	6245(3)	4514(11)	6344.0(15)	33.7(9)
C10	5680(3)	5437(12)	5848.9(16)	38.2(9)
C11	5990(3)	6862(12)	5465.5(15)	38.5(10)
C12	6877(3)	7084(10)	5522.9(14)	32.9(9)
C13	7219(3)	8254(10)	5108.4(14)	36.7(9)
C14	8064(3)	8151(11)	5132.9(15)	37.6(10)
C15	8608(3)	6649(10)	5591.4(15)	33.5(9)
C16	8332(3)	5548(10)	6020.7(14)	29.9(8)
C17	7458(2)	5949(10)	6007.3(14)	29.5(8)
C18	7111(2)	5025(10)	6439.2(14)	30.0(8)
C19	8412(3)	9378(12)	4681.5(17)	46.9(11)
C20	9620(3)	5051(12)	6736.7(17)	39.8(10)

Table 3 Anisotropic Displacement Parameters ($Å^2×10^3$) for 21mb_cdk6_FJN288B1_xtal3_0f. The Anisotropic displacement factor exponent takes the form: $-2\pi^2[h^2a^{*2}U_{11}+2hka^*b^*U_{12}+\ldots]$.

Atom	U_{11}	U_{22}	U_{33}	U_{23}	U_{13}	U_{12}
Cl1	68.1(8)	42.9(6)	23.0(5)	5.6(4)	1.8(4)	3.2(5)
Cl2	46.5(6)	53.8(7)	43.8(6)	-3.8(5)	21.6(5)	-4.9(5)
O1	39.8(15)	34.0(15)	24.1(13)	-0.7(11)	3.8(11)	2.1(12)
O2	35.6(17)	73(2)	41.9(17)	-3.7(16)	10.6(13)	-5.6(15)
O3	34.8(14)	30.4(14)	30.3(14)	-0.3(11)	7.0(11)	-0.6(11)
O4	42.7(16)	44.9(18)	26.8(14)	-0.9(13)	-2.9(12)	2.4(13)
C1	35(2)	23.3(18)	29.0(18)	-2.0(15)	11.2(16)	3.8(15)
C2	45(2)	29(2)	20.8(17)	-1.1(15)	9.6(16)	8.1(16)
C3	43(2)	32(2)	31(2)	-1.5(17)	8.1(17)	7.4(17)
C4	61(3)	37(2)	24.7(19)	3.1(17)	10.5(19)	10(2)
C5	61(3)	39(2)	32(2)	2.7(18)	20(2)	6(2)
C6	49(2)	33(2)	38(2)	-1.9(18)	17.4(19)	2.9(18)
C7	41(2)	25.3(19)	31.6(19)	-2.4(16)	15.9(16)	5.1(16)
C8	37(2)	39(2)	33(2)	-5.2(18)	11.3(17)	1.3(18)
C9	38(2)	35(2)	27.0(19)	-3.7(16)	7.7(16)	2.9(17)
C10	34(2)	46(2)	31(2)	-4.9(18)	1.5(16)	1.5(18)
C11	41(2)	43(2)	25.6(19)	-1.4(17)	-0.4(16)	4.3(18)
C12	47(2)	26.1(19)	23.2(18)	-2.5(15)	5.0(16)	2.2(17)
C13	60(3)	26(2)	21.6(18)	-3.2(15)	7.0(18)	-1.9(18)
C14	60(3)	28(2)	26.5(19)	-6.3(16)	14.4(18)	-9.3(18)
C15	45(2)	26.3(19)	31.4(19)	-6.6(16)	14.5(17)	-3.3(17)
C16	40(2)	24.7(18)	23.8(18)	-5.5(15)	7.0(15)	-2.2(15)
C17	41(2)	22.5(18)	25.0(18)	-2.3(14)	9.0(16)	0.0(15)
C18	35(2)	26.5(19)	27.1(18)	-0.7(15)	5.9(15)	3.2(15)
C19	73(3)	40(3)	32(2)	-0.6(19)	22(2)	-10(2)

Table 3 Anisotropic Displacement Parameters ($Å^2×10^3$) for 21mb_cdk6_FJN288B1_xtal3_0f. The Anisotropic displacement factor exponent takes the form: $-2\pi^2[h^2a^{*2}U_{11}+2hka^*b^*U_{12}+\ldots]$.

Atom	U_{11}	U_{22}	U_{33}	U_{23}	U_{13}	U_{12}
C20	36(2)	41(2)	37(2)	-1.5(19)	0.9(17)	-1.1(18)

Table 4 Bond Lengths for 21mb_cdk6_FJN288B1_xtal3_0f.

Atom	Atom	Length/Å	Atom	Atom	Length/Å
Cl1	C13	1.754(4)	C7	C8	1.470(5)
Cl2	C15	1.734(4)	C8	C9	1.493(6)
O1	C1	1.241(5)	C9	C10	1.417(5)
O2	C8	1.221(5)	C9	C18	1.380(6)
O3	C16	1.354(5)	C10	C11	1.352(6)
O3	C20	1.440(5)	C11	C12	1.414(6)
O4	C3	1.321(5)	C12	C13	1.417(6)
C1	C2	1.467(5)	C12	C17	1.430(5)
C1	C18	1.490(5)	C13	C14	1.361(6)
C2	C3	1.392(5)	C14	C15	1.408(6)
C2	C7	1.402(6)	C14	C19	1.513(6)
C3	C4	1.403(6)	C15	C16	1.382(5)
C4	C5	1.363(7)	C16	C17	1.422(6)
C5	C6	1.386(6)	C17	C18	1.435(5)
C6	C7	1.393(6)			

Table 5 Bond Angles for 21mb_cdk6_FJN288B1_xtal3_0f.

Atom	Atom	Atom	Angle/°	Atom	Atom	Atom	Angle/°
C16	O3	C20	119.6(3)	C10	C11	C12	121.3(4)
O1	C1	C2	120.8(3)	C11	C12	C13	122.5(4)
O1	C1	C18	120.1(3)	C11	C12	C17	119.4(4)

Table 5 Bond Angles for 21mb_cdk6_FJN288B1_xtal3_0f.

Atom	Atom	Atom	Angle/°	Atom	Atom	Atom	Angle/°
C2	C1	C18	118.7(3)	C13	C12	C17	118.1(4)
C3	C2	C1	119.5(4)	C12	C13	Cl1	117.6(3)
C3	C2	C7	119.7(4)	C14	C13	Cl1	118.7(3)
C7	C2	C1	120.7(3)	C14	C13	C12	123.7(4)
O4	C3	C2	124.0(4)	C13	C14	C15	116.7(4)
O4	C3	C4	117.3(4)	C13	C14	C19	122.6(4)
C2	C3	C4	118.7(4)	C15	C14	C19	120.6(4)
C5	C4	C3	120.9(4)	C14	C15	Cl2	117.9(3)
C4	C5	C6	121.3(4)	C16	C15	Cl2	118.6(3)
C5	C6	C7	118.6(4)	C16	C15	C14	123.3(4)
C2	C7	C8	119.7(3)	O3	C16	C15	122.2(4)
C6	C7	C2	120.7(4)	O3	C16	C17	117.8(3)
C6	C7	C8	119.5(4)	C15	C16	C17	119.2(3)
O2	C8	C7	121.6(4)	C12	C17	C18	117.7(4)
O2	C8	C9	120.5(4)	C16	C17	C12	118.3(3)
C7	C8	C9	117.9(4)	C16	C17	C18	123.8(3)
C10	C9	C8	117.4(4)	C9	C18	C1	117.0(3)
C18	C9	C8	121.8(4)	C9	C18	C17	119.5(3)
C18	C9	C10	120.8(4)	C17	C18	C1	122.7(3)
C11	C10	C9	119.8(4)				

Table 6 Torsion Angles for 21mb_cdk6_FJN288B1_xtal3_0f.

A	B	C	D	Angle/°	A	B	C	D	Angle/°
Cl1	C13	C14	C15	-175.0(3)	C8	C9	C18	C1	-20.9(6)
Cl1	C13	C14	C19	1.5(6)	C8	C9	C18	C17	169.2(4)
Cl2	C15	C16	O3	-5.9(5)	C9	C10	C11	C12	7.5(7)

Table 6 Torsion Angles for 21mb_cdk6_FJN288B1_xtal3_0f.

A	B	C	D	Angle/°	A	B	C	D	Angle/°
Cl2	C15	C16	C17	-175.6(3)	C10	C9	C18	C1	159.5(4)
O1	C1	C2	C3	-17.3(5)	C10	C9	C18	C17	-10.4(6)
O1	C1	C2	C7	161.2(4)	C10	C11	C12	C13	173.8(4)
O1	C1	C18	C9	-149.2(4)	C10	C11	C12	C17	-3.4(6)
O1	C1	C18	C17	20.3(6)	C11	C12	C13	Cl1	4.9(5)
O2	C8	C9	C10	9.0(6)	C11	C12	C13	C14	-172.9(4)
O2	C8	C9	C18	-170.7(4)	C11	C12	C17	C16	167.9(4)
O3	C16	C17	C12	-162.6(3)	C11	C12	C17	C18	-7.4(5)
O3	C16	C17	C18	12.4(5)	C12	C13	C14	C15	2.7(6)
O4	C3	C4	C5	176.8(4)	C12	C13	C14	C19	179.2(4)
C1	C2	C3	O4	1.8(6)	C12	C17	C18	C1	-155.2(3)
C1	C2	C3	C4	-178.5(4)	C12	C17	C18	C9	14.1(5)
C1	C2	C7	C6	-179.3(4)	C13	C12	C17	C16	-9.4(5)
C1	C2	C7	C8	-3.5(6)	C13	C12	C17	C18	175.3(3)
C2	C1	C18	C9	23.8(5)	C13	C14	C15	Cl2	170.4(3)
C2	C1	C18	C17	-166.6(3)	C13	C14	C15	C16	-4.8(6)
C2	C3	C4	C5	-2.9(6)	C14	C15	C16	O3	169.4(3)
C2	C7	C8	O2	-176.6(4)	C14	C15	C16	C17	-0.4(6)
C2	C7	C8	C9	6.8(6)	C15	C16	C17	C12	7.6(5)
C3	C2	C7	C6	-0.8(6)	C15	C16	C17	C18	-177.4(4)
C3	C2	C7	C8	175.1(4)	C16	C17	C18	C1	29.8(6)
C3	C4	C5	C6	0.7(7)	C16	C17	C18	C9	-160.9(4)
C4	C5	C6	C7	1.6(6)	C17	C12	C13	Cl1	-177.9(3)
C5	C6	C7	C2	-1.5(6)	C17	C12	C13	C14	4.3(6)
C5	C6	C7	C8	-177.3(4)	C18	C1	C2	C3	169.7(3)
C6	C7	C8	O2	-0.7(6)	C18	C1	C2	C7	-11.8(5)

Table 6 Torsion Angles for 21mb_cdk6_FJN288B1_xtal3_0f.

A	B	C	D	Angle/°	A	B	C	D	Angle/°
C6	C7	C8	C9	-177.3(4)	C18	C9	C10	C11	-0.5(6)
C7	C2	C3	O4	-176.7(4)	C19	C14	C15	Cl2	-6.1(5)
C7	C2	C3	C4	2.9(6)	C19	C14	C15	C16	178.6(4)
C7	C8	C9	C10	-174.4(4)	C20	O3	C16	C15	61.7(5)
C7	C8	C9	C18	6.0(6)	C20	O3	C16	C17	-128.4(4)
C8	C9	C10	C11	179.8(4)					

Table 7 Hydrogen Atom Coordinates (Å×10^4) and Isotropic Displacement Parameters (Å^2×10^3) for 21mb_cdk6_FJN288B1_xtal3_0f.

Atom	*x*	*y*	*z*	U(eq)
H4	8688.76	5592.95	7851.83	61
H4A	7829.49	999.11	8648.02	49
H5	6439.61	-881.36	8436.97	51
H6	5534.35	-26.99	7586.71	47
H10	5084.83	5054.64	5786.46	46
H11	5604.87	7732.73	5151.49	46
H19A	9004.81	10126.82	4822.91	70
H19B	8069.38	11341.9	4499.73	70
H19C	8385.89	7460.6	4429.44	70
H20A	10095.65	4038.74	6623.55	60
H20B	9685.07	4496.65	7111.6	60
H20C	9617.9	7590.57	6690.88	60

Experimental

Single crystals of $C_{20}H_{12}Cl_2O_4$ **[21mb_cdk6_FJN288B1_xtal3_0f]** were **[]**. A suitable crystal was selected and **[]** on a **Bruker APEX-II CCD** diffractometer. The crystal was kept at 123.00 K during data collection. Using Olex2 [1], the structure was solved with the XT [2] structure solution program using Intrinsic Phasing and refined with the SHELXL [3] refinement package using Least Squares minimisation.

1. Dolomanov, O.V., Bourhis, L.J., Gildea, R.J, Howard, J.A.K. & Puschmann, H. (2009), J. Appl. Cryst. 42, 339-341.
2. Sheldrick, G.M. (2015). Acta Cryst. A71, 3-8.
3. Sheldrick, G.M. (2015). Acta Cryst. C71, 3-8.

Crystal structure determination of [21mb_cdk6_FJN288B1_xtal3_0f]

Crystal Data for $C_{20}H_{12}Cl_2O_4$ (*M* =387.20 g/mol): monoclinic, space group $P2_1/c$ (no. 14), *a* = 16.284(3) Å, *b* = 3.8310(7) Å, *c* = 26.131(4) Å, *β* = 105.538(5)°, *V* = 1570.6(5) $Å^3$, *Z* = 4, *T* = 123.00 K, μ(MoKα) = 0.439 mm^{-1}, *Dcalc* = 1.637 g/cm^3, 22112 reflections measured ($4.66° \leq 2\Theta \leq 51.998°$), 3094 unique ($R_{int}$ = 0.0917, R_{sigma} = 0.0945) which were used in all calculations. The final R_1 was 0.0700 ($I > 2\sigma(I)$) and wR_2 was 0.1910 (all data).

Refinement model description

Number of restraints - 0, number of constraints - unknown.

Details:

1. Fixed Uiso at 1.2 times of all C(H) groups and at 1.5 times of all C(H,H,H) groups, all O(H) groups
2a. Aromatic/amide H refined with riding coordinates:
C4(H4A), C5(H5), C6(H6), C10(H10), C11(H11)
2b. Idealised Me refined as rotating group C19(H19A,H19B,H19C), C20(H20A,H20B,H20C)
2c. Idealised tetrahedral OH refined as rotating group O4(H4)

Crystal structure for compound 170

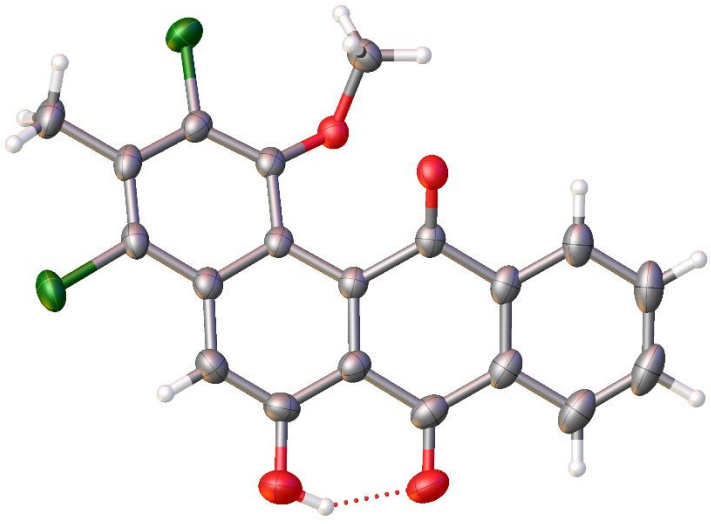

Table 1 Crystal data and structure refinement for 21mb_cdk5_FJN289C_0f.

Identification code	21mb_cdk5_FJN289C_0f
Empirical formula	$C_{20}H_{12}Cl_2O_4$

Formula weight	387.20
Temperature/K	173.0
Crystal system	monoclinic
Space group	$P2_1/c$
a/Å	3.8487(2)
b/Å	25.7577(15)
c/Å	15.8388(10)
α/°	90
β/°	92.616(2)
γ/°	90
Volume/Å^3	1568.52(16)
Z	4
ρ_{calc}g/cm^3	1.640
μ/mm^{-1}	0.440
F(000)	792.0
Crystal size/mm^3	0.363 × 0.064 × 0.04
Radiation	MoKα (λ = 0.71073)
2Θ range for data collection/°	3.162 to 53.996
Index ranges	$-4 \leq h \leq 4$, $-32 \leq k \leq 32$, $-20 \leq l \leq 20$
Reflections collected	29351
Independent reflections	3399 [R_{int} = 0.0639, R_{sigma} = 0.0474]
Data/restraints/parameters	3399/0/238
Goodness-of-fit on F^2	1.107
Final R indexes [I>=2σ (I)]	R_1 = 0.0616, wR_2 = 0.1623
Final R indexes [all data]	R_1 = 0.0726, wR_2 = 0.1692
Largest diff. peak/hole / e Å^{-3}	0.55/-0.35

Table 2 Fractional Atomic Coordinates (×10^4) and Equivalent Isotropic Displacement Parameters (Å^2×10^3) for 21mb_cdk5_FJN289C_0f. U_{eq} is defined as 1/3 of of the trace of the orthogonalised U_{IJ} tensor.

Atom	*x*	*y*	*z*	U(eq)
Cl1	-1388(3)	2262.5(3)	7547.4(6)	44.0(3)
Cl2	1044(3)	3162.0(4)	4574.2(5)	44.3(3)
O1	405(6)	4765.2(9)	6514.2(15)	33.8(5)
O2	6940(8)	4478.3(12)	9484.5(17)	51.2(7)
O3	3634(6)	4047.8(9)	5637.1(14)	30.7(5)
O4	4369(10)	3570.0(13)	9548.0(18)	59.8(9)
C1	2570(8)	4678.9(12)	7084(2)	29.0(7)
C2	4347(9)	5117.8(13)	7530(2)	32.6(7)
C3	4373(10)	5604.4(13)	7156(3)	40.6(8)
C4	5995(11)	6018.6(15)	7583(3)	49.3(10)
C5	7473(11)	5947.7(16)	8388(3)	50.3(11)
C6	7432(10)	5472.5(16)	8776(3)	45.8(9)
C7	5871(9)	5050.2(14)	8344(2)	35.9(8)
C8	5662(9)	4543.5(15)	8759(2)	36.4(8)
C9	4066(9)	4103.5(13)	8291(2)	31.8(7)
C10	3520(10)	3626.1(14)	8720(2)	35.6(8)
C11	1976(10)	3217.3(14)	8303(2)	36.1(8)
C12	1276(9)	3233.4(12)	7422(2)	30.4(7)
C13	-142(9)	2802.8(12)	6966(2)	31.8(7)
C14	-495(9)	2786.9(12)	6106(2)	32.7(7)
C15	764(9)	3221.6(12)	5660(2)	30.5(7)
C16	2021(8)	3664.8(12)	6052(2)	27.6(6)
C17	2073(8)	3692.5(12)	6959(2)	26.8(6)
C18	3127(8)	4143.8(12)	7427(2)	27.8(6)
C19	-1948(11)	2322.8(14)	5628(3)	43.2(9)

Table 2 Fractional Atomic Coordinates (×10^4) and Equivalent Isotropic Displacement Parameters (Å^2×10^3) for 21mb_cdk5_FJN289C_0f. U_{eq} is defined as 1/3 of of the trace of the orthogonalised U_{IJ} tensor.

Atom	*x*	*y*	*z*	U(eq)
C20	1737(10)	4323.5(14)	4971(2)	35.6(8)

Table 3 Anisotropic Displacement Parameters (Å^2×10^3) for 21mb_cdk5_FJN289C_0f. The Anisotropic displacement factor exponent takes the form: -2π^2[h^{2}a*^{2}U$_{11}$+2hka*b*U$_{12}$+…].

Atom	U_{11}	U_{22}	U_{33}	U_{23}	U_{13}	U_{12}
Cl1	46.9(6)	27.0(4)	57.8(6)	9.6(4)	-0.1(4)	-3.4(4)
Cl2	56.6(6)	41.5(5)	34.4(4)	-10.1(4)	-2.7(4)	-0.1(4)
O1	33.4(13)	28.0(11)	39.6(13)	-0.2(10)	-1.2(10)	4.0(10)
O2	58.8(18)	55.4(17)	38.3(14)	-8.4(12)	-11.2(12)	0.1(14)
O3	29.4(12)	29.3(11)	33.4(11)	0.9(9)	1.6(9)	-0.6(9)
O4	84(3)	55.4(18)	39.2(15)	4.7(13)	-10.8(14)	1.8(17)
C1	24.7(16)	27.3(15)	35.5(16)	-2.8(12)	5.9(13)	2.1(12)
C2	25.1(17)	29.2(16)	44.0(18)	-9.6(14)	7.2(13)	1.9(13)
C3	37(2)	29.0(17)	56(2)	-6.4(15)	11.3(16)	0.2(15)
C4	44(2)	28.1(18)	77(3)	-9.1(18)	18(2)	-3.9(16)
C5	39(2)	42(2)	71(3)	-28(2)	14.3(19)	-10.3(17)
C6	36(2)	48(2)	54(2)	-21.7(18)	7.9(17)	-5.5(17)
C7	26.4(17)	38.2(18)	43.5(18)	-13.4(15)	6.7(14)	-3.1(14)
C8	30.3(18)	45(2)	34.2(17)	-9.6(14)	1.9(14)	0.5(15)
C9	30.8(18)	32.5(16)	31.9(16)	-4.9(13)	-0.5(13)	3.8(13)
C10	38.2(19)	39.4(18)	28.9(16)	2.2(14)	-0.7(13)	5.5(15)
C11	40(2)	31.9(17)	37.0(17)	5.8(14)	3.2(14)	2.3(14)
C12	27.3(17)	26.4(15)	37.3(17)	-0.1(13)	-1.7(13)	4.4(13)
C13	26.1(17)	23.3(15)	45.9(18)	2.2(13)	0.1(13)	0.8(12)
C14	26.0(17)	24.2(15)	47.4(19)	-4.7(13)	-4.0(14)	1.3(12)

Table 3 Anisotropic Displacement Parameters ($Å^2×10^3$) for 21mb_cdk5_FJN289C_0f. The Anisotropic displacement factor exponent takes the form: $-2\pi^2[h^2a^{*2}U_{11}+2hka^*b^*U_{12}+\ldots]$.

Atom	U_{11}	U_{22}	U_{33}	U_{23}	U_{13}	U_{12}
C15	28.7(17)	29.0(16)	33.4(16)	-4.9(13)	-2.7(13)	3.8(13)
C16	23.3(16)	25.3(15)	34.0(16)	-1.0(12)	-1.8(12)	4.9(12)
C17	20.9(15)	25.1(14)	34.1(16)	-1.6(12)	-2.4(12)	3.2(11)
C18	22.7(16)	27.3(15)	33.6(16)	-1.7(12)	1.8(12)	1.3(12)
C19	43(2)	29.4(17)	57(2)	-8.3(16)	-6.2(17)	-3.4(15)
C20	34.3(19)	36.6(18)	35.8(17)	6.8(14)	2.1(14)	0.0(14)

Table 4 Bond Lengths for 21mb_cdk5_FJN289C_0f.

Atom	Atom	Length/Å	Atom	Atom	Length/Å
Cl1	C13	1.748(3)	C7	C8	1.465(5)
Cl2	C15	1.734(3)	C8	C9	1.473(5)
O1	C1	1.220(4)	C9	C10	1.425(5)
O2	C8	1.241(4)	C9	C18	1.403(4)
O3	C16	1.352(4)	C10	C11	1.365(5)
O3	C20	1.442(4)	C11	C12	1.410(5)
O4	C10	1.345(4)	C12	C13	1.419(5)
C1	C2	1.484(4)	C12	C17	1.432(4)
C1	C18	1.493(4)	C13	C14	1.364(5)
C2	C3	1.387(5)	C14	C15	1.421(5)
C2	C7	1.402(5)	C14	C19	1.509(5)
C3	C4	1.395(5)	C15	C16	1.377(4)
C4	C5	1.384(6)	C16	C17	1.437(4)
C5	C6	1.370(6)	C17	C18	1.427(4)
C6	C7	1.406(5)			

Table 5 Bond Angles for 21mb_cdk5_FJN289C_0f.

Atom	Atom	Atom	Angle/°	Atom	Atom	Atom	Angle/°
C16	O3	C20	119.1(3)	C10	C11	C12	121.1(3)
O1	C1	C2	119.9(3)	C11	C12	C13	122.1(3)
O1	C1	C18	121.3(3)	C11	C12	C17	119.7(3)
C2	C1	C18	118.3(3)	C13	C12	C17	118.2(3)
C3	C2	C1	119.8(3)	C12	C13	Cl1	117.6(3)
C3	C2	C7	119.6(3)	C14	C13	Cl1	119.0(3)
C7	C2	C1	120.5(3)	C14	C13	C12	123.4(3)
C2	C3	C4	119.7(4)	C13	C14	C15	116.9(3)
C5	C4	C3	120.1(4)	C13	C14	C19	122.9(3)
C6	C5	C4	121.2(4)	C15	C14	C19	120.2(3)
C5	C6	C7	119.1(4)	C14	C15	Cl2	117.5(2)
C2	C7	C6	120.2(4)	C16	C15	Cl2	119.0(3)
C2	C7	C8	119.6(3)	C16	C15	C14	123.4(3)
C6	C7	C8	120.1(3)	O3	C16	C15	123.0(3)
O2	C8	C7	120.6(3)	O3	C16	C17	117.6(3)
O2	C8	C9	120.0(3)	C15	C16	C17	118.7(3)
C7	C8	C9	119.3(3)	C12	C17	C16	118.5(3)
C10	C9	C8	119.4(3)	C18	C17	C12	118.0(3)
C18	C9	C8	121.1(3)	C18	C17	C16	123.4(3)
C18	C9	C10	119.5(3)	C9	C18	C1	116.7(3)
O4	C10	C9	121.6(3)	C9	C18	C17	120.0(3)
O4	C10	C11	118.1(3)	C17	C18	C1	122.0(3)
C11	C10	C9	120.3(3)				

Table 6 Torsion Angles for 21mb_cdk5_FJN289C_0f.

A	B	C	D	Angle/°	A	B	C	D	Angle/°
Cl1	C13	C14	C15	-176.0(3)	C8	C9	C18	C17	170.6(3)
Cl1	C13	C14	C19	0.5(5)	C9	C10	C11	C12	7.8(5)
Cl2	C15	C16	O3	-3.4(4)	C10	C9	C18	C1	159.1(3)
Cl2	C15	C16	C17	-174.4(2)	C10	C9	C18	C17	-8.3(5)
O1	C1	C2	C3	-19.3(5)	C10	C11	C12	C13	176.3(3)
O1	C1	C2	C7	157.9(3)	C10	C11	C12	C17	-2.3(5)
O1	C1	C18	C9	-146.7(3)	C11	C12	C13	Cl1	5.8(5)
O1	C1	C18	C17	20.5(5)	C11	C12	C13	C14	-172.6(3)
O2	C8	C9	C10	9.6(5)	C11	C12	C17	C16	167.3(3)
O2	C8	C9	C18	-169.3(3)	C11	C12	C17	C18	-8.2(5)
O3	C16	C17	C12	-162.9(3)	C12	C13	C14	C15	2.4(5)
O3	C16	C17	C18	12.3(4)	C12	C13	C14	C19	178.9(3)
O4	C10	C11	C12	-174.8(3)	C12	C17	C18	C1	-153.3(3)
C1	C2	C3	C4	178.9(3)	C12	C17	C18	C9	13.5(5)
C1	C2	C7	C6	-177.5(3)	C13	C12	C17	C16	-11.4(4)
C1	C2	C7	C8	-0.8(5)	C13	C12	C17	C18	173.1(3)
C2	C1	C18	C9	24.8(4)	C13	C14	C15	Cl2	168.9(3)
C2	C1	C18	C17	-168.0(3)	C13	C14	C15	C16	-5.5(5)
C2	C3	C4	C5	-2.1(6)	C14	C15	C16	O3	171.0(3)
C2	C7	C8	O2	-178.7(3)	C14	C15	C16	C17	0.0(5)
C2	C7	C8	C9	4.3(5)	C15	C16	C17	C12	8.6(4)
C3	C2	C7	C6	-0.3(5)	C15	C16	C17	C18	-176.2(3)
C3	C2	C7	C8	176.4(3)	C16	C17	C18	C1	31.4(5)
C3	C4	C5	C6	1.1(6)	C16	C17	C18	C9	-161.8(3)
C4	C5	C6	C7	0.3(6)	C17	C12	C13	Cl1	-175.6(2)
C5	C6	C7	C2	-0.7(5)	C17	C12	C13	C14	6.0(5)

Table 6 Torsion Angles for 21mb_cdk5_FJN289C_0f.

A	B	C	D	Angle/°	A	B	C	D	Angle/°
C5	C6	C7	C8	-177.4(3)	C18	C1	C2	C3	169.1(3)
C6	C7	C8	O2	-2.0(5)	C18	C1	C2	C7	-13.6(5)
C6	C7	C8	C9	-179.0(3)	C18	C9	C10	O4	-179.8(3)
C7	C2	C3	C4	1.7(5)	C18	C9	C10	C11	-2.5(5)
C7	C8	C9	C10	-173.3(3)	C19	C14	C15	Cl2	-7.7(4)
C7	C8	C9	C18	7.7(5)	C19	C14	C15	C16	177.8(3)
C8	C9	C10	O4	1.2(5)	C20	O3	C16	C15	62.1(4)
C8	C9	C10	C11	178.6(3)	C20	O3	C16	C17	-126.8(3)
C8	C9	C18	C1	-21.9(5)					

Table 7 Hydrogen Atom Coordinates (Å×10^4) and Isotropic Displacement Parameters (Å^2×10^3) for 21mb_cdk5_FJN289C_0f.

Atom	*x*	*y*	*z*	U(eq)
H4	5468.34	3833.19	9724.13	90
H3	3290.24	5655.49	6611.22	49
H4A	6086.29	6349.7	7320.77	59
H5	8535.54	6233.86	8676.48	60
H6	8444.4	5429.04	9329.72	55
H11	1364.47	2917.02	8610.79	43
H19A	-32.15	2114.5	5421.91	65
H19B	-3436.46	2441.04	5147.51	65
H19C	-3321.25	2111.29	6004.66	65
H20A	-763.06	4298.39	5057.5	53
H20B	2244.92	4170.26	4424.27	53
H20C	2438.61	4689.28	4979.82	53

Experimental

Single crystals of $C_{20}H_{12}Cl_2O_4$ **[21mb_cdk5_FJN289C_0f]** were **[]**. A suitable crystal was selected and **[]** on a **Bruker APEX-II CCD** diffractometer. The crystal was kept at 173.0 K during data collection. Using Olex2 [1], the structure was solved with the SHELXT [2] structure solution program using Intrinsic Phasing and refined with the SHELXL [3] refinement package using Least Squares minimisation.

1. Dolomanov, O.V., Bourhis, L.J., Gildea, R.J, Howard, J.A.K. & Puschmann, H. (2009), J. Appl. Cryst. 42, 339-341.
2. Sheldrick, G.M. (2015). Acta Cryst. A71, 3-8.
3. Sheldrick, G.M. (2015). Acta Cryst. C71, 3-8.

Crystal structure determination of [21mb_cdk5_FJN289C_0f]

Crystal Data for $C_{20}H_{12}Cl_2O_4$ (M =387.20 g/mol): monoclinic, space group $P2_1/c$ (no. 14), a = 3.8487(2) Å, b = 25.7577(15) Å, c = 15.8388(10) Å, β = 92.616(2)°, V = 1568.52(16) Å^3, Z = 4, T = 173.0 K, μ(MoKα) = 0.440 mm^{-1}, *Dcalc* = 1.640 g/cm^3, 29351 reflections measured ($3.162° \leq 2\Theta \leq 53.996°$), 3399 unique ($R_{int}$ = 0.0639, R_{sigma} = 0.0474) which were used in all calculations. The final R_1 was 0.0616 ($I > 2\sigma(I)$) and wR_2 was 0.1692 (all data).

Refinement model description

Number of restraints - 0, number of constraints - unknown.

Details:

1. Fixed Uiso at 1.2 times of all C(H) groups and at 1.5 times of all C(H,H,H) groups, all O(H) groups
2a. Aromatic/amide H refined with riding coordinates:
C3(H3), C4(H4A), C5(H5), C6(H6), C11(H11)
2b. Idealised Me refined as rotating group:
C19(H19A,H19B,H19C), C20(H20A,H20B,H20C)
2c. Idealised tetrahedral OH refined as rotating group:
O4(H4)

References

1. Asimov, I., *A short history of chemistry*. Praeger, New York: 1979.

2. Warren, W., Contemporary reception of Wohler's discovery of the synthesis of urea. *Journal of Chemical Education* **1928,** *5* (12), 1539.

3. Rocke, A. J., *The quiet revolution: Hermann Kolbe and the science of organic chemistry*. Univ. of California Press, Berkeley: 1993.

4. Russell, C. A., The changing role of synthesis in organic chemistry. *Ambix* **1987,** *34* (3), 169-180.

5. Nicolaou, K. C.; Sorensen, E. J., *Classics in total synthesis: targets, strategies, methods*. John Wiley & Sons, Inc., Weinheim: 1996.

6. Poliakoff, M.; Fitzpatrick, J. M.; Farren, T. R.; Anastas, P. T., Green chemistry: science and politics of change. *Science* **2002,** *297* (5582), 807-810.

7. Török, B.; Dransfield, T., Green chemistry: Historical perspectives and basic concepts. In *Green Chemistry*, Elsevier, Boston: 2018; pp 3-16.

8. Stolarski, R. S., The Antarctic ozone hole. *Scientific American* **1988,** *258* (1), 30-37.

9. Solomon, S., Stratospheric ozone depletion: A review of concepts and history. *Reviews of Geophysics* **1999,** *37* (3), 275-316.

10. Weatherhead, E. C.; Andersen, S. B., The search for signs of recovery of the ozone layer. *Nature* **2006,** *441* (7089), 39-45.

11. Schneider, S. H., The greenhouse effect: science and policy. *Science* **1989,** *243* (4892), 771-781.

12. Lashof, D. A.; Ahuja, D. R., Relative contributions of greenhouse gas emissions to global warming. *Nature* **1990,** *344* (6266), 529-531.

13. Broughton, E., The Bhopal disaster and its aftermath: a review. *Environmental Health* **2005,** *4* (1), 1-6.

14. Varma, R.; Varma, D. R., The Bhopal disaster of 1984. *Bulletin of Science, Technology & Society* **2005,** *25* (1), 37-45.

15. Beach, E. S.; Cui, Z.; Anastas, P. T., Green Chemistry: A design framework for sustainability. *Energy & Environmental Science* **2009,** *2* (10), 1038-1049.

16. Anastas, P. T.; Warner, J. C., *Green chemistry : theory and practice*. Oxford University Press, Oxford: 1998.

17. Anastas, P.T.; Eghbali, N., Green chemistry: principles and practice. *Chemical Society Reviews* **2010,** *39* (1), 301-312.

18. Anastas, P. T.; Kirchhoff, M. M.; Williamson, T. C., Catalysis as a foundational pillar of green chemistry. *Applied Catalysis A: General* **2001,** *221* (1-2), 3-13.

19. Anastas, P. T.; Bartlett, L. B.; Kirchhoff, M. M.; Williamson, T. C., The role of catalysis in the design, development, and implementation of green chemistry. *Catalysis Today* **2000,** *55* (1-2), 11-22.

20. Knowles, W. S., Asymmetric hydrogenations (Nobel lecture). *Angewandte Chemie International Edition* **2002,** *41* (12), 1998-2007.

21. Knowles, W. S., Application of organometallic catalysis to the commercial production of L-DOPA. *Journal of Chemical Education* **1986,** *63* (3), 222.

22. Noyori, R., Asymmetric hydrogenation. *Acta Chemica Scandinavica* **1996,** *50*, 380-390.

23. Sharpless, K. B., Searching for new reactivity. *Tetrahedron* **1994,** *50*, 4235.

24. Sheldon, R. A., E factors, green chemistry and catalysis: an odyssey. *Chemical Communications* **2008,** (29), 3352-3365.

25. Sheldon, R. A., Green chemistry and resource efficiency: towards a green economy. *Green Chemistry* **2016,** *18* (11), 3180-3183.

26. Pereira, C. J., Environmentally friendly processes. *Chemical Engineering Science* **1999,** *54* (13-14), 1959-1973.

27. Varma, R. *The presidential green chemistry challenge awards program, summary of 1997 award entries and recipients*; EPA744-S-97-001. US Environmental Protection Agency, Office of Pollution and Prevention of Toxins, Washington, DC: 1997.

28. Cann, M.; Connelly, M., The BHC company synthesis of Ibuprofen, a greener synthesis of Ibuprofen which creates less waste and fewer byproducts. In *Real World Cases in Green Chemistry*, American Chemical Society, Washington DC: 2000; pp 19-24.

29. Dasari, M. A.; Kiatsimkul, P.-P.; Sutterlin, W. R.; Suppes, G. J., Low-pressure hydrogenolysis of glycerol to propylene glycol. *Applied Catalysis A: General* **2005,** *281* (1-2), 225-231.

30. The Nobel Prize in Chemistry 2005. https://www.nobelprize.org/prizes/chemistry/2005/summary/ (accessed 2021-09-15).

31. Schuster, M.; Blechert, S., Olefin metathesis in organic chemistry. *Angewandte Chemie International Edition* **1997,** *36* (19), 2036-2056.

32. Fürstner, A., Olefin metathesis and beyond. *Angewandte Chemie International Edition* **2000,** *39* (17), 3012-3043.

33. Natta, G.; Dall'Asta, G.; Bassi, I. W.; Carella, G., Stereospecific ring cleavage homopolymerization of cycloolefins and structural examination of the resulting homologous series of linear crystalline *trans* polyalkenamers. *Die Makromolekulare Chemie: Macromolecular Chemistry and Physics* **1966,** *91* (1), 87-106.

34. Natta, G.; Dall'Asta, G.; Mazzanti, G., Stereospecific homopolymerization of cyclopentene. *Angewandte Chemie International Edition* **1964,** *3* (11), 723-729.

35. Natta, G.; Dall'Asta, G.; Mazzanti, G.; Motkoni, G., Stereospecific Polymerization oí Cyclobutene. *Die Makromolekulare Chemie: Macromolecular Chemistry and Physics* **1963,** *69*, 163-179.

36. Sutthasupa, S.; Shiotsuki, M.; Sanda, F., Recent advances in ring-opening metathesis polymerization, and application to synthesis of functional materials. *Polymer Journal* **2010,** *42* (12), 905-915.

37. Nicolaou, K.C.; Bulger, P. G.; Sarlah, D., Metathesis reactions in total synthesis. *Angewandte Chemie International Edition* **2005,** *44* (29), 4490-4527.

38. Grubbs, R. H.; Chang, S., Recent advances in olefin metathesis and its application in organic synthesis. *Tetrahedron* **1998,** *54* (18), 4413-4450.

39. Mortier, J., *Arene chemistry: reaction mechanisms and methods for aromatic compounds*. John Wiley & Sons, Inc.,Hoboken: 2015.

40. Jean-Louis Hérisson, P.; Chauvin, Y., Catalyse de transformation des oléfines par les complexes du tungstène. II. Télomérisation des oléfines cycliques en présence d'oléfines acycliques. *Die Makromolekulare Chemie: Macromolecular Chemistry and Physics* **1971,** *141* (1), 161-176.

41. Pelly, S. C.; Parkinson, C. J.; van Otterlo, W. A.L.; de Koning, C. B., Metathesis reactions for the synthesis of ring-fused carbazoles. *The Journal of Organic Chemistry* **2005,** *70* (25), 10474-10481.

42. Grubbs, R.; Wenzel, A., Handbook of Metathesis 2nd Ed.; Vol. 1. Wiley-VCH: Weinheim, Germany: 2015.

43. Ravindar, L.; Lekkala, R.; Rakesh, K.; Asiri, A. M.; Marwani, H. M.; Qin, H.-L., Carbonyl–olefin metathesis: A key review. *Organic Chemistry Frontiers* **2018,** *5* (8), 1381-1391.

44. Scharf, D.; Korte, F., Photosensibilisierte cyclodimerisierung von norbornen. *Tetrahedron Letters* **1963,** *4* (13), 821-823.

45. Albright, H.; Davis, A. J.; Gomez-Lopez, J. L.; Vonesh, H. L.; Quach, P. K.; Lambert, T. H.; Schindler, C. S., Carbonyl–Olefin Metathesis. *Chemical Reviews* **2021,** *121*, 9359-9406.

46. Jones, G.; Schwartz, S. B.; Marton, M. T., Regiospecific thermal cleavage of some oxetan photoadducts: carbonyl–olefin metathesis in sequential photochemical and thermal steps. *Journal of the Chemical Society, Chemical Communications* **1973,** (11), 374-375.

47. Jones, G.; Acquadro, M. A.; Carmody, M. A., Long-chain enals via carbonyl–olefin metathesis. An application in pheromone synthesis. *Journal of the Chemical Society, Chemical Communications* **1975,** (6), 206-207.

48. Stille, J. R.; Grubbs, R. H., Synthesis of (±)- $\Delta^{(9,\,12)}$-capnellene using titanium reagents. *Journal of the American Chemical Society* **1986,** *108* (4), 855-856.

49. Nicolaou, K.C.; Postema, M. H.; Claiborne, C. F., Olefin metathesis in cyclic ether formation. Direct conversion of olefinic esters to cyclic enol ethers with Tebbe-type reagents. *Journal of the American Chemical Society* **1996,** *118* (6), 1565-1566.

50. Griffith, A. K.; Vanos, C. M.; Lambert, T. H., Organocatalytic carbonyl-olefin metathesis. *Journal of the American Chemical Society* **2012,** *134* (45), 18581-18584.

51. Hong, X.; Liang, Y.; Griffith, A. K.; Lambert, T. H.; Houk, K., Distortion-accelerated cycloadditions and strain-release-promoted cycloreversions in the organocatalytic carbonyl-olefin metathesis. *Chemical Science* **2014,** *5* (2), 471-475.

52. Jermaks, J.; Quach, P. K.; Seibel, Z. M.; Pomarole, J.; Lambert, T. H., Ring-opening carbonyl–olefin metathesis of norbornenes. *Chemical science* **2020,** *11* (30), 7884-7895.

53. Zhang, Y.; Jermaks, J.; MacMillan, S. N.; Lambert, T. H., Synthesis of 2*H*-Chromenes via hydrazine-catalyzed ring-closing carbonyl-olefin metathesis. *ACS Catalysis* **2019,** *9* (10), 9259-9264.

54. Zhang, Y.; Sim, J. H.; MacMillan, S. N.; Lambert, T. H., Synthesis of 1,2-dihydroquinolines via hydrazine-catalyzed ring-closing carbonyl-olefin metathesis. *Organic letters* **2020,** *22* (15), 6026-6030.

55. Demole, E.; Enggist, P.; Borer, M. C., Applications synthétiques de la cyclisation d'alcools tertiaires γ-éthyléniques en α-bromotétrahydrofurannes sous l'action du N-bromosuccinimide. II. Cyclisation du (±)-nérolidol en diméthyl-2,5-(méthyl-4-pentène-3-yl)-2-cycloheptène-4-one, tétraméthyl-3,3,7,10-oxa-2-tricyclo [5.5.0.01,4]-dodécène-9, β-acoratriène, cédradiène-2,8, épi-2-α-cédrène et α-cédrène. *Helvetica Chimica Acta* **1971,** *54* (7), 1845-1864.

56. Jackson, A. C.; Goldman, B. E.; Snider, B. B., Intramolecular and intermolecular Lewis acid catalyzed ene reactions using ketones as enophiles. *The Journal of Organic Chemistry* **1984,** *49* (21), 3988-3994.

57. van Schaik, H. P.; Vijn, R. J.; Bickelhaupt, F., Acid-catalyzed olefination of benzaldehyde. *Angewandte Chemie International Edition* **1994,** *33* (15-16), 1611-1612.

58. Khripach, V. A.; Zhabinskii, V. N.; Kuchto, A. I.; Zhiburtovich, Y. Y.; Gromak, V. V.; Groen, M. B.; van der Louw, J.; de Groot, A., Intramolecular cycloaddition/cycloreversion of (*E*)-3β, 17β-diacetoxy-5,10-secoandrost-1(10)-en-5-one. *Tetrahedron letters* **2006,** *47* (38), 6715-6718.

59. Soicke, A.; Slavov, N.; Neudörfl, J.-M.; Schmalz, H.-G., Metal-free intramolecular carbonyl-olefin metathesis of *ortho*-prenylaryl ketones. *Synlett* **2011,** *2011* (17), 2487-2490.

60. Ludwig, J. R.; Zimmerman, P. M.; Gianino, J. B.; Schindler, C. S., Iron (III)-catalysed carbonyl–olefin metathesis. *Nature* **2016,** *533* (7603), 374-379.

61. Ludwig, J. R.; Schindler, C. S., Lewis acid catalyzed carbonyl–olefin metathesis. *Synlett* **2017,** *28* (13), 1501-1509.

62. Becker, M. R.; Reid, J. P.; Rykaczewski, K. A.; Schindler, C. S., Models for understanding divergent reactivity in Lewis acid-catalyzed transformations of carbonyls and olefins. *ACS Catalysis* **2020,** *10* (7), 4387-4397.

63. Ludwig, J. R.; Phan, S.; McAtee, C. C.; Zimmerman, P. M.; Devery III, J. J.; Schindler, C. S., Mechanistic investigations of the iron (III)-catalyzed carbonyl-olefin metathesis reaction. *Journal of the American Chemical Society* **2017,** *139* (31), 10832-10842.

64. Ma, L.; Li, W.; Xi, H.; Bai, X.; Ma, E.; Yan, X.; Li, Z., $FeCl_3$-catalyzed ring-closing carbonyl–olefin metathesis. *Angewandte Chemie International Edition* **2016,** *55* (35), 10410-10413.

65. McAtee, C. C.; Riehl, P. S.; Schindler, C. S., Polycyclic aromatic hydrocarbons via iron (III)-catalyzed carbonyl–olefin metathesis. *Journal of the American Chemical Society* **2017,** *139* (8), 2960-2963.

66. Groso, E. J.; Golonka, A. N.; Harding, R. A.; Alexander, B. W.; Sodano, T. M.; Schindler, C. S., 3-Aryl-2,5-dihydropyrroles via catalytic carbonyl-olefin metathesis. *ACS catalysis* **2018,** *8* (3), 2006-2011.

67. Watson, R. B.; Schindler, C. S., Iron-catalyzed synthesis of tetrahydronaphthalenes *via* 3,4-dihydro-2*H*-pyran intermediates. *Organic letters* **2018,** *20* (1), 68-71.

68. Watson, R. B.; Golonka, A. N.; Schindler, C. S., Iron (III) chloride catalyzed formation of 3, 4-dihydro-2*H*-pyrans from α-alkylated 1,3-dicarbonyls. Selective synthesis of α-and β-lapachone. *Organic letters* **2016,** *18* (6), 1310-1313.

69. Rohr, J.; Thiericke, R., Angucycline group antibiotics. *Natural Product Reports* **1992,** *9* (2), 103-137.

70. Drautz, H.; Zähner, H.; Rohr, J.; Zeeck, A., Metabolic products of microorganisms. 234 Urdamycins, new angucycline antibiotics from *streptomyces fradiae* I. Isolation, characterization and biological properties. *The Journal of Antibiotics* **1986,** *39* (12), 1657-1669.

71. Dann, M.; Lefemine, D.; Barbatschi, F.; Shu, P.; Kunstmann, M.; Mitscher, L.; Bohonos, N., Tetrangomycin, a new quinone antibiotic. *Antimicrobial Agents and Chemotherapy* **1965,** *5*, 832-835.

72. Kuntsmann, M.; Mitscher, L., The structural characterization of tetrangomycin and tetrangulol. *The Journal of Organic Chemistry* **1966,** *31* (9), 2920-2925.

73. Bowie, J.; Johnson, A., The structure of ochromycinone. *Tetrahedron Letters* **1967,** *8* (16), 1449-1452.

74. Liu, W.-C.; Parker, W. L.; Slusarchyk, D. S.; Greenwood, G. L.; Graham, S. F.; Meyers, E., Isolation, characterization, and structure of rabelomycin, a new antibiotic. *The Journal of Antibiotics* **1970,** *23* (9), 437-441.

75. Sezaki, M.; Kondo, S.; Maeda, K.; Umezawa, H.; Ohno, M., The structure of aquayamycin. *Tetrahedron* **1970,** *26* (22), 5171-5190.

76. Henkel, T.; Rohr, J.; Beale, J. M.; Schwenen, L., Landomycins, new angucycline antibiotics from *Streptomyces sp*. *The Journal of Antibiotics* **1990,** *43* (5), 492-503.

77. Kharel, M. K.; Pahari, P.; Shepherd, M. D.; Tibrewal, N.; Nybo, S. E.; Shaaban, K. A.; Rohr, J., Angucyclines: Biosynthesis, mode-of-action, new natural products, and synthesis. *Natural Product Reports* **2012,** *29* (2), 264-325.

78. Luzhetskyy, A.; Vente, A.; Bechthold, A., Glycosyltransferases involved in the biosynthesis of biologically active natural products that contain oligosaccharides. *Molecular BioSystems* **2005,** *1* (2), 117-126.

79. Korynevska, A.; Heffeter, P.; Matselyukh, B.; Elbling, L.; Micksche, M.; Stoika, R.; Berger, W., Mechanisms underlying the anticancer activities of the angucycline landomycin E. *Biochemical Pharmacology* **2007,** *74* (12), 1713-1726.

80. Cottreau, K. M.; Spencer, C.; Wentzell, J. R.; Graham, C. L.; Borissow, C. N.; Jakeman, D. L.; McFarland, S. A., Diverse DNA-cleaving capacities of the jadomycins through precursor-directed biosynthesis. *Organic Letters* **2010,** *12* (6), 1172-1175.

81. Hall, S. R.; Blundon, H. L.; Ladda, M. A.; Robertson, A. W.; Martinez-Farina, C. F.; Jakeman, D. L.; Goralski, K. B., Jadomycin breast cancer cytotoxicity is mediated by a copper-dependent, reactive oxygen species–inducing mechanism. *Pharmacology Research & Perspectives* **2015,** *3* (2), e00110.

82. Hasinoff, B. B.; Wu, X.; Yalowich, J. C.; Goodfellow, V.; Laufer, R. S.; Adedayo, O.; Dmitrienko, G. I., Kinamycins A and C, bacterial metabolites that contain an unusual diazo group, as potential new anticancer agents: antiproliferative and cell cycle effects. *Anti-Cancer Drugs* **2006,** *17* (7), 825-837.

83. Rohr, J.; Beale, J. M.; Floss, H. G., Urdamycins, new angucycline antibiotics from *Streptomyces fradiae*. *The Journal of Antibiotics* **1989,** *42* (7), 1151-1157.

84. Sasaki, E.; Ogasawara, Y.; Liu, H.-W., A biosynthetic pathway for BE-7585A, a 2-thiosugar-containing angucycline-type natural product. *Journal of the American Chemical Society* **2010,** *132* (21), 7405-7417.

85. Brown, P. M.; Thomson, R. H., Naturally occurring quinones. Part XXVI. A synthesis of tetrangulol (1,8-dihydroxy-3-methylbenz[α]anthracene-7,12-quinone). *Journal of the Chemical Society, Perkin Transactions 1* **1976,** (9), 997-1000.

86. Nicolaou, K. C.; Snyder, S. A.; Montagnon, T.; Vassilikogiannakis, G., The Diels–Alder reaction in total synthesis. *Angewandte Chemie International Edition* **2002,** *41* (10), 1668-1698.

87. Guingant, A.; Barreto, M. M., A new route for the efficient synthesis of (±) ochromycinone, a naturally occurring benz[α]anthraquinone. *Tetrahedron letters* **1987,** *28* (27), 3107-3110.

88. Krohn, K.; Micheel, J.; Zukowski, M., Total synthesis of angucyclines. Part 15: A short synthesis of (±)-6-deoxybrasiliquinone B. *Tetrahedron* **2000,** *56* (27), 4753-4758.

89. Kaliappan, K. P.; Ravikumar, V., Angucyclinone antibiotics: Total syntheses of YM-181741, (+)-ochromycinone, (+)-rubiginone B2, (−)-tetrangomycin, and MM-47755. *The Journal of Organic Chemistry* **2007,** *72* (16), 6116-6126.

90. Matsumoto, T.; Sohma, T.; Yamaguchi, H.; Kurata, S.; Suzuki, K., Total synthesis of antibiotic C104: Benzyne-furan cycloaddition approach to the angucyclines. *Tetrahedron* **1995,** *51* (27), 7347-7360.

91. Kraus, G. A.; Wu, Y., The synthesis of angularly fused aromatic ring systems. The synthesis of 3-deoxyrabelomycin. *Tetrahedron Letters* **1991,** *32* (31), 3803-3806.

92. Hauser, F. M.; Rhee, R. P., New synthetic methods for the regioselective annelation of aromatic rings: 1-hydroxy-2,3-disubstituted naphthalenes and 1,4-dihydroxy-2,3-disubstituted naphthalenes. *The Journal of Organic Chemistry* **1978,** *43* (1), 178-180.

93. Mal, D.; Roy, H. N.; Hazra, N. K.; Adhikari, S., A rapid access to hydroxylated benz [α]anthraquinones: Hypervalent iodine oxidation of β-naphthols. *Tetrahedron* **1997,** *53* (6), 2177-2184.

94. Mal, D.; Dey, S., Synthesis of chlorine-containing angucycline BE-23254 and its analogs. *Tetrahedron* **2006,** *62* (41), 9589-9602.

95. Roush, W. R.; Neitz, R. J., Studies on the synthesis of landomycin A. Synthesis of the originally assigned structure of the aglycone, landomycinone, and revision of structure. *The Journal of Organic Chemistry* **2004,** *69* (15), 4906-4912.

96. Katsuura, K.; Snieckus, V., Directed *ortho* metalation reactions. Synthesis of the naturally-occurring benz[α]anthraquinones X-14881 C and ochromycinone. *Tetrahedron Letters* **1985,** *26* (1), 9-12.

97. Kimura, S.; Kobayashi, S.; Kumamoto, T.; Akagi, A.; Sato, N.; Ishikawa, T., Syntheses of prekinamycin and a tetracyclic quinone from common synthetic intermediates. *Helvetica Chimica Acta* **2011,** *94* (4), 578-591.

98. Kesenheimer, C.; Kalogerakis, A.; Meißner, A.; Groth, U., The cobalt way to angucyclinones: Asymmetric total synthesis of the antibiotics (+)-rubiginone B2, (−)-tetrangomycin, and (−)-8-O-methyltetrangomycin. *Chemistry–A European Journal* **2010,** *16* (29), 8805-8821.

99. Sato, K.; Asao, N.; Yamamoto, Y., Efficient method for synthesis of angucyclinone antibiotics via gold-catalyzed intramolecular [4+ 2] benzannulation: enantioselective total synthesis of (+)-ochromycinone and (+)-rubiginone B2. *The Journal of Organic Chemistry* **2005,** *70* (22), 8977-8981.

100. Nicolaou, K. C.; Bulger, P. G.; Sarlah, D., Palladium-catalyzed cross-coupling reactions in total synthesis. *Angewandte Chemie International Edition* **2005,** *44* (29), 4442-4489.

101. Ding, C.; Tu, S.; Li, F.; Wang, Y.; Yao, Q.; Hu, W.; Xie, H.; Meng, L.; Zhang, A., Synthesis study on marmycin A: preparation of the C3′-desmethyl analogues. *The Journal of Organic Chemistry* **2009,** *74* (16), 6111-6119.

102. Kotha, S.; Lahiri, K.; Dhurke, K., Recent applications of the Suzuki–Miyaura cross-coupling reaction in organic synthesis. **2002,** *58* (48), 9633-9695.

103. Blakemore, D. Suzuki–Miyaura coupling. In *Synthetic Methods in Drug Discovery: Volume 1;* Royal Society of Chemistry, 2015; pp 1-69. DOI: 10.1039/9781782622086-00001.

104. Miyaura, N.; Suzuki, A., Stereoselective synthesis of arylated (*E*)-alkenes by the reaction of alk-1-enylboranes with aryl halides in the presence of palladium catalyst. *Journal of the Chemical Society, Chemical Communications* **1979,** (19), 866-867.

105. Miyaura, N.; Yamada, K.; Suzuki, A., A new stereospecific cross-coupling by the palladium-catalyzed reaction of 1-alkenylboranes with 1-alkenyl or 1-alkynyl halides. *Tetrahedron Letters* **1979,** *20* (36), 3437-3440.

106. Miyaura, N.; Yanagi, T.; Suzuki, A., The palladium-catalyzed cross-coupling reaction of phenylboronic acid with haloarenes in the presence of bases. *Synthetic Communications* **1981,** *11* (7), 513-519.

107. Watanabe, T.; Miyaura, N.; Suzuki, A., Synthesis of sterically hindered biaryls via the palladium-catalyzed cross-coupling reaction of arylboronic acids or their esters with haloarenes. *Synlett* **1992,** *1992* (03), 207-210.

108. Miyaura, N., Cross-coupling reaction of organoboron compounds via base-assisted transmetalation to palladium (II) complexes. *Journal of Organometallic Chemistry* **2002,** *653* (1-2), 54-57.

109. Martin, R.; Buchwald, S. L., Palladium-catalyzed Suzuki-Miyaura cross-coupling reactions employing dialkylbiaryl phosphine ligands. *Accounts of Chemical Research* **2008,** *41* (11), 1461-1473.

110. Johnson, M. M.; Ngwira, K. J.; Rousseau, A. L.; Lemmerer, A.; de Koning, C. B., Novel methodology for the synthesis of the benz[α]anthracene skeleton of the angucyclines using a Suzuki-Miyaura/isomerization/ring closing metathesis strategy. *Tetrahedron* **2018,** *74* (1), 12-18.

111. Ngwira, K. J.; Rousseau, A. L.; Johnson, M. M.; de Koning, C. B., Reactions of [2-(2-naphthyl) phenyl] acetylenes and 2-(2-naphthyl)benzaldehyde-*O*-phenyloximes: Synthesis of the angucycline tetrangulol and 1,10,12-trimethoxy-8-methylbenzo[*c*]phenanthridine. *European Journal of Organic Chemistry* **2017,** *2017* (11), 1479-1488.

112. Heinzman, S. W.; Grunwell, J. R., Regiospecific synthesis of bromojuglone derivatives. *Tetrahedron Letters* **1980,** *21* (45), 4305-4308.

113. Brimble, M. A.; Bachu, P.; Sperry, J., Enantioselective synthesis of an analogue of nanaomycin A. *Synthesis* **2007,** *2007* (18), 2887-2893.

114. Anderson, J. M.; Kochi, J. K., Silver (I)-catalyzed oxidative decarboxylation of acids by peroxydisulfate. Role of silver (II). *Journal of the American Chemical Society* **1970,** *92* (6), 1651-1659.

115. Kesteleyn, B.; De Kimpe, N.; Van Puyvelde, L., Total synthesis of two naphthoquinone antibiotics, psychorubrin and pentalongin, and their C(1)-substituted alkyl and aryl derivatives. *The Journal of Organic Chemistry* **1999,** *64* (4), 1173-1179.

116. Brimble, M. A.; Elliott, R. J., Stereoselective synthesis of deoxy analogues of the 3C-protease inhibitor thysanone. *Tetrahedron* **2002,** *58* (1), 183-189.

117. Moriarty, E.; Aldabbagh, F., Synthesis of aryl ring-fused benzimidazolequinones using 6-exo-trig radical cyclizations. *Tetrahedron Letters* **2009,** *50* (37), 5251-5253.

118. Moriarty, E.; Carr, M.; Bonham, S.; Carty, M. P.; Aldabbagh, F., Synthesis and toxicity towards normal and cancer cell lines of benzimidazolequinones containing fused aromatic rings and 2-aromatic ring substituents. *European Journal Of Medicinal Chemistry* **2010,** *45* (9), 3762-3769.

119. Sweeney, M.; Gurry, M.; Keane, L.-A. J.; Aldabbagh, F., Greener synthesis using hydrogen peroxide in ethyl acetate of alicyclic ring-fused benzimidazoles and anti-tumour benzimidazolequinones. *Tetrahedron Letters* **2017,** *58* (36), 3565-3567.

120. Pathak, R.; Vandayar, K.; van Otterlo, W. A.L.; Michael, J. P.; Fernandes, M. A.; de Koning, C. B., The synthesis of angularly fused polyaromatic compounds by using a light-assisted, base-mediated cyclization reaction. *Organic & Biomolecular Chemistry* **2004,** *2* (23), 3504-3509.

121. Braverman, S.; Duar, Y., Thermal rearrangements of allenes. Synthesis and mechanisms of cycloaromatization of pi and heteroatom bridged diallenes. *Journal of the American Chemical Society* **1990,** *112* (15), 5830-5837.

122. McMurry, J. E.; Fleming, M. P., New method for the reductive coupling of carbonyls to olefins. Synthesis of *beta*-carotene. *Journal of the American Chemical Society* **1974,** *96* (14), 4708-4709.

123. Mukaiyama, T.; Sato, T.; Hanna, J., Reductive coupling of carbonyl compounds to pinacols and olefins by using $TiCl_4$ and Zn. *Chemistry Letters* **1973,** *2* (10), 1041-1044.

124. Tyrlik, S., Application des complexes de metaux de transition de bas degre d'oxydation en synthese organique. I. Nouvelle synthese d'olefines a partir de derives carbonyles. *Bulletin de la Societe Chimique de France* **1973,** *6*, 2147-2148.

125. McMurry, J. E., Carbonyl-coupling reactions using low-valent titanium. *Chemical Reviews* **1989,** *89* (7), 1513-1524.

126. Bensari, A.; Zaveri, N. T., Titanium (IV) chloride-mediated *ortho*-acylation of phenols and naphthols. *Synthesis* **2003,** *2003* (02), 0267-0271.

127. Rayment, E. J.; Summerhill, N.; Anderson, E. A., Synthesis of phenols via fluoride-free oxidation of arylsilanes and arylmethoxysilanes. *The Journal of Organic Chemistry* **2012,** *77* (16), 7052-7060.

128. De Koning, C. B., The syntheses of some naturally derived naphthoquinones. Ph.D. Thesis, The University of Cape Town., 1987.

129. Liu, G.; Xu, B., Hydrogen-bond donor solvents enabled metal and halogen-free Friedel–Crafts acylations with virtually no waste stream. *Tetrahedron Letters* **2018,** *59* (10), 869-872.

130. Sheldon, R. A., The greening of solvents: Towards sustainable organic synthesis. *Current Opinion in Green and Sustainable Chemistry* **2019,** *18*, 13-19.

131. Byrne, F. P.; Jin, S.; Paggiola, G.; Petchey, T. H.; Clark, J. H.; Farmer, T. J.; Hunt, A. J.; McElroy, C. R.; Sherwood, J., Tools and techniques for solvent selection: green solvent selection guides. *Sustainable Chemical Processes* **2016,** *4* (1), 1-24.

132. Hauser, F. M.; Ellenberger, S. R., Regiospecific oxidation of methyl groups in dimethylanisoles. *Synthesis* **1987,** (8), 723-724.

133. Li, T.; Li, J.; Zhu, Z.; Pan, W.; Wu, S., Cobalt (II)-catalyzed benzylic oxidations with potassium persulfate in TFA/TFAA. *RSC Advances* **2019,** *9* (36), 20879-20883.

134. Nicolaou, K.C.; Montagnon, T.; Baran, P.; Zhong, Y.-L., Iodine (V) reagents in organic synthesis. Part 4. *o*-Iodoxybenzoic acid as a chemospecific tool for single electron transfer-based oxidation processes. *Journal of the American Chemical Society* **2002,** *124* (10), 2245-2258.

135. Torii, S.; Tanaka, H.; Inokuchi, T.; Nakane, S.; Akada, M.; Saito, N.; Sirakawa, T., Indirect electrooxidation (an ex-cell method) of alkylbenzenes by recycle use of diammonium hexanitratocerate in various solvent systems. *The Journal of Organic Chemistry* **1982,** *47* (9), 1647-1652.

136. Yoshino, Y.; Hayashi, Y.; Iwahama, T.; Sakaguchi, S.; Ishii, Y., Catalytic oxidation of alkylbenzenes with molecular oxygen under normal pressure and temperature by *N*-hydroxyphthalimide combined with $Co(OAc)_2$. *The Journal of Organic Chemistry* **1997,** *62* (20), 6810-6813.

137. Ishii, Y.; Sakaguchi, S., A new strategy for alkane oxidation with O_2 using *N*-hydroxyphthalimide (NHPI) as a radical catalyst. *Catalysis Surveys from Asia* **1999,** *3* (1), 27-35.

138. Ishiyama, T.; Murata, M.; Miyaura, N., Palladium (0)-catalyzed cross-coupling reaction of alkoxydiboron with haloarenes: a direct procedure for arylboronic esters. *The Journal of Organic Chemistry* **1995,** *60* (23), 7508-7510.

139. Jacob III, P.; Callery, P. S.; Shulgin, A. T.; Castagnoli Jr, N., A convenient synthesis of quinones from hydroquinone dimethyl ethers. Oxidative demethylation with ceric ammonium nitrate. *The Journal of Organic Chemistry* **1976,** *41* (22), 3627-3629.

140. Shan, G.; Yang, X.; Ma, L.; Rao, Y., Pd-catalyzed C-H oxygenation with TFA/TFAA: Expedient access to oxygen-containing heterocycles and late-stage drug modification. *Angewandte Chemie* **2012,** *124* (52), 13247-13251.

141. Thirunavukkarasu, V. S.; Ackermann, L., Ruthenium-catalyzed C–H bond oxygenations with weakly coordinating ketones. *Organic Letters* **2012,** *14* (24), 6206-6209.

142. Dias, G. G.; Rogge, T.; Kuniyil, R.; Jacob, C.; Menna-Barreto, R. F.; da Silva Júnior, E. N.; Ackermann, L., Ruthenium-catalyzed C–H oxygenation of quinones by weak O-coordination for potent trypanocidal agents. *Chemical Communications* **2018,** *54* (91), 12840-12843.

143. Roudesly, F.; Oble, J.; Poli, G., Metal-catalyzed CH activation/functionalization: The fundamentals. *Journal of Molecular Catalysis A: Chemical* **2017,** *426*, 275-296.

144. Gontijo, T. B.; de Carvalho, R. L.; Dantas-Pereira, L.; Menna-Barreto, R. F.; Rogge, T.; Ackermann, L.; da Silva Júnior, E. N., Ruthenium (II)-and Palladium (II)-catalyzed position-divergent CH oxygenations of arylated quinones: Identification of hydroxylated quinonoid compounds with potent trypanocidal activity. *Bioorganic & Medicinal Chemistry* **2021,** *40*, 116164.

145. Potterat, O.; Puder, C.; Wagner, K.; Bolek, W.; Vettermann, R.; Kauschke, S. G., Chlorocyclinones A−D, chlorinated angucyclinones from *Streptomyces sp*. strongly antagonizing rosiglitazone-induced PPAR-γ activation. *Journal of Natural Products* **2007,** *70* (12), 1934-1938.

146. Anastas, P. T.; Kirchhoff, M. M., Origins, current status, and future challenges of green chemistry. *Accounts of Chemical Research* **2002,** *35* (9), 686-694.

147. Ellabban, O.; Abu-Rub, H.; Blaabjerg, F., Renewable energy resources: Current status, future prospects and their enabling technology. *Renewable and Sustainable Energy Reviews* **2014,** *39*, 748-764.

148. Kühlborn, J.; Groß, J.; Opatz, T., Making natural products from renewable feedstocks: back to the roots? *Natural Product Reports* **2020,** *37*, 380-424.

149. Stubba, D.; Lahm, G.; Geffe, M.; Runyon, J. W.; Arduengo III, A. J.; Opatz, T., Xylochemistry—Making Natural Products Entirely from Wood. *Angewandte Chemie International Edition* **2015,** *54* (47), 14187-14189.

150. Anastas, P. T.; Warner, J. C., *Green chemistry: Theory and practice*. Oxford University Press, Oxford: 1998.

151. Gallezot, P., Process options for converting renewable feedstocks to bioproducts. *Green Chemistry* **2007,** *9* (4), 295-302.

152. Baeyer, A., Ueber die beziehungen der zimmtsäure zu der indigogruppe. *Berichte der Deutschen Chemischen Gesellschaft* **1880,** *13* (2), 2254-2263.

153. Huisgen, R., Adolf von Baeyer's scientific achievements—a legacy. *Angewandte Chemie International Edition* **1986,** *25* (4), 297-311.

154. de Meijere, A., Adolf von Baeyer: winner of the nobel prize for chemistry 1905. *Angewandte Chemie International Edition* **2005,** *44* (48), 7836-7840.

155. Metzger, J. O., Fats and oils as renewable feedstock for chemistry. *European Journal of Lipid Science and Technology* **2009,** *111* (9), 865-876.

156. Biermann, U.; Bornscheuer, U.; Meier, M. A.; Metzger, J. O.; Schäfer, H. J., Oils and fats as renewable raw materials in chemistry. *Angewandte Chemie International Edition* **2011,** *50* (17), 3854-3871.

157. Kiguchi, T.; Shirakawa, M.; Honda, R.; Ninomiya, I.; Naito, T., Total synthesis of (+)-azimic acid, (+)-julifloridine, and proposed structure of *N*-methyl julifloridine via cycloaddition of nitrone to a chiral dipolarophile. *Tetrahedron* **1998,** *54* (51), 15589-15606.

158. Bardhan, S. K.; Gupta, S.; Gorman, M.; Haider, M. A., Biorenewable chemicals: Feedstocks, technologies and the conflict with food production. *Renewable and Sustainable Energy Reviews* **2015,** *51*, 506-520.

159. Calvo-Flores, F. G.; Dobado, J. A., Lignin as renewable raw material. *ChemSusChem* **2010,** *3* (11), 1227-1235.

160. Torres, L. A. Z.; Woiciechowski, A. L.; de Andrade Tanobe, V. O.; Karp, S. G.; Lorenci, L. C. G.; Faulds, C.; Soccol, C. R., Lignin as a potential source of high-added value compounds: A review. *Journal of Cleaner Production* **2020,** *263*, 121499.

161. Zakzeski, J.; Jongerius, A. L.; Bruijnincx, P. C.; Weckhuysen, B. M., Catalytic lignin valorization process for the production of aromatic chemicals and hydrogen. *ChemSusChem* **2012,** *5* (8), 1602-1609.

162. Mgaya, J.; Shombe, G. B.; Masikane, S. C.; Mlowe, S.; Mubofu, E. B.; Revaprasadu, N., Cashew nut shell: a potential bio-resource for the production of bio-sourced chemicals, materials and fuels. *Green Chemistry* **2019,** *21* (6), 1186-1201.

163. Lubi, M. C.; Thachil, E. T., Cashew nut shell liquid (CNSL)-a versatile monomer for polymer synthesis. *Designed Monomers and polymers* **2000,** *3* (2), 123-153.

164. Mubofu, E. B., From cashew nut shell wastes to high value chemicals. *Pure and Applied Chemistry* **2016,** *88* (1-2), 17-27.

165. Deutsch, J.; Köckritz, A., Synthesis of novel chemicals from cardanol as a product of cashew nutshell processing. *Food Science & Nutrition* **2020,** *8* (7), 3081-3088.

166. Paramashivappa, R.; Kumar, P. P.; Vithayathil, P.; Rao, A. S., Novel method for isolation of major phenolic constituents from cashew (*Anacardium occidentale* L.) nut shell liquid. *Journal of Agricultural and Food Chemistry* **2001,** *49* (5), 2548-2551.

167. Amorati, R.; Attanasi, O. A.; Favi, G.; Menichetti, S.; Pedulli, G. F.; Viglianisi, C., Amphiphilic antioxidants from "cashew nut shell liquid"(CNSL) waste. *Organic & Biomolecular chemistry* **2011,** *9* (5), 1352-1355.

168. Stadeler, J., Uber die eigenthumlichen Bestandtheile der Anacardium Fruchte. *Ann Chemie Pharmacie* **1847,** *63*, 117-165.

169. Ruhemann, S.; Skinner, S., LXVI.—Anacardic acid. *Journal of the Chemical Society, Transactions* **1887,** *51*, 663-665.

170. Harvey, M.; Caplan, S., Cashew nut shell liquid. *Industrial & Engineering Chemistry* **1940,** *32* (10), 1306-1310.

171. Backer, H.; Haack, N., Composants du latex de l'*Anacardium Occidentale* Linn. *Recueil des Travaux Chimiques des Pays-Bas* **1941,** *60* (9), 661-677.

172. Tyman, J. H., Long-chain phenols. Part III. Identification of the components of a novel phenolic fraction in *Anacardium occidentale* (cashew nut-shell liquid) and synthesis of the saturated member. *Journal of the Chemical Society, Perkin Transactions 1* **1973**, 1639-1647.

173. Balachandran, V. S.; Jadhav, S. R.; Vemula, P. K.; John, G., Recent advances in cardanol chemistry in a nutshell: from a nut to nanomaterials. *Chemical Society Reviews* **2013,** *42* (2), 427-438.

174. Ribeiro, V. G. P.; Marcelo, A. M. P.; Da Silva, K. T.; Da Silva, F. L. F.; Mota, J. P. F.; Do Nascimento, J. P. C.; Sombra, A. S. B.; Clemente, C. d. S.; Mele, G.; Carbone, L., New ZnO@ Cardanol porphyrin composite nanomaterials with enhanced photocatalytic capability under solar light irradiation. *Materials* **2017,** *10* (10), 1114.

175. Moreira, L. F. B.; Lucas, E. F.; González, G., Stabilization of asphaltenes by phenolic compounds extracted from cashew-nut shell liquid. *Journal of Applied Polymer Science* **1999,** *73* (1), 29-34.

176. Costa, K. d. P.; de Viveiros, B. M.; Junior, M. A. S. S.; Suarez, P. A.; Rezende, M. J., Chemical transformations in technical cashew nut shell liquid and isolated mixture of cardanols, evaluation of the antioxidant activity and thermal stability of the products for use in pure biodiesel. *Fuel* **2019,** *235*, 1010-1018.

177. Chen, H.; Sun, J., Selective hydrogenation of phenol for cyclohexanone: A review. *Journal of Industrial and Engineering Chemistry* **2021,** *94*, 78-91.

178. Shi, Y.; Kamer, P. C.; Cole-Hamilton, D. J., Synthesis of pharmaceutical drugs from cardanol derived from cashew nut shell liquid. *Green Chemistry* **2019,** *21* (5), 1043-1053.

179. Ngwira, K. J.; Kühlborn, J.; Mgani, Q. A.; de Koning, C. B.; Opatz, T., Valorisation of cashew nut shell liquid phenolics in the synthesis of UV absorbers. *European Journal of Organic Chemistry* **2019,** *2019* (30), 4778-4790.

180. Roberts, J. C., Naturally occurring xanthones. *Chemical Reviews* **1961,** *61* (6), 591-605.

181. Pinto, M. M.; Palmeira, A.; Fernandes, C.; Resende, D. I.; Sousa, E.; Cidade, H.; Tiritan, M. E.; Correia-da-Silva, M.; Cravo, S., From natural products to new synthetic small molecules: a journey through the world of xanthones. *Molecules* **2021,** *26* (2), 431.

182. El-Seedi, H. R.; El-Ghorab, D. M.; El-Barbary, M. A.; Zayed, M. F.; Goransson, U.; Larsson, S.; Verpoorte, R., Naturally occurring xanthones; latest investigations: isolation, structure elucidation and chemosystematic significance. *Current Medicinal Chemistry* **2009,** *16* (20), 2581-2626.

183. Vieira, L.; Kijjoa, A., Naturally-occurring xanthones: recent developments. *Current Medicinal Chemistry* **2005,** *12* (21), 2413-2446.

184. Resende, D. I.; Durães, F.; Maia, M.; Sousa, E.; Pinto, M. M., Recent advances in the synthesis of xanthones and azaxanthones. *Organic Chemistry Frontiers* **2020,** *7* (19), 3027-3066.

185. Leconte, C., Beiträge zur chemischen Geschichte der Gentianwurzel. *Archiv der Pharmazie* **1838,** *63* (2), 184-192.

186. Hostettmann, K.; Hostettmann, M., Xanthones. In *Methods in plant biochemistry*, Academic press: 1989; Vol. 1, pp 493-508.

187. Bringmann, G.; Lang, G.; Steffens, S.; Günther, E.; Schaumann, K., Evariquinone, isoemericellin, and stromemycin from a sponge derived strain of the fungus *Emericella variecolor*. *Phytochemistry* **2003,** *63* (4), 437-443.

188. Pinto, M.; Sousa, E., Natural and synthetic xanthonolignoids: chemistry and biological activities. *Current Medicinal Chemistry* **2003,** *10* (1), 1-12.

189. Gottlieb, O.; Mesquita, A. L.; da Silva, E. M.; de Melo, M. T., Xanthones of *Kielmeyera ferruginea*. *Phytochemistry* **1969,** *8* (3), 665-666.

190. Zhou, H.-M.; Liu, Y.-L.; Blaskó, G.; Cordell, G. A., Swertiabisxanthone-I from *Swertia macrosperma*. *Phytochemistry* **1989,** *28* (12), 3569-3571.

191. Finnegan, R.; Stephani, R.; Ganguli, G.; Ganguly, S.; Bhattacharya, A., Occurrence of mangiferin in *Hiptage madablota Geartn*. *Journal of Pharmaceutical Sciences* **1968,** *57* (6), 1039-1040.

192. Loureiro, D. R.; Soares, J. X.; Costa, J. C.; Magalhães, Á. F.; Azevedo, C. M.; Pinto, M. M.; Afonso, C. M., Structures, activities and drug-likeness of anti-infective xanthone derivatives isolated from the marine environment: A review. *Molecules* **2019,** *24* (2), 243.

193. Feng, Z.; Lu, X.; Gan, L.; Zhang, Q.; Lin, L., Xanthones, a promising anti-inflammatory scaffold: structure, activity, and drug likeness analysis. *Molecules* **2020,** *25* (3), 598.

194. Zhou, B.-D.; Zeng, L.-L.; Tong, Y.-G.; Fang, J.-Y.; Ruan, Z.-P.; Zeng, X.-Y.; Fang, Y.-Y.; Xu, G.-F.; Hu, D.-B., Synthesis and antitumor, antityrosinase, and antioxidant activities of xanthone. *Journal of Asian Natural Products Research* **2018,** *20* (5), 467-476.

195. Salman, Z.; Yu-Qing, J.; Bin, L.; Cai-Yun, P.; Iqbal, C. M.; Atta-ur, R.; Wei, W., Antioxidant nature adds further therapeutic value: an updated review on natural xanthones and their glycosides. *Digital Chinese Medicine* **2019,** *2* (3), 166-192.

196. Shan, T.; Ma, Q.; Guo, K.; Liu, J.; Li, W.; Wang, F.; Wu, E., Xanthones from mangosteen extracts as natural chemopreventive agents: potential anticancer drugs. *Current Molecular Medicine* **2011,** *11* (8), 666-677.

197. Klein-Júnior, L. C.; Campos, A.; Niero, R.; Corrêa, R.; Vander Heyden, Y.; Filho, V. C., Xanthones and cancer: from natural sources to mechanisms of action. *Chemistry & Biodiversity* **2020,** *17* (2), e1900499.

198. Urbatzka, R.; Freitas, S.; Palmeira, A.; Almeida, T.; Moreira, J.; Azevedo, C.; Afonso, C.; Correia-da-Silva, M.; Sousa, E.; Pinto, M., Lipid reducing activity and toxicity profiles of a library of polyphenol derivatives. *European Journal of Medicinal Chemistry* **2018,** *151*, 272-284.

199. Michael, A., On the action of aromatic oxy-acids on phenols. *Am. Chem. J* **1883,** *5*, 81-97.

200. v. Kostanecki, S.; Nessler, B., Synthesen von oxyxanthonen. *Berichte der Deutschen Chemischen Gesellschaft* **1891,** *24* (1), 1894-1897.

201. Grover, P.; Shah, G.; Shah, R., Xanthones. Part IV. A new synthesis of hydroxyxanthones and hydroxybenzophenones. *Journal of the Chemical Society* **1955**, 3982-3985.

202. Sousa, M.; Pinto, M., Synthesis of xanthones: an overview. *Current Medicinal Chemistry* **2005,** *12* (21), 2447-2479.

203. Miguel Goncalves Azevedo, C.; Manuel Magalhaes Afonso, C.; Maria Magalhaes Pinto, M., Routes to xanthones: an update on the synthetic approaches. *Current Organic Chemistry* **2012,** *16* (23), 2818-2867.

204. Ramakrishnan, S.; Paramewaran, S.; Nasir, N. M., Synthetic approaches to biologically active xanthones: An update. *Chemical Papers* **2021,** *75* (2), 455-470.

205. Mroß, G.; Reinke, H.; Fischer, C.; Langer, P., Synthesis of functionalized 2-alkoxybenzoates, 2-aryloxybenzoates and xanthones based on formal [3+ 3] cyclocondensations of 3-alkoxy-and 3-aryloxy-1-silyloxy-1,3-butadienes with 3-silyloxy-2-en-1-ones. *Tetrahedron* **2009,** *65* (19), 3910-3917.

206. Kelly, T. R.; Jagoe, C. T.; Li, Q., Synthesis of (±) cervinomycins A1 and A2. *Journal of the American Chemical Society* **1989,** *111* (12), 4522-4524.

207. Goodell, J. R.; Madhok, A. A.; Hiasa, H.; Ferguson, D. M., Synthesis and evaluation of acridine-and acridone-based anti-herpes agents with topoisomerase activity. *Bioorganic & Medicinal Chemistry* **2006,** *14* (16), 5467-5480.

208. Granoth, I.; Segall, Y.; Kalir, A., Friedel–Crafts acylation–cyclisation reactions of 3-bromophenyl ethers with phosphorus trichloride and oxalyl chloride to give the corresponding phenoxaphosphine and xanthen-9-one derivatives. *Journal of the Chemical Society, Perkin Transactions 1* **1973**, 1972-1974.

209. Ma, R. Y.; Chen, Y. F.; Wang, J. R.; Du, Z. T., Synthesis of xanthones by palladium-catalyzed tandem carbonylation/C–H activation via 2-iodo diaryl ethers. *Journal of the Chinese Chemical Society* **2018,** *65* (1), 28-32.

210. Zhao, J.; Yue, D.; Campo, M. A.; Larock, R. C., An aryl to imidoyl palladium migration process involving intramolecular C− H activation. *Journal of the American Chemical Society* **2007,** *129* (16), 5288-5295.

211. Wang, P.; Rao, H.; Hua, R.; Li, C.-J., Rhodium-catalyzed xanthone formation from 2-aryloxybenzaldehydes via cross-dehydrogenative coupling (CDC). *Organic Letters* **2012,** *14* (3), 902-905.

212. Johnson, M. M.; Naidoo, J. M.; Fernandes, M. A.; Mmutlane, E. M.; van Otterlo, W. A.L.; de Koning, C. B., CAN-mediated oxidations for the synthesis of xanthones and related products. *The Journal of Organic Chemistry* **2010,** *75* (24), 8701-8704.

213. Mondal, M.; Puranik, V. G.; Argade, N. P., Facile synthesis of 1,3,7-trihydroxyxanthone and its regioselective coupling reactions with prenal: Simple and efficient access to osajaxanthone and nigrolineaxanthone F. *The Journal of Organic Chemistry* **2006,** *71* (13), 4992-4995.

214. Iikubo, K.; Ishikawa, Y.; Ando, N.; Umezawa, K.; Nishiyama, S., The first direct synthesis of α-mangostin, a potent inhibitor of the acidic sphingomyelinase. *Tetrahedron Letters* **2002,** *43* (2), 291-293.

215. Zhou, C.; Larock, R. C., Synthesis of aryl ketones or ketimines by palladium-catalyzed arene C− H addition to nitriles. *The Journal of Organic Chemistry* **2006,** *71* (9), 3551-3558.

216. Dai, M.; Yuan, X.; Kang, J.; Zhu, Z.-J.; Yue, R.-C.; Yuan, H.; Chen, B.-Y.; Zhang, W.-D.; Liu, R.-H.; Sun, Q.-Y., Synthesis and biological evaluation of phenyl substituted polyoxygenated xanthone derivatives as anti-hepatoma agents. *European Journal of Medicinal Chemistry* **2013,** *69*, 159-166.

217. Hintermann, L.; Masuo, R.; Suzuki, K., Solvent-controlled leaving-group selectivity in aromatic nucleophilic substitution. *Organic Letters* **2008,** *10* (21), 4859-4862.

218. Dam, J.; Bode, M. L.; de Koning, C. B., Ceric ammonium sulfate (CAS) mediated oxidations of benzophenones possessing a phenolic substituent for the synthesis of xanthones and related products. *The Journal of Organic Chemistry* **2018,** *84* (1), 150-160.

219. Frederick, J.; Snell, H.; Haywood, E., Solar ultraviolet radiation at the earth's surface. *Photochemistry and Photobiology* **1989,** *50* (4), 443-450.

220. Korać, R. R.; Khambholja, K. M., Potential of herbs in skin protection from ultraviolet radiation. *Pharmacognosy Reviews* **2011,** *5* (10), 164.

221. Gallagher, R. P.; Lee, T. K., Adverse effects of ultraviolet radiation: a brief review. *Progress in Biophysics and Molecular Biology* **2006,** *92* (1), 119-131.

222. Haywood, R.; Wardman, P.; Sanders, R.; Linge, C., Sunscreens inadequately protect against ultraviolet-A-induced free radicals in skin: implications for skin aging and melanoma? *Journal of Investigative Dermatology* **2003,** *121* (4), 862-868.

223. Shaath, N. A., Ultraviolet filters. *Photochemical & Photobiological Sciences* **2010,** *9* (4), 464-469.

224. Casiraghi, G.; Casnati, G.; Puglia, G.; Sartori, G.; Terenghi, G., Selective reactions between phenols and formaldehyde. A novel route to salicylaldehydes. *Journal of the Chemical Society, Perkin Transactions 1* **1980**, 1862-1865.

225. Nowrouzi, N.; Motevalli, S.; Tarokh, D., Palladium-catalyzed direct CH arylation of 2-hydroxybenzaldehydes with organic halides in neat water. *Journal of Molecular Catalysis A: Chemical* **2015,** *396*, 224-230.

226. Wakaki, T.; Togo, T.; Yoshidome, D.; Kuninobu, Y.; Kanai, M., Palladium-catalyzed synthesis of diaryl ketones from aldehydes and (hetero) aryl halides via C–H bond activation. *ACS Catalysis* **2018,** *8* (4), 3123-3128.

227. Kühlborn, J.; Groß, J.; Opatz, T., Making natural products from renewable feedstocks: back to the roots? *Natural Product Reports* **2020,** *37* (3), 380-424.

228. Eaton, P. E.; Carlson, G. R.; Lee, J. T., Phosphorus pentoxide-methanesulfonic acid. Convenient alternative to polyphosphoric acid. *The Journal of Organic Chemistry* **1973,** *38* (23), 4071-4073.

229. Ouchene, L.; Litvinov, I. V.; Netchiporouk, E., Hawaii and other jurisdictions ban oxybenzone or octinoxate sunscreens based on the confirmed adverse environmental effects of sunscreen ingredients on aquatic environments. *Journal of Cutaneous Medicine and Surgery* **2019,** *23* (6), 648-649.

230. Chawla, H.; Pant, N.; Kumar, S.; Mrig, S.; Srivastava, B.; Kumar, N.; Black, D. S., Synthesis and evaluation of novel tetrapropoxycalix[4]arene enones and cinnamates for protection from ultraviolet radiation. *Journal of Photochemistry and Photobiology B: Biology* **2011,** *105* (1), 25-33.

231. Jagot, F.; Minnie, I.; Rahman, A.; Ntsimango, S.; Ngwira, K. J.; de Koning, C. B., Hydrogen-bonded xanthones as potential UV absorbers: The synthesis of xanthones from bio-renewable cardanol utilizing a ceric ammonium sulfate (CAS)-mediated oxidation reaction. *SynOpen* **2022,** *6* (01), 58-66.

232. Pulikottil, F. T.; Pilli, R.; Suku, R. V.; Rasappan, R., Nickel-catalyzed cross-coupling of alkyl carboxylic acid derivatives with pyridinium salts via C–N bond cleavage. *Organic Letters* **2020,** *22* (8), 2902-2907.

233. Dickschat, J. S.; Wang, T.; Stadler, M., Volatiles from the xylarialean fungus *Hypoxylon invadens*. *Beilstein Journal of Organic Chemistry* **2018,** *14* (1), 734-746.